UNDERSTANDING THE PROGRESSION OF CML THROUGH THE REGULATION OF SELF-RENEWAL AND CELL SURFACE MARKERS

Dr Gillian A. Horne

MRCP MRes MBChB BSc (Med Sci)

Submitted in fulfilment of the requirements for the degree of Doctor of Philosophy

August 2017

Section of Experimental Haematology
Institute of Cancer Sciences
College of Medical, Veterinary and Life Sciences
University of Glasgow

‘All truths are easy to understand once they are discovered; the point is to discover them’

Galileo Galilei

In memory of Professor Tessa L. Holyoake
1963 - 2017

Abstract

Chronic myeloid leukaemia (CML) is a clonal myeloproliferative disorder that is associated with a reciprocal translocation between the long arms of chromosomes 22 and 9, giving rise to the Philadelphia (Ph) chromosome and the subsequent formation of the *BCR-ABL* fusion gene, encoding the constitutively active oncogenic tyrosine kinase, BCR-ABL. Advances in targeted therapies in chronic phase (CP) CML, notably the use of tyrosine kinase inhibitors (TKI), have led to a ten-fold reduction in disease progression to an accelerated or blast phase (BP). However, if left untreated, or in patients where resistance to TKIs exists or develops, the disease eventually progresses. BP can be myeloid, lymphoid or of an undifferentiated immunophenotype and, despite chemotherapeutic agents, will often end with a terminal outcome.

Progression to BP disease is thought to arise for three reasons: patient non-compliance, TKI resistance, which may be *BCR-ABL* dependent or independent, and disease persistence. Disease persistence suggests that a small population of cells survive despite TKI therapy, gain or have self-renewal properties, and reside in select haemopoietic bone marrow niches. These cells, termed leukaemic stem cells (LSCs), are not fully dependent on *BCR-ABL*, relying on deregulation of stem cell intrinsic pathways for their survival.

Within this thesis, we have explored the role of the self-renewal pathway, Notch, in the maintenance and progression of stem and progenitor populations within primary CML samples. We firstly identified, through focussed gene expression analysis, a deregulation of Notch pathway components within CP-CML samples. The Notch receptor, *NOTCH2*, was upregulated within this population. This was confirmed at protein level. The pathway was, however, deemed not to be activated through *in vitro* experimental assessment of proliferation, apoptosis, and cell cycle analysis in CP primary samples treated with the gamma-secretase inhibitor, DAPT. In view of the abundant expression of the receptor, we hypothesised that the pathway could be reactivated through exogenous stimulation upon ligand binding. An OP9 co-culture system, as well as plate-bound recombinant ligand, were utilised to allow for the overexpression of the Notch ligands, Delta-like 1 and Jagged1. We have demonstrated that Notch signalling can be reactivated within CP-CML samples, and that cellular function upon reactivation is dependent on cell maturity, i.e. immature $Lin^-CD34^+CD38^-$ and mature $Lin^-CD34^+CD38^+$ cells. The short-term effects of Notch activation through Jagged1 in $CD34^+$ CP-CML cells led to early erythroid differentiation that is blocked in an immature state. This was determined through cell surface identification of

erythroid markers. There was an increase in expression of both CD71 and GlyA with the addition of stromal co-culture. As CD33 expression was maintained, it suggested that although the samples had initiated differentiation, they could not progress beyond an immature phenotype. To corroborate the possible involvement of Notch activation through Jagged1 interaction in early differentiation, gene expression was investigated in primary $CD34^+$ CP-CML patient samples. There was a statistically significant increase in expression of key genes involved in early erythroid differentiation, namely, *p38* and *PU.1*, which have notable involvement in development of (pro)erythroblasts. Further to this, within the Lin^- $CD34^+CD38^-$ population, short-term activation of Notch through Jagged1 led to a significant reduction in colony formation with long-term colony initiating cell assays. This suggests that pulsed Notch activation may exhaust stem cell activity within the CP-CML phenotype and represent a possible targeted approach towards the CML LSC.

These findings did not translate on disease progression to a myeloid BP phenotype. Notch could not be reactivated despite the presence of the Notch receptor, *NOTCH2*. To investigate this further, we sorted CP (n=12), myeloid BP (n=11), and lymphoid BP (n=5) into stem and progenitor populations, before undertaking quantitative PCR of 90 self-renewal gene components of Wnt/β-catenin, Notch, Hedgehog, and BMP signalling pathways. The self-renewal pathways were highly deregulated between CP and BP, and suggested a two-phase disease process (i.e. CP and AP/BP), rather than triphasic (i.e. CP, AP and BP). There was statistically significant upregulation in Wnt/β-catenin components in myeloid BP compared to CP, particularly *TCF7*. We hypothesised that Wnt upregulation was preventing Notch activation in myeloid BP-CML. Further to this, transcriptional expression of self-renewal and cell survival pathways was compared between the Ph positive (+) acute leukaemias, namely, myeloid BP, lymphoid BP and Ph+ acute lymphoblastic leukaemia (ALL) (n=5). There was limited change in gene expression profiles of the self-renewal pathway components between myeloid and lymphoid BP disease, but gene expression could segregate Ph+ ALL from lymphoid BP upon gene clustering. This suggests that self-renewal gene components may offer diagnostic implications in the diagnosis of lymphoid BP and Ph+ ALL.

We next sought to provide further functional data as to the immunophenotypic marker of the CML LSC within CP disease. Our group has previously identified that CD93 is highly upregulated in CP-CML LSCs. Furthermore, using flow cytometry, we demonstrated significant upregulation of CD93 protein expression on $lin^-CD34^+CD38^-CD45RA^-CD90^+$ CML LSCs from peripheral blood and bone marrow of CP-CML patients (n= 17) compared

to normal HSC from healthy peripheral blood stem cell donors (n=7) and bone marrow donors (n=4). FISH confirmed that 100% of $lin^{-}CD34^{+}CD38^{-}CD45RA^{-}CD90^{+}CD93^{+}$ CML cells were BCR-ABL+ in all samples assessed. This thesis has further highlighted the LSC capability of a $CD93^{+}$-selected population through functional *in vitro* and *in vivo* analysis. We have demonstrated that $CD93^{+}$ CML-LSCs have increased colony-forming capability within long-term colony initiating cell assays. Furthermore, in xenograft transplantation experiments (n = 5), after 16 weeks, $CD34^{+}CD93^{+}$ CML LSC engrafted lethally irradiated NOD/SCID/IL-2Rg-/- (NSG) mice with BCR-ABL positive cells, whereas $CD34^{+}CD93^{-}$ cells from the same patient samples failed to engraft to significant levels. FISH confirmed that engrafted human cells were BCR-ABL positive. We further highlighted the immature LSC phenotype of CD93-selected cells through bulk and single cell gene expression analysis of 90 cell survival and self-renewal pathway components.

Overall the work presented in this thesis has furthered our understanding of the role of self-renewal within CML maintenance and progression, as well as further implicating the use of the cell surface marker, CD93, in the identification of the CML-LSC. This data will help guide novel therapeutic approaches towards the CML LSC in future experimental work, as well as guide further development in the transcriptional differences and potential targets in the Ph+ acute leukaemias.

Acknowledgements

As I reflect on the last few years of this PhD, I am reminded of the family, friends (old and new) and colleagues that have helped through the good times, the frustrating times, the repetitive times, and the late nights. This thesis is as much theirs, helping me in my clinical, academic and personal development.

It is with immense gratitude that I thank the following people who have supported me throughout this PhD, from the initial grant applications to the end. First and foremost, I would like to thank my supervisors, Professor Mhairi Copland and Professor Tessa Holyoake. Your guidance has been instrumental in allowing me to continue on this career path. Mhairi, thank you for listening to me and allowing me to develop my ideas. I feel privileged to have you as my primary supervisor and mentor for this thesis and for many years to come. Tessa, your work ethic inspires me - as well as your running! Your questioning only made me better and I thank you for this. To my 'third' supervisor, Dr Helen Wheadon, thank you for your constant guidance – you went above and beyond to develop me as a scientist. Thank you also to Dr Karen Keeshan, Dr Alison Michie, Dr David Vetrie, Dr Heather Jorgenson and Dr Graham Hamilton, who have offered guidance and have always shown an interest in my ideas.

To my 'lab family' – thanks for the banter! Dr Victoria Campbell - my night time and early morning lab buddy – thanks for your help (clinically and academically), and always being able to hold a conversation about celebrity gossip! Dr Ross Kinstrie and (almost) Dr Chris Estell – my gossipy girl pals who listen to me moan and help me out of any scientific conundrum! Miss Heather Morrison (my gene expression guru) and Miss Jen Cassels (my flow cytometry queen) – you two could rule the world (if only with your cheesy music taste). Thank you to Mrs Karen Dunn for teaching me all things mouse – I look forward to more mousey adventures! Dr Alan Hair, Mrs Diane Verrecchia, Mrs Angela Newlands, and Ms Michelle Bradley – the POG would be lost without you, and I thank you for being just really nice people! There are too many of the POG team to thank by name, but each of our 'lab family' has helped me at various stages and I am immensely grateful to each PI, PhD, postdoc, and masters student I have come in contact with. To my clinical colleagues – thank you for understanding.

To my EHA-ASH TRTH family – your guidance has helped me develop this project and make it better (hopefully). Every single person I have met through this program is

inspirational and makes me strive to do better. The collaborations and connections that have been developed will last a lifetime. Thank you to the Wellcome Trust who funded this fellowship, and to the patients who have donated samples to enable the research within the Paul O'Gorman Leukaemia Research Centre to be so world-renowned.

To 'the girls' (Eilidh, Bee, and Katie) – thanks for not forgetting I existed when I was working 'all' the time and for getting me out for a cocktail or two! To my mum, dad, David, Mo, and Les…thanks for listening to me and keeping me grounded. Dad, thanks for asking me repeatedly if it is done yet – it is! And finally, to my husband, Dan - thank you for always being there with the tea on!

To finish, in the words of F. Scott Fitzgerald, 'you don't write because you want to say something; you write because you've got something to say'.

Publication research output 2013-2017

Publications

Horne GA, Copland M. Approaches for targeting self-renewal pathways in cancer stem cells: implications for haematological treatments. *Expert Opin Drug Discov*. 2017; 12(5): 465-474

Horne GA, Jackson L, Helgason V, Holyoake TL. Stem Cell Guardians – Old and new Perspectives in LSC Biology. *Curr Drug Targets*. 2017;18(4):405-413

Igbineweka NE, Horne GA, Jackson MB, Chevassut TJ. Low Oxygen Affinity Variant Haemoglobin in an elderly woman presenting with low oxygen saturation. *Acute Med*. 2015;14(2):72-6

Horne GA, Chevassut TJ, Fidler K, Wynne C. Haemolytic anaemia: don't leave it out in the cold. *Arch Dis Child Educ Pract Ed*. 2015; 100(6):323-30

Horne GA, Kinstrie R, Copland M. Novel drug therapies in myeloid leukemia. *Pharm Pat Anal*. 2015;4(3):187-205

Horne GA, Steward HJ, Dickson J, Knapp S, Ramsahoye B, Chevassut T. Nanog required BRD4 to maintain murine embryonic stem cell pluripotency and is suppressed by bromodomain inhibitor JQ1 together with Lefty1. *Stem Cells*. Dec. 2015;24(7):879-91

Bisling KE, Brewin JN, McGovern AP, Horne GA et al. DNMT3A mutations at R882 hotspot are only found in major clones of acute myeloid leukemia. *Leuk Lymphoma.* 2014 Mar;55(3):711-4

Steward HJ, Horne GA, Bastow S, Chevassut TJ. BRD4 associates with p53 in DNMT3A-mutated leukemia cells and is implicated in apoptosis by the bromodomain inhibitor JQ1. *Cancer Med*. 2013;2(6):826-35

Brewin J, Horne G, Chevassut T. Genomic landscapes and clonality of de novo AML. *N Engl J Med*. 2013 Oct 10;369(15):1472-3

Publications in preparation

Kinstrie R*, Horne GA*, Morrison H, Irvine D, Munje C, Dunn K, Cassels JE, Holyoake TL, Wheadon H, Copland M. CD93 – a novel biomarker for chronic phase CML stem cells.

Horne GA, Morrison H, Kinstrie R, Hair A, Cassels JE, Wheadon H, Holyoake TL, Copland M. Notch pathway activation targets leukemic stem cells in chronic phase CML, but cannot be activated upon disease progression to myeloid blast phase.

Horne GA, Hamilton G, Holyoake TL, Copland M. Whole exome sequencing maps progression to myeloid and lymphoid blast phase in an unusual presentation of progressive CML.

Dobbin E, Tarafdar A, Zimmermann M, Morrison H, Toofan P, Horne GA, Copland M, Freeburn R, Wheadon H. Redirecting oncogene driven hematopoietic differentiation: Role of Wnt mediated transcriptional changes in self-renewal, early myeloid commitment and leukaemia progression.

Declaration

I declare that, except where explicit reference is made to the contribution of others, that this dissertation is the result of my own work and has not been submitted for any other degree at the University of Glasgow or any other institution.

Dr Gillian A. Horne

Table of contents

List of figures

List of tables

List of abbreviations

°C	Celsius
7AAD	7 amino actinomycin D
ABL	Abelson murine leukaemia viral oncogene homolog
ADAM	a disintegrin and metalloproteinase
ALL	acute lymphoblastic leukaemia
AML	acute myeloid leukaemia
AP	accelerated phase
ATCC	American Type Culture Collection
BCR	breakpoint cluster region protein
BM	bone marrow
BMP	bone morphogenic protein
BP	blast phase
CCyR	complete cytogenetic response
CFC	colony forming cells
CFSE	carboxyfluorescein diacetate succinimidyle ester
CHR	complete haematological response
CK1	casein kinase 1
CLL	chronic lymphocytic leukaemia
CLP	common lymphoid progenitors
CML	chronic myeloid leukaemia
CMP	common myeloid progenitors
CMR	complete molecular response
CO_2	carbon dioxide
CP	chronic phase
CSC	cancer stem cells
CSL	CBF-1-Suppressor of Hairless/lag1
CXCL12	stromal cell-derived factor 1
DAPI	4’,6-diamidino-2-phenyloindole
DAPT	N-[N-(3,5-Difluorophenacetyl-L-alanyl)]-(S)-phenylglycine t-butyl ester
DHH	desert hedgehog
DLL	delta-like
DMSO	dimethylsulphoxide
DSMZ	Deutsche Sammlung von Mikroorganismen und Zellkulturen
ELN	European Leukemia Net
FACS	fluorescence activated cell sorting
FISH	fluorescence In Situ Hybridisation
FMO	fluorescence minus one
FSC	forward-angle scatter
fucose-GIcNAc	fucose-N-acetylglucosamine
GCSF	granulocyte colony stimulating factor
Gfi1	growth factor independence 1
GMP	granulocyte-monocyte progenitors
GO	gemtuzumab ozogamicin
GSC	gamma secretase complex
GSK3β	glycogen synthase kinase 3β
HBSS	hanks balanced salt solution

CD34-	CD34 negative
CD34+	CD34 positive
DADI	The DAsatinib DIscontinuation study
DESTINY	DeEscalation and Stopping Treatment of Imatinib, Nilotinib or sprYcel in chronic myeloid leukaemia
EURO-ski	The European Stop Kinase Inhibitor trial
GlyA	glycophorin A
GSI	gamma secretase inhibitor
Hh	hedgehog
HRP	horseradish-peroxidase
HSC	haemopoietic stem cell
HSPC	haemopoietic stem and progenitor cells
IF	immunofluorescence
IFC	integrated fluidic circuit
IHH	indian hedgehog
IS	international scale
JAG	jagged
JAK-STAT	janus kinase/signal transducers and activators of transcription
LMPP	lymphoid-primed multipotent progenitors
LSCs	leukaemic stem cells
LTC-IC	long-term culture initiating cell assays
LTMCM	long-term myeloid culture medium
MAML	mastermind-like
MCyR	major cytogenetic response
MEP	megakaryocyte-erythroid progenitors
MFI	mean fluorescence intensity
MMR	major molecular response
MNC	mononuclear cells
MPP	multipotent progenitors
MRD	minimal residual disease
MSCs	mesenchymal stem cells
Msi-1	Musashi-1
MSPC	mesenchymal stem and progenitor cells
NCCN	National Comprehensive Cancer Network
NOD-SCID	non-obese diabetic severe combined immunodeficient
PB	peripheral blood
PCA	principal component analyses
PCR	polymerase chain reactions
PF4	platelet factor 4
Ph+	philadelphia positive
PI	propidium iodide
PTCH1	Patched1
PTCH2	Patched2
PVDF	immune-Bot polucinyliden difluoride
R-Jag1	recombinant jagged1
SCF	stem cell factor
SDS-PAGE	sodium dodecyle sulphate-polyacrylamide gel electrophoresis
SFM+5GF	serum free media and 5 growth factor
SFM+LGF	low growth factor SFM

SHH	sonic hedgehog
SMO	smoothened
SRC	SCID-repopulating cells
SSC	side-angle scatter
STIM	STop IMatinib
STK36	serine threonine kinase 36
TCF/LEF	T-cell factor/lymphoid enhancer factor
Tel	translocation Ets leukaemia
TGF-β	transforming growth factor beta
TGF-β1	transforming growth factor beta 1
TKI	tyrosine kinase inhibitor

1. Introduction

1.1. Haemopoiesis

1.1.1. Hierarchical haemopoiesis

The generation of mature and differentiated blood cells from a haemopoietic stem cell (HSC) is one of the best-characterised hierarchical systems. It relies on an intricate balance between self-renewal and differentiation, highlighting key features that have been critical to our understanding of how stem cells are maintained, differentiate, and are altered during haematological disease (Bhatia et al, 1997a; Bhatia et al, 1997b; Doulatov et al, 2010; Kiel et al, 2005; Majeti et al, 2007; Notta et al, 2011; Notta et al, 2016; Spangrude et al, 1988; Till & McCulloch, 1961).

In general, self-renewing cell types with extended life spans are rare and remain at the theoretical peak of the hierarchy (figure 1-1). These include long-term HSCs, as well as short-term HSCs, and intermediates with less durable self-renewal potential, termed multipotent progenitors (MPPs). They are defined by the capacity to perpetually self-renew, whilst contributing to a pool of differentiating cells. Oligoclonal progenitors (i.e. common myeloid progenitors (CMP) and common lymphoid progenitors (CLP)) appear in increased numbers below the self-renewing cell types. They have a shorter life-span and it is from these the common lineages for myelopoiesis (Akashi et al, 2000) and lymphopoiesis (Kondo et al, 1997) are isolated. Oligopotent CMPs undergo further constraint into megakaryocyte-erythroid progenitors (MEPs) that make platelets and erythrocytes, and granulocyte-monocyte progenitors (GMPs) that make granulocytes and monocytes.

Much of this understanding was developed within murine models using *in vivo* repopulating assays to assess sustained self-renewal and multipotent differentiation capacity. Subsequently, xenotransplantation models and robust *in vitro* colony assays, including long-term culture initiating cell assays (LTC-IC), have translated these findings into a humanised model (Copland et al, 2008; Doulatov et al, 2010; Galy et al, 1995; Laurenti et al, 2013; Manz et al, 2002; Sutherland et al, 1990).

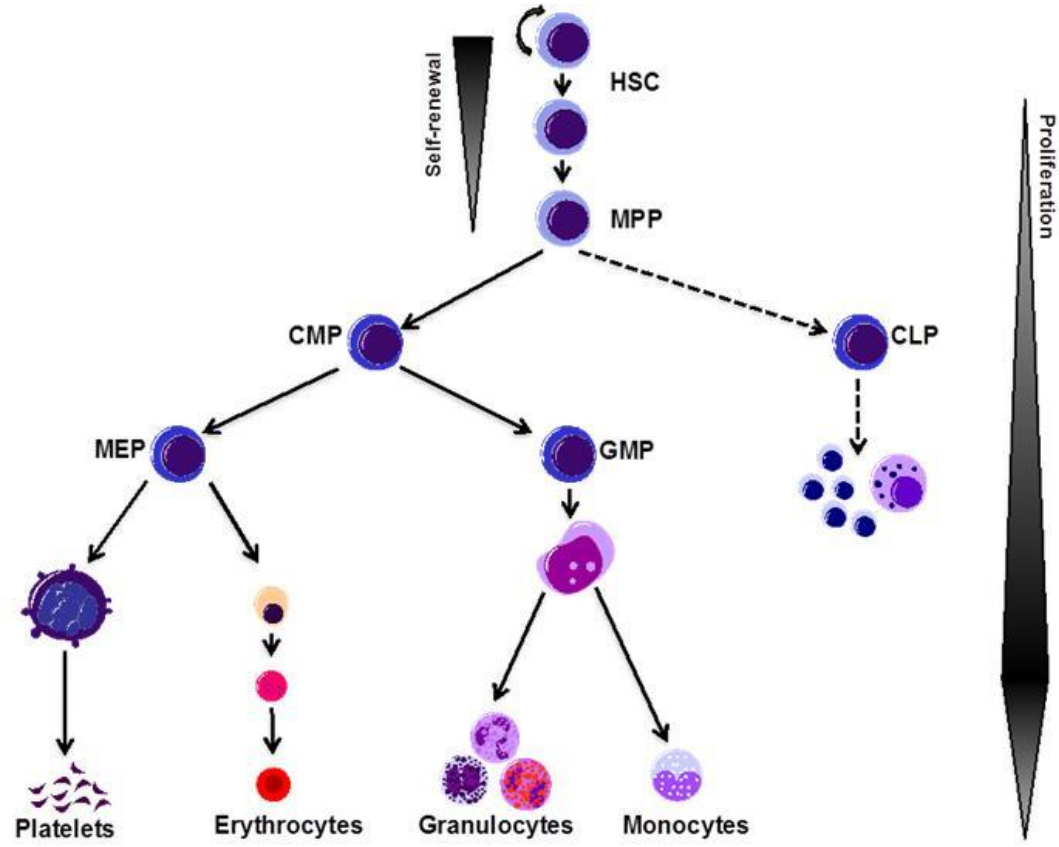

Figure 1-1 Simplified hierarchical model of haemopoiesis
Schematic diagram of a hierarchical model of haemopoiesis. HSCs reside at the peak of the hierarchy and have maximal self-renewal potential. They give rise to the MPP population. From MPPs, lineage committed progenitors are derived and from them more differentiated intermediate progenitors (not shown) before terminally differentiated cells are generated.

Although, this hierarchical idea was first postulated in 1909 (Konstantinov, 2000; Maximow, 1909), the continual advancement of scientific technique has led to an increased understanding of haemopoiesis, and its re-development. Although the standard model is used extensively as an operational paradigm, experimental data have challenged it. For example, the identification of a population of cells that have lymphoid developmental capacities, but can also give rise to granulocytes and macrophages, but not to megakaryocytes or erythrocytes, has been identified in both murine and human studies (Adolfsson et al, 2005; Ceredig et al, 2006; Doulatov et al, 2010; Reynaud et al, 2003). This population of cells, termed lymphoid-primed multipotent progenitors (LMPP), are not consistent with the established concept of dichotomous lineage segregation and remain contentious. However, their identification questions the mechanism through which MPPs lose lineage specific potential.

Furthermore, uncertainty remains concerning the myelo-erythro-megakaryocytic arm of the hierarchy, in part due to the fact that clonogenic *in vitro* assays do not read out all colony types at the same time making it difficult to account for all cells within a phenotypically pure

population. Paired daughter analysis of mouse HSC cell divisions have demonstrated that MEPs can be derived from HSCs directly without progressing through conventional MPPs and CMPs (Yamamoto et al, 2013). Transcriptional studies of highly purified or single-cell murine HSCs have established that molecular programmes corresponding to myeloid-erythroid-megakaryocyte fates can directly emerge in multipotent cells, arguing that cellular differentiation is not a gradual process and that myeloid differentiation can occur without progressing through the CMP stage (Guo et al, 2013; Månsson et al, 2007; Pronk et al, 2007; Yamamoto et al, 2013). Most recently, Notta et al mapped the lineage potential of nearly 3000 single cells from 33 different cell populations of stem and progenitor cells to obtain a two-tier hierarchy for development in early and late haemopoiesis (Notta et al, 2016). Regardless, although these data challenge the standard model, a clear consensus has yet to be made on a revised model of haemopoiesis and for the purpose of this thesis, the former hierarchical model will be used.

1.1.2. Phenotypic characterisation of human HSCs

As already described, murine models remain an indispensable approach for studying haemopoiesis, with loss or gain of gene function models allowing precise determination of the cellular components essential in its maintenance and deregulation. Human studies, however, remain imperative in our understanding of the haemopoietic hierarchy in view of the complex interactions within the bone marrow (BM) and peripheral blood (PB), as well as the differences that are noted between murine and human models. For example, tumourigenesis or epigenetic vulnerability in species that vary in size, ecology, age to reproductive maturity, and lifespan will lead to differing cellular responses (Hahn & Weinberg, 2002).

The phenotypic characterisation of human HSCs has been fundamental in the pursuit to understand normal and abnormal haemopoiesis. CD34, a surface glycoprotein, was initially discovered to be expressed on primitive haemopoietic tissues, but absent on mature differentiated cells, representing only 1-4% of BM haemopoietic cells (Civin et al, 1984). This population has been shown to be multipotent, highly enriched for colony forming cell (CFC) activity in assays *in vitro* and having the capacity for long-term haemopoietic reconstitution in murine xenograft models and clinical HSC transplantation studies (Hogan et al, 2002; Kang et al, 2008; Krause et al, 2013a; Lu et al, 1993; Sutherland et al, 1989; Sutherland et al, 1990; Vogel et al, 2000). Its physiological function is poorly understood, but roles in adhesion and differentiation have been described (Belay et al, 2017; Domogala et al, 2017; Ohnishi et al, 2013; Salati et al, 2008). However, it has been demonstrated that

CD34-deficient mice retain normal PB counts and a response to haemopoietic stress (Cheng et al, 1996). This may be, in part, due to the observation that CD34 positive ($CD34^+$) cells appear to be a heterogeneous population, with some evidence to suggest that CD34 negative ($CD34^-$) cells may be more primitive (Anjos-Afonso et al, 2013; Bhatia et al, 1998; Bonnet & Dick, 1997; Matsuoka et al, 2015; Zanjani et al, 1998). Within human studies, Zajani et al demonstrated *in vivo* engraftment potential of some Lin^-CD34^- BM cells in foetal sheep in primary and secondary recipients, and Bhatia et al showed engraftment of human cord blood Lin^-CD34^- cells in NOD/SCID mice (Bhatia et al, 1998; Zanjani et al, 1998). Within the latter, $CD34^+$ cells were noted from the Lin^-CD34^- transplanted animals, suggesting $CD34^-$ to be more primitive. These studies suggest that Lin^-CD34^- possess *in vivo* repopulating activity, rather than clonogenic and LTC-IC activity. Because these findings have been shown within *in* vivo models, it may suggest that cell-to-cell interaction within the BM microenvironment can influence self-renewal and repopulating potential, and this will be explored later in this chapter.

In view that the specificity of CD34 within an HSC population has yet to be fully determined, other surface markers in combination have been used to identify an HSC population. These include CD38, CD90, CD49f and CD45RA. Between 90 and 99% of $CD34^+$ cells express CD38; these cells have been shown not to possess self-renewal potential. Subsequently, it is the $Lin^-CD34^+CD38^-$ cells which are enriched in LTC-IC and have engraftment potential (Bhatia et al, 1997a; Hao et al, 1995; Huang & Terstappen, 1994a). In combination with CD34, CD90 demarcates a population of immature cells, with expression reducing in the presence of markers of maturing lineage commitment (Baum et al, 1992; Chen et al, 1995; Murray et al, 1995; Negrin et al, 2000). Further studies have introduced CD45RA as a marker of more differentiated cells (Bhatia et al, 1997b; Conneally et al, 1997; Craig et al, 1994; Lansdorp et al, 1990; Majeti et al, 2007; Schiavone et al, 1995). Similarly, CD49f expression has been described with enriched long-term HSC activity (van Galen et al, 2014; Yu et al, 2012), although its precision is variable between samples and, therefore, it is not typically used to define an HSC population in refined sorting strategies of human samples. Therefore, a current phenotype for human HSCs can be identified as $Lin^-CD34^+CD38^-CD90^+CD45RA^-$ (figure 1-2).

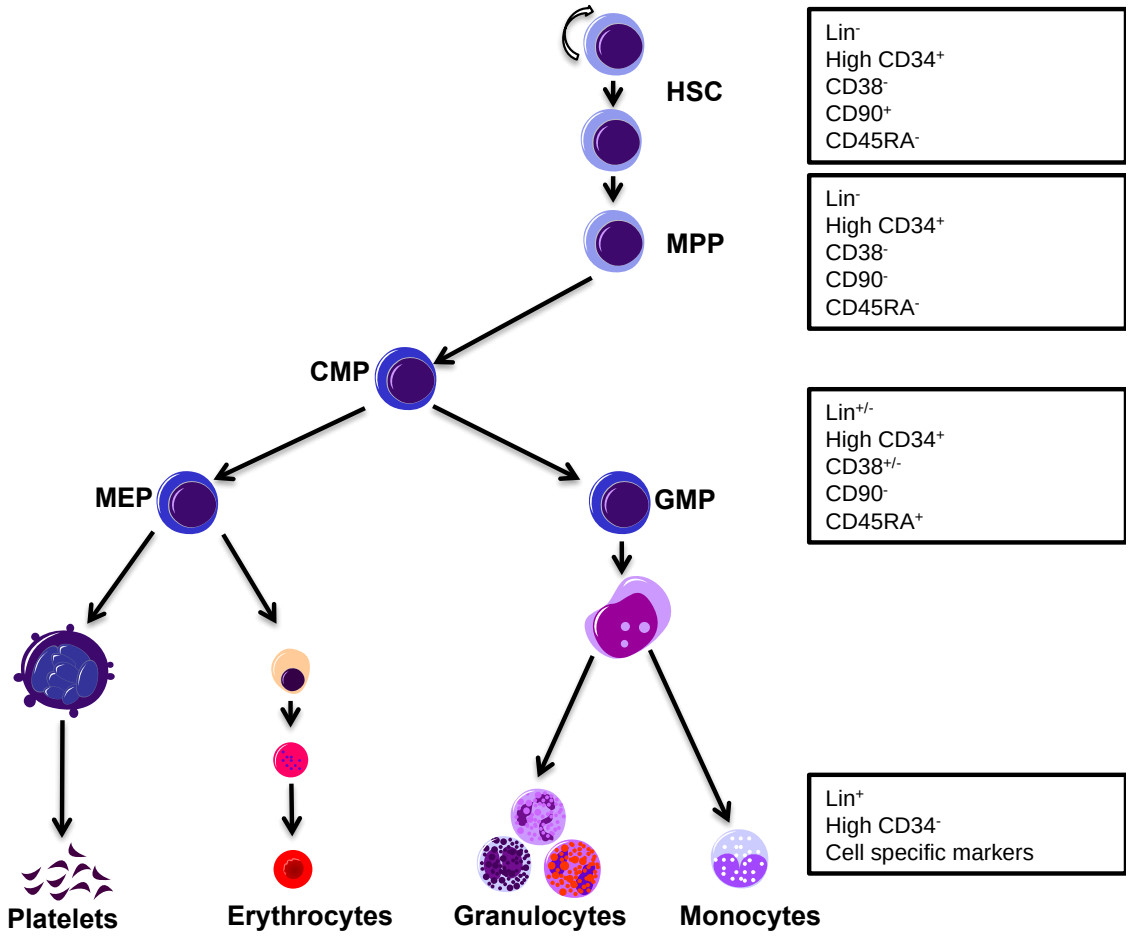

Figure 1-2 Phenotypic characterisation of the haemopoietic hierarchy
Schematic diagram depicting a phenotypic characterisation classification for an adult human haemopoietic hierarchy. For the purpose of this thesis, HSCs can be phenotypically classified as $Lin^-CD34^+CD38^-CD90^+CD45RA^-$, with MPP population classified as $Lin^-CD34^+CD38^-CD90^-CD45RA^-$, and mature populations classified by cell specific surface makers. Each population used within experimental design is described within both the methods and results chapters, with appropriate sorting strategies defined.

1.1.3. The maintenance of HSCs through quiescence and self-renewal

A refined cell sorting strategy to isolate highly purified stem and progenitor cell populations has led to an increased understanding of their functional and molecular properties, particularly within an HSC population. In order for an HSC population to be maintained, HSC loss through apoptosis, senescence or commitment to differentiation must be balanced with self-renewal capability (Goodell et al, 1996; Orford & Scadden, 2008; Passegué et al, 2005). HSCs are mainly quiescent (i.e. residing in G0 phase of the cell cycle). However, as they differentiate, a progressive reduction in the percentage of G0 cells is noted with a corresponding increase in the proliferation rate of each progenitor population (Catlin et al, 2011; Nygren et al, 2006). Although quiescence in itself does not define a stem cell, it is a major regulator of HSC function, with the ability to promote higher engraftment potential in

in vivo models, and its loss resulting in an imbalance of progenitor cells leading to HSC depletion (Cheshier et al, 1999; Mahmud et al, 2001; Orford & Scadden, 2008; Vanegas & Vernot, 2017; Wang et al, 2015). At a molecular level, cell cycle regulators play an integral role. As expected within a non-proliferative state, there are higher levels of the negative cell cycle regulators and lower levels of genes involved in DNA replication, for example *CyclinA2* and *CyclinB1* are downregulated owing to their role in cell cycle progression and proliferation (Forsberg et al, 2010; Kalaszczynska et al, 2009). Genes integral in transcriptional regulation, such as *Foxo3* and *Ezh1* are conversely upregulated within an HSC population (Miyamoto et al, 2007; Mochizuki-Kashio et al, 2011). In keeping with this, expression of positive cell cycle regulators, such as *CyclinD1*, has been shown to increase during differentiation (Passegué et al, 2005).

Although quiescence is a major regulator of HSCs, it is the cell's capacity for self-renewal that defines it. This function is critical to sustaining a hierarchical cell population. Self-renewal can be achieved through symmetric and asymmetric cell division, but the regulation of this has yet to be fully elucidated (Caussinus & Hirth, 2007; Daynac & Petritsch, 2017; Morrison & Kimble, 2006; Wu et al, 2007). Recent evidence suggests that ligand-dependent signalling pathways', such as Notch, Hedgehog (Hh), and Wnt/β-catenin, play a pivotal role (Campbell et al, 2008; Duncan et al, 2005; Staal et al, 2016; Weli et al, 2010). These pathways are often controlled through cell-to-cell interaction in the BM microenvironment, where the HSCs reside. Further to this, external signals from epigenetic modification and hypoxia, as well as intrinsic factors of the HSCs are deemed important (Belle et al, 2016; Bourdieu et al, 2017; Hasemann et al, 2014; Kramer & Challen, 2017; Vukovic et al, 2016).

1.2. Intrinsic and extrinsic regulation of HSC function

1.2.1. *The bone marrow microenvironment*

Haemopoietic stem and progenitor cells (HSPC) reside within the BM, which harbours distinct areas (or 'niches') that allow for the exogenous regulation of HSPC behaviour. Schofield first postulated this in 1978 (Schofield, 1978); however, it has only been in recent years with the advances in imaging techniques and selective genetic manipulation of specific cell populations that detailed insights of the BM anatomy and physiology have been generated (Kim et al, 2017; Le et al, 2017; Malide et al, 2014; Pang et al, 2015; Wang et al, 2017).

The BM microenvironment (figure 1-3) is composed of extracellular matrix proteins, including collagen, fibronectin, laminin and hyaluronic acid, as well as cellular elements, including haemopoietic and non-haemopoietic cells. Non-haemopoietic cells include mesenchymal stem and progenitor cells (MSPC), osteoprogenitors, osteocytes, endothelial cells, adipocytes, sympathetic nerve fibres, and non-myelinating Schwann cells (Smith & Calvi, 2013). These cells make up two distinct, yet controversial, niche types, namely the vascular and osteoblastic niches (Calvi et al, 2003; Kiel et al, 2005; Leatherman, 2013; Nilsson, 2001; Zhang et al, 2003). The exact roles that each niche contribute in the maintenance of haemopoietic cells, and indeed HSCs, remains contentious, with it being suggested that the more primitive cells mainly reside in one niche (i.e. the osteoblastic niche) and then migrate on their development (Ding & Morrison, 2013; Ehninger & Trumpp, 2011).

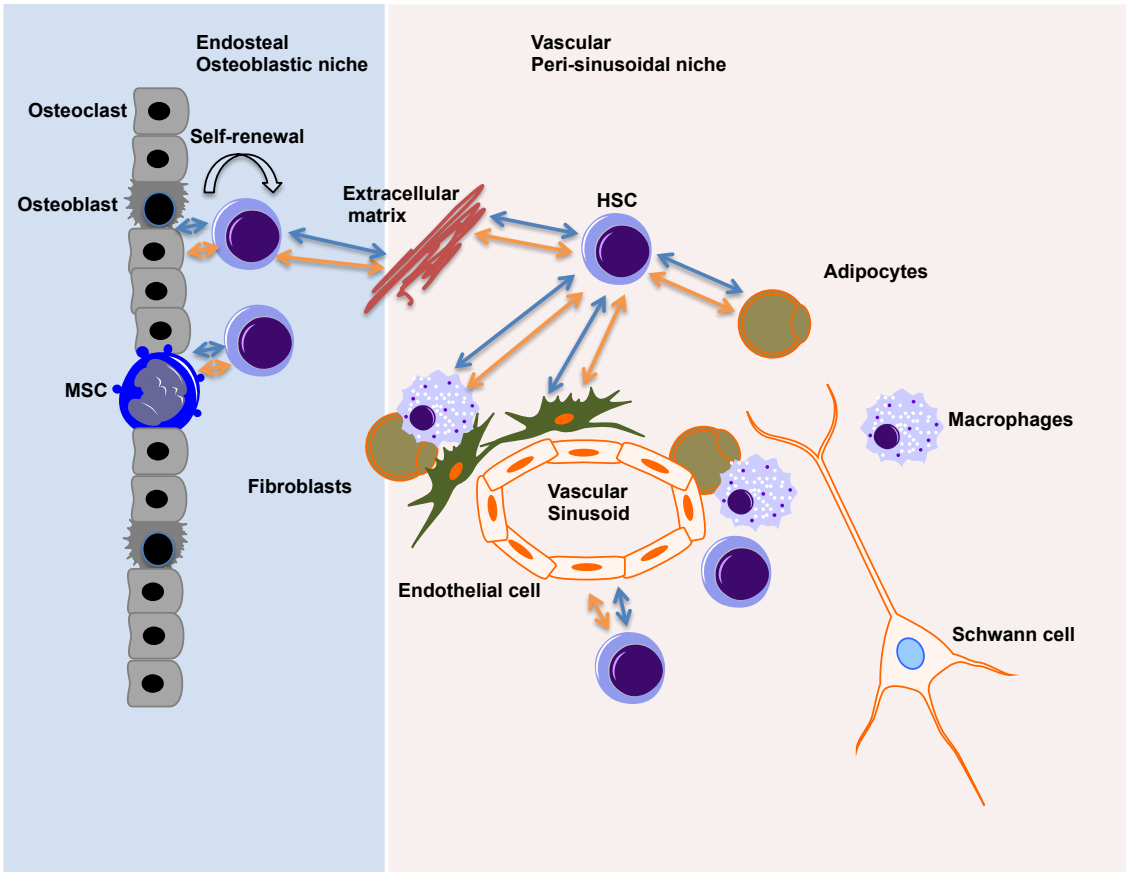

Figure1-3 Simplified representation of the bone marrow microenvironment
Schematic representation of the BM microenvironment. The BM consists of two niche-types, namely the osteoblastic and vascular niche. Within both niches is a collection of cells that lead to the secretion of chemokines, cytokines, and ligand interaction that governs HSC maintenance, expansion and self-renewal.

The niche cells bi-directionally communicate with haemopoietic cells via a number of different mechanisms. One such mechanism is through secreted factors, such as stem cell factor (SCF), transforming growth factor beta 1 (TGF-β1), and platelet factor 4 (PF4 also called CXCL4), and chemokines, such as stromal cell-derived factor 1 (CXCL12) (Camacho et al, 2017; Schroeder et al, 2016). Furthermore, sympathetic nerve fibres can modulate HSPC function via the secretion of noradrenaline, as well as oxygen tension within the niche (Yamazaki et al, 2011). Beside these mechanisms, cell-bound molecules such as adhesion molecules and ligands play an important role in HSPC maintenance and development, leading to both self-renewal and differentiation properties.

MSPC have a clear functional role within normal and deregulated haemopoiesis (Friedenstein et al, 1968). It has been shown that the simultaneous injection of donor MSCs with HSCs accelerates the recovery of haemopoiesis after lethal total body irradiation (Noort et al, 2002; Zhang et al, 2004). Similarly marrow stromal cells can maintain haemopoiesis *in vitro* for periods longer than 6 months (Dexter et al, 1977).

Further to this, it is known that HSPC fate can be influenced by different tissue environments (Trentin, 1971), and indeed deregulated states can influence the environment in which they reside. This highlights the role for bi-directional communication as being integral in the maintenance and development of HSCs in haematological disease. For example, the first evidence for niche-driven deregulation of haemopoiesis was demonstrated in mice with deletions in the retinoblastoma gene, the retinoic acid receptor gamma, or the Notch ligand endocytosis regulator, *Mib1* (Kim et al, 2008; Walkley et al, 2007). Deletions in these genes led to a myeloproliferative disease phenotype and highlighted that deletions in non-haemopoietic cells could contribute to hematological disease initiation. Furthermore, alterations in evolutionary conserved self-renewal pathways have been shown to predispose to leukaemia induction. For example, constitutively active β-catenin in osteoblasts has been demonstrated to induce an acute myeloid leukaemic (AML) phenotype (Kode et al, 2014). Furthermore, within this paper was the observation that *Jagged1* was increased in osteoblasts, which, in turn increased Notch signalling in HSC progenitors. It was subsequently suggested within this paper that Notch activation led to the development of genomic instability and chromosomal deregulation leading to the development of AML.

Further to this, many examples have been presented to demonstrate that leukaemic HSPCs can also remodel the BM microenvironment. For example, within chronic phase (CP) chronic myeloid leukaemia (CML), it has been shown that CML cells secrete granulocyte colony stimulating factor (GCSF) that results in decreased expression of CXCL12 and impairment of HSPC function (Zhang et al, 2012). Moreover, CML cells can stimulate the expansion of osteoblasts by a number of mechanisms, including cell-to-cell contact between leukaemic cells and mesenchymal stem cells (MSCs) (Schepers et al, 2013). This data suggests that remodeling of the BM microenvironment by leukaemia cells or other disease processes may reduce its ability to support normal haemopoiesis.

Taken together, these data demonstrate the importance of, not only HSC to the BM microenvironment, but also how deregulated cells can influence their surroundings, and vice versa.

1.2.2. *Intrinsic regulation of HSC function*

As has previously been determined, haemopoiesis and HSC activity relies on an intricate balance of self-renewal and differentiation. This is achieved through both intrinsic and extrinsic mechanisms that act as regulating controls. As has been described above, extrinsic

regulation is imperative in this process; however, it is known that external regulatory signals must integrate with intrinsic mechanisms to have their effect.

There are many intrinsic factors that have been shown to be implicated in the regulation of self-renewal and differentiation. For example, in brief, translocation Ets leukaemia (Tel) has been demonstrated to be required for HSC self-renewal, with its inactivation leading to the depletion of HSCs in the BM (Hock et al, 2004). Furthermore, overexpression of the transcription factor, *HoxB4* has been shown to increase the self-renewal potential of HSCs in both *in vitro* and *in vivo* models (Hong et al, 2014; Magnusson et al, 2007; Oshima et al, 2011; Sharma et al, 2006; Yu et al, 2014). Growth factor independence 1 (Gfi1) has been identified as a positive regulator of HSC self-renewal that functions to restrain HSC proliferation through upregulation of the cell cycle inhibitor, p21, since its expression is decreased in Gfi1 null HSCs (Zeng et al, 2004). As has previously been described, cell cycle regulators are imperative within this process. In keeping with this is the balance of cell survival pathways, such as Janus kinase/signal transducers and activators of transcription (JAK-STAT) (amongst others), with Stat3 and Stat5 being shown to be positive regulators of HSC self-renewal (Kato et al, 2005; Schuringa et al, 2004a; Schuringa et al, 2004b). This list is not exhaustive but highlights the importance of intrinsic regulation within the process of HSC function.

1.2.3. Haemopoiesis and developmental signalling pathways

Data has been presented above that highlights the critical role for extrinsic and intrinsic signals in the maintenance and function of HSCs. Within this discussion has been the importance of cell-to-cell interaction between HSCs and the BM microenvironment where they reside. Included in these are the ligand-dependent evolutionary conserved self-renewal pathways, Notch, Wnt/β-catenin, bone morphogenic protein (BMP), and Hh. All have been implicated in the regulation of HSC self-renewal and stem cell expansion (Campbell et al, 2008; Delaney et al, 2010; Delaney et al, 2005; Duncan et al, 2005; Staal et al, 2016; Weli et al, 2010).

1.2.3.1. The Notch signalling pathway

The Notch signalling pathway has a recognised role in the maintenance and expansion of HSCs. It is an evolutionary conserved signalling pathway that was first discovered in 1917 by Thomas Hunt Morgan in *Drosophila melanogaster* with observations of a notched phenotype in the wings of flies with the Notch gene mutation (Morgan, 1917). Notch

signalling has been shown to be involved in a variety of cell-fate decisions that influence the development and function of many organs, including stem cell maintenance, cell proliferation, haemopoiesis and apoptosis (Capaccione & Pine, 2013; Chiba, 2006; Cowart et al, 2012; Ohishi et al, 2003; Schwanbeck & Just, 2011; Yugawa et al, 2013).

It is a ligand-dependent signalling pathway that activates as a result of cell-to-cell interaction between the Notch receptor on the target cell and the ligand on the adjacent cell (figure 1-4). Mammals express four transmembrane Notch receptors (Notch 1-4) and five transmembrane ligands (Delta-like (DLL) 1, DLL3, DLL4, Jagged (JAG) 1, and JAG2). The ligands differ in their extracellular domains and functional capability dependent on cell contact. For example, Delta family ligands can mediate Notch activation *in trans* and Notch inhibition *in cis* (Espinoza et al, 2013). The relative affinity of Notch receptors for Notch ligands is controlled by receptor glycosylation mediated by the addition of fucose-N-acetylglucosamine (fucose-GIcNAc) moieties (Stanley, 2007). Three intracellular proteolytic cleavages occur to alter downstream gene expression.

Firstly, Notch precursor proteins, processed in the trans-Golgi apparatus, are cleaved by a furin-like convertase to produce the mature Notch receptor, consisting of Notch extracellular and Notch transmembrane subunits. Mature receptors are then taken to the plasma membrane, with subsequent membrane-associated ligand engagement. Upon ligand-receptor interaction, extracellular Notch is dissociated from the intracellular subunit. This triggers cleavage by a disintegrin and metalloproteinase (ADAM) protease (either ADAM 10 or 17). This cleavage allows release of a short extracellular peptide that is then immediately cleaved by the gamma secretase complex (GSC), liberating intracellular Notch to translocate to the nucleus and initiate Notch signalling by binding to the CBF-1-Suppressor of Hairless/lag1 (CSL), a constitutive transcriptional repressor, displacing co-repressors and recruiting co-activators, such as Mastermind-like (MAML) proteins. The Notch-CSL-MAML complex, in turn, recruits transcriptional regulators forming the Notch transcriptional complex. It is this that activates Notch downstream target genes, including *HES1* (Ohishi et al, 2003). Notch signalling, particularly in the haemopoietic system is complicated by the number of Notch receptors and ligands expressed by both haemopoietic and stromal cells within the microenvironment, as well as the interaction between Notch and other key self-renewal signalling pathways, namely, Hh and Wnt/β-catenin (Campbell et al, 2008; Duncan et al, 2005).

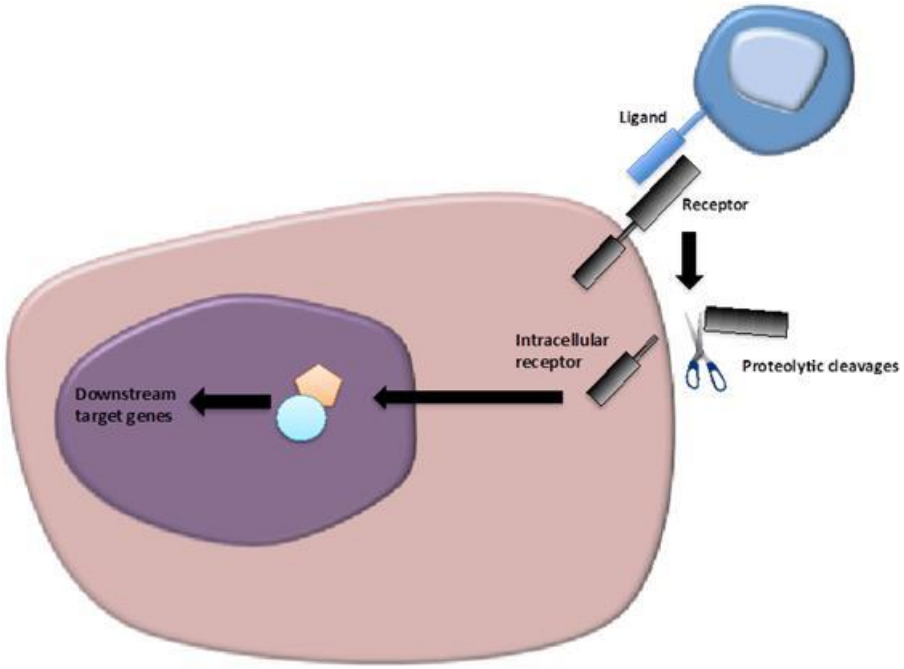

Figure1-4 Simplified representation of the Notch signalling pathway
At the plasma membrane, Notch extracellular domain binds to the relevant ligand to facilitate ADAM protease activity and GSC cleavage. Intracellular Notch is dissociated and translocated to the nucleus, and forms a transcriptional activation complex with CSL (blue circle) and MAML (orange hexagon), which recruit co-activators that activate Notch target genes. Phosphorylation of the intracellular Notch promotes FBXW7-mediated ubiquitination and degradation of intracellular Notch, terminating Notch signalling.

Aside from ligands, Notch signalling is positively regulated by Musashi-1 (Msi-1), an RNA-binding protein belonging to a conserved family of neural RNA-binding proteins. Msi-1 binds and represses the translation of Numb. Numb is a membrane associated negative regulator of Notch that prevents the intracellular domain of the Notch receptor migrating to the nucleus (Imai et al, 2001; Pasto et al, 2014). Furthermore, other negative regulators exist in this complex system. Phosphorylation of the intracellular domain by CDK8 promotes FBXW7-modified ubiquitination and degradation of the intracellular Notch receptor, which subsequently terminates Notch signalling (Hannon et al, 2012; King et al, 2013; Takeishi et al, 2013). To add another level of complexity, the addition of one of the fringe N-acetylglucosamine (GIcNAc)-transferases (lunatic, manic, or radical) leads to the 'fringe effect' whereby the addition of GIcNAc to the O-fucose sugar can either inhibit Notch signalling when interacting with the JAG ligand, or initiate Notch signalling when interacting with the DLL ligand (LaVoie & Selkoe, 2003; Thomas & van Meyel, 2007).

There is a documented role for Notch signalling in haemopoiesis, with differing roles in HSCs and differentiated cells described. For example, forced activation of Notch1 in haemopoietic cells has been shown to increase HSC self-renewal capacity (Kunisato et al, 2003). However, in differentiated cells, Notch1 activation favours lymphoid lineage

commitment (Stier et al, 2002), particularly within early T-lineage development. Furthermore, *in vivo* exposure of mouse or human haemopoietic progenitors to Notch ligands has been shown to enhance cytokine-mediated expansion and, thus has led to clinical trials assessing the role of Notch within haemopoietic recovery after cord blood transplantation (Dahlberg et al, 2011; Delaney et al, 2010; Delaney et al, 2005; Varnum-Finney et al, 2003).

Within HSC regulation, the role of Notch signalling remains controversial. Several *in vivo* studies have demonstrated preserved HSC function despite genetic strategies to block transcriptional activation of all Notch receptors (Maillard et al, 2008). However, inactivation of *Notch2* has also been shown to delay reconstitution (Varnum-Finney et al, 2011). Further to this, there is a noted role of cell-to-cell interaction between osteoblasts that express Jagged1, and HSCs, maintaining a self-renewal HSC state (Benveniste et al, 2014; Poulos et al, 2013). In keeping with this, pan inhibition of activated Notch blocks both T cell development and HSC maintenance and expansion, demonstrating the role of Notch within the HSC-BM environment. However, there have been published reports that suggest the contrary – that inhibition of Notch1 or Jagged1 has no effect on HSC self-renewal capacity (Mancini et al, 2005).

The role of Notch is complex with divergent reports both from *in vitro* and *in vivo* experiments. The reasons for this are numerous. Firstly, the pathway can generate numerous ligand-receptor interactions, each with differing functional relevance, with expression on the tissue of interest being integral in its assessment. For example, in murine B cell development, DLL1 functions as the main ligand for Notch2 whereas in T cell development DLL4 interacts with Notch1 (Kang et al, 2014; Meng et al, 2016; Ting et al, 2017). Furthermore, differing experimental design can lead to variation in Notch signal intensity (Delaney et al, 2010; Gama-Norton et al, 2015; Varnum-Finney et al, 2003); for example, it has never been formally shown if signal intensity varies *in vitro* or *in vivo.* There will also be varying signalling intensity between plate-bound 'isolated' ligands versus stromal support from *in vivo* experiments, which will have a much wider array of ligands and self-renewal pathway interactions. A further explanation could come from non-canonical Notch signalling, whereby downstream signalling molecules can be activated through bypassing the co-complex formation with MAML. For example, DLL1 ligands have been suggested to activate IL-6 mediated signalling in $CD34^+$ cells, but not in purified HSCs. This not only suggests a potential for non-canonical activation, but also highlights the differing roles one may see in immature and mature populations (Csaszar et al, 2014). There remains much to

be gained through the understanding of this pathway and its interactions in normal and malignant HSCs.

1.2.3.2. The Wnt/β-catenin signalling pathway

The Wnt/β-catenin signalling pathway (figure 1-5) has been shown to be integral in haemopoiesis and malignant haematology (Galán-Díez et al, 2016; Richter et al, 2017; Staal et al, 2016). In the absence of Wnt/β-catenin signalling, free cytoplasmic β-catenin is degraded by a multiprotein complex, including glycogen synthase kinase 3β (GSK3β), casein kinase 1 (CK1) alpha, and scaffold proteins (including adenomatous polypopsis coli (APC) and axin). Phosphorylation is initiated by CK1 alpha, which primes β-catenin for GSK3β-dependent phosphorylation of Ser33, Ser37 and Thr41 residues. Receptor-ligand interaction allows for the stabilisation of β-catenin via the recruitment of axin and inhibition of GSK3β (Li et al, 2012a). This allows β-catenin to accumulate within the cytoplasm and translocate to the nucleus where it interacts with members of the T-cell factor/lymphoid enhancer factor (TCF/LEF) subfamily of transcription factors to induce expression of Wnt downstream target genes (Willert & Nusse, 1998).

It has been demonstrated that many cellular proteins can directly and indirectly interact with β-catenin and other components of the Wnt/β-catenin pathway. Further to this, the intensity of the signal can have a concentration-dependent effect on cell fate (Luis et al, 2011). It is well established that there is a role for Wnt/β-catenin signalling in embryonic haemopoiesis (Austin et al, 1997; Cheng et al, 2008; Corrigan et al, 2009; Tran et al, 2010), however, its role in adult haemopoiesis is yet to be fully determined. In the adult BM microenvironment, the ligands, Wnt2b, Wnt5a, and Wnt10b are expressed (Van Den Berg et al, 1998), with evidence to suggest a role in lineage commitment. Wnt5a is expressed by mature B cells, while Wnt10b is produced by myeloid cells, erythrocytes and immature B cells (Congdon et al, 2008; Liang et al, 2003). Further to this, Wnt10b has been shown to be upregulated within BM regeneration (Congdon et al, 2008).

In vitro experiments and gain- or loss-of-function *in vivo* studies have yielded differing results as to the role of Wnt/β-catenin signalling in HSC function (Kirstetter et al, 2006; Luis et al, 2009; Reya et al, 2003). For example, constitutively active β-catenin *in vivo* in a Bcl2-transgenic model increases HSC proliferation, and repopulation capacity upon transplantation into lethally irradiated mice (Reya et al, 2003). However, conditional overexpression of a stabilised form of β-catenin led to a block in multi-lineage differentiation, transient HSC expansion, and long-term HSC exhaustion (Kirstetter et al,

2006; Scheller et al, 2006). Additionally, HSCs from *Wnt3a* knockout murine foetal liver reconstituted haemopoiesis in primary transplant, but had severely impaired secondary transplant capacity, suggesting impaired self-renewal potential (Luis et al, 2009). In some respects these results mirror the inconsistencies found in the similar experiments interrogating self-renewal pathways, including Notch (described above) and Hh signalling, as described below (Gao et al, 2009; Hofmann et al, 2009b; Merchant et al, 2010).

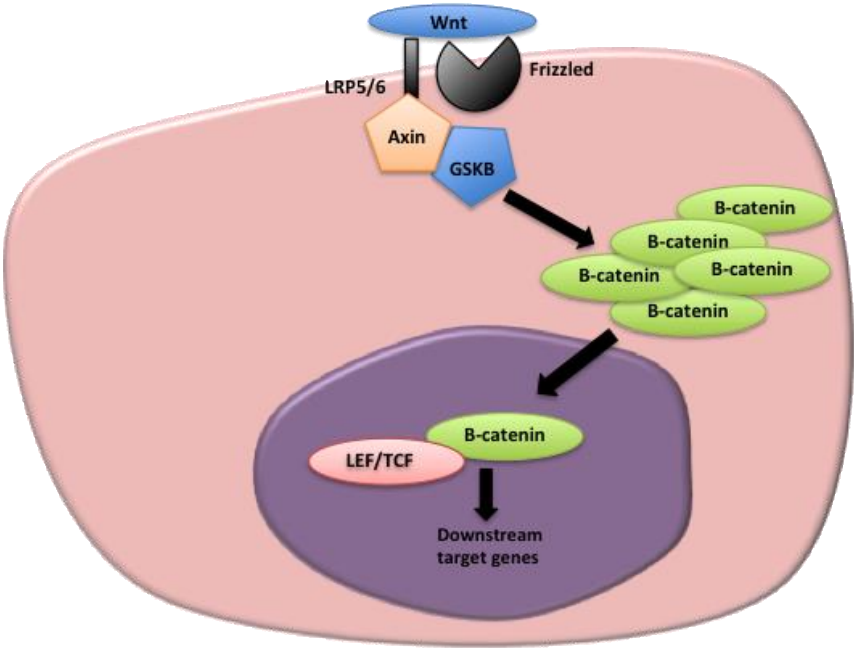

Figure1-5 Simplified representation of the Wnt/β-catenin signalling pathway
In the absence of Wnt signalling, free cytoplasmic β-catenin is degraded by a multiprotein complex. Receptor-ligand interaction allows for the stabilisation of β-catenin via the recruitment of axin and inhibition of GSK3β. This allows β-catenin to accumulate within the cytoplasm and translocate to the nucleus where it interacts with members of the T-cell factor/lymphoid enhancer factor (TCF/LEF) subfamily of transcription factors to induce expression of Wnt downstream target genes.

1.2.3.3. The Hedgehog signalling pathway

The Hh signalling pathway (figure 1-6) is an evolutionarily conserved signalling pathway that was first discovered during the study of embryonic patterning in *Drosophila* (Nusslein-Volhard, 1980). It is critical for both embryonic development and adult tissue homeostasis, including chromatin formation (Zhan et al, 2011), cell cycle regulation (Kenney, 2000; Roy & Ingham, 2002) and stem cell self-renewal (Memmi et al, 2015). In the adult, its functions are cell and tissue dependent, with its activation being implicated in the maintenance of cancer stem cells (CSC) in both solid (Ischenko et al, 2008; Samadani & Akhavan-Niaki, 2015) and haematological malignancies (Irvine et al, 2016; Long et al, 2011; Zhao et al, 2009). Activation of the canonical Hh pathway appears to be linked to primary immotile cilia, with documented reports of primary cilia within haemopoietic tissue (Irvine et al, 2016;

Singh et al, 2016a). The canonical pathway is ligand-dependent, relying upon receptor-ligand interaction between one of the three possible ligand isoforms – Sonic (SHH), Desert (DHH), and Indian (IHH) – to the Hh receptors, Patched1 (PTCH1) and Patched2 (PTCH2). In the absence of ligand support, PTCH1 is located within the primary cilia, emphasising the importance of cilia within the canonical route. Ligand-PTCH1 interaction causes the internalisation of PTCH and the subsequent activation of Smoothened (SMO). Activated SMO then moves into the cilium allowing for the accumulation of the active forms of GLI2 and GLI3 in the nucleus. This potentiates the activity of other positive regulators, including serine threonine kinase 36 (STK36), resulting in activation of key downstream targets (Ischenko et al, 2008).

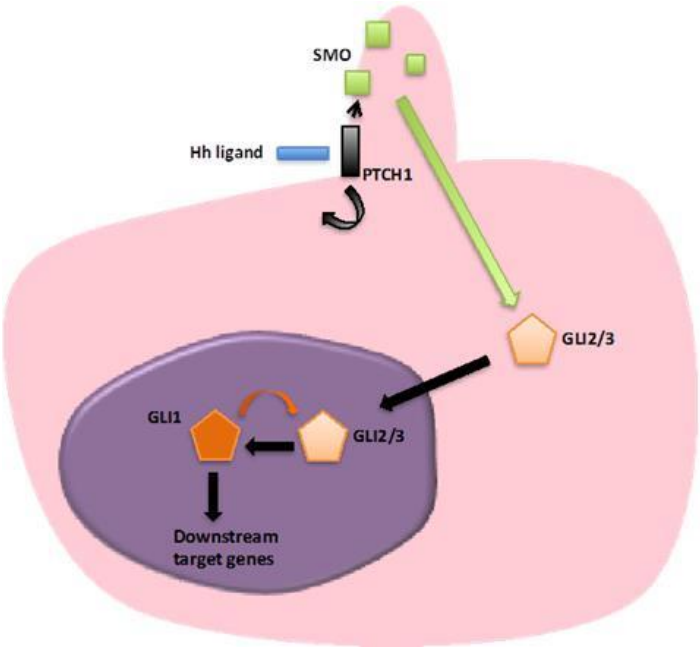

Figure1-6 Simplified representation of the Hh signalling pathway
Upon receptor-ligand interaction, PTCH1 is internalised and there is subsequent activation of SMO. Activated SMO moves into the cilium allowing for the accumulation of the active forms of GLI2 and GLI3 in the nucleus. This potentiates the activity of other positive regulators, including STK36, resulting in activation of key downstream targets.

The role of Hh signalling in haemopoiesis is complex and has been shown to be dependent on developmental stage, cell lineage, and extrinsic factors, for example, under regenerative stress (Bhardwaj et al, 2001; Trowbridge et al, 2006a). Evidence suggests that Hh plays a vital role in early haemopoietic development (Cridland et al, 2009). However, its role within adult haemopoiesis is controversial, with some reports suggesting a dispensable role within normal haemopoiesis (Gao et al, 2009; Hofmann et al, 2009b; Trowbridge et al, 2006a). For example, knockout of *SMO* in *in vivo* models has been shown not to adversely affect steady-state normal haemopoiesis (Gao et al, 2009; Hofmann et al, 2009b). Furthermore, SMO

inhibition within early phase clinical trials has shown little or no haemopoietic toxicity (Cohen, 2012; Feldmann et al, 2007).

1.2.3.4. The BMP signalling pathway

Like the self-renewal signalling pathways described above, there is a complex role noted within BMP signalling and haemopoiesis. The BMPs belong to the transforming growth factor beta (TGF-β) superfamily and have been shown to be involved in diverse cellular functions, including cell proliferation, differentiation, apoptosis, and stem cell self-renewal, in both embryonic and adult phenotypes (Herpin & Cunningham, 2007; Miyazono et al, 2005). The BMP pathway functions through receptor-mediated intracellular signalling (figure 1-7) (Toofan et al, 2014). Two types of receptors have been identified; namely type I receptors (Alk2, Alk3, and Alk6) and the type II receptors (Bmpr2a and Bmpr2b) (Kirmizitas et al, 2017). Different combinations of type II receptors with any of the type I receptors confers specificity and cellular consequence. Within the canonical system, upon ligand binding with BMP2 or 4, type I receptors become phosphorylated, leading to the heterodimerisation with the type II receptor. This, in turn, phosphorylates the corresponding Smad proteins and drives the formation of the Smad-Smad complex (Blank & Karlsson, 2011). This complex translocates to the nucleus where it regulates transcription of the downstream target genes (Derynck & Zhang, 2003).

Canonical BMP signalling has been shown to be important in both early embryonic and adult haemopoiesis (Crisan et al, 2015). BMP4 maintains the reconstitutive ability of HSCs *in vitro* (Bhatia et al, 1999). Furthermore, Smad5 has been shown to negatively regulate the proliferation and self-renewal of early yolk sac derived multipotent haemopoietic progenitors (Khurana et al, 2014; Liu et al, 2003) with inhibition of Smad-dependent BMP signalling enhancing homing and engraftment of BM HSCs (Monteiro et al, 2008). *In vivo*, in conditional *Bmpr1a* mutant mice, the pool size of HSCs is controlled by trabecular bone volume (Zhang, 2003). Thereby suggesting that BMP signalling mediated by Bmpr1a controls HSC number through regulation of the niche. This is consistent with previous findings using a transgenic mouse model in which parathyroid hormone receptor is expressed (Calvi et al, 2003).

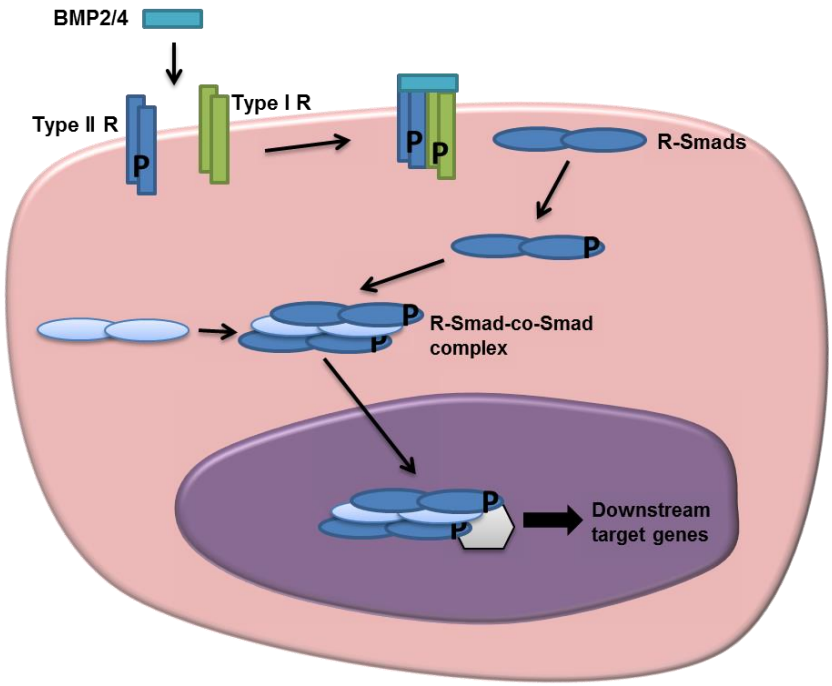

Figure1-7 Simplified representation of the BMP signalling pathway
Upon ligand binding, type I receptors become phosphorylated, which leads to the heterodimerization of these receptors with type II receptors. This in turn phosphorylates the corresponding R-Smads and drives the formation of R-Smad–co-Smad complex. The Smad–Smad complex then translocates to the nucleus where it forms a complex with transcription factors and cofactors to regulate the transcription of BMP target genes involved in the cell cycle, proliferation and self-renewal.

1.2.4. Integration of signalling pathways

The evolutionary-conserved self-renewal pathways' described above have a clear, yet complex, role within haemopoiesis. The complexity to understand their role in haemopoiesis lies in the fact that they do not act in isolation, relying on interactions between pathways to maintain a balance between self-renewal and differentiation. This is particularly relevant within the BM microenvironment, where intracellular signalling proteins can impact on one or more of the pathways. But while many of the phenotypic and functional properties have been determined, the regulation of how these pathways interact has not been fully elucidated (Reya, 2003). The complexity of the interconnectivity between self-renewal pathways can be demonstrated on basic proteomic analysis of self-renewal pathway proteins in normal HSCs, as demonstrated in figure 1-8. Although gene and protein interconnectivity can be hypothesised through bioinformatic analysis, ongoing experimental analysis of the functional output has allowed some of these interactions to be validated.

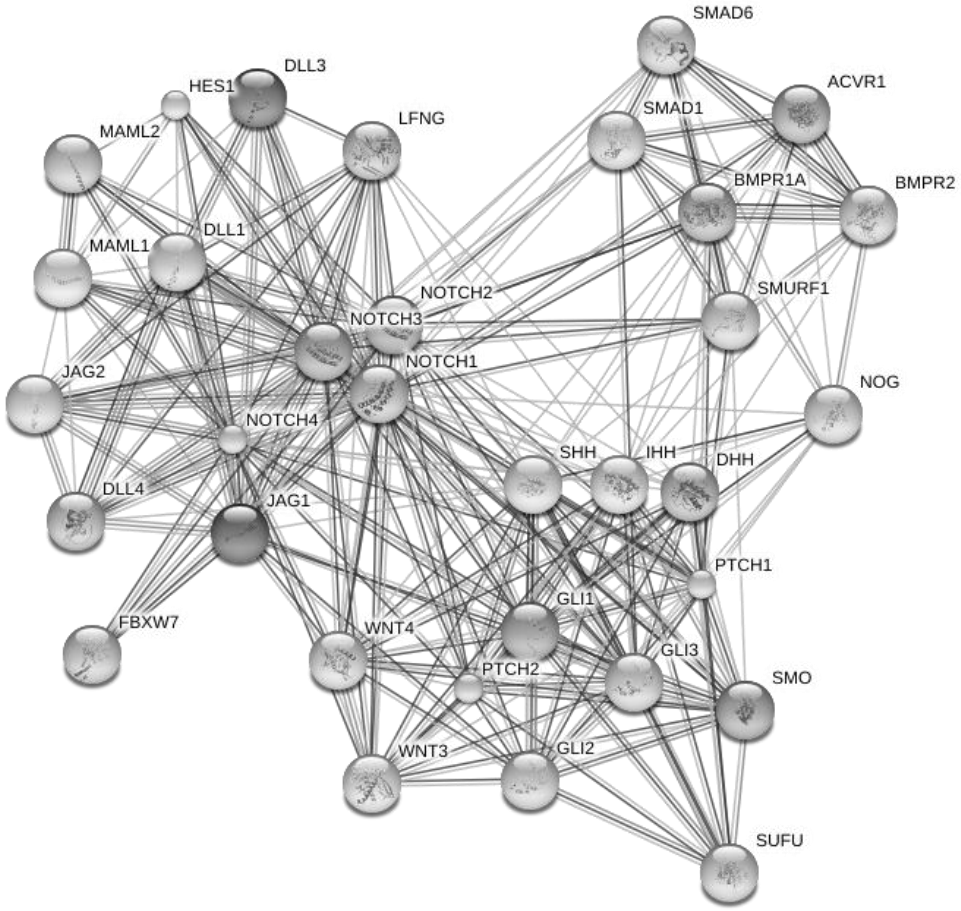

Figure1-8 Protein interconnectivity of self-renewal pathways in normal HSCs
Protein interconnectivity analysis of self-renewal pathways in normal HSCs as determined by proteinstring.com. There is a clear interconnectivity between proteins of the self-renewal pathways depicted, namely, Notch, Wnt/β-catenin, Hh, and BMP.

Many of these interactions are dependent on communication between the BM microenvironment and the cell of interest, as described above. Also, hypoxia has been shown to promote an undifferentiated state in a Notch-dependent manner, likely owing to the activation of HIF-1α (Gustafsson et al, 2005). Furthermore, downstream targets of Notch signalling are Hh and Wnt/β-catenin components, including Gli2, Gli3, and TCF4 (Li et al, 2012b). Further to this, Wnt/β-catenin signalling influences Notch1 expression, with manipulation of the pathway by overexpression of β-catenin promoting significant expansion of murine HSCs *in vitro* (Reya, 2003). However, its role, as stated above *in vivo* has been questioned since β-catenin has been conditionally expressed or deleted without having an effect on haemopoiesis (Cobas et al, 2004; Kirstetter et al, 2006). Again, this suggests a complex role in an *in vivo* setting and influence through the BM microenvironment. As described previously, axin and GSK3β mediate the phosphorylation and degradation of β-catenin in a basal state. Inhibitors of GSK3β gene have been shown to promote human and mouse HSC maintenance (Sato et al, 2004) and haemopoietic

repopulation in transplanted mice (Trowbridge et al, 2006b) by modulating gene targets of Wnt/β-catenin, Notch and Hh pathways. Furthermore, Wnt/β-catenin signalling influences the stability of GLI1 allowing for its accumulation (Nakamura et al, 2013; Noubissi et al, 2009).

As well as direct interactions between pathways, it has been shown that protein concentration influences cellular function. For example, BMP4 has differential effects on human HSCs depending on concentration, maintaining but not expanding human HSCs *in vitro* (Bhatia et al, 1999). Cross talk between hypoxia, HIF-1α, and TGF-β/Smad signalling has, in fact, been demonstrated in relation to CXCL12 induction and subsequent HSC induced homing towards this chemokine (Tabatabai et al, 2006). Furthermore, Wnt/β-catenin signalling and BMP cooperate to influence HOX activity.

This data demonstrates the complexities of interactions between self-renewal pathways at a basal HSC level, but it is the alterations and interconnectivity within haematological malignancy that may warrant further investigation when considering potential therapeutic targets, particularly within a stem cell driven disease phenotype, such as CML.

1.2.5. Cancer stem cells in haematological malignancy

CSC offer the concept that a small population of cells sharing characteristics of differentiation, self-renewal and homeostatic control, allow for the maintenance and dissemination of disease (Alison et al, 2011; Reya et al, 2001). Within haematological disease, these are referred to as leukaemic stem cells (LSCs). LSCs are mostly quiescent, in G0-phase and out of the cell cycle, and home to the BM microenvironment, in which they are protected from apoptosis and conventional treatments (Busfield et al, 2014; Crews & Jamieson, 2012; Zhang et al, 2013). Within a variety of haematological malignancies, including AML (Bonnet & Dick, 1997), CML (Graham et al, 2007; Zhang et al, 2013), and multiple myeloma (Yaccoby et al, 1998), the existence of LSCs has been identified. *In vivo* and *in vitro* experimental models have demonstrated that LSCs share many features with HSCs (Bhatia et al, 1997c), including self-renewal and engraftment potential, but have also offered critical differences in functional properties (Jordan et al, 2006), which allows for a therapeutic index of intervention, that would permit targeting of LSCs, whilst maintaining normal haemopoiesis. For the purpose of this thesis, only AML and CML LSCs will be discussed in detail.

1.2.5.1. The identification and origin of LSCs

AML LSCs were one of the first CSC populations to be characterised within haematological and solid malignancy (Bonnet & Dick, 1997; Lapidot et al, 1994). The complexity in morphological, genetic, and epigenetic heterogeneity within AML makes identifying an appropriate therapeutic target challenging, but may allow for LSC characterisation if the AML LSCs have distinct features according to their subtype. However, the immunophenotypic identification of the AML LSC remains a persistent area of debate (Blair et al, 1997; Blair et al, 1998; Bonnet & Dick, 1997; Jordan et al, 2000). Historically, LSCs (both in AML and CML) have been characterised within the $CD34^{+}CD38^{-}$ population, where their presence has been shown to be capable of generating leukaemic primary, secondary and tertiary engraftment in non-obese diabetic severe combined immunodeficient (NOD-SCID) mice (Bonnet & Dick, 1997; Lapidot et al, 1994). However, recent studies have suggested that LSC activity can extend into the $CD34^{+}CD38^{+}$ population, with data indicating that leukaemia-initiating capacity could be present in a mature $CD34^{-}$ population (Sarry et al, 2011; Taussig et al, 2010). This suggests that LSCs can either be derived from HSCs or from progenitor cells that acquire self-renewal properties.

Additional markers of AML LSCs have been identified, including CD123 (Al-Mawali et al, 2016; Ehninger et al, 2014), CD33 (Ehninger et al, 2014), CD45RA (Kersten et al, 2016), CD47 (Majeti et al, 2009), CD96 (Hosen et al, 2007), and CD93 (Iwasaki et al, 2015). Some are currently being translated into the clinical setting for identification or targeting of the LSC, including monoclonal antibodies towards CD47 (NCT02678338) and CD123 (NCT02848248), as well as anti-CD123-chimeric antigen receptor-T (CART) cells (NCT03114670; NCT02159495) (Luo et al, 2015; Mardiros et al, 2013). However, safety concerns have been described. For example, CD47 is expressed on the majority of normal tissues and may prevent the ability to achieve a therapeutic level of antibody (Jaiswal et al, 2009; Oldenborg, 2013). Further to this, CD123 has been demonstrated to be expressed on HSCs, and not on all LSCs, therefore inhibition of CD123 may have some consequences in normal haemopoiesis (Gill et al, 2014; Taussig et al, 2005).

Probably the most well established of these approaches, is the use of gemtuzumab ozogamicin (GO), an anti-CD33 monoclonal antibody conjugated with calicheamicin, which remains under clinical evaluation. There have been large randomised studies of the use of GO in newly diagnosed patients with AML (Burnett et al, 2011; Burnett et al, 2012; Castaigne et al, 2012; Petersdorf et al, 2013b). Within the AML15 clinical trial (Burnett et al, 2011), a subgroup analysis revealed an improved overall survival at 5 years for patients

with favourable cytogenetics (79% versus 71%, p=0.001), but no benefit for patients with unfavourable cytogenetics. Furthermore, 70% of all intermediate-risk patients had a 10% improvement in 5-year overall survival if given GO during induction, but this seemed dependent on white cell count, performance status, or secondary disease. Within AML16 (Burnett et al, 2012), there was no difference in the initial response rate, and the treatment-related mortality was similar, without any increase in toxicity with GO. However, at a median follow-up of 30 months, the relapse rate was significantly lower with GO (68% versus 76%, p=0.007), and the 3-year overall survival was significantly better (25% versus 20%, p=0.05).

The difficulties in identifying a universal marker of AML LSCs are, in part, due to the intra-patient and inter-patient heterogeneity identified within AML LSC populations (Eppert et al, 2011; Taussig et al, 2010) and has been particularly noted within relapse, where AML LSC frequency and phenotypic diversity have been shown to be much greater compared to the initial diagnostic LSC (Mendler et al, 2015; van Rhenen et al, 2007).

Regardless of these complexities, the importance of AML LSCs clinically is well established. Most pertinently, within the identification of minimal residual disease (MRD) (i.e. submicroscopic disease identified using molecular and immunophenotypic techniques), which resembles that of the diagnostic disease population, allows response to therapy to be followed over time, and offers a prognostic indicator for adverse outcome (Feller et al, 2004; Ivey et al, 2016). It seems reasonable that LSCs reside within this population, having only been minimally impacted by conventional chemotherapy that targets dividing cells, and therefore, it stands that treatments focussing on the elimination of LSCs will reduce MRD and ultimately improve disease outcomes. Furthermore, it has been shown that AML patients with a greater number of LSCs or a more prevalent stem cell phenotype at diagnosis have inferior clinical outcomes compared to those who have fewer LSCs or a less prevalent stem cell phenotype (Eppert et al, 2011; van Rhenen et al, 2005).

Although the most historic evidence of LSCs within haematological disease arise within AML, much insight into potential therapeutic strategies can be acquired from CML, where the CP disease represents a classic example of the stochastic CSC hypothesis model, without the molecular, epigenetic and genetic heterogeneity seen within AML. Furthermore, it is known that as the disease progresses to the acute BP, committed progenitors gain self-renewal function; again highlighting the potential for LSC to be derived from a more mature progenitor population (Jamieson et al, 2004; Kinstrie et al, 2016; Radich et al, 2006).

Therefore, understanding the LSC in CML may be clinically transferable to other stem cell-driven diseases, including AML.

In CML, low-level *BCR-ABL* positive LSCs, as defined within a $CD34^{+}CD38^{-}$ population, have been identified in the BM of tyrosine kinase inhibitor (TKI)-treated CP-CML patients in deep molecular response (i.e. those that achieve a 4-log or greater reduction of quantitative *BCR-ABL* expression from standardised baseline over a prolonged period) (Bhatia et al, 2003a; Chomel et al, 2011; Chomel et al, 2016; Chu et al, 2011). These cells have been shown to be capable of growth in LTC-IC assays and have murine engraftment potential, demonstrating their self-renewal capability. The demonstration that CML LSCs persist in the presence of a targeted therapy explains the phenomenon of disease persistence, and highlights that LSCs are BCR-ABL independent, relying on other pathways to sustain their survival (Corbin et al, 2011; Hamilton et al, 2012). The concept of disease persistence through quiescent LSCs has been further highlighted in recent years by trials exploring the discontinuation of TKIs in CP-CML patients with sustained deep molecular response; these will be described in detail within a later section in this introduction (Mahon et al, 2010; Richter et al, 2016; Ross et al, 2013; Takahashi et al, 2012).

A number of challenges remain within both the scientific and clinical communities in the eradication of LSCs, in both AML and CML. Firstly, in the identification of an appropriate specific target, or pan-target, that will enable permanent eradication of the LSCs. Secondly, when an appropriate target is identified that is clinically justifiable, the timings of intervention must be deduced, as well as the evaluation of disease persistence. This will remain a huge clinical challenge, especially in view that therapies that are only effective against the stem cell compartment (which represents 1-2% of bulk) may be difficult to evaluate due to the persistence of bulk malignant cells and concordant chemotherapy-based treatment.

1.2.5.2. Self-renewal pathways in LSCs – a potential target

As discussed, self-renewal is considered to be the integral property of the LSC, and its deregulation is known to affect the development, maintenance, and persistence of LSCs in both AML and CML. To date, a number of aberrant signalling pathways have been proposed to contribute to the LSC phenotype (Liao et al, 2012; Martelli et al, 2010; Naughton et al, 2009; Sengupta et al, 2007; Zhao et al, 2007). These pathways, including Hh, Notch and Wnt/β-catenin, are known regulators of self-renewal, and are often differentially expressed following genetic events. A number of deregulated proteins within these pathways may represent a broadly applicable therapeutic strategy, however, it is well known that these pathways rarely work in isolation, and rely on a web of activity leading to disease maintenance, persistence, and progression. The complexities in interaction between these pathways in LSCs are well documented and will be discussed under each heading below (figure 1-9).

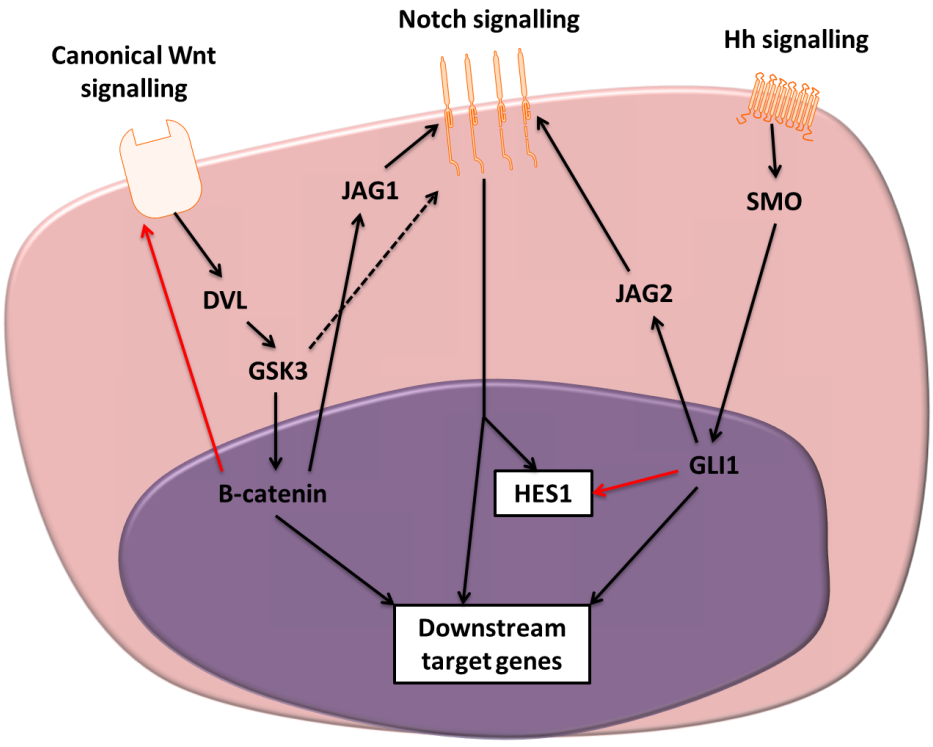

Figure1-9 Complex interactions between self-renewal pathways.
The interconnectivity between self-renewal pathways is well documented within the LSC. It is known that proteins within each of the pathways, namely Hh, Wnt/β-catenin, and Notch, can both antagonise and agonise the other pathways by cross talk leading to both up- and downregulation of downstream targets.

To add to this complexity in AML is the genetic variation that is seen, as this can mediate the proliferative and anti-apoptotic signals. Expression of specific oncogenes, such as

FLT3, *RAS*, and *MLL*, may create new dependencies on specific signalling pathways in LSCs, and activate signalling pathways in isolation or simultaneously (Somervaille et al, 2009; Stirewalt et al, 2001). Therefore, developing a therapeutic intervention that is efficacious in all activated pathways remains unachievable. Our best option remains to understand the acquired vulnerability in the mechanisms of the signalling pathways, which may offer a therapeutic window to eradicate the LSCs and plan for clinical translation.

1.2.5.3. Evolutionary conserved self-renewal pathways in LSCs

1.2.5.3.1. Hedgehog signalling and the LSC

The Hh signalling pathway has been shown to be inappropriately activated in a number of malignancies, including AML and CML, where it is intrinsically involved in the maintenance and expansion of the LSC compartment (Dierks et al, 2008; Long et al, 2011; Zhao et al, 2009). Within haematological malignancy, activation of the pathway has been shown to be linked to primary immotile cilia (Campbell et al, 2016; Singh et al, 2016), where the receptor-ligand interaction causes the internalisation of PTCH1 and subsequent activation of SMO. This enables SMO to move into the cilium allowing for the accumulation of the active forms and the activation of key downstream targets (Irvine & Copland, 2012). SMO is the critical mediator in the canonical pathway and, therefore, represents a key therapeutic target to prevent the pathway's activation. SMO can be readily targeted with pharmacological agents, including cyclopamine, and clinical grade agents, such as LDE225 (sonidegib) (Irvine et al, 2016) or PF-04449913 (glasdegib) (Irvine & Copland, 2012; Martinelli et al, 2015).

However, the pathway's complexity lies in its interactions and dependency with other key survival pathways. It has been suggested that the survival of CML progenitor cells is maintained by both the auto-activation of Hh and β-catenin (Su et al, 2012). Furthermore, Hh activation modulates NUMB-p53 responses, therefore, Hh suppression will subsequently alter p53 target genes; p53 is referred to as the guardian of the genome, therefore, careful evaluation of modulation of its function needs to be gained (Colaluca et al, 2008; Sheng et al, 2013). p53 as a modulatory target in leukaemia is an area which is becoming of increasing interest; both in CML (Abraham et al, 2016) and AML (Latif et al, 2015).

The importance of Hh signalling in CML is well established, with SMO inhibition leading to reduced self-renewal capacity of CML LSCs in both *in vitro* models with clinical grade SMO antagonists, and *in vivo*¸ where Smo-deficient mice have reduced leukaemogenesis in primary and secondary transplantation models (Dierks et al, 2008; Irvine et al, 2016; Zhao

et al, 2009). Furthermore, combination of SMO antagonists with TKIs has been demonstrated to lead to a synergistic reduction of CP CML LSCs in patient samples *in vitro* and CP and BC CML xenograft transplantation models (Irvine et al, 2016; Sadarangani et al, 2015). Our group has recently demonstrated that LDE225, a small molecule clinically investigated SMO inhibitor, used alone and in combination with the TKI, nilotinib, inhibited the Hh pathway in $CD34^+$ CP-CML cells, reducing the number and self-renewal capacity of CML LSC *in vitro* (Irvine et al, 2016). The combination had no effect on normal HSCs and when combined, these agents reduced $CD34^+$ CP-CML cell engraftment in NSG mice. Furthermore, upon administration to EGFP+/SCLtTA/TRE-BCR-ABL mice, the combination enhanced survival with reduced leukaemia development in secondary transplant recipients.

Importantly, deregulation of Hh may potentially contribute to disease progression, with differential Hh activity increasing as CML progresses to blast phase (BP) (Su et al, 2012), and increased gene expression of *PTCH1* has been observed in BP samples (Sengupta et al, 2007). Therefore, early targeting of the pathway may be therapeutically viable to reduce disease progression.

Whilst preclinical data appears promising to support the Hh pathway as a therapeutic target in CML, clinical trials utilising SMO antagonists as a therapeutic option have halted in early phases. Within solid tumors, these inhibitors have successfully been translated into clinical practice (Rudin et al, 2009; Von Hoff et al, 2009), however, within CML when combined with TKI, toxicity has been a major limitation (Ottmann et al, 2015; Shah et al, 2014).

In AML, the role of Hh has not been fully elucidated, with limited data available on the implications of Hh deregulation on disease biology, perhaps due to the vast heterogeneity seen within the disease. Activation of Hh, through *SMO* and *GLI* expression, has been described within primary AML samples, particularly acute promyelocytic leukaemia (APML) (Bai et al, 2008; Yang et al, 2013); no *SMO* mutations have been identified to account for this increase in activity (Campbell et al, 2016). It is clear, however, that there is a prognostic significance in its expression, with increased *GLI1* and *GLI2* being associated with reduced overall survival and as a marker of prognosis, respectively (Wellbrock et al, 2015).

Studies suggest that HHIP, a membrane-associated or soluble glycoprotein that functions to bind Hh ligands, can suppress leukaemic cell proliferation (Kobune et al, 2012);

furthermore, within the same study, reduced stromal HHIP expression was shown to contribute towards the development of AML. *HHIP* can be modulated through standard chemotherapy agents, where it has been demonstrated that 5-azacitadine-mediated amplification of stromal cell *HHIP* expression led to attenuated leukaemic cell proliferation potential.

The biological significance of pathway modulation has yet to be fully understood, with varying results available. Genetic inactivation of *SMO* in MLL-AF9-transformed LSCs does not affect AML development in primary recipient mice (Hofmann et al, 2009). Conversely, SMO inhibition with cyclopamine has been shown to reduce proliferation in myelomonocytic cell lines (Campbell et al, 2016). AML, as a disease, shows great heterogeneity and, therefore, focused evaluation through each of the classified disease entities needs to be undertaken, but it appears that there may be a therapeutic role for Hh inhibitors within a myelomonocytic phenotype. It is more clear that pharmacologic inhibition of Hh signalling appears to enhance AML 'gold-standard' therapy by sensitising LSCs to chemotherapy within the BM microenvironment (Fukushima et al, 2016a), which may lead to clinical advances in the eradication of AML LSCs. Currently, clinical trials are under way to investigate Hh inhibitors in AML, and early phase 1/2 results appear promising (Cortes et al, 2016a; Martinelli et al, 2015). Of note, a subsequent phase 2 clinical trial of LDE225 in AML, NCT01826214, recently closed due to lack of efficacy as a single agent; perhaps highlighting the limited activity of SMO inhibition on bulk disease.

1.2.5.3.2. Wnt/β-catenin Signalling and the LSC

The Wnt/β-catenin signalling pathway plays an essential role in the maintenance and differentiation of LSCs and the propagation of malignancies (Clevers, 2006; Jamieson et al, 2004). Its activation has been demonstrated in acute disease, namely AML LSCs and within myeloid BC CML (Ho et al, 2016; Jamieson et al, 2004). Furthermore, it has been suggested that a deletion within β-catenin reduces the ability of mice to develop *Bcr-Abl* positive leukaemia, which is suggestive of a role in the pathogenesis of chronic disease (Zhao et al, 2007). Therefore, targeting Wnt/β-catenin is a viable option in eradication of the LSC and in the prevention of disease progression and dissemination.

Within CML, loss of β-catenin in a murine model of CML impaired the development of the disease by inhibiting LSC self-renewal, and genetic and pharmacological inhibition of β-catenin activity synergised with TKI to target the loss of CML LSCs (Heidel et al, 2012; Jamieson et al, 2004). CBP/catenin antagonists have demonstrated efficacy in eliminating the CML and acute lymphoblastic leukaemia (ALL) LSC population *in vitro* and *in vivo*

(Gang et al, 2014; Zhao et al, 2016). A similar importance is seen within AML, where high expression of Ctnnb1 has been reported to correlate with poor prognosis (Ysebaert et al, 2006). Deletion of β-catenin within murine models has been shown to significantly reduce development and transplantation of AML driven by *MLL-AF9* or *HoxA9* (Wang et al, 2010; Yeung et al, 2010). In turn, within murine models of MLL-rearrangement AML it has been shown that self-renewal of LSCs is mediated, in part, by Ctnnb1, suggesting that Ctnnb1 may represent a therapeutic target within this subtype. Genetic and pharmacological inhibition of Ctnnb1 leads to decreased leukaemia formation. Interference with prostaglandin signalling has been shown to target the Wnt/β-catenin axis in HSCs (Goessling et al, 2009), and treatment with COX inhibitors, such as indomethacin, has been shown to lead to a decrease of LSCs in secondary recipients (Wang et al, 2010). This is mediated through Ctnnb1, although translating this clinically would be a challenge in view of adverse risk of bleeding. Inhibitors of canonical Wnt/β-catenin signalling are currently undergoing phase I clinical trials in AML (NCT01398462) (Cortes et al, 2014b).

Again, the interactions with other survival pathways, complicates antagonising Wnt/β-catenin. For example, within CML, TKI exposure has been shown to upregulate CD27 signalling, resulting in activation of Wnt target genes, which include Notch and c-Myc (Riether et al, 2015; Schurch et al, 2012). Wnt/β-catenin-Notch interaction is well documented, particularly within the BM microenvironment, where mutations of Ctnnb1 have been found in osteoblasts resulting in overexpression of Notch ligands and activation of the Notch pathway in HSCs (Kode et al, 2014).

The non-canonical Wnt (i.e. β-catenin independent) signalling pathways are diverse and can be initiated by WNT interaction with Frizzled receptors, or RYK and ROR receptor tyrosine kinases, to regulate small GTPases, as well as calcium flux and kinase cascades (Ford et al, 2013). This area is not as well characterised in LSC maintenance as the canonical pathway (Shen et al, 2014). Non-canonical signalling has been shown to exert an antagonistic effect on canonical signalling, with Wnt5a promoting GSK3β independent degradation of β-catenin and competing with Wnt3a for binding to the receptor complex (Anastas & Moon, 2013). A greater understanding of the non-canonical pathway may decipher an interesting therapeutic approach in β-catenin inhibition.

1.2.5.3.3. Notch signalling and the LSC

Notch signalling is involved in a variety of cell-fate decisions that influence the development and function of many organs, including stem cell maintenance, cell proliferation, haemopoiesis and apoptosis (Bray, 2016; Chiba, 2006).

Its role in malignancy has been shown to be cell and tissue-dependent, with the pathway playing both oncogenic and tumour suppressive roles depending on cell and cancer type (Capaccione & Pine, 2013; Pancewicz & Nicot, 2011; Schwanbeck & Just, 2011; Yugaw et al, 2013). In haemopoietic malignancies, accumulating evidence demonstrates its importance in growth, differentiation, and apoptosis (Chiang et al, 2013; Etet et al, 2012; Hannon et al, 2012; Kamdje et al, 2011; Pancewicz & Nicot, 2011; Schwanbeck & Just, 2011), with its role in T-ALL, chronic lymphocytic leukaemia (CLL), and B cell leukaemias and lymphomas well documented (Ellisen et al, 1991; Etet et al, 2012; Hannon et al, 2012; Kamdje & Krampera, 2011). Improved understanding of the Notch signalling pathway in these malignancies suggests that the Notch pathway may be a prime drug target; however, the therapeutic role of Notch inhibition may be directly dictated by its toxicities and the influence of its inhibition on other cell lineages, including the myeloid lineage (Deangelo et al, 2006; Krop et al, 2012).

Reports about the role which Notch plays in myeloid disease are conflicting, as Notch activation in myeloid precursors has been shown to promote self-renewal, induce and inhibit differentiation to monocytes, or induce apoptosis (Carlesso et al, 1999; Li et al, 1998; Sarmento et al, 2005; Schroeder et al, 2003). Early observations suggested that Notch signalling may play a role in myeloid progression (Milner et al, 1996; Schroeder et al, 2003; Tan-Pertel et al, 2000), with its role best characterised within AML. Importantly, it has been shown that exposing AML cells to plate-bound Notch ligands led to a full range of responses from proliferation to growth arrest that varied with patient sample, suggesting again the difficultly evaluating signalling pathways due to inter-patient heterogeneity (Tohda & Nara, 2001). More recently, observations have supported a tumour suppressive role for Notch signalling in immature LSC compartments of AML disease models (Chen et al, 2008; Kannan et al, 2013; Klinakis et al, 2011; Lobry et al, 2013; Tohda & Nara, 2001). Furthermore, in AML cell lines and primary patient blasts, downregulation of Notch1 expression was associated with a decrease in PU.1-mediated differentiation capacity, indicating a pivotal role in maintenance of an immature state (Chen et al, 2008).

Within CML, the data is limited. In another myeloproliferative disorder, chronic myelomonocytic leukaemia, a tumour suppressor role for the Notch pathway was again described, supporting a loss-of-function hypothesis (Klinakis et al, 2011). Conversely, however, a recent paper has identified an antagonistic role between Notch and TKIs within primitive samples; although the mechanisms have not been fully elicited, this perhaps is representative of crosstalk between signalling pathways (Aljedai et al, 2015). Recent data from our group has suggested the importance of Notch activation within LTC-IC assays, where activation of the $CD34^{+}38^{-}$ population through *Jagged1* led to a statistically significant reduction in colonies (Horne et al, 2016). It remains to be seen if this pathway has a functional and, indeed, therapeutic role, within CML biology. There are no clinical trials underway evaluating Notch modulation in myeloid disease.

1.2.5.3.4. BMP signalling and the LSC

BMP have been shown to be involved in diverse cellular functions, from apoptosis to self-renewal, in embryonic and adult phenotypes. Dysregulation within the BMP-TGF-β pathway is critical in LSC survival (Laperrousaz et al, 2013; Miyanari & Torres-Padilla, 2012; Naka et al, 2010), particularly mediated by its downstream target genes in the Cdx-Hox axis.

Interaction between Wnt/β-catenin and BMP signalling regulates the Cdx family of homeobox transcription factors – the master regulators of Hox gene expression (Lengerke et al, 2008). Cdx2 is aberrantly expressed in AML and promotes leukaemia propagation through deregulation of Hox genes (Scholl et al, 2007), with its overexpression demonstrated in 90% of AML patients and overexpression *in vivo* leading to increased engraftment in NSG murine models. Aberrant expression of HOX genes has been linked to both AML and CML (Grier et al, 2005; Scholl et al, 2007), with overexpression of HoxB3 (Sauvageau et al, 1997), HoxB8 (Perkins et al, 1990), or HoxA10 (Sauvageau et al, 1997) leading to the generation of acute leukaemia in murine models, as well as being associated with expansion of the HSC compartment in *in vitro* and *in vivo* models (Antonchuk et al, 2002; Thorsteinsdottir et al, 2002). Although this represents an interesting target of both Wnt/β-catenin and BMP, no translational evidence is available for an antagonistic influence in LSC regression.

Genomic studies within primary $CD34^{+}$ CML samples suggest that components of the pathway, including target genes, are downregulated (Gerber et al, 2013; Radich et al, 2006; Toofan et al, 2014). This raises the possibility that the pathway can be activated through extrinsic mechanisms, and emphasises the role of the BM microenvironment in the

protection of LSCs against TKI-mediated apoptosis. It has been shown that type 1 receptors are present on LSCs in primary CML samples, with an associated downregulation of BMP ligands (Laperrousaz et al, 2013; Toofan et al, 2014). CML aspirate and trephine BM samples had significantly higher levels of BMP2 and BMP4 compared to normal donors. This suggests that there is the ability to upregulate the BMP pathway and that it is via extrinsic mechanisms within the diseased BM microenvironment/niche. Laperrousaz *et al* (Laperrousaz et al, 2013) demonstrated that expression of BMP2 and BMP4 varied depending on niche cell type, with BMP2 and BMP4 being more highly expressed in polymorphonuclear cells and endothelial sinusoid cells, respectively. In response to increased levels of soluble BMP2 and BMP4, they showed that CML LSCs maintained their primitive phenotypes and enhanced LTC-IC potential, indicating that the BMP pathway can suppress differentiation and potentiate LSC survival.

1.2.6. Clinical implications of LSC and drug targets

The above suggests that as LSCs retain dependency on self-renewal pathways, they could be selectively targeted if the complexities in their interactions are fully understood. Disappointingly, despite strong *in vitro* and *in vivo* preclinical data, drugs against these targets have yet to be implemented in the clinical setting as a standard of care. This is, in part, due to trial design, as well as toxicities that are generated, particularly in areas with high cell turnover, such as within the gastrointestinal tract.

The clinical need for alternative and more effective therapies in AML and CML are different. AML represents a disease where there has been little progress in therapeutic strategies, with improvement in survival likely secondary to better supportive measurements rather than improvements in standard chemotherapeutics. The need for targeted and individualised treatments is a necessity in the disease for improved outcome and eventual cure. However, the targeting of LSCs is likely only to be effective in a minority of patients and will vary, dependent on the sub-class of disease. The difficulty remains in 1) identification of LSC in bulk samples with no established immunophenotype, and 2) understanding the differences in signalling pathways within an epigenetic, genetic, and morphologically heterogeneous disease.

Within CML, there has been an overall improvement in survival of approximately ten-fold since the introduction of targeted therapy against *BCR-ABL* (Bower et al, 2016). This has led to the majority of patients achieving close to normal life expectancy, when treated with TKIs. The need for eradication of the LSC is necessary to enable complete eradication of

CML and subsequent cure, allowing patients to stop therapy, and to alleviate a financial burden within healthcare systems. Like AML, a biomarker of the LSC needs to be identified and sensitive enough to identify CML LSCs at low level following treatment. Although many labs have performed extensive analysis to identify markers of a primitive cell population in the preclinical setting, including CD26 (Culen et al, 2016; Herrmann et al, 2015; Warfvinge et al, 2017) and IL1-RAP (Järås et al, 2010; Landberg et al, 2016; Warfvinge et al, 2017; Ågerstam et al, 2016), none have been shown, as yet, to be robust enough at clinical translation. CD26, however, is showing increasing promise in this area with recent data suggesting a correlation between CD26 expression and treatment response, as well as $Lin^{-}CD34^{+}CD38^{-/low}CD45RA^{-}cKIT^{-}CD26^{+}$ population being identified as a potential therapeutic target at a single cell level (Culen et al, 2016; Warfvinge et al, 2017). Although identification of the CML LSC appears to be within reach, little is known about the biology of the LSC in those patients that are in deep molecular response, with much of our understanding and the previous data coming from a drug-naïve population. Clinically, the therapeutic need will be in those that are on TKI therapy.

The biological understanding of aberrant self-renewal pathways within the LSC and potential targets is well underway; however the preparation for translation into the clinical setting needs to be considered. Firstly, as stated above, within each disease the immunophenotypic characterisation of the LSC needs to be established. When this is verified and supported internationally, there are considerations that need to be addressed to translate targeted inhibition or activation clinically.

Firstly, decisions regarding evaluation of response to self-renewal modulation. Within an *in vivo* and *in vitro* setting, these responses are often generated by utilising immature populations of sorted cells or genetically manipulating murine models. Within a clinical setting, the response of bulk disease cannot be used as a surrogate for the clinical effect on the LSC population as there are differential sensitivities between the bulk and LSC populations, nor can evaluation of survival be used as a surrogate in treatment evaluation. Clearly, established markers of the LSC (e.g. murine engraftment, LTC-IC assessment, re-plating efficiency) may be used as a surrogate for response, or an MRD evaluation could be used to generate some understanding of the proportion of LSC at diagnosis and then following treatment.

Secondly, comparing new, targeted approaches to standardised chemotherapy regimens needs to be carefully executed. The use of GO in AML has directed understanding of the

evaluation of a targeted response compared to standard treatments (Petersdorf et al, 2013; Rowe & Lowenberg, 2013), with a realisation that often a targeted therapeutic approach within bulk samples will require a longer treatment period to achieve a clinical response. Can overall survival be used as an endpoint if standard chemotherapy eradicates bulk disease, whereas targeted approaches are acting as an adjunctive therapy that requires longer duration to see an effect?

Thirdly, treatment timings of intervention will be essential in the understanding of disease biology. The treatments could be started simultaneously to allow for the likely longer duration needed for the targeted therapy to achieve a response. But this would cause difficulties in an appropriate primary clinical end-point and evaluation of the LSC response to therapy. Alternatively, the treatments could be sequenced to allow for identification of those patients, particularly with CML, where targeted therapy (in addition to BCR-ABL TKI) is not needed, and in AML, in those that have MRD positivity despite chemotherapy. This would, however, open the potential for clonal evolution of the disease, which may render it more difficult to treat and skew results of an LSC-targeted approach. With a concurrent approach, it is likely that drug toxicities may be a clinical issue, rendering the approach undeliverable as a standard-of-care.

Therefore, not only is an in-depth understanding of aberrant signalling pathway biology within LSCs required for generation of appropriate and justifiable therapeutic targets in the eradication of LSCs, careful consideration in the isolation and identification of LSCs, endpoint response, and timing of therapy is needed to enable translation of the therapeutic targets into a clinical setting.

1.2.7. Chronic myeloid leukaemia as a paradigm for a cancer stem cell malignancy

As described above, increasing evidence suggests that many malignancies function through primitive cell populations that share properties with somatic stem cells, termed CSCs (LSCs for leukaemias). Conventional chemotherapy is unable to eradicate these and, therefore, development of targeted therapies is a necessity to lead to cure. CML represents an excellent disease model of LSCs, as it is a clonal disorder with its origin traceable to the very primitive multipotent stem cell (Fialkow et al, 1967; Fitzgerald et al, 1971; Yamamoto et al, 2013). Furthermore, CML is a well understood disease, with numerous well validated experimental models that can be manipulated, when compared to the heterogeneity seen within AML

(Clarke & Holyoake, 2017; Daley et al, 1990; Eaves et al, 1998; Gelebart et al, 2016; Holyoake & Vetrie, 2017; Milne, 2017; Sontakke et al, 2016; Van Etten, 2001).

Much evidence has been provided to demonstrate a functional role of CML as a paradigm for a stem cell disease. Clinically, it has been observed that packed red cell transfusions from cells derived from CML patients could lead to temporary homologous BM engraftment and Philadelphia positive (Ph+) progeny in the PB of severely neutropenic recipients' (Levin et al, 1963). The first experimental evidence came from *in vivo* transplantation and *in vitro* stem cell assays (Copland et al, 2008; Daley et al, 1990; Foley et al, 2013; Graham et al, 2007a; Holyoake et al, 1999; Koschmieder et al, 2005). Furthermore, unlike other oncogenes, *Bcr-Abl* expression in murine haemopoietic progenitors fails to confer self-renewal capability and fails to induce leukaemia *in vivo*, confirming a stem cell origin of disease (Foley et al, 2013; Huntly et al, 2004).

Although it is generally accepted that the cell of origin within CML is the HSC, its clonal origin is traceable to the multipotent stem cell, giving rise to both haemopoietic and endothelial cells (Fang et al, 2005; Fialkow et al, 1967; Gunsilius et al, 2000). This highlights evidence presented in the previous section of the thesis of the importance of the BM microenvironment within the disease process, altering intra-cellular signalling and protein expression that may affect cross talk between the LSC and BM microenvironment. The interactions between LSCs and the BM remain an important area of research and may determine the best strategy for eradication of the LSC. In many myeloid leukaemias' there is enhanced osteoblastic proliferation and a marked increase in LSCs and progenitor expansion (Krause et al, 2013). LSCs rely on the BM niche for their persistence and modulate it to enhance survival, and a number of key interactions with self-renewal pathways contribute to the chemo-resistance that is seen. Deregulation of BMP has been shown in murine models where *Bmpr1a/Alk3* conditional knockout mice have impaired BMP signalling, which leads to increased niche size and thereby enhanced numbers of HSCs (Zhang et al, 2003b). Furthermore, a number of ligand-receptor mediated pathways regulate CML LSC, and in turn alter signalling pathways responsible for their maintenance, including the thrombopoietin receptor, MPL, which regulates JAK-STAT signalling (Zhang et al, 2016). MPL has been shown in high levels to lead to reduced TKI sensitivity in CML, although, in turn, a higher sensitivity to JAK inhibitors. Expansion of the osteoblast layer of the CML BM microenvironment can contribute to creating a hostile environment for HSC, mediated through alterations in TGF-β, Notch and pro-inflammatory signalling (Bowers et al, 2015; Krause et al, 2013). However, there are difficulties in utilising the BM

microenvironment therapeutically – how should the pathways within the marrow be targeted? Would peripheral injections suffice to produce a large enough concentration of blockade without leading to adverse effects? Signalling pathways clearly play an important role in determining cell survival, proliferation and differentiation of the leukaemic clone. Therefore, it seems pertinent to understand the role of differing signals within a CML LSC population, to fully identify potential therapeutic targets.

1.3. Chronic myeloid leukaemia

CML is an acquired myeloproliferative disorder that originates from a constitutively active oncogenic tyrosine kinase, BCR-ABL. It was first identified in the mid-1800s, where descriptions of splenomegaly and leucocytosis were described by independent physicians' (Bennett, 1845; Craigie, 1845; Kampen, 2012; Virchow, 1845). Although Bennett initially described his case as an infective process, Virchow suspected a neoplastic disorder that he called 'white blood cell disease' or 'leukaemia'. Following this, the Philadelphia chromosome was identified, where the observation of an abnormally small G-group chromosome was made – this was the first link between chromosomal abnormalities and human cancer (Nowell, 1962; Nowell & Hungerford, 1960) and paved the way in the understanding that cancer could be of genetic consequence. However, despite these initial discoveries, it was only in 1973 that Janet Rowley recognised that the Ph chromosome was the product of a reciprocal translocation between chromosome 9 and 22 (Rowley, 1973). The translocation partners were later identified as *BCR* and *ABL*, with the associated upregulation of tyrosine kinase activity leading to the cell's proliferation and survival (Groffen et al, 1984; Heisterkamp et al, 1983; Melo et al, 1993; Shtivelman et al, 1985).

CML accounts for 15-20% of all adult leukaemias', with an incidence of approximately 1 in 100,000. The median age of presentation is between 40 and 60 years. The disease normally runs a triphasic course from an initial CP to an accelerated phase (AP), and then to the acute phase of the disease, termed BC or BP. Without treatment, disease progression is inevitable. Duration of disease, before progression or death has been shown to be 4-6 years, 1 year, and 3-6 months, if left untreated for CP, AP and BP, respectively, but this remains highly variable between patients (Jabbour & Kantarjian, 2014). Expansion of the myeloid compartment in the BM characterises the CP of the disease and leads to a left shift of the myeloid lineage in the PB and resultant accumulation of mature neutrophils, often with the presence of basophilia and thrombocytosis. Splenomegaly is often detected on clinical examination. On progression to AP and BP, there is a block in differentiation and leukaemic blasts accumulate in the BM and PB, leading to a similar clinical presentation as seen in acute leukaemia, with severe BM failure (Sawyers, 1999), and a very poor prognosis.

1.3.1. Molecular biology and clinical pathogenesis of CML

The Philadelphia chromosome is pathognomonic of CML (Nowell, 1962; Nowell & Hungerford, 1960; Rowley, 1973). It consists of a shortened chromosome 22, resulting from a reciprocal translocation, t(9,22)(q34;q11), between the long arms of chromosome 9 and 22 (figure 1-9) (Rowley, 1973). The Philadelphia translocation adds a 3' segment of the Abelson murine leukemia viral oncogene homolog (*ABL)* gene from chromosome 9q34 to the 5' segment of the breakpoint cluster region protein (*BCR)* gene on chromosome 22q11. This creates a hybrid *BCR-ABL* that can be subsequently transcribed into mRNA which gives rise to the BCR-ABL protein. More than 95% of patients with CML harbour this mutation, along with 15-30% of adults with ALL, and 2% of adults with de novo AML (Crews & Jamieson, 2012).

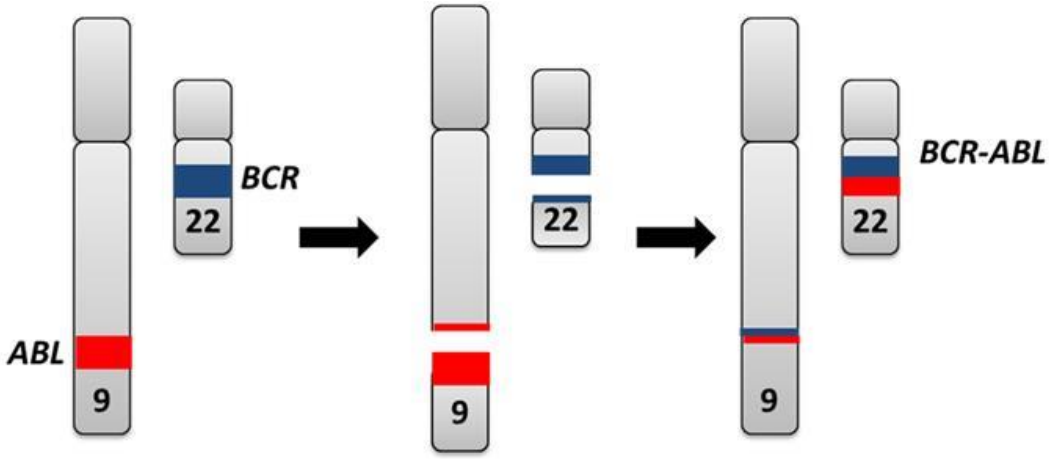

Figure1-10 The development of *BCR-ABL through the translocation of chromosome 9 and 22*
The reciprocal translocation between chromosome 9 and 22 results in the formation of the Philadelphia chromosome (shortened 22) and the *BCR-ABL* fusion transcript.

The *ABL* gene encodes a 145kD non-receptor kinase and contains 3 SRC homology (SH) domains, SH1, SH2, and SH3 (Van Etten, 1999). SH1 is the functionally active tyrosine kinase domain, with SH2 important in protein-protein interactions, and SH3 regulating tyrosine kinase activity through an inhibitory function. The main function of the ABL protein is to integrate signals from intra- and extracellular sources to affect survival, proliferation and apoptosis (Brasher & Van Etten, 2000; Hantschel et al, 2012; Nagar et al, 2003). The *BCR* gene encodes a 160kD protein that acts as a serine threonine kinase via a domain at the N-terminus. Further to this, it has a dimerisation domain, as well as central and C-terminal domains that allow interaction with signalling proteins (Hantschel & Superti-Furga, 2004). The phosphorylation of BCR itself can activate signalling pathways, including RAS, as well as JAK-STAT and PI3k-AKT, maintaining the cell's proliferation and survival (Danial & Rothman, 2000).

As discussed, the translocation of the 3' portion of *ABL* to 5' portion of *BCR* leads to the formation of a *BCR-ABL* transcript, which gives rise to the BCR-ABL protein. Different breakpoints within the *BCR* sequence have been identified and, depending on where the break occurs, three chimeric BCR-ABL proteins of different molecular weight can be produced (p190, p210, and p230 BCR-ABL) (Melo, 1997). Most CML patients harbour the p210 BCR-ABL protein, while the p190 BCR-ABL is mainly seen in patients with Philadelphia chromosome positive (Ph+) ALL, and rarely patients with CML. p230 BCR-ABL has been associated with a variant form of CML, termed chronic neutrophilic leukaemia, which tends to run an indolent course, although classical cases of CML in association with p230 BCR-ABL have been described (Arana-Trejo et al, 2002; Bertorelle et al, 2001; Elliott et al, 2005). All three proteins have been shown to have *in vitro* transformation properties and *in vivo* leukaemogenic activity, although have different kinase affinity (Clark et al, 1988; Daley et al, 1990; Konopka et al, 1984; Li et al, 1999). Via autophosphorylation and substrate phosphorylation, BCR-ABL can directly and indirectly activate the signalling pathways central to its transforming activity (Cai et al, 2017; Cutler et al, 2017; Horne et al, 2017). Further to the activation of signalling pathways, various structural alterations of ABL and BCR can facilitate leukaemogenic activity. For example, the N-terminal coiled-coil motif of BCR increases its tyrosine kinase activity and enables binding by ABL (Dorey et al, 2001; Hantschel, 2012; Hantschel & Superti-Furga, 2004; Schindler et al, 2000). Structurally, these alterations allow for multiple protein-protein interactions and activation of downstream signalling pathways that confer a survival and proliferative advantage. Furthermore, BCR interferes with the adjacent SH3 kinase regulatory domain, which in turn causes ABL to become constitutively active.

There is a clear pathognomonic role for BCR-ABL in CML. Furthermore, it also enables diagnostic certainty and an ability to monitor disease response to treatment via assessment of quantitative (q)*BCR-ABL*.

1.3.2. Defining treatment response

It has been well described that patient outcome correlates with speed and depth of treatment response (Druker et al, 2006; Hanfstein et al, 2012; Hochhaus et al, 2009; Hughes et al, 2010). The aim of treatment is to achieve haematological, cytogenetic and molecular response at critical time points from treatment initiation (table 1-1). Molecular measurements utilise qRT-PCR to estimate the amount of *BCR-ABL* mRNA relative to an internal reference gene/housekeeping, most commonly *ABL1* or *GUSB*. The results are

expressed on an International Scale (IS) as a percentage, with 100% *BCR-ABL* IS corresponding to the International Randomized Study of Interferon and STI571 (IRIS) study (NCT00333840) standardized baseline and 0.1% *BCR-ABL* IS being defined as a major molecular response (MMR or MR3; 3 log reduction from the standardized baseline) (Hughes et al., 2006). An International Scale has been developed to ensure molecular responses across laboratories are consistent (Branford et al, 2008).

Response	Criteria
Complete haematological response (CHR)	Normalisation of peripheral blood Resolution of splenomegaly
Minimal cytogenetic response	>65-95% Ph+ metaphases in bone marrow
Minor cytogenetic response	>35-65% Ph+ metaphases in bone marrow
Partial cytogenetic response	1-35% Ph+ metaphases in bone marrow
Major cytogenetic response (MCyR)	0-35% Ph+ metaphases in bone marrow
Complete cytogenetic response (CCyR)	0% Ph+ metaphases in bone marrow
Major molecular response (MMR) or MR3.0	3 log reduction in *BCR-ABL* relative to control
MR4.0	*BCR-ABL* <0.01% or undetectable disease in cDNA with 10,000–31,999 *ABL1* transcripts or 24,000–76,999 *GUSB* transcripts
MR4.5	*BCR-ABL* <0.0032% or undetectable disease in cDNA with 32,000–99,999 *ABL1* transcripts or 77,000–239,999 *GUSB* transcripts
MR5	*BCR-ABL*<0.001% or undetectable disease in cDNA with greater than or equal to100,000 *ABL1* transcripts, or greater than or equal to240,000 *GUSB* transcripts

Table 1-1 Definitions of treatment response in CML
European Leukemia Net (ELN) criteria detailing definitions of response to TKI. *BCR-ABL* is the quantitative RT-PCR assessment of *BCR-ABL1:ABL1* (or other housekeeping gene) in the International Scale. Ph+; Philadelphia chromosome positive (Baccarani et al, 2013; Cross et al, 2015).

Evidence and guidelines suggest that at 3 months, a *BCR-ABL* of greater than 10% should trigger an examination of compliance and, if indicated, TKI resistance. Within the German CML IV study, amongst the patients that did not achieve a *BCR-ABL* of less than 10% at 3 months, overall survival at 5 years was poorer (87% versus 97% for patients with a *BCR-ABL* of less than 1%) (Hanfstein et al, 2012). Furthermore, a *BCR-ABL* of greater than 9.84% has been demonstrated to be the strongest predictor of inferior event free survival and overall survival (Marin et al, 2012).

Within Europe, these findings have been adopted and formalised into guidelines developed by the ELN (Baccarani et al, 2013) and the National Comprehensive Cancer Network (NCCN), recommending key treatment milestones which form the basis of CML monitoring, enabling an objective and internationally validated assessment of response to therapy, and early recognition of those being treated sub-optimally or failing therapy and would warrant a change in therapy or further investigation (table 1-2).

Time	Optimal	Warning	Failure
Baseline		High risk; CCA	
3 months	*BCR-ABL1* ≤ 10% +/- Ph+ ≤ 35%	*BCR-ABL1* > 10% +/- Ph+ 36-95%	No CHR, and/or Ph+ >95%
6 months	*BCR-ABL1* <1% +/- Ph+ 0	*BCR-ABL1* >10% +/- Ph+ 1-35%	*BCR-ABL1* >10% and/or Ph+ >35%
12 months	*BCR-ABL1* ≤ 0.1%	*BCR-ABL1* >0.1-1%	*BCR-ABL1* >1% and/or Ph+ >0
Then, and at any time	*BCR-ABL1* ≤ 0.1%	Confirmed clonal abnormalities, Ph-	Loss of CHR Loss of CCyR Confirmed loss of MMR

Table 1-2 Definition of minimum required response to TKI therapy
ELN criteria detailing minimum required response to first-line TKI therapy from initiation (Baccarani et al, 2013).

Molecular monitoring is the most sensitive approach in determining TKI-failure and disease progression, and enables salvage therapy to be commenced at loss of molecular rather than loss of cytogenetic or haematological response. (Branford et al, 2012; Hanfstein et al, 2012; Hughes et al, 2010; Milojkovic et al, 2012). However, at present, cytogenetic response remains included in the guidelines, and BM examinations are still recommended in a diagnostic approach. This is particularly important at baseline to assess for additional cytogenetic abnormalities. Current guidelines suggest performing a BM examination at baseline, 3, 6, and 12 months to ensure CCyR has been achieved (Baccarani et al, 2013). There is evidence to support the association between event free survival and overall survival with cytogenetic response, as demonstrated within the 6 year follow-up for the IRIS trial, where the event free survival rate was 59%, 85%, and 91% for patients with no cytogenetic response, MCyR, or CCyR at 6 months, respectively (Hochhaus et al, 2009). For second generation TKIs, these milestones occur earlier (Kantarjian et al, 2012; Larson et al, 2012). However, with advances and increased sensitivity in molecular monitoring, most centres, including our own, are moving away from this frequency of BM assessment. An alternative method to determine cytogenetic response is with the use of Fluorescence In Situ

Hybridisation (FISH) on PB, and when combined with a *BCR-ABL* transcript level of ≤1% (IS) leads to reassurance that the disease is being adequately treated (Oehler, 2013).

1.3.3. Treatment of CML

The introduction of TKIs in the management of CML is one of the greatest advances in the treatment of leukaemia. Since their introduction, there has been at least a 10-fold increase in survival rates compared to the pre-TKI era, where initial treatment was based on standard cytotoxic chemotherapy, such as busulphan and hydroxycarbamide. Although these treatments allowed for a haematological response, no cytogenetic response could be achieved as the pathognomonic insult was not being targeted (Hehlmann et al, 1993). Furthermore, these treatments are associated with numerous side-effects, including myelosuppression. Interferon alpha was introduced as a standard of care in the mid-80s, and demonstrated a significant improvement compared to preceding therapies, with a 15% higher 5-year survival (Talpaz et al, 1986). Cytogenetic response and overall survival were improved when combined with systemic chemotherapy, such as cytarabine (Beck et al, 2001). Within the 1980s, it also became clear that allogeneic stem cell transplantation could result in long-term disease-free survival and probably cure the disease for selected patients, though not without significant risk of morbidity and mortality (Clift et al, 1982; Fefer et al, 1979; Goldman et al, 1982).

With the discovery of BCR-ABL activation, came the hypothesis that targeting BCR-ABL could eliminate disease, and in 1996 preclinical data demonstrated that a modified 2-phenylaminopyrimidine induced apoptosis of *BCR-ABL* positive human cells, including primary CML cells, with little toxicity on normal cells (Druker et al, 1996). This compound, now known as imatinib, specifically inhibited BCR-ABL tyrosine kinase activity by competitive inhibition at the ATP-binding site of the BCR-ABL protein. This subsequently resulted in the inhibition of phosphorylated proteins from downstream signalling pathways. Although it effectively inhibits BCR-ABL, it blocks other kinases, including platelet-derived growth factor receptor and c-KIT (Giles et al, 2009). Its clinical ability was demonstrated in the International Randomized Study of Interferon and STI571 (IRIS) study, where imatinib (STI571) was shown to induce significantly higher rates of haematological and cytogenetic responses, and subsequently overall survival compared to the interferon-alpha plus low-dose cytarabine; the gold-standard therapy prior to TKIs (O'Brien et al, 2003; O'Brien, 2008). Initial assessment at 19 months, demonstrated a CCyR rate of 74% versus 9% ($p<0.001$) and failure to progress at 12 months of 99% versus 93% ($p<0.001$) in the imatinib arm compared to interferon-alpha plus low-dose cytarabine, respectively.

Importantly this response was durable, with an 8-year follow-up demonstrating an event free survival rate of 91% and overall survival rate of 93% (Hochhaus et al, 2009; O'Brien, 2008). Now, off pharmaceutical patent (2016), imatinib is the current gold standard for first line therapy of CML in UK. However, 8-year follow-up within the trial highlighted that only 55% of patients enrolled remained on imatinib therapy, highlighting potential issues with tolerability and adverse events amongst this patient group. Although dose escalation of imatinib can improve response rates in patients with a sub-optimal response, switching to second or third generation TKIs can be more effective (Cortes et al, 2010a; Cortes et al, 2010b; Kantarjian et al, 2012; Larson et al, 2012). Since the introduction of imatinib, second and third generation TKIs have been developed. Current guidelines suggest that for first-line therapy, dasatinib and nilotinib can be used as an alternative or for treatment of cases with TKI failure (Baccarani et al, 2013).

Dasatinib is a second generation TKI that has been shown to be significantly more potent than imatinib *in vitro*. Again, like imatinib, dasatinib has been shown to target other tyrosine kinases, including the Src family, which influences the increased incidence of TKI-related side-effects, such as pleural effusions (Aplenc et al, 2011; Hantschel et al, 2007; Kantarjian et al, 2012; Lindauer & Hochhaus, 2010; Shah et al, 2004) seen with dasatinib. The DASISION trial (NCT00481247) compared dasatinib 100mg OD and imatinib 400mg OD in the setting of front-line treatment (Kantarjian et al, 2010). At 12 months, the primary outcome of confirmed CCyR was 83% versus 72% (p=0.007) (Jabbour et al, 2014) in the dasatinib and imatinib arms, respectively. Five year follow-up demonstrated that dasatinib achieved deeper responses at earlier time points, with a higher proportion of patients achieving MMR at 3 months in the dasatinib arm (84% versus 64%, $p<0.0001$) (Cortes et al, 2016b). Correlating with this was a decreased progression to BC. Rates of grade 3 or 4 haematologic adverse events were higher for dasatinib versus imatinib. Drug related pleural effusion was more common with dasatinib (28%) than with imatinib (0.8%), but did not impair the achievement of cytogenetic and molecular response (Cortes et al, 2016b). The UK STI571 Prospective International RandomIsed Trial 2 (SPIRIT2) phase 3 clinical trial (NCT01460693) confirmed these results, with 12 month MMR being achieved in 57.5% versus 46% in the dasatinib and imatinib arms, respectively ($p<0.001$). Again treatment toxicity played a major role in dasatinib treatment, with pleural effusions occurring more frequently with dasatinib than imatinib (24.1% versus 1.2%) (Osborne et al, 2015). In patients intolerant or resistant to imatinib, dasatinib has demonstrated durable response rates, with the START-C phase 2 study demonstrating a 2 year CCyR rate of 53%, with 90% of these being maintained at 24 months. Furthermore, the START-R study demonstrated

significantly higher rates of CCyR comparing dasatinib 70mg twice daily with high dose imatinib at 2 years (i.e. 400mg twice daily)(44% versus 18%, p=0.0025) (Kantarjian et al, 2009; Mauro et al, 2008; Milojkovic et al, 2012)

Nilotinib, a structural analogue to imatinib, has increased affinity for BCR-ABL *in vitro* compared to imatinib (Weisberg et al, 2005). Like dasatinib, nilotinib has been shown to induce a sustained haematological and cytogenetic response in more patients, when compared with imatinib. The Evaluating Nilotinib Efficacy and Safety in Clinical Trials – Newly Diagnosed patients (ENESTnd) study (NCT00471497) presents the mainstay of this data. This phase 3, randomised clinical trial compared two doses of nilotinib (300mg BD, and 400mg BD) to imatinib (400mg OD). The use of nilotinib was associated with significantly higher MMR at 12 months compared to imatinib, with limited change between the two doses of nilotinib used (44% versus 43% versus 22% for nilotinib 300mg BD, nilotinib 400mg BD and imatinib 400mg OD, respectively; $p<0.001$) (Kantarjian et al, 2011b; Saglio et al, 2010). Five-year follow-up demonstrated the cumulative incidence of MMR to be 77% for both doses of nilotinib and 60% with imatinib ($p<0.0001$) (Kantarjian et al, 2011b; Saglio et al, 2010). Although, event free survival was not statistically changed between trial arms, there was an advantage with reducing rates of disease progression in those with intermediate and high-risk disease receiving nilotinib, as estimated through the Sokal score. This highlights the role for second generation TKIs in prevention of disease transformation. As with dasatinib, adverse events and toxicity with nilotinib use is significant. Within the ENESTnd study, the 6 year cumulative cardiovascular side effect event rate was significantly increased in the nilotinib arm, with a concentration effect of increasing doses (Hochhaus et al, 2016). Other notable side-effects, included skin rash, headaches, and pancreatitis (rarely). As well as first line therapy, like dasatinib, nilotinib has been shown to offer an alternative for a second-line approach (Kantarjian et al, 2011a).

As well as the first and second generation TKIs, bosutinib and ponatinib are available for use in treatment failure, or, in the case of ponatinib, with the detection of a *T315I* mutation (Brümmendorf et al, 2015; Cortes et al, 2014a; Cortes et al, 2012; Cortes et al, 2013). Bosutinib, a dual Src/Abl TKI, demonstrates a more potent *in vitro* activity against Bcr-Abl than imatinib (Golas et al, 2003; Puttini et al, 2006; Rassi & Khoury, 2013). Like other TKIs, bosutinib has activity against a wide range of tyrosine kinases, including c-KIT and platelet-derived growth factor receptor (Puttini et al, 2006). The phase 3 clinical trial, Bosutinib Efficacy and Safety in newly diagnosed chronic myeloid leukemia (BELA) (NCT00574873), compared the efficacy and safety of bosutinib against imatinib (Cortes et

al, 2012). Following a dose escalation to 500mg OD, the trial allowed the potential for further increase to 600mg OD for patients with inadequate molecular and cytogenetic response. At 24 months, cumulative CCyR were similar in bosutinib (79%) and imatinib (80%) arms; however, cumulative MMR rates were significantly higher with bosutinib (59% versus 49%) (Brümmendorf et al, 2015). Importantly, bosutinib appeared to retain activity across mutations that confer imatinib resistance (see section 1.3.4.2), with the exception of T315I and responses were independent of whether patients had resistance or intolerance to imatinib. The most common side effects have been shown to include, diarrhoea, nausea, and vomiting (Gambacorti-Passerini et al, 2014; Nakaseko et al, 2015). Diarrhoea is the most common side-effects noted clinically with bosutinib. Within the BELA trial, it occurred in 84% of patients, with 9% experiencing grade 3 symptoms. It is generally self-limiting and patients should be warned of this prior to drug initiation and given prophylactic loperamide.

Ponatinib is currently the only TKI active against the T315I mutation (O'Hare et al, 2009; Zhou et al, 2011), and therefore remains an important treatment modality in CML. The Ponatinib Ph-positive ALL and CML Evaluation (PACE) trial (NCT01207440) evaluated approximately 500 patients that were considered resistant or intolerant of dasatinib and nilotinib or if they had CML with a *T315I* mutation (Cortes et al, 2013). The trial used a dose of 45mg OD ponatinib and patients were stratified into both disease phase and mutational state. Within our own clinical practice, this dose can be reduced to 30mg with good effect, and clinical trials assessing this lower dose are currently ongoing. In the PACE trial, at 12 months, MCyR was achieved in 56% of the patient cohort, with 75% of patients harbouring the T315I mutation achieving MCyR. Long-term follow-up confirmed a sustained response, with 83% of these patients remaining in MCyR at 3 years (Cortes et al, 2014a) and 39% of patients achieving MMR or better. Within this trial, patients responded more favourably if they had received fewer prior TKIs. As with other TKIs, significant adverse events were noted. Particularly, arterial occlusive events occurred in 28% of patients, with the most common treatment adverse events being abdominal pain, rash, headache, and constipation (Cortes et al, 2014a). Severe hypertension occurred in 20% of the cohort taking ponatinib. Vascular occlusion and cardiovascular events occurred more commonly with increasing age and prior cardiovascular co-morbidities. Clearly, for our own clinical practice, cardiovascular side effects must be considered and in early 2014, a revised warning was issued regarding ponatinib and the risk of thrombotic events, vascular occlusions, and heart failure (Gainor & Chabner, 2015). The indications for ponatinib use according to manufacturers prescribing information (www.iclusig.com) include the

treatment of adult patients with T315I-positive CML or Ph+ ALL, or in the treatment of adults with any stage of CML or Ph+ ALL for whom no other TKI therapy is indicated.

With the information depicted above, figure 1-10 represents a schematic plan for TKI therapy within CP-CML according to ELN guidelines and current evidence.

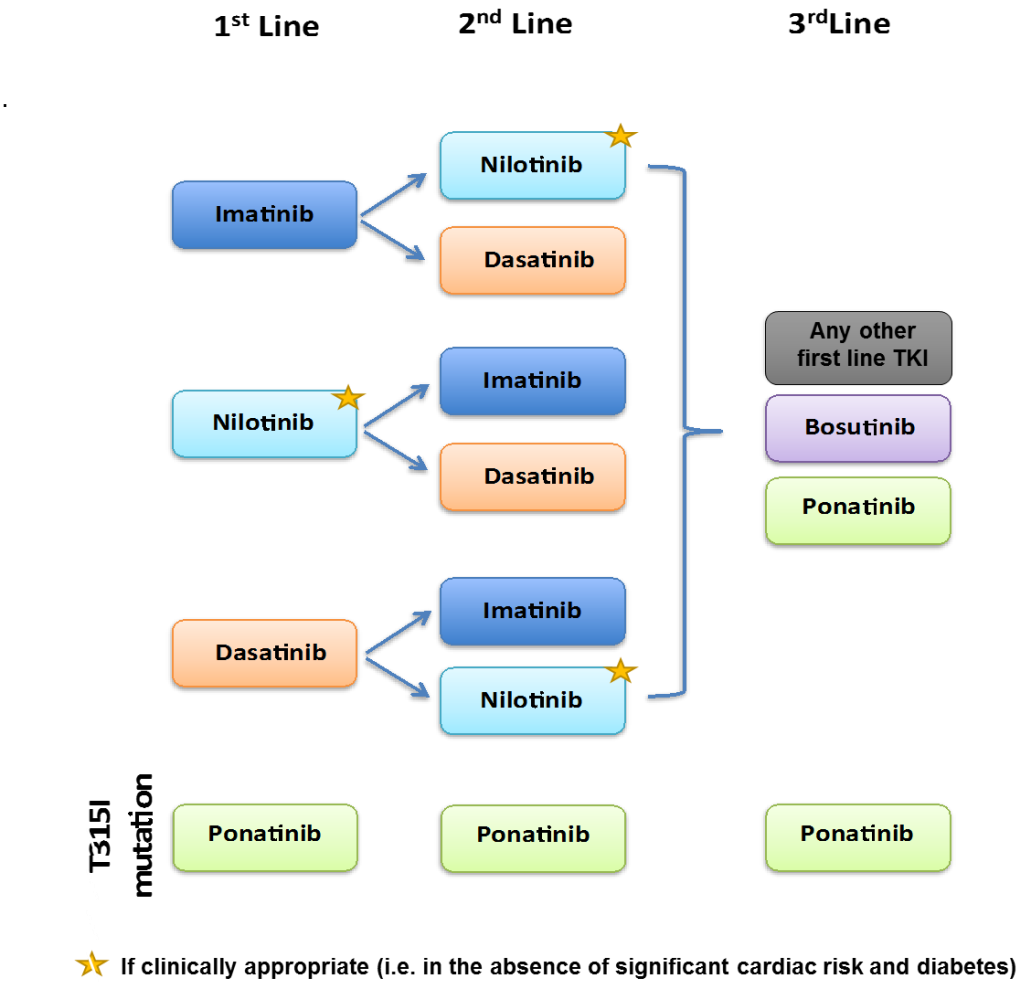

Figure 1-11 Schematic diagram of a treatment algorithm for TKI use in CML
Schematic for TKI use in CP-CML, with 1st, 2nd and 3rd line therapy available. TKI choice should be based on a individual-basis, with co-morbid conditions carefully evaluated. For example, cardiovascular disease and diabetes should be considered prior to initiating nilotinib in view of significant adverse events. This is based on current ELN guidelines

With such an array of TKIs available and a significant increase in survival compared to the pre-TKI era, the role of allogeneic transplant is more limited than in the pre-TKI era. It remains an important treatment option however, with high-risk disease, and those with T315I positive advanced CML. Outcomes following transplantation remain superior for patients in CP compared to advanced phase disease, with a 5-year survival of approximately 90% in those with CP compared to 10-20% with BP. However, in view that TKI therapy is generally well tolerated and not associated with the significant morbidity and mortality seen with allogeneic transplantation, the question remains whether there is a role for transplantation in CP-CML at all. Targeted therapy in CP-CML is clearly a great medical achievement and success. However, despite a targeted therapeutic approach, a small number of patients will not respond, or sub-optimally respond, to TKI therapy.

1.3.4. Why does treatment fail?

It has been estimated that about 30% of patients' fail to achieve an MMR at 2 years (Kantarjian & Cortes, 2011). The reasons for this are three fold, relying on patient compliance to TKI, resistance to therapy, and disease persistence.

1.3.4.1. Patient compliance

Patient compliance remains integral to achieving adequate response. Indeed, it has been estimated that non-compliance with TKI increases sub-optimal response by approximately 3-fold (Noens et al, 2009). The Adherence Assessment with Glivec: Indicators and Outcomes (ADAGIO) study allowed assessment of compliance in a cohort of 169 CML patients over a 90-day period. Only 14.2% of the cohort was found to be completely compliant with TKI, while 71% took less than recommended, and 14.8% more than recommended. Non-compliance was associated with sub-optimal response to TKI (Noens et al, 2009).

The assessment of compliance remains a difficult area of clinical evaluation. However, microelectronic monitoring has allowed observation of the number of times a bottle cap is removed, and serves as a marker of compliance within a population. In a study by Marin et al, it was determined that treatment compliance is a critical factor in achieving and maintaining a deep molecular response, with the probability of achieving MMR and complete molecular response (CMR) significantly better in those with compliance of greater than 90%. Furthermore, compliance was the only independent predictor for achieving CMR (Marin et al, 2010). Compliance of 85% or less and having never achieved MMR have been shown to be the only independent predictors of TKI failure (Ibrahim et al, 2011).

Non-compliance remains a complex clinical issue with a number of factors demonstrated to influence this. Included in this are complex psychological issues, such as depression, disbelief of disease, as well as polypharmacy, longevity of taking the medication, and side-effects, to name a few. In view of its importance clinically, methods have, and are, being introduced to provide patients with increasing support (Bordonaro et al, 2014; Cornelison et al, 2012). For example, within our own services at the West of Scotland Cancer Centre, increased support is being made available through the introduction of CML-specific nurse specialists that give ongoing psychological support, as well as phone-consultations and the development of support groups. This has allowed for increased home support, as well as peer-to-peer support in CML community groups, to enable better compliance. It has been demonstrated that increased accessibility to pharmacists, behavioural specialists, and other healthcare professionals assists with the identification of an individual's reasons behind non-compliance and ultimately, development of individualised care plans to overcome it (Eliasson et al, 2011; Osterberg & Blaschke, 2005).

1.3.4.2. Resistance to therapy

Non-compliance can be managed within a multidisciplinary team if identified promptly. However, despite good compliance, a number of patients' will respond sub-optimally or fail therapy. This can be due, in part, to developing resistance to TKI therapy. Inherent or acquired resistance to therapy has been demonstrated in *in vitro* cell line models and primary samples (Mahon et al, 2000). There has been increasing interest in resistance to TKI therapy of late, but in depth discussion is beyond the scope of this thesis. However, to aid understanding of the reasons for disease progression and the complex nature of its underlying mechanisms, this will be discussed in brief. Resistance to therapy can occur via BCR-ABL-dependent or BCR-ABL-independent mechanisms.

1.3.4.2.1. BCR-ABL-dependent mechanisms

The most common mechanism of resistance to TKI is the development of point mutations or amplification of the *BCR-ABL* gene, which alters the kinase domain of BCR-ABL rendering the TKI ineffective. These mutations can develop at any stage of disease, and can be utilised clinically to guide TKI choice.

To date, more than 90 *BCR-ABL* point mutations have been identified, with a lesser number biologically characterised (Azevedo et al, 2017; Cavelier et al, 2015; Gibbons et al, 2014; Khorashad et al, 2013; Shah et al, 2002; Szankasi et al, 2016). Four different clusters of

BCR-ABL kinase domain mutations have been described, and include those that affect the P-loop, the SH2 domain, the SH3 domain, and the activation loop (Branford et al, 2003; Schindler et al, 2000; Soverini et al, 2011). The T315I mutation that results from the replacement of threonine by isoleucine at ABL amino acid position 315 is arguably the most therapeutically relevant mutation within CML, as ponatinib remains the only therapeutic option. Although many mutations have been identified, their clinical significance varies, with not all mutations resulting in relapse or disease progression (Hughes et al, 2006; Jabbour et al, 2006; Nicolini et al, 2006). Identification of specific mutations, including T315I, F317L/V/I/C, Y253H, F359V/C/I, V299L, and E255K, however remains imperative to TKI choice (table 1-3; figure 1-11).

Mutation	Action
T315I	Consider ponatinib
T315A **F317L/V/I/C**	Consider nilotinib or bosutinib (rather than dasatinib)
Y253H **F359V/C/I**	Consider dasatinib or bosutinib (rather than nilotinib
V299L	Consider nilotinib
E255K/V	Consider dasatinib
Any other mutation	Consider dasatinib, nilotinib, bosutinib, ponatinib

Table 1-3 Point mutation and recommended action for TKI choice (Ai & Tiu, 2014)

Furthermore, the type of mutation can be associated with phase of disease, with mutations at M244, M351, and G250 frequently detected in CP, and mutations at T315, E255, and Y253 being found in AP and BP (Branford et al, 2009; Soverini et al, 2006). The ELN recommends screening for mutations in any patient with treatment failure or sub-optimal response, including rise in *BCR-ABL* transcript levels to allow for early detection of mutations and appropriate change in therapy.

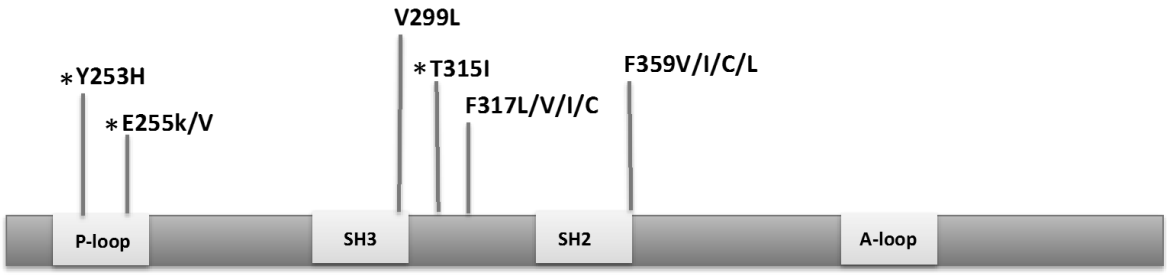

Figure 1-11 Schematic of point mutations according to position
Schematic of point mutations associated with clinically relevant TKI choice. Asterisks are amino acid substitutions more associated with advanced disease stage.

Further to this, additional mechanisms have been postulated to confer TKI resistance. For example, within the BP cell line, K562, it has been demonstrated that there is an increase in expression of the P-glycoprotein efflux pump when passaged through increasing doses of imatinib (Mahon et al, 2000). However, this same cell line also demonstrated a 6-fold amplification of the *BCR-ABL* gene, and no discrimination between the imatinib resistance versus the P-glycoprotein overexpression was made.

1.3.4.2.2. BCR-ABL-independent mechanisms

As well as BCR-ABL-dependent mechanisms, BCR-ABL-independent mechanisms of resistance have been described that rely on the alteration of cellular signalling, and cell cycle regulation within the downstream pathways that have been altered with activation of the protein and inhibition of multiple non-BCR-ABL kinases (Li & Li, 2007). The BCR-ABL protein activates alternative signalling pathways, including SRC kinase, RAS, and JAK-STAT signalling (Cortez et al, 1997; Gallipoli et al, 2014; Pendergast et al, 1993). The aberrant activation of these pathways leads to the CML cell's proliferation and enhanced survival.

The activation of the SRC family kinases has been shown to promote both disease progression, as well as TKI-unresponsiveness. BCR-ABL directly interacts with SRC family kinases resulting in both a conformational change in the ABL kinase domain through phosphorylation of SH2 and SH3, as well as activation of SRC family kinases, Hck, Lyn, and Fyn), leading to cell growth, differentiation and survival (Danhauser-Riedl et al, 1996; Hu et al, 2006; Meyn et al, 2006; Stanglmaier et al, 2003). Additionally, while there have been no clinical examples of SRC-activating mutations in imatinib-resistant cell lines or primary CML specimens, cellular activation of this pathway through numerous other cross-talk networks may still facilitate resistance (Donato et al, 2003; Ptasznik et al, 2004; Wu et

al, 2008). RAS signalling has also shown to be activated through Grb2-mediated binding of the Y177 moiety in the BCR sequence (Cortez et al, 1997; Pendergast et al, 1993), however, the specific mitogen-activated protein kinases that Ras activates in CML are yet to be fully elucidated. Furthermore, studies have demonstrated that Grb2 can recruit Gab-2 with subsequent activation of both PI3k and ERK pathways (Sattler et al, 2002). The mechanism by which these signalling pathways are activated has been shown to be through the expression of plasma membrane transporter molecules, including the ABC family of transporters, ABCG2 and MDR-1. It has been suggested that overexpression of these protein complexes might confer resistance through reducing intracellular imatinib concentration (Mahon et al, 2003). However, a clear correlation between transporter molecule expression and patient response to imatinib has not been fully elucidated.

Furthermore, clonal evolution occurs when CML cells acquire additional chromosomal abnormalities, or epigenetic modulation. Cytogenetic aberrations have been described in an increasing percentage in BP compared to CP, with some, such as aberrations within chromosome 17 leading to changes within the *TP53* gene, and subsequent poor outcome (Cortes et al, 2003; Lahaye et al, 2005; O'Dwyer et al, 2002; Wendel et al, 2006). Epigenetic methylation and post-translation acetylation alter gene expression and subsequent protein function. Within CML, the role of epigenetic modification at a biological and therapeutic level are becoming of increasing interest (Bixby & Talpaz, 2011; Lee et al, 2007; Scott et al, 2016).

1.3.4.3. Disease persistence

TKI resistance and activation of alternative signalling pathways has been shown to be involved in failure to respond to TKI therapy. However, in addition to this is the phenomenon of disease persistence, which suggests that despite a targeted therapeutic approach, BCR-ABL-independent mechanisms are being exploited to sustain the survival of LSC (Bhatia et al, 2003b; Chomel et al, 2011; Deininger, 2012). As described, these cells are resistant to therapy, meaning that on cessation of TKI treatment the disease is likely to return (Chu et al, 2011; Deininger, 2012; Graham et al, 2008; Hamilton et al, 2012; Ross et al, 2013). The role of LSCs has been extensively described above, and highlights that further information and understanding is needed to identify the underlying mechanisms that confer survival to CML LSCs under TKI therapy.

1.3.4.4. Stopping trials

Multiple clinical trials exploring the discontinuation of TKIs in CP patients with sustained molecular remission (Etienne et al, 2017; Mahon et al, 2014; Mahon, 2015; Mahon et al, 2010; Mahon et al, 2016; Rea et al, 2012; Ross et al, 2010; Ross et al, 2013; Takahashi et al, 2012) have been performed. These trials have demonstrated that discontinuation of therapy can be selectively achieved, with most recent 'Stop Imatinib' (STIM) trial (NCT00478985) data stating the cumulative incidence of molecular relapse at 60 months was 61% (CI 52-70%), with few cases of late relapse being observed (Mahon et al, 2014). This suggests that if molecular relapse is to occur, it happens early. Comparable results have been reported worldwide (Mahon et al, 2014; Mahon et al, 2010; Rea et al, 2012; Ross et al, 2010; Ross et al, 2013; Takahashi et al, 2012). The European Stop Kinase Inhibitor (EURO-SKI) trial (NCT01596114) is the largest study to date, with recruitment of over 800 patients. Most recent analysis demonstrated a molecular-recurrence free survival of 62% at 6 months, 56% at 12 months, and 52% at 24 months (Mahon et al, 2016). The DAsatinib DIscontinuation (DADI) study (NCT01627132) analysed molecular-relapse free survival after stopping dasatinib as second-line therapy or beyond. The probability of molecular-recurrence free survival was 49% at 6 months, and 48% at 12 months, with all molecular relapses occurring within 7 months of stopping therapy. All patients with molecular relapse regained deep molecular response within 6 months (Imagawa et al, 2015). The UK equivalent trial currently in process (DESTINY – DeEscalation and Stopping Treatment of Imatinib, Nilotinib or sprYcel in chronic myeloid leukaemia: NCT01804985) and is analysing the role of dose reduction before complete suspension of TKI treatment. Interim data suggested that decreasing TKI treatment to half the standard dose was associated with improvement in TKI adverse events, in patients with stable MR3 or more. This suggested that many patients are being overtreated and that there is scope for TKI dose reduction prior to discontinuation to assess response (Clark et al, 2016).

Although these results indicate the possibility for TKI discontinuation in a small subset of CML patients, they highlight an uncertainty surrounding the 'trigger' event(s) in molecular relapse, and question if sustained BCR-ABL expression, LSC persistence, microenvironmental factors or, indeed, multiple factors are the cause. Within the TWISTER trial (Ross et al, 2013), LSCs could still be identified by functional assays in all undetectable (by quantitative-polymerase chain reactions (qPCR)) MRD samples derived from patients' no longer on TKI treatment, suggesting that these cells, although present, were not yet driving a leukaemic process. But then, it is known that in up to 30% of normal individuals, low level of BCR-ABL expression can be identified (Bose et al, 1998; Takahashi et al, 2012),

perhaps suggesting that *BCR-ABL* transcript level alone is not sufficient for CML maintenance. It is unknown, however, what cell types these transcripts are originating from and if this is significant long-term. Interestingly, a single copy of *Bcr-Abl* expressed from the endogenous BCR locus in a knock-in murine model is not sufficient to induce leukaemia (Foley et al, 2013). Therefore, although it is clear that a certain level of *BCR-ABL* needs to be expressed at the stem cell level to cause CML, it is unclear if further molecular changes or aberrant signalling is needed to drive molecular relapse and disease progression. Furthermore, it is unknown if *BCR-ABL* is the initiating insult, or if host factors, such as epigenetic and genetic changes influence disease outcome and precede the acquisition of *BCR-ABL*. Regardless, it is apparent, that further insight into why LSCs survive TKIs is vital in the quest for cure.

1.3.5. Ph+ Acute leukaemia

As has been previously described, CML runs a triphasic disease course. If left untreated, the disease will inevitably progress to the more acute form of the disease, termed BC or BP. The median survival remains poor, with most treatments ineffective in this phase of disease. BP CML does not represent the only Ph+ acute leukaemia, with both Ph+ ALL and *de novo* Ph+ AML described within the literature. Within this group of diseases, the treatment approaches differ, although survival advantage remains poor in all groups. This section will describe each disease entity separately to aid understanding of their similarities and differences at a molecular level.

1.3.5.1. Blast phase CML

Despite a targeted therapeutic approach with TKIs in CML, a small number of patients will present in or progress to the acute phase of the disease, termed BC or BP. BP is defined by the World Health Organisation (Arber et al, 2016) as the presence of at least one of

- blasts comprising approximately 20% of PB white cells or nucleated BM cells,
- extramedullary blast proliferation, or
- large foci or clusters of blasts in the BM

The ELN diagnostic criteria rests on at least 30% blasts in PB white cells or nucleated BM cells, or the demonstration of extramedullary blastic infiltrates (Baccarani et al, 2013). Regardless, if progression to BP is suspected, it needs to be acted on with immediate effect to aid outcome. It can present as either myeloid or lymphoid in lineage, with approximately two-thirds of cases being found to be of a myeloid phenotype (Kinstrie et al, 2016).

Approximately 25% of patients present with a pre B-lymphoblastic phenotype, with occasional cases of T-cell transformation having been identified (Atallah et al, 2002; Rosenthal et al, 1977). This suggests that within BP, LSCs may play an important role in view of the ability to differentiate to both lineages. However, a high degree of heterogeneity has been recognised, with multiple immunophenotypically distinct populations identified (Kinstrie et al, 2016). Furthermore, it has been shown that within BP disease, committed progenitors can acquire self-renewal properties (Jamieson et al. 2004). As such, the LSC in BP-CML may reside in at least 3 subsets, namely $Lin^{-}CD34^{+}CD38^{-}$, $Lin^{-}CD34^{+}$ cells remaining from CP, and the disease-driving $Lin^{-}CD34^{+}CD38^{+}$ granulocyte-macrophage progenitors/common myeloid progenitors (GMPs/CMPs) (Jamieson et al, 2004).

The incidence of progression to BP under TKI treatment ranges between 0.7 and 4.5% (Cortes et al, 2013; Hehlmann et al, 2011; Hughes et al, 2014). As expected, there is a great reduction in incidence of progression on treatment compared to the pre-TKI era, where, within the German CML study group, it was shown that incidence of progression decreased from 1.5-3.7% (CML studies I-IIIA (Hehlmann et al, 1994a; Hehlmann et al, 2003; Hehlmann et al, 1994b)) to 0.3-2.2% (CML IV (Hehlmann et al, 2014)) per year. The rate of progression falls sharply when MMR is obtained (Hehlmann et al, 2011; Hehlmann et al, 2014). Reported incidence of CML presentation in BP ranges from 0.9 to 6.7% (Hoffmann et al, 2015).

Responses to TKIs in BP are transitory, and median survival following diagnosis of BP remains only 6.5 to 11 months in those treated with TKI alone (Hehlmann, 2012). This is, in part, secondary to the development of additional mutations within the BCR-ABL kinase domain leading to TKI resistance. As such, the mainstay of treatment remains TKI plus conventional aggressive chemotherapy, followed by allogeneic stem cell transplantation (if able) (Hehlmann et al, 2012). Despite this approach, 5-year survival rates have been shown to be less than 20%, therefore, deciphering a therapeutic strategy remains of utmost importance for this patient group.

The mechanisms responsible for progression to BP remain poorly understood, particularly when determining why patients progress to either lymphoid or myeloid lineage BP. Although, the risk of progression to BP on TKI therapy is greatly reduced if MMR is reached, there has been no correlation found between *BCR-ABL* expression and either progression or the development of secondary genetic changes. It is thought that *BCR-ABL* expression provides a favourable environment for genetic instability and maintenance of

secondary DNA modifications (Bacher et al, 2005a; Bacher et al, 2005b; Bacher et al, 2005c; Radich, 2007). Although this, in itself, does not explain why some of these mutations are lineage-specific. However, common mutations have been identified within phenotypes, with 20-30% and 38% generating mutations in *TP53* and *RUNX1*, respectively, within a myeloid phenotype and almost 50% of lymphoid BP cases having a *CDKN2A/B* or *IKZF1* mutation (Bacher et al, 2005c; Mullighan et al, 2008; Roche-Lestienne et al, 2008).

As described, studies to identify the LSC population in BP disease are more limited when compared to the information available for CP. Jamieson *et al* found that the HSC population ($lin^-CD34^+CD38^-CD90^+CD45RA^-$) was not expanded in myeloid BP-CML and identified the GMP population as a potential source of LSCs in myeloid BP (Jamieson et al, 2004). However, this study did not assess the multipotent progenitor (MPP; lin-CD34+CD38-CD90-CD45RA-)/LMPP-like subpopulations, nor did it assess *in vivo* LSC activity. Further studies by the Jamieson group identified activation of β-catenin as the likely mechanism of enhanced self-renewal capacity in the myeloid BP GMP cells (Jamieson et al, 2004; Minami et al, 2008). Less information is available regarding the LSC populations in lymphoid BP-CML. A case report of a patient with imatinib-resistant lymphoid BP-CML indicated that the imatinib-resistant sub-clone (E255K kinase domain mutation) likely originated in the B-cell committed progenitor compartment, but no functional stem cell assays were performed (Kobayashi et al, 2011). The LSC is, however, likely to be fundamental in view of the role it plays in disease development and persistence. From the literature, it can be gleaned that in BP-CML, the LSC subsets are $Lin^-CD34^+CD38^-$ and Lin^-CD34^+ cells remaining from CP-CML and the disease-driving $Lin^-CD34^+CD38^+$ GMP/CMPs. Each of these has deregulated self-renewal. However, understanding their role is made hugely complicated by the inter-connectivity seen between self-renewal pathways (Radich, 2007), and also the heterogeneity seen between cases (Kinstrie et al, 2016). Various self-renewal pathways have been implicated in this, including Wnt-β-catenin, which is probably the most established (Abrahamsson et al, 2009; Radich et al, 2006; Sengupta et al, 2007; Zhao et al, 2007). Other self-renewal pathways', including Hh and BMP, have been linked to this process, but their exact role has yet to be fully elucidated (Jamieson et al, 2004; Radich et al, 2006; Su et al, 2012). Certainly, it may arise that the role for self-renewal pathways will be determined from which subset the LSC derives. For example, accumulation of β-catenin in the nucleus of GMPs leads to increased self-renewal potential (Abrahamsson et al, 2009; Ysebaert et al, 2006). It seems pertinent, therefore, that the role for each evolutionary conserved self-renewal pathway be determined, as this will aid understanding and the development of therapeutic strategies for BP CML.

1.3.5.2. Ph+ acute lymphoblastic leukaemia

Ph+ acute lymphoid-phenotype leukaemias encompass both lymphoid BP CML (described above) and Ph+ ALL. These two diseases are clinically distinct, but can often be mislabelled. Ph+ ALL accounts for approximately 25-30% of ALL diagnosed in adults. Although 70-90% of cases will achieve a complete remission with conventional chemotherapy, long-term survival remains poor, reflecting high rates of relapse and failure of salvage regimens. It encompasses three main phenotypes:

- a lymphoid lineage restricted phenotype with either p190 or p210 BCR-ABL fusion variants
- a stem cell phenotype with either p190 or p210 BCR-ABL fusion variant, or
- misclassified lymphoid BP CML, which has a stem cell phenotype and expresses p210 BCR-ABL fusion variant.

The differences between both lymphoid BP and Ph+ ALL lie in the BCR-ABL fusion variants and activation of other kinases, particularly SRC kinases, as well as potentially within the cell of origin (Hu et al, 2004). The two BCR-ABL fusion variants, p190 and p210, are determined by the different amounts of BCR that they include, leading to different molecular weights (Soekarman et al, 1990). The larger 210kD fusion protein (p210) is almost always found in CML, but is also present in approximately 10-15% of Ph+ ALL. Inversely, the 190kD fusion protein is found in the majority of paediatric Ph+ ALL, 25-30% of adult Ph+ ALL, and only rarely in CML (Advani & Pendergast, 2002). In both, the signalling pathways involved in cell proliferation and survival are deregulated, leading to the phosphorylation of many proteins (Mullighan, 2012a; b; Radich et al, 2006). Included in this is the activation and phosphorylation of STAT5, which has been demonstrated to be required for progression to lymphoid transformation (Hantschel et al, 2012). The JAK-STAT pathway is integral to disease progression, but it is also known to have many interactions with self-renewal pathways that have not yet been fully described. Further to this, attempts to address the differences between lymphoid BP and Ph+ ALL have focussed on studies to address the cell of origin, with conflicting results. As CML is known to be a stem cell disease, *BCR-ABL* should theoretically be identified in all cell types. Similarly, with ALL being lineage-restricted, it would be anticipated that *BCR-ABL* would be restricted to the lymphoid lineage. However, there is data to suggest that both produce a multi-lineage involvement. Furthermore, it has been shown that Ph+ cells within a myeloid compartment

in ALL may correlate with a more favourable prognosis (Secker-Walker, 1984; Secker-Walker et al, 1978), although this remains contentious (Cuneo et al, 1994b).

1.3.5.3. De Novo Ph+ acute myeloid leukaemia

De novo Ph+ AML accounts for 0.5-3% of all AML cases and by definition has no evidence of CML either before the onset of AML or after successful treatment (Keung et al, 2004; Soupir et al, 2007). Its pathogenesis remains controversial with some reports suggesting that it represents a de novo myeloid BP of CML rather than signifying an isolated disease entity (Neuendorff et al, 2016). Indeed, although p190 *BCR-ABL* transcripts have been described, most cases express the p210 *BCR-ABL* transcript (Neuendorff et al, 2016). Further to this, it has been suggested that age-dependent clonal haemopoiesis may play a role, with previous data demonstrating that 'healthy' individuals harbour *BCR-ABL*. Thus, the co-occurrence of *BCR-ABL* within age-dependent clonal haemopoiesis could lead to the development of disease. Despite limited experimental and clinical data, the WHO classification has acknowledged de novo Ph+ AML in its most recent guidelines.

In view that clinical descriptions of de novo Ph+ AML are so few, little is known about its characteristic features. Clinical presentations, however, are similar to that of AML, with no difference in morphology and immunophenotypic analysis to differentiate it. The criteria to differentiate it from BP-CML include an acute presentation, lack of previous history of CP-CML and no splenomegaly. In general, PB count will not demonstrate a basophilia and there will be a lower mature myeloid cell count.

Cytogenetic and molecular features may differentiate between BP-CML and de novo Ph+ AML (Berger et al, 1993; Bacher et al, 2011). For example, in CML, clonal evolution occurs in 60-80%, with a lower percentage in Ph+ AML. Deletions in 7q have been described in Ph+ AML, but remain rare with BP-CML. Molecular mutations such as *NPM1* and *FLT3*, are more common in Ph+ AML. Furthermore, deletions of *IKZF* and *CDKN2A/B* have been described in Ph+ AML, as well as the concomitant loss within immunoglobulins and T cell receptor gene complexes (Nacheva et al, 2013).

Currently, no standardised treatment for de novo Ph+ AML exists, although given the small numbers, it would be difficult to conduct a randomised clinical trial to determine this. From the limited data available, TKI-alone does not achieve a sustained response. Although this is perhaps unsurprising as *BCR-ABL* is not thought to be the clinical driver of the disease,

but most likely provides a proliferative advantage. The addition of TKI to standardised AML conventional chemotherapy seems a reasonable approach allowing treatment of an acute phenotype with the addition of a targeted TKI. Prognosis, however, seems to be poor with induction failure and relapse common in cases of de novo Ph+ AML described (Keung et al, 2004; Soupir et al, 2007). In keeping with this, the NCCN clinical guidelines in oncology recognise it as a poor-risk group, comparable with complex karyotype AML.

1.3.5.4. The unanswered questions

Ph+ acute leukaemias' clearly represent a spectrum of disease entities, including myeloid and lymphoid BP-CML, Ph+ ALL, and de novo Ph+ AML. All have a poor prognosis, but due to the paucity of patients and heterogeneity of disease, randomised controlled trials are difficult to initiate and evaluate. Furthermore, the pathophysiology of each disease has not yet been fully elucidated.

Within BP-CML, there is limited evidence on the factors that drive disease progression from a CP myeloid phenotype to an acute disease entity that can present in either lineage. It has been hypothesised that LSCs are imperative as a causative mechanism, and that the initiating lesion remains at a stem cell level, rather than a more differentiated phenotype. However, there is no real documented evidence to how lineage decision is driven within this subset. Furthermore, there is little to no evidence on the variation of self-renewal and survival signalling pathways between phenotypes, and if lymphoid BP should be managed as per a disease of lymphoid origin, rather than that of myeloid. Without a randomised control trial, it is difficult to justify this treatment decision. Perhaps understanding genomic regulation between myeloid and lymphoid BP disease and other acute Ph+ acute diseases will guide diagnostic strategies and potential therapeutic strategies.

1.4. Aims

The following thesis is an investigation into the identification and eradication of the CML LSC in CP through evaluation of the self-renewal pathway, Notch, and the cell surface marker, CD93. Further to this, it has enabled investigation into the genomic differences of self-renewal and survival pathways in both the progression of disease and between subsets of Ph+ acute leukaemia.

Experiments were designed to address the following specific aims:

1. **To examination the role of the Notch signalling pathway in CP-CML and in the progression of disease to a myeloid BP phenotype**

As has been described through the introduction of this thesis, self-renewal pathways remain fundamental in the maintenance and propagation of the LSC in CML. However, despite much experimental evidence into the role of Hh, Wnt/β-catenin and BMP signalling, there is limited and conflicting data on the role of Notch signalling within this disease model, or within disease progression. Within this thesis I have extensively evaluated the role of Notch signalling within CP-CML and through disease progression to a myeloid BP phenotype.

2. **To examine the genomic variation in self-renewal signalling pathways in**
    a. **Disease progression to myeloid BP disease**
    b. **Between myeloid BP and lymphoid B**
    c. **Lymphoid BP and Ph+ ALL**

The role which self-renewal pathways play within disease progression and between Ph+ acute leukaemias has yet to be fully elucidated. Within this thesis, I have analysed the genomic variation of self-renewal pathways through Fluidigm analysis in primary samples. This has allowed some understanding of the interconnectivity within and between diseases, and provides preliminary data to enable further targeted investigation.

3. **To evaluate the functional role of CD93 in CML LSC *in vitro* and *in vivo***

Our group has recently identified upregulation of CD93 within a LSC phenotype in CP-CML. This data has been extended to include functional *in vitro* and *in vivo* experimentation, as well as single cell genomic analysis to validate this finding and examine the heterogeneity of the CP CML LSC.

2. Materials and Methods

2.1. Materials

The names and addresses of the suppliers are listed below.

Company	Address
Applied Biosystems	Lingley House, 120 Birchwood Boulevard, Warrington, WA3 7QH, UK
BD Biosiences	The Danby Building, Edmund Halley Road, Oxford, OX4 4DQ, UK
BioRad	Maxted Rd, Hemmel Hempstead, West Sussex, HP2 7DX, UK
Bioscience Lifescience Ltd	10 Orchard Place, Nottingham Business Park, Nottingham, NG8 6PX, UK
Cell Signalling Technology	2316 ZA Leiden, The Netherlands
Cellagen Technology	5940 Pacific Mesa Court, San Diego, CA 92121, USA
eBioscience	3 Fountain Drive, Paisley, PA4 9RF, UK
New England Biolabs	75-77 Knowl Piece, Wilbury Way, Hitchin, Herts SG4 0TY, UK
Eppendorf UK Ltd	Endurance House, Vision Park, Histon, Cambridge, CB24 9ZR
Eurofins MWG Operon	Westway Estate 28-32 Brunel Road, Acton, London, W3 7XR, UK
Fisher Scientific UK	Bishop Meadow Road, Loughborough, Leicestershire, LE1 5RG, UK
Fluidigm UK Ltd	90 Fetter Lane, London, EC4A 1EQ, UK
Fred Baker Scientific Ltd	3 Kancer Court, Cheshire, WA17 1PN, UK
GraphPad Software, Inc.	7825 Fay Avenue, Suite 230 La Jolla, CA 92037 USA
Greiner Bio-One Ltd.	Unit 5, Stroudwater Business Park, Gloucestershire, GL10 3SX, UK
Invitrogen, Paisley, UK Ltd. Part of Life Technologies	3 Foundation Drive, Paisley, UK
Jackson ImmunoResearch, Laboratories, Inc.	UK distributor; Stratech Scientific Limited
Labtech International Ltd.	Acorn House, The Broyle, Ringmer, East Sussex, BN8 5NN, UK
Millipore (U.K.) Limited	Suite 3 & 5, Croxley Green Buisiness Park, Watford, WD18 8YH, UK
Miltenyi Biotec Ltd.	Almac House, Church Lane, Bisley, Surrey, GU24 9DR, UK
Novartis Pharmaceuticals UK Ltd	Frimley, Camberley, Surrey, GU16 7SR, UK
Peprotech EC Ltd.	Peprotech House, 29 Margavine Road, London, W6 8LL, UK
Promega UK	Delta House, Southampton Science Park, Southampton, SO16 7NS, UK

Qiagen	Fleming Way, Crawley, West Sussex, RH10 9NQ, UK
R&D Systems	19 Barton Lane, Abingdon Science Park, Abingdon, OX14 3NB, UK
Santa Cruz Biotechnology, Inc	Heidelberg, 69115, Germany
Scientific Lab Supplies Ltd	204 Main St, Coatbridge, ML5 3RB, UK
Sigma-Aldrich	The Old Brickyard, New Rd, Gillingham, Dorset, SP8 4XT, UK
Stem Cell Technologies	40 Rues des Berges, Miniparc Polytec, Bâtiment Sirocco, 38000 Genoble, France
Stratech Scientific Limited	Oaks Drive, Newmarket, Suffolk, CB8 7SY, UK 340 A Street #101 Ashland, OR97520, USA
ThermoFisher Scientific	3 Fountain Drive, Paisley, PA4 9RF, UK

2.1.1. Tissue culture

2.1.1.1. Tissue culture materials

Plastics	Supplier
Blunt ended needles	Invitrogen, Paisley, UK
Cryotubes	Fisher Scientific, Loughborough, UK
Eppendorf tubes (0.5 / 1.5ml)	Invitrogen, Paisley, UK
FACS tubes (sterile/unsterile)	BD Biosciences, Oxford, UK
Falcon tubes (15, 50ml)	Fred Baker Scientific, Cheshire, UK
Flat bottomed culture plates (6, 12, 24, 48, 96 well)	Greiner Bio-One, Gloucestershire, UK
Flat bottomed culture plates coated with collagen type 1 (6 and 24 well)	Scientific Lab supplies, Coatbridge, UK
Haemocytometer	Hawksey, UK
Media filtration system	Scientific Lab supplies, Coatbridge, UK
Non-adherent tissue culture dishes (35mm / 100mm)	Scientific Lab supplies, Coatbridge, UK
Non-adherent tissue culture flasks ($75cm^3$)	Scientific Lab supplies, Coatbridge, UK
Pipette tips (p10, p20, p100, p200, p1000)	Greiner Bio-One, Gloucestershire, UK
Sterile tissue culture pipettes (5, 10, 25, 50ml)	Scientific Lab supplies, Coatbridge, UK
Syringe filters (22 micron)	Invitrogen, Paisley, UK
Syringes (5, 10, 20, 50 ml)	Invitrogen, Paisley, UK
Tissue culture flasks (25, 75, 150 cm^3)	Greiner Bio-One, Gloucestershire, UK

2.1.1.2. Tissue culture reagents

Reagent	Supplier
Alpha MEM medium	Invitrogen, Paisley, UK
BIT 9500 serum substitute (BIT)	Stem Cell Technologies, British Columbia, Canada
Bovine serum albumin (BSA)	Sigma-Aldrich, Dorset, UK
CliniMACS $CD34^+$ beads	Miltenyi Biotec, Auburn CA
CliniMACS PBS/EDTA buffer	Miltenyi Biotec, Auburn CA
CliniMACS tubing set and columns	Miltenyi Biotec, Auburn CA
Demecolcine (Colcemid; N-Deacetyl – N – Methylcolchicine)	Invitrogen, Paisley, UK
Dimethylsulphoxide (DMSO)	Sigma-Aldrich, Dorset, UK
DNase I (Recombinant human DNAse)	Stem Cell Technologies, British Columbia, Canada
Dulbecco's modified eagle medium (DMEM)	Sigma-Aldrich, Dorset, UK
Dulbecco's phosphate buffered saline (PBS)	Sigma-Aldrich, Dorset, UK
Dulbecco's phosphate buffered saline without Ca^{2+} and Mg^{2+} (DPBS)	Invitrogen, Paisley, UK
Ethanol 100%	Sigma-Aldrich, Dorset, UK
Foetal bovine serum (FBS)	Invitrogen, Paisley, UK
Genetecin G418 (1013-027)	Invitrogen, Paisley, UK
Ham's F12 / DMEM (F12/DMEM)	Invitrogen, Paisley, UK
Hanks balanced salt solution (Ca^{2+} Mg^{2+} free) (HBSS-CMF)	Invitrogen, Paisley, UK
Histopaque	Miltenyi Biotec, Auburn CA
Horse serum	Invitrogen, Paisley, UK
Human serum albumin 20% (HSA 20%)	University of Glasgow
Human serum albumin 4.5% (HSA 4.5%)	University of Glasgow
Hydrocortisone 21 – Hemisuccinate (Sodium salt)	Stem Cell Technologies, British Columbia, Canada
Hygromycin B	Invitrogen, Paisley, UK
Imatinib	Novartis, Frimley, UK
Iscove's modified dulbecco's medium (IMDM)	Invitrogen, Paisley, UK
L-glutamine 200mM (100x)	Invitrogen, Paisley, UK
Magnesium chloride (1.25M)	Sigma-Aldrich, Dorset, UK
Methocult H4034	Stem Cell Technologies, British Columbia, Canada
Mitomycin C	Invitrogen, Paisley, UK
Myelocult 5100	Stem Cell Technologies, British Columbia, Canada
N-[N-(3,5-Difluorophenacetyl-L-alanyl)]-(S)-phenylglycine t-butyl ester (DAPT)	Cellagen Technology, USA
Penicillin (5000u)/ streptomycin (5mg/ml) solution (Pen/Strep)	Invitrogen, Paisley, UK

Recombinant human Flt-3 ligand (Flt3L)	Peprotech EC Ltd, UK
Recombinant human G-CSF (G-CSF)	NHS pharmacy
Recombinant human IL-3 (IL-3)	Peprotech EC Ltd, UK
Recombinant human IL-6 (IL-6)	Peprotech EC Ltd, UK
Recombinant human SCF (SCF)	Peprotech EC Ltd, UK
Recombinant Jagged1	R&D systems, Abingdon, UK
RPMI 1640 medium (RPMI)	Invitrogen, Paisley, UK
Sodium azide	Sigma-Aldrich, Dorset, UK
Sterile water (dH_20)	Invitrogen, Paisley, UK
Tri-sodium citrate (0.155M)	Sigma-Aldrich, Dorset, UK
Trypan blue solution (8mM)	Sigma-Aldrich, Dorset, UK
Trypsin- EDTA (0.25%)	Sigma-Aldrich, Dorset, UK
β-mercaptoethanol (200mM)	Invitrogen, Paisley, UK

2.1.1.3. Tissue culture media components (not listed within text)

2.1.1.3.1. Serum free media (SFM)

	Volume
IMDM	97.25ml
BIT	25ml
L-Glutamine	1.25ml
Penicillin/streptomycin	1.25ml
β-mercaptoethanol (200mM)	250ul (i.e. 400uM)
Low density lipoprotein (10mg/ml)	250ul (40ug/ml)
Filter sterilise through 0.22um filter before use	

2.1.1.3.2. SFM with high growth factor (SFM+5GF)

	Volume	Final Concentration
SFM	10ml	
IL-3 (50ug/ml)	4ul	20ng/ml
IL-6 (50ug/ml)	4ul	20ng/ml
G-CSF (50ug/ml)	10ul	50ng/ml
SCF (50ug/ml)	20ul	100ng/ml
Flt3L (50ug/ml)	20ul	100ng/ml

2.1.1.3.3. MSC media

	Volume	Final Concentration
DMEM	400ml	
Hyclone FBS	100ml	20%

2.1.1.3.4. Long-term myeloid culture medium (LTMCM)

	Volume concentration	Final Concentration
Myelocult	500ml	

Hydrocortisone 21 – Hemisuccinate ($1x10^{-4}$M)	1ml	$0.2x10^{-6}$M

2.1.1.4. Tissue culture solutions

2.1.1.4.1. Thawing solution of primary samples (DAMP)

	Volume concentration	Final Concentration
PBS	418.75ml	
Tri-sodium citrate (0.155M)	53ml	8.2mM
HSA 20%	24ml	1%
DNase I (~2500U/1ml)	2ml	10U/ml
$MgCl_2$ (1M)	1.25ml	2.5mM

2.1.1.4.2. PBS/2% FBS washing solution

	Volume
PBS	490ml
FBS	10ml

2.1.1.4.3. PBS/20% FBS quenching solution

	Volume
PBS	400ml
FBS	100ml

2.1.1.4.4. Freezing solution for primary samples

	Volume
4.5% HSA	80ml
DMSO	20ml

2.1.1.4.5. Freezing solution for cell lines

	Volume
FBS	80ml
DMSO	20ml

2.1.1.4.6. LTC-IC harvest washing buffer

	Volume
IMDM	500ml
FBS	2ml

2.1.2. Immunofluorescence

2.1.2.1. Immunofluorescence reagents

Reagent	Supplier
100% ethanol	University of Glasgow
100% methanol	University of Glasgow
Acetic acid	University of Glasgow
4',6-diamidino-2-phenyloindole (DAPI)	Invitrogen, Paisley, UK
Fix and Perm Reagents A/B	Invitrogen, Paisley, UK
Formamide	Invitrogen, Paisley, UK
KCL 0.75M	University of Glasgow
LS1 BCR-ABL Dual Colour FISH probe set	Abbott Diagnostics, Maidenhead, UK
Poly-L-Lysine	Invitrogen, Paisley, UK
Rubber cement	Halfords, Braehead, UK
SSC	Invitrogen, Paisley, UK

2.1.2.2. FISH solutions

2.1.2.2.1. Hypotonic KCL solution

	Volume
KCl 0.75M	1ml
dH_2O	10ml

2.1.2.2.2. Fixative

	Volume
Acetic acid	2ml
Methanol	9ml

2.1.2.2.3. Stock SSC buffer (x20 concentration) (20X SSC)

	Volume
SSC	132g
dH_2O	500ml
Pure HCl	Titrate to pH 5.3

2.1.2.2.4. FISH wash buffer I (2xSSC 0.1% NP40)

	Volume
20X SSC	100ml
dH_2O	899ml
NP40	1ml
Pure HCl	Titrate to pH7

2.1.2.2.5. FISH wash buffer 2 (0.4xSSC 0.3% NP40)

	Volume
20X SSC	10ml

dH_2O	493.5ml
NP40	1.5ml
Pure HCl	Titrate to pH7

2.1.2.2.6. FISH denaturation buffer

	Volume
Formamide 70%	49ml
20X SSC	7ml
dH_2O	14ml
Pure HCl	Titrate to pH7

2.1.3. Flow cytometry

2.1.3.1. Flow cytometry reagents

Reagent	Supplier
7 amino actinomycin D (7-AAD, Viaprobe solution)	BD Biosciences, Oxford, UK
AnnexinV – FITC or Annexin V - APC	BD Biosciences, Oxford, UK
Anti-goat FITC	BD Biosciences, Oxford, UK
Anti-mouse IgG2a FITC	BD Biosciences, Oxford, UK
Anti-mouse IgG2a FITC	BD Biosciences, Oxford, UK
Anti-rabbit IgG FITC or PE	Sigma-Aldrich, Dorset, UK
Anti-rabbit IgG PE	BD Biosciences, Oxford, UK
Carboxyfluorescein diacetate succinimidyl diester (CFSE)	Invitrogen, Paisley, UK
FACS clean solution	Becton Dickinson, Oxford, UK
FACS flow solution	Becton Dickinson, Oxford, UK
Fix and Perm Kit	Invitrogen, Paisley, UK
HBSS-CMF	Invitrogen, Paisley, UK
Propidium Iodide (PI)	BD Biosciences, Oxford, UK

2.1.3.2. Flow cytometry antibodies

Reagent	Supplier
Mouse anti-human CD19-V450 (HIB19)	BD Biosciences, Oxford, UK
Mouse anti-human CD33-PerCP-Cy5.5 (P67.6)	BD Biosciences, Oxford, UK
Mouse anti-human CD34-APC (581)	BD Biosciences, Oxford, UK
Mouse anti-human CD34-PerCP (8G12)	BD Biosciences, Oxford, UK
Mouse anti-human CD36-APC (CB38)	BD Biosciences, Oxford, UK
Mouse anti-human CD38-V450 (HIT2)	BD Biosciences, Oxford, UK
Mouse anti-human CD45-FITC (H130)	BD Biosciences, Oxford, UK
Mouse anti-human CD45RA-APC H7 (HI100)	BD Biosciences, Oxford, UK
Mouse anti-human CD71-FITC (M-A712)	BD Biosciences, Oxford, UK
Mouse anti-human CD73-V450 (AD2)	BD Biosciences, Oxford, UK
Mouse anti-human CD90-PE Cy7 (5E10)	BD Biosciences, Oxford, UK
Mouse anti-human CD93-PE (R3)	eBioscience, ThermoFisher Scientific, Paisley, UK

Mouse anti-human DLL1-PE (MHD1-314)	BD Biosciences, Oxford, UK
Mouse anti-human glycophorin A-PE (GA-R2)	BD Biosciences, Oxford, UK
Mouse anti-human Jagged1-PE (MHJ1-152)	BD Biosciences, Oxford, UK
Mouse anti-human Lineage cocktail-FITC (CD3 (MϕP9), 14 (3G8), 16 (NCAM16.2), 19 (SJ25C1), 20 (SK7), 56 (L27))	BD Biosciences, Oxford, UK
Rat anti-mouse CD45-APC-Cy7 (30-F11)	BD Biosciences, Oxford, UK
Rat anti-mouse DLL1-PE (3OB11.1O)	BD Biosciences, Oxford, UK

2.1.4. Western blotting

2.1.4.1. Western blotting reagents

Reagent	Supplier
2-mercaptoethanol (50ul/ml)	Sigma-Aldrich, Dorset, UK
Ammonium persulphate (APS)	Sigma-Aldrich, Dorset, UK
Bromophenol blue	Sigma-Aldrich, Dorset, UK
BSA protein	BioRad, Hampstead, UK
ECL	BioRad, Hampstead, UK
Glycerol	Sigma-Aldrich, Dorset, UK
horseradish-peroxidase (HRP)-labelled secondary antibodies	Sigma-Aldrich, Dorset, UK
Immune-blot polyvinyliden difluoride (PVDF) membrane	BioRad, Hampstead, UK
Milli Q ultrapure water	Sigma-Aldrich, Dorset, UK
NaCl	Sigma-Aldrich, Dorset, UK
NP40	Sigma-Aldrich, Dorset, UK
Ovalbumin	Sigma-Aldrich, Dorset, UK
Phosphatase inhibitor cocktail	Sigma-Aldrich, Dorset, UK
Protease inhibitor cocktail	Sigma-Aldrich, Dorset, UK
Quickstart Bradford Dye Reagent	BioRad, Hampstead, UK
Sodium dodocyl sulphate (SDS)	Sigma-Aldrich, Dorset, UK
SRX-101A medical film processor	Konica Minolta Medical Graphic, Inc., Banbury, UK
Stripping solution	Sigma-Aldrich, Dorset, UK
TEMED	Sigma-Aldrich, Dorset, UK
Trisma base	Sigma-Aldrich, Dorset, UK
Tween 20	Sigma-Aldrich, Dorset, UK

2.1.4.2. Western blotting antibodies

Antibody	Reactive Species	Dilution	Block	Supplier
ADAM10, C-terminus	Rabbit	1:1000	5% Milk	Millipore
Anti-mouse IgG (H+L)- HRP conjugated	Horse	1:10000	5% BSA	Cell Signalling
Anti-rabbit IgG (H+L)- HRP conjugated	Goat	1:10000	5% BSA	Cell Signalling

Cleaved Notch1 (Val1744) (D3B8)	Rabbit	1:500	5% BSA	Cell Signalling
GAPDH (D16H11)	Rabbit	1:1000	5% Milk	Cell Signalling
Notch1 (A-8)	Mouse	1:500	5% BSA	Santa Cruz
Notch2 (D67C8)	Rabbit	1:1000	5% BSA	Cell Signalling

2.1.4.2.1. Western blotting solutions

2.1.4.2.1.1. 1M Tris HCl

	Volume
Trisma base	60.6g
dH_2O	500ml
HCl/NaCl	To appropriate PH

2.1.4.2.1.2. 10% SDS

	Volume
SDS	10g
dH_2O	91ml

2.1.4.2.1.3. 10% APS

	Volume
APS	0.1g
dH_2O	1000ul

2.1.4.2.1.4. 10X TBS

	Volume
NaCl	87.6g
Tris	58.1g
dH_2O	1000ml

2.1.4.2.1.5. 1X TBSN

	Volume
NP40 10% (25ml NP40/250ml H2O)	5ml
1xTBS	1000ml

2.1.4.2.1.6. Semi-dry transfer buffer (10X)

	Volume
Glycine	29.3g
Tris	58.1g
SDS	3.75g
dH_2O	1000ml

2.1.4.2.1.7. Semi-dry transfer buffer (1X)

	Volume
Methanol	200ml
10X Transfer buffer stock	100ml
dH$_2$O	700ml

2.1.4.2.1.8. Blocking solution (5X)

	Volume
BSA	25g
Ovalbumin	5g
1xTBS	500ml
Sodium azide	Sprinkle

2.1.5. Molecular biology

2.1.5.1. Molecular biology reagents

Reagent	Supplier
20X taqman gene expression assay	Applied Biosystems, Warrington, UK
2X assay loading reagent	Applied Biosystems, Warrington, UK
2X taqman universal PCR mastermix	Applied Biosystems, Warrington, UK
Applied Bioscience micro RNA kit	Applied Biosystems, Warrington, UK
Arcturus picopure RNA isolation kit	Applied Biosystems, Warrington, UK
Boric acid	Sigma-Aldrich, Dorset, UK
DNAse1	Qiagen, Crawley, UK
dNTP mix	Applied Biosystems, Warrington, UK
EDTA	Sigma-Aldrich, Dorset, UK
GE loading reagent	Applied Biosystems, Warrington, UK
Gene expression master mix	Applied Biosystems, Warrington, UK
Molecular biology grade 100% ethanol	Qiagen, Crawley, UK,
Molecular biology grade H_2O	Qiagen, Crawley, UK
Random primers	Applied Biosystems, Warrington, UK
Reverse transcriptase	Applied Biosystems, Warrington, UK
RNA easy micro kit	Qiagen, Crawley, UK
RNA easy mini kit	Qiagen, Crawley, UK
RNase inhibitor	Applied Biosystems, Warrington, UK
RNeasy mini kit	Qiagen, Crawley, UK
Taqman gene expression assay	Applied Biosystems, Warrington, UK
TE buffer, pH 8	Applied Biosystems, Warrington, UK
Tris base	Sigma-Aldrich, Dorset, UK

2.1.5.2. Molecular biology solutions

2.1.5.2.1. 10X TBE buffer

	Volume
Boric acid	55g
EDTA (0.5M, pH 8.0)	40ml
Tris base	108g
dH_2O	1000ml

2.1.5.2.2. 2X reverse transcription mastermix

	Volume
10X RT Buffer	2ul
25X dNTP mix	0.8ul
10X RT Random primers	2ul
Reverse transcriptase 50u/ul	1ul
RNase inhibitor	1ul
Nuclease free water	3.2ul

2.1.5.2.3. Fluidigm assay mix

	Volume
2X assay loading reagent	2.5ul
20X TaqMan Gene expression assay	2.5ul

2.1.5.2.4. Fluidigm sample mix

	Volume
2X TaqMan universal PCR Mastermix	2.5ul
20X GE sample loading reagent	0.25ul
cDNA	2.25ul

2.1.5.3. Primers

	Forward	Reverse
ABL-A3-B	GTTTGGGCTTCACACCATTCC	-
ACVR2A	ACCATGGCTAGAGGATTGGC	GCCAACCCAAAGTCAGCAAT
ACVR2B	CTGCAACGAACGCTTCACTC	CAGGACGATGAGGGAAAGGC
ADAM 10	ATGGCAAAGATGATAAAGAATTATGCC	AATCGTTGCAAGGGGATCC
ADAM 17	CTTCTACAGATACATGGGCAGAG	CTCTATCTGTATTCCATAGCCTTTAA
ADAM19	GTTTACACAACAGACCAAGAAGC	CTTGTGTTTGGTGGCGTCC
AKT1	TGGACTACCTGCACTCGGAGAA	GTGCCGCAAAAGGTCTTCATGG
AKT2	CCAACACCTTTGTCATACGCTGC	GCTTCAGACTGTTGGCGACCAT
AKT3	GATGCCTCTACAACCCATCAT	GTCCATGCAGTCCATACCATCCT
ATM	CGGAGCTGATTGTAGCAACATACTA	CAGATAGAGCCTGAAGTACACAGAG
ATR	CAGCTCTCTATGAAGGCCATTCAA	GTTCTACTGTTTCACTGTCTGTTGC

B2M	TTGTCTTTCAGCAAGGACTGG	ATCCGGCATCTTCAAACCTCC
BCL2	ATCGCCCTGTGGATGACTGAGT	GCCAGGAGAAATCAAACAGAGGC
BCR-C5R	BCR-C5R	-
BMI1	GCATCGAACAACGAGAATCA	GCTGGTCTCCAGGTAACGAA
BMI1	AACTGATGATGAGATAATAAGC	CTTCTGAGAAACTTTCTTAAGTGC
BMP10	ACCCACCAGAGTACATGTTGG	GCCCATTAAAACTGACCGGC
BMP7	CAGGCCTGTAAGAAGCACGA	TGGTTGGTGGCGTTCATGTA
C-JUN	CTTGAAAGCTCAGAACTCGGAG	CTGCGTTAGCATGAGTTGGC
CCDN1	CAGAAGGAGATTGTGCCATCC	GAAGCGGTCCAGGTAGTTCA
CCNA1	CTCGTAGGAACAGCAGCTATGC	GCTAGAACTTTCAGAAGCAAGTGTTC
CCNA2	TGGCGGTACTGAAGTCCGG	CAAGGAGGAACGGTGACATGC
CCNB1	CAGCTCTTGGGGACATTGGTAAC	ACTGGCACCAGCATAGGTACC
CCNE1	CAACGTGCAAGCCTCGGA	CAAAGTGCTGATCCCTTAAGTATGTC
CCNE2	CAAGTTGATGCTCTTAAAGATGCTCC	GCAGCAGTCAGTATTCTGTACTGG
CD79A	GAACGAGAAGCTCGGGTTG	TGCCCACATCCTGGTAGGT
CD93	GGCAGACAGTTACTCCTGGGTT	GGAGTTCAAAGCTCTGAGGATGG
CDC25A	GTCTAGATTCTCCTGGGCCATTG	CAGAATGGCTCCTCTTCAGAGC
CDC25B	GGATTTGTGGACATCCTAGAGAGT	ACTTGCTGTACATGACGAGGT
CDC25C	CACTCAGCTTACCACTTCTGCAG	GGGCTACATTTCATTAGGTGCTGG
CDK2	GCCTGATTACAAGCCAAGTTTCC	TCCGCTTGTTAGGGTCGTAGT
CDK4	GAAACTCTGAAGCCGACCAG	AGGCAGAGATTCGCTTGTGT
CDK4	CCCATCAGCACAGTTCGTGA	AACACCAGGGTTACCTTGATCTC
CDK6	CCTGCAGGGAAAGAAAAGTGC	CCTCCTCTTCCCTCCTCGAA
CDK6	CCGAAGTCTTGCTCCAGTCC	GTTGATCAACATCTGAACTTCCACG
CDKN1A	GTGGACCTGGAGACTCTCAG	CCTCTTGGAGAAGATCAGCCG
CDKN1C	CACGATGGAGCGTCTTGTC	CCTGCTGGAAGTCGTAATCC
CDKN2A	CCGAATAGTTACGGTCGGAGG	CACGGGTCGGGTGAGAGT
CDKN2B	GGTGGCTACGAATCTTCCG	CCTAAGTTGTGGGTTCACCA
CDKN3A	GGTTTATGTGCTCTTCCAGGTTG	GTGCAGCTAATTTGTCCCGAAAC
CHEK1	CCATCAGCAAGAATTACCATTCCAG	CTGGGAGACTCTGACACACC
CHEK2	ATGAGAACCTTATGTGGAACCCC	GCTCAGAGAAAGGTGGATACCC
CSF1R	GGACATTCATCAACGGCTCT	GCTCAGGACCTCAGGGTATG
CSF2R	GTTACCACACCCAGCATTCC	TTGGCAGTCCCAGCTTAAAT
CSF3R	TGGGACCCAGGAATCTATCA	ATGAGGCAGGAGAGGTTGTG
CYC1	ACTGCGGGAAGGTCTCTACTT	GGGTGCCATCGTCAAACTCTA
CYCLIN D3	TGGATGCTGGAGGTATGTGA	TGCACAGTTTTTCGATGGTC
CYCLIN E1	GTCCTGGCTGAATGTATACATGC	CCCTATTTTGTTCAGACAACATGGC
DAAM1	AGAAGTATGCCAGCGAAAGG	TCTCCACTCCTGCACCTTGG
DKK3	GCATCATCGACGAGGACTGT	GTCTCCACAGCACTCACTGT
DLL1	GCCTGGATGTGATGAGCAGC	ACAGCCTGGATAGCGGATACAC
DLL3	CACTCAACAACCTAAGGACGCAG	GAGCGTAGATGGAAGGAGCAGA
DLL4	TCGCTCATCATCGAAGCTTGG	CAGTTCTGACCCACAGCTAGG
DTX1	AATCCCGAGGATGTGGTTCG	GTAGCCTGATGCTGTGACCA
E2F1	GGACCTGGAAACTGACCATCAG	CAGTGAGGTCTCATAGCGTGAC
E2F2	CTCTCTGAGCTTCAAGCACCTG	CTTGACGGCAATCACTGTCTGC

E2F3	AGCGGTCATCAGTACCTCTCAG	TGGTGAGCAGACCAAGAGACGT
EFNA1	GTCTGAGAAGTTCCAGCGCT	CACTGACAGTCACCTTCAACC
EFNA4	GAGGCTCCAGGTGTCTGTCT	AATGCTCCATCTTGTCGGTCTG
EGR1	TGACCGCAGAGTCTTTTCCT	TGGGTTGGTCATGCTCACTA
EGR2	CTGACACTCCAGGTAGCGAG	GTTGATCATGCCATCTCCGGC
ENOX2	GAGCTGGAGGGAACCTGATTT	CACTGGCACTACCAAACTGCA
ETS1	GAGTCAACCCAGCCTATCCA	ATGGGATGGAGCGTCTGATA
FAT1	ATCTGTGGAGCCTCCTGGCATA	CATCTGTAGCCTCGACTGTGAG
FAT2	CACTGACAGTCATGGTCCGA	GTGTCAGGAACACTTGCCTC
FAT3	GACAGAGACACATCCGACGTT	GCCTCTTCACATAGACCTTCCAC
FAT4	CCCACATTTGCCAGTAAAGCG	GTGAACTGAGAGTTTCCACCG
FBXW7	CCTTCTCTGGAGAGAGAAATGC	CTGTCTGATGTATGCACTTTTCC
FOS	AGGAGAATCCGAAGGGAAAGG	TAGTTGGTCTGTCTCCGCTTG
FOXM1	TCAAAACCGAACTCCCCCTG	GCAGCACTGATAAACAAAGAAAGA
FOXO1	CTACGAGTGGATGGTGAAGAGC	CCAGTTCCTTCATTCTGCACTCG
FOXO3	CCTACTTCAAGGATAAGGGCGAC	GCCTTCATTCTGAACGCGCATG
FURIN	CCACATGACTACTCCGCAGAT	TACGAGGGTGAACTTGGTCAG
GATA3	CGAACTGTCAGACCACCACA	GGTTTCTGGTCTGGATGCCTT
GEMIN2	TTGTTACCTGAGGCTCATTCAC	TCATCAGCTAAATCACGTTGGT
GFI1	GCTCCCCAGGACCAGACTAT	CTTCGGTCAGCTGCGATT
GLI1	AGCCAAGCACCAGAATCGG	TCTTGACATGTTTTCGCAGCG
GLI3	CTCCTATGGTCACTTATCTGCAAGT	TGAACCTAAGCTCTGTTGTCGG
GNB2L1	TCCATACCTTGACCAGCTTG	GCAGATTGTCTCTGGATCTC
GSK3B	CGACTAACACCACTGGAAGCT	GGATGGTAGCCAGAGGTGGAT
HES1	GGAGAAAAATTCCTCGTCCC	CGCGAGCTATCTTTCTTCAG
HEY1	CCGTGGATCACCTGAAAATGC	GGCATCTAGTCCTTCAATGATGC
HEY2	GAAGATGCTCCAGGCTACAGG	CCTTCCACTGAGCTTAGGTACC
HHIP	GCCATTCAGTAATGGTCCTTTGG	CCACTGCTTTGTCACAGGAC
HIF1A	TACTCATCCATGTGACCATGAGG	TAGTTCTTCCTCGGCTAGTTAGG
HIPK1	GCCACTACAGATTCAGTCAGGAG	GTGTGATGGTGGCTACTTGAGG
HLF	GCCCATGATCAAGAAAGCTC	GGCGATCTGGTTCTCTTTCA
HOXA4	ATGTCAGCGCCGTTAACCC	TGTTGGGCAGTTTGTGGTCT
HOXA5	AAGTCATGACAACATAGGCGGC	GATACTCAGGGACGGAAGGC
HOXA6	TGCGCGGGTGCTGTGTAT	GCTGCGTGGAATTGATGAGC
HOXB4	CTGGATGCGCAAAGTTCACGTG	CGTGTCAGGTAGCGGTTGTAGT
ICAT	CATGCTGCGGAAGATGGGAT	GGAAAACGCCATCACCACGT
IHH	GGACGCTATGAAGGCAAGATCG	CAGCGAGTTCAGGCGGTCCTT
IKZF1	AACGTCGCCAAACGTAAGAG	AGTTGATGGCGTTGTTGATG
INHB1	AAGTCGGGGAGAACGGGTAT	GGTCACTGCCTTCCTTGGAA
INK4A	CTCGTGCTGATGCTACTGAGGA	GGTCGGCGCAGTTGGGCTCC
INK4C	CGTCAATGCACAAAATGGATTTGG	GAATGACAGCGAAACCAGTTCGG
INK4D	GTGCATCCCGACGCCCTCAAC	TGGCACCTTGCTTCAGCAGCTC
JAG1	TGGGATTCCAGTAATGACACCG	GTAGTCATCACAGGTCACGC
JAG2	CAAAAACCTGATTGGCGGCT	CACACACTGGTACCCGTTCA
LEF1	CACTGACAGTGACCTAATGC	CAACGACATTCGCTCTCATT
LEF1	CTACCCATCCTCACTGTCAGTC	GATGTTCCTGTTTGACCTGAGG

LFNG	GCCACAAGGAGATGACGTT	GAGCAGTTTGTGATGACCACG
MAML	GCAACAGCAGTTCCTTCAGAGG	GTGAACTGTCCAACCTGCTGTG
MDM2	TGTTTGGCGTGCCAAGCTTCTC	CACAGATGTACCTGAGTCCGATG
MEIS1	AAGCAGTTGGCACAAGACACGG	CTGCTCGGTTGGACTGGTCTAT
MEIS1	AAGACACGGGACTCACCATC	TGACCGTCCATTACGAAACC
MFNG	CTGGTACAGTTCTGGTTTGC	ATGTGTCCATGAAACGGGAGC
MPL	ACTCAGCGAGTCCTCTTTGTGG	CATAGCGGAGTTCGTACCTCAG
MPO	GCATCATCGGTACCCAGTTC	GTGGTGATGCCTGTGTTGTC
MTOR	AGCATCGGATGCTTAGGAGTGG	CAGCCAGTCATCTTTGGAGACC
MYC	GACTCTGAGGAGGAACAAGA	TTGGCAGCAGGATAGTCCTT
NFKB1	AGATGATCCATATTTGGGAAGGC	TTGCTCTAATATTTGAAGGTATGGGC
NOTCH 1	TCCACTGTGAGAACAACACGC	ACTCATTGACATCGTGCTGGC
NOTCH 2	GCAAAGTGTATCGATCACCCGA	TGCAGGTGTAGGAATCAATACCATC
NOTCH 3	TACTGGTAGCCACTGTGAGCAG	CAGTTATCACCATTGTAGCCAGG
NOTCH 4	TTCCACTGTCCTCCTGCCAGAA	TGGCACAGGCTGCCTTGGAATC
NUMB	CCAAACCAGTGACAGTGGTGGC	CCCAAGGGTTGGTTTCACGC
P190 BCR-e1-A	GACTGCAGCTCCAATGAGAAC	-
P210 BCR-e1-A	GAAGTGTTTCAGAAGGCTTCTCC	-
p38	GAGCGTTACCAGAACCTGTCTC	AGTAACCGCAGTTCTCTGTAGGT
PBX1	GGAGGATACAGTGATGGACTCG	GGAGGTATCAGAGTGAACACTGC
PML	CCGTCATAGGAAGTGAGGTCTTC	GTTTTCGGCATCTGAGTCTTCCG
PREP1	ATTGCATCAGGAGTCGCACAGC	GAGACTGAAGGCTGTCCACGTT
PSEN1	GGTGGTTCTGTATAAATACAGGTGC	AACAGTAATGTAGTCCACAGCAA
PTCH1	ACATTTGTGTTACAAATCAGGAGAGC	CTGTCCCAGACTGTAATTTCGC
PTCH2	TGTGGTGGGAGGCTATCTG	GCATGGTCACACAGGCATAG
RFNG	CTCTCACCTGGAGAACCTGCA	TCTTGATGCAGGCTGAAGCCT
RPS6kB1	TACTTCGGGTACTTGGTAA	GATGAAGGGATGCTTTACT
RUNX1	CACCTACCACAGAGCCATCAA	CTCGGAAAAGGACAAGCTCC
RUNX1T1	ATCACAACAGAGAGGGCCAA	CTGCAGGTTTCACTCGCTTT
RUNX2	AACAAGACCCTGCCCGTGG	CATTCAGCAGAGGCATTCCGG
SHH	CGAGCGATTTAAGGAACTCACC	GCGTTCAACTTGTCCTTACACC
SMAD6	CTCCCTACTCTCGGCTGTCT	AGAATTCACCCGGAGCAGTG
SMAD7	CCATCACCTTAGCCGACTCT	CCAGGGGCCAGATAATTCGT
SMO	CTGACCGCTTCCCTGAAGG	CGTCCTCGTACCAGCTCTTGG
SMURF1	ATGCAGTTCGTGGCCAGATA	CAGGCCCGGAGTCTTCATAC
SMURF2	GACAGGATCCTCTCGAGTGC	AGCTTTCATAGGGTGGAATGTCT
SPI1	GTGCCCTATGACACGGATCT	AAGCTCTCGAACTCGCTGTG
STAT3	CCTAGATCGGCTAGAAAACTGG	GGGTCCCCTTTGTAGGAAAC
STIL	GACACAGTGCAAGCTGGAAGAC	AGTCAGGCTCTTGATCCTCACC
SUFU	CTCCAGGTTACCGCTATCGTCA	TGCTCAGGGATGTTGGCAGAAG
TAZ	CCGTGTCCAATCACCAGTCCT	CTTGGTGAAGCAGATGTCTGC
TCF3	TGACCTCCTGGACTTCAGC	ACCTGAACCTCCGAACTGC
TCF4	AATCAAAACAGCTCCTCCGATT	CCATCTTGCCTCTTGGCCG
TCF7	TCAACCAGATCCTGGGTCGC	CCTTTCCTTGCGGGCCAG

TEAD1	CCTGGCTATCTATCCACCATGTG	CTGGTCCTCGTCTTGCCTGT
TEAD3	GCAGTAGATGTGCGCCAGAT	TGGATGGTGCTGTTGAGGT
TEAD4	GCTCTGGATGTTGGAGTTCTCG	GGCTTGACTGGCTGATGTG
TLE1	TGTCATATGGATTAAACATTGAAATGC	CACGTTCAACAGCCTGGG
TLE2	TATGAGATGTCGTACGGGC	CAGGAAGGGGATAATCTGAGC
TLE3	GTCTTGTGACAGGATCAAAGACG	CATTTCAATGTTCAAGCCATAGGA
TLE4	GAAAACCACCAGGAGTTGACC	GTCAGCTCTCCGTTCATTCC
TP53	TTCTTGCATTCTGGGACAGCC	GGGGGTGTGGAATCAACCC
TP73	ACTTTGAGATCCTGATGAAGC	GAGGACCGGCCCGTAGGA
TYW1	ATTGTCATCAAGACGCAGGGC	GTTGCGAATCCCTTCGCTGTT
UBE2D2	CCATGGCTCTGAAGAGAATCC	GATAGGGACTGTCATTTGGCC
VEGF	AGAAGGAGGAGGGCAGAATCA	AGGGTACTCCTGGAAGATGTCC
WWTR1	GAGGACTTCCTCAGCAATGTGG	CGTTTGTTCCTGGAAGACAGTCA
YAP1	GCAGTTGGGAGCTGTTTCTC	GCCATGTTGTTGTCTGATCG
ZEB2	CCGCCACGAGAAGAATGAAG	TACCTGCTCCTTGGGTTAGC

2.2. Methods

2.2.1. Drugs and reagents

N-[N-(3,5-Difluorophenacetyl-L-alanyl)]-(S)-phenylglycine t-butyl ester (DAPT) was made into stock dilutions of 10mM in dimethylsulphoxide (DMSO) and stored at -20 degrees Celsius (°C). Imatinib was made into stock dilutions of 10mM in DMSO. Dilutions to working concentrations were made with media. DMSO was used as a negative control dependent on drug concentration. Growth factors were reconstituted as per manufacturer's guidelines.

2.2.2. General tissue culture

A list of the materials used for tissue culture can be seen in section 2.1.1.1 and 2.1.1.2. Media composition (not listed within table 2-4) and specific solutions can be seen in section 2.1.1.3 and 2.1.1.4.

2.2.2.1. Standard cell culture conditions

All cell culture procedures were performed using sterile technique in a laminar airflow hood. All cell culture was incubated in a humidified atmosphere at 37°C in 5% carbon dioxide (CO_2).

2.2.2.2. Culture of cell lines

A variety of cell lines were used and are listed below (table 2-2). All culture conditions were as described by either American Type Culture Collection (ATCC), Deutsche Sammlung von Mikroorganismen und Zellkulturen (DSMZ), or from the originating institution. OP9-GFP and OP9-DLL1 stromal cells were a kind gift from Professor Zúñiga-Pflücker (University of Toronto). OP9-JAG1 stromal cells were a kind gift from Dr Bianca Blom (University of Amsterdam). The overexpression of DLL1 and JAG1 was initially confirmed using Western blotting or flow cytometry protein quantification.

Cell Line	Origin	Culture conditions	
M210B4	Cell line derived from BM stromal cells from a (C57BL/6J X C3H/HeJ)F1 mouse; the cells express laminin and collagen IV, but do not express collagen I or Factor VIII. These cells have	90% RPMI 1640 + 10% FBS; maintain cells until 80% confluency; split cell 1:6 to 1:10 every 2 to 3 days. Every 2 weeks, 160uL of genetecin and 25uL hygromycin B per 2ml media was added for cell selection.	Stem Cell Technologies

	been engineered to secrete human IL-3 and human G-CSF.		
SL/SL	Cell line derived from BM stromal cells from the SL/SL mouse; these cells have been engineered to produce IL-3 and human SCF.	90% RPMI 1640 + 10% FBS; maintain cells until 80% confluency; split cell 1:6 to 1:10 every 2 to 3 days. Every 2 weeks, 320uL of genetecin and 50uL hygromycin B per 2ml media was added for cell selection.	Stem Cell Technologies
OP9GFP	Murine embryonic stem cells from BM/stroma	Alpha Minimum Essential Medium without ribonucleosides and deoxyribonucleosides and with 2.2 g/L sodium bicarbonate. To make the complete growth medium, add the following components to the base medium: FBS to a final concentration of 20% ; Maintain cultures at a cell concentration between $4x10^3$ and $1x10^4$ cells/cm^2.	University of Toronto
OP9DLL1	Murine embryonic stem cells from BM/stroma with retroviral stable expression of the notch ligand, DLL1.	Alpha Minimum Essential Medium without ribonucleosides and deoxyribonucleosides and with 2.2 g/L sodium bicarbonate. To make the complete growth medium, add the following components to the base medium: FBS to a final concentration of 20%; maintain cultures at a cell concentration between $4x10^3$ and $1x10^4$ cells/cm^2.	University of Toronto
OP9JAG1	Murine embryonic stem cells from BM/stroma with	Alpha Minimum Essential Medium without ribonucleosides and deoxyribonucleosides and	University of Amsterdam

	retroviral stable expression of the notch ligand, JAG1.	with 2.2 g/L sodium bicarbonate. To make the complete growth medium, add the following components to the base medium: FBS to a final concentration of 20%; maintain cultures at a cell concentration between $4x10^3$ and $1x10^4$ cells/cm^2.	

Table 2- 1 Cell line origin and culture conditions

2.2.2.3. Primary CML and normal CD34+ cell collection and enrichment

Leukapheresis samples were obtained with written informed consent, in accordance with the declaration of Helsinki and with Greater Glasgow and Clyde NHS Trust Ethics Committee approval from patients with CML.

In brief, on attainment of the sample, 6ml of histopaque solution was added to a 15ml falcon tube and allowed to warm to room temperature. The whole blood sample was diluted 1 in 2 with PBS, and carefully layered drop-wise onto the histopaque solution. Samples were centrifuged at 400xg for 30min at room temperature. Following this, the opaque interface containing the mononuclear cells (MNC) was carefully aspirated with a 3ml sterile pastette and transferred to a sterile 15ml falcon tube. These cells were then washed twice with sterile PBS at a centrifugation force of 300xg for 5 min.

Large volume samples from leukapheresis were CD34-purified directly through the CliniMACS system (Miltenyi Biotec, Bisley, UK) by Dr Alan Hair. The CliniMACs system is an immune-magnetic beads system that positively selects $CD34^+$ cells using super-paramagnetic beads coupled with a suitable $CD34^+$ monoclonal antibody. Briefly, super-paramagnetic $CD34^+$ beads (~50nM diameter) were added to the primary cell MNC sample and the resulting suspension passed through a high-gradient magnetic separation column, which resulted in the retention of the magnetic beads as the sample passed through. Purity was assessed by flow cytometry, which confirmed all samples were >95% $CD34^+$ post selection. A representative example is shown in figure 2-1. If the sample was not to be immediately used *in vitro,* samples were stored in cryotubes at -185°C until required for use. Each sample was determined to be Ph+ by FISH following $CD34^+$ enrichment.

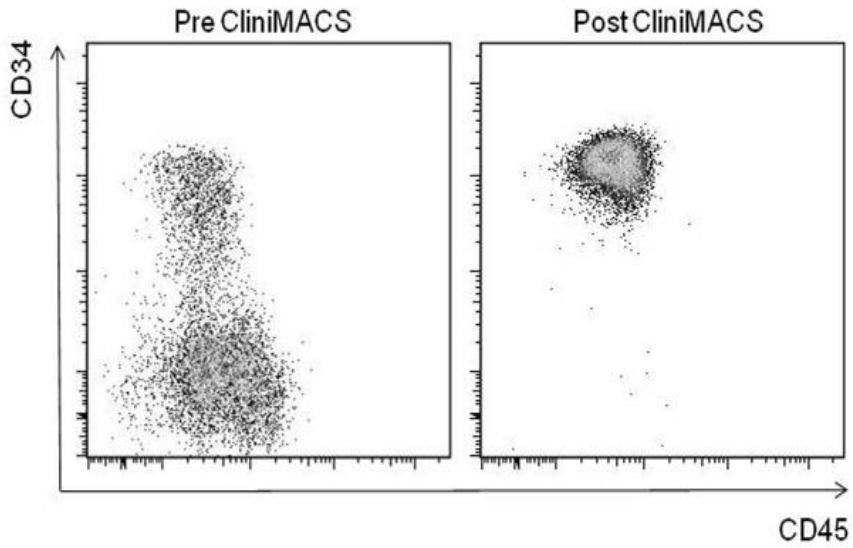

Figure 2- 1 Representative flow cytometry plots pre and post CliniMACS system of a primary CML sample.
CD34 expression is plotted against CD45 expression to assess the purity of the population.

The CP-CML samples used within this thesis are listed in table 2-3, with AP and BP samples in table 2-4, and Ph+ ALL samples in table 2-5. Ph+ ALL samples were kindly gifted to us from the UKALL14 clinical trial by Professor Adele Fielding.

Identifier	Chapter	Experiment	Age	Gender	Subtype	Breakpoint	WCC at diagnosis	Pre Treatment
CML110	6	Microarray validation	48	F	CP	p210	-	none
CML111	6	Microarray validation	-	-	CP	p210	-	-
CML112	4	Gene expression	-	-	CP	p210	-	none
CML113	3,4	Gene expression/functional data	53	F	CP	p210	-	-
CML269	4	Gene expression	74	M	CP	p210	312	none
CML273	4	Gene expression	60	F	CP	p210	307	none
CML332	6	TKI effect	62	F	CP	p210	132	none
CML339	6	NSG	34	F	CP	p210	-	none
CML340	6	NSG	55	M	CP	p210	-	none
CML342	6	Cell cycle	54	M	CP	p210	-	none
CML343	6	LT-CIC	46	M	CP	p210	4.8	none
CML347	6	LT-CIC	34	F	CP	p210	385.8	Imatinib
CML350	6	LT-CIC	-	-	CP	p210	-	-
CML351	6	NSG	-	-	CP	p210	-	-
CML366	4	Gene expression	41	F	CP	p210	-	none
CML368	4	Gene expression	51	M	CP	p210	-	-
CML373	6	NSG	48	M	CP	p210	-	none
CML385	6	NSG	51	M	CP	p210	-	none
CML388	6	TKI effect	61	F	CP	p210	227.6	none
CML391	6	NSG	33	F	CP	p210	141	Interferon
CML393	6	NSG	35	M	CP	p210	-	none
CML395	6	NSG	34	M	CP	p210	-	none

CML399		6	TKI effect	51	M	CP	p210	214	none
CML407		6	Cell cycle	50	M	CP	p210	-	none
CML436	3,4		Gene expression/functional data	18	F	CP	p210	300	none
CML441	3,4		Gene expression/functional data	66	F	CP	p210	-	none
CML443	3,4		Gene expression/functional data	63	M	CP	p210	-	none
CML444	3,4		Gene expression/functional data	47	M	CP	p210	313.4	none
CML446	3,4		Gene expression/functional data	35	M	CP	p210	65.5	none
CML452	3,4		Gene expression/functional data	45	M	CP	p210	275	none
CML456	3,4		Gene expression/functional data	64	M	CP	p210	-	none

Table 2- 2 CP-CML samples used, including age, gender, breakpoint BCR-ABL mutation, WCC at diagnosis if known and pre-treatment.

Identifier	Chapter	Experiment	Breakpoint	Subtype	Additional Chromosomal Abnormalities
CML184	4	Gene expression	p210	AP	none
CML402	4	Gene expression/functional data	p210	AP	none
CML403	4	Gene expression/functional data	p210	AP	none
CML404	4	Gene expression	p210	AP	none
CML TN04	4,5	Gene expression/functional data	p210	mBP	none
CML371	4,5	Gene expression/functional data	p210	mBP	none
CML384	4,5	Gene expression	p210	mBP	none
CML405	4,5	Gene expression	p210	mBP	-
CML406	4,5	Gene expression	p210	mBP	yes
R6900	4,5	Gene expression	p210	mBP	-
RB810	4,5	Gene expression/functional data	p210	mBP	-
RB900	4,5	Gene expression	p210	mBP	-
CML TN08	5	Gene expression/functional data	p210	lBP	yes
050-04	5	Gene expression	p210	lBP	none
CML267	5	Gene expression	p210	lBP	none
CML407	5	Gene expression/functional data	p210	lBP	none
CML408	5	Gene expression/functional data	-	lBP	-

Table 2- 3 AP and BP samples used within this thesis

Identifier	Chapter	Experiment	UKALL14 trial nos	Breakpoint
ALL1	5	Gene expression	14-1-432	p190
ALL2	5	Gene expression	14-1-467	p190
ALL3	5	Gene expression	14-1-475	p190
ALL4	5	Gene expression	14-1-479	p190
ALL5	5	Gene expression	14-1-490	p210

Table 2- 4 Ph+ ALL samples used within this thesis

2.2.2.4. Cryopreservation of cells

Cryopreservation, in liquid nitrogen at -185°C, of both cell lines and fresh primary cells was used for long-term storage. $4x10^6$ to $2x10^7$ $CD34^+$-selected cells or $1x10^8$ unselected MNC were suspended in 1 to 2ml of an equal volume primary cell freezing solution (section 2.1.1.4.4; 20% DMSO in 4.5% HSA giving a final concentration of 10% DMSO) and aliquoted into cryotubes.

Cell lines were cyropreserved as per guidelines from ATCC or DSMZ. In brief, $5x10^6$-$1x10^7$ cells were suspended in cell line freezing solution (section 2.1.1.4.5; 90% FBS and 10% DMSO). Cells were then transferred to a cryofreezer container ('Mr Frosty') and slowly cooled at a controlled rate to -80 °C before being transferred to -185 °C freezer for long-term storage.

2.2.2.5. Cell recovery post cryopreservation

$CD34^+$ primary cells were removed from liquid nitrogen and immediately thawed at 37 °C in a water bath. Following this, 10ml of thawing solution (DAMP; section 2.1.1.4.1) was gradually added to the cells over 10 min with constant gentle agitation to prevent clumping. The cells were then centrifuged at 210xg for 10 min and washed a further twice in 10ml DAMP. Finally, the cell pellet was re-suspended in SFM and 5 Growth Factor (SFM+5GF) (section 2.1.1.3.2); cell number and viability was assessed by trypan blue exclusion and the cells cultured overnight at 37°C with 5% CO_2 in a non-adherent tissue culture flask at a maximum density of $1x10^6$ cells/ml. Culture in SFM+5GF maximises cell recovery post thaw. The following day these cells were washed twice in PBS with 2% FBS, re-suspended in fresh low growth factor SFM (SFM+LGF) (i.e. 1 in 100 dilution of SFM+5GF) and a viable cell count performed.

2.2.2.6. FACS of Primary CD34+ cells

Cell sorting was kindly performed by Miss Jennifer Cassels. Fluorescence activated cell sorting (FACS) was utilised in a number of experiments to isolate $CD34^+38^+$ and $CD34^+38^-$ fractions, as well as in the isolation of $Lin^-CD34^+CD38^-CD90^+CD93^+$ and $Lin^-CD34^+CD38^-CD90^+CD93^-$ cell populations. In brief, fresh or recovered $CD34^+$ cells were washed and resuspended in PBS/2%FBS. Cells were counted and stained with appropriate antibodies (depending on the experiments) for 30 minutes (min) at room temperature in the dark. $2x10^4$ cells were used for relevant single colour controls to define positive and negative staining for each marker and to set compensation. Further to this, a fluorescence minus one (FMO) control was used to ensure the proper identification of appropriate gating strategy. Stained cells were washed and filtered through a 0.22uM filter prior to sorting with a BD FACS Aria with Diva software. Figure 2-2 demonstrates a representative example for sorting of $CD34^+CD38^-CD90^+CD93^{-/+}$ populations. All CML samples were assessed for Ph+ status, confirmed by dual colour FISH.

Figure 2- 2 Representative flow cytometry analysis of cell sorting with a BD FACS Aria and DIVA software.

Following antibody staining as described within the text, samples were analysed and sorted with a BD FACS Aria and DIVA software. FMO controls were utilised for an accurate gating strategy. Cell sorting was performed by Miss Jennifer Cassels.

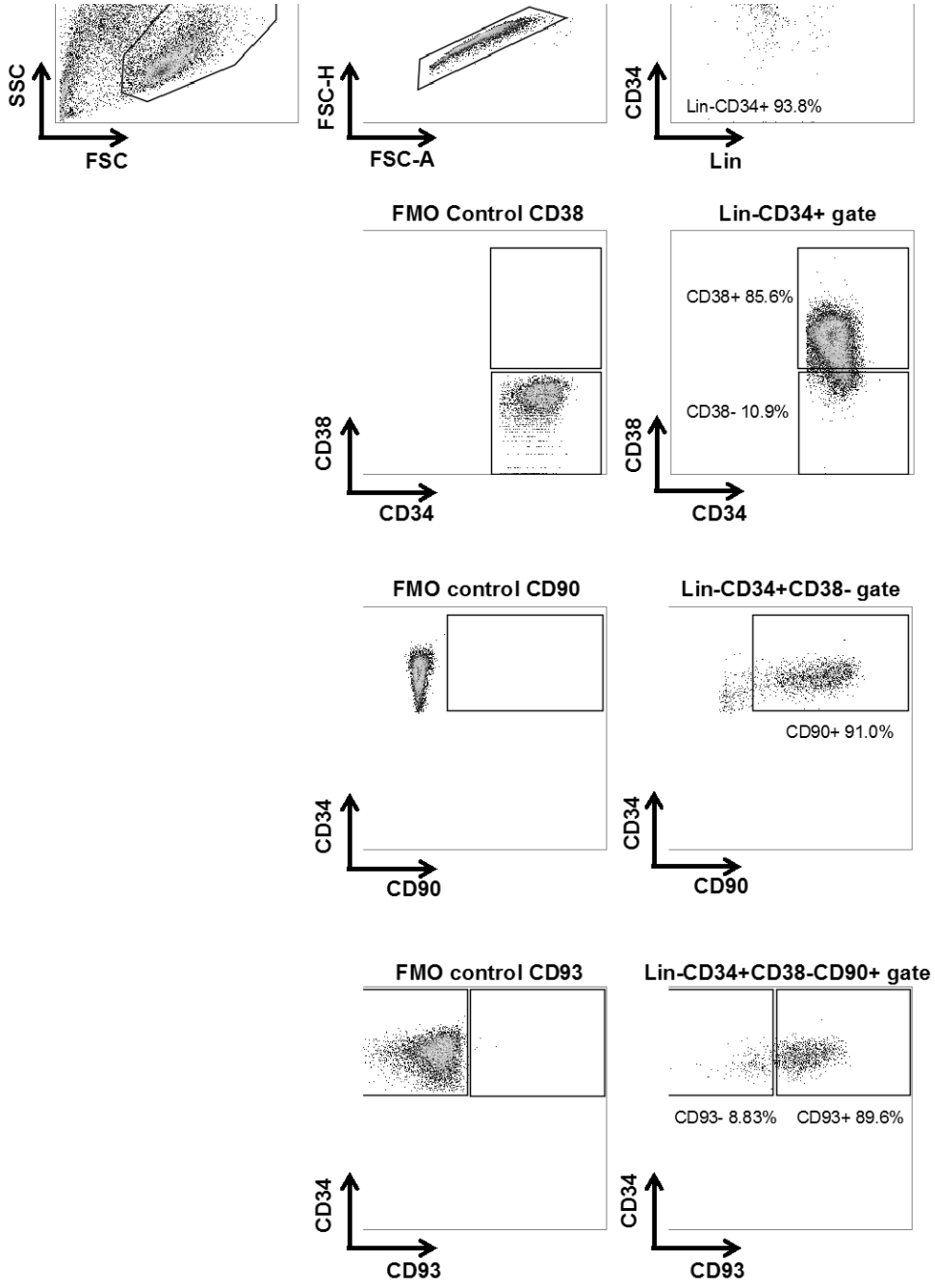

2.2.2.7. Culture of primary cells

$CD34^+$ cells or sorted populations were maintained in suspension culture in SFM+LGF at 37°C with 5% CO_2 in tissue culture hydrophobic flasks prior to experimental set-up. Prior to each experiment, cells were washed in PBS/2%FBS and resuspended in fresh medium at the desired density for each experimental arm. Cells were harvested at different time points for RNA, protein and functional assays as dictated by the experimental design.

2.2.2.8. Mesenchymal stem cells

2.2.2.8.1. MSC Isolation

Human MSCs were isolated from CP CML patient BM samples after written informed consent in accordance with the declaration of Helsinki and with Greater Glasgow and Clyde NHS Trust Ethics Committee approval. Cells were placed into a T75 NunC flask in DMEM medium in the presence of 20% Hyclone FBS and incubated at 37°C with 5% CO_2 for >7days until cell populations had adhered. Suspension cells were subsequently removed and the adherent cells washed with PBS. Cells were characterised in accordance with the International Society for Cellular Thearpy and cyropreserved at early passage number (i.e. passage 1 to 3) to maintain viability on thaw.

2.2.2.8.2. MSC Characterisation

MSC phenotype was confirmed according to the International Society for Cellular Therapy, with confirmation of $CD45^-CD34^-Lin^-CD90^+CD73^+CD105^+$ phenotype and positive Nestin immunofluorescence (Figure 2-3).

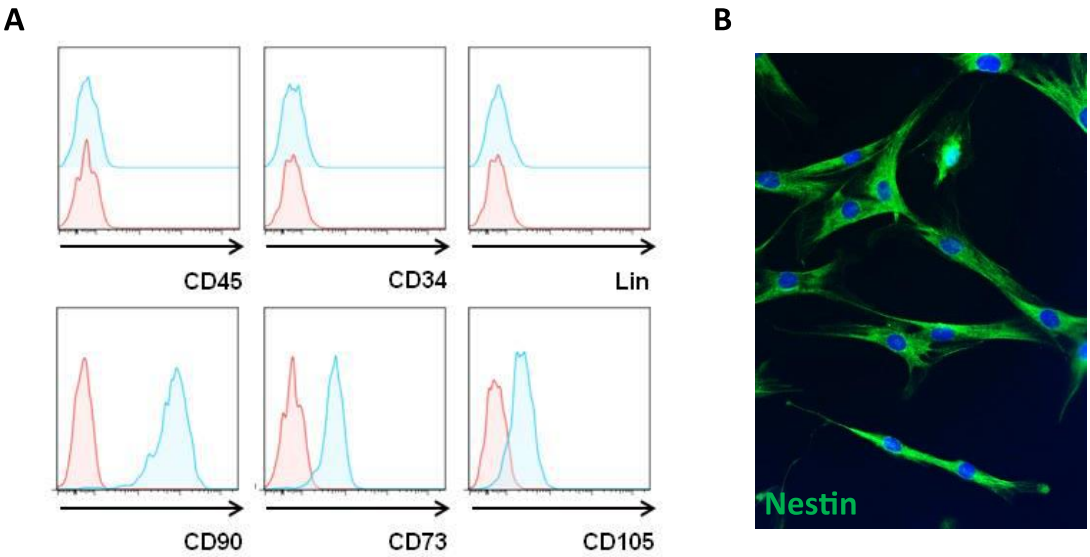

2.2.2.9. Co-culture

Figure 2- 3 Confirmation of MSC phenotype according to the International Society for Cellular Therapy
(A) Flow cytometry of markers used in the identification of a confirmed MSC phenotype; pink represents the isotype control. (B) Immunofluorescence (IF) of MSCs from a CP-CML patient stained with Nestin.

Stromal cells were seeded onto sterile tissue culture flat bottom plastic (6 well/12 well plates). OP9 stromal cells were seeded at a 1 in 24 ratio with suspension cells (i.e. 1 stromal cell per 24 suspension cells) 24 hours prior to co-culture. All experiments were performed in at least experimental triplicate. M210B4 and SL/SL were seeded at 75000 cells per 24 well plate as per the LTC-IC protocol. When recombinant ligand was used, sterile tissue culture flat bottom plates were coated in differing concentrations of recombinant Jagged1 (R-Jag1) (10-50ng/ml), left at 37°C for 12 hours prior to removing the excess ligand, and then adding suspension cells. Binding the ligand to the plate ensures that they are competent to deliver a signal. It has been previously demonstrated that soluble Notch ligands can act as dominant negative inhibitors, and therefore, assessment of activation was undertaken in all samples with IF of the cleaved form of the receptor.

2.2.2.10. Cell counting and viability assessment

All cell counts were performed using a haemocytometer. Cell viability was assessed by trypan blue dye exclusion, utilising the finding that non-viable cells absorb trypan blue due to damaged membranes, whereas viable cells do not. Trypan blue stock solution (8mM) was diluted 1:10 with PBS to give a working solution of 0.8mM. 10ul of this solution was added to 10ul of cell suspension to give a 1:2 dilution of cells, prior to being added to a haemocytometer counting chamber. A minimum of 100 viable cells were counted, and where necessary, the cell suspension solution diluted if needed. Cell count was performed on an inverted microscope. Given that the cover-slide is held 0.1mm above the counting surface, each $1mm^2$ has a volume of 0.1uL. The absolute viable cell count per ml was the number of unstained cells per mm^2 multiplied by the trypan blue dilution factor and then by 10^4.

2.2.2.11. Colony forming cell assay

Colony forming cell (CFC) assays are clonal progenitor assays that measure the proliferation capacity and multipotency of haemopoietic progenitors. Methylcellulose supplemented with growth factors (methocult H4034) was thawed at 4°C overnight, well mixed and divided into 2.6ml tubes. These aliquots could then be stored at -20°C until required. Following recovery, $CD34^+$ CML cells were cultured for 5 days with or without stromal support (OP9GFP, OP9JAG1, OP9DLL1, R-Jag1) in SFM+LGF. The cells were then harvested, washed in PBS, re-suspended in fresh SFM and viable cell counts performed. Each of the different cell suspensions was inoculated into a single tube of methocult to give a final concentration of $4x10^3$ cells/ml and the final volume of inoculums made up with SFM to equal 10% of the original volume of methocult. These tubes were thoroughly mixed and 1.1ml of resultant single cell suspension plated in duplicate into 35mm culture dishes. The duplicate assays were placed in a 100mm culture dish with a further 35mm dish containing 3ml sterile water to maximise humidity. These were cultured under standard conditions for 14-18 days prior to colony

assessment using an inverted microscope and a counting grid. Following culture, all progenitor cells with colony forming potential in that specific GF context will have proliferated and differentiated fully. The resultant colonies can then be assessed for size (broadly reflective of original proliferative capacity) and constituent cell types from which can inferred the degree of lineage commitment and hence the maturity of the cell of origin.

The capacity of an individual haemopoietic progenitor cell colony to replate in a CFC assay has been used as an indicator of the self-renewal potential of that progenitor. CFC replating assays were performed to assess effects on self-renewal capacity. In replating experiments, 50 single colonies from each experimental arm were harvested/'plucked' from methocult between days 10-12 of primary culture. Each single colony was resuspended in 20uL of fresh SFM, before being plated in 100uL of methocult within each well of a 96-well plate. The plates were incubated for 12-14 days at 37°C and 5% CO_2 prior to counting the number of wells with viable colonies.

2.2.2.12. Long-term culture-initiating cell assay

The LTC-IC assay has been demonstrated to maintain human HSCs *in* vitro for at least 8-10 weeks with extended culture of cells in the presence of a suitable supportive stromal environment. It is an established technique that allows assessment of the maintained self-renewal potential of cells in prolonged culture.

The assay (figure 2-4) utilises an irradiated adherent feeder layer of M210B4 and SL/SL cells to support myelopoiesis (Hogge et al, 1996), with these stromal cells being genetically modified to stably express IL-3 and G-CSF, and IL-3 and SCF, respectively. Stromal cell lines were maintained under selection with geneticin and hygromycin B. Early passage was used within all experiments (i.e. <6 passage). Stromal cells were initially irradiated under a cobalt γ-ray source for a total of 80Gy to prevent proliferation within the prolonged culture. A viable cell count of both irradiated cells was performed and the concentration of each adjusted to $1.5x10^5$ per ml. Cell suspensions were mixed in a 1 to 1 ratio before 1ml was plated to each central well of a 24-well type 1 collagen coated plate (i.e. 8 central wells). This created a fully confluent layer. Humidity was maximised with the addition of 1ml sterile water to the remaining wells. Plates were maintained in an incubator for up to 1 week until required. LTMCM was prepared by adding 1uM hydrocortisone to myelocult. This media was made up fresh on each media change.

In general, primary cells were cultured within their experimental condition for 5 days. Viable cell counts were performed. $1x10^5$ cells from each experimental condition were washed in PBS/2%FBS and resuspended in 2ml LTMCM. The LTMCM was carefully aspirated from the

adherent cells, prior to 1ml of our primary cell suspension being added (i.e. 50,000 cells per well; each arm performed in at least duplicate). The plates were cultured under standard conditions for 6 weeks. Each week, 500uL media was removed carefully in an attempt not to disturb the adherent layer, and replaced with fresh LTMCM. After 6 weeks in culture, the entire contents of each well was harvested. The supernatant from each well was collected into a 15ml falcon tube. The wells were washed twice with 1ml HBSS and added directly into the 15ml falcon tube. 500uL 0.25% trypsin/EDTA was added to each well and incubated at 37°C. Following trypsinisation, 25uL of FBS was added to each well and the entire contents collected to the falcon tube. The wells were washed with 1ml IMDM/2% FBS twice, with both washes transferred to the 15ml falcon tube. The falcon tubes were centrifuged for 10 min at 210xg and the supernatant dispensed. Cells were resuspended in 1ml IMDM/2% FBS and viable cell counts performed. 50,000 viable cells in 30uL of SFM were inoculated into 3ml methocult. These tubes were then thoroughly mixed, left to settle at room temperature and 1.1ml of the resultant single cell suspension was plated into duplicated 35mm culture dishes. The assays were then placed in 100mm culture dishes with a 35mm dish containing 3ml sterile water to maximise humidity. Assays were cultured under standard conditions for 12-14 days prior to colony assessment using an inverted microscope and counting grid. Colony numbers were then counted and comparison between treatment arms was made.

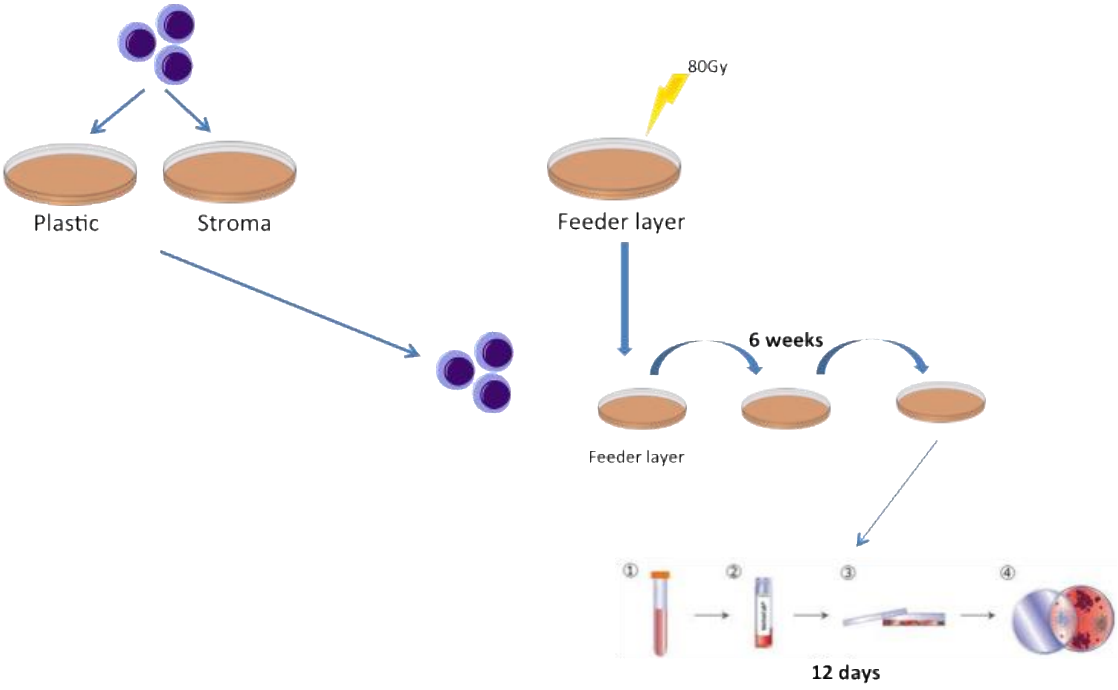

Figure 2- 4 The long-term culture initiating cell assay
Schematic representation of the long-term culture initiating cell (LTC-IC) assay, where suspension cells (namely, sorted populations of CML cells) are cultured in the presence of an irradiated stromal layer that is necessary to maintain myelopoieiss. Cells are cultured under specific conditions for 6 weeks prior to assessment with colony forming cell assays.

2.2.3. Fluorescence in situ hybridisation

FACS-sorted cells were incubated at 37°C for 15 min in a hypotonic solution of 0.075M KCl. Cells were centrifuged at 1500rpm for 5 min and supernatant carefully removed. Cells were re-suspended in fixative (3:1 methanol: acetic acid) added in a drop wise manner, with constant vortexing. Cells were then incubated for 5 min at room temperature, centrifuged at 12000rpm for 2 min and supernatant removed. Cells were washed twice in fixative before re-suspension in 1ml fixative. Fixed cells were centrifuged at 12000rpm for 2 min and re-suspended in fresh fixative. 3µl of fixed cell suspension was dropped onto a glass slide, air-dried and cell density checked using a phase contrast microscope. Probe mixes were prepared according to manufacturer's instructions and 2µl added to cells on slide and coverslips placed and sealed with rubber solution. Slides were heated in a hybridisation chamber for 5 min at 72°C and then 37°C overnight. Coverslips were removed and slides washed in a 0.4x SSC/3% NP40 wash buffer at 72° for 2 min and then washed in a 2x SSC/ 1% NP40 wash buffer at room temperature for 2 min. DAPI mounting medium (Vector Laboratories) was applied, a coverslip attached and the slide analysed using an AXIOvision AX10 fluorescent microscope and AXIOvision software. Chromosome t(9;22) BCR-ABL fusion was detected by a dual colour dual fusion probe (figure 2-5).

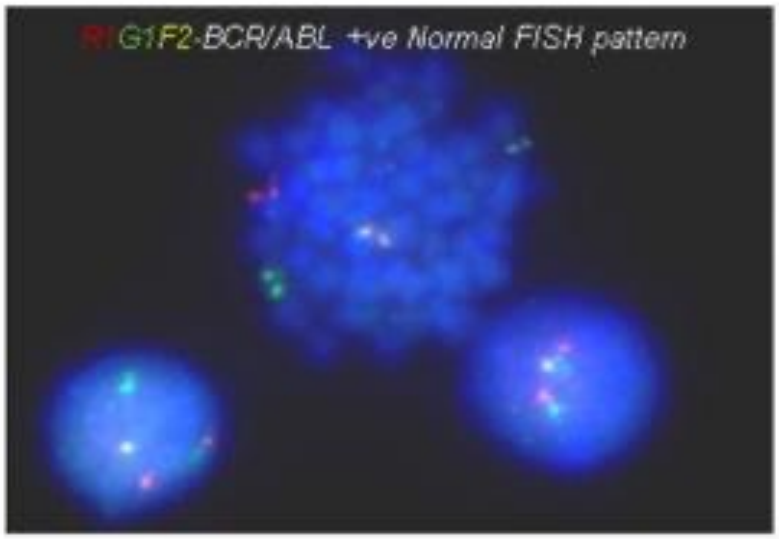

Figure 2- 5 Representative example for FISH within CP-CML cells
The identification of *BCR-ABL* is diagnostic of CML. In order to effectively analyse the CML samples, FISH was utilised as per clinical protocol in the assessment of activated protein.

2.2.4. Flow cytometry

2.2.4.1. Detection and quantification of protein expression

Flow cytometry allows for the characterisation of both chemical and physical properties of a single cell through the use of fluorochrome-labelled antibodies. In brief, a single cell suspension is presented to at least one laser leading to the excitation of the fluorochrome. Light is emitted at different wavelengths allowing for simultaneous measurement of cellular properties. For example, size and granularity of single cells can be measured by the forward-angle scatter (FSC), and side-angle scatter (SSC), respectively. Typically, this can be used to identify cell types in PB for diagnostic purposes. Furthermore, identification of specific cell surface and intracellular proteins can be utilised in sorting of cells phenotypically (described above), or into single cells, for diagnostic and experimental data.

To detect and quantify levels of protein expression, cells were harvested and washed in PBS/2%FBS. To allow for a precise gating strategy, a FMO control was used, whereby all antibodies bar one is used for each antibody in the series to allow for precise gating strategy (figure 2-2). A single stain control was also used as an internal antibody control.

Following washing, $5x10^4$ cells were used within each unstained, single-stained and FMO control, where cells were re-suspended in 100ul PBS/2%FBS prior to the addition of antibody (concentration calculated in previous dilution experiments'). The 'bulk-stain' sample was re-suspended in 100-450ul PBS/2%FBS prior to the addition of antibody - this volume was dependent on cell number. Samples were stained for 30 min at 4°C and then washed twice with PBS/2%FBS before being filtered through a 0.22uM filter. Cells were resuspended in 100-500uL of PBS/2%FBS and analysed immediately using a FACSCantoII flow cytometer (BD Biosciences), data was acquired using BD FACSDiva (BD Biosciences) software, and analysed using FlowJo (Tree Star Inc, Ashland, USA) software. When an unconjugated primary antibody was used, the cells were washed and resuspended in 100µL of PBS/1%BSA with either 2µL of the secondary anti-rabbit IgG FITC conjugate (1:50 dilution), or 10µL of the secondary anti-rabbit IgG PE conjugate (1:10 dilution), depending on the requirement for multi-parametric flow cytometry analysis, at 4°C in the dark for 30 min. A range of antibodies used is detailed in section 2.1.2.2.

Quantification of the protein of interest within each sample was calculated in relative terms, using the ratio between the geometric mean fluorescence intensity (MFI) of the antibody labelled live cells and the geometric MFI of the isotype labelled live cells. When measuring changes in levels of protein within each sample following treatment, the MFI ratio (calculated as explained above) for each treatment arm was expressed as a percentage.

2.2.4.2. Apoptosis assays

Apoptosis was measured by flow cytometry using annexinV and 7-amino actinomycin D (7AAD) staining. AnnexinV is a phospholipid binding protein that has a high affinity for phosphatidylserine in the presence of physiological calcium concentration. As cells apoptose, there is a shift and translocation of phosphatidylserine to the external surface of the phospholipid layer that comprises the plasma membrane. 7AAD is only able to stain dead or late apoptotic cells, and therefore, when combined with annexinV allows for the detection of early and late apoptosis (figure 2-6). Practically, following a wash in PBS/2%FBS 0.5-1x10^5 cells were resuspended in 100µL of annexinV buffer containing 5µL annexinV conjugated to relevant fluorochrome and 5µL 7AAD and incubated at room temperature for 15 min in the dark. Following incubation, 400µL of HBSS was added to the cell suspension and analysis was immediately performed by flow cytometry. Unstained and single stained cells were used to set voltages and compensation.

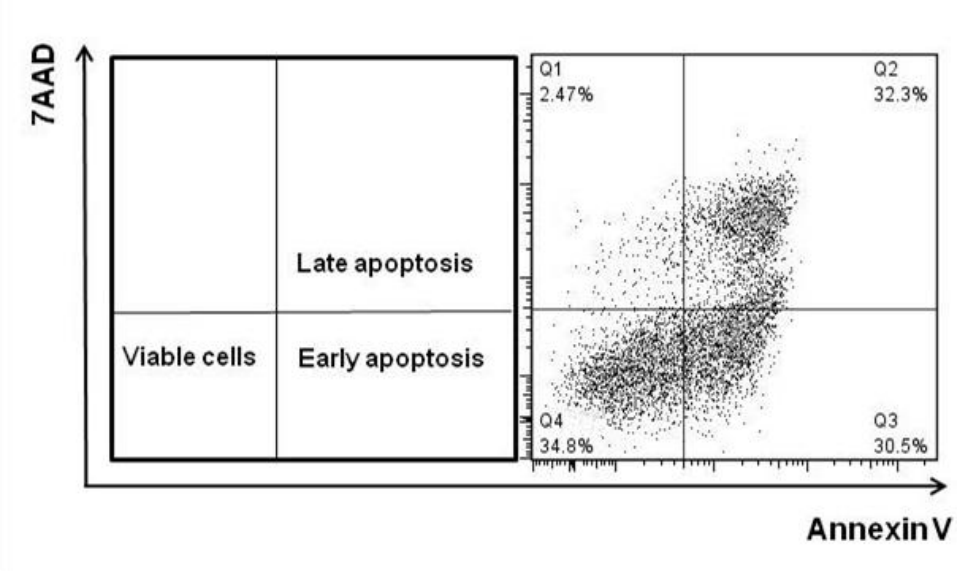

Figure 2- 6 Representative example of AnnexinV/7AAD staining in the context of apoptosis
Representative example of annexinV/7AAD staining. Viable cell populations will be negative for both annexinV and 7AAD, cells in early apoptosis would be annexinV positive but 7AAD negative, and cells in late apoptosis would be positive for both annexinV and 7AAD.

2.2.4.3. Cell cycle analysis

Flow cytometry can be used in the assessment of the cell cycle status of cells within each sample and following treatment and varying culture conditions. To do this, a DNA-binding fluorescent dye was used, termed propidium iodide (PI).

Practically, cells were fixed with ice-cold 100% ethanol. Ethanol allows cells to be fixed and permeabilised in a one-step process. Samples were stored at -20°C for no more than 5 days before analysis. When ready to be analysed, samples were washed twice in PBS/2%FBS. To

ensure only DNA was stained, cells were treated with ribonuclease (100ug/ml), and then stained with PI (50ug/ml), before being immediately analysed using the FACSCantoII flow cytometer; data was acquired using BD FACSDiva software, and analysed using FlowJo software (figure 2-7).

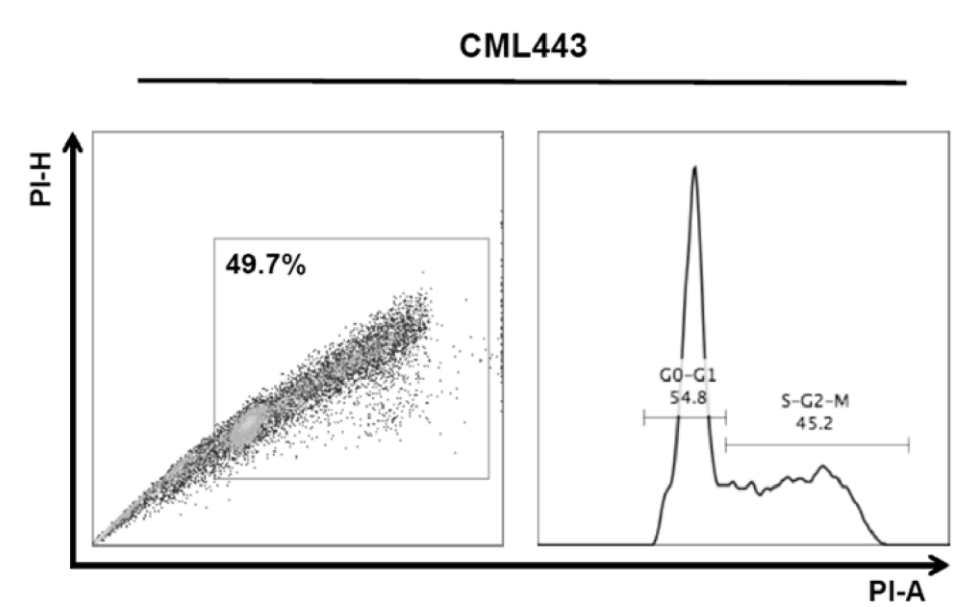

Figure 2- 7 Representative example of PI staining and cell cycle analysis
PI was used to assess cell cycle status within both primary and cell line samples. Using FlowJo technology, samples were gated according to their PI content that can depict cells in G0-G1 and S-G2-M. Gates were fixed following first analysis (i.e. plastic or untreated control) to allow comparison with differing experimental conditions.

2.2.4.4. CFSE

Carboxyfluorescein diacetate succinimidyle ester (CFSE) is an intracellular dye used to track cell divisions of heterogeneous and asynchronous cell populations by flow cytometry. It is a lipophilic molecule that upon entering the cell, intracellular esterases cleave the acetate groups to yield the fluorescent carboxyfluorescein molecule. Further to this, the succinimidyl ester group reacts with primary amines on intracellular proteins, cross-linking the dye and fixing it within the cytoplasm of the cell. It allows for stable cell staining, and upon division, the dye is equally divided between the two daughter cells determining a serial dilution of the dye with each division, and hence allowing a measure of the number of divisions a sample has undergone in culture (figure 2-8).

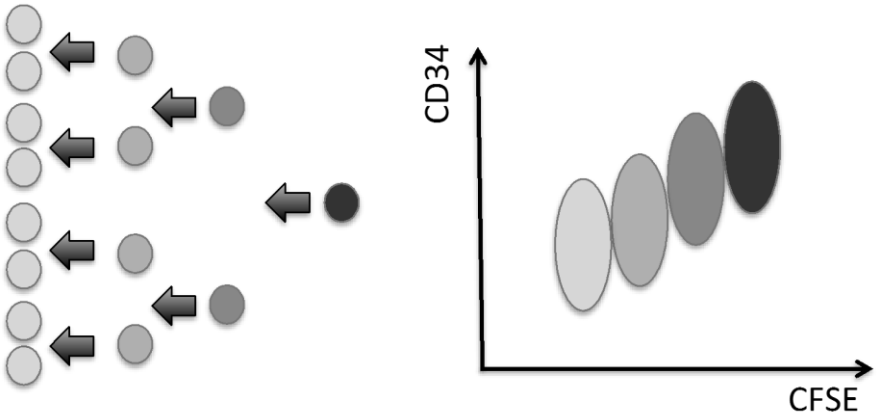

Figure 2- 8 Schematic representation of CFSE assay by flow cytometry
When cells are stained with CFSE, it allows for stable intracellular staining, thereby on each cell division, the dye is equally shared between the two daughter cells.

Practically, the cell sample was resuspended in 5ml PBS/2%FBS and stained with 10uL of a 500uM solution of CFSE dye to give a final concentration of 1uM. Cells were stained for 10 min at 37°C in a water bath, while a small aliquot of cells was kept unstained to allow for a control in analysis. Following the 10 min incubation, CFSE was quenched by adding 10X volume of ice cold PBS/20%FBS and then washed once more in fresh PBS/2%FBS. Cells were analysed every 24 hours to allow identification of cell divisions. To identify the undivided cell population following treatment, a control well was set up to which 100ng/ml of colcemid was added which effectively blocks cells proliferation. In some cases, cells were also stained with cell surface markers to allow for identification of differentiation with proliferation.

2.2.5. Immunofluorescence

Cells were plated on poly-lysine-coated slides at 60,000 cells/well at baseline and following 5 days with or without treatment. Preparations were fixed in 4% paraformaldehyde for 15 min then permeabilised with 0.2% TritonX100 (Sigma-Aldrich, Dorset) for 10 min. Cells were blocked for 2 hours prior to primary antibodies being applied for 12 hours at 4^0C. After washing fives times with PBS, cells were incubated in Alexa fluor linked secondary antibodies for 2 hours. After a final wash with PBS, the slides were mounted in 0.1ug/ml DAPI (4',6-diamidino-2-phenyloindole) mounting medium and viewed by fluorescence microscopy using a Zeiss imager M1 microscope. To illustrate intensity of immunolabelling digital images were captured at identical exposure times.

2.2.6. Western blotting

Western blotting allows for a measure of a fractionated protein component. Proteins are first separated according to their molecular weight, before being transferred onto a nitrocellulose or polyvinylidene fluoride (PVDF) membrane, which will contain all proteins in the sample being analysed. The use of primary antibodies and the crosslinking with a secondary antibody that contains a detectable enzyme allows for the identification of specific proteins within each

sample. Samples are quantified against a housekeeping gene that is stably expressed within the cells, such as *GAPDH* or *SHP2*.

2.2.6.1. Preparation of protein lysates

Protein lysates were prepared as follows; cells were harvested and washed twice in cold PBS (1200 rpm for 5 min). They were then re-suspended in freshly made lysis buffer with protease inhibitors (approximately 50ul per $1x10^6$ cells) and mixed thoroughly. The lysate preparations were then incubated on ice for 30 min; then spun at 14000 rpm at 4ºC for 10 min. The supernatants were then decanted into 500uL eppendorf tubes and stored in aliquots at -80ºC prior to use. Samples were thawed and quantified prior to use to allow equal expression within the experimental design.

2.2.6.2. Protein quantification

Protein lysates were quantified using Quickstart Bradford Dye Reagent. Following the manufacturers protocol, a standard curve was prepared using BSA protein standards, at concentrations ranging from 0 to 20ug/ml. Absorbance was read at 595 nM on a Spectramax M5 plate reader and analysed with SoftMax Pro 5.2 software.

2.2.6.3. Gel electrophoresis and immunolabelling

Between 10-20ug of protein lysate was made up to a final volume of 12ul in solubilisation buffer and 3ul of sample buffer reducing agent. Samples were heated to 95°C for 5 min prior to Sodium Dodecyle Sulphate-polyacrylamide gel electrophoresis (SDS-PAGE). 7.5% acrylamide gels were used to separate proteins larger than 50kDa and 10% gels for proteins smaller that 50kDa. Cell lysates were fractionated by SDS-PAGE in 1x running buffer at 80V for 30 min and 180V for 45 min. Separated proteins were transferred onto PVDF membrane using a semi-dry transfer method. PVDF was immersed in 100% methanol for 1 min before being saturated in 1x semi-dry transfer buffer. Four 1.0 mm Whatman paper strips were placed below the PVDF membrane, the gel was then added on top of the membrane followed by four more paper strips, the stack was then compressed to remove air bubbles. Proteins were transferred onto the membranes at 40mA/gel for 60 min. Blots were washed with 1xTBST, blocked in TBST containing either 5% BSA or 5% milk for 1 hour at room temperature. Following block, the blots were incubated with primary antibody overnight at 4°C. Blots were then washed four times with TBST and incubated with horseradish-peroxidase (HRP)-labelled secondary antibodies for 1 hour at room temperature. Secondary antibody was washed four times with TBST, followed by two washes with TBS and then blots were developed using Bio-Rad ECL and developed on a SRX0101A Medical Film Processor.

2.2.6.4. Membrane re-probing

Membrane re-probing allows sequential incubation of a membrane with different antibodies by removing antibodies bound into the membrane without removing the actual protein. This was performed by incubating the PVDF membrane with the Re-Blot Plus Strong stripping solution diluted 1:10 with distilled water. Following two brief washes (5 min per wash) in TBST, the membrane was re-blocked for 1 hour and finally incubated with a different primary antibody.

2.2.7. Gene expression analysis

All reagents and primers used can be found in section 2.1.3.

Gene expression is assessed through polymerase chain reaction (PCR) technology, a technique used to amplify short specific regions of DNA, provided at least part of the sequence is known. In general, two short oligonucleotide primers are designed to capture complimentary areas on each of the DNA strands of the double helix; these are at opposite ends of the sequence to be amplified. In the presence of the primers and excess nucleotides, as well magnesium chloride, heating causes the double stranded DNA to separate. Cooling allows the primers to anneal to their complimentary sequences. The DNA sequence 3' to the primer can be copied by polymerase (such as Taq) forming new complete double stranded DNA molecules extended from forward to reverse primary sequences. Successive rounds of this process leads to amplification of the target gene.

2.2.7.1. Primer design

Primers were designed using NCBI software; all sequences can be seen in section 2.1.3.3. Primers were synthesised commercially using Eurofins MWG Operon and were reconstituted with the appropriate volume of nucleic acid free water to achieve a stock concentration of 100uM. Dilutions were made to achieve the appropriate working concentration of 25uM and aliquots prepared to ensure sterility and prevent numerous freeze-thaw events.

2.2.7.2. RNA extraction

Total RNA was isolated from pellets using either the Qiagen RNeasy Mini Kit or the Applied Biosystems Arcturus Picopure RNA isolation kit (depending on sample size) according to the manufacturer's instructions. The quantity and purity of the extracted RNA was measured using a nanodrop spectrophotometer Nd-1000 (Labtech International, East Sussex, UK). An absorbance at 260nm quantified nucleic acid and the ratio of 260/280 determined purity (pure RNA ratio is 2.0).

2.2.7.3. cDNA synthesis

Reverse transcription of RNA into cDNA was carried out by using the High Capacity cDNA Reverse Transcription Kit. 10µL of the extracted RNA was mixed with 10µL of 2X Reverse

Transcription Mastermix (2.2.4.8) in a PCR tube and reaction carried out as per manufacturer's protocol (i.e. 25°C for 10 min, 37°C for 120 min and 85°C for 5 seconds (secs)). cDNA was kept at -20°C for long-term storage.

2.2.7.4. Target amplification

Due to the low level of expression of target genes of interest and for consistency throughout experimental design, a preamplification step of the cDNA was carried out using Qiagen Multiplex PCR plus kit. The manufacturers protocol was followed. Pre-amplification cycling conditions involved an initial PCR activation step for 5 min at 95°C, then 14 cycles of: 30 secs at 95°C, 90 secs at 60°C, and 90 secs at 72°C; the reaction was then finished with an extension of 10 min at 68°C.

2.2.7.5. Real time- PCR (RT-PCR)

RT-PCR allows detection of messenger RNA expression following reverse transcription into cDNA. Following a PCR reaction, the PCR products are run on an agarose gel by electrophoresis and separated according to their size and stained with ethidium bromide prior to their detection. This is a qualitative analysis, and was used within this thesis to ensure primers were specific, and working prior to quantitative analysis.

Practically, 50-100ng of cDNA was used and mixed with the RT-PCR mix in a PCR tube. Following cycling conditions, the PCR products were run in 2% agarose gel in order to visualise the individual DNA bands. The gel was prepared with 1g agarose powder in 50ml of 1X TBE buffer. The mixture was heated in a microwave until the agarose powder had completely dissolved. 2uL ethidium bromide (10mg/ml) was added and the mix poured into a casting tray. The gel was left to set for about 30 min. Each well of the gel was loaded with 10uL of PCR product mixed with 2ul loading dye (6X); 2uL of 100bp DNA ladder was loaded in a separate lane and then run at 50V in a tank filled with 1x TBE buffer. The PCR products were detected using an ultraviolet light source.

2.2.7.6. Fluidigm gene expression

Quantitative RT-PCR allows for the quantification of the cDNA products in a sample by detection of increasing level of fluorescence during the reaction, as the PCR products accumulate during amplification. By plotting fluorescence against the number of cycles of the PCR reaction, it is possible to determine the cycle number at which the increase in fluorescence is exponential and exceeds the set background fluorescence threshold. This is termed the Ct threshold. During an exponential phase of the reaction, the reaction has not yet reached its saturation and the DNA target doubles every cycle so that the quantity of the PCR product is

directly proportional to the amount of template nucleic acid, with any differences in fluorescence signal secondary to different starting amounts of cDNA in the samples tested.

The Fluidigm BioMark HD system integrates thermal cycling and fluorescence detection in a Fluidigm dynamic array integrated fluidic circuit (IFC) and provides a high-throughput qRT-PCR using standard primers or TaqMan gene expression assays. The system allows simultaneous PCR reactions in nanolitre volumes on a single microfluidic device. Prior to Fluidigm analysis, all cDNA samples were preamplified as described above. Unincorporated primers were removed using Exonuclease I, following the manufacturers protocol. The thermal cycling conditions were 30 min at 37°C (digestion), then 15 min at 80°C (enzyme inactivation).

Gene expression levels were determined by 48:48 or 96:96 Dynamic Biomark Array, following the manufacturer's defined protocols for primer-based assays. Sample mixes and assay mixes were loaded into the wells of a previously primed dynamic array integrated fluidic circuit. The sample and assay mixes were combined through the IFC chip network of the microfluidic channels, chambers and valves automatically assembling individual PCR reactions. Thereafter, cycling conditions involved 60 secs hot start at 95°C, and then 30 cycles of: 5 secs at 96°C and 20 secs at 60°C, followed by a melting curve step for 3 secs at 60°C.

Relative gene expressions were analysed by the delta delta (ΔΔ) Ct method using an average of five to six housekeeping genes (*UBE2D2*, *B2M*, *ENOX2*, *GN2B1*, *TYW1*, and *CYC1*) as a reference control and an assigned calibrator. This allows analysis of the relative change in expression between samples by calculating the difference in delta Ct values between the cell types. Fold change between samples can then be assessed as each cycle represents a doubling, assuming that the relative amplification efficiencies are similar between comparators.

Primers were purchased from Eurofins MWG Operon shown in section 2.1.3.3. Heat maps were produced using PermutMatrix software or heatmap.2 in R/Bioconductor; these used Pearson distance for dissimilarity and complete linkage for hierarchical clustering.

2.2.7.7. Fluidigm C1 Single cell gene expression

Advances in single cell analysis have allowed for a more complete investigation of the cellular heterogeneity that may exist within populations and enables a more detailed examination of the homogeneity or heterogeneity of a population than was previously possible.

To assess single cell gene expression, Fluidigm C1 single cell gene expression was used to isolate single cells into individual reaction chambers using an IFC-based system. Following capture, cells were examined by microscopy for viability and to ensure single cell capture. Any concern over single cell status led to the well being withdrawn from examination. The C1 single cell auto prep system allows a reliable approach to reproducibly process 96 cells in parallel with minimal user intervention that could lead to contamination.

Practically, following sorting into appropriate populations, 4000 cells were loaded into a 10-17 micron Fluidigm C1 single cell auto prep IFC, and cell capture performed according to the manufacturer's instructions. Capture efficiency was determined using microscopy to exclude samples from the analysis with no or more than one cell captures or samples where in addition to cell there was cellular debris. Upon capture, reverse transcription and cDNA preamplifcaition were performed in the Fluidigm C1 single cell auto prep IFC, as per manufacturers instructions. Relative gene expressions were analysed by the ΔΔ Ct method as described above. All statistical analysis was performed through R/Bioconductor. The statistical analyses were performed using Limma modified t-test applying Benjamini-Hochberg adjustment for multiple hypothesis testing.

2.2.8. In vivo experimentation

2.2.8.1. Xenotransplantation model

The NSG mouse model was used to assay human LSCs with *in vivo* engraftment capacity (SCID-repopulating cells or SRC). CP-CML $Lin^-CD34^+CD93^+$ or $Lin^-CD34^+CD93^-$ cells were isolated by FACS sorting ($1x10^6$ cells/ mouse), washed and transplanted via tail vein injection into sublethally irradiated (200 cGy) 8-12 week old NSG mice. Mice were euthanised after 16 weeks and marrow contents of femurs were obtained. To assess human cell engraftment, cells were labeled with anti-human CD45, CD33 and CD19 antibodies prior to analysis by flow cytometry. Human $CD45^+CD33^+$ cells were isolated by FACS sorting and analysed by FISH for the *BCR-ABL* gene rearrangement.

2.2.8.2. Notch2 overexpression model

Rosa-Inl N2IC mouse – these mice were generated in the Aifantis lab (NYU) by the insertion of a loxP flanked splice acceptor NEO-ATG cassette with two polyA sites followed by ICN2 into the ROSA26 locus, allowing the ROSA26 promoter to drive expression of the NEO-ATG

cassette. Cre recombinase-mediated excision of NEO-ATG results in use of the splice acceptor in the ICN2 cassette and irreversible expression of the transgene

2.2.9. Statistics

All results shown are the mean +/- standard error of the mean (mean +/- SEM) unless otherwise stated. All statistical analysis was performed with Graph Pad prism software using the two-sided unpaired or paired student's t-test when two groups were compared. When multiple groups were compared, a one-way ANOVA with correction for multiple groups' comparison was used. Within single cell gene expression analysis, a Limma modified t-test applying Benjamini-Hochberg adjustment for multiple hypothesis testing was used. A p value of <0.05 was considered significant.

3. Results I

3.1. Introduction

The introductory chapter to this thesis has clearly demonstrated that despite TKI therapy being highly efficacious at eradicating *BCR-ABL* positive proliferative cells, they are unable to eradicate the most primitive quiescent LSCs in *in vitro* and *in vivo* assays (Bhatia et al, 2003b; Chomel et al, 2016; Chu et al, 2011; Graham, 2002). These residual cells underpin the phenomenon of disease persistence. This has been further highlighted in recent TKI discontinuation clinical trials, where more than half of patients developed an early molecular relapse upon discontinuation of therapy in the context of a deep molecular response (Clark et al, 2016; Imagawa et al, 2015; Mahon et al, 2010; Mahon et al, 2016; Rea et al, 2012; Ross et al, 2010; Ross et al, 2013; Ross, 2015; Takahashi et al, 2012). This evidence concludes that CML LSCs are independent of BCR-ABL kinase activity for their survival, and imply that when BCR-ABL is inhibited through maximal pharmacological intervention with TKI therapy, other factors drive cell survival through genetic, epigenetic or alternative signalling pathways (Corbin et al, 2011b; Foley et al, 2013; Hamilton et al, 2012).

As previously discussed, self-renewal is considered to be an integral property of the LSC, and its deregulation is known to affect the development, maintenance, and persistence of the CML LSCs within the context of disease persistence. To date, a number of aberrant signalling pathways have been proposed to contribute to the LSC phenotype. These pathways, including Hh, Wnt/β-catenin and BMP, are known regulators of cell survival, and are often differentially expressed following genetic events (Fukushima et al, 2013; Irvine et al, 2016; Laperrousaz et al, 2013; Liao et al, 2012; Lu et al, 2013; Sengupta et al, 2007; Zhao et al, 2007). A number of deregulated proteins within these pathways may represent a broadly applicable therapeutic strategy; however, it is well known that these pathways rarely work in isolation, and rely on an interconnecting web of activity leading to disease maintenance, persistence, and progression (Sengupta et al, 2007; Sinclair et al, 2013; Zon, 2008). To understand the true potential of targeting an individual self-renewal pathway protein, one must ascertain the impact of manipulating an individual pathway in a given disease. This will allow for better understanding of the acquired vulnerability in the mechanisms of the signalling pathway, which will, in turn, allow for a therapeutic window to eradicate the LSCs. Although, our lab and others have documented the effects of many signalling

pathways in CML, including Hh, Wnt-β-catenin, and BMP, the role that the Notch signalling pathway plays in myeloid disease remains controversial.

The Notch signalling pathway has been implicated in a number of malignancies with its role being cell- and tissue-dependent. In cancer biology, Notch signalling has been demonstrated to play both an oncogenic and tumour suppressive role, depending on cell and cancer type (Al-Hajj et al, 2003; Leong & Karsan, 2006; Miele, 1999; Pancewicz & Nicot, 2011; Pasto et al, 2014; Prasetyanti et al, 2013; Suman et al, 2013). In haemopoietic malignancies, accumulating evidence demonstrates its importance in growth, differentiation, and apoptosis (Chiang et al, 2013; Hannon et al, 2012b; Nwabo Kamdje et al, 2011; Pancewicz & Nicot, 2011; Seke Etet et al, 2012).

Notch receptors 1-3 are expressed in both immature and mature blood cells (Chiba). Deregulation of Notch was first identified in T-cell ALL where mutation rates in *NOTCH1* have been reported in 50-70% of cases (Ellisen et al, 1991; Hannon et al, 2012b; Nwabo Kamdje et al, 2011; Roma et al, 2012). Similarly, Notch receptor mutations have been identified in a range of mature B cell leukaemias and lymphomas (Crews & Jamieson, 2012). Improved understanding of the Notch signalling pathway in these malignancies suggests that the Notch pathway may be a prime drug target; however, the therapeutic role of Notch inhibition may be directly dictated by the effects of its inhibition on other cell lineages, including the myeloid lineage (Deangelo et al, 2006; Tosello & Ferrando, 2013).

Reports about the role which Notch plays in myeloid disease are conflicting, as Notch activation in myeloid precursors has been shown to promote self-renewal, induce or inhibit differentiation to monocytes, or induce apoptosis (Carlesso et al, 1999; Li et al, 1998; Sarmento et al, 2005; Schroeder et al, 2003). Early observations suggested that Notch signalling may play a role in myeloid progression (Schroeder et al, 2003; Tan-Pertel et al, 2000). For example, Tan-Pertel *et al* demonstrated that Notch enhanced cell survival of the 32D cell line and promoted entry into a myeloid cell fate. 32D cells proliferate as blasts in the presence of the cytokines GM-CSF and IL-3, but initiate differentiation and undergo granulopoeisis in the presence of G-CSF. Interestingly, an earlier study contradicted this, observing that an activated form of Notch1 could inhibit G-CSF-induced granulocytic differentiation of 32D myeloid progenitors (Milner et al, 1996). It should be noted, however, that both studies used a truncated form of Notch

rather than inhibition of full-length Notch and inhibition of full-length Notch in this cell line has yet to be described.

Importantly, in 2001, Todha *et al* showed that exposing AML cells to plate-bound Notch ligands led to a full range of responses from proliferation to growth arrest that varied with patient sample, suggesting a combinatorial role between self-renewal pathways and molecular disease (Tohda & Nara, 2001). More recently, observations have supported a tumour suppressive role for Notch signalling in myeloid disease (Chen et al, 2008; Kannan et al, 2013; Klinakis et al, 2011; Lobry et al, 2013; Yin et al, 2009). A recent study identified a tumour suppressor role for the Notch pathway in another myeloproliferative disorder, chronic myelomonocytic leukaemia (CMML). This offers evidence for the existence of inactivating Notch mutations in CMML, and is supportive of a loss-of-function mechanism in myeloid disease (Klinakis et al, 2011). Furthermore, in AML cell lines and primary patient blasts, downregulation of Notch1 expression was associated with decrease in PU.1-mediated differentiation capacity, indicating a pivotal role in maintenance of an immature state (Chen et al, 2008). Recently, it was observed that human AML samples, isolated into stem and progenitor populations, express Notch receptors, however activation of downstream Notch targets was low, suggesting that Notch is present but not active in the samples analysed (Kannan et al, 2013; Lobry et al, 2013). Subsequent activation of the Notch receptors or Notch targets led to AML growth arrest *in vivo* and conversely Notch inhibition via dnMAML enhanced proliferation (Kannan et al, 2013), again suggesting a role of Notch in myeloid neoplastic proliferation.

Data is limited within CML. Notch has been shown to inhibit growth of the CML cell line, K562, although the authors do not assess endogenous active Notch signalling, instead only analysing Notch receptors at an mRNA level (Yin et al, 2009). Furthermore, it has been demonstrated that, using an *in vivo* model of CP-CML and BP-CML, that Numb, a Notch antagonist, was present at low levels in CP disease, but at high levels in BP, suggesting that there is a change in Notch signalling with progression of disease (Ito et al, 2010).

Unpublished microarray studies by the Copland laboratory confirm that *HES1*, a Notch downstream target gene, expression is increased in very primitive $lin^{-}CD34^{+}CD38^{-}CD90^{+}$ CML stem/progenitor cells compared to normal. Furthermore, there is a progressive increase in *HES1* expression as CML progresses. Additional unpublished

microarray studies have shown that TKI treatment of $CD34^+$ CML stem/progenitor cells regulates gene expression in pathways critical for self-renewal, including Notch. In addition, *HES1* was found to be highly expressed in CML blast crisis. This has been further demonstrated *in vivo*, where retroviral co-expression of *Hes1* with *Bcr-Abl* resulted in generation of an aggressive acute leukaemia. However, the question remains, if *HES1* is being regulated by the Notch pathway or, indeed, another signalling mechanism, as recent evidence suggests that despite relatively high levels of Notch1 receptor in a panel of primary AML patients, *HES1* was expressed at low levels (Chiaramonte et al, 2005).

These differing observations could be explained by existence of multiple molecular interactions between Notch signalling and other self-renewal pathways, which are likely to correlate with the ability of Notch to function as an oncogene or a tumour suppressor. The role that Notch is playing within CP-CML in isolation or in combination with other self-renewal pathways, if any, remains unanswered.

3.2. Aims

Based on the evidence provided above, the specific aims set out in this chapter are:

1. To assess the expression of the Notch signalling pathway elements in $CD34^+$ CP-CML patient samples;
2. To assess the functional role, if any, of the Notch signalling pathway in $CD34^+$ CP-CML patient samples;
3. To assess differences in the functional role of the Notch signalling pathway between stem and progenitor cells in CP-CML.

3.3. Results

3.3.1. *The Notch signalling pathway is silenced in CD34⁺ CP-CML patient samples*

To address the possible involvement of the Notch signalling pathway in CML, Notch pathway gene expression was investigated in primary CML patient samples. Using Fluidigm technology, mRNA expression of 24 $CD34^+$ CP-CML patient samples was compared to normal BM $CD34^+$ samples, purchased from Stem Cell Technologies. Relative gene expression levels were determined using the average normal $CD34^+$ value as a calibrator, calculated using the delta delta (ΔΔ) CT method (Schmittgen & Livak, 2008), using an average of six housekeeping genes as reference. The CP-CML samples had no preceding treatment prior to analysis. 4 samples failed the analysis.

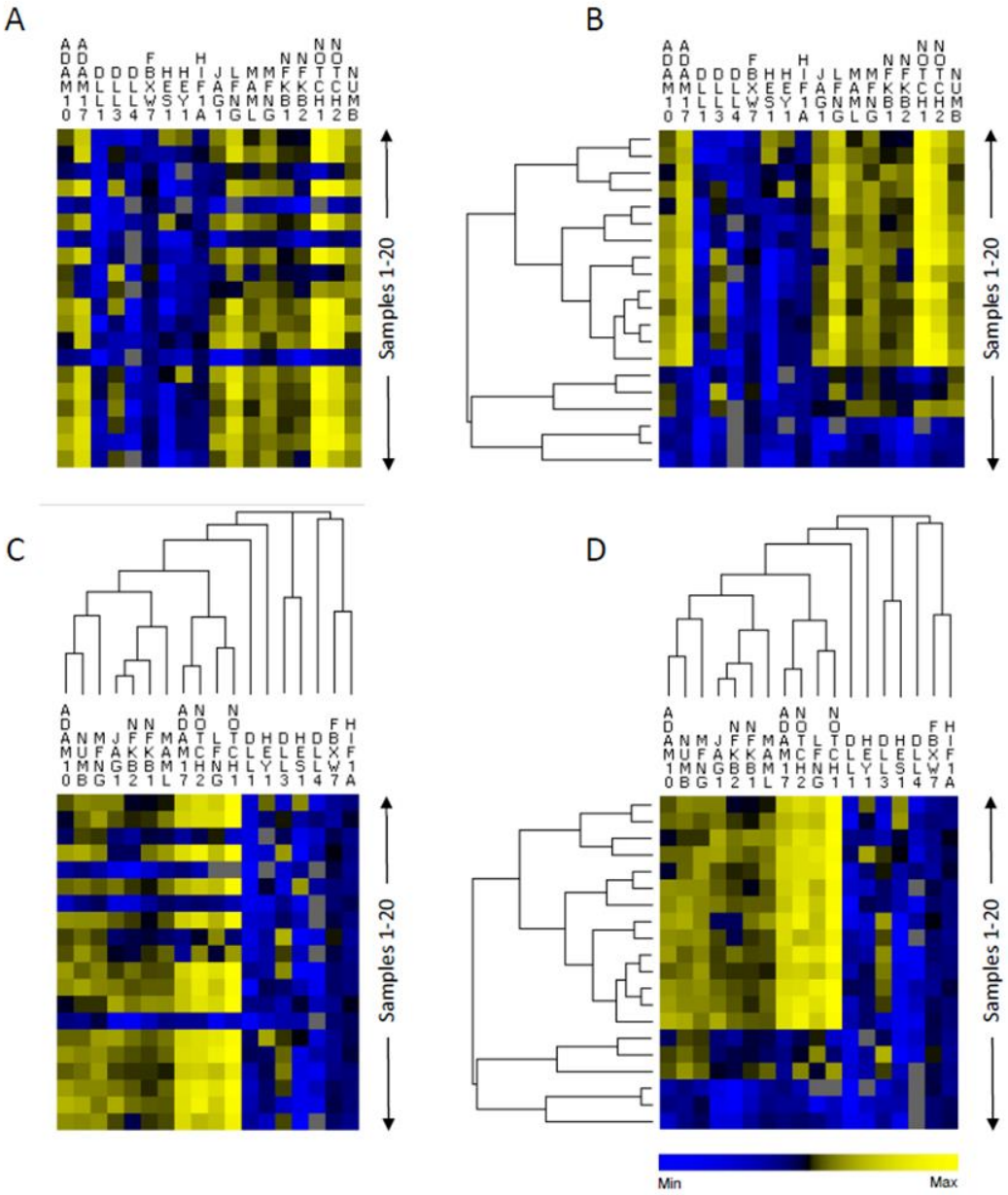

Figure 3 - 1 Notch pathway components are differentially expressed between CP-CML CD34$^+$ and normal CD34$^+$ samples

Gene expression profiling (GEP) for Notch pathway components was determined from normal CD34$^+$ BM samples (n=6), and CML cells after CD34$^+$-selection from peripheral blood (n=20). Gene expression was determined by Fluidigm array analysis. Relative gene expression levels were determined by the average normal CD34$^+$ value as a calibrator calculated using the ΔΔCT method, with an average of six housekeeping genes as reference. CP-CML CD34$^+$ samples had no preceding treatment prior to analysis. Heatmaps were produced using PermutMatrix software. (A) Heatmap representation of fold change between CP-CML and normal CD34$^+$ sample. (B) Heatmap representation of Notch pathway components between CP-CML and normal CD34$^+$ samples with sample clustering. (C) Heatmap representation of Notch pathway components between CP-CML and normal CD34$^+$ samples with gene clustering. (D) Heatmap representation of Notch pathway components between CP-CML and normal CD34$^+$ samples with gene and sample clustering. There was no prognostic significance between quantitative *BCR-ABL* level and Notch pathway components at 6, 12, and 18 months as determined by ELN guideline criteria (Baccarani et al. 2013).

This demonstrated that the Notch signalling pathway components are highly deregulated at the mRNA level in CP-CML compared to normal (figure3-1A). Gene clustering methods determined that patient samples (figure 3-1B) and Notch pathway components (figure 3-1C) could be clustered upon gene expression, however, on analysis of quantitative *BCR-ABL* expression at 6, 12, and 18 months, there was no prognostic relevance noted on clustering in isolation or together (figure 3-1D).

Focussed gene analysis established that the Notch signalling pathway was inactive, as demonstrated through downregulation of the Notch target genes, *HES1* ($p<0.0001$; figure 3-2A), and *HIF1A* ($p=0.0029$). Decreased expression compared to normal was shown in other downstream targets, including *HEY1*, but this was not determined to be statistically significant ($p=0.3019$). In parallel, the Notch negative regulators, *MFNG* ($p=0.0108$), and *NUMB* ($p=0.0114$) were upregulated (figure 3-2B). Taken together, these data suggests that the pathway may be silenced in CP-CML.

In these patient samples, the Notch receptor, *NOTCH2*, was significantly upregulated compared to normal CD34$^+$ samples, $p=0.0001$ (figure 3-2C). As Notch ligand expression was also downregulated at an mRNA level (figure 3-2D), this was highly suggestive that the downregulation of the pathway was not secondary to *cis*-inhibitory mechanisms (del Álamo et al, 2011).

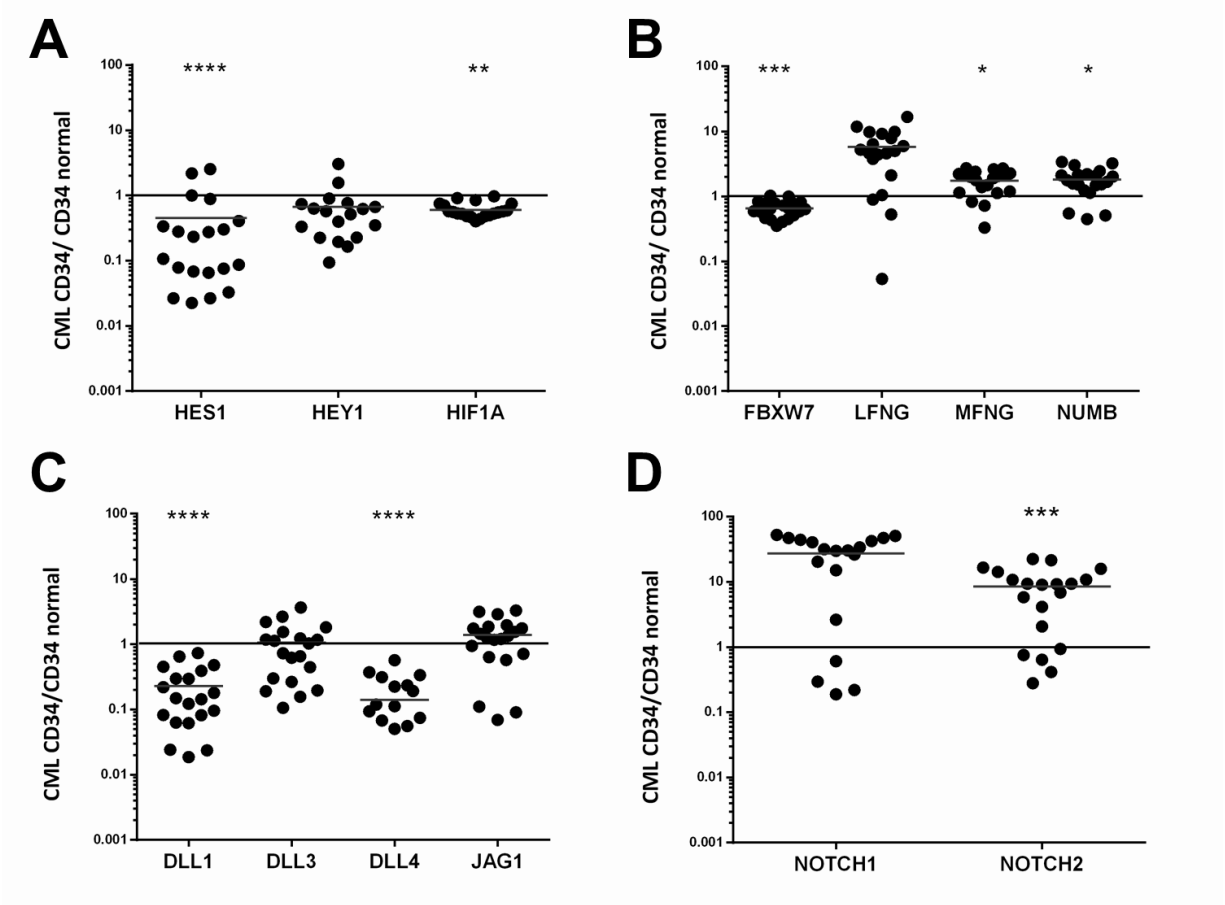

Figure 3 - 2 Focussed gene analysis identifies that the Notch signalling pathway is silenced in CD34⁺ CP-CML

Relative gene expression levels for 20 CD34⁺ CP-CML samples were determined against the average normal CD34⁺ values calculated using the ΔΔCT method with an average of six housekeeping genes as reference. Fold change is relative to normal CD34⁺ samples (n=6). (A) Dot plot representing fold change expression values for Notch target genes. (B) Dot plot representing fold change expression values for negative regulators of the Notch pathway. (C) Dot plot representing fold change expression for Notch ligands. (D) Dot plot representing fold change expression of Notch receptors. P values were determined by an unpaired t-test with Welch correction (* p<0.05, ** p<0.01, *** p<0.001, **** p<0.0001).

Noted within this mRNA expression data were two distinct populations of low and high expression of the metalloprotease, *ADAM17* (figure 3-3). On further examination of these patient samples, it was noted that *ADAM17* expression correlated with Notch receptor mRNA expression, as demonstrated through spearman rank correlation (R) (R = 0.7717 [p=0.0001], R= 0.8255 [p<0.0001] with *NOTCH1* and *NOTCH2*, respectively). However, this did not correlate to prognostic relevance in terms of quantitative *BCR-ABL* expression at 18 months. Furthermore, there was no correlation with the downstream target gene, *HES1*. Again, highlighting that the pathway is silenced within the samples analysed.

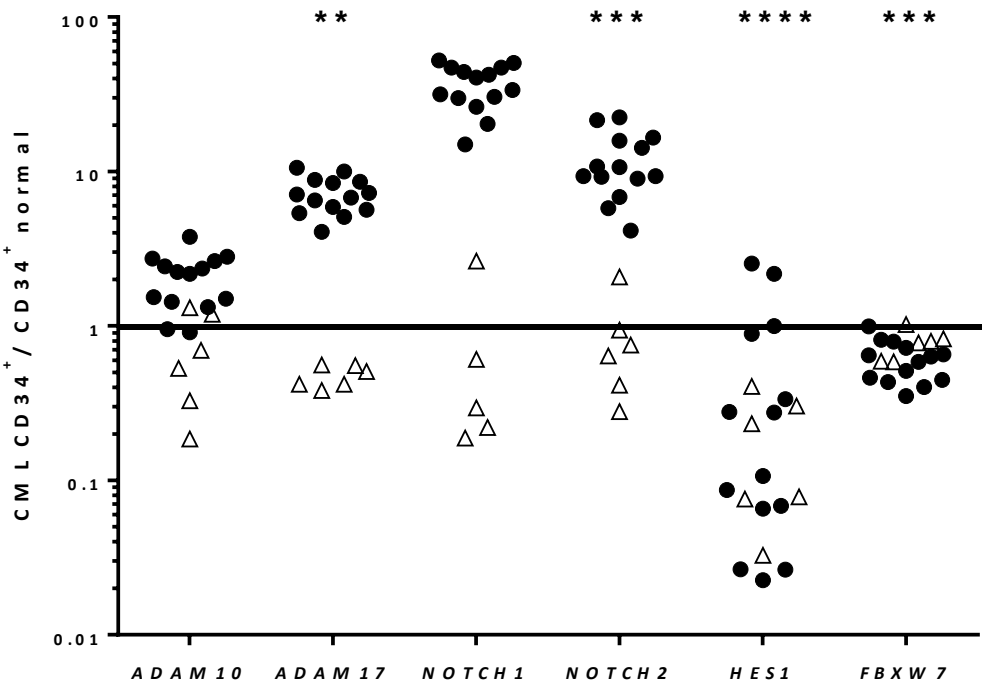

Figure 3 - 3 Focussed gene analysis identifies that the metalloprotease, ADAM17, statistically correlates with Notch receptor expression

Relative gene expression levels for 20 $CD34^+$ CP-CML samples were determined against the average normal $CD34^+$ values calculated using the ΔΔCT method with an average of six housekeeping genes as reference. Fold change is relative to normal $CD34^+$ samples (n=6). P values were generated relative to normal $CD34^+$ samples. P values were determined by an unpaired t-test with Welch correction (* $p<0.05$, ** $p<0.01$, *** $p<0.001$). The triangles represent samples with low *ADAM17* expression, and the the circles represent samples with high *ADAM17* expression. Pearson's correlation coefficient between *ADAM17* and *NOTCH1* demonstrated an R-value of 0.7717 ($p=0.0001$), and between *ADAM17* and *NOTCH2* 0.8255 ($p<0.0001$).

3.3.2. *FBXW7* confers prognostic relevance at 12 and 18 months

FBXW7 is an E3 ubiquitin ligase and is a substrate recognition component of the Cullin-1/SCF complex that targets specific substrate proteins for poly-ubiquination and degradation of the 26S proteasome. Fbxw7 has been shown *in vivo* to target many proto-oncoproteins, growth promoters, and anti-apoptotic molecules, including Cyclin E, c-Myc, Notch1, c-Jun, mTOR, and Mcl1 (King et al. 2013; Nakayama & Nakayam 2006; Matsuoka et al. 2008; Reavie et al. 2010). Within the same dataset used in section 3.3.1, we analysed the expression of *FBXW7* in the 20 CML patient samples, where quantitative *BCR-ABL* expression was known at 6, 12, and 18 months. Classifying these samples into good and intermediate/poor responders, in accordance with the ELN guidelines for management of CML (Baccarani et al. 2013), it was shown that *FBXW7* represents a prognostic indicator of *BCR-ABL* response at 12 and 18 months (figure 3-4). *FBXW7* has an indispensable role in the maintenance of quiescence, with deletions

in Fbxw7 leading to cell exhaustion. This, perhaps, highlights the potential role of *FBXW7* as a therapeutic modality within CP-CML in the eradication of the LSCs.

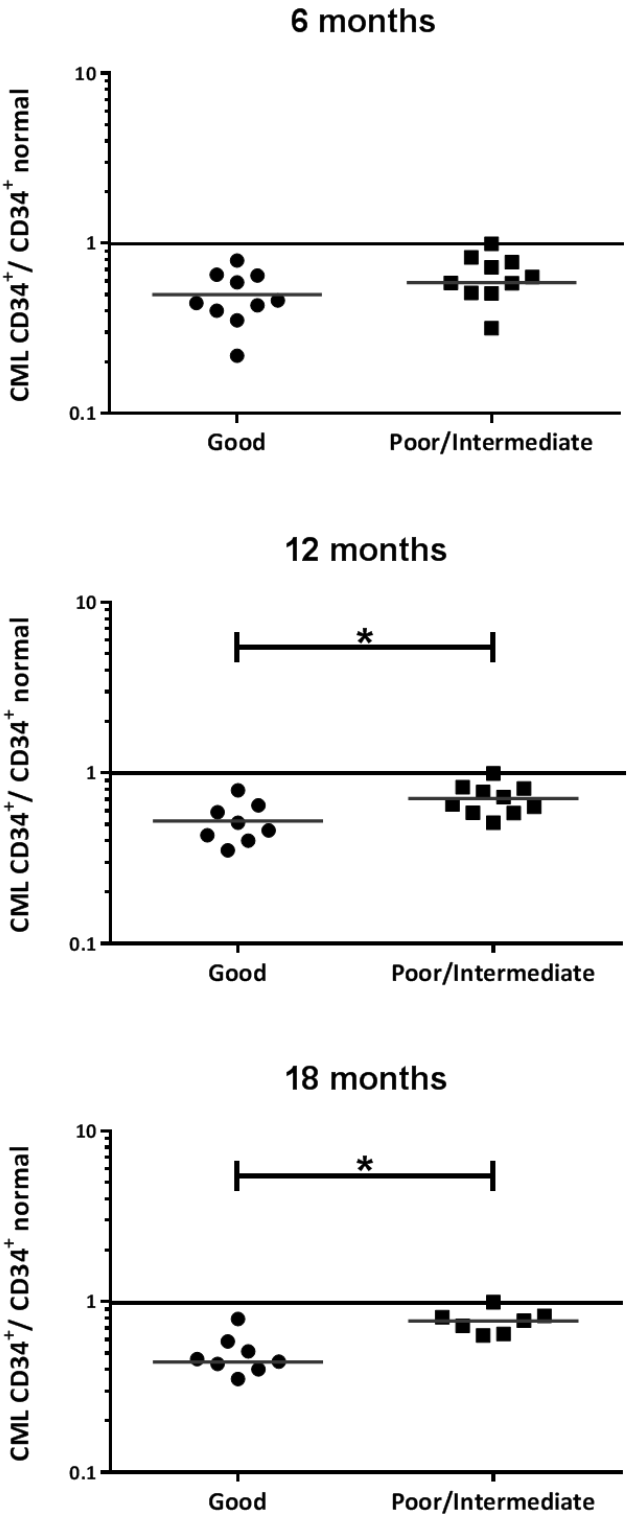

Figure 3 - 4 *FBXW7* represents a prognostic indicator at 12 and 18 months
Relative gene expression levels for 20 $CD34^+$ CP-CML samples were determined against the average normal $CD34^+$ values calculated using the ΔΔCT method with an average of six housekeeping genes as reference. Fold change is relative to normal $CD34^+$ samples (n=6).

3.3.3. *Upregulation of Notch receptors are present at protein level*

The upregulation of *NOTCH1* and *NOTCH2* genes was confirmed at protein level through IF. Using an antibody for the full-length receptor, IF was performed on 4 $CD34^+$ CP-CML samples. Within all samples, a punctate appearance was noted for both NOTCH1 and NOTCH2 full-length receptors within the cytoplasm of the cells, with varying expression levels noted across patient samples, consistent with the gene expression findings (figure 3-5). In view that the pathway was inactive by gene expression, we confirmed this at protein level with the cleaved, activated form of the Notch receptor, val1744, which was absent on $CD34^+$ CP-CML cells by either IF (n=4) or western blotting (n=2). These results supported the gene expression data that the Notch receptors, *NOTCH1* and *NOTCH2*, are present on the cell surface of CP-CML samples, but are not activated.

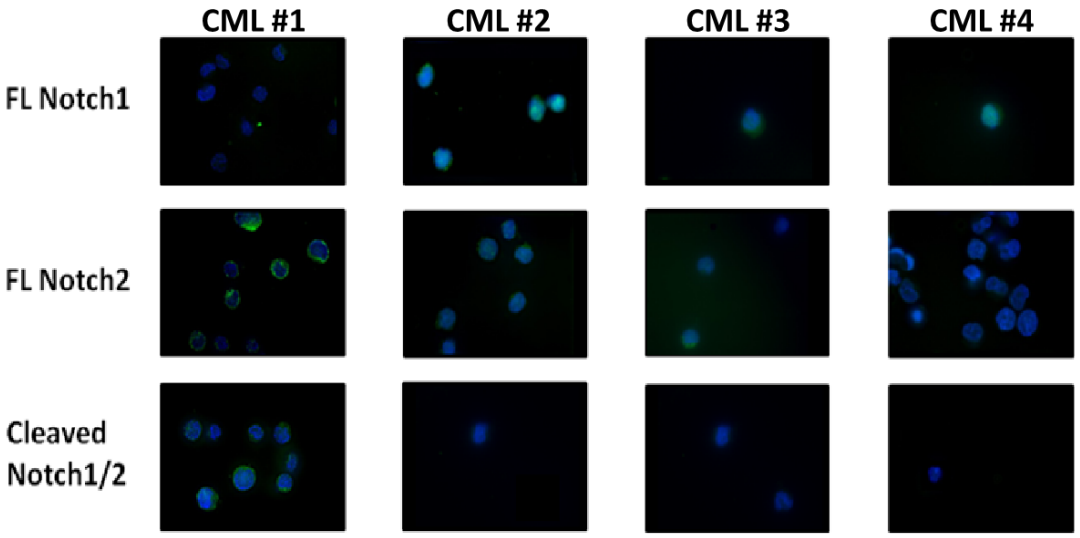

Figure 3 – 5 Upregulation of Notch receptors was confirmed by IF
To illustrate intensity of immunolabelling, digital images were captured at identical exposure times. The expression of full length (FL) Notch1, FL Notch2, and cleaved Notch 1/2 (val1744) are depicted here for 4 CP-CML samples. The punctate appearance of the FL receptor is visible in a cytoplasmic distribution in all samples. There was no activation of cleaved Notch present.

3.3.4. *Pharmacological inhibition of Notch does not alter cellular growth in CD34⁺ CP-CML in plastic culture conditions*

To ensure that Notch signalling was not active in CP-CML and gain further insight into the functional role of the Notch pathway in CP-CML, 5 $CD34^+$ primary samples were cultured with and without the pharmacological Notch inhibitor, DAPT; a gamma secretase inhibitor (GSI) that prevents the dissociation and translocation of the intracellular aspect of the Notch receptor to the nucleus. Cells (n=5) were thawed or used fresh from $CD34^+$-selection and cultured in low growth factor SFM on non-stromal conditions (i.e. plastic culture without stromal support) with and without 10uM DAPT for 7 sequential days. Trypan blue exclusion cell counts every 24 hours showed that there was no statistically significant difference between untreated and treated samples in terms of cell growth (figure 3-6).

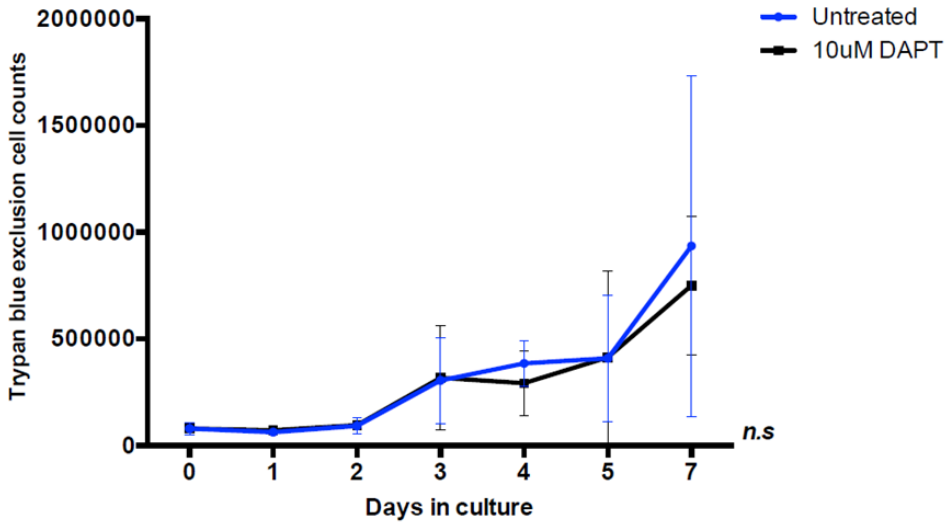

Figure 3 - 6 Pharmacological inhibition of Notch does not alter cellular growth in $CD34^+$ CP-CML cells in plastic culture

$CD34^+$ CP-CML cells were used from isolation of fresh peripheral blood samples or thawed and cultured in low growth factor SFM with or without the presence of 10uM DAPT (n=5). DMSO treated cells were used as an 'untreated' control. Cells were counted using trypan blue exclusion cell counts every 24 hours. No statistical difference was seen with the addition of DAPT over sequential days in culture as analysed using a paired student's t-test at each time-point (n=5; $p>0.05$).

Furthermore, analysis of cell cycle (figure 3-7) and apoptosis (figure 3-8) following up to 7 days of culture in these patient samples did not demonstrate any statistical change in cell cycle components or apoptotic ability with the addition of DAPT. Together, these results, as expected, demonstrate that pharmacological inhibition of the Notch signalling pathway does not alter cellular growth function in $CD34^+$ CP-CML samples in plastic culture conditions and validated our gene expression data.

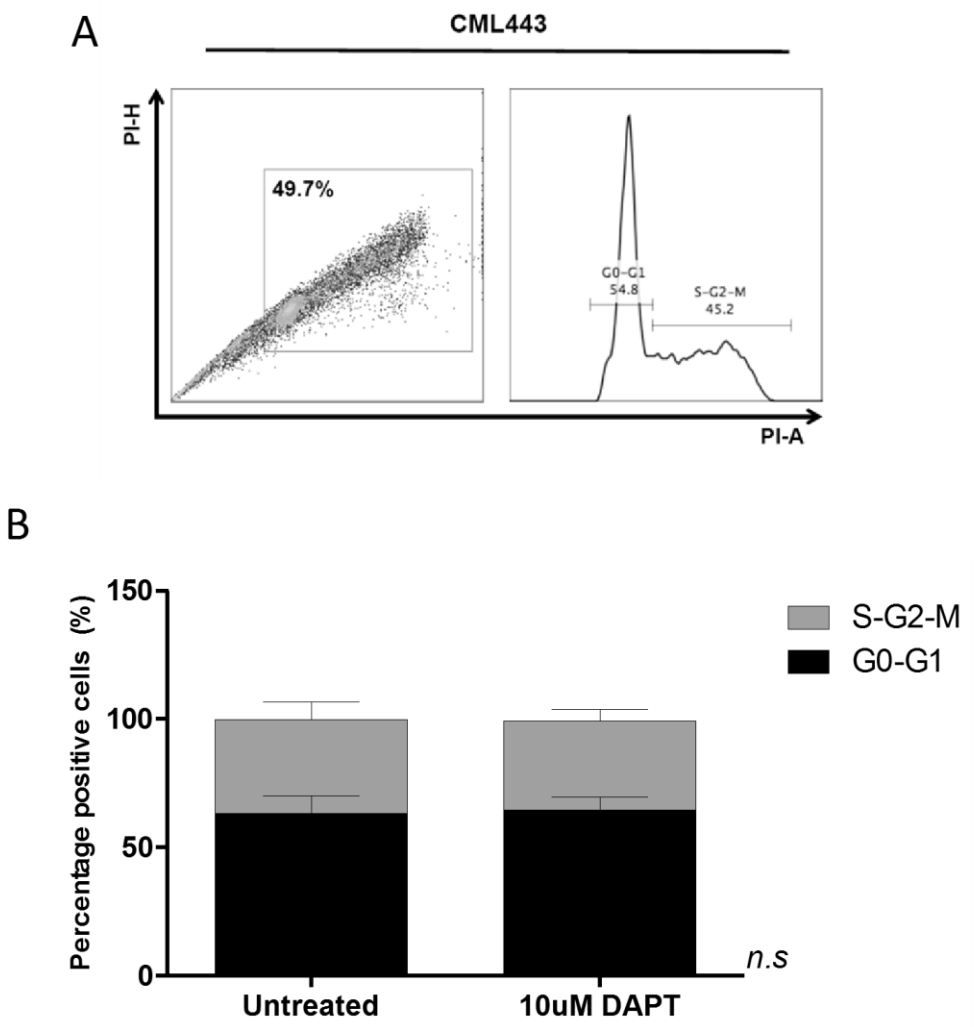

Figure 3 - 7 Pharmacological inhibition of Notch does not alter the cell cycle in CD34$^+$ CP-CML cells in plastic culture

CD34$^+$ CP-CML cells were used from isolation of fresh peripheral blood samples and cultured in low growth factor SFM with or without the presence of 10uM DAPT (n=5). DMSO treated cells were used as 'untreated' control. Following five days in culture, cells were washed with 2ml 2%FBS/PBS, and then fixed with ice-cold ethanol prior to freezing. Within 48 hours of freezing, samples were centrifuged at 300g for 5 min prior to being washed with 2%FBS/PBS and PI stain added. Samples were incubated for 15 min before being immediately analysed by flow cytometry. (A) Representation of flow cytometry analysis of cell cycle. (B) There was no statistical difference seen in cell cycle status between populations as determined by a student's t test (p=0.9, n=5).

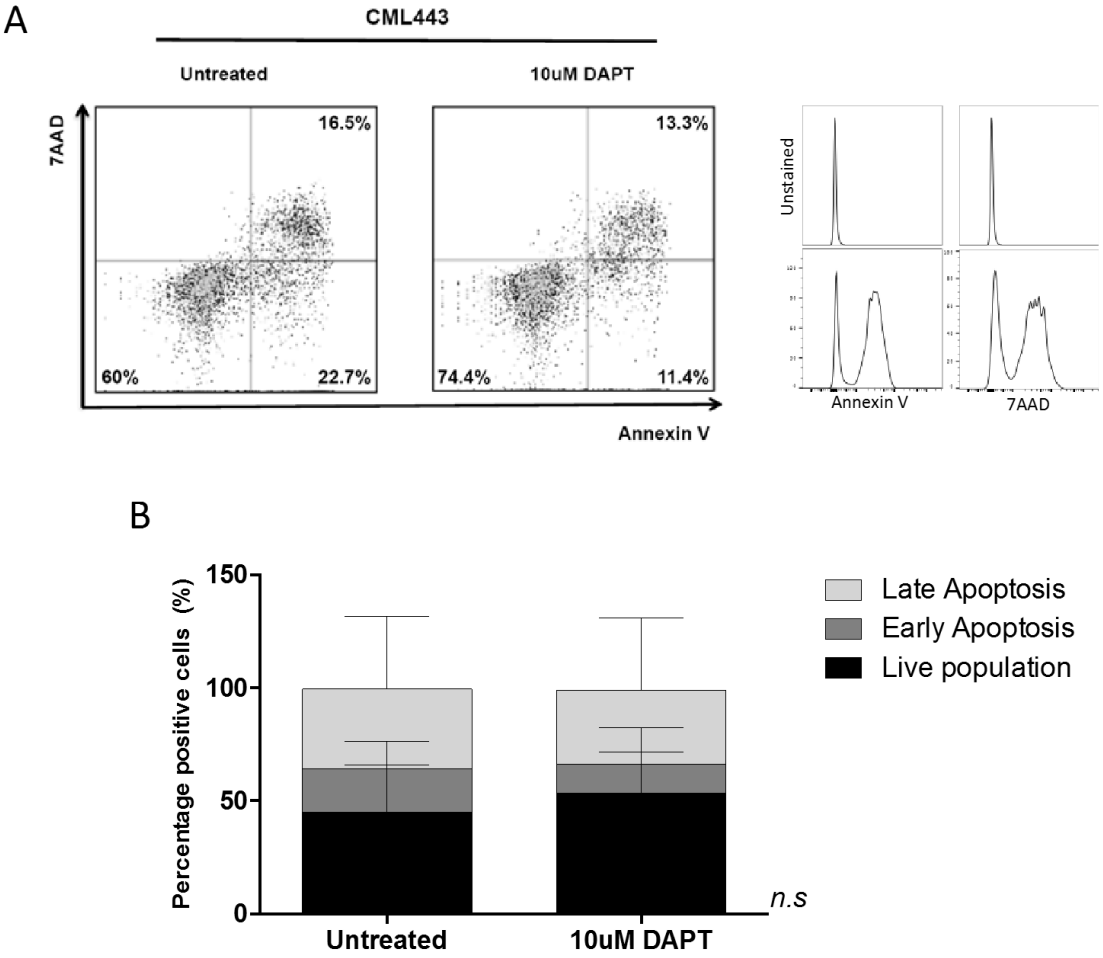

Figure 3 - 8 Pharmacological inhibition of Notch does not affect apoptotic potential of CD34$^+$ CP-CML cells in plastic culture conditions

CD34$^+$ CP-CML cells were used from thaw or isolation of CD34$^+$-selected fresh peripheral blood samples and cultured in low growth factor SFM with or without the presence of 10uM DAPT (n=5). DMSO treated cells were used as 'untreated' control. Following five days in culture, following a 2% FBS/PBS wash, 0.5-1x10^5 cells were re-suspended in 100µL of annexinV buffer containing 5µL annexin-V conjugated to relevant fluorochrome and 5µL 7AAD. Samples were incubated at room temperature for 15 min in the dark. Following incubation, further 200µL of annexinV buffer was added to the cell suspension and analysis was immediately performed by flow cytometry. Unstained and single stained cells were used to set voltages and compensation. (A) Representation of flow cytometry analysis of CML443; side panel demonstrates single stain controls. (B) Combined data collection of annexinV/7AAD staining. There was no statistical difference between populations ($p>0.05$, n=5).

3.3.5. *Notch pathway silencing within CP-CML is not secondary to increased methylation of the receptor*

It was next sought to investigate if the Notch pathway was silenced by increased methylation of the Notch components. To do this, H3K27me3 and H3K4me3 levels of the Notch components were interrogated within the E-MTAB-2581 microarray dataset. On global analysis, the Notch pathway was globally downregulated. H3K27me3 was statistically significantly increased for *LFNG* only, with no increase in H3K4me3 between normal (n=3) and CP (n=3) samples. This suggests that there were no aberrant methylation patterns to disrupt normal Notch signalling events and that, therefore, inferred that the Notch pathway could be exogenously activated in CP-CML samples.

3.3.6. *In vitro activation of the Notch pathway through ligand binding alters the growth potential of CP-CML CD34$^+$ patient samples*

In view that the CP-CML CD34$^+$ cells specifically and abundantly express the Notch receptor, *NOTCH2*, and that the pathway was confirmed to be functionally inactive at basal state (i.e. on plastic culture without stromal support), it was hypothesised that Notch signalling could be reactivated through exogenous activation in CP-CML CD34$^+$ cells upon ligand binding to the Notch receptor. As both the osteoblastic niche and MSCs express the Notch ligands, DLL1 and JAG1, it was decided to focus our experimental upregulation of the Notch pathway through these ligand interactions. The OP9 co-culture system was utilised, to allow for the overexpression of the DLL1 or JAG1 proteins, using OP9-GFP cells as control stroma (figure 3-9).

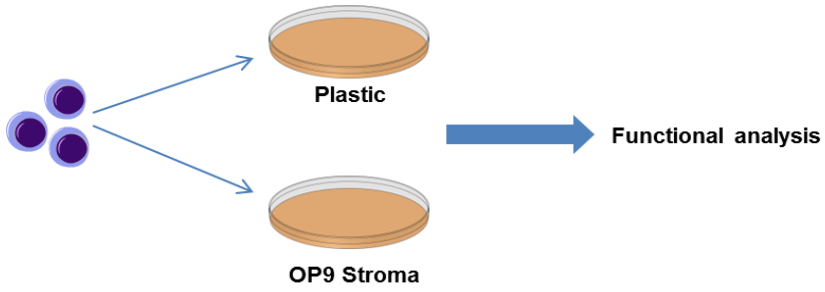

Figure 3 - 9 Schematic representation of co-culture experimentation
CD34$^+$ CP-CML samples were thawed or used fresh from CD34$^+$-isolation, and cultured on plastic or on OP9 stromal conditions in low growth factor SFM for the duration of the experiment. Functional analysis was then performed as described within each experimental model.

The DLL1 protein was only expressed within the OP9DLL1 stroma; whereas, both OP9GFP and OP9JAG1 expressed the JAG1 protein, with a concentration effect seen

within the expression between the GFP and JAG1 cell line (i.e. increased expression within OP9JAG1).

Compared to non-stromal conditions, culturing over 7 days on OP9-GFP led to a significant increase in growth as assessed by trypan blue exclusion cell counts (p=0.02, n=5). The overexpression of JAG1 led a further increase compared to OP9-GFP (p=0.002), suggesting that the increase in growth potential was secondary to culturing in the presence of increasing concentrations of the JAG1 protein, and not due to 'stromal' effects alone (figure 3-10).

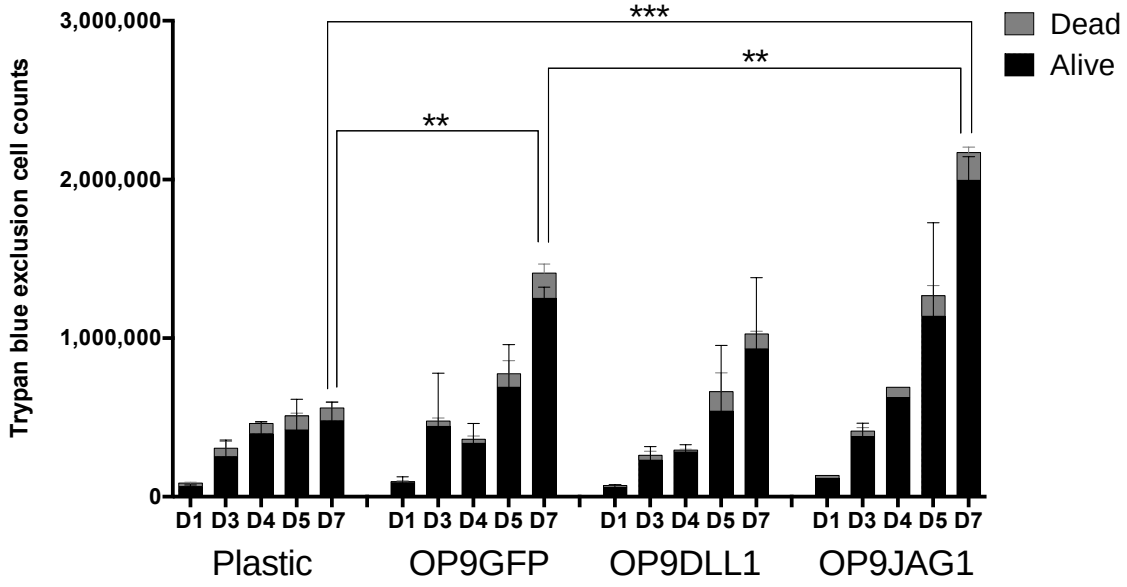

Figure 3 - 10 *In vitro* activation of the Notch pathway through ligand binding alters the growth potential of CP-CML CD34$^+$ patient samples

CD34$^+$ CP-CML cells were used from isolation of fresh peripheral blood samples or thawed and cultured in low growth factor SFM with or without the presence of stroma. Within each co-culture experiment, OP9 stromal cells only underwent a maximum of 8 passages before use. OP9 stromal cells were seeded at a 1 in 24 ratio with suspension cells (i.e. 1 stromal cell per 24 suspension cells) 24 hours prior to co-culture. 50,000 CD34$^+$ cells were seeded onto plastic or stromal conditions in 12 well plates and counted every 24 hours using trypan blue exclusion cell counts. Compared to non-stromal conditions, culturing over 7 days on OP9GFP led to a statistically significant increase in growth (p=0.02, n=5). The overexpression of JAG1 led to a further increase compared to OP9GFP (p=0.002, n=5), suggesting that the increase in growth potential was secondary to culturing in the presence of increasing concentrations of JAG1 protein.

In view of patient variability, the cell counts were normalised to their non-stromal control at day 5 (figure 3 – 11). With this, it was clear, that there was a statistical significant increase in trypan blue exclusion cell count following 5 days of culture between the OP9GFP and OP9JAG1 experimental arms. Subsequently, experiments following this were conducted for between five and seven days.

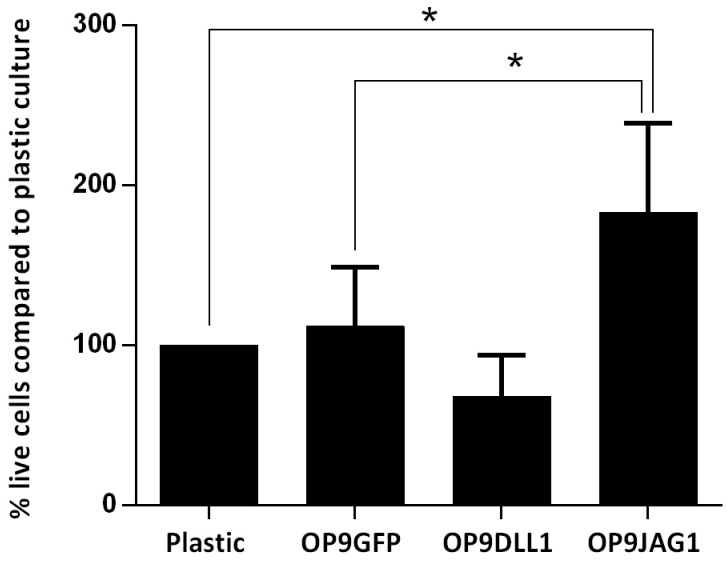

3 - 11 *In vitro* activation of the Notch pathway through ligand binding alters the growth potential at 5 days when samples are normalised to non-stromal conditions
Cell counts taken from figure 3-10 were normalised to their plastic/non-stromal control. This was to allow for sample variation. Upon normalisation, on day 5 of culture, there was a statistically significant increase in trypan blue exclusion cell counts between the OP9GFP and OP9JAG1 ($p<0.05$, $n=5$) by one way ANOVA. Subsequently, experiments following this were conducted for between five and seven days.

Upregulation of the pathway was confirmed with increased expression of *HES1*, a downstream target of the Notch pathway, at the gene level (n=6 plastic conditions; n=4 OP9JAG1 co-culture, p=0.001), and overexpression of the val1744 protein by IF (n=4) (figure 3-12). Co-culturing with OP9GFP also led to an increase in expression compared to normal, consistent with the expression of JAG1 in the cell line. There was no increase expression of *HES1* in those CML cells co-cultured with OP9DLL1 cells.

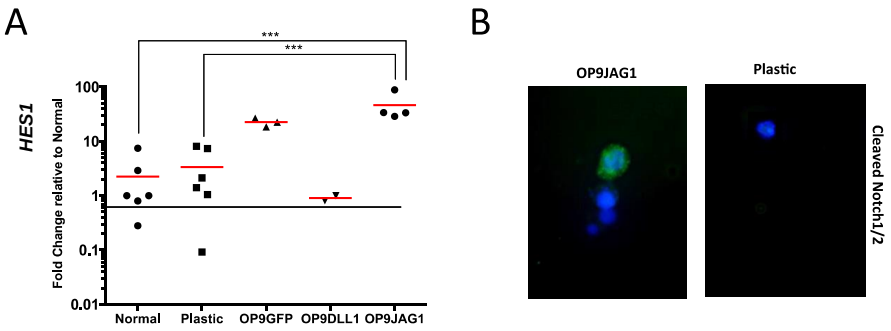

Figure 3 - 12 Co-culturing on OP9JAG1 stroma is associated with increase activation of the Notch pathway at gene and protein level

(A) Relative gene expression levels of *HES1* for n=5 $CD34^+$ CP-CML samples co-cultured against the average normal $CD34^+$ values calculated using the ΔΔCT method with an average of six housekeeping genes as reference. Fold change is relative to normal $CD34^+$ samples (n=5). 1 samples cultured on OP9JAG1, 2 samples cultured on OP9GFP, and 3 samples cultured on OP9DLL1 failed the analysis. There was a statistically significant increase in *HES1* in samples cultured on OP9JAG1 compared to non-stromal conditions. P values were determined by an unpaired t-test (* p<0.05, ** p<0.01, *** p<0.001). (B) Immunofluorescence of val1744 protein, the active form of the Notch receptor, suggested an increase in Notch activity in cells cultured with OP9GFP (not shown) and OP9JAG1.

Activation of the pathway through JAG1, and not DLL1, was further confirmed by utilising DAPT, where we observed a significant decrease in live cell counts within the OP9GFP (p=0.01) and OP9JAG1 (p=0.018) experimental arms (figure 3-13). There was no decrease in cell counts observed on non-stromal conditions (i.e. plastic), nor culturing on OP9DLL1 stroma, which was consistent with the *HES1* gene expression data.

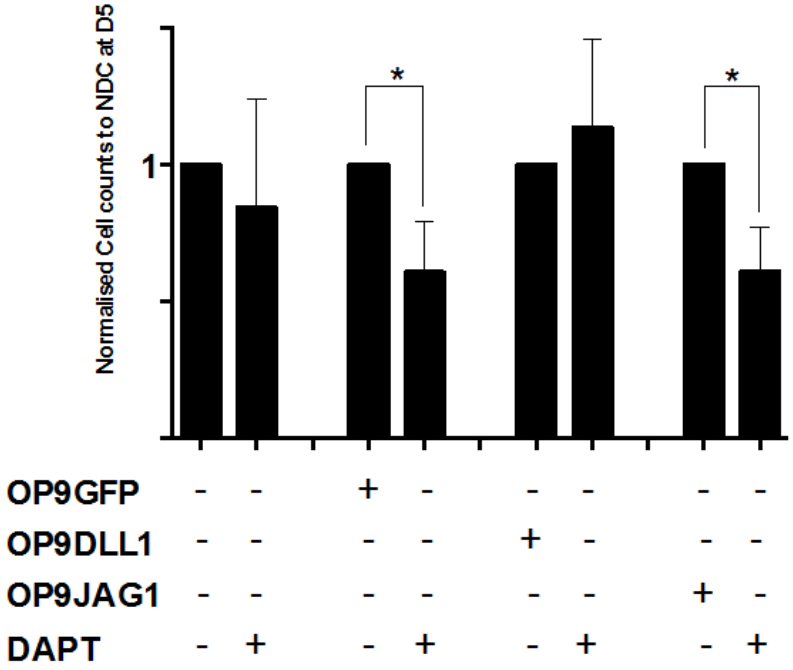

Figure 3 - 13 The Notch pathway can be activated in CD34$^+$ CP-CML cells through the Jagged1 protein
CD34$^+$ CP-CML cells were used from isolation of fresh peripheral blood samples and cultured in low growth factor SFM with or without the presence of stroma. Within each co-culture experiment, stroma only underwent a maximum of 8 passages before use. OP9 stromal cells were seeded at a 1 in 24 ratio with suspension cells (i.e. 1 stromal cell per 24 suspension cells) 24 hours prior to co-culture. Within each condition, 10uM DAPT, was added to one arm of the experiment. Cells were subsequently counted at sequential days using trypan blue exclusion. Results are shown at day 5. In view of patient variability, within each co-culture condition, counts were normalised to the untreated control. There was a statistically significant decrease in cell number in the OP9GFP and OP9JAG1 on addition of DAPT, suggesting that the activated pathway was being inhibited causing a reduction in cell number. (n=5, $p<0.05$; p value determined by a students t-test).

3.3.7. *In vitro activation of the Notch pathway through ligand binding does not alter cell cycle status in CP-CML CD34$^+$ patient samples*

From this, it was questioned if activation of the Notch pathway through exogenous ligands pushed the CD34$^+$ CP-CML cells into cycle (i.e. S-G2-M phase) leading to increased growth potential. CP-CML CD34$^+$ cells were cultured from thaw or used fresh from CD34$^+$-isolation in low growth factor SFM, with or without stromal conditions and fixed prior to PI staining and flow cytometry analysis. Culturing on stromal conditions with active Notch ligands did not influece the cell cycle distribution of CD34$^+$ CP CML cells in short term *in vitro* culture ($p > 0.05$, n=3) (figure 3-14).

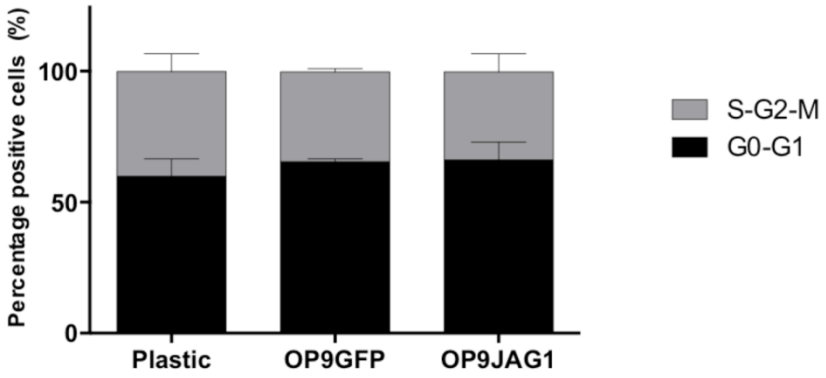

Figure 3 - 14 Notch activation through exogenous ligand binding does not influence cell cycle distribution of CD34$^+$ CP-CML cells in short term culture
CD34$^+$ CP-CML cells were used from isolation of fresh peripheral blood samples or thawed and cultured in low growth factor SFM with or without the presence of stroma. Within each co-culture experiment, stroma only underwent a maximum of 8 passages before use. OP9 stromal cells were seeded at a 1 in 24 ratio with suspension cells (i.e. 1 stromal cell per 24 suspension cells) 24 hours prior to co-culture. Cells were cultured between five and seven days before fixed with ethanol in preparation for PI staining (method 2.3.3.4). On flow cytometry analysis, there was no statistical difference, as assessed by multiple comparison ANOVA, between different culture conditions ($p>0.05$, n=3).

3.3.8. *In vitro activation of the Notch pathway through ligand binding leads to a decrease in CD34 positivity and early erythroid differentiation*

Next, it was questioned if the increased growth potential noted within the initial trypan blue exclusion cell counts could be explained by alteration in cell division kinetics. This was in the knowledge that activation of the Notch pathway through Jagged1 ligand-receptor interaction in other disease processes has been shown to alter symmetric and asymmetric division, which has accounted for proliferation states (Srinivasan et al. 2016; Costa et al. 2016).

In order to investigate the effect of exogenous Notch ligands on the cell division kinetics of $CD34^+$ CP-CML cells, CFSE dye incorporation was used with flow cytometry analysis. Briefly, CP-CML $CD34^+$ cells were thawed or used fresh, stained with CFSE and cultured in the presence of non-stromal or stromal conditions. Following 5 days in culture, cells were harvested for viable cell count and flow cytometry analysis. $CD34^+$ expression was assessed with a monoclonal $CD34^+$ antibody conjugated to the fluorescent dye APC. Only cells in the viable gate (set by FSC and SSC criteria) were included in the analysis. Three samples were analysed.

Although no statistical difference was noted between the three populations, there was a trend towards an increase in the percentage of viable cells in later divisions on stromal co-culture compared to non-stromal conditions, suggesting that cells are protected somewhat to enable increased divisions. However, this was not dependent on activated Notch signalling with no statistical difference noted between OP9GFP and OP9JAG1 co-cultures (figure 3-15).

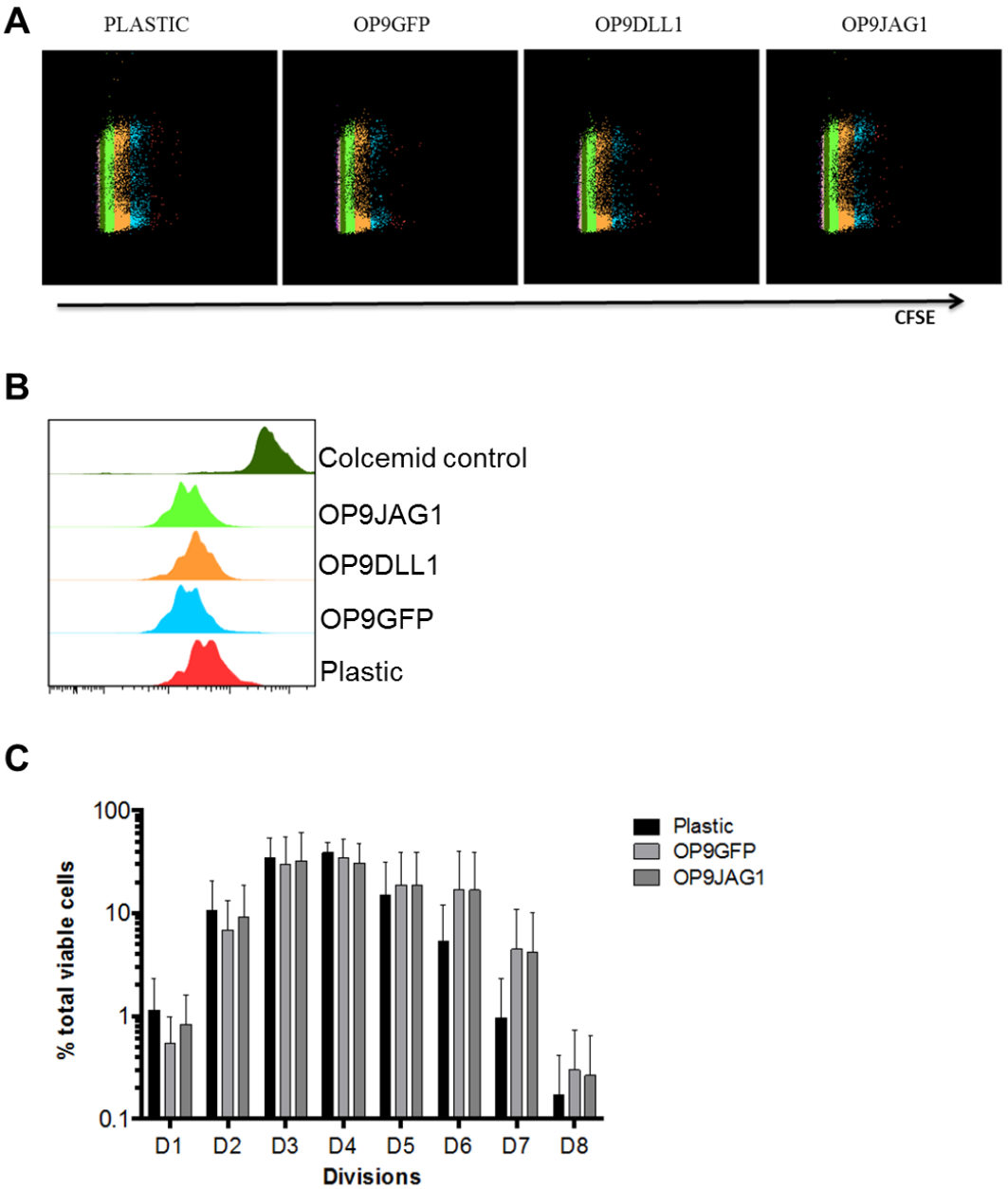

Figure 3 – 15 Stromal co-culture with OP9 cells increases percentage of total viable cells in later cell divisions

$CD34^+$ CP-CML cells were stained with CFSE and cultured with or without stromal for five days before analysis using flow cytometry. (A) Rainbow dot plot representing cells within each cell division for each of the co-culture conditions. (B) Histogram representation of total divisions and colcemid control for each non-stromal and stromal condition. From this visual representation, stromal co-culture can be seen to increase total cell divisions compared to culture on plastic only. (C) Percentage of total viable cells within each division for each condition. The bars represent the mean value from 3 primary samples, while the error bars represent SEM. There was no statistical difference between cell divisions and experimental conditions, but sample variability was extensive.

With a trend towards increased viable cells at day 5 on stromal co-culture with OP9 cells, we hypothesised that this could be extended to a primitive population with the knowledge that if activation of the Notch signalling pathway was altering the balance between the number of self-renewal and commitment divisions that are occurring, there would be less primitive cells at each division gate due the resultant increased differentiation. This was measured through reduced expression of primitive surface phenotypic markers, such as CD34 and, more primitively, CD38.

Within the same samples used above (n=3, $CD34^+$ CP-CML), there was an overall statistically significant decrease in overall expression of CD34 within the viable cell population (figure 3-16A) in cells cultured on OP9JAG1 stroma compared to plastic control. However, due to sample variability, differences in CD34 expression for each cell division were not significant. (figure 3-16B).

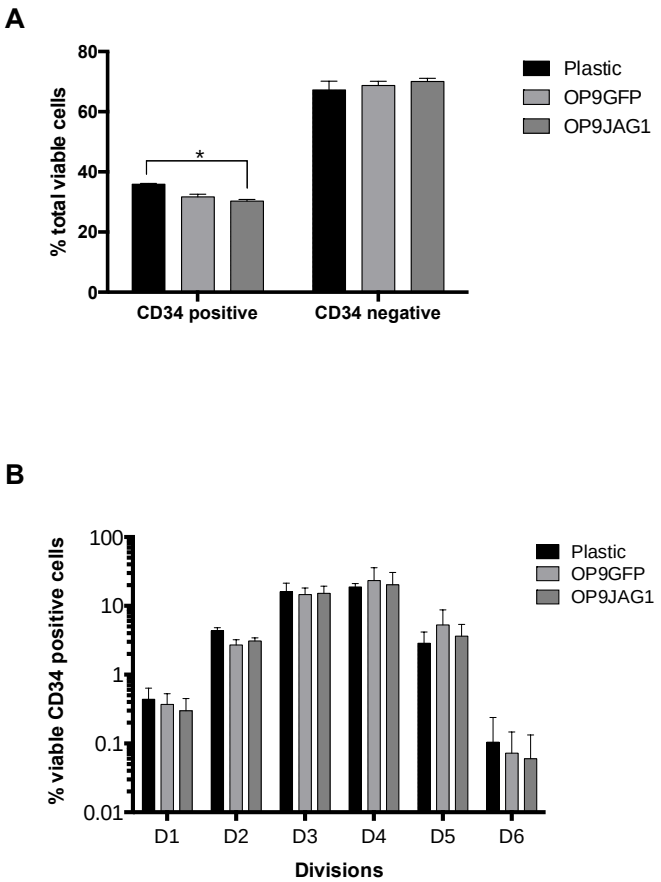

Figure 3 – 16 Activation of Notch through Jagged1 leads to decreased expression of CD34 within a bulk viable cell population

$CD34^+$ CP-CML cells (n=3) were stained with CFSE and cultured with or without stroma for five days before analysis using flow cytometry. (A) Percentage of total viable cells within CD34 positive and negative gates. Error bars represent SEM. There was a statistically significant decrease in CD34 positive cells between plastic and OP9JAG1 co-culture as determined by an unpaired student's t-test ($p<0.05$, n=3). (B) Percentage of total viable cells within each division for each condition. The bars represent the mean value from 3 primary samples, while the error bars represent SEM. There was no statistical difference between cell divisions and experimental conditions, but sample variability was extensive.

This led us to question if the decrease in CD34 positivity in the viable cell populations was secondary to cell differentiation or if there was an element of apoptosis within the samples to account for this loss.

To investigate this, apoptosis was first analysed using annexinV and 7AAD staining in $CD34^+$ samples following 5 days of co-culture with and without stromal conditions (n=3). There was an increase in percentage of cells in late apoptosis in those cultured in the presence of OP9JAG1 compared to OP9GFP; this was evident in both raw and normalised values (figure 3-17); this was not statistically significant.

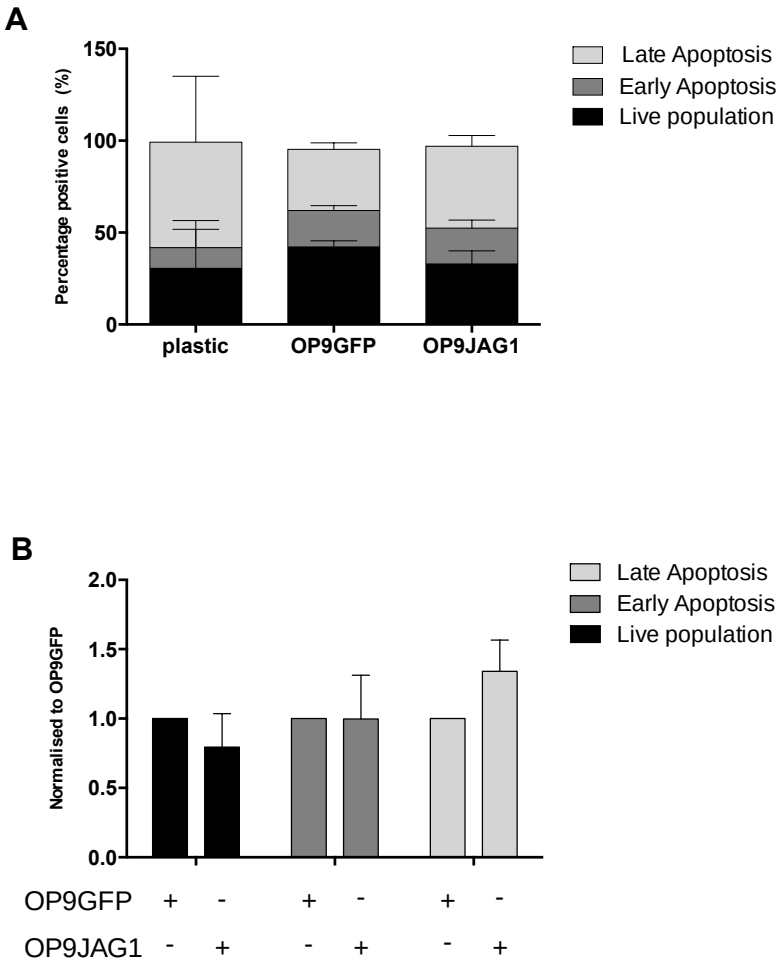

Figure 3 – 17 Activation of Notch through Jagged1 potentially increases late apoptosis

$CD34^+$ CP-CML cells were used from thaw or isolation of $CD34^+$-selected fresh peripheral blood samples and cultured in low growth factor SFM with or without the presence of stromal conditions (n=3). Following five days in culture, following a 2% FBS/PBS wash, 0.5-1x10^5 cells were re-suspended in 100µL of annexinV buffer containing 5µL annexinV conjugated to relevant fluorochrome and 5µL 7AAD. Samples were incubated at room temperature for 15 min in the dark. Following incubation, further 200µL of annexinV buffer was added to the cell suspension and analysis was immediately performed by flow cytometry. Unstained and single stained cells were used to set voltages and compensation. (A) Combined data collection of annexinV/7AAD staining. There was no statistical difference between populations as analysed by a multicomparison ANOVA ($p>0.05$, n=3). (B) OP9JAG1 percentages normalised to OP9GFP to allow for sample variability. There was no statistical difference between populations ($p>0.05$, n=3)

To evaluate if this could be translated to co-culture within a 'human' co-culture model, human MSCs were isolated from CP-CML patient BM and authenticated with the $CD45^{-}CD34^{-}Lin^{-}CD90^{+}CD73^{+}CD105^{+}$ phenotype (figure 3-18A) and positive Nestin IF (chapter 2.3.2.8.2). JAG1 expression was confirmed through IF (figure 3-18B), before $CD34^{+}$ CP-CML samples (n=4) were cultured with and without the presence of MSCs, and with and without 5uM IM. MSC co-culture protected from IM-induced apoptosis, as has previously been described ($p<0.0001$, n=4) (Zhang et al, 2013). There was a modest increase in early apoptosis between untreated non-stromal and stromal co-cultures, which may represent the release of cytokines from the stromal cells or activation through JAG1 (p.0.008, n=4) (figure 3-18C).

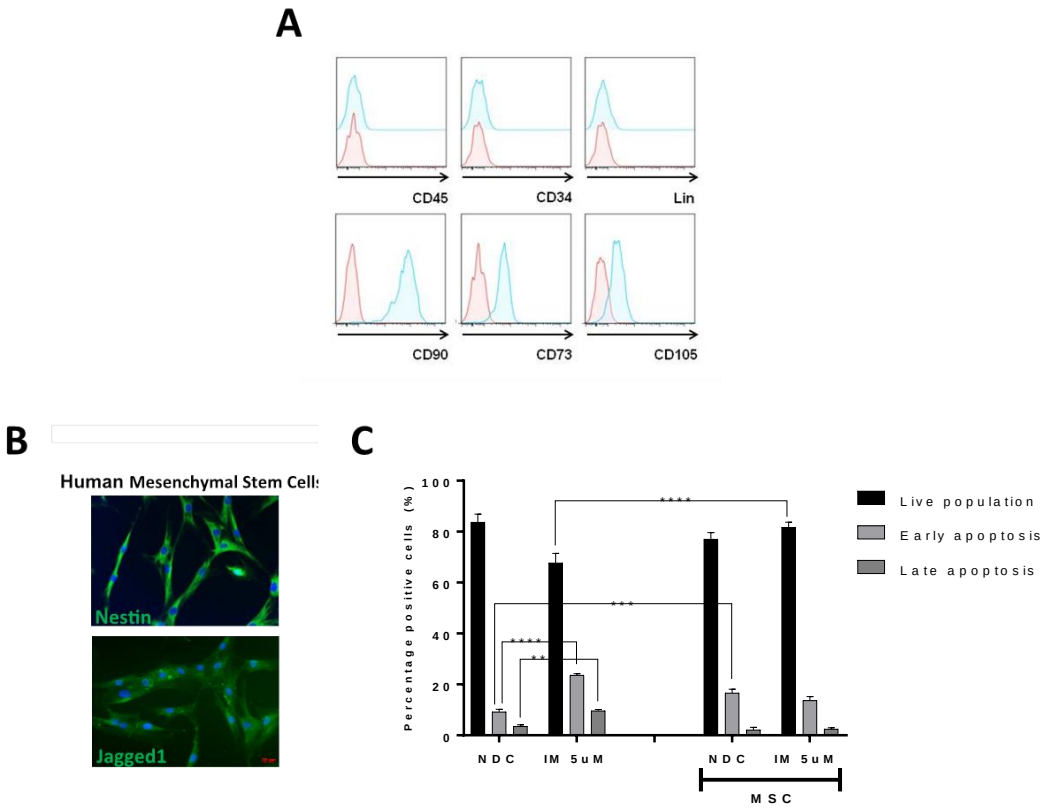

Figure 3 – 18 Co-culture with CP-CML MSCs demonstrated expression of JAG1 and protection against IM.

(A) Human MSCs were isolated from CP-CML patient bone marrow and authenticated with the $CD45^{-}CD34^{-}Lin^{-}CD90^{+}CD73^{+}CD105^{+}$ phenotype. (B) Immunofluorescence demonstrated expression of Nestin and JAG1. (C) AnnexinV and 7AAD analysis of apoptosis by flow cytometry demonstrated protection against IM-induced cell death ($P<0.0001$; viable cells), but an increase in early apoptosis on MSC was noted between untreated cultures (p.0.008, n=4)

In view that there was only a modest increase in apoptotic ability in activation of Notch through JAG1, cell surface expression was next determined for myeloid and erythroid differentiation markers; namely, CD33, CD36, Glycophorin A (GlyA), and CD71. Four $CD34^+$ CP-CML samples were thawed or used fresh from $CD34^+$-isolation and cultured with or without stroma for 5 days. Suspension cells were washed with PBS/2%FBS solution and stained with the appropriate antibody and analysed with flow cytometry, as described within chapter 2.3.2.6. Absolute percentage of positive cells is demonstrated in figure 3-19A. In view of sample variability, values were normalised to the non-stromal control (i.e. plastic culture) (figure 3-19B). This demonstrated that there was no significant change in CD33 or CD36 expression with the addition of co-culture and exogenous activation of Notch through ligand binding with JAG1. However, there was an increase in expression of both CD71 and GlyA with the addition of stromal co-culture, specifically JAG1. This was statistically significant for CD71 ($p<0.05$, $n=4$), where a significant increase in expression was noted in association with activation of Notch through JAG1 interaction. GlyA expression was not significantly increased, suggesting that although the samples had initiated erythroid differentiation, they were halted at an immature erythroid state.

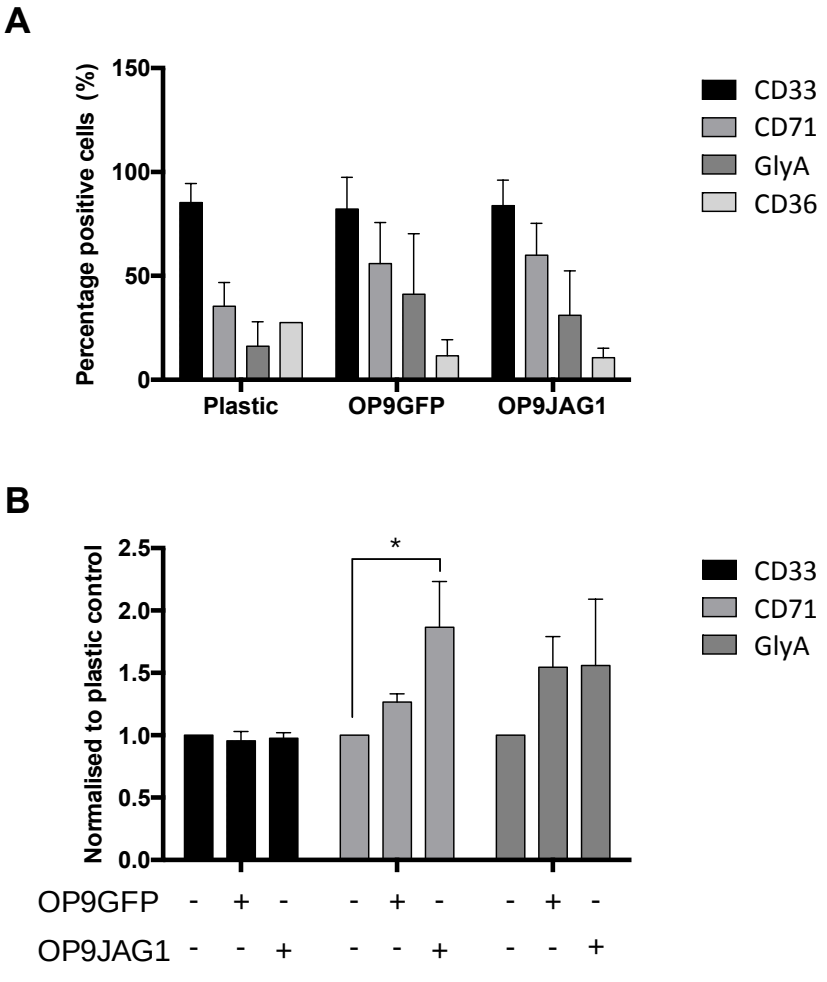

Figure 3 – 19 In vitro activation of Notch through JAG1 induces early differentiation of CD34+ CP-CML primary samples

Four CD34+ CP-CML samples were thawed or used fresh from CD34+-isolation and cultured with or without stroma for 5 days. Suspension cells were washed with 2%FBS/PBS solution and stained with the appropriate antibody and analysed with flow cytometry, as described within chapter 2.3.2.6. (A) Absolute percentage of positive cells within each experimental arm for each cell surface marker. No statistical difference was noted between samples. (B) values were normalised to the non-stromal control. There was no significant change in CD33 expression with the addition of co-culture and exogenous activation of Notch through ligand binding with Jagged1. However, there was an increase in expression of both CD71 and GlyA with the addition of stromal co-culture. There was a statistically significant increase in CD71 expression ($p<0.05$, Tukey's multicomparison ANOVA) with activation of Notch.

If short-term culture, allowed for early myeloid/erythroid differentiation, it was hypothesised that long-term differentiation assays would yield an increase in erythroid colony formation with the exogenous activation of Notch signalling through co-culture. CFC assays are clonal progenitor assays that measure the proliferation capacity and multi-potency of haemopoietic progenitors. $CD34^+$ CP-CML cells (n=5) following co-culture in non-stromal and stromal conditions were inoculated into a semi-solid culture medium containing a standard growth factor cocktail. Following culture for 12 days, colonies were evaluated and counted. Each condition was set up in duplicate and mean between plates calculated. There was a huge variation between samples, but no statistical change was noted between OP9GFP and OP9JAG1 ($p=0.7$, n=5), and furthermore between the non-stromal and OP9JAG1 experimental arms ($p=0.068$, n=5). No difference noted in GM or GEMM colonies (data not shown). Colonies were BCR-ABL positive in all conditions, as determined by FISH (figure 3-20).

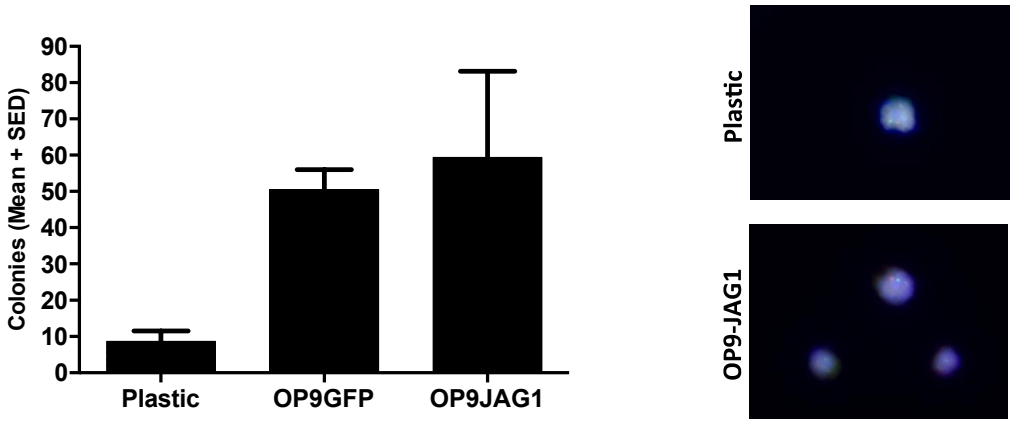

Figure 3 – 20 Notch activation within CD34+ CP-CML leads to a trend towards increased erythroid colony formation, although this was not statistically significant.

CFC assays were performed with $CD34^+$ CP-CML cells (n=5) following co-culture in non-stromal and stromal conditions. There was a huge variation between samples, but no statistical change was noted between OP9GFP and OP9JAG1 ($p=0.7$, n=5), and furthermore between the non-stromal and OP9JAG1 experimental arms ($p=0.068$, n=5). Colonies were BCR-ABL positive in all conditions, as determined by FISH.

To corroborate the possible involvement of Notch activation through JAG1 interaction in early erythroid differentiation, gene expression was investigated in primary $CD34^+$ CP-CML patient samples (n=5). Using Fluidigm technology, mRNA expression of baseline/plastic culture, OP9GFP co-culture and OP9JAG1 co-culture after 5 days was compared to normal peripheral blood $CD34^+$ samples. Relative gene expression levels were determined using the average normal $CD34^+$ value as a calibrator, calculated using the ΔΔ CT method, using an average of six housekeeping genes as reference. The patients had had no TKI treatment prior to sample collection and analysis.

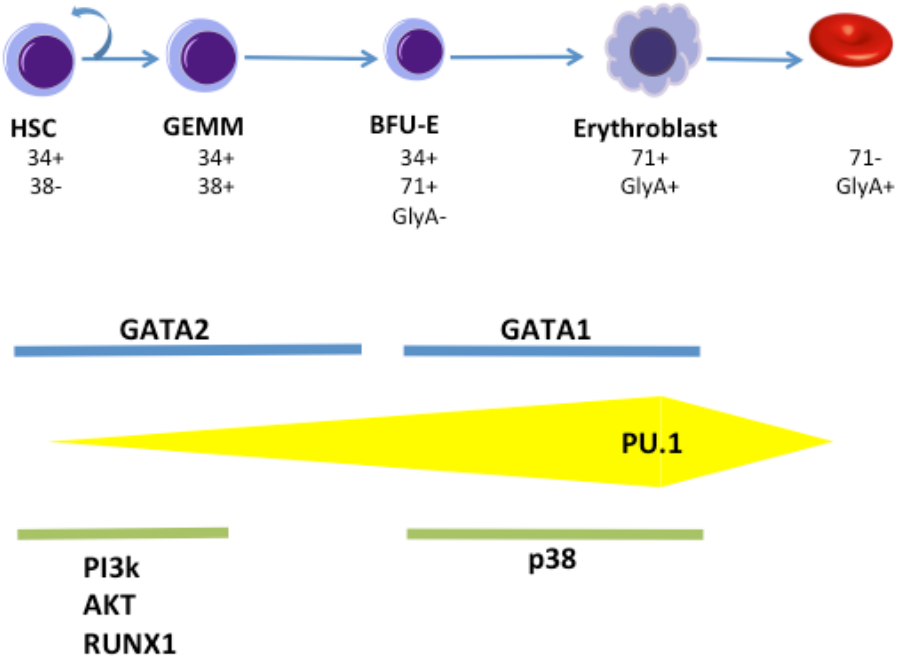

Figure 3 – 21 Schematic representation of erythroid differentiation and associated gene changes.
Schematic representation of erythroid differentiation according to cell surface expression. Regulatory genes are depicted dependent on activity within the differentiation path. PU.1 is a key regulatory gene within erythroid function, with noted increased expression driving towards an erythroblast phase (Chen et al, 2008).

Previous data available on gene transcription involved in differentiation through myeloid and erythroid phenotype was utilised to identify the major players in early erythroid differentiation (figure 3-21). There was a statistically significant increase in expression of key genes involved in early erythroid differentiation, namely, *p38* ($p<0.05$ between baseline and OP9JAG1 culture) and *PU.1* ($p<0.05$ between baseline and OP9JAG1 culture), which has known involvement in development of erythroblasts (figure 3-22). Furthermore, there was little change in gene expression in regulators of the stem cell phenotype, namely *GATA2*, *NFKB1*, and *PI3K*. Interestingly, there was a statistically significant increase in *TP53* between culture on plastic alone and OP9JAG1

co-culture ($p<0.05$). There was no statistical change between OP9GFP and OP9JAG1 co-culture, but this may be explained by the amount of JAG1 that is present in OP9GFP compared to OP9JAG1 stromal cells (figure 3-22).

In turn, these results, suggest the hypothesis that activation of Notch through Jagged1 in CP-CML $CD34^+$ cells may lead to halted early erythroid differentiation with a possible increase in apoptosis. However, the difficulty in assessing Notch activation in $CD34^+$ CP-CML cells is that the influence of the pathway is likely to change between a self-renewing population and a more mature population. Therefore, it is not surprising that experiments using bulk $CD34^+$ cells produce large inter-patient variability, with a non-conclusive role of the pathway in short term *in vitro* culture.

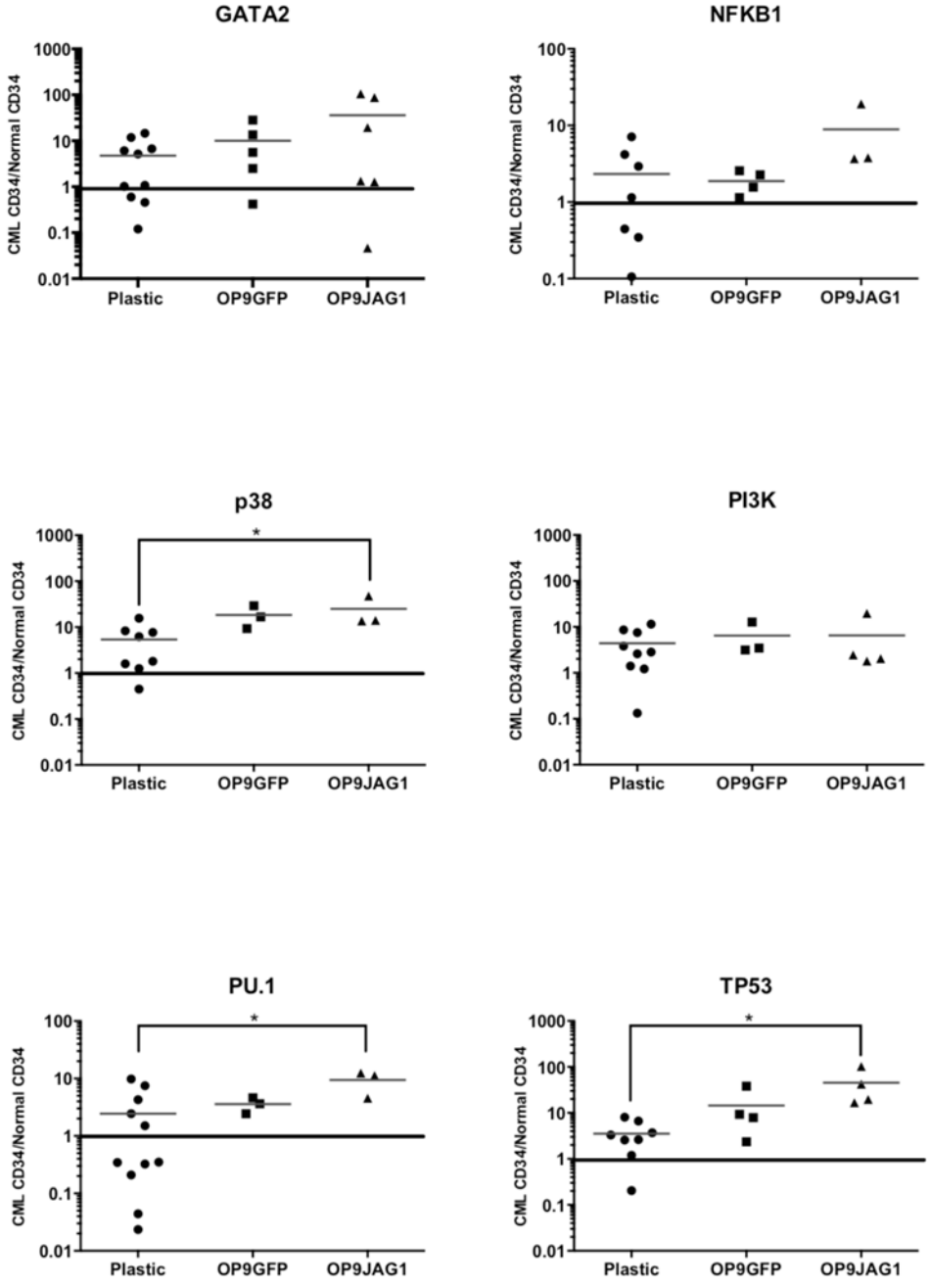

Figure 3 – 22 Gene expression of regulatory erythroid differentiation genes confirms functional data

Using Fluidigm technology, mRNA expression of culture on plastic, OP9GFP co-culture and OP9JAG1 co-culture after 5 days was compared to normal peripheral blood CD34+ samples. Relative gene expression levels were determined using the average uncultured normal CD34+ value as a calibrator calculated using the ΔΔ Ct method, using an average of six housekeeping genes as reference. There was a statistically significant increase in overexpression of key genes involved in early erythroid differentiation, namely, *p38* ($p<0.05$ between baseline and OP9JAG1 culture) and *PU.1* ($p<0.05$ between baseline and OP9JAG1 culture), which has known involvement in development of erythroblasts (figure 3-22). Furthermore, there was little change in gene expression in regulators of the stem cell phenotype, namely *GATA2*, *NFKB1*, and *PI3K*. Interestingly, there was a statistically significant increase in *TP53* between baseline and OP9JAG1 co-culture ($p<0.05$). There was no statistical change between OP9GFP and OP9JAG1 co-culture.

3.3.9. *In vitro activation of the Notch pathway has differing function in short and long-term culture, and in immature and mature populations*

To address if Notch signalling impacts stem and progenitor populations differently, CP-CML patient samples (n=3) were sorted into immature and mature cell populations, namely $Lin^-CD34^+CD38^-$ and $Lin^-CD34^+CD38^+$, using FACS. In brief, fresh or recovered $CD34^+$ cells were washed and resuspended in 2%FBS/PBS. Cells were counted and stained with appropriate antibodies for 30 min at room temperature in the dark. $2x10^4$ cells were used for relevant single colour controls to define positive and negative staining for each marker and to set compensation. Stained cells were washed and filtered through a 0.22uM filter prior to sorting with a BD FACS Aria with Diva software. Figure 3-23 demonstrates a representative example for the sorted populations. All CML samples were assessed for Ph+ status, confirmed by dual colour FISH.

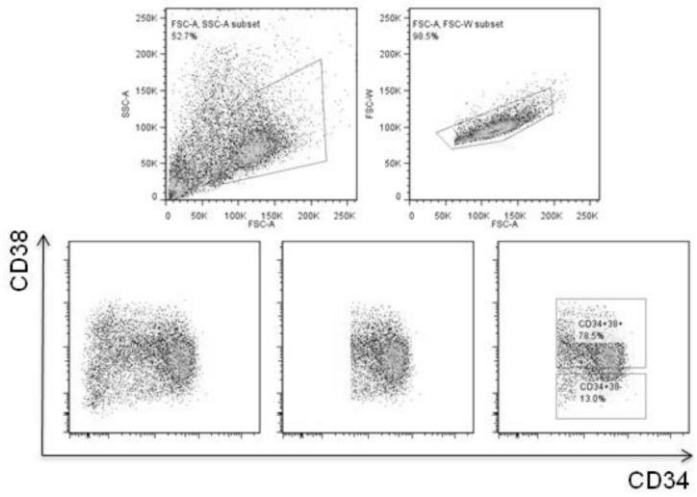

Figure 3 - 23 Representation of flow activated cell sorting to Lin-CD34+CD38- population

Representative example of FACS sorting to $Lin^-CD34^+CD38^-$ cell populations.

Following cell sorting, cells were co-cultured on non-stromal or stromal conditions for 5 days. At day 5, there was a statistically significant increase in cell growth of the $CD34^{+}CD38^{+}$ population between the non-stromal (i.e. plastic) and OP9JAG1 stromal conditions ($p<0.05$, n=3). There was a trend towards increased growth in the OP9JAG1 experimental arm compared to OP9GFP, although this was not significant, likely in keeping with basal levels of JAG1 on the OP9GFP stroma. This was, however, not statistically significant (figure 3-24). Within the $CD34^{+}CD38^{-}$ experimental arm, there was no statistical difference in trypan blue exclusion cell counts over the five days analysed, but there was a trend towards reduced cell counts in the OP9JAG1 arm compared to the OP9GFP arm (figure 2-24).

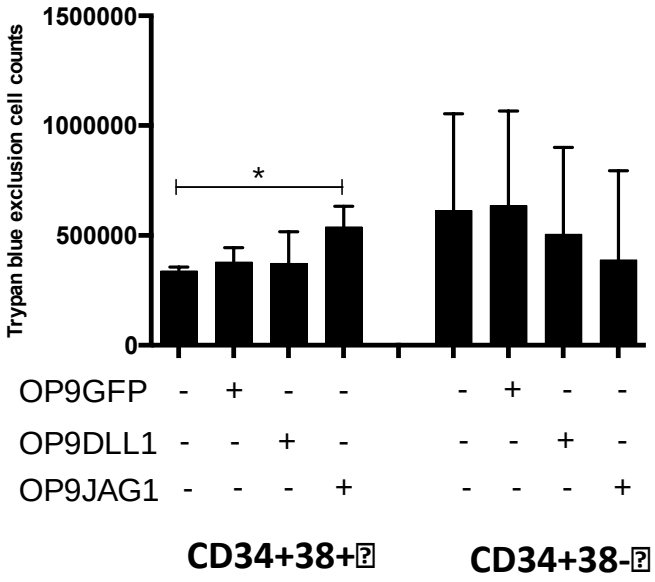

Figure 3 – 24 *In vitro* activation of Notch increases growth potential in mature CP-CML populations, and not immature populations
Following FACS sorting, $CD34^{+}$ CP-CML cells were cultured with or without the presence of stroma. At day 5, there was a statistically significant increase in cell growth of the $CD34^{+}CD38^{+}$ population between the non-stromal (i.e. plastic) and OP9JAG1 stromal conditions ($p<0.05$, n=3). Within the $CD34^{+}CD38^{-}$ experimental arm, there was no statistical difference in trypan blue exclusion cell counts.

In view of the decreased trend in growth potential in the $CD34^{+}CD38^{-}$ population with OP9JAG1 co-culture, apoptotic ability was next analysed using annexinV and 7AAD staining between the stromal conditions in the mature and immature experimental arms. There was no statistical change within the $CD34^{+}CD38^{+}$ populations, but an increase trend in both early and late apoptosis with the $CD34^{+}C38^{-}$ ($p>0.05$, n=3) (figure 3-25). This was important because it suggested that activation of the pathway within an immature LSC population was toxic to the cells in short-term *in vitro* culture. In view

of this, it was hypothesised that Notch activation through OP9JAG1 may lead to decrease in self-renewal capacity in long-term assays.

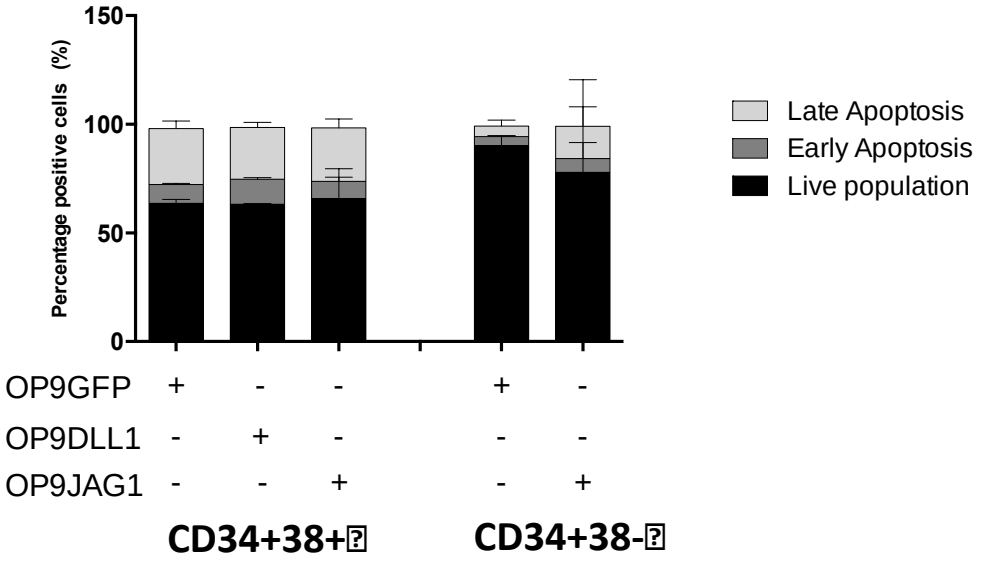

Figure 3 – 25 *In vitro* activation of Notch increases apoptotic ability in immature CP-CML populations

$CD34^+$ CP-CML cells were sorted into $CD34^+CD38^+$ and $CD34^+CD38$- populations and cultured in low growth factor SFM with or without the presence of stroma (n=3). Within each co-culture experiment, OP9 stromal cells only underwent a maximum of 8 passages before use. OP9 stromal cells were seeded at a 1 in 24 ratio with suspension cells (i.e. 1 stromal cell per 24 suspension cells) 24 hours prior to co-culture for 5 days. Following five days in culture, following a 2% FBS/PBS wash, 0.5-1x10^5 cells were re-suspended in 100µL of annexinV buffer containing 5µL annexin-V conjugated to relevant fluorochrome and 5µL 7AAD. Samples were incubated at room temperature for 15 minutes in the dark. Following incubation, further 200µL of annexinV buffer was added to the cell suspension and analysis was immediately performed by flow cytometry. Unstained and single stained cells were used to set voltages and compensation. There was no statistical change within the $CD34^+CD38^+$ populations, but an increase trend in both early and late apoptosis with the $CD34^+C38^-$ when co-cultured with OP9JAG1 cells ($p>0.05$, n=3).

Self-renewal activity can be measured both *in vitro* and *in vivo* in assays that approximate stem cell activity in the original population by observing the behaviours of their progeny under various conditions. As discussed within the methods section, the most robust demonstration and quantification of self-renewal activity is from limited dilution xenograft transplantation. However, within our model of exogenous activation in an immature phenotype, this is impractical and infeasible. *In vitro* assays offer a surrogate measure of self-renewal activity and allow for small cell numbers as well as co-culture conditions. To question if exogenous activation would affect the long-term culture ability of an immature stem cell population, LTC-IC assays were used. Following extended culture over 6 weeks in a supportive stromal co-culture, cells with residual colony forming capacity can be assessed and their prevalence in the initial sample inferred.

In brief (figure 3-26), CP-CML $Lin^{-}CD34^{+}CD38^{+}$ and $Lin^{-}CD34^{+}CD38^{-}$ were co-cultured for 7 days on non-stromal and stromal conditions as previously described. To ensure no OP9-effect, cells were also cultured on plate-bound recombinant JAG1; this allowed for true representation of JAG1 exogenous activation without stromal influence. Hygromycin and geneticin-selected M210B4 and SL-SL fibroblast stromal cells were irradiated at 80Gy 24 hours prior to use within the assay, before being plated on gelatin-coated plates at a confluence of each cell type adjusted to $1.5x10^{5}$/ml. 50,000 of the cultured CP-CML-selected cells were suspended in 1ml myelocult/hydrocortisone media in duplicate, and then seeded onto the M210B4/SL-SL irradiated stroma for 6 weeks. Weekly, 500ul media was carefully changed with fresh myelocult/hydrocortisone media ensuring that the stromal and suspension cells were not disturbed. Following 6 weeks in culture, cells were harvested and inoculated into methocult as per the CFC assay protocol, before colonies counted between 12-14 days following harvest.

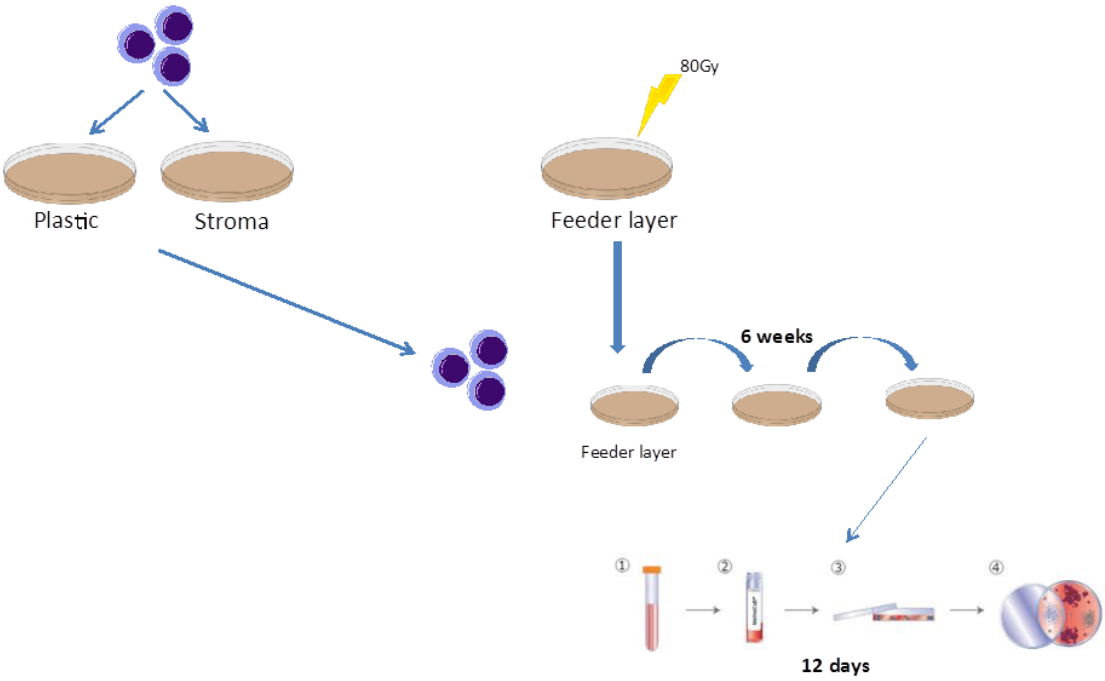

Figure 3 – 26 Schematic of long-term culture initiating cell assay experimental design

Schematic representation of the LTC-IC assay, where suspension cells (namely, sorted populations of CML cells) are cultured in the presence of an irradiated stromal layer that is necessary to maintain myelopoieiss. Cells are cultured under specific conditions for 6 weeks prior to assessment with colony forming cell assays.

Three CP-CML samples were analysed, with 4 replicates per experimental arm. Colony numbers were counted following 12 -14 days in methocult. Data was presented normalised to the plastic control. Within the $Lin^{-}CD34^{+}38^{+}$ population, there was no significant reduction in colony number in the samples cultured on OP9GFP or OP9JAG1 stroma. On plate-bound recombinant JAG1 co-culture there was a decrease in colony number, although this was not statistically significant. The addition of DAPT in the initial co-culture with OP9GFP and OP9JAG1, rescued the effect on colony formation in those that were co-cultured with OP9JAG1 stroma (figure 3-27).

Within the $Lin^{-}CD34^{+}38^{-}$ experimental arm there was no change in colony formation between non-stromal conditions and co-culture with OP9GFP. However, there was a statistically significant reduction in colony formation between both plastic and OP9GFP compared to OP9JAG1 or recombinant JAG1 co-culture ($p<0.05$ in both comparisons) (figure 3-27). This suggested that short-term activation of Notch in *in vitro* culture led to a statistically significant reduction in self-renewal and the ability to form colonies, and therefore, suggests that short-term activation of Notch may represent a therapeutic modality towards the CML LSC.

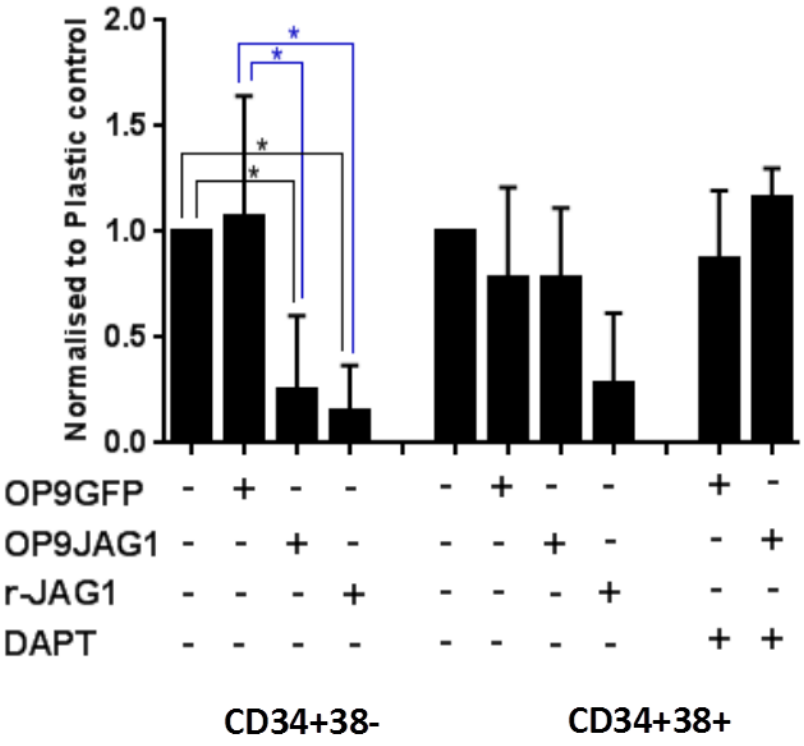

Figure 3 – 27 *In vitro* activation of Notch through JAG1 significantly decreases colony formation in LTC-IC assays in an immature population, suggesting a possible therapeutic target towards the CP-CML LSC

3 CP-CML samples were used in analysis, with 4 replicates per experimental arm. Colony numbers were counted following 12 -14 days in methocult. Data was presented normalised to the plastic control. Within the $Lin^{-}CD34^{+}38^{+}$ population, there was no significant reduction in colony number in the samples cultured on OP9GFP or OP9JAG1 stroma. On plate-bound recombinant JAG1 co-culture there was a decrease in colony number, although this was not statistically significant. The addition of DAPT in the initial co-culture with OP9GFP and OP9JAG1, rescued the effect on colony formation in those that were co-cultured with OP9JAG1 stroma. Within the $Lin^{-}CD34^{+}38^{-}$ experimental arm there was no change in colony formation between non-stromal conditions and co-culture with OP9GFP. However, there was a statistically significant reduction in colony formation on both plastic and OP9GFP compared to OP9JAG1 or recombinant JAG1 co-culture ($p<0.05$ in both experimental arms as per ANOVA).

3.4. Discussion

For the first time, within this chapter, we present data that suggests a functional action of Notch signalling within CP-CML, and confirm previously suggested findings that there is, indeed, a role for Notch signalling within myeloid disease.

Using $CD34^+$ CP-CML primary samples, it was demonstrated that Notch receptors were present, but not active, within CP-CML at both mRNA and protein level. This was shown through mRNA expression of the Notch receptors, *NOTCH1* and *NOTCH2*, which were significantly overexpressed within a CP-CML population. Protein expression of the extracellular receptor was validated using IF. The pathway was inactive, as evidenced through the expression of the downstream targets, *HES1* and *HIF1A*, and with absent expression, through IF and western blotting, of val1744, which represents the cleaved Notch receptor upon canonical pathway activation (Chiang et al, 2013). This was again shown on evaluation of microarray datasets, which showed the pathway was globally downregulated. I next validated this gene and protein expression data through functional evaluation of the pathway on non-stromal culture conditions (i.e. plastic culture) with and without the addition of the pharmacological Notch inhibitor, DAPT. Addition of DAPT on non-stromal *in vitro* culture conditions did not functionally alter cell growth, cell cycle, or apoptosis in $CD34^+$ CP-CML samples, suggesting that Notch signalling is silenced in $CD34^+$ CP-CML and excludes a "positive" role for Notch signalling in CML disease progression or treatment resistance.

Overexpression of Notch receptors has previously been described in CP-CML (Aljedai et al, 2015). However, within this paper, it was suggested that the pathway was active within the disease subset, through expression of *HES1* transcripts compared to housekeeping genes in 4 samples ($p<0.05$). This, however, was not consistent through samples, nor consistent within the subpopulations analysed. Furthermore, the overexpression of *HES1* was not described at a protein level and the protein expression of the receptor was identified using a monoclonal antibody that targets the extracellular aspect of the receptor, which does not confirm activation, merely the presence of an extracellular receptor. Our results were more consistent with the data described in AML, where it has been shown that there is an upregulation of *NOTCH2*, but with no confirmed activation at basal cell level (Klinakis, 2011; Lobry et al, 2013; Oh et al, 2013).

Analysis of global gene expression of Notch signalling components demonstrated no statistical correlation with *BCR-ABL* expression at 12 and 18 months. However, *FBXW7* was shown to be a prognostic indicator between good and poor responders in accordance to ELN guidelines (Baccarani et al, 2013). *FBXW7* is not unique to Notch signalling and has been shown *in vivo* to target many proto-oncogenes, growth promoters, and anti-apoptotic molecules. Furthermore, *FBXW7* has been shown to have an indispensable role in the maintenance of adult HSC quiescence (Matsuoka et al, 2008; Thompson et al, 2008). Deletions of Fbxw7 in HSCs and CML LSCs have been shown to lead to c-Myc accumulation, activation of the TP53 signalling pathway, aberrant cell cycle entry and eventual exhaustion (Reavie et al, 2013; Reavie, 2010). TP53 mutations can accompany disease progression in human CML and TP53 loss in some cases impedes the anti-leukaemic response to BCR-ABL inhibition (Kelman et al, 1989; Wendel et al, 2006), suggesting that loss of TP53 in some tumours could constitute an adaptive response to the increase in the levels of c-Myc during CML progression.

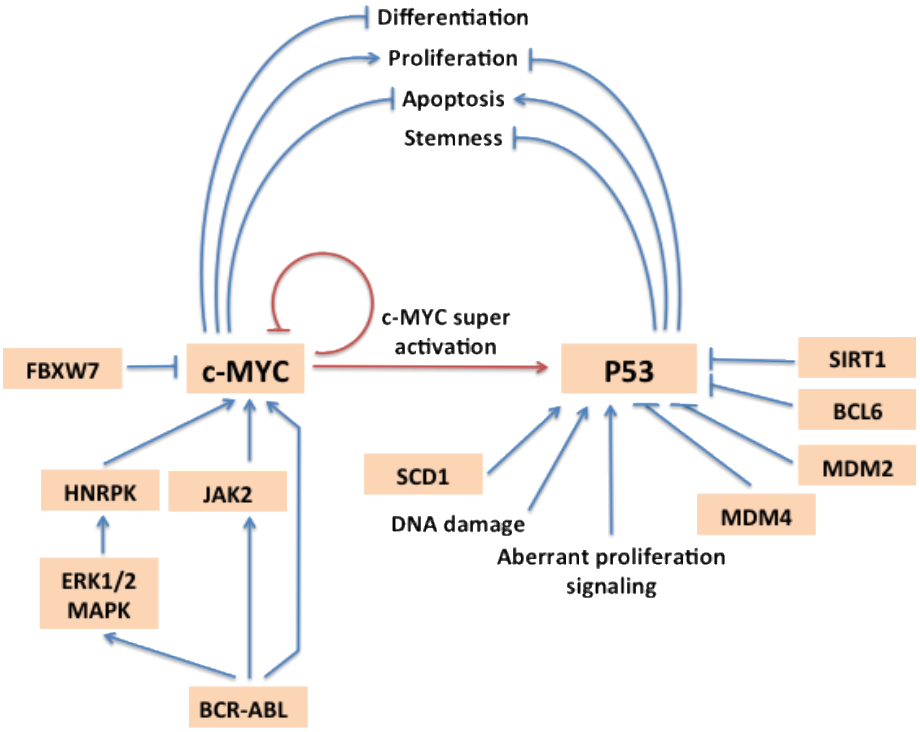

Figure 3 – 28 Schematic representation of c-MYC and p53 within CP-CML

Recently, published work within the Holyoake group has highlighted the association between c-Myc and p53 within CML LSCs, functioning as central hubs within the regulatory process of disease maintenance (Abraham et al, 2016) (figure 3-28). Using clinically tractable inhibitors, namely the HDM2 inhibitors, RG7112 (Roche), and BET inhibitors, CPI-203 and CPI-0610 (Constellation Pharmaceuticals), it was shown that

selectively targeting these transcription factors could lead to elimination of the CML LSC both *in vitro and in vivo*. Our data, perhaps, highlights further the potential role now of FBXW7 as a therapeutic modality within CP-CML in the eradication of the LSCs, or at least in the identification of those who will inevitably be poor responders in accordance with *BCR-ABL* activity.

In view that the CP-CML $CD34^+$ cells specifically and abundantly express the Notch receptor, *NOTCH2*, and that the pathway was confirmed to be functionally inactive at basal state (i.e. on plastic culture without stromal support), it was then hypothesised that Notch signalling could be reactivated through exogenous activation in CP-CML $CD34^+$ cells upon ligand binding to the Notch receptor. As has been described in detail within the introductory chapter, multiple cell types within the BM microenvironment express Notch receptors and ligands. This could be of particular importance in CML, where emerging evidence indicates that not only do the CML LSCs strongly rely on the BM niche for their self-renewal and proliferation, but they also modify the BM to their advantage (Bhatia et al, 1995; Krause et al, 2013b). The BM contains an endosteal osteoblastic niche, which supports quiescence and self-renewal and a more vascular/peri-sinusoidal niche that promotes proliferation and differentiation; both associate with supporting MSCs. Notch plays an important role in osteogenesis and angiogenesis, and can influence osteoblast differentiation positively or negatively (Ramasamy et al, 2014). Despite the abundance of data on Notch and HSC function, controversy remains regarding the precise role of Notch signalling in normal physiology owing to the intricacies of some Notch-related phenotypes (Dahlberg et al, 2011; Delaney et al, 2005). For example, the effects of Notch ligand activation vary based on the relative density of Notch surface receptors (Delaney et al, 2005). Also, there is precedence for differential effects by various Notch ligands, with distinct roles of JAG1/2 versus DLL in lymphoid development. For example, Delta1-induced signalling completely inhibits the differentiation of human haemopoietic progenitors into the B cell lineage and promotes the emergence of cells with a phenotype of T cell/natural killer (NK) precursors, while JAG1-induced signalling does not disturb B or T cell/NK development (Jaleco et al, 2001). It was, therefore, decided to focus our experimental upregulation of the Notch pathway through JAG1 and DLL1 ligands utilising an OP9 co-culture system and plate-bound recombinant ligand approach in an *in vitro* setting. This was of particular importance as manipulation of Notch ligands influences both haemopoietic and mesenchymal stromal cell fates and ultimately, alters the microarchitecture of the BM microenvironment, thereby altering the dynamics of the

same regulatory interactions under investigation. We first needed to understand how upregulation through ligand binding could alter the myeloid $CD34^+$ cells before trying to tackle a 3D *in vitro* or *in vivo* approach.

Our data demonstrated that upon JAG1 activation of the Notch pathway, as demonstrated by differences between OP9GFP and OP9JAG1 experimental arms, there was increased growth potential of $CD34^+$ cells, although this was not explained by CFSE assays to confirm proliferation rates, nor change in cell cycle distribution. This can, in part, be explained by the basal concentration of JAG1 within the OP9GFP experimental arm. Activation of the pathway was confirmed at gene level with increased expression of *HES1* and the val1744 protein in both the OP9GFP and OP9JAG1 experimental arms. To overcome the basal levels of JAG1 in the OP9GFP cell line, we adopted two approaches: the first was to assess all experiments against a non-stromal control, and then compare to plate-bound recombinant JAG1 in isolated experiments. Recombinant JAG1 allowed for assessment of the influence of Notch activation negating the contributing factors from stromal cells, such as expression of other self-renewal pathways and cytokine release.

CFSE assays showed a number of interesting findings. Firstly, it demonstrated an increased trend towards percentage of viable cells in later division on stromal co-culture compared to non-stromal conditions, suggesting that in stromal conditions, cells are protected somewhat to enable increased divisions. This was again confirmed within MSC experiments where co-culture on MSC led to protection of $CD34^+$ against TKI-induced apoptosis. Within our experiments, this was not clearly dependent on activation of Notch through JAG1 expression. This suggests that Notch activation is not solely responsible for protection of LSC within disease states. Previously, it has been suggested that this protection of CML stem and progenitor cells from TKIs is through a close interplay between N-cadherin and the Wnt pathway (Zhang et al, 2013), amongst other pathways (Agarwal & Bhatia, 2015; Perrotti et al, 2016; Toofan et al, 2014; Zhou et al, 2016). Secondly, this data demonstrated that globally, JAG1-induced Notch activation led to a decrease in the percentage of total viable $CD34^+$ cells. This is perhaps, not surprising, in that Notch activation may be altering the balance between the number of self-renewal cells and commitment divisions that are occurring. The normal function of Notch within HSCs has previously been discussed, but to recap, this is largely dependent on activating ligand strength that controls specifying haemopoietic fate (Gama-Norton et al, 2015). It has been suggested that canonical Notch signalling is

dispensable for the maintenance of HSCs in the adult BM under physiologic conditions (Maillard et al, 2008), with further support found in the conditional deletion of *Notch1* or *Notch1* plus *Notch2* under the control of the interferon-dependent expression of Mx-Cre that specifically and exclusively affected lymphoid differentiation, but not other haemopoietic lineages (Besseyrias et al, 2007; Radtke et al, 1999).

This data led us to establish that upon JAG1 activation, cells undergo a degree of apoptosis, but more significantly, it causes a push towards early erythroid differentiation that is blocked in an immature state (i.e. proerythroblast phase). This was determined through cell surface identification of erythroid markers. There was an increase in expression of both CD71 and GlyA with the addition of stromal co-culture. This was only statistically significant with CD71 surface expression. As CD33 expression was maintained, it suggested that although the samples had initiated differentiation, they could not progress beyond an immature phenotype. To corroborate the possible involvement of Notch activation through JAG1 interaction in early differentiation, gene expression was investigated in primary $CD34^+$ CP-CML patient samples. There was a statistically significant increase in overexpression of key genes involved in early erythroid differentiation, namely, *p38* ($p<0.05$) and *PU.1* ($p<0.05$), which have notable involvement in development of (pro)erythroblasts. Furthermore, there was little change in gene expression in regulators of the stem cell phenotype, namely *GATA2* and *NFKB1*. This is the first time this has been proposed within a CML phenotype.

Literature evidence remains conflicting regarding the role of Notch activation in normal differentiation models (Schroeder et al, 2003; Tan-Pertel et al, 2000; Zeuner et al, 2011). Initial *in vitro* studies suggested that Notch signalling accelerated myeloid differentiation (Schroeder et al, 2003; Tan-Pertel et al, 2000), with subsequent studies contesting this conclusion, with one study suggesting that Notch can suppress myelopoiesis *in vitro* (de Pooter et al, 2006) and further studies suggesting it can induce a megakaryocyte differentiation. Within an AML subset, Notch activation through DLL4 led to leukaemia initiating cells differentiating into more mature cell types with morphology resembling macrophages or dendritic cells, and an increased proportion of cells undergoing apoptosis (Lobry et al, 2013). Erythropoiesis involves the progressive differentiation of uncommitted progenitors to mature erythrocytes. However, not only differentiation but also apoptosis participates in the regulation of cell survival and mature red cell turnover. The amount of Epo mainly dependent on hypoxia, is one of the key factors in controlling the survival of erythroid cells. Other transcription factors

including *GATA1* and, more recently, *TP53* have been implicated in regulating apoptosis at different stages of erythroid maturation (Robert-Moreno et al, 2007); again consistent with the data presented within this chapter.

The difficulty in assessing Notch activation in $CD34^+$ CP-CML cells is that the influence of the pathway is likely to change between a self-renewing population and a more mature population. Therefore, it is unsurprising that experiments using bulk $CD34^+$ cells produce large inter-patient variability, with a non-conclusive role of the pathway in short term *in vitro* culture.

Analysis of sorted immature and mature populations, suggested that the cellular function of Notch through Jagged1 interaction was variable dependent on cell maturity, with activation in mature progenitors leading to increased growth by trypan blue exclusion cell counts, and within an immature population, leading to apoptosis. We next questioned if exogenous activation would affect the long-term culture ability of an immature stem cell population; LTC-IC assays were used. Notably, there was a statistically significant reduction in colony formation between both plastic and OP9GFP compared to OP9JAG1 or recombinant JAG1 co-culture. This suggested that short-term activation of Notch in an *in vitro* co-culture system led to a statistically significant reduction in self-renewal and the ability to form colonies. This has not previously been described, and although it provides a potential therapeutic role in the eradication of the LSC, I have failed to present the mechanism by which this occurs. A hallmark feature of adult stem cells is their relative proliferative quiescence. Although these cells are considered immortal, HSCs can exhaust and this is frequently hastened by proliferative stress. For example, HSCs are capable of reconstituting the haemopoietic system following transplantation. However, after serial transplantation, HSCs gradually decline and are eventually exhausted. I propose that activation of the Notch pathway through the JAG1 protein leads to increased cell growth, differentiation and apoptosis in CP-CML cells, that ultimately leads to LSC exhaustion and a decrease in colony formation.

3.5. Future Work

In order to evaluate the function of Notch activation as a therapeutic modality, we have firstly embarked on translating the *in vitro* findings to an *in vivo* setting. This will allow for evaluation within a BM microenvironment. With thanks to the Aifantis laboratory (NYU), we have utilised the ROSA26-ICN2 murine model, which were generated by insertion of a loxP flanked splice acceptor NEO-ATG cassette with two polyA sites followed by ICN2 into the ROSA26 locus, allowing the ROSA26 promoter to drive expression of the NEO-ATG cassette. Cre-recombinase–mediated excision of NEO-ATG results in use of the splice acceptor in the ICN2 cassette and irreversible expression of the transgene (Lobry et al. 2013; Klinakis et al. 2011). Following confirmed activation of Notch, animals will be sacrificed and BM cells retrovirally transduced with *BCR-ABL* as described (Mizuno et al. 2008; Li et al. 1999), and monitored for leukaemic progression.

In order to prove that stem cell exhaustion is the mechanism by which Notch activation reduces LSC colony formation long-term, serial BM transplantation into lethally irradiated mice would be undertaken. However, this is most likely going to be inhibited by cell numbers needed, as one would have to isolate the LSC population in view of the proposed dual functions of Notch. A simpler approach in an *in vitro* setting is to use serial CFC assays following LTC-IC assays to mimic the *in vivo* approach. This would provide evidence that the cells are becoming more exhausted within the Notch activated samples (i.e. colonies will not form in serial CFC assays in the Notch activated experimental arm).

Further to this, we have recently set-up a 3D *in vitro* model to allow for evaluation of cell interactions between different niche components. This will allow for a detailed evaluation of activating Notch on different cell types, as well as cell interactions. Our quiescent 3D BM niche uses magnetic nanoparticles to form MSC spheroids via magnetic levitation (Lewis et al, 2017). On implantation into a type I collagen gel (stiffness akin to BM), the cells in the spheroids are viable, but quiescent, express high levels of STRO-1 and nestin, can be tracked/sorted (due to their fluorescent tag) and respond to stimulation. These are then co-cultured above a monolayer of osteoblasts or endothelial cells, recapitulating the endosteal and perivascular components of the BM niche, respectively. LSC are then introduced into the system and cultured on the collagen matrix, allowing homing and migration towards the MSC spheroid. By

fluorescently tagging MSC and LSC cell populations (using fluorescent magnetic nanoparticles (mNPs)), this system uniquely enables the migration/interaction with the various cell populations to be monitored over time by live imaging using Incucyte Zoom™ system. Following disaggregation using collagenase, self-renewal and differentiation of the cell populations can be monitored and enumeration using specific markers by multi-parameter flow cytometry performed. The major advantages of this 3D system are (1) all the cells used are human, derived from primary patient samples enabling the leukaemia cells to interact with osteoblasts, MSC and endothelial cells within an extracellular matrix, creating a physiological environment mimicking the human in vivo BM niche. (2) By creating MSC spheroids using magnetic nanoparticles the MSC survive in an immature dormant quiescent state until stimulated by cell-to-cell interactions, tissue damage or extrinsic stimulation. The MSC then have the capacity to divide and differentiate appropriately akin to the natural BM microenvironment. (3) By fluorescently tagging MSC and HSC/LSC cell populations this system uniquely enables the migration, interaction and remodelling within the various cell populations to be monitored over time by live imaging. (4) Scale, sufficient cells can be co-culture using this system to enable the detailed biochemical and molecular assays to be performed-thus advancing research into the pathophysiology of leukaemia initiation and progression. (5) Microinjection of growth factors/small molecule inhibitors using hydrogel systems will enable localised effects to be monitored. (6) This model provides an ideal platform for drug screening with the potential to be adopted for high throughput screening of small molecule inhibitors or siRNA libraries by pharmaceutical companies. (7) This system will provide a valid alternative to mouse models and allows for limited cell numbers. Development of this project is currently underway in collaboration with Drs Helen Wheadon and Catherine Berry (both University of Glasgow).

4. Results II

4.1. Introduction

Despite a targeted therapeutic approach with TKIs in CML, a small number of patients will present in or progress to the acute phase of the disease, termed BC or BP. The incidence of progression to BP under TKI treatment ranges between 0.7 and 4.5% (Cortes et al, 2013; Hehlmann et al, 2011; Hughes et al, 2014) and is defined, as described within the introduction, according to the World Health Organisation (Arber et al, 2016) by the presence of at least one of

1. Blasts comprising approximately 20% of peripheral blood (PB) white cells or nucleated bone marrow cells,
2. Extramedullary blast proliferation, or
3. Large foci or clusters of blasts in the bone marrow.

Responses to TKIs in BP are transitory, and median survival following diagnosis of BP remains at only 6.5 to 11 months in those treated with TKI alone (Hehlmann, 2012). Therefore, if progression is suspected, it needs to be acted on with immediate effect to optimise outcome. As previous described within the introductory chapter, it can present as either myeloid, lymphoid, or biphenotypic in lineage, with approximately two-thirds of cases being found to be of a myeloid phenotype (Atallah et al, 2002; Kinstrie et al, 2016; Rosenthal et al, 1977). This suggests that within BP, LSCs may play an important role in view of the ability to differentiate to both lineages. However, a high degree of heterogeneity has been recognised, with multiple immunophenotypically distinct populations identified (Kinstrie et al, 2016). Furthermore, it has been shown that within BP disease, committed progenitors can acquire self-renewal properties (Jamieson et al, 2004; Kinstrie et al, 2016). As such, the LSC in BP-CML may reside in at least 3 subsets, namely $Lin^{-}CD34^{+}CD38^{-}$, $Lin^{-}CD34^{+}$ cells remaining from CP, and the disease-driving $Lin^{-}CD34^{+}CD38^{+}$ GMPs and CMPs (Jamieson et al, 2004; Kinstrie et al, 2016).

To date, it remains unclear the mechanisms responsible for progression to BP, nor those that determine lineage decision. This has been discussed within the introductory section 1.3.5.1. It is clear, however, there may be a role for self-renewal pathways within this process, which remains unsurprising in view of the role that the LSC plays within disease development and persistence. Most of the data available surrounds myeloid BP, which is more common. In BP-CML, the LSC subsets has been shown to result in

multiple populations with the immunophenotype of normal progenitors, as well as stem cells (Kinstrie et al, 2016). Various self-renewal pathways have been implicated in this, including Wnt/β-catenin, which is probably the most well established (Abrahamsson et al, 2009; Radich et al, 2006b; Sengupta et al, 2007; Zhao et al, 2007). Other self-renewal pathways, including Hh and BMP, have been linked to this process, but their exact role has yet to be fully elucidated (Jamieson et al, 2004; Radich et al, 2006; Su et al, 2012). Certainly, it may be shown that the role for different self-renewal pathways will be determined dependent upon which subset the LSC derives from. For example, accumulation of β-catenin in the nucleus of GMPs leads to increased self-renewal potential (Abrahamsson et al, 2009; Ysebaert et al, 2006). It seems pertinent, therefore, that the role for each evolutionary conserved self-renewal pathway be determined, as this will aid understanding and the development of therapeutic strategies.

In view of the finding that within a CP-CML model Notch activation, through JAG1, led to early differentiation and reduction in colony formation in short-term and long-term *in vitro* culture, respectively, we questioned if this could be translated to a BP phenotype, and indeed lead to a therapeutic advantage. There is a documented role for Notch pathway components in the progression of disease; however, the reports remain conflicting. It has been documented that within the K562 cell line, Notch inhibition can induce erythroid maturation (Lam et al, 2000). However, within the same cell line, activation of the pathway through a lentiviral model has led to a reduction in colony formation (Suresh & Irvine, 2015). Furthermore, activated intracellular Notch has been shown to cooperate with Bcr-Abl contributing to CML blast crisis in an *in vivo* model (Mizuno et al, 2008). Contrary to these observations, inactivation of Notch1 in mouse HSCs induced CMML and Notch1 here has been suggested to have a tumour suppressor role (Klinakis et al, 2011). In this study, conditional knockdown of Notch1/2/3 genes in mouse models induced CMML-like disease and introduction of Notch1 or Notch2 could rescue the disease phenotype. This study also reported that intracellular Notch1 expression in murine leukaemia-initiating cells upregulated Hes1 levels, which led to the repression of myeloid expansion. However, *Hes1* has been previously reported to cause CML BP transformation in mice (Nakahara et al, 2010).

The data presented within results I suggests a potential role for the eradication of the LSC in CP disease; therefore, it was sought to determine if this could be translated into a myeloid BP phenotype, where there is huge need for novel therapeutic agents.

4.2. Aims

Based on the evidence provided above, the specific aims set out in this chapter are:

1. To assess the expression of the Notch signalling pathway elements in myeloid BP-CML patient samples;
2. To determine the functional role, if any, of the Notch signalling pathway in myeloid BP-CML patient samples;
3. To assess the interconnectivity between self-renewal pathways through gene expression analysis between CP and myeloid BP.

4.3. Results

4.3.1. *The Notch signalling pathway is silenced in primary myeloid BP CML*

To evaluate the role of Notch signalling within a myeloid BP phenotype, Notch pathway gene expression was investigated in primary myeloid BP-CML samples. Using Fluidigm technology, mRNA expression of 11 myeloid BP-CML patient samples was compared to normal PB $CD34^+$ samples. Relative gene expression levels were determined using the average normal $CD34^+$ value as a calibrator calculated using the ΔΔCt method (Schmittgen & Livak, 2008), using an average of five housekeeping as reference. All but one patient sample had been exposed to TKI prior to analysis.

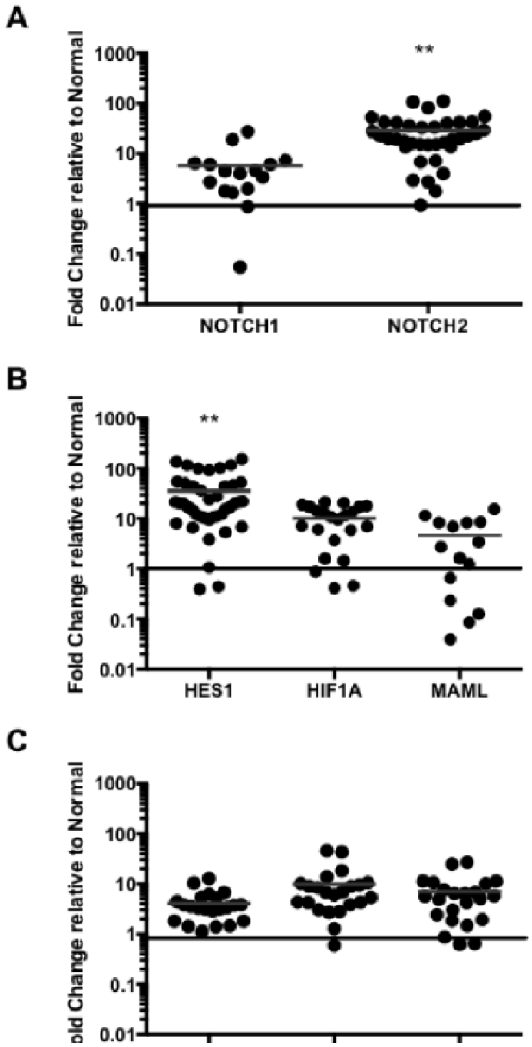

Figure 4 - 1 Focussed gene expression analysis demonstrates that the Notch pathway components are likely silenced within primary myeloid BP samples

Relative gene expression levels for 11 CD34+ BP-CML samples were determined against the average normal CD34+ PB values calculated using the ΔΔCt method with an average of five housekeeping genes as reference. Fold change is relative to normal CD34+ PB samples (n=3). (A) Dot plot showing fold change expression values for Notch receptors. (B) Dot plot showing fold change expression values for Notch downstream targets and *MAML.* (C) Dot plot showing fold change expression of negative regulators of the pathway. P values were determined by an unpaired t-test (* $p<0.05$, ** $p<0.01$).

Focussed gene analysis confirmed that the Notch receptor, *NOTCH2*, was statistically upregulated compared to normal $CD34^+$ PB samples (p=0.0035; figure 4-1A). *NOTCH1* was overexpressed, but this was not deemed statistically significant (p=0.21; figure 4-1A). The downstream target, *HES1*, was statistically upregulated within the myeloid BP samples (p=0.0023; figure 4-1B); however, the pathway was deemed to be silenced with no statistical change shown in gene expression of other downstream targets, such as *HIF1A* (p=0.3632; figure 4-1B). Furthermore, the intracellular complex of the pathway necessary for downstream activation, *MAML* was not significantly overexpressed within this population (p=0.96; figure 4-1B). Negative regulators were overexpressed compared to normal samples, but this was not statistically significant (figure 4-1C).

Although the gene expression analysis was suggestive that the majority of myeloid BP samples did not demonstrate active Notch signalling through gene expression analysis, it was not conclusive, as *HES1*, a major downstream target of the Notch pathway was significantly upregulated. Furthermore, although *HIF1A* and *MAML* did not demonstrate a statistically significant upregulation, they had increased expression compared to the normal PB samples. The cleaved aspect of the intracellular NOTCH2 receptor, val1744, was absent through IF and western blotting.

Therefore, to confirm that the pathway was not upregulated, the pharmacological Notch inhibitor, DAPT, was utilised. Three myeloid BP-CML primary samples were thawed or used fresh, and sorted into $CD34^+$ populations, as previously described. Cells were cultured in low growth factor SFM on non-stromal conditions (i.e. plastic culture without stromal support) with and without 10uM DAPT for five sequential days. Trypan blue exclusion cell counts showed that there was no statistically significant difference between untreated and treated samples in terms of cell growth; however, there was notable heterogeneity between samples (figure 4-2). Of note, there was a slight increase in growth potential amongst those samples treated with DAPT for 5 days *in vitro*.

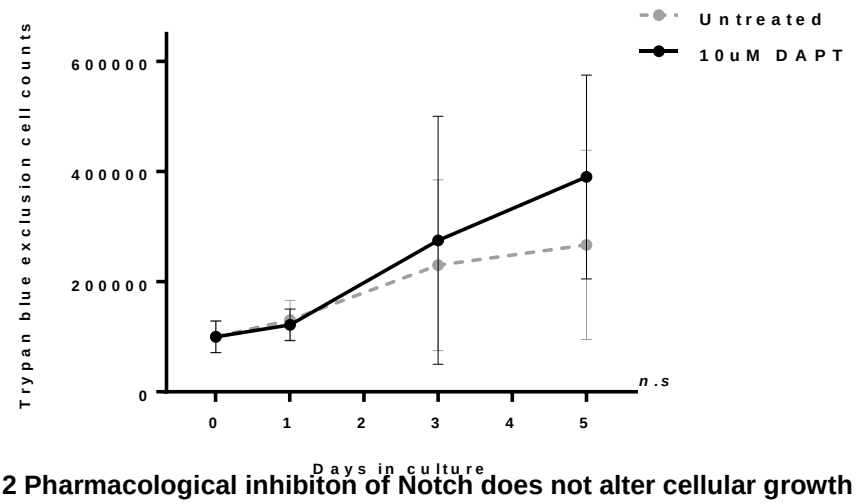

Figure 4 - 2 Pharmacological inhibiton of Notch does not alter cellular growth in myeloid BP samples in plastic culture

$CD34^+$ myeloid BP cells were cultured in low growth factor SFM with or without the presence of 10uM DAPT (n=3). DMSO treated cells were used as an 'untreated' control. Cells were counted using trypan blue exclusion cell counts every 24 hours. No significant difference was seen with the addition of DAPT over sequential days in culture as analysed using a paired student's t-test at each time-point (n=3; p>0.05).

To determine if the increase in growth potential was a 'true' finding, annexinV and 7AAD were utilised to assess apoptosis and live cell populations. There was no change in apoptotic ability, nor percentage of live cells, between experimental arms using flow cytometry measurement of annexinV and 7AAD, suggesting that Notch inhibition on plastic culture does not alter apoptotic ability, within a myeloid BP phenotype (figure 4-3).

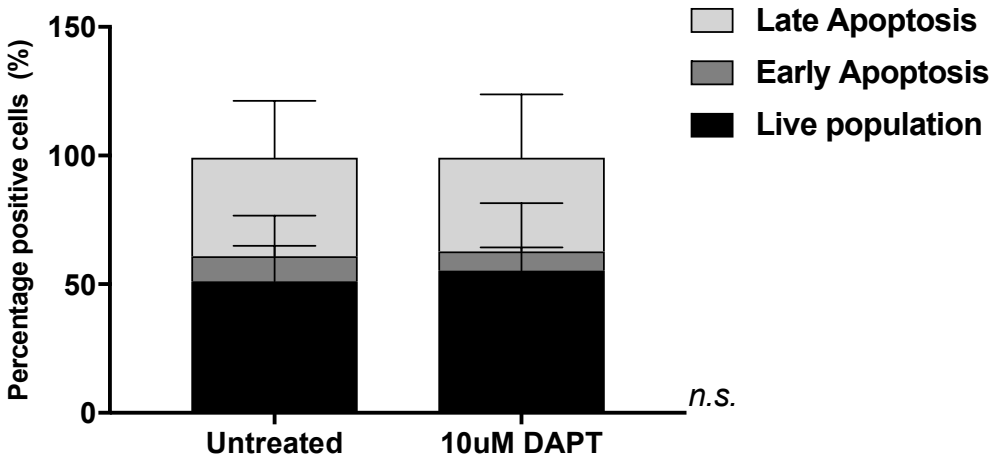

Figure 4 - 3 Pharmacological inhibition of Notch does not affect apoptotic ability of myeloid BP samples in plastic culture conditions

Myeloid BP cells were cultured in low growth factor SFM with or without the presence of 10uM DAPT for 5 days (n=3). DMSO treated cells were used as 'untreated' control. Samples were stained with annexinV and 7AAD as previously described. Unstained and single stained cells were used to set voltages and compensation. There was no significant difference between populations as analysed using a paired student's t-test at each time-point (n=3; p>0.05).

4.3.2. *In vitro activation of Notch through ligand binding does not alter cellular function in primary myeloid BP samples*

In view that myeloid BP CD34^{+} cells specifically and abundantly express the Notch receptor, *NOTCH2*, and that the pathway was deemed functionally inactive at basal state (i.e. on plastic culture without stromal support), it was hypothesised that Notch signalling could be reactivated exogenously by altering cellular function, as had been demonstrated within a CP phenotype. As within the CP experimental model, an OP9 co-culture system was used to allow for the overexpression of the DLL1 and JAG1 proteins, using OP9-GFP cells as control stroma. CP-CML samples had demonstrated changes between a mature and immature population, therefore myeloid BP-CML samples were sorted into these populations using CD34 and CD38 expression. Three samples were used.

Following cell sorting, cells were cultured on non-stromal and stromal conditions for six sequential days in low growth factor SFM. Trypan blue exclusion cell counts were conducted every 24 hours to assess cell growth between experimental arms. There was no statistical change in cell growth between non-stromal and stromal conditions ($p>0.05$; figure 4-4).

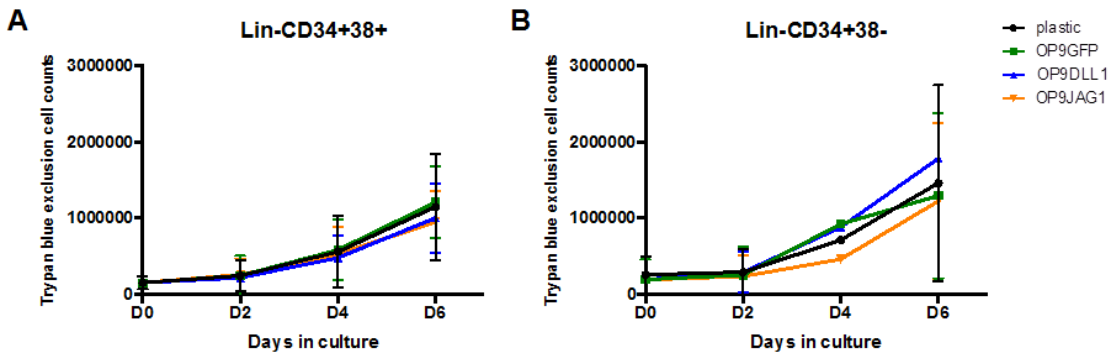

Figure 4 - 4 Co-culture with Notch ligand support does not alter the growth potential in mature and immature myeloid BP cells

Myeloid BP progenitor cells were sorted by CD34 and CD38 expression before being cultured in low growth factor SFM with or without the presence of stroma. Within each co-culture experiment, OP9 stromal cells underwent a maximum of 8 passages before use. OP9 stromal cells were seeded at a 1 in 24 ratio with suspension cells (i.e. 1 stromal cell per 24 suspension cells) 24 hours prior to co-culture. 50,000 myeloid cells were seeded onto plastic or stromal conditions in 12 well plates and counted every 24 hours using trypan blue exclusion cell counts. There was no signficant change between co-culture conditions, nor between mature and immature populations as assessed by a multiple comparison ANOVA at each time-point (n=3; $p>0.05$).

To confirm this pattern, apoptosis assays were used to determine live population percentage and apoptotic ability within a co-culture system. AnnexinV and 7AAD was assessed by flow cytometry as previously described. Within both populations, culturing on stroma led to an apparent increase in live cells, however this was not significant, nor dependent on activation of the Notch signalling pathway (figure 4-5).

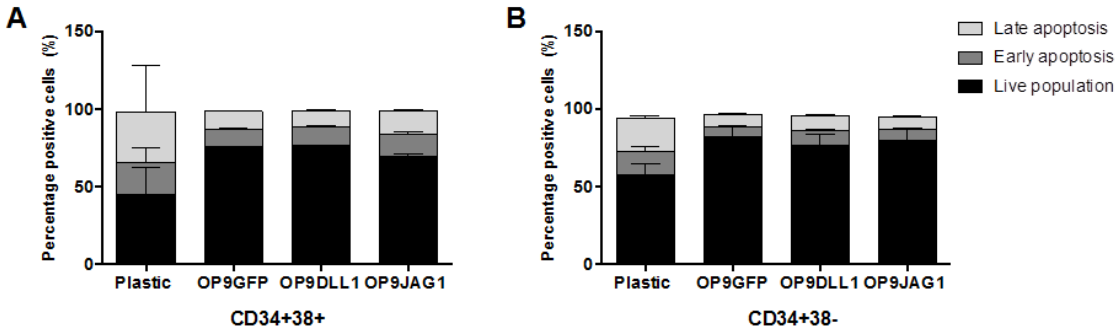

Figure 4 - 5 Co-culture with Notch ligand support does not alter the apoptotic ability in mature and immature myeloid BP progenitor cells

Myeloid BP cells were cultured in low growth factor SFM with or without the presence of stromal conditions for five days (n=3). Samples were stained with AnnexinV and 7AAD as previously described. Unstained and single stained cells were used to set voltages and compensation. There was no statistical difference between populations, nor stromal conditions, as analysed using a multiple comparison ANOVA at each time-point (n=3; $p>0.05$).

CFC assays were used to assess the capacity for proliferation and differentiation within both population subsets. This was in view of the differentiation potential seen within a CP phenotype. $CD34^+$ BP-CML cells following co-culture in non-stromal and stromal conditions were inoculated into a semi-solid culture medium containing a standard growth factor cocktail. Following culture for 12 days, colonies were evaluated and counted. Each condition was in duplicate and mean between plates calculated. Over four BP-CML samples, there was no statistical change between colony formation upon co-culture (figure 4-6).

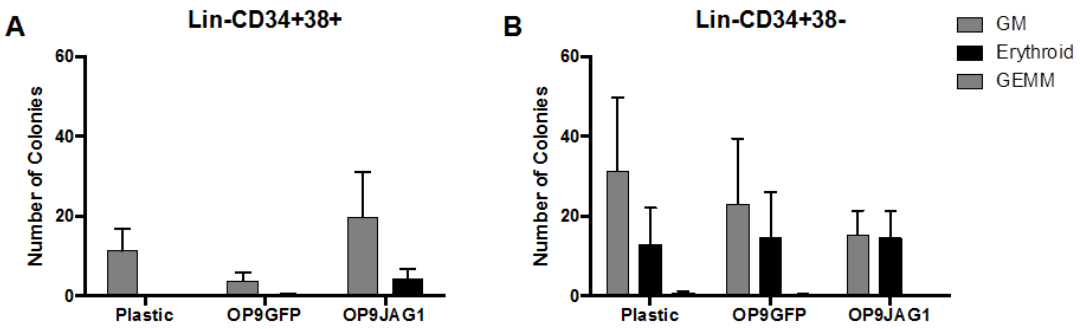

Figure 4 - 6 Co-culture with Notch ligand support does not alter colony formation in mature and immature myeloid BP cells

Myeloid BP cells were sorted by CD34 and CD38 expression. Following co-culture in non-stromal and stromal conditions for five days, cells were inoculated into a semi-solid culture medium containing a standard growth factor cocktail. Following culture for 12 days, colonies were evaluated and counted. Each condition was in duplicate and mean between plates calculated. There was no difference between co-culture conditions ($p>0.05$; $n=3$). Colonies were BCR-ABL positive in all conditions, as determined by FISH.

This was suggestive that either the pathway was not being activated by the co-culture conditions or that activation had no effect on cellular function. To determine this, RNA was extracted from the previously co-cultured samples and analysed for both the downstream Notch target, *HES1,* and the intracellular complex necessary for target activation, *MAML*. This was to determine if there were changes at a gene level between co-culture conditions. There was no statistical change between experimental arms (figure 4-7). This was corroborated at protein level using IF of val1744, the intracellular component of the Notch receptor, which showed no activity. This confirmed that the pathway was not being activated in any of the co-culture conditions, nor between immature and mature populations. This was not comparable to the CP-CML data.

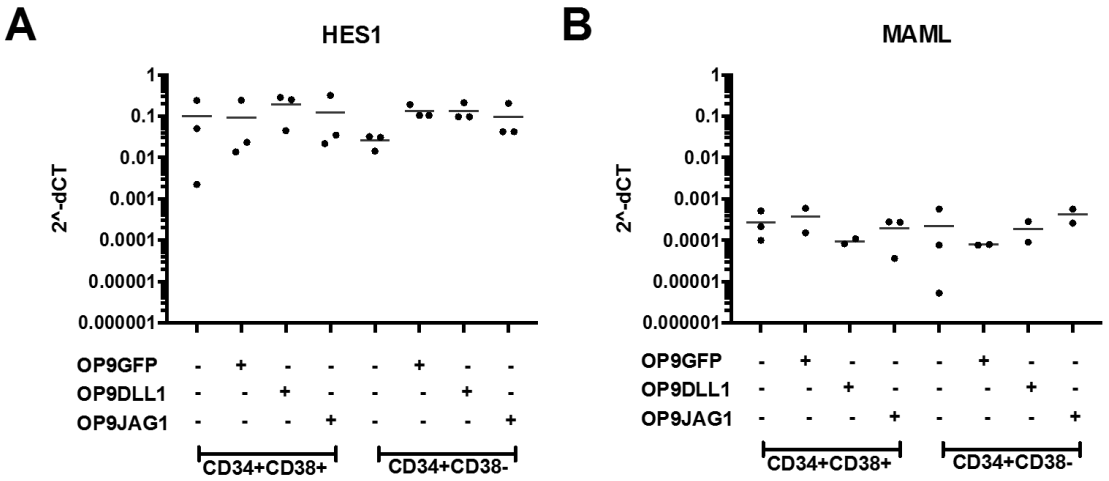

Figure 4 - 7 Gene expression of *HES1* and *MAML* confirms that the Notch pathway is not actviated through exogenous ligand expression

Using Fluidigm technology, mRNA expression of $CD34^+CD38^+$ and $CD34^+CD38^-$ culture on plastic, OP9GFP co-culture, OP9DLL1 and OP9JAG1 co-culture after 5 days was compared to normal peripheral blood $CD34^+$ samples. Relative gene expression levels were determined using the average normal $CD34^+$ value as a calibrator calculated using the ΔΔ Ct method, using an average of five housekeeping genes as reference. There was no difference between populations, nor within co-culture conditions, as determined by a multiple comparison ANOVA ($p>0.05$).

4.3.3. *Gene expression analysis of evolutionary conserved self-renewal pathways between CP and myeloid BP disease*

The functional data generated above did not demonstrate a clear functional role for Notch signalling within myeloid BP primary samples. In part, this could be due to the heterogeneity that is seen between BP samples (Kinstrie et al, 2016). It can be concluded, however, that activation of the pathway does not have the same functional relevance as within CP (Results I). It was hypothesised at this juncture that the Notch signalling pathway could not be activated in the same way as a CP phenotype due to aberrancies of other self-renewal pathways and/or upregulation of negative regulators. It is well documented that as CML progresses, self-renewal pathways are deregulated (Sengupta et al. 2007; Jamieson et al. 2004). Self-renewal pathways are modulated by interconnecting signals within the microenvironment. This, subsequently means, that upregulation of downstream targets, such as *HES1*, can be acquired via other pathways. Moreover, understanding the interconnectivity between pathways, may, in turn, help understand the reasons that CP disease can progress to either myeloid or lymphoid lineage BP.

To try and delineate interconnections between self-renewal pathways, RNA was extracted from CP, AP, and myeloid BP before assessing gene expression of self-renewal pathway components, including components of the Notch, Wnt/β-catenin, Hh, and BMP pathways, as well as the main apoptotic regulators, including *TP53*. This was to determine gene expression changes between CP, AP, and myeloid BP disease.

Using Fluidigm technology, quantitative PCR of 90 self-renewal and cell survival genes was performed with the primary sample RNA. 100ng was transcribed to cDNA across all samples to enable comparison between groups. Samples were plated in duplicate, and as more than one Fluidigm plate was to be used, an internal sample control was used across plates to enable comparison. On global gene expression analysis, CP could be segregated from AP and myeloid BP by differential gene expression through gene clustering of the fold change compared to the PB $CD34^+$ population (figure 4-8). AP and myeloid BP could not be distinguished through this method, suggesting that the differential gene expression in CML progression is a two-step phenomenon rather than three; this has been previously described (Radich et al. 2006).

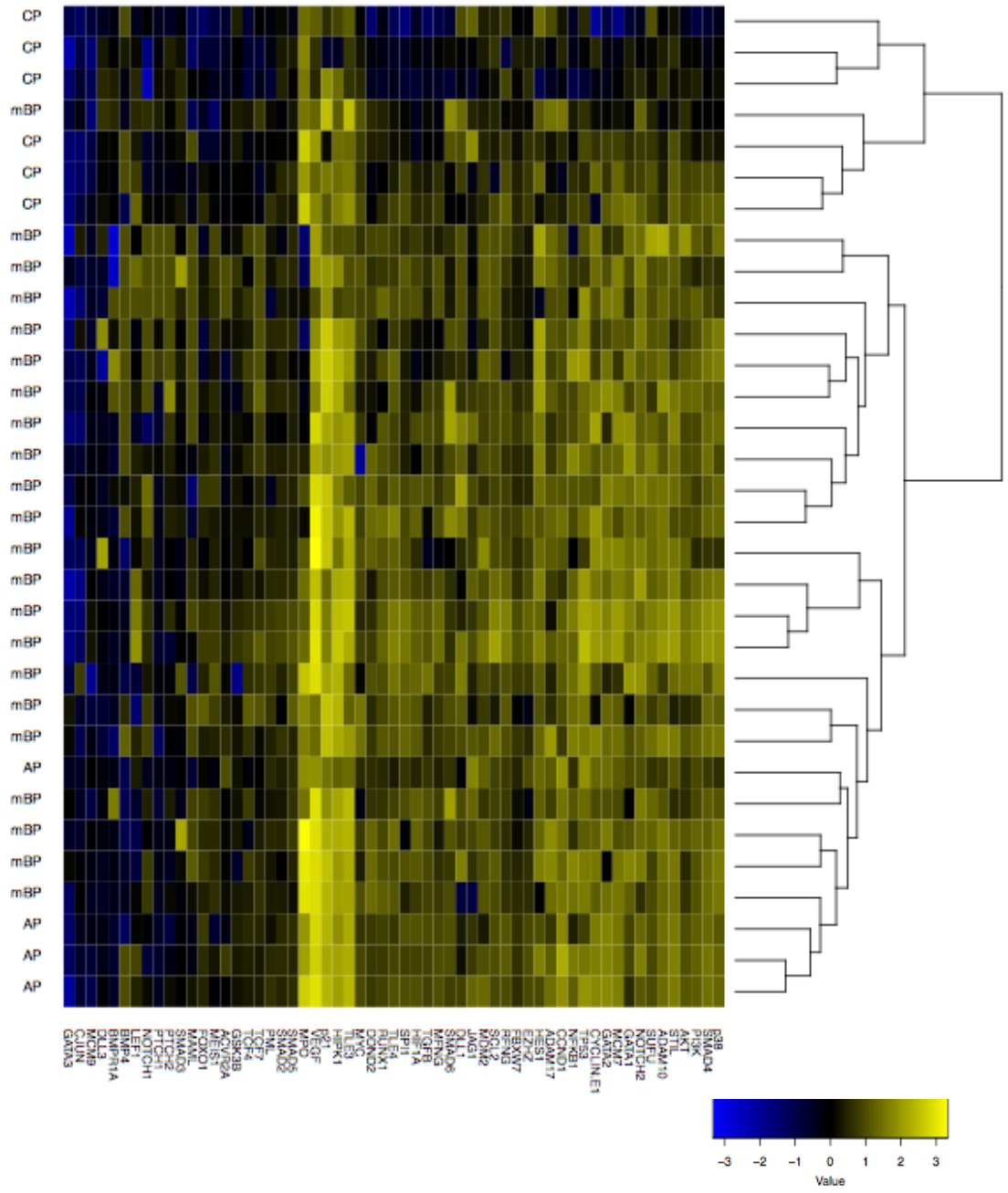

Figure 4 - 8 Gene expression clustering suggests a two-stage disease process within CML

Gene expression profiles (GEPs) were determined from CP, AP, and myeloid BP populations. Gene expression levels were determined by Fluidigm array analysis. Relative gene expression levels were determined by ΔΔCt method using an average of five housekeeping genes as reference and the average $CD34^{+}$ value as the calibrator for fold change. Heat maps and gene clustering were produced by using heatmap.2 in R/Bioconductor.

Focussed gene analysis of this dataset demonstrated that there was a notable deregulation of all self-renewal pathways between CP and myeloid BP disease. The Notch pathway was no exception. There was a statistically significant increase in the Notch receptors, *NOTCH1* and *NOTCH2*, between CP and myeloid BP disease (p=0.007 and p=0.03, respectively; figure 4-9 A-B). However, there was no statistical

change in the Notch ligands (figure 4-9 C-E). Furthermore, there was a statistically significant increase in gene expression of the metalloproteases necessary for proteasome cleavage of the pathway on activation, namely *ADAM10* (p=0.0004; figure 4-10A) and *ADAM17* (p=0.0043; figure 4-10B).

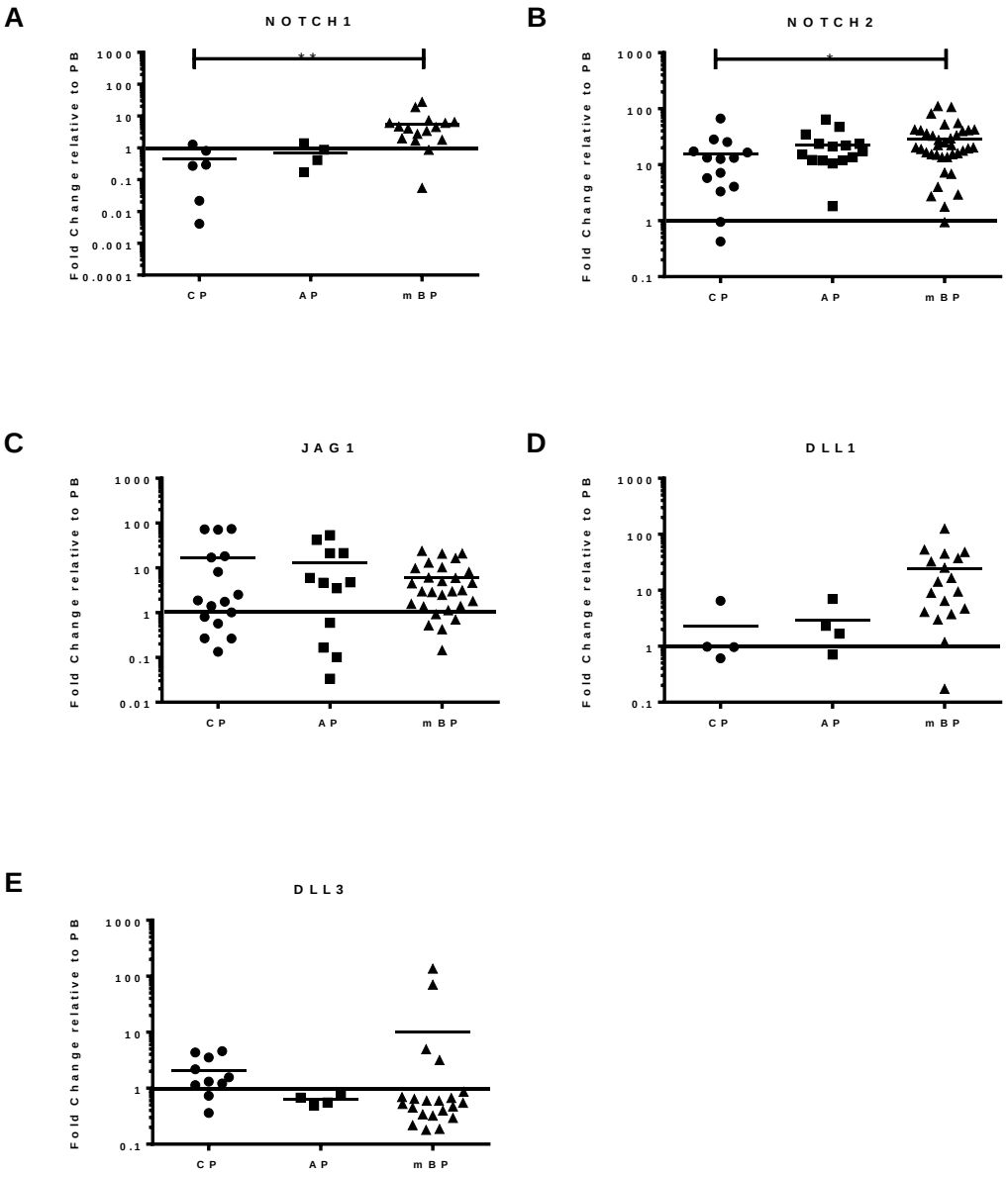

Figure 4 - 9 Focussed gene expression of Notch receptors and ligands

Using Fluidigm technology, mRNA expression was determined for CP, AP, and myeloid BP compared to normal PB CD34+ samples. Relative gene expression levels were determined using the average normal CD34+ value as a calibrator calculated using the ΔΔCT method, using an average of five housekeeping genes as reference. Statistical significance was generated by unpaired t test between populations to enable determination of significance gene changes within disease progression. (A) Dot plot showing gene expression of *NOTCH1.* (B) Dot plots showing gene expression of *NOTCH2*. (C) Dot plots showing gene expression of *JAG1.* (D) Dot plots showing gene expression of *DLL1.* (E) Dot plots showing gene expression of *DLL3.* P values were determined by an unpaired t-test between populations (* p<0.05, ** p<0.01, *** p<0.001).

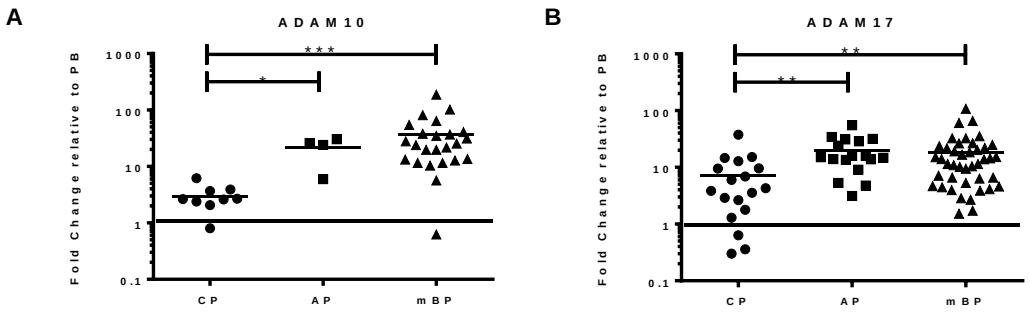

Figure 4 - 10 Focussed gene expression of the metalloproteases, *ADAM10* and *ADAM17,* in CML progression to myeloid BP

Analysis of gene expression was determined using the ΔΔCt method as previously described. (A) Dot plot showing gene expression of *ADAM10.* (B) Dot plots showing gene expression of *ADAM17*. P values were determined by an unpaired t-test between populations (* p<0.05, ** p<0.01, *** p<0.001).

There was a statistically significant increase in *MAML* between CP and myeloid BP. However, compared to normal PB samples, these were not significant as stated above (figure 4-11). This suggests that although there is a shift in Notch signalling through progression to myeloid BP disease, the pathway is not likely active as this critical co-activator is not elevated compared to normal.

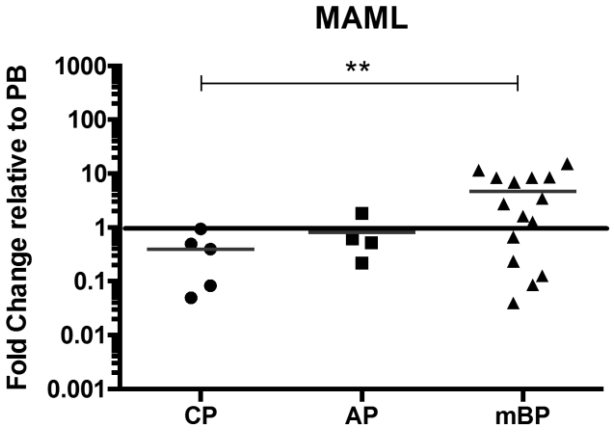

Figure 4 - 11 Focussed gene expression of *MAML*

Analysis of gene expression was determined using the ΔΔCt method as previously described. Dot plot represents gene expression of *MAML* compared to normal PB $CD34^+$ samples in the three phases of disease. P values were determined by an unpaired t-test between populations (** p<0.01).

Interestingly, the negative regulators, *FBXW7* and *MFNG,* were increased in myeloid BP compared to CP (p=0.02, and p=0.007, respectively), and between CP and AP,

suggesting that this could potentially be a mechanism to its silencing (figure 4-12A-B). Expression of the negative regulator, *RFNG*, was not altered in any phase of disease (figure 4-12C).

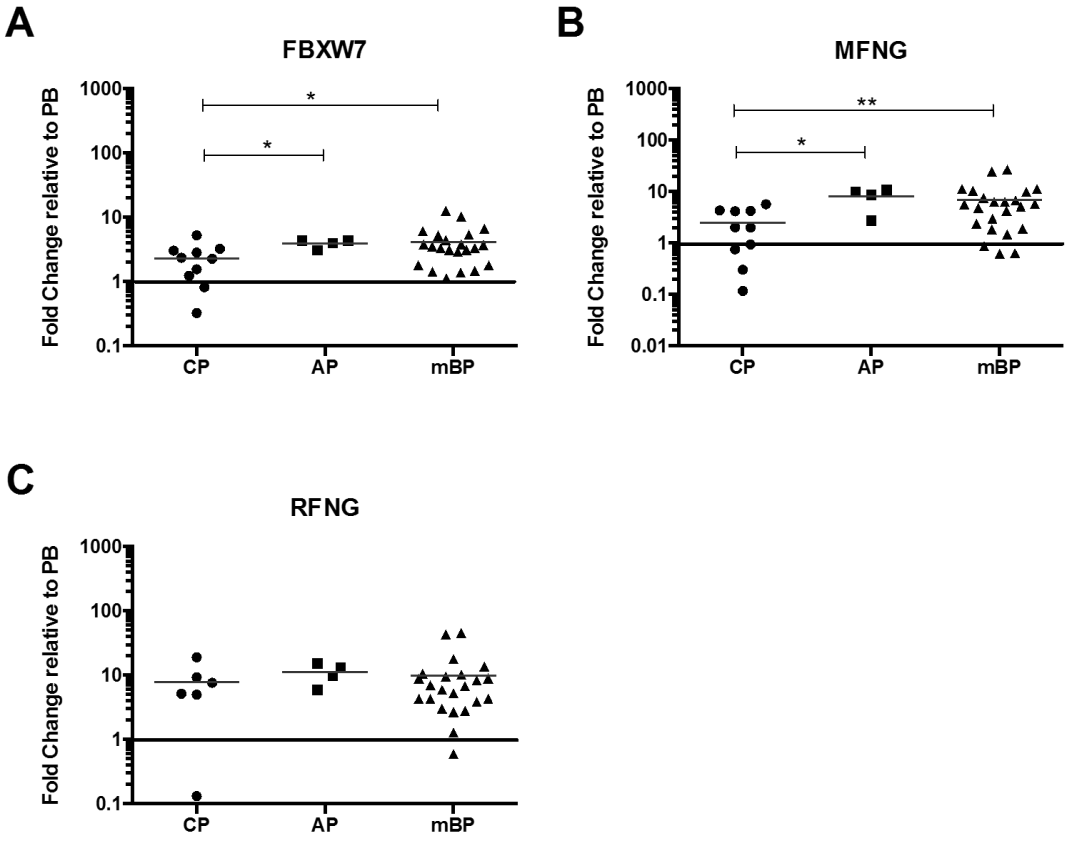

Figure 4 - 9 Focussed gene expression of negative regulators of the Notch pathway
Analysis of gene expression was determined using the ΔΔCt method as previously described. (A) Dot plot showing gene expression of *FBXW7* compared to normal PB CD34$^+$ samples in the three phases of disease. (B) Dot plot showing gene expression of *MFNG* compared to normal PB CD34$^+$ samples in the three phases of disease. (C) Dot plot showing gene expression of *RFNG* compared to normal PB CD34$^+$ samples in the three phases of disease. P values were determined by an unpaired t-test between the experimental population and normal, with an ANOVA used to determine significance between phase of disease (* $p<0.05$, ** $p<0.01$).

As previously documented, the Notch downstream target, *HES1*, has a statistically significant increase in expression within myeloid BP compared to normal PB CD34$^+$ samples. Furthermore, the gene expression data demonstrated a statistically significant increase in expression of the Notch downstream targets, *HES1* ($p=0.0008$) and *HIF1A* ($p<0.0001$), in progression from CP to myeloid BP (figure 4-12). This cannot be explained by the gene expression of the Notch pathway components demonstrated above.

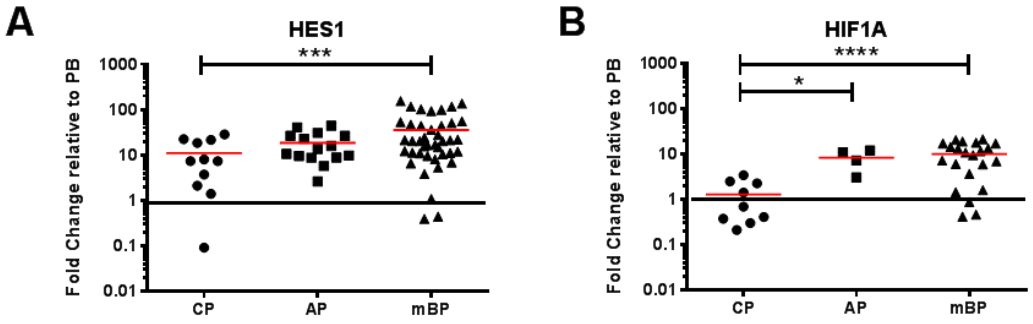

Figure 4 - 13 Focussed gene expression of the Notch downstream targets, *HES1* and *HIF1A*

Analysis of gene expression was determined using the ΔΔCt method as previously described. (A) Dot plot showing gene expression of *HES1* compared to normal PB $CD34^+$ samples in the three phases of disease. (B) Dot plot showing gene expression of *HIF1A* compared to normal PB $CD34^+$ samples in the three phases of disease. P values were determined by an unpaired t-test between the experimental population and normal, with an ANOVA used to determine significance between phase of disease (* $p<0.05$, *** $p<0.001$, **** $p<0.0001$).

This led to the question also whether the upregulation of both *HES1* and *HIF1A* was secondary to the activation of other self-renewal pathways. Furthermore, it was hypothesised that the activation of other self-renewal pathways was preventing activation of Notch components. For example, if considering *HES1*, the gene can be upregulated by numerous mechanisms (figure 4-14). These include through the BMP, Wnt/β-catenin and Hh pathways, as well as directly through *HIF1A*. Within each pathway, there is influence in the negative regulation of Notch.

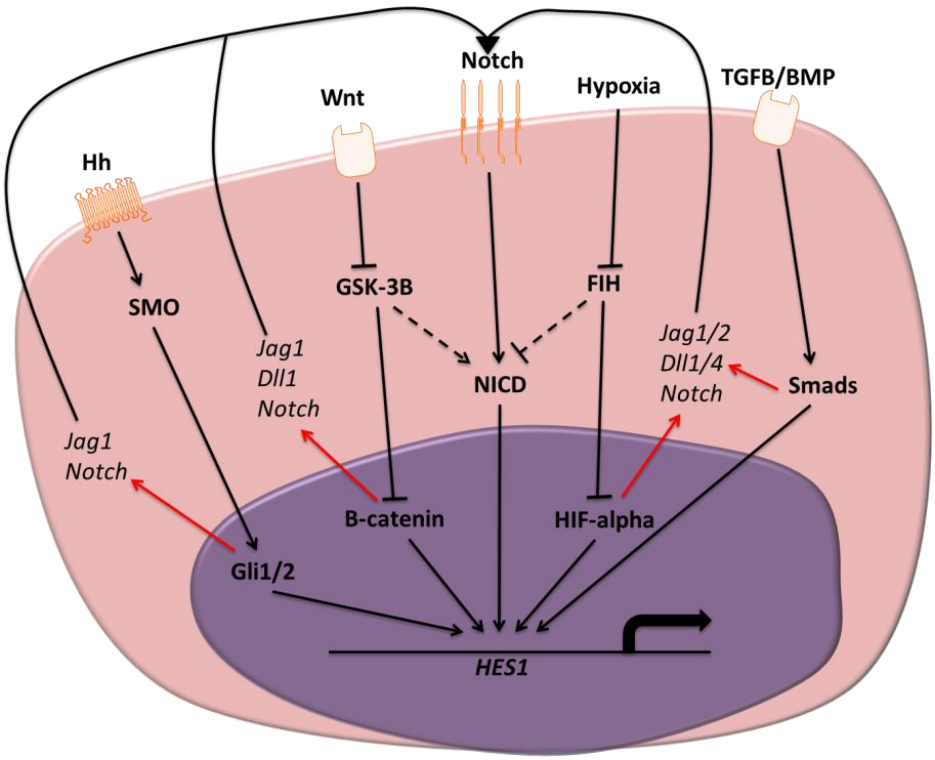

Figure 4 - 14 The interconnectivity between self-renewal pathwyas and activation of *HES1*

Notch activates *HES1* through a canonical signalling approach that involves proteolytic cleavages as described within the introductory chapter. The Wnt signalling pathway interconnects with Notch via activation of Notch target genes, including *HES1 or* from Notch signalling components, like Notch receptors and ligands. *GSK3β* potentiates Notch-dependent gene expression via phosphorylation of Notch1, but can also reduce the transcriptional activity of Notch2. The Hh pathway induces *HES1* and Notch pathway components. Hypoxia cross talks with the Notch pathway via induction of Notch receptors and ligands, and common downstream targets, such as *HES1*.

Components of the canonical Wnt/β-catenin pathway were examined in view of previous literature evidence suggesting the pathway's involvement in CML progression (Abrahamsson et al, 2009; Radich et al, 2006). There was a statistically significant increase in expression of *TCF4* (p=0.0002) and *TCF7* (p=0.0005), the major endpoint mediators of Wnt/β-catenin signalling, between CP and myeloid BP (figure 4-15A-B). *TCF7* was signifcantly increased between CP and AP (p=0.04; figure 4-15B). Lymphoid enhancer factor 1 (*LEF1*) was unchanged (figure 4-15C). This indicated that the Wnt/β-catenin pathway was activated during disease progression. *GSK3*β was statistically significantly increased between CP and both AP (p=0.02) and myeloid BP disease (p=0.02) (figure 4-15D). It is, however, difficult to correlate gene expression of GSK3β, as it is the phosphorylated protein that accumulates during canonical Wnt/β-catenin activation.

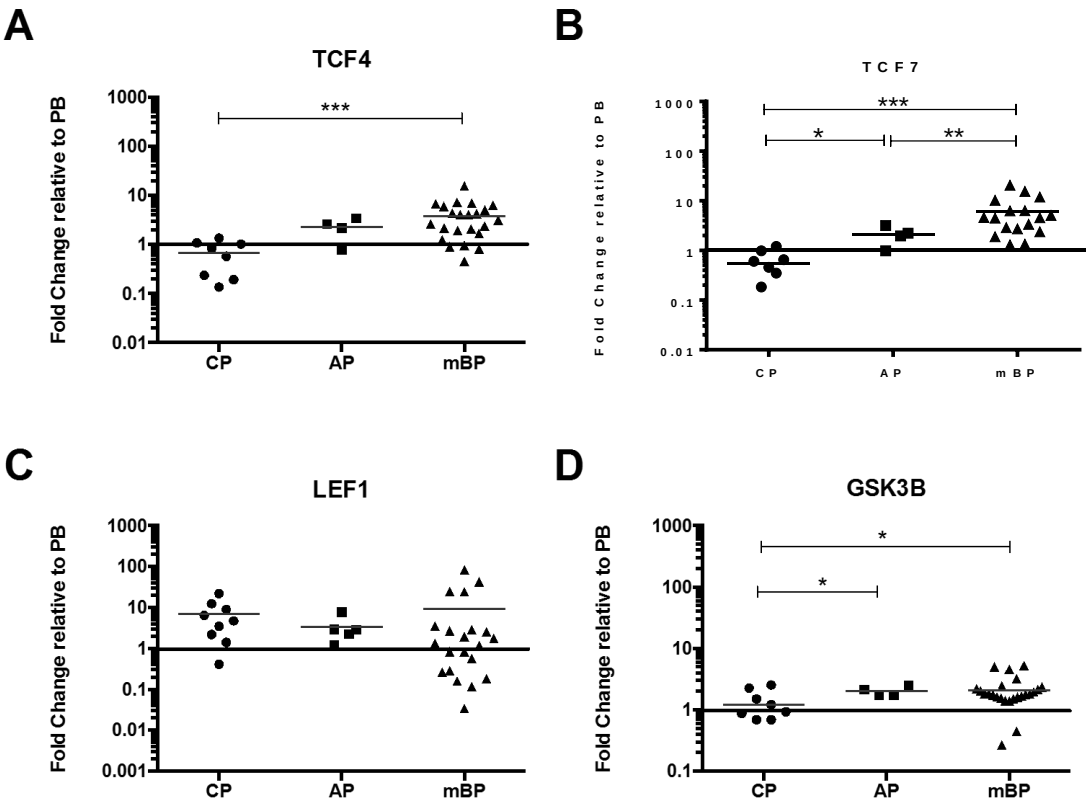

Figure 4 - 15 Focussed gene expression of components of Wnt/β-catenin canonical signalling

Analysis of gene expression was determined using the ΔΔCt method as previously described. Dot plots showing gene expression of (A) *TCF4* (B) *TCF7* (C) *LEF1* and (D) *GSK3β* compared to normal PB CD34$^+$ samples in the three phases of disease P values were determined by an unpaired t-test between the experimental population and normal, with an ANOVA used to determine significance between phase of disease (* p<0.05, ** p<0.01, *** p<0.001).

Furthermore, *TLE3* and *TLE4* had increased expression in myeloid disease progression, with a statistical increase in expression between CP and myeloid BP for both (p=0.0001 and p=0.0003, respectively; figure 4-16A-B), and between AP and myeloid BP for *TLE4* (p=0.01) (figure 4-16A). This data validates that canonical Wnt/β-catenin components are deregulated within a myeloid BP phenotype.

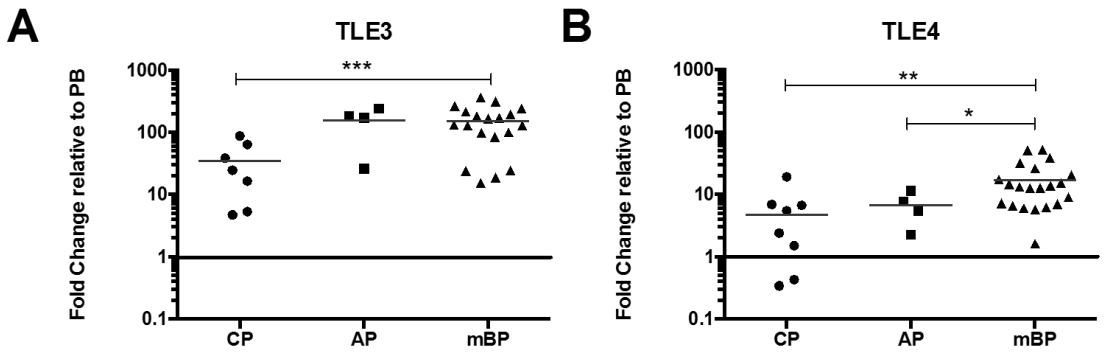

Figure 4 - 16 Focussed gene expression of components of Wnt-β-catenin canonical signalling

Analysis of gene expression was determined using the ΔΔCt method as previously described. (A) Dot plot showing gene expression of *TLE3* compared to normal PB CD34$^+$ samples in the three phases of disease. (B) Dot plot showing gene expression of *TLE4* compared to normal PB CD34$^+$ samples in the three phases of disease. P values were determined by an unpaired t-test between the experimental population and normal, with an ANOVA used to determine significance between phase of disease (** p<0.01, *** p<0.001).

Wnt/β-catenin activity influences Hh activity and vice versa. It has been shown that Wnt/β-catenin signalling can influence the stability of *GLI1* allowing for its cellular accumulation. To investigate this, the Hh pathway was next analysed. The Hh receptors, *PTCH1* and *PTCH2* were not statistically changed between CP, AP, and myeloid BP (figure 4-17A-B). As expected, *GLI1* was significantly overexpressed in myeloid BP compared to CP disease (p=0.01; figure 4-17C). Interestingly, *SUFU*, a negative regulator of Hh was increased in myeloid BP compared to CP and AP (p=0.02 and p=0.01, respectively; figure 4-17D). This may suggest that *GLI1* is being regulated through another self-renewal pathway, such as Wnt/β-catenin, or that *SUFU* has a dual role in the regulation of Hh.

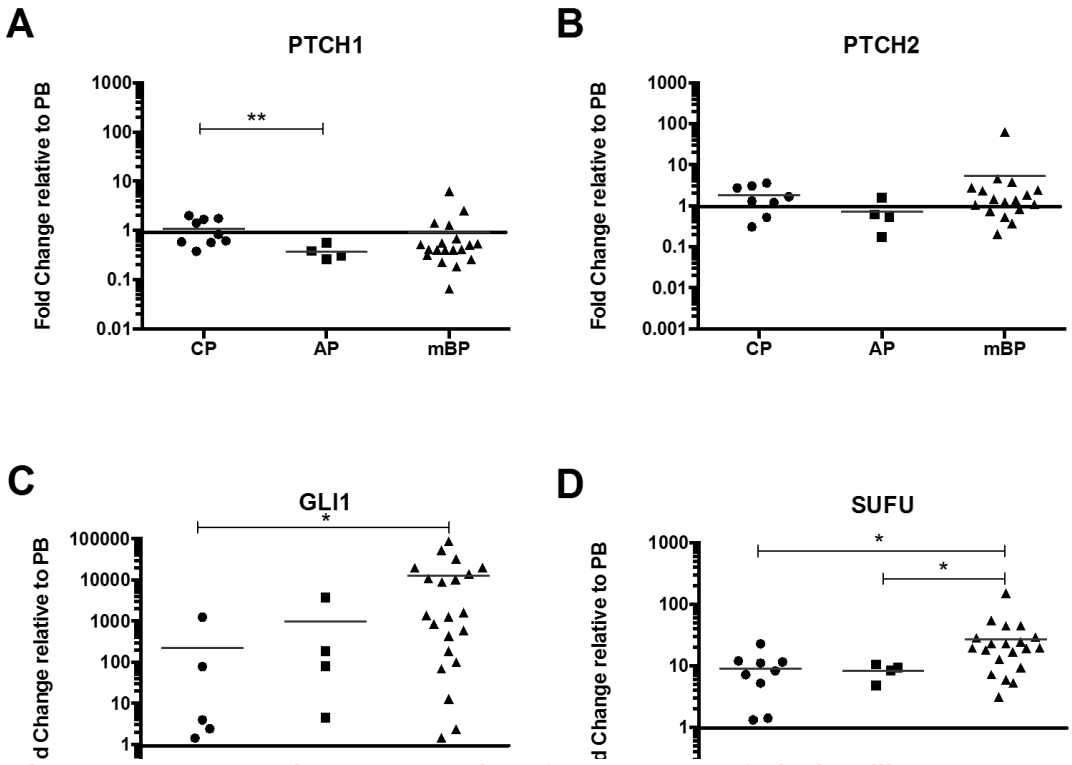

Figure 4 - 17 Focussed gene expression of components of Hh signalling

Analysis of gene expression was determined using the ΔΔCt method as previously described. (A) Dot plot representing gene expression of *PTCH1* compared to normal PB CD34$^+$ samples in the three phases of disease. (B) Dot plot showing gene expression of *PTCH2* compared to normal PB CD34$^+$ samples in the three phases of disease. (C) Dot plot showing gene expression of *GLI1* compared to normal PB CD34$^+$ samples in the three phases of disease. (D) Dot plot showing gene expression of *SUFU* compared to normal PB CD34$^+$ samples in the three phases of disease. P values were determined by an unpaired t-test between the experimental population and normal, with an ANOVA used to determine significance between phase of disease (* p<0.05, ** p<0.01).

There is known cooperation between *BMP4* and both Hh and Wnt/β-catenin signalling. *BMP4* expression associates with Hh signalling in determining HSC fate, both in embryonic and adult haemopoiesis. There was no statistical change in *BMP4* expression in progression of disease (figure 4-18).

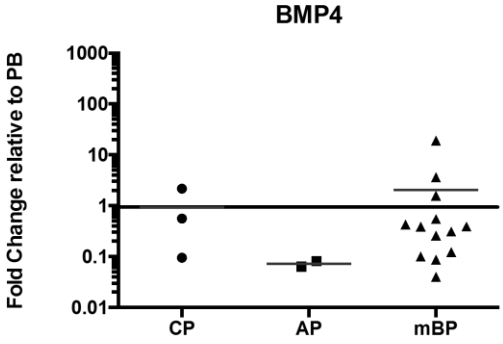

Figure 4 - 18 Focussed gene expression of *BMP4*

Analysis of gene expression was determined using the ΔΔCt method as previously described. Dot plot represents gene expression of *BMP4* compared to normal PB CD34$^+$ samples in the three phases of disease (* p<0.05, ** p<0.01, *** p<0.001, **** p<0.0001).

Within the canonical BMP pathway, SMADs are the major signal transducers. Upon phosphorylation of type I receptors, SMAD1, 5, and 7 become phosphorylated and form a complex with SMAD4. Within our data, there was no increase in *SMAD5* between CP and AP/myeloid BP (figure 4-19D). *SMAD1* and *7* were not analysed. *SMAD4* had increased expression in myeloid BP (p=0.005) compared to CP (figure 4-19C), and this may suggest that a complex between SMAD1/5/7 and SMAD4 was not formed. Interestingly *SMAD6* was statistically significantly upregulated in advanced phases compared to CP (p=0.04 between CP and AP; p=0.01 between CP and myeloid BP) (figure 4-19E). The BMP pathway is inhibited by *SMAD6*, which inhibits phosphorylation of SMAD1/5/7. Therefore, this gene expression data may suggest that the pathway is downregulated in all stages of CML.

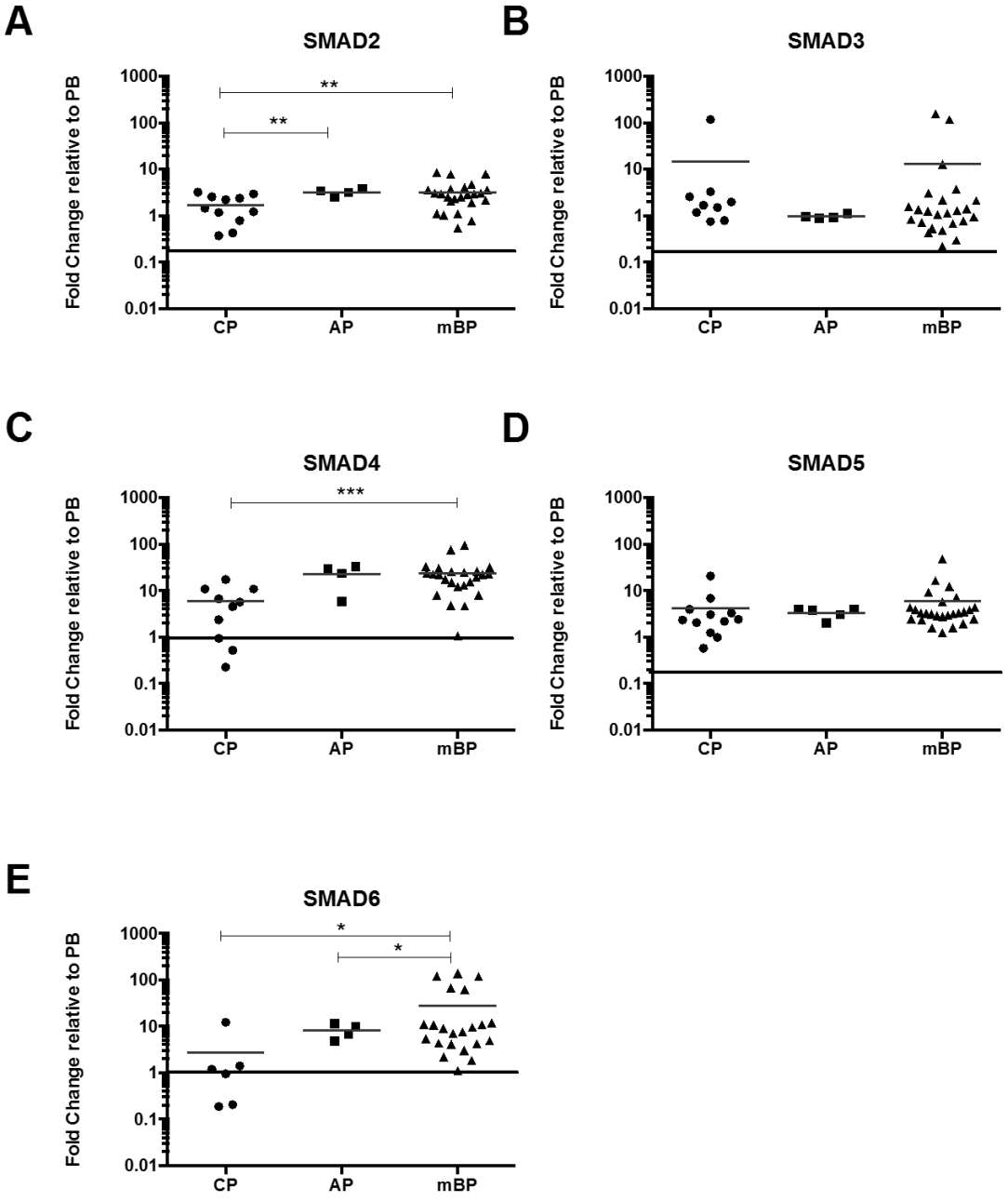

Figure 4 - 19 Focussed gene expression of components of BMP signalling
Analysis of gene expression was determined using the ΔΔCt method as previously described. Dot plots showing gene expression of (A) *SMAD2,* (B) *SMAD3*, (C) *SMAD4,* (D) *SMAD5,* and (E) *SMAD6,* compared to normal PB $CD34^+$ samples in the three phases of disease. P values were determined by an unpaired t-test between the experimental population and normal, with an ANOVA used to determine significance between phase of disease (* $p<0.05$, ** $p<0.01$, *** $p<0.001$).

It is clear from the gene expression data presented above, that varying components of self-renewal pathways' are deregulated between CP and advanced CML. It is this deregulation that makes deciphering a therapeutic target within a self-renewal pathway challenging. We next analysed the downstream targets of these pathways that have a function in cell cycle, differentiation, and apoptosis, in an attempt to determine the cause of deregulation within CML progression.

CCND1, CCND2, and *CYCLIN E1* were picked to assess G0-G1 phase of the cell cycle; *STIL* was chosen to assess cell cycle regulation through mitosis; and *p21* was used to determine cell cycle inhibition (although varying reports suggest that within CML, this is increased in proliferative capacity, as considered within the discussion). The cell cycle genes, including *CCND1*¸ *CCND2*, *p21*, *CYCLIN E1*, and *STIL* were statistically and significantly upregulated during disease progression, in keeping with the increased proliferative rate seen within an acute phase phenotype. *CCND1* and *CCND2* were upregulated between myeloid BP and CP ($p<0.0001$ and $p=0.03$, respectively; figure 4-20A-B), with a statistically significant increase in expression of *CCND1* between CP and AP ($p=0.04$; figure 4-20A). *CYCLIN E1* was also significantly upregulated between CP and AP ($p=0.01$), as well as CP and myeloid BP disease ($p=0.002$; figure 4-20E). These findings are in keeping with increased cell cycle transition and proliferative capacity seen with disease progression. *p21* is known to confer resistance to TKI in disease progression (Ferrandiz et al, 2010). Within our dataset, it was shown to have an increased expression compared to normal PB and between CP and myeloid BP disease ($p=0.0001$; figure 4-20C)). *FOXO1* was not statistically increased in disease progression (figure 4-20D).

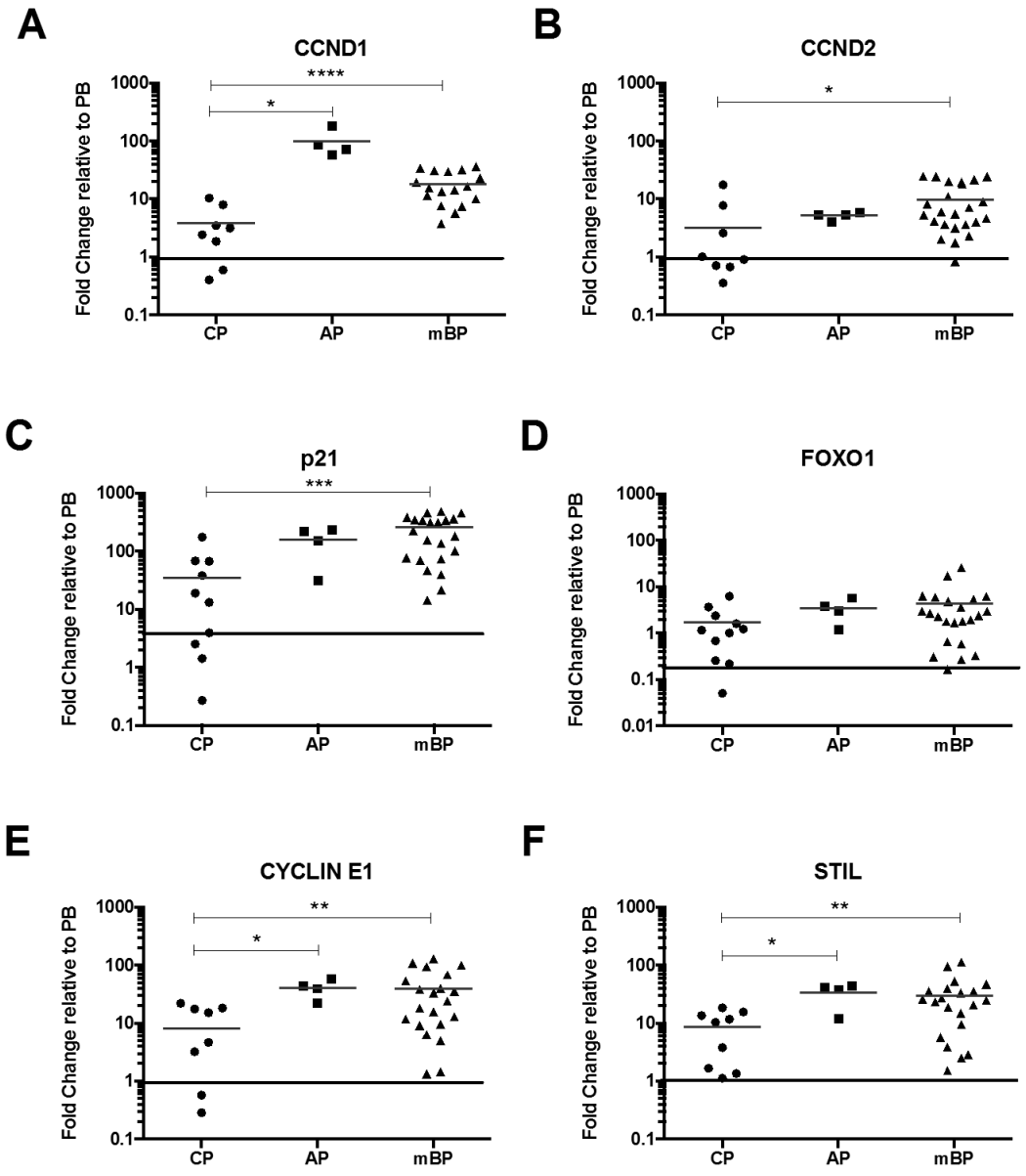

Figure 4 - 20 Focussed gene expression of cell cycle components

Analysis of gene expression was determined using the ΔΔCt method as previously described. Dot plot showing gene expression of (A) *CCND1,* (B) *CCND2*, (C) *p21,* (D) *FOXO1,* (E) *CYCLIN E1,* and (F) *STIL*, compared to normal PB $CD34^{+}$ samples in the three phases of disease. P values were determined by an unpaired t-test between the experimental population and normal, with an ANOVA used to determine significance between phase of disease (* $p<0.05$, ** $p<0.01$, *** $p<0.001$, **** $p<0.0001$).

It is known that as CML progresses abnormalities develop within DNA replication and subsequent formation of DNA double stranded breaks, leading to cellular instability. In keeping with this, *MCM7* and *MCM9* were analysed. *MCM7* has been demonstrated to encode the protein essential for the initiation of genomic replication, with *MCM9* required as a pre-replication complex. Both were increased between CP and myeloid BP (p=0.002 and p=0.005, respectively; figure 4-21).

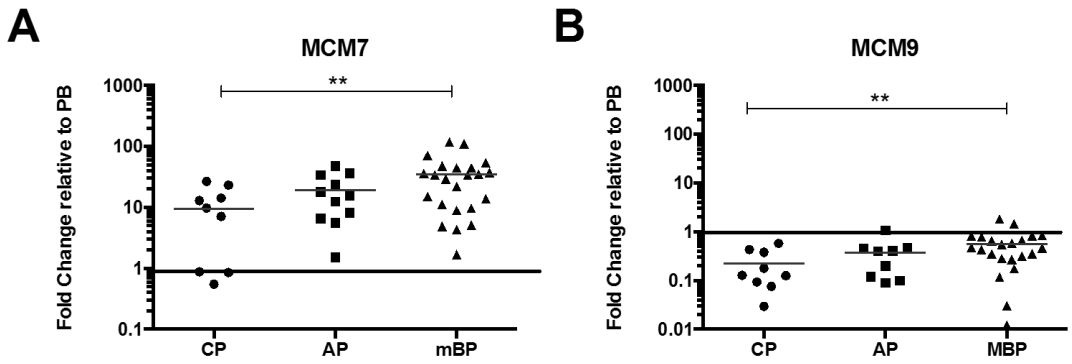

Figure 4 - 21 Focussed gene expression of *MCM7* and *MCM9*
Analysis of gene expression was determined using the ΔΔCt method as previously described. (A) Dot plot representing gene expression of *MCM7* compared to normal PB CD34$^+$ samples in the three phases of disease. (B) Dot plot representing gene expression of *MCM9* compared to normal PB CD34$^+$ samples in the three phases of disease. P values were determined by an unpaired t-test between the experimental population and normal, with an ANOVA used to determine significance between phase of disease (** p<0.01)

RUNX1, a downstream target of BMP, was evaluated as it has been previously shown that abnormalities with *RUNX1* expression may promote CML disease progression, with mutations demonstrated within progressive phenotypes. In keeping with this, *RUNX1* was statistically increased between CP and myeloid BP (p=0.008) and between AP and myeloid BP (p=0.0093; figure 4-22A). We next analysed markers of a proliferative phenotype, namely the *GATA* gene family, where *GATA2* has been shown previously to be involved in evolution to myeloid BP, and *cJUN*, which has been demonstrated to regulate cell cycle. There was no change in expression of *cJUN* or *GATA1* (figure 4-22B-C). *GATA2* has been shown to correlate with prognosis within CML progression (Giotopoulos et al, 2015). Within our dataset, there was increased expression between CP and AP (p=0.01), as well as CP and myeloid BP, as expected (p<0.0001; figure 4-22D). *GATA3* was also increased between CP and both AP and myeloid BP, but the overall expression was lower compared to normal PB CD34$^+$ cells (figure 4-22E).

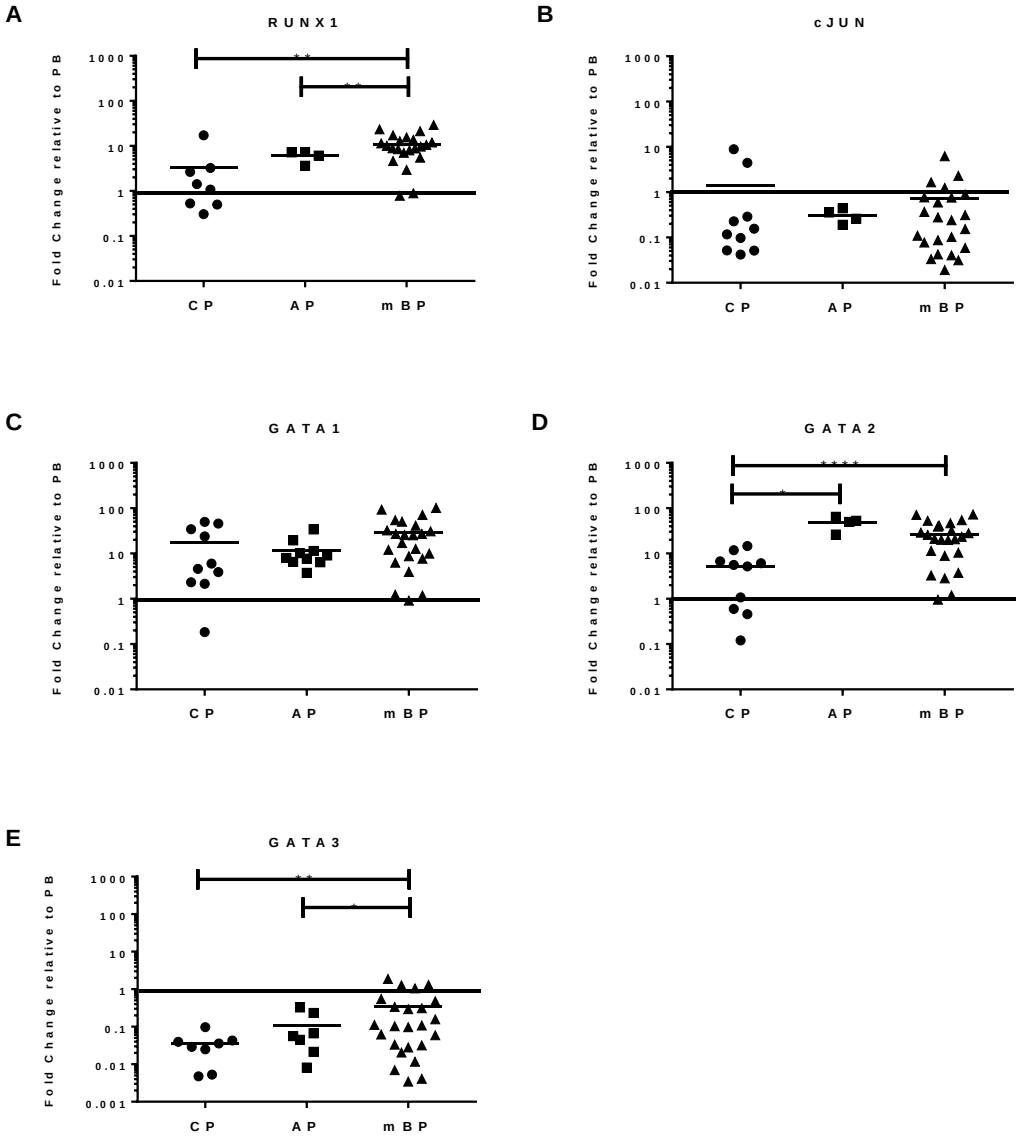

Figure 4 - 22 Focussed gene expression of differentiation components
Analysis of gene expression was determined using the ΔΔCt method as previously described. Dot plots showing (A) RUNX1, (B) cJUN, (D) *GATA1,* (E) *GATA2,* and (F) *GATA 3,* compared to normal PB CD34^{+} samples in the three phases of disease. P values were determined by an unpaired t-test between the experimental population and normal, with an ANOVA used to determine significance between phase of disease (* p<0.05, ** p<0.01, **** p<0.0001).

MPO expression was comparable between disease stages, in keeping with the myeloid phenotype of the samples (figure 4-23A); there was no significant change in expression between phases. Both *MEIS1* and *SPI1* have been implicated in the balance of differentiation and disease progression. Within our data, there was an increase in expression of *MEIS1* through disease progression, although there was no significant change compared to normal PB (figure 4-23B). *SPI1* demonstrated an increase between

myeloid BP and normal PB, as well as between CP and myeloid BP disease (p=0.01; figure 4-23C).

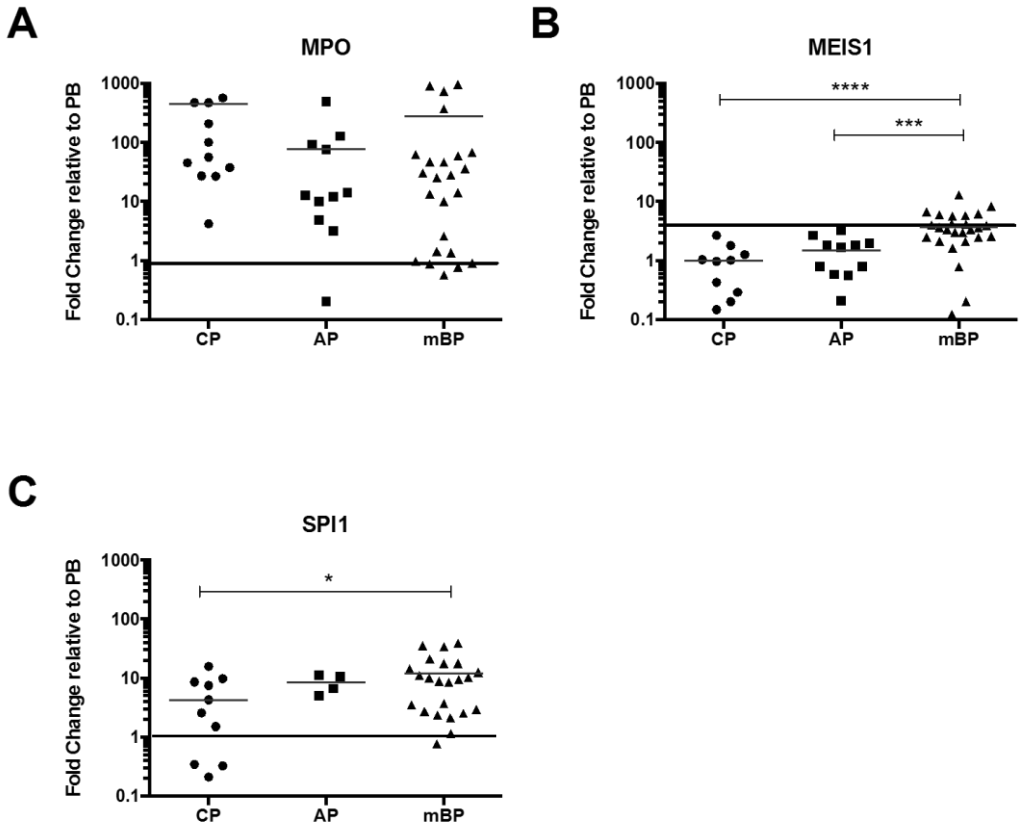

Figure 4 - 23 Focussed gene expression of differentiation components
Analysis of gene expression was determined using the ΔΔCt method as previously described. (A) Dot plot representing gene expression of *MPO* compared to normal PB CD34⁺ samples in the three phases of disease. (B) Dot plot representing gene expression of *MEIS* compared to normal PB CD34⁺ samples in the three phases of disease. (C) Dot plot representing gene expression of *SPI1* compared to normal PB CD34⁺ samples in the three phases of disease. P values were determined by an unpaired t-test between the experimental population and normal, with an ANOVA used to determine significance between phase of disease (* p<0.05, *** p<0.001, **** p<0.0001).

Transcription factors necessary for apoptosis were significantly increased between CP and myeloid BP disease. *HIPK1*, which is downstream of Hh, has been shown to activate Wnt/β-catenin. It was statistically increased between CP and myeloid BP disease (p<0.0001; figure 4-24A). *NFKβ* activity has been shown to be present within a blast phenotype; in keeping with this, there was a statistically significant increase in expression between CP and myeloid BP (p=0.0002; figure 4-24B). *TP53* and *MYC* have been demonstrated within our group to be key 'hubs' within LSC persistence and targeting these has been shown to lead to LSC eradication (Abraham et al, 2016). Within our data, there was increased expression of *TP53* between CP and AP, as well as myeloid BP disease (figure 4-24C). However, there was also increased expression of *MDM2* with disease progression (figure 4-24D); this was not significant in

comparison to normal PB. *MYC* showed increased expression between CP and myeloid BP (p=0.01 (figure 4-24E); again, this was not significant compared to normal PB controls, as was also the case for *TGF-β* which showed a statistically significant increase between CP and both AP (p=0.006) and myeloid BP (p=0.001; figure 4-24F).

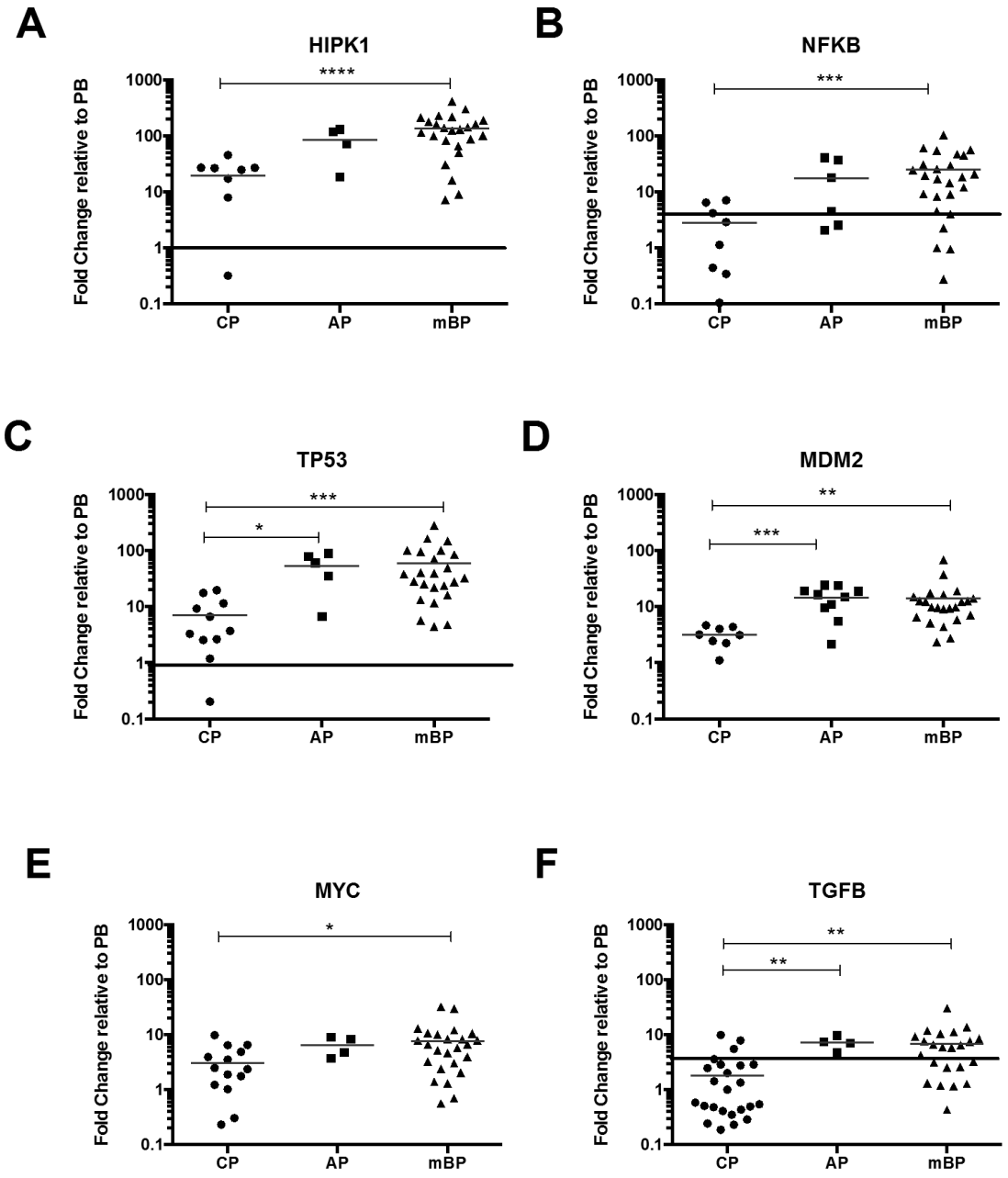

Figure 4 - 24 Focussed gene expression of components involved in apoptosis

Analysis of gene expression was determined using the ΔΔCt method as previously described. Dot plots showing (A) *HIPK1,* (B) *NFKβ,* (C) *TP53,* (D) *MDM2,* (E) *MYC*, and (F) *TGF-β* compared to normal PB $CD34^+$ samples in the three phases of disease. P values were determined by an unpaired t-test between the experimental population and normal, with an ANOVA used to determine significance between phase of disease (* p<0.05, ** p<0.01, *** p<0.001, **** p<0.0001).

EZH2 has been demonstrated to result in myeloprolifeative neoplasm and has been shown to mediate activity of methyltransferase activity. Our data showed statistically significant increase in expression in all phases of disease, compared to normal. (CP, p=0.0066, AP, p=0.012, mBC, p= 0.0005), although this was not significant between stage of disease.

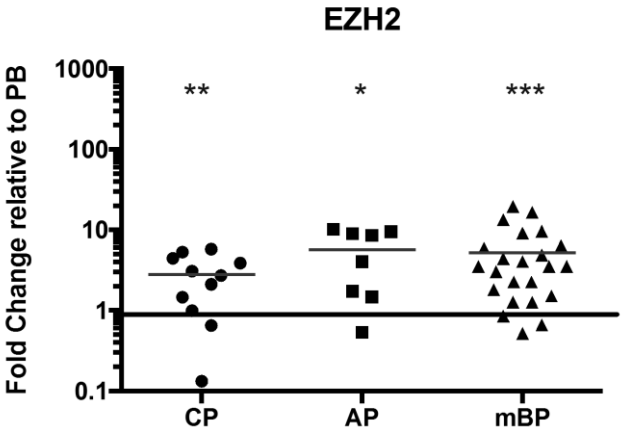

Figure 4 – 25 Focussed gene expression of *EZH2* in CML disease progression
Analysis of gene expression was determined using the ΔΔCt method as previously described. Dot plot representing gene expression of *EZH2* compared to normal PB $CD34^+$ samples in the three phases of disease. P values were determined by an unpaired t-test between the experimental population and normal, with an ANOVA used to determine significance between phase of disease (* $p<0.05$, ** $p<0.01$, *** $p<0.001$).

4.4. Discussion

Within this chapter, data is presented that suggests the Notch pathway has a differing functional role in myeloid BP-CML compared to CP-CML. This is the first time that primary myeloid BP cells have been used to understand this pathway in this phase of the disease. Previous literature evidence relies on cell line data or *in vivo* retroviral models and provides conflicting outcomes.

Firstly, our data suggests that within primary myeloid cells, the Notch pathway is inactive at a basal state (i.e. on plastic non-stromal culture). This was based on gene expression data, where, despite a statistically significant increase in the Notch downstream target, *HES1*, there was no objective evidence of the pathway being activated, with no statistical change in other downstream targets, such as *HIF1A*, and no increase in expression of *MAML*, the intracellular complex necessary for downstream activation. This was confirmed through functional analysis, which suggested that despite inhibition of the pathway using the gamma-secretase inhibitor, DAPT, there was no statistically significant change in trypan blue cell counts or apoptotic ability over six days in *in vitro* culture.

As there was an abundance of the Notch receptor, *NOTCH2*, on the myeloid BP cells, we next questioned if the pathway could be upregulated through exogenous expression of the Notch ligands, DLL1 and JAG1, as had been demonstrated within CP-CML. An OP9 co-culture system was used as previously described within chapter 3, and samples were sorted into immature and mature progenitor phenotypes using CD34 and CD38 expression. In cell proliferation, apoptosis, and differentiation assays, there was no change in cellular function within any co-culture model. The pathway was not deemed to be upregulated through exogenous activation with Notch ligands, by both gene expression of *HES1* and *MAML*, as well as IF of the val1744 protein.

This was, somewhat, surprising, in view of the mounting evidence that Notch signalling plays a role in acute myeloid disease, namely AML, with increasing and convincing evidence suggesting that Notch activation in myeloid precursors promotes self-renewal, induces and inhibits differentiation to monocytes, or can induce apoptosis (Carlesso et al, 1999; Li et al, 1998; Sarmento et al, 2005; Schroeder et al, 2003). Furthermore, early observations have shown that Notch signalling may play a role in myeloid progression (Schroeder et al, 2003; Tan-Pertel et al, 2000). More recently, observations have

supported a tumour suppressive role for Notch signalling in AML (Chen et al, 2008; Kannan et al, 2013; Klinakis et al, 2011; Lobry et al, 2013; Yin et al, 2009). It was observed that human AML samples expressed Notch receptors, however activation of downstream Notch targets was low, suggesting that Notch was present but not active in the samples analysed (Kannan et al, 2013; Lobry et al, 2013). Subsequent activation of the Notch receptors or Notch targets led to AML growth arrest *in vivo* and conversely Notch inhibition via dnMAML enhanced proliferation (Kannan et al, 2013), again suggesting a role of Notch in myeloid neoplastic proliferation. Within CML itself, there is a clear role for *Hes1* within an acute phenotype, with *in vivo* data using a retroviral model resulting in an aggressive acute *Bcr-Abl* positive leukaemia, and as our data has suggested, myeloid BP disease is associated with an increasing activation of *HES1*. It is likely, as our data suggests, that this is not being mediated by Notch signalling and the question remains, what is driving its expression.

To evaluate this, it was next questioned if other signalling pathways were driving the increasing expression of *HES1*. This was in the knowledge that aberrancies within signal transduction pathways are the key in self-renewal, proliferative, and anti-apoptotic potential within CML progression and the CML LSC (Crews & Jamieson, 2012; Radich et al, 2006; Steelman et al, 2004; Zon, 2008). These pathways include the evolutionary conserved self-renewal pathways, Hh, Wnt/β-Catenin, TGF-β, BMP, and Notch, as well as survival pathways, such as MAPK and JAK-STAT signalling, leading to the upregulation of oncogenic transcription factors, such as c-MYC. It is known that these pathways and transcription factors do not act in isolation, relying on interconnective networks between them (Sinclair et al, 2013). RNA was extracted from CP, AP, and myeloid BP samples before being transcribed into cDNA at equal concentrations to allow for comparison between samples. Gene clustering of the data generated suggested that CML progression is a two-step phenomenon from CP to advanced/acute phase disease. This has previously been documented within the GSE1470 microarray dataset (Radich et al, 2006) and suggested that our dataset would be comparable in determining changes in gene expression through focussed gene analysis. Gene expression demonstrated notable deregulation of all evolutionary conserved self-renewal pathways between CP and AP/myeloid BP. Within the Notch pathway, there was a statistically significant increase in *NOTCH1, NOTCH2, ADAM10, and ADAM17*, which suggested that these cells had the machinery to allow for upregulation of the

pathway. In conjunction with this, there was a statistically significant increase in expression of the negative regulators, *MFNG* and *FBXW7.*

In addition to the core components of the Notch pathway, additional proteins modulate its activity; these include the Fringe family of glucosyltransferases (Haltiwanger & Stanley, 2002; Thomas & van Meyel, 2007). Fringe molecules, including *MFNG*, glycosylate Notch, thereby modifying the receptor's response to its ligands. In general, glycosylation increases the response of Notch to Delta-like, but decreases Jagged-induced Notch signalling. In mammals, this decrease in Jagged-induced Notch cleavage occurs with no reduction in Jagged-Notch binding (Hicks et al, 2000; Yang et al, 2005). This perhaps offers an explanation for the inability of the Notch receptors to activate through JAG1, as would have been expected following the CP data generated in the previous chapter.

As has been discussed within earlier chapters, *FBXW7* is not unique to Notch signalling and has been shown *in vivo* to target many proto-oncogenes, growth promoters, and anti-apoptotic molecules. Furthermore, *FBXW7* has been shown to have an indispensable role in the maintenance of adult HSC quiescence (Matsuoka et al, 2008; Thompson et al, 2008). Deletions of Fbxw7 in HSCs and CML LSCs have been shown to lead to c-Myc accumulation, activation of the TP53 signalling pathway, aberrant cell cycle entry and eventual exhaustion (Reavie et al, 2013; Reavie, 2010). Within our dataset, there was a small but statistically significant increase in *MYC* expression between CP and myeloid BP. c-MYC is activated through direct BCR-ABL-mediated phosphorylation and the MAPK and JAK-STAT pathways to induce growth-factor independent proliferation and has been shown to be a key mediator of leukaemogenesis in CML (Afar et al, 1994; Askew et al, 1991; Notari et al, 2006; Xie et al, 2002). In keeping with this, *p38* was statistically and significantly increased between CP and myeloid BP. c-MYC has been also implicated in driving disease progression, as elevated expression confers an increased risk of progression to BP (Calabretta, 2004; Lucas et al, 2015; Radich, 2007). Additionally, inhibition of c-MYC is able to target TKI-resistant CML cells (Abraham et al, 2016; Winter et al, 2012), indicating that inhibition of c-MYC may have further therapeutic applications in advanced stage or TKI resistant disease. Activation of c-MYC has been shown to increase TP53 and, indeed, this is apparent within our own dataset. TP53 mutations can accompany disease progression in human CML and *TP53* loss in some cases impedes the anti-leukaemic

response to BCR-ABL inhibition (Kelman et al, 1989; Wendel et al, 2006), suggesting that loss of p53 in some tumours could constitute an adaptive response to the increase in the levels of c-Myc during CML progression. Within our own dataset, although there is a statistically significant increase in *TP53*, we cannot correlate this as being clinically relevant without the *TP53* mutational status of each of the samples used and evaluation at a protein level.

The gene expression data demonstrated a statistically significant increase in expression of the Notch downstream targets, *HES1* and *HIF1A*, in progression from CP to myeloid BP. Both may be modulated through other self-renewal pathways. Their importance, however, in CML proliferation and progression is well documented, as described for *HES1* earlier in this chapter (Jamieson, 2010; Nakahara et al, 2010). *HIF1A* has been shown to promote chronic CML cell proliferation by upregulating *p21* expression (Zhang et al, 2012). *p21*, a cell cycle inhibitor has been shown to be upregulated with high levels of *Bcr-Abl* and that retaining *p21* in a cytosolic location can allow *Bcr-Abl* to evade the cell cycle arrest normally induced by nuclear *p21* (Keeshan et al, 2003). To understand the potential mechanisms for upregulation of *HES1* and *HIF1A*, we next assessed self-renewal components of other pathways in view that the interconnectivity between self-renewal pathway components has been shown to alter expression of these genes.

We demonstrated that Wnt/β-catenin expression was increased between CP and myeloid BP disease. This was through the statistically increased expression of *TCF4* and *TCF7*. There was no statistically significant change in LEF expression. The Wnt/β-catenin pathway plays an essential role in the maintenance and differentiation of LSCs and the propagation of malignancies (Clevers, 2006). Its activation has been shown to be critical within the previously mentioned GSE1470 dataset (Radich et al, 2006). The importance of deregulation of Wnt/β-catenin has been described in both disease initiation and disease progression within CML (Zhao et al, 2007). It has been previously reported that *TLE3* expression can be directly induced by Wnt/β-catenin signalling, as part of a negative feedback loop within the canonical pathway (Kokabu et al, 2014). It is, therefore, unsurprising that both *TLE3* and *TLE4* have increased expression within our dataset. Furthermore, in unpublished data, with our collaborator, Dr Helen Wheadon, *TLE3* has been shown to be of prognostic relevance in the determination of poor responders to TKIs. In the absence of Wnt/β-catenin signalling, cytoplasmic β-catenin is ultimately phosphorylated by GSK3β and targeted for degradation by an

actin-mediated multimeric complex. GSK3β can, therefore be increased within the context of Wnt/β-catenin activation. GSK3β is an interesting area of leukaemia research because of its role in preserving a quiescent HSC despite having negative effects on self-renewal (through inhibitory phosphorylation of Hh, Notch and Wnt/β-catenin signalling) (Foltz et al, 2002; Grimes & Jope, 2001; Jia et al, 2002). Retrospectively, it is difficult to ascertain any functional relevance from gene expression data of *GSK3β* because its function is from a phosphorylated protein. This is despite data suggesting that the ability of self-renewal in Ph+ precursors being linked to Wnt/β-catenin activation through *GSK3β* missplicing, or via impairment in binding through a BCR-ABL-mediated phosphorylation (Abrahamsson et al, 2009; Jamieson et al, 2004; Reddiconto et al, 2012). *NFKβ* was shown to be upregulated within our data between CP and myeloid BP. Increased *GSK3β* has been shown to upregulate *NFKβ* leading to increased proliferation and aggressiveness of solid tumours, such as Gliomas (Hoesel & Schmid, 2013). Furthermore, GSK3β has been shown to bind and phosphorylate the intracellular Notch component, and attenuation of GSK3β activity reduces phosphorylation of intracellular Notch *in* vivo, suggesting a dual functional role in Notch inhibition and activation (Foltz et al, 2002; McCubrey et al, 2013).

Wnt/β-catenin signalling can influence the stability of *GLI1* allowing for its intracellular accumulation (Noubissi et al, 2009). Furthermore, downstream Hh targets have been shown to modulate Wnt/β-catenin signalling. Within our gene expression data, *GLI1* was statistically overexpressed when CP was compared to myeloid BP. However, *SUFU*, a negative regulator of Hh, was significantly increased within a myeloid phenotype and between CP and myeloid BP. This could suggest that Wnt/β-catenin signalling, in part, is driving the expression of *GLI1* within our subset. However, *HIP1K,* a downstream target of Hh was also upregulated between CP and myeloid BP. *HIP1K* has been shown to both promote and antagonise Wnt/β-catenin signalling, as well as its autophosphorylation being shown to drive *TP53* expression. Mutations within *SUFU* have been demonstrated to drive hyperactivation of the pathway in basal cell carcinomas and medulloblastomas, which may offer an explanation (Taylor et al, 2002). Regardless, there is a clinical role for inhibition of Hh signalling within a myeloid BP phenotype as discussed within the introductory chapter (Cortes et al, 2016a; Fukushima et al, 2013; Fukushima et al, 2016b; Jamieson et al, 2011).

The BMPs belong to the TGF-β superfamily and have been shown to be involved in a huge array of diverse cellular functions, including cell proliferation, differentiation, apoptosis, and stem cell self-renewal, in both embryonic and adult phenotypes (Herpin & Cunningham, 2007; Miyazono et al, 2005). Dysregulation within the BMP-TGF-β pathway has been shown to be critical in LSC survival (Laperrousaz et al, 2013; Miyazono, 2012; Naka et al, 2010). The BMP pathway functions through receptor-mediated intracellular signalling (Toofan et al, 2014). It has been shown that type 1 receptors are present on LSCs in primary CML samples, with an associated downregulation of BMP ligands (Laperrousaz et al, 2013). Within the same study, CML aspirate and trephine BM samples had significantly higher levels of BMP2 and BMP4 compared to normal donors. Our data suggested that *BMP4* was upregulated compared to normal PB, but that there was no change between CP and AP/advanced disease. SMADs are the major signal transducers in the canonical BMP pathway. Upon phosphorylation of type I receptors, SMAD1/5/7 become phosphorylated and form a complex with SMAD4. Within our data set, there was no increase in *SMAD5*. *SMAD4* had increased expression in myeloid BP, but this may suggest that the SMAD-complex was not formed. Interestingly *SMAD6* was statistically significantly upregulated in all phases compared to CP. The BMP pathway is inhibited by *SMAD6* and *SMAD7* which inhibits phosphorylation of SMAD1/5/8. Therefore this suggests, as previous functional data has, that within isolated CML cells, the pathway is not activated, but has the ability to be activated through receptor-ligand binding, and this may represent a therapeutic modality.

Cell cycle gene expression favoured a positive regulation of cell cycle progression (i.e. progression through all phases of the cell cycle, mitosis, and proliferation), with statistically significant increased expression of *CCND1*¸ *CCND2*, *CYCLIN E1*, and *STIL*. This is in keeping with an increased proliferative rate seen within an acute disease setting. For example, *CCND2* has been shown to be increased in *BCR-ABL* expressing lymphoblasts and required for their proliferation (Deininger et al, 2001). The regulation of quiescence remains important despite the increased proliferation seen within BP disease. Interestingly, *p21*, a cell cycle inhibitor, is increased in myeloid BP compared to CP as the disease balances acute proliferation with stem cell quiescence. Furthermore, the location of *p21* seems to be integral in its function, as described above, with cytosolic *p21* allowing *Bcr-Abl* to evade the cell cycle arrest normally induced by

nuclear *p21* (Keeshan et al, 2003). Furthermore, *p21* is known to confer resistance to TKI in disease progression. In keeping with this idea, *TGF-β* was increasingly upregulated between CP and myeloid BP. *TGF-β* has a key role in maintenance of quiescence and has been hugely implicated in LSC survival (Miyazono, 2012; Naka et al, 2010).

The transition of CML from CP to BP is characterised by the accumulation of molecular and chromosomal abnormalities, but the molecular mechanisms underlying this genetic instability are poorly understood. There is some evidence as to the relationship between *BCR-ABL* expression and activity of proteins involved in DNA repair (Radich, 2007; Shet et al, 2002). To this avail, our data demonstrated an increased expression in the DNA replication genes, *MCM7 and MCM9,* between CP and myeloid BP disease. There is accumulating evidence that suggests that BCR-ABL causes this directly through induction of ROS inducing DNA breaks requiring repair and by interacting directly with the repair machinery to inhibit performance (Skorski, 2008). It has also been shown that BCR-ABL directly drives expression of certain members of the DNA repair pathways resulting in increased DNA instability (Skorski, 2008). The uncontrolled activity of *MCM7* and *MCM9* may represent an interesting therapeutic target in myeloid BP disease in the control of genomic instability.

Interestingly, our data revealed that EZH2 was significantly and consistently upregulated through all phases of CML. Within our centre, and others, recently published data has described the use of global and transcriptomic analysis to determine the functional dependency of LSCs on EZH2 and its use as a therapeutic modality. Our group showed that combining an EZH2 inhibitor with TKI was highly effective at eradicating the LSC population (Scott et al, 2016). Our data, therefore, may suggest the possibility of expanding this therapeutic modality to a myeloid BP phenotype.

Our gene expression data highlights the difficulty in understanding the interconnectivity between signalling pathways. This is an area of research that needs further investigation and understanding to enable the development of therapeutic agents to eradicate myeloid BP. Our data has shown that Notch signalling has no relevance within this model. This may, in part be due to the increase of *MFNG* and *FBXW7,* but will be largely due to modification of other self-renewal pathways', such as Wnt/β-catenin and Hh.

4.5. Future work

The data presented above raises interesting possibilities for further research into the regulation of self-renewal pathways within myeloid BP. The mechanism by which Notch is inhibited within myeloid BP disease has not been fully elucidated. The role which the Fringe process plays in this offers exciting potential as glycosylation is an elegant means for regulating self-renewal pathways, particularly Notch. Although the functional relevance of this within myeloid BP is unlikely to offer a practical therapeutic advantage as, not only would a two-step approach need to be utilised to inhibit the fringe affect, followed by Notch activation. As we demonstrate no functional relevance to either inhibition or activation of the pathway, it is difficult to predict if this will yield therapeutic potential.

More relevant to therapeutic intervention is the continued understanding of gene regulation within disease progression. The regulation of DNA repair genes, including *MCM7* and *MDM9,* may prove an interesting area of therapeutic advantage and experimental models analysing their inhibition are currently under investigation within our group.

5. Results III

5.1. Introduction

As has previously been discussed within this thesis, the transformation of CP CML to BP, or the presentation of CML in BP, is associated with a high mortality despite therapeutic intervention with TKIs (Radich, 2007; Saußele & Silver, 2015). Progression to BP may present as either myeloid, lymphoid, or an undifferentiated phenotype. This variation can be, somewhat, anticipated in view of the importance of the LSC in CML pathogenesis (Crews & Jamieson, 2012; Graham et al, 2008; Holyoake et al, 1999; Jamieson et al, 2004). The pathophysiology of what drives disease progression, however, remains poorly understood. Furthermore, the literature available determining factors that induce lineage potential within the disease phenotype is limited (Wang et al, 2015).

It is thought that *BCR-ABL* provides a favourable environment for the development and maintenance of secondary DNA modifications (Bacher et al, 2005a; Radich, 2007). Although this, in itself, does not explain why some of these mutations are lineage-specific. Numerous genetic mutations have been identified in BP disease. Some are common to both lineages, and it has been hypothesised that these merely act as a surrogate for genomic instability rather than the genes pivotal for progression. Others are implicated more commonly in either myeloid or lymphoid disease, such as *TP53* and *RUNX1*, respectively (Calabretta, 2004; Roche-Lestienne et al, 2008). Within myeloid BP, deregulation of self-renewal and cell survival pathways can be correlated with progression, as described in Results II. However, the exact mechanisms by which they act have not been fully elucidated. Within lymphoid BP, less information is available and, therefore, it is difficult to hypothesise cause and effect of genetic mutations or indeed alteration of signalling pathways.

Further to this, studies to identify the LSC population in BP disease are more limited when compared to the information available for CP. Jamieson *et al* found that the HSC population ($lin^-CD34^+CD38^-CD90^+CD45RA^-$) was not expanded in myeloid BP-CML and identified the GMP population as a potential source of LSCs in myeloid BP (Jamieson et al, 2004). However, this study did not assess the multipotent progenitor (MPP; $lin^-CD34^+CD38^-CD90^-CD45RA^-$)/LMPP-like subpopulations, nor did it assess *in vivo* LSC activity. Further studies by the Jamieson group identified activation of β-catenin as the likely mechanism of enhanced self-renewal capacity in the myeloid BP

GMP cells (Jamieson et al, 2004; Minami et al, 2008). Less information is available regarding the LSC populations in lymphoid BP CML. A case report of a patient with imatinib-resistant lymphoid BP-CML indicated that the imatinib-resistant sub-clone (E255K kinase domain mutation) likely originated in the B-cell committed progenitor compartment, but no functional stem cell assays were performed (Kobayashi et al, 2011). In order to increase understanding of the lineage-specificity within CML progression, one must understand not only the differences in cell survival and self-renewal pathway components that may occur between a myeloid and lymphoid phenotype, but also the heterogeneity that is seen within Ph+ acute leukaemias, especially if the cell of origin is not the LSC, as would be expected. This will allow understanding for alternative therapeutic strategies between the conditions.

Ph+ acute lymphoid-phenotype leukaemias encompass both lymphoid BP CML and Ph+ ALL. These two diseases are clinically distinct, but can often be mislabelled. Ph+ ALL accounts for approximately 25-30% of ALL diagnosed in adults. Although 70-90% of cases will achieve a complete remission with conventional chemotherapy, long-term survival remains poor reflecting high rates of relapse and failure of salvage regimens. It encompasses three main phenotypes:

- A lymphoid lineage restricted phenotype with either p190 or p210 *BCR-ABL* fusion variant*;*
- A stem cell phenotype with either p190 or p210 *BCR-ABL* fusion variant, or
- Misclassified lymphoid BP CML, which has a stem cell phenotype and expresses p210 *BCR-ABL* fusion variant.

The differences between both lymphoid BP and Ph+ ALL lie in the BCR-ABL fusion variants, as described within the introduction to this thesis, as well as potentially within the cell of origin. The two *BCR-ABL* fusion variants, p190 and p210, are determined by the different amounts of BCR that they include, leading to different molecular weights (Soekarman et al. 1990). The larger 210kD fusion protein (p210) is almost always found in CML, but is also present in approximately 30% of Ph+ ALL. Inversely, the 190kD fusion protein is found in the majority of paediatric Ph+ ALL, 25-30% of adult Ph+ ALL, and only rarely in CML (Advani & Pendergast, 2002). In both, the signalling pathways involved in cell proliferation and survival are deregulated, leading to the phosphorylation of many proteins (Mullighan, 2012a; Radich et al, 2006). Included in this is the activation and phosphorylation of STAT5, which has been

demonstrated to be required for progression to lymphoid transformation (Hantschel et al, 2012). The JAK-STAT pathway is integral part to disease progression, but it is also known to have many interactions with self-renewal pathways that have not yet been fully described. Further to this, attempts to address the differences between lymphoid BP and Ph+ ALL have focussed on studies to address the cell of origin, with conflicting results (Hovorkova et al, 2017; Hunger, 2017; Thomas, 2012). As CML is known to be a stem cell disease, *BCR-ABL* should theoretically be identified in all cell types. Similarly, with ALL being lineage restricted, it would be anticipated that the *BCR-ABL* would be restricted to the lymphoid lineage. However, there is evidence to suggest that both produce a multi-lineage involvement (Anastasi et al, 1996; Cuneo et al, 1994a; Pajor et al, 2000; Schenk et al, 1998).

Based on this information, we firstly hypothesised that there would be changes between gene expression patterns of cell survival and self-renewal pathways between myeloid and lymphoid BP disease. Furthermore, we hypothesised that the gene expression patterns would be different between Ph+ ALL and lymphoid BP, in keeping with the idea that these are distinct disease subtypes.

5.2. Aims

Based on the evidence provided above, the specific aims set out in this chapter are:

1. To evaluate the heterogeneity of lymphoid progenitor sub-populations within lymphoid BP disease;
2. To evaluate the gene expression changes of self-renewal and cell survival signalling pathways between myeloid and lymphoid BP;
3. To evaluate the gene expression changes of self-renewal and cell survival signalling pathways between lymphoid BP and Ph+ ALL.

5.3. Results

5.3.1. Lymphoid BP is an immunophenotypically heterogeneous disease

To identify if lymphoid BP samples were heterogeneous at an immunophenotypic level, samples were thawed and cultured in high growth factor SFM overnight. This was to ensure the samples had been under the same conditions to allow gene expression comparison with myeloid BP samples in later experiments. Samples were sorted by FACS into HSC, MPP, CMP, CLP ($lin^-CD34^+CD38^+CD45RA^+CD10^+CD19^-CD33^-$), and pro B ($lin^-CD34^+CD38^+CD45RA^+CD10^+CD19^+CD33^-$) cell populations (figure 5-1).

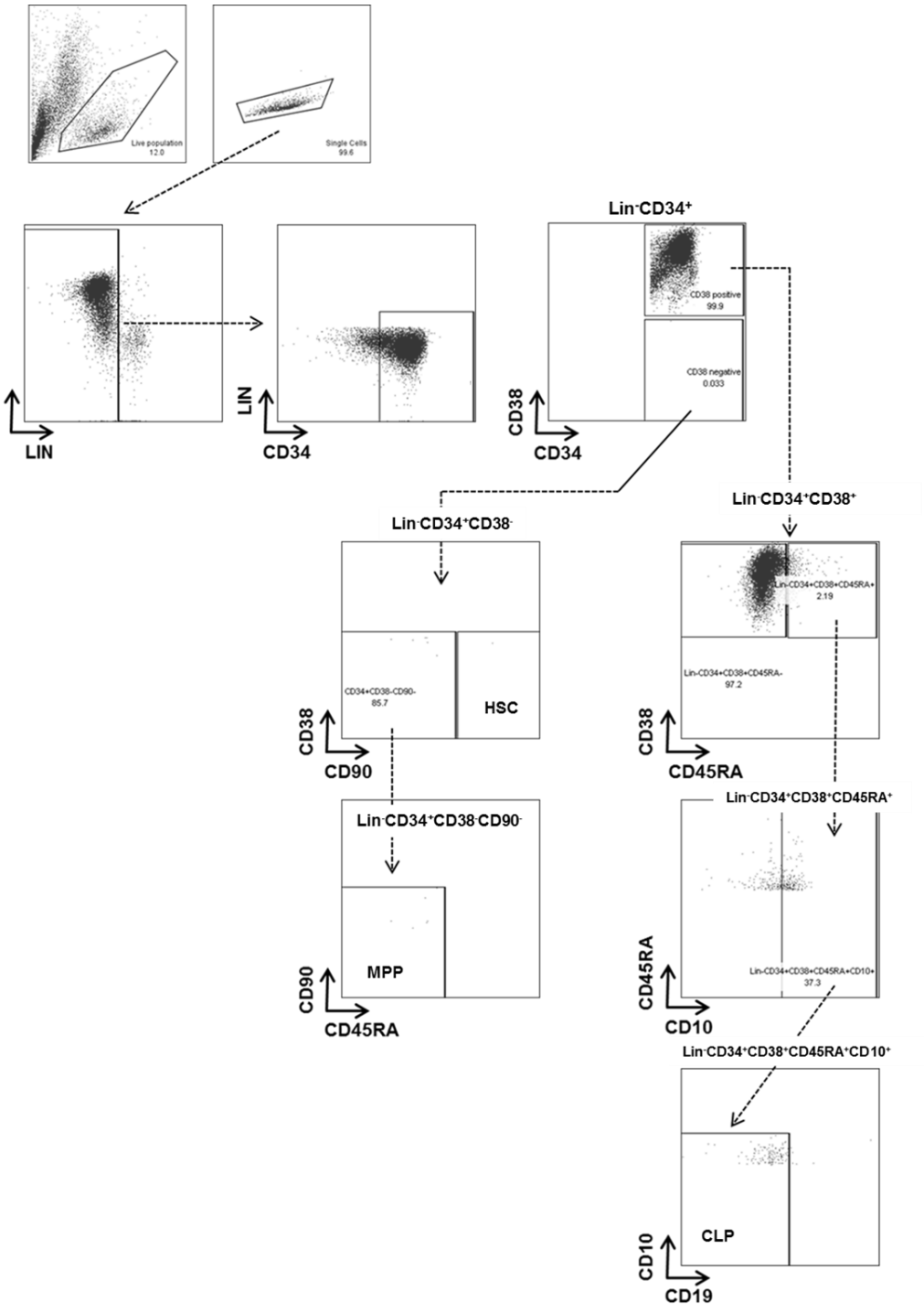

Figure 5 - 1 FACS strategy for lymphoid BP samples
Cells were washed in PBS/2%FBS and counted following thawing. $5x10^4$ cells were used within each unstained and single-stained control, where cells were re-suspended in 100ul PBS/2%FBS prior to the addition of antibody. The 'multi-stain' sample was re-suspended in 450ul PBS/2%FBS prior to the addition of antibody. Samples were stained for 30 min at 4°C and then washed twice with PBS/2%FBS before being filtered through a 0.22uM filter. Cells were sorted with a BD FACS Aria with Diva software.

Samples were analysed using FlowJo software to determine heterogeneity. Four samples were analysed in detail; however, two of these samples had a recovery rate of only 10% and only $Lin^-CD34^+CD38^+$ and $Lin^-CD34^+CD38^-$ populations identified and, therefore, are not included in the detailed immunophenotypic analysis. Of the two remaining samples, recovery rate was low, as has been previously demonstrated with BP samples (figure 5-2A). Furthermore, there was a variation in percentage of lineage negative cells within the live population (range between 43% and 85%) (figure 5-2B).

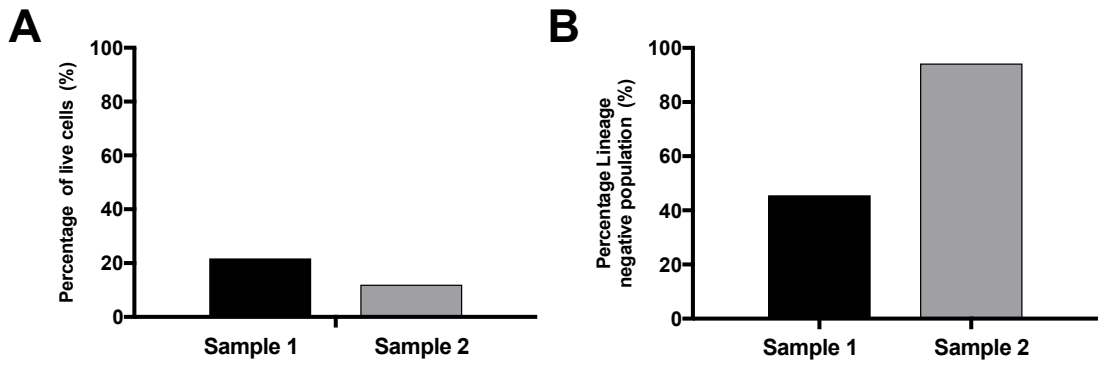

Figure 5 - 2 Following thaw, lymphoid BP samples have a low recovery rate with a variation in percentage of a lineage negative population
Cells were thawed and sorter as per figure 5-3. Immediately after FACS sorting, cells were analysed using FlowJo v7 software. (A) Percentage of live cells in each sample. (B) Percentage of lineage negative cells isolated and FACS sorted into sub-populations.

Next, the percentage of $CD34^+$ and $CD34^+CD38^-$ populations was assessed in comparison to the lineage negative population (figure 5-3). There was again a variation between the two samples, with CD34 and $CD34^+CD38^-$ expression of lineage negative cells. There appeared to be a lower immature component (i.e. $CD34^+CD38^-$) compared to previous experiments within myeloid BP CML, with the population ranging between 0.03 and 1%.

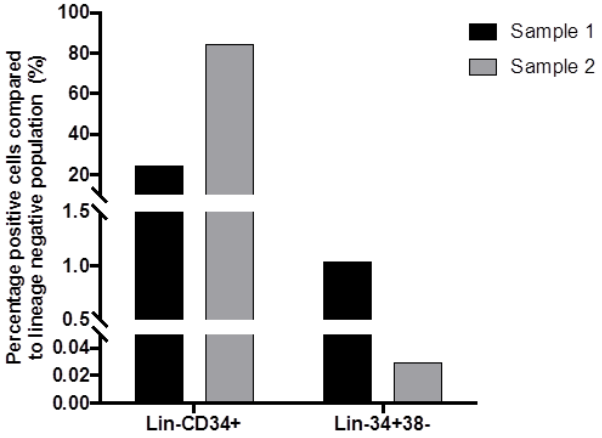

Figure 5 - 3 Lymphoid BP samples have a varying percentage of $CD34^+$ and $CD34^+CD38^-$ cells

Cells were thawed and sorted as per figure 5-1. Immediately after FACS sorting, cells were analysed using FlowJo v7 software. The percentage of CD34+ and CD34+CD38- populations were calculated against the lineage negative population. There was variation in both with CD34+ cells ranging between 22 and 83%, and CD34+CD38- cells ranging between 0.03 and 1%.

Between the samples, there were differences in the proportion of immature and mature populations (figure 5-4). For example, sample 1 had an increased percentage of immature cells, with an increased percentage of HSCs and MPPs, whereas sample 2 had a greater number of differentiated cells (i.e. CMP). The CLP populations were comparable between samples. Neither sample had a pro-B population. Despite this, the majority of cells within both samples were akin to a CMP population, namely 20-83% of cells when compared to the $lin^-CD34^+CD38^+$ population. Samples were collected and immediately isolated into RNA samples due to small cell numbers following sorting.

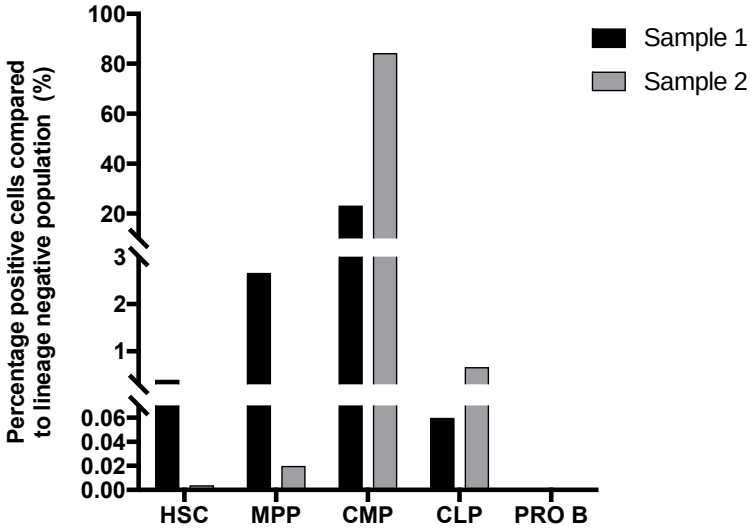

Figure 5 - 4 The CMP population is the largest of the lymphoid BP sub-populations

Cells were thawed and FACS sorted as per figure 5-3. Immediately after FACS sorting, cells were analysed using FlowJo v7 software. The percentages of sub populations were gated in the lineage negative population according to the sorting strategy.

5.3.2. Self-renewal gene expression is equivalent between myeloid and lymphoid BP

As described, myeloid (n=11), lymphoid BP (n=4) and normal PB (n=3) samples were thawed, cultured, and sorted into stem and progenitor populations as previously described and RNA extracted. Using Fluidigm technology, quantitative PCR of 90 self-renewal and cell survival signalling genes was performed. 100ng of RNA was transcribed to cDNA across all samples to enable comparison between groups. Samples were plated in duplicate or triplicate, and as more than one Fluidigm plate was to be used, an internal sample control was used across plates to enable comparison. Myeloid and lymphoid BP sub-populations were pooled for analysis to ascertain a global expression pattern between disease phenotypes, rather than between sub-populations. The sub-population data will be presented within publication. On global gene expression analysis, myeloid and lymphoid BP could not be distinguished by gene clustering methods (figure 5-5). Each duplicate or triplicate was represented independently within all analysis. This is perhaps, unsurprising, in view that the cell of origin will be the same for both populations and in view that on immunophenotypic analysis, the majority of cells were within a CMP population.

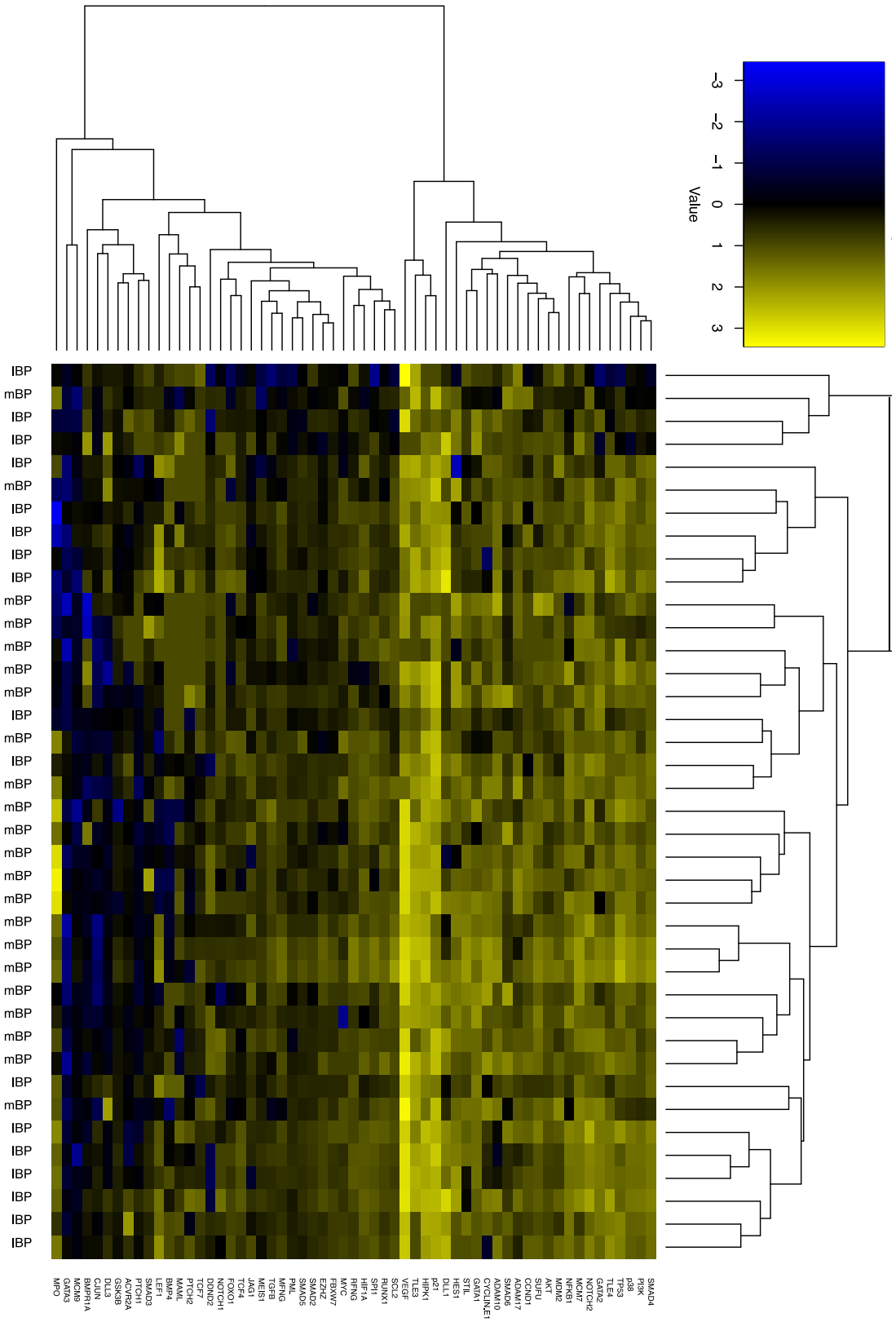

Figure 5 - 5 Gene clustering could not segregate myeloid and lymphoid BP disease
Gene expression profiles (GEPs) were determined from myeloid BP and lymphoid BP populations. GEP levels were determined by Fluidigm array analysis. Relative gene expression levels were determined by ΔΔCt method using an average of five housekeeping genes as reference and the average Normal PB value as the calibrator for fold change. Heat maps and gene clustering were produced by using heatmap.2 in R/Bioconductor.

For the purpose of this chapter, focussed gene expression results will be presented as fold change against normal to represent the change associated with a malignant phenotype. Black asterisks above the gene of interest represent statistically significant change between leukaemic samples and normal $CD34^+$ PB. These were determined using an unpaired student's t-test between experimental arms on the delta CT values. Black asterisks with a contector represent statistically significant change between myeloid and lymphoid BP. This was again done using an unpaired student's t-test between myeloid and lymphoid BP samples on the delta CT value. Although, there were many genes that were statistically significantly changed between leukaemic and normal, the main question in this chapter was surrounding gene expression changes between myeloid and lymphoid BP disease.

In keeping with the global gene expression analysis, there was little difference in gene expression of the key self-renewal and cell survival signalling pathway components between myeloid and lymphoid BP disease. For example, within the Notch pathway, there was little statistically significant difference in Notch components between myeloid and lymphoid BP (figure 5-6). This was, despite, statistically significant changes in the pathway's components between leukaemic samples and normal PB samples. Interestingly, *MAML* was statistically significantly upregulated compared to normal PB in the lymphoid BP subset, but not within myeloid BP. This, perhaps, suggests that there is activated expression of the pathway in lymphoid BP disease and may represent an interesting therapeutic target.

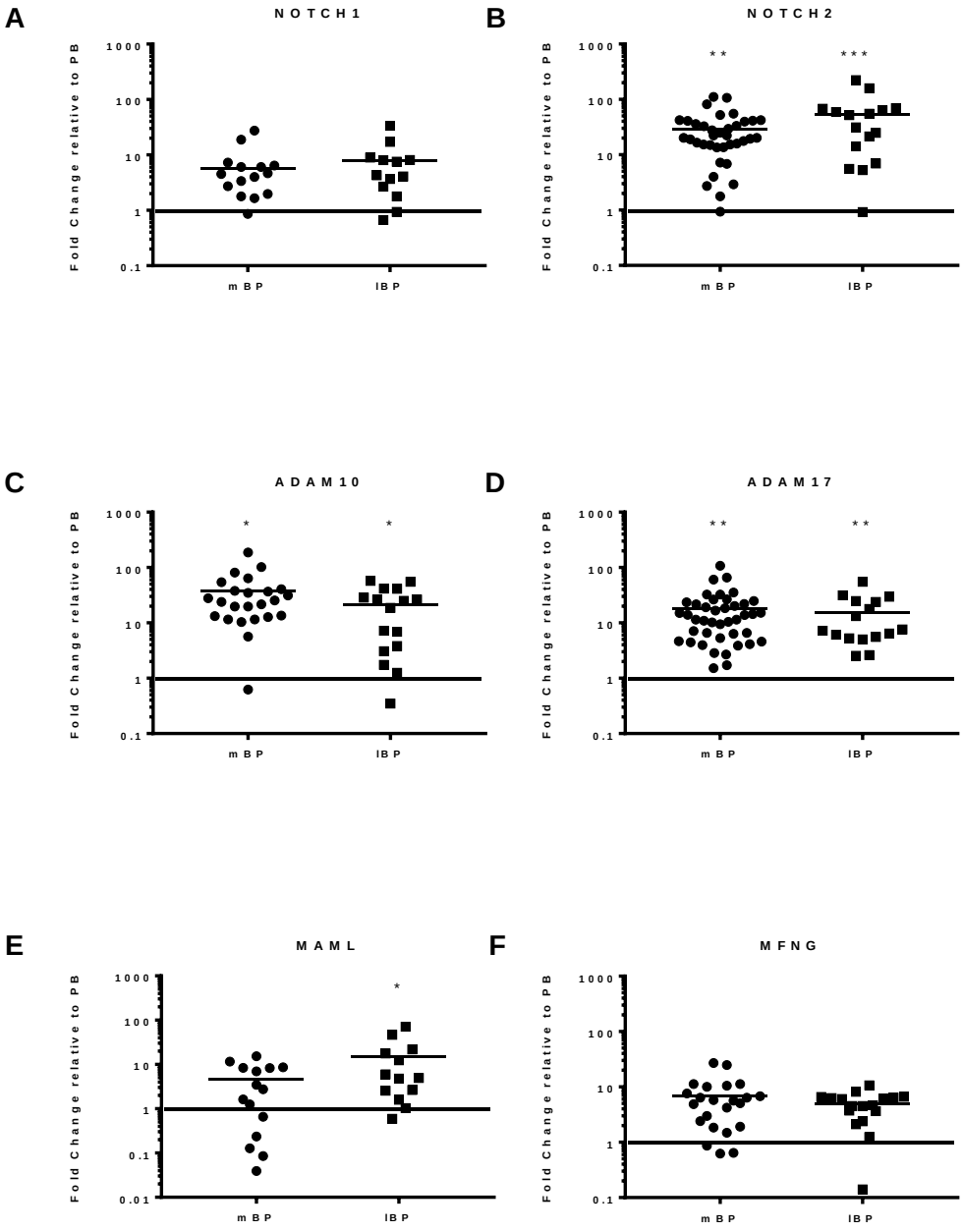

Figure 5 - 6 Focused gene expression of Notch pathway components suggests active Notch in a lymphoid phenotype

Using Fluidigm technology, mRNA expression was determined for myeloid and lymphoid BP compared to normal PB $CD34^+$ samples. Relative gene expression levels were determined using the average normal PB value as a calibrator calculated using the ΔΔCt method, using an average of five housekeeping genes as reference. (A-B) Dot plots showing gene expression of *NOTCH1* and *NOTCH2.* (C-F) Dot plots showing gene expression of Notch components, *ADAM10*, *ADAM17*, *MAML* and *MFNG*. P values were determined by an unpaired t-test (* $p<0.05$, ** $p<0.01$).

HES1 was statistically significantly upregulated in both myeloid and lymphoid disease compared to normal PB. There was no statistically significant increase in *HES1* expression in lymphoid compared to myeloid BP (figure 5-7). This is, perhaps, surprising in view of its known influence in lineage commitment inducing normal HSCs to move into a lymphoid path.

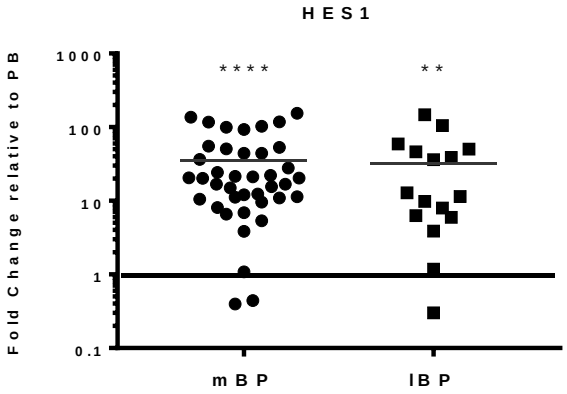

Figure 5 - 7 Focussed gene expression of *HES1* between myeloid BP and lymphoid BP

Using Fluidigm technology, mRNA expression was determined for myeloid and lymphoid BP compared to normal PB $CD34^+$ samples. Relative gene expression levels were determined using the average normal PB value as a calibrator calculated using the ΔΔCt method, using an average of five housekeeping genes as reference. P values were determined by an unpaired t-test (** $p<0.01$, **** $p<0.0001$).

Similarly, the Notch downstream target, *HIF1A*, was upregulated in both lymphoid and myeloid BP; however, there was no change in expression between disease phenotypes (figure 5-8). Together, this suggests that the downstream targets of Notch and the pathway components do not necessarily influence lineage specificity between myeloid and lymphoid BP disease.

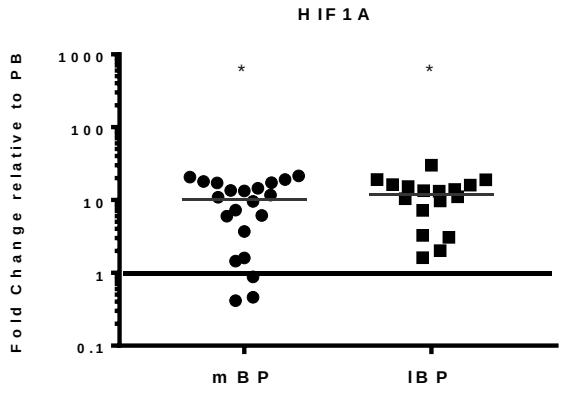

Figure 5 - 8 Focussed gene expression of *HIF1A* between myeloid BP and lymphoid BP

Using Fluidigm technology, mRNA expression was determined for myeloid and lymphoid BP compared to normal PB samples. Relative gene expression levels were determined using the average normal PB value as a calibrator calculated using the ΔΔCt method, using an average of five housekeeping genes as reference. Statistical significance was generated by unpaired t-test to enable determination of significant gene changes between disease phenotypes (* p<0.05).

Again, in keeping with the global gene expression analysis, there was only significant statistical change in a small number of genes from components of self-renewal pathways' between disease phenotypes. This is not in keeping with our initial hypothesis and, perhaps suggests a limited dependence on self-renewal pathways in myeloid and lymphoid BP. Furthermore, it suggests that self-renewal pathways do not seem to be important in terms of lineage specificity in driving the disease phenotype.

Of the genes assessed, the only significant change in the self-renewal pathways was within the Wnt/β-catenin pathway, with increased expression of *LEF1* (p=0.02) and *TLE4* (p=0.04) within the lymphoid BP samples (figure 5-9). There was a statistically significant increased expression of *TLE4* in both disease phenotypes compared to normal PB. There is a noted role of *LEF1* is B-cell lineage commitment through the activation of Pax5, and loss of *TLE4* enables stem cell self-renewal (Laing et al, 2015; Nutt et al, 1999).

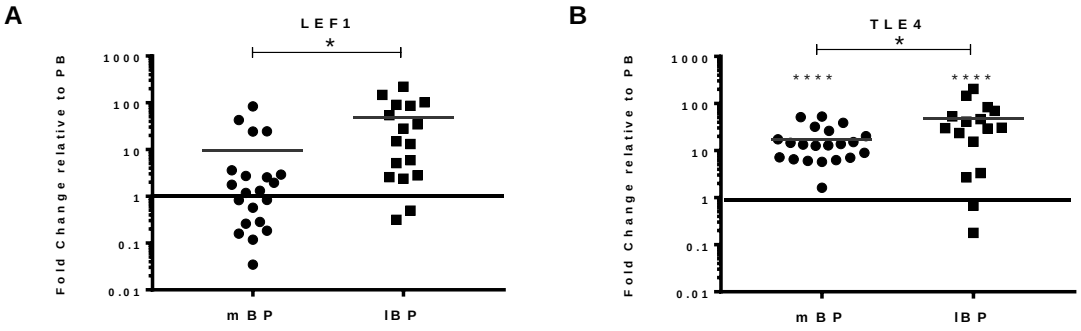

Figure 5 – 9 Focussed gene expression of Wnt/β-catenin pathway components between myeloid BP and lymphoid BP

Using Fluidigm technology, mRNA expression was determined for myeloid and lymphoid BP compared to normal PB samples. Relative gene expression levels were determined using the average normal PB value as a calibrator calculated using the ΔΔCt method, using an average of five housekeeping genes as reference. (A) Focussed gene expression of *LEF1*. (B) Focussed gene expression of *TLE4*. P values were determined by an unpaired t-test (p<0.05, **** p<0.0001).

Although, there was only minimal statistically significant change in a small number of self-renewal pathway components, a number of the downstream targets were statistically changed between myeloid and lymphoid lineage. These included *STIL,* which was statistically significantly decreased in lymphoid disease (figure 5-10). This is in keeping with its role in the regulation of lineage commitment, with increased expression favouring myeloid differentiation.

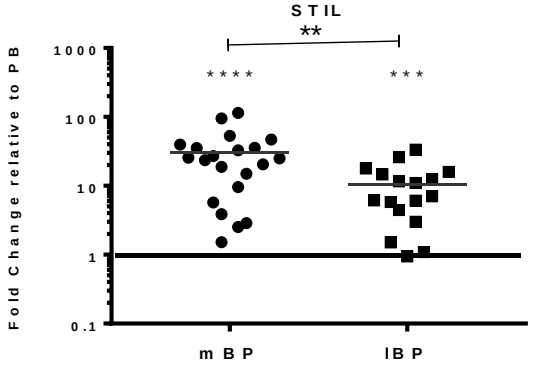

Figure 5 - 10 Focussed gene expression of *STIL* between myeloid BP and lymphoid BP

Using Fluidigm technology, mRNA expression was determined for myeloid and lymphoid BP compared to normal PB samples. Relative gene expression levels were determined using the average normal PB value as a calibrator calculated using the ΔΔCt method, using an average of five housekeeping genes as reference. P values were determined by an unpaired t-test (** p<0.01, *** p<0.001, **** p<0.0001).

Further to this, a statistically significant decrease in expression was noted in *TGF-β* and *p38* within in lymphoid BP samples compared to myeloid BP (p=0.02 and p=0.04, respectively; figure 5-11). Both genes were increased in expression compared to normal PB, but this was not statistically significant.

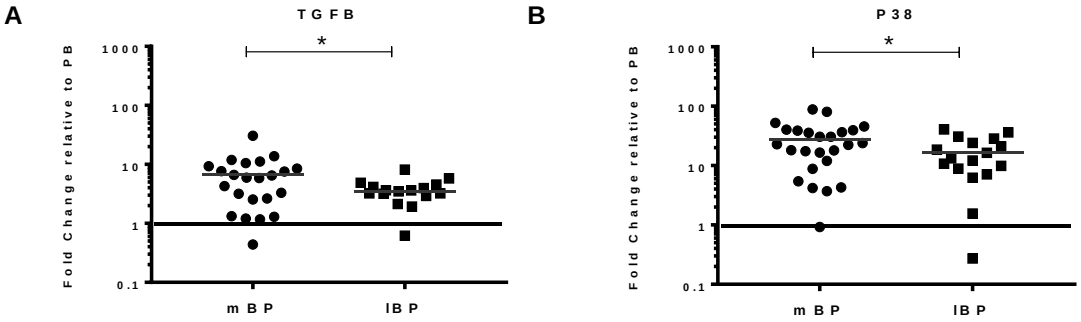

Figure 5 - 11 Focussed gene expression of *TGFB* and *p38* between myeloid BP and lymphoid BP

Using Fluidigm technology, mRNA expression was determined for myeloid and lymphoid BP compared to normal PB samples. Relative gene expression levels were determined using the average normal PB value as a calibrator calculated using the ΔΔCt method, using an average of five housekeeping genes as reference. (A) Focussed gene expression of *TGF-B*. (B) Focussed gene expression of *p38.* P values were determined by an unpaired t-test (* p<0.05).

The cell cycle regulators, *CCND1* and *CCND2*, were significantly decreased in lymphoid compared to myeloid BP samples (p=0.05 and p=0.0001, respectively; figure 5-12A and B). *CCND1* was statistically significantly increased in both disease phenotypes compared to normal PB, with *CCND2* statistically significantly increased compared to normal in the lymphoid BP samples alone. Moreover, *RUNX1* and *CYCLIN E1* were significantly decreased in the lymphoid BP compared to myeloid (p=0.002 and p=0.002, respectively; figure 5-12C and D). *CJUN* and *FOXO1* were significantly increased in lymphoid BP compared to myeloid (p=0.003 and p=0.05, respectively; figure 5-12E and F), although there was no statistically significant change compared to normal PB. The difficulty in ascertaining information from cell cycle regulators is the large degree of variation that is seen between samples. This is highlighted when analysing samples at a ΔCt level. For examples, within *CCND2* and *FOXO1* (figure 5-13), the ΔCt levels are presented for all populations within the analysis. ΔCt was used to acquire statistical change as described above.

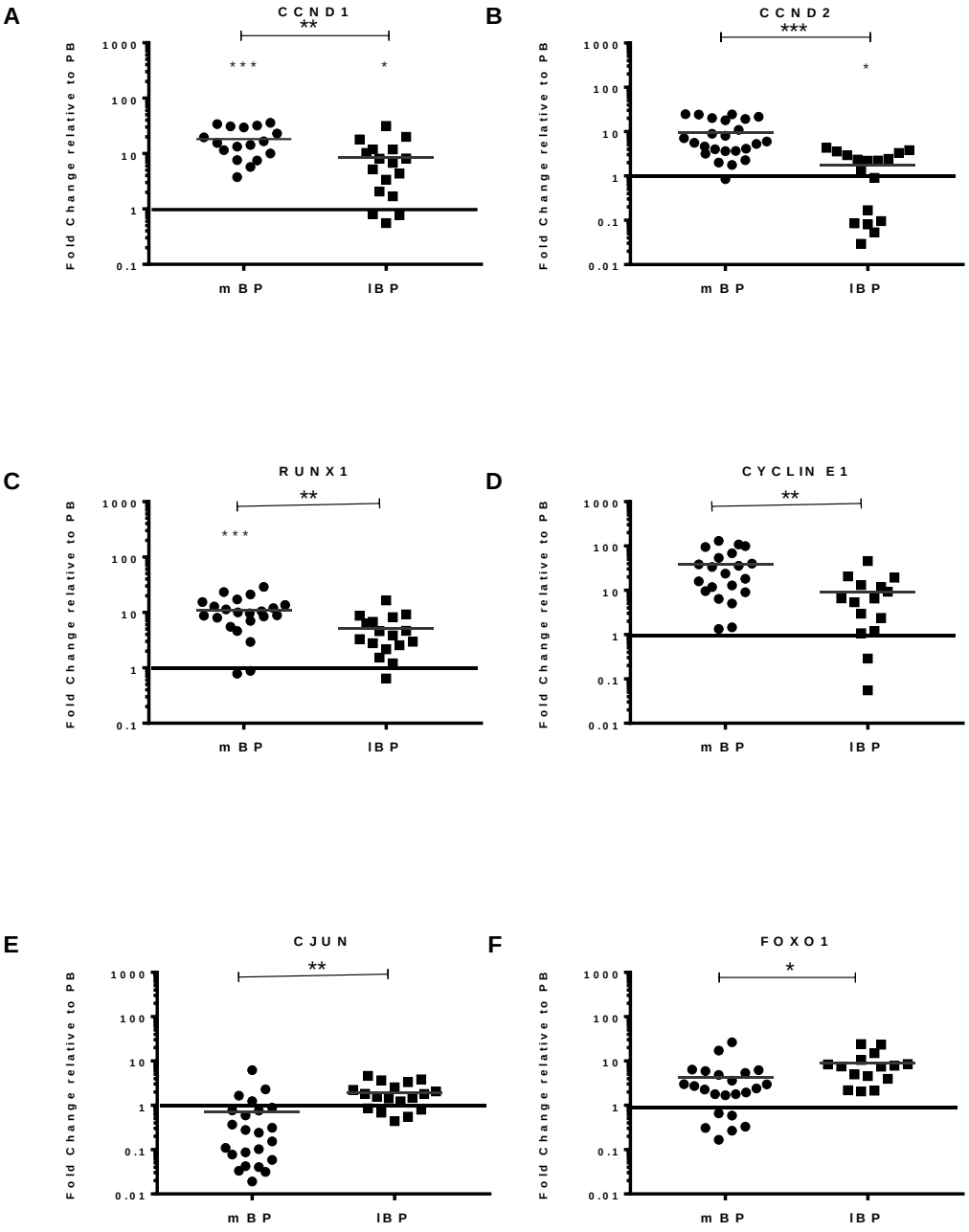

Figure 5 - 12 Focussed gene expression of cell cycle regulators between myeloid BP and lymphoid BP

Using Fluidigm technology, mRNA expression was determined for myeloid and lymphoid BP compared to normal PB samples. Relative gene expression levels were determined using the average normal PB value as a calibrator calculated using the ΔΔCT method, using an average of five housekeeping genes as reference. (A) Focussed gene expression of CCND1. (B) Focussed gene expression of *CCND2.* (C) Focussed gene expression of *RUNX1.* (D) Focussed gene expression of *CYCLINE1*. (E) Focussed gene expression of *CJUN.* (F) Focussed gene expression of *FOXO1.* P values were determined by an unpaired t-test (* p<0.05, ** p<0.01, *** p<0.001, **** p<0.0001).

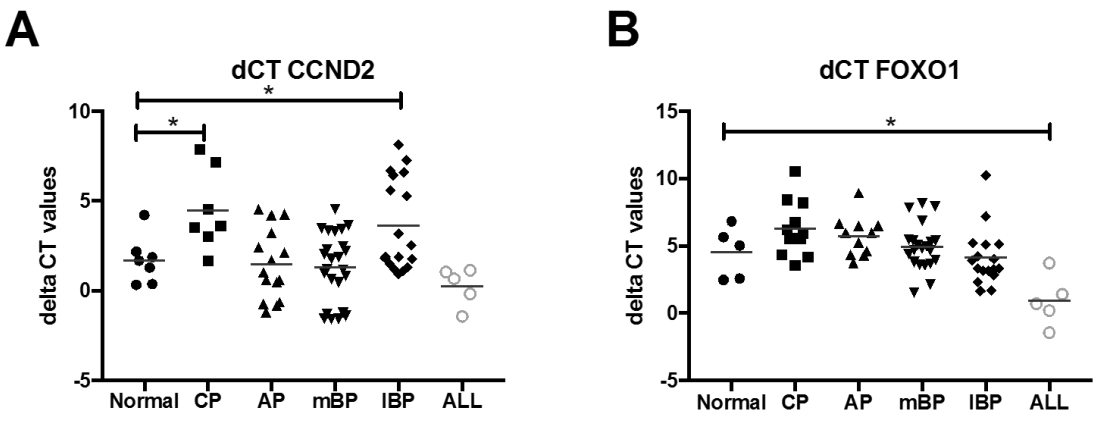

Figure 5 – 13 ΔCT values for all populations within gene expression analysis
ΔCT values for all populations within gene expression analysis demonstrate the variability between samples

The changes in the downstream target genes listed above are unlikely to represent a change in cell lineage specificity, but merely describe the differences in cell cycle pattern between the two BP phenotypes.

Within our dataset, the most striking finding was that there was no change between BP phenotypes for genes known to be involved in lineage commitment. Most notably, the *GATA* genes (*GATA1, GATA2, and GATA3)*, and *MYC,* which have a known effect on myeloid commitment, were not statistically changed between myeloid and lymphoid BP (figure 5-14). Together these data suggest that lymphoid BP disease has a similar gene expression pattern to myeloid BP. This is, perhaps, in keeping with its stem cell origin.

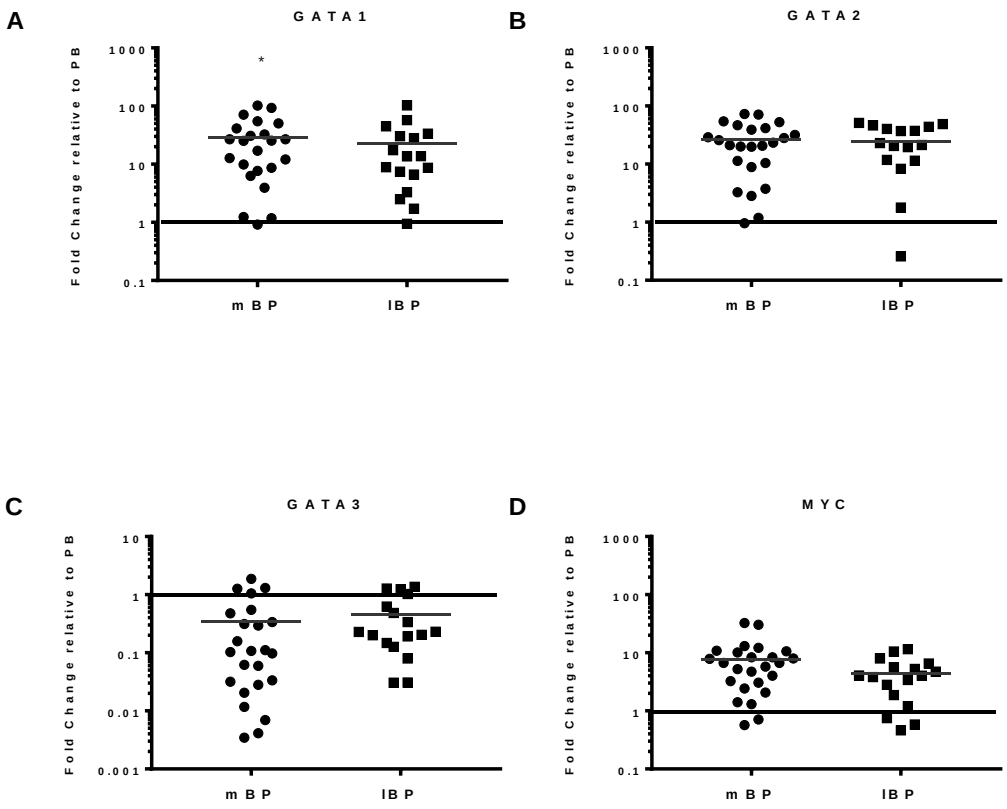

Figure 5 – 14 Focussed gene expression of lineage commitment regulators between myeloid BP and lymphoid BP

Using Fluidigm technology, mRNA expression was determined for myeloid and lymphoid BP compared to normal PB samples. Relative gene expression levels were determined using the average normal PB value as a calibrator calculated using the ΔΔCT method, using an average of five housekeeping genes as reference. (A) Focussed gene expression of *GATA1*. (B) Focussed gene expression of *GATA2.* (C) Focussed gene expression of *GATA3.* (D) Focussed gene expression of *MYC*. P values were determined by an unpaired t-test (* $p<0.05$, ** $p<0.01$, *** $p<0.001$, **** $p<0.0001$).

5.3.3. Lymphoid BP and Ph+ ALL have distinct gene expression alterations of self-renewal and cell survival signalling pathway components

Because of the similarities in self-renewal and cell survival gene expression between myeloid and lymphoid BP, we next questioned if there was a significant change between Ph+ ALL samples and lymphoid BP disease. This was with the view that the cell of origin differs between lymphoid BP and Ph+ ALL and it may guide potential future therapeutic targets, as well as increasing the understanding of the gene expression differences between them.

Ph+ ALL sample RNA (n=5) was kindly gifted to us from the UKALL14 clinical trial by Professor Adele Fielding. All samples were of B cell origin and treatment naive. Again, 100ng of RNA was used in keeping with previous experiments. Lymphoid BP sample RNA (n=5) were used in duplicate or triplicate and generated as previously. Again, Fluidigm technology was used to determine the quantitative gene expression of 90 self-renewal and cell survival signalling genes. Relative gene expression levels were determined using the average normal PB samples as a calibrator calculated using the $\Delta\Delta$Ct method, using an average of five housekeeping genes as reference.

Global gene analysis demonstrated that Ph+ ALL and lymphoid BP could be segregated by gene clustering methods (figure 5-15). This suggests that these are distinct disease entities as described by self-renewal and cell survival signalling pathways.

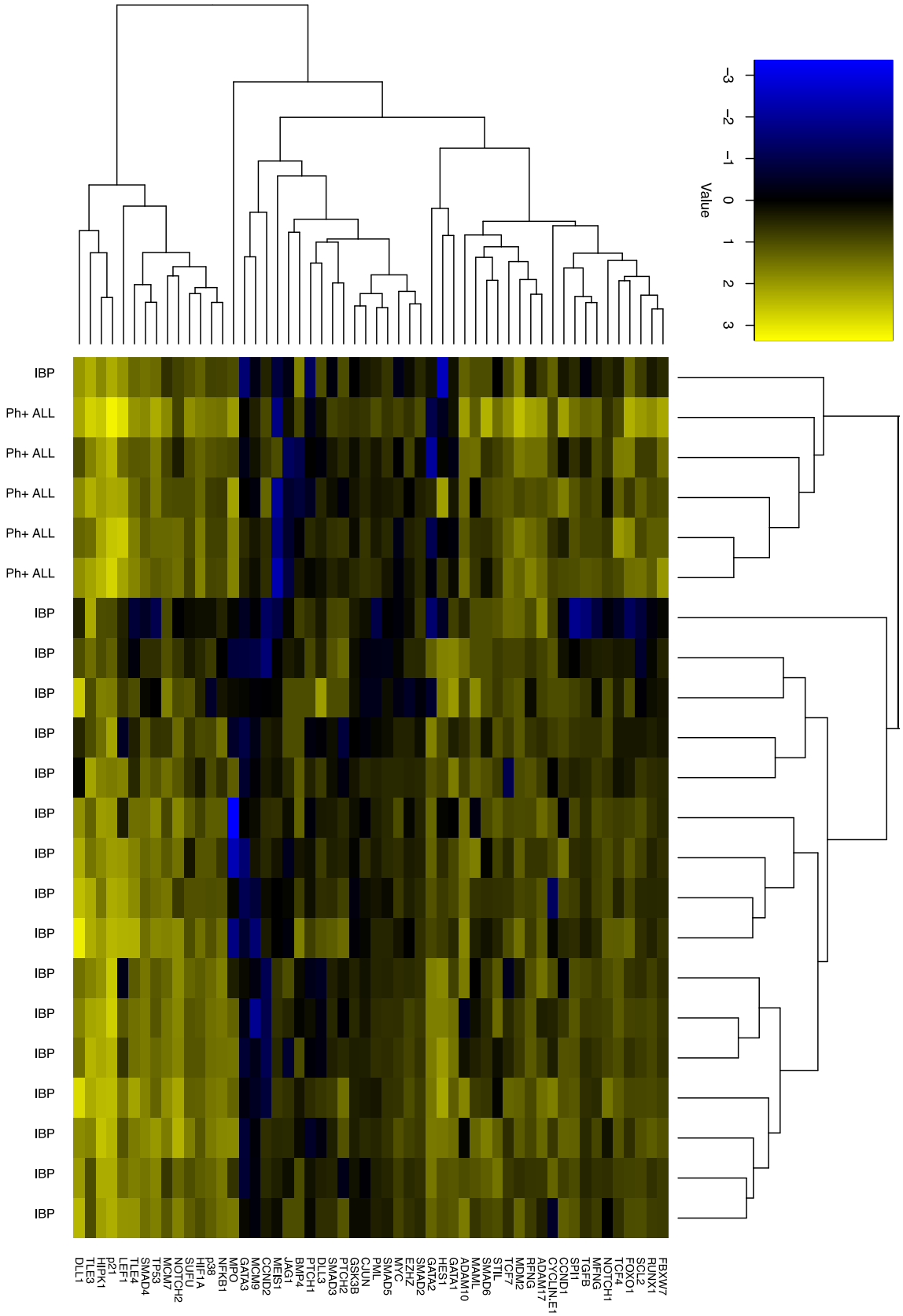

Figure 5 – 15 Gene clustering of self-renewal and cell survival components can segregate lymphoid BP and Ph+ ALL

Gene expression profiles (GEPs) were determined from lymphoid BP and Ph+ ALL samples. GEP levels were determined by Fluidigm array analysis. Relative gene expression levels were determined by ΔΔCt method using an average of five housekeeping genes as reference and the average normal PB value as the calibrator for fold change. Heat maps and gene clustering were produced using heatmap.2 in R/Bioconductor.

Focussed gene expression analysis of the Ph+ ALL and lymphoid BP samples demonstrated that there was little change in self-renewal pathway components between the two diseases. For example, within the Notch pathway (figure 5-16), a pathway with a noted role within T-cell ALL, the only gene to be significantly altered was the Notch receptor, *NOTCH2*, which was significantly lower in the Ph+ ALL arm (p=0.02; figure 5-16B). However, compared to normal PB samples, *NOTCH2, ADAM10,* and *ADAM17* were significantly overexpressed in both lymphoid BP and Ph+ ALL. Compared to normal PB, *MAML* was significantly increased in lymphoid BP, but not within Ph+ ALL.

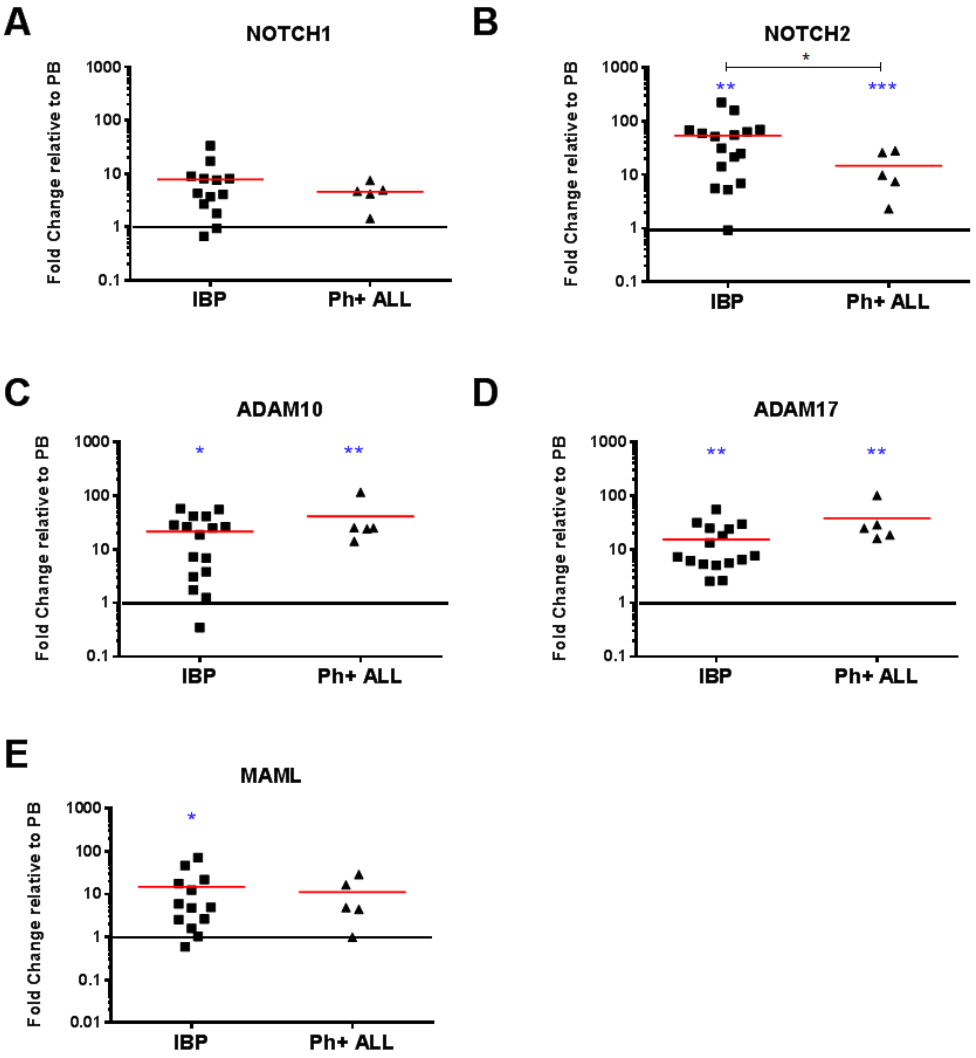

Figure 5 – 16 Focussed gene expression of lineage commitment regulators between myeloid BP and lymphoid BP

Using Fluidigm technology, mRNA expression was determined for lymphoid BP and Ph+ ALL samples compared to normal PB samples. Relative gene expression levels were determined using the average normal PB value as a calibrator calculated using the ΔΔCt method, using an average of five housekeeping genes as reference. Statistical significance was generated by unpaired t-test to enable determination of significant gene changes between disease phenotypes (* p<0.05, ** p<0.01, *** p<0.001).

Expression of *JAG1* was significantly lower in Ph+ ALL compared to lymphoid BP (p=0.017; figure 5-17A), although neither disease phenotype had altered expression in comparison to normal PB. No change was noted for *DLL1* or *DLL3* between lymphoid BP and Ph+ ALL; however, a statistically significant increase in *DLL1* was noted compared to normal for both (figure 5-17B and C). This may have implications in *cis*-inhibitory mechanisms within the cells, especially if translated to protein level.

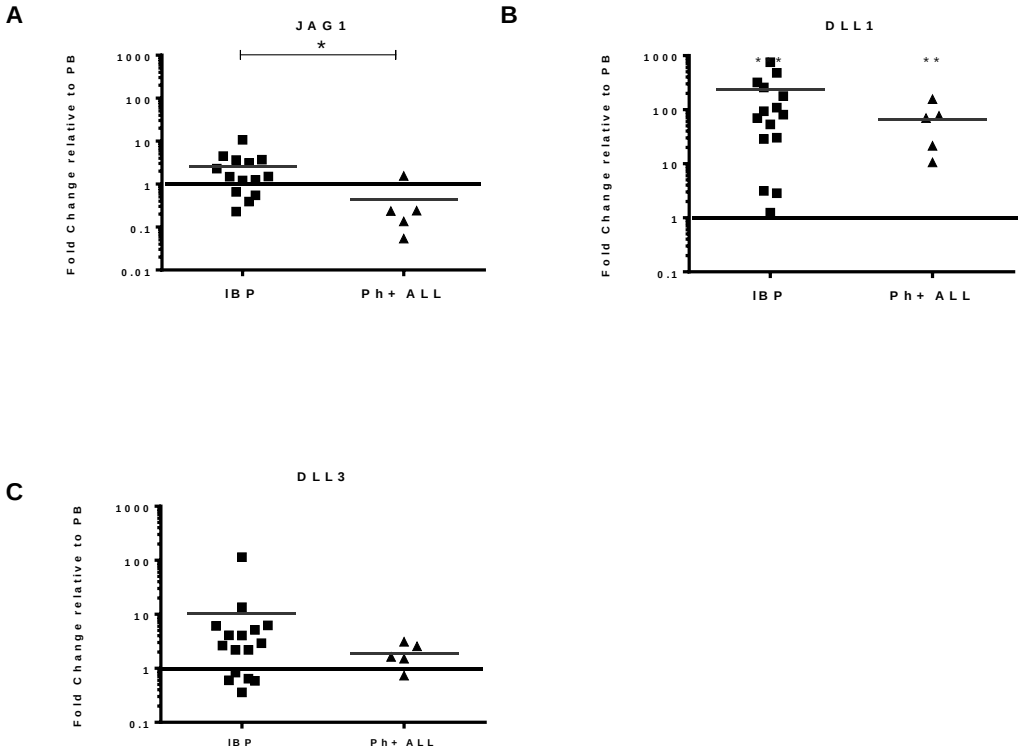

Figure 5 - 17 Focussed gene expression of Notch ligands between lymphoid BP and Ph+ ALL

Using Fluidigm technology, mRNA expression was determined for lymphoid BP and Ph+ ALL samples compared to normal PB samples. Relative gene expression levels were determined using the average normal PB value as a calibrator calculated using the ΔΔCt method, using an average of five housekeeping genes as reference. (A) Focussed gene expression of *JAG1*. (B) Focussed gene expression of *DLL1.* (C) Focussed gene expression of *DLL3.* P values were determined by an unpaired t-test (* p<0.05, ** p<0.01, *** p<0.001, **** p<0.0001).

To investigate this further, the downstream targets of the Notch signalling pathway were evaluated. Interestingly, compared to normal PB, there was no statistical change in *HES1* expression in Ph+ ALL, suggesting that the Notch pathway was not activated within this disease phenotype (figure 5-18A). There was, however, a statistically significant increase in expression of *HIF1A* in both diseases (p=0.03 for lymphoid BP and p=0.001 for Ph+ ALL), and of *HES1* in the lymphoid BP population (p=0.01),

compared to normal PB (figure 5-18). This is perhaps suggestive that there are not the same interactions between self-renewal pathways' in different Ph+ acute leukaemias; furthermore, as discussed within the introduction to this thesis, the BM niche has been shown to be remodelled differently in disease and perhaps this varies between the Ph+ acute leukaemias. There was a statistically significant increase in expression of *HIF1A* in Ph+ ALL compared to lymphoid BP which may suggest an interesting therapeutic target in Ph+ ALL pending further functional experiments' (p=0.01; figure 5-18B).

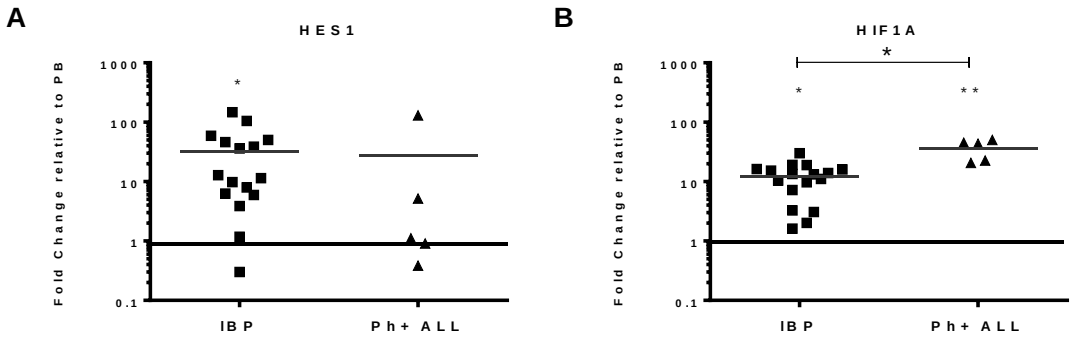

Figure 5 – 18 Focussed gene expression of *HES1* and *HIF1A* between lymphoid BP and Ph+ ALL

Using Fluidigm technology, mRNA expression was determined for lymphoid BP and Ph+ ALL samples compared to normal PB samples. Relative gene expression levels were determined using the average normal PB value as a calibrator calculated using the ΔΔCT method, using an average of five housekeeping genes as reference. Statistical significance was generated by unpaired t-test to enable determination of significant gene changes between disease phenotypes. (A) Focussed gene expression of *HES1*. (B) Focussed gene expression of *HIF1A.* P values were determined by an unpaired t-test (* p<0.05, ** p<0.01).

There was a statistically significant increase in *FBXW7* compared to normal PB within the Ph+ ALL (p=0.002; figure 5-19A), but there was no change in expression between lymphoid BP and Ph+ ALL of the Notch negative regulators, *FBXW7, MFNG,* and *RFNG* (figure 5-19).

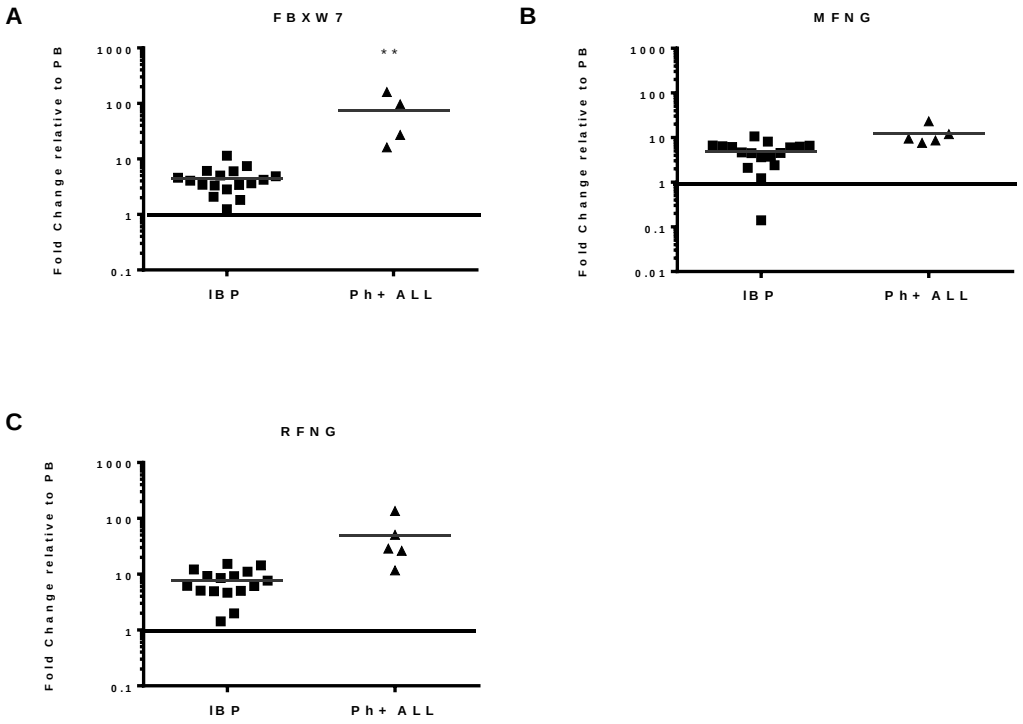

Figure 5 – 19 Focussed gene expression of Notch negative regulators between lymphoid BP and Ph+ ALL

Using Fluidigm technology, mRNA expression was determined for lymphoid BP and Ph+ ALL samples compared to normal PB samples. Relative gene expression levels were determined using the average normal PB value as a calibrator calculated using the ΔΔCt method, using an average of five housekeeping genes as reference. (A) Focussed gene expression of *FBXW7*. (B) Focussed gene expression of *MFNG.* (C) Focussed gene expression of *RFNG.* P values were determined by an unpaired t-test (** $p<0.01$).

As per previous results, self-renewal pathway components and downstream targets were next analysed to determine interaction and potential therapeutic targets within both diseases. Within the Wnt/β-catenin pathway, there was no statistical difference between lymphoid BP and Ph+ ALL; however, in keeping with other results, statistically significant change was noted for both conditions compared to normal PB. This is in keeping with the leukaemic phenotype. Notably, *TCF4* ($p=0.012$; figure 5-20A), *TCF7* ($p=0.0055$; figure 5-20B), *LEF1* ($p=0.04$; figure 5-20C), *TLE3* ($p=0.008$; figure 5-20E), and *TLE4* ($p=0.0002$; figure 5-20F) were statistically significantly upregulated within Ph+ ALL compared to normal PB, suggesting a dependence on the Wnt pathway in the leukaemic phenotype. *TLE3* ($p=0.04$; figure 5-20E) and *TLE4* ($p<0.0001$; figure 5-20F) were overexpressed in lymphoid BP compared to normal.

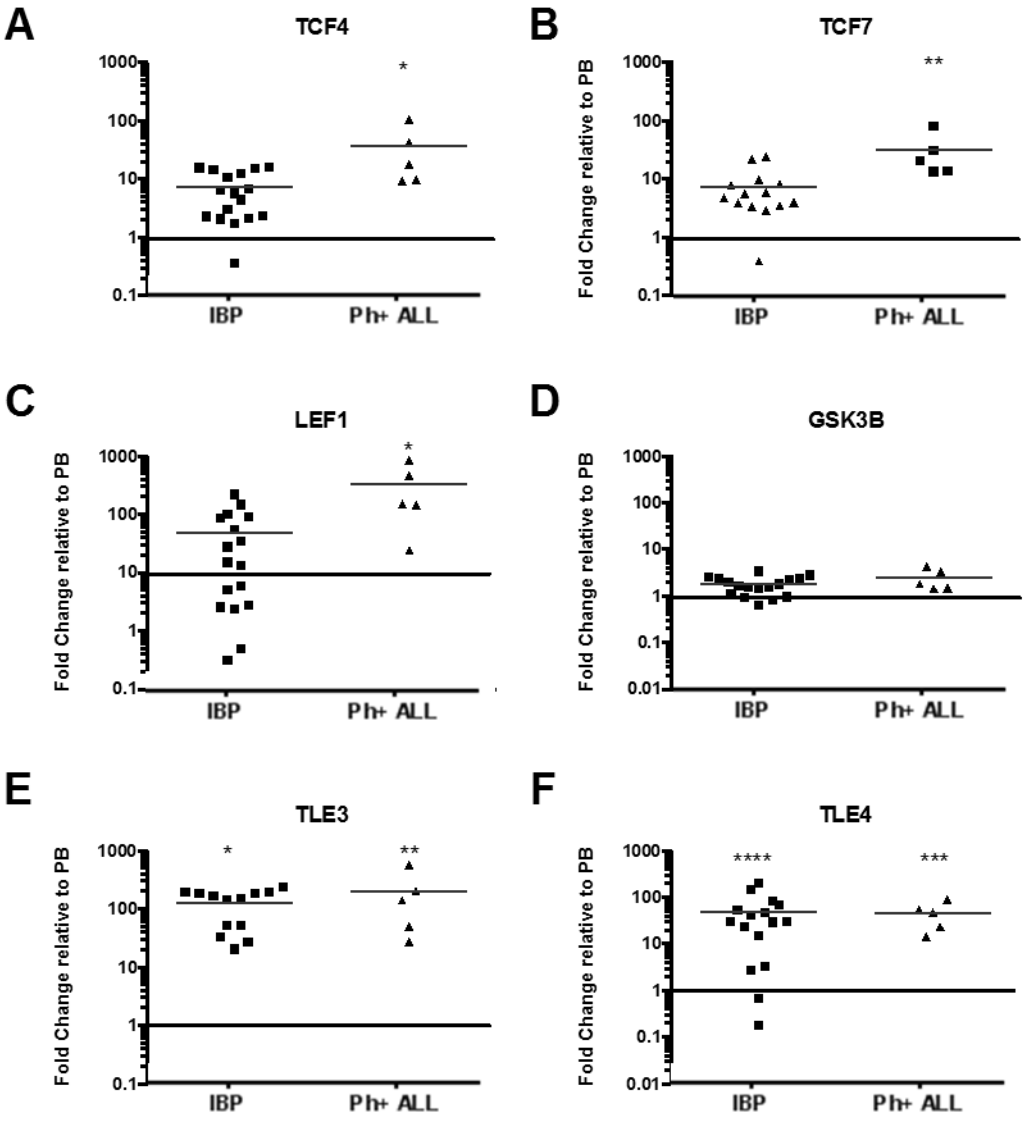

Figure 5 - 20 Focussed gene expression of Wnt/β-catenin pathway components between lymphoid BP and Ph+ ALL

Using Fluidigm technology, mRNA expression was determined for lymphoid BP and Ph+ ALL samples compared to normal PB samples. Relative gene expression levels were determined using the average normal PB value as a calibrator calculated using the ΔΔCT method, using an average of five housekeeping genes as reference. (A) Focussed gene expression of *TCF4*. (B) Focussed gene expression of *TCF7.* (C) Focussed gene expression of *LEF1.* (D) Focussed gene expression of *GSK3β*. (E) Focussed gene expression of *TLE3.* (F) Focussed gene expression of *TLE4.* P values were determined by an unpaired t-test (* p<0.05, ** p<0.01, *** p<0.001, **** p<0.0001).

Similarly, within the components of the Hh pathway, there was no change in expression between lymphoid BP and Ph+ ALL (figure 5-21). There was, however, an increased expression of *SUFU* (p<0.0001 in lymphoid BP, p=0.0032 in Ph+ ALL; figure 5-21A) in both experimental arms compared to normal PB, with no statistically significant increase in the expression of the downstream target, *HIPK1*.

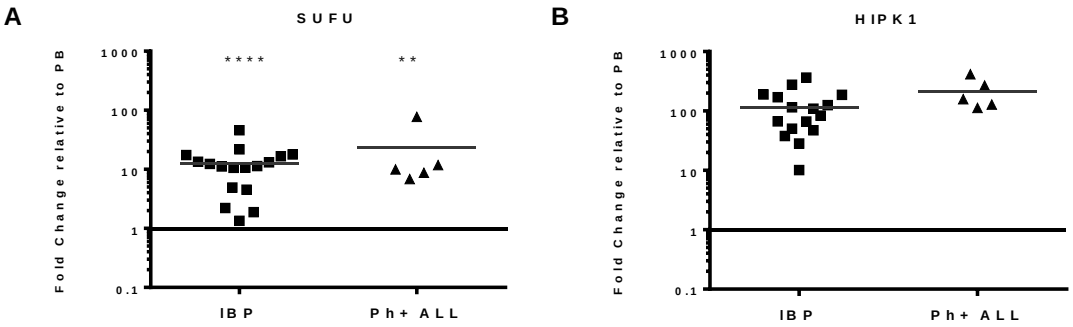

Figure 5 – 21 Focussed gene expression of Hh pathway components between lymphoid BP and Ph+ ALL

Using Fluidigm technology, mRNA expression was determined for lymphoid BP and Ph+ ALL samples compared to normal PB samples. Relative gene expression levels were determined using the average normal PB value as a calibrator calculated using the ΔΔCt method, using an average of five housekeeping genes as reference. (A) Focussed gene expression of *GLI1*. (B) Focussed gene expression of *SUFU.* (C) Focussed gene expression of *HIPK1.* P values were determined by an unpaired t-test (** p<0.01, **** p<0.0001).

As previously described, there is known cooperation between *BMP4* and both Hh and Wnt/β-catenin signalling. There was no statistical change between lymphoid BP and Ph+ ALL in *BMP4* expression, or between the Ph+ leukaemias and normal PB (figure 5-22). Furthermore, there were no significant difference in the SMADs analysed between lymphoid BP and Ph+ ALL, or compared to normal PB (data not shown). This suggests that there is a limited role for BMP within lymphoid BP and Ph+ ALL.

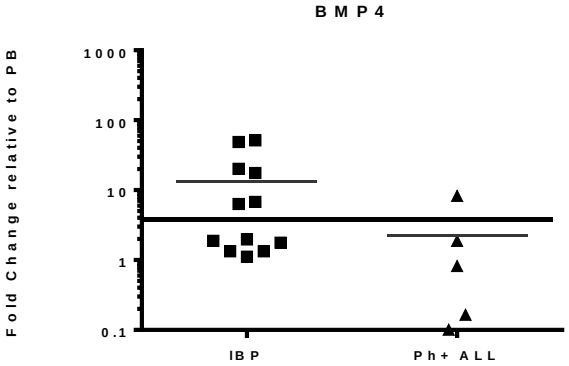

Figure 5 - 22 Expression of *BMP4* in lymphoid BP and Ph+ ALL

Relative gene expression levels were determined using the average normal PB value as a calibrator calculated using the ΔΔC method, using an average of five housekeeping genes as reference. Statistical significance was generated by unpaired t-test to enable determination of significant gene changes between disease phenotypes. There was no statistical change between experimental arms, nor compared to normal PB.

As expected, there was significant difference in stem cell survival regulators, namely *GATA1* (p=0.004) and *GATA2* (p<0.0001), which had a statistically significant lower expression in Ph+ ALL compared to lymphoid BP disease (figure 5-23). This is perhaps representative of the stem cell origin of lymphoid BP disease, compared to Ph+ ALL. Compared to normal, there was no statistical change between normal and lymphoid BP for *GATA1* expression, likely owing to the degree of variation noted within samples. There was, however, a statistically significant increase in expression of *GATA1* (p<0.05) and a decrease in *GATA2* (p<0.05), when comparing Ph+ ALL to normal. There was no change in *GATA3* expression between lymphoid BP and Ph+, nor compared to normal. *GATA3* has a known role within the T-lymphocyte lineage, but its role within self-renewal and the HSC population remains unclear.

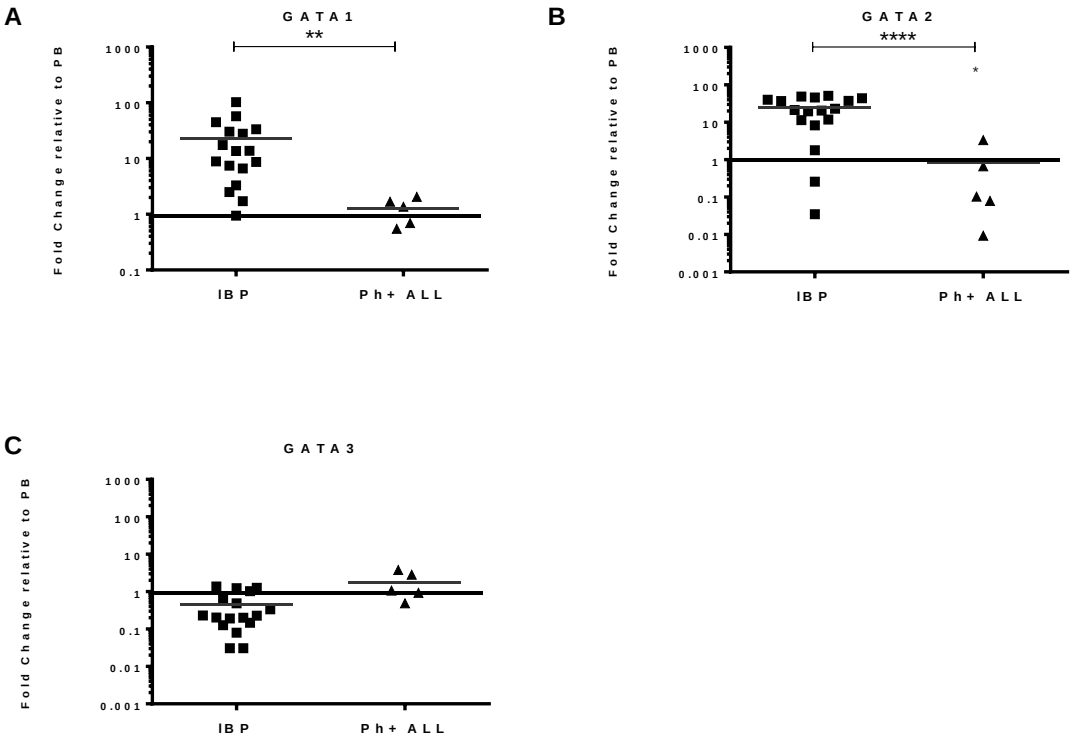

Figure 5 – 23 Focussed gene expression of stem cell survival components between lymphoid BP and Ph+ ALL

Using Fluidigm technology, mRNA expression was determined for myeloid and lymphoid BP compared to normal PB samples. Relative gene expression levels were determined using the average normal PB value as a calibrator calculated using the ΔΔCt method, using an average of five housekeeping genes as reference. (A) Focussed gene expression of *GATA1*. (B) Focussed gene expression of *GATA2.* (C) Focussed gene expression of *GATA3.* P values were determined by an unpaired t-test (* p<0.05, *** p<0.001, **** p<0.0001).

Contrary to data in AML, which suggests a clinical significance in increased expression of *GATA1*, *GATA2* and *SCL* expression (Shimamoto et al, 1994), there was no statistically significant change in expression of *SCL* compared to normal or between disease phenotypes (figure 5-24).

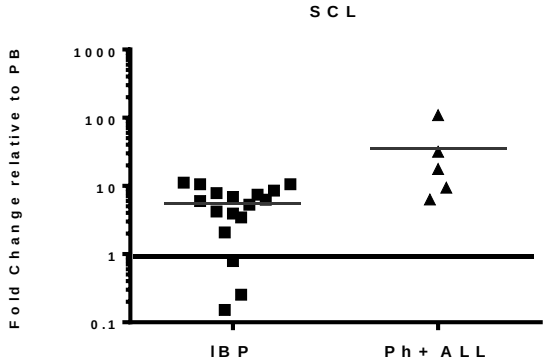

Figure 5 – 24 Focussed gene expression of *SCL* between lymphoid BP and Ph+ ALL
Relative gene expression levels were determined using the average normal PB value as a calibrator calculated using the ΔΔCT method, using an average of five housekeeping genes as reference. Statistical significance was generated by unpaired t test between populations to enable determination of significance gene changes within disease phenotype. There was no statistical change between experimental arms, or compared to normal PB.

No significant change was noted between other cell cycle regulators in the two Ph+ leukaemias, including *CCND1*, *CCND2*, *p21*, *FOXO1*, *STIL* and *CYCLINE1* (figure 5-25). There was a statistically significant increase expression in *p21* ($p=0.01$ for lymphoid BP and $p=0.001$ for Ph+ ALL) and *STIL* ($p=0.0002$ for lymphoid BP and $p<0.0001$ for Ph+ ALL) in both populations, with statistically significant increase expression in *FOXO1* ($p<0.05$) within Ph+ ALL.

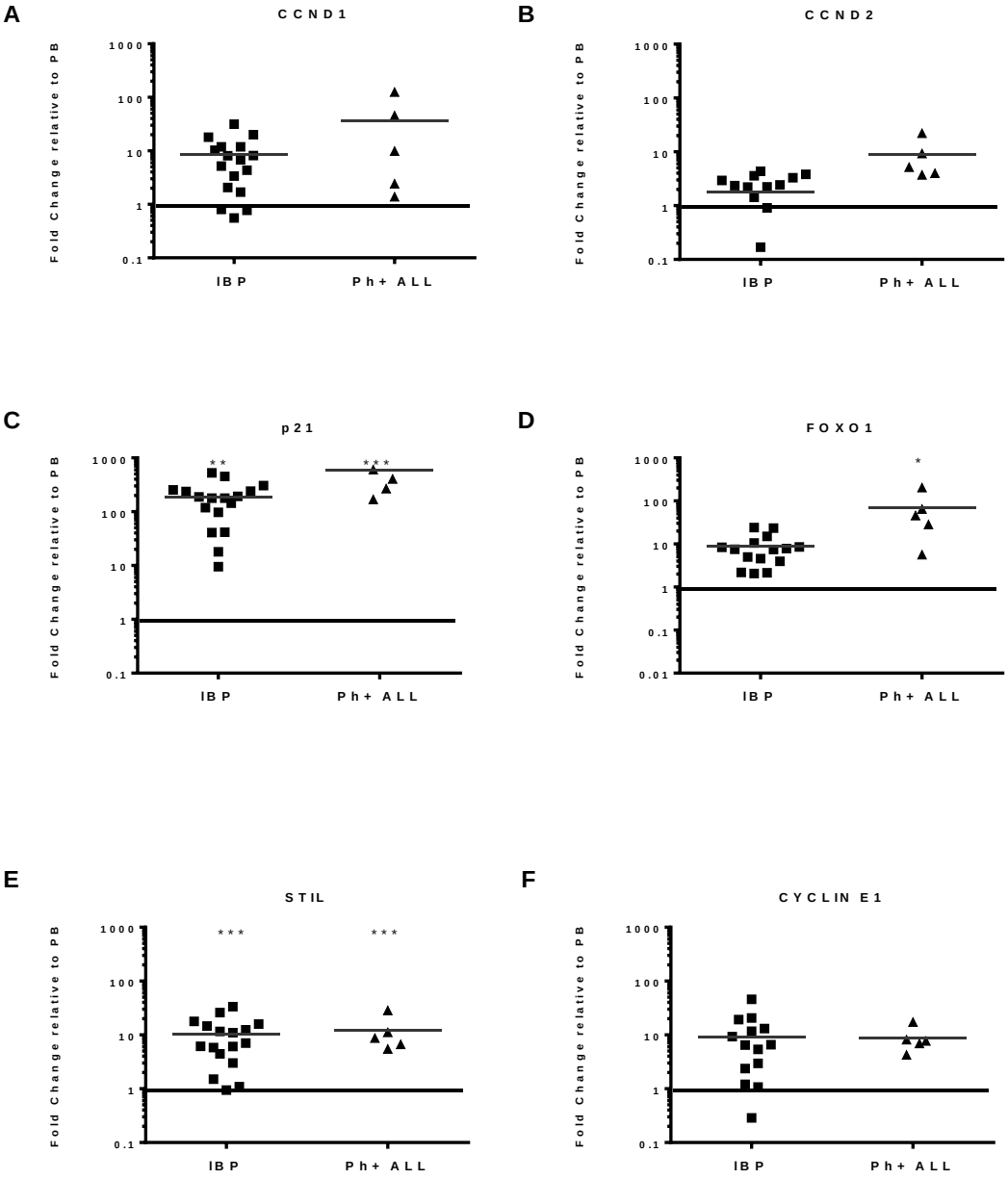

Figure 5 – 25 Focussed gene expression of cell cycle regulators between lymphoid BP and Ph+ ALL

Relative gene expression levels were determined using the average normal PB value as a calibrator calculated using the ΔΔCT method, using an average of five housekeeping genes as reference. (A) Focussed gene expression of *CCND1*. (B) Focussed gene expression of *CCND2*. (C) Focussed gene expression of *p21*. (D) Focussed gene expression of *FOXO1*. (E) Focussed gene expression of *STIL.* (F) Focussed gene expression of *CYCLIN E1.* P values were determined by an unpaired t-test (* $p<0.05$, ** $p<0.01$, *** $p<0.001$).

5.4. Discussion

The data presented above raises the possibility that lymphoid BP and myeloid BP samples are similar in gene expression of self-renewal and cell survival pathway components. This suggests that the two disease processes are, perhaps, more similar than previously anticipated. Furthermore, it provides evidence to suggest that perhaps the treatment of lymphoid BP should be based on chemotherapeutic agents used within acute myeloid disease, rather than acute lymphoblastic disease. In keeping with this, the current UK BP clinical trial, MATCHPOINT (Management of Transformed Chronic myeloid leukaemia: Ponatinib and Intensive chemotherapy: a dose finding study), utilises a chemotherapy regimen commonly used for high risk and relapsed/refractory AML (FLAG-Ida) in both disease subtypes (Bergua et al, 2016; Burnett et al, 2013).

Furthermore, both myeloid and lymphoid BP are heterogeneous diseases encompassing immature and mature phenotypes within the same population (Kinstrie et al, 2016). The heterogeneity described within lymphoid BP in this chapter is only based on two samples, and clearly this needs to be expanded to encompass other samples to understand the true heterogeneity that is present. There are some difficulties in this, however, as lymphoid BP disease is a rare entity and, therefore, this will be a longstanding endeavour. Although our group has recently published with regards to heterogeneity in myeloid BP disease (Kinstrie et al, 2016), within lymphoid BP this data is limited to case-based analysis and immunophenotypic change (Bettelheim et al, 1985; Cervantes et al, 1998; Ilaria, 2005). Within the Cervantes study, 17 out of 19 patients were of B-lineage phenotype, with the other 2 being T-lineage. Similar to our own data, all the samples had one or more myeloid markers expressed (Cervantes et al, 1998). This report also suggested that lymphoid BP was seldom associated with an AP, which clearly has an implication in management. Subsequently, being able to identify a gene expression profile within lymphoid BP may help in the earlier diagnosis of the disease and quick initiation of treatment.

To determine this, we assessed the gene expression of 90 self-renewal and cell survival components between myeloid and lymphoid BP disease. This was with the initial hypothesis that there would be aberrancies between the two disease phenotypes that may guide earlier diagnosis and novel therapeutic approaches. Self-renewal pathways were utilised because of the known association of acquisition of self-renewal properties, specifically of Wnt/β-catenin pathway, within BP disease (Jamieson et al, 2004).

Although there is some data to describe this within myeloid BP, there is inadequate data within lymphoid BP, with even less known about the genes responsible for determining lineage-selectivity. As described within the introductory paragraph to this discussion, the gene expression data, firstly, demonstrated that the 90 self-renewal and cell survival components could not segregate myeloid and lymphoid BP phenotypes on global gene analysis through gene clustering methods. This is in keeping with recent single cell transcriptomic data within a *BCR-ABL*+ population, where lymphoid (n=2) and myeloid (n=1) BP samples were clustered together (Giustacchini et al, 2017). Furthermore, our data suggests that the cells have limited alteration in self-renewal components, likely owing to the LSC in the disease pathogenesis. It is known that the LSC in BP-CML may result in at least 3 subsets, namely $Lin^{-}CD34^{+}CD38^{-}$, $Lin^{-}CD34^{+}$ cells remaining from CP, and the disease-driving $Lin^{-}CD34^{+}CD38^{+}$ GMPs (Jamieson et al, 2004). Our data, in some respects, reflects this, as there were no statistical differences between both myeloid and lymphoid BP disease. Furthermore, as the data was pooled, it suggests that there are similar degrees of immature and mature populations in both disease phenotypes.

All key self-renewal pathway components of Notch, Wnt/β-catenin, Hh, and BMP, were analysed, although not all were reported within this results section due to statistical significance not being achieved. The Notch signalling pathway has a known role within lineage decision making of the normal HSC population, particularly towards a lymphoid bias (Delaney et al, 2010; Jaleco et al, 2001; Ohishi et al, 2003a; Ohishi et al, 2002). The main components of the pathway were not statistically changed between myeloid and lymphoid BP disease. However, as there was a statistically significant increased expression of *NOTCH2*, *ADAM10*, and *ADAM17* compared to normal PB, it suggested that within BP disease these may be the components to upregulate the pathway. Interestingly, *MAML*, the intracellular component of Notch required for canonical activation of its downstream targets, was signficantly increased in lymphoid BP compared to normal, but not within myeloid BP. This perhaps suggests that the Notch pathway is, indeed, upregulated within lymphoid BP disease, however, further functional analysis is required to fully determine this and we are currently in the process of extending this experimental work. Despite this, there was no statistically significant increase in the downstream targets of Notch, *HES1* and *HIF1A*, between myeloid and lymphoid disease. Within the previous chapter, the complex activation of these downstream targets was explored and therefore, although *HES1* was statistically significantly increased in both myeloid and lymphoid BP compared to normal, this

could be driven through a number of different mechanisms within each phenotype; for example, through the activation of other self-renewal pathways.

Assessing a role for the Notch signalling pathway using gene expression data is difficult due to differing ligand-receptor interactions leading to varying functional roles. For example, although within previous chapters, we have demonstrated the potential for LSC eradication with NOTCH2-JAG1 interaction in CP disease, it is known that Notch-Delta1 interactions can promote T-cell lineage commitment and maturation (Besseyrias et al, 2007). Further functional analysis needs to be evaluated within Lymphoid BP as to the effect of differing ligand-receptor binding.

In keeping with the global gene expression analysis through clustering methods between myeloid and lymphoid BP, there were limited changes between self-renewal pathway components in other pathways analysed. Only within the Wnt/β-catenin pathway were there significant changes between myeloid and lymphoid BP disease. Within lymphoid BP, there was a statistically significant increase in *LEF1* and *TLE4*. Furthermore, *TLE4* was shown to be statistically significantly increased within both myeloid and lymphoid BP compared to normal PB. The importance of deregulation in Wnt/β-catenin has been described in disease initiation and progression of CML (Abrahamsson et al, 2009; Radich et al, 2006; Zhao et al, 2007). Furthermore, *LEF1* has been shown to regulate accumulation of β-catenin intracellularly and be important in leukaemogenesis. In murine experiments, increased LEF1 led to abnormalities of haemopoietic differentiation and developed B-ALL and AML, with the LSC exhibiting lymphoid characteristics (Petropoulos et al, 2008). Furthermore, there has shown to be inactivation of *LEF1* in T-cell ALL (Gutierrez et al, 2010a; Gutierrez et al, 2010b), with overexpression perhaps highlighting the B-cell phenotype of our Ph+ ALL samples. *TLE4* has been previously demonstrated to enable stem cell differentiation.

Within our dataset, *STIL* was significantly unregulated in both myeloid and lymphoid BP compared to normal PB. *STIL* has a noted role in the regulation of lineage commitment, with increased expression favouring myeloid differentiation. In keeping with this, expression in lymphoid BP was significantly lower compared to the myeloid BP samples. The increase in expression in comparison to normal may be explained by the mixed population seen within lymphoid BP samples, with the identification of a CMP populton in the samples extensively immunophenotyped. *TGF-β* was noted to be significantly decreased in lymphoid BP compared to myeloid BP. *TGFβ* has been

shown to maintain leukaemic initiating cell potential within CML CP (Miyazono, 2012; Naka et al, 2010) and the decreased expression in lymphoid BP may be in keeping with a more differentiated phenotype. Within our dataset, the most striking area was that there was no change between populations of genes known to be involved in lineage commitment. Most notably, the *GATA* genes (*GATA1, GATA2, and GATA3)*, and *MYC,* which have a known effect on myeloid commitment, did not significantly change between myeloid and lymphoid BP. Together this data suggests that lymphoid BP disease has a similar gene expression pattern to myeloid BP. This is, perhaps, in keeping with its stem cell and myeloid origin.

These data presented emphasise the similarities between myeloid BP and lymphoid BP disease, with only minimal changes suggestive of novel therapeutic targets. In view of this, we next sought to question if there were differing gene expression profiles of self-renewal and cell survival pathways within the Ph+ acute leukaemias'. This was in view of the known differences in cell of origin between them, with lymphoid BP representing a distinctly stem cell disease, and Ph+ ALL a more differentiated phenotype. Indeed, on global gene expression of the 90 self-renewal and cell survival components, the two diseases could be segregated with gene clustering methods.

On focussed gene analysis, there were similar expression patterns of the self-renewal pathway components between lymphoid BP and Ph+ ALL. Although there was a statistically significant decrease in *NOTCH2* expression in Ph+ ALL compared to lymphoid BP. *NOTCH2, ADAM10,* and *ADAM17* were significantly upregulated compared to normal PB samples in both Ph+ leukaemias. This suggests that, as with lymphoid BP, Ph+ ALL has the components necessary for Notch activation. However, despite this, only lymphoid BP had a statistically significant increase in expression of *MAML* compared to normal. In keeping with this, *HES1* was not statistically significantly increased in Ph+ ALL samples, suggesting that the pathway was not active at a gene level. *FBXW7*, a negative regulator of Notch, was statistically significantly increased in Ph+ ALL compared to normal. As there was no statistical change in *TP53* and *MYC,* this suggests that *FBXW7* is acting independently of these survival mechanisms, and may offer a therapeutic target within the disease.

HIF1A is important within leukaemogenesis, particularly in CML (Zhang et al, 2012; Zhou et al, 2016). Within our dataset, *HIF1A* was statistically significantly increased in Ph+ ALL compared to both lymphoid BP and normal PB. Although further investigation is required to ascertain its importance in Ph+ ALL, it seems an exciting area of development. It has been shown that within ALL, blockade of *HIF1A*-mediated signalling may play an important role in chemo-sensitisation of ALL cells under hypoxic conditions of the BM (Frolova et al, 2012). Furthermore, within childhood B-ALL, high expression of *HIF1A* is associated with a good prognosis (Silveira et al, 2014), as well as being required for active Wnt signalling in T-ALL (Giambra et al, 2015). Although our focussed gene analysis demonstrated no significant difference between lymphoid BP and Ph+ ALL within Wnt/β-catenin pathway components, there appeared to be an increased dependency on the Wnt/β-catenin pathway within Ph+ ALL, with a statistically significant increase in key Wnt components, namely *TCF4, TCF7,* and *LEF1,* compared to normal PB. There is clearly an identified role for the Wnt pathway in the propagation of malignancy (Clevers, 2006; van Rhenen et al, 2007), but there is only limited data of its role within Ph+ ALL (Gregory et al, 2010). There is increasing evidence of its reliance, however, in normal B-cell development and, therefore, it represents a potential area of interesting further development in its role as a novel therapeutic intervention.

As expected, there was significant change in the cell survival regulators, namely *GATA1* and *GATA2*, which had a statistically significant decrease in expression in Ph+ ALL compared to lymphoid BP disease. This is likely in keeping with the myeloid and stem cell component noted within lymphoid BP. For example, *GATA1* is known to play an essential role in the commitment to, and subsequent differentiation within, myeloid lineages, particularly, erythroid, megakaryocyte and eosinophilic (Drissen et al, 2016; Ferreira et al, 2005). Contrary to AML data, which suggests a clinical significance of *GATA1*, *GATA2* and *SCL* expression (Shimamoto et al, 1994), there was no statistical difference in *SCL* expression compared to normal or between lymphoid BP and Ph+ ALL. Furthermore, there was no significant change between other cell cycle regulators in the Ph+ acute lymphoid leukaemias, including *CCND1*, *CCND2*, *FOXO1*, *STIL* and *CYCLINE1*. This is in keeping with the leukaemic phenotype of the diseases.

Together, this data confirms that lymphoid BP and Ph+ ALL are distinct disease entities and offers potentially interesting targets for further evaluation. This chapter has offered novel insight into the similarities between myeloid and lymphoid BP disease, which has not been previously described. Further to this, it has allowed discussion into the differences between self-renewal pathways between the Ph+ acute lymphoid leukaemias, which may guide potential therapeutic targets in the future, including *FBXW7* and components of the Wnt/β-catenin pathway within Ph+ ALL.

6. Results IV

6.1. Introduction

The concept of disease persistence through quiescent LSCs has been highlighted in recent years by trials exploring the discontinuation of TKIs in CP-CML patients with sustained deep molecular response (i.e. those that achieve a 4 log or greater reduction of quantitative *BCR-ABL* expression from standardised baseline over a prolonged period) (Etienne et al, 2017; Mahon et al, 2014; Mahon, 2015; Mahon et al, 2010; Mahon et al, 2016; Rea et al, 2012; Ross et al, 2010; Ross et al, 2013; Takahashi et al, 2012). These trials have demonstrated that discontinuation of therapy can be selectively achieved, with STIM trial data stating the cumulative incidence of molecular relapse at 60 months was 61% (CI 52-67%), with few cases of late relapse being observed (Mahon et al, 2014). This suggests that if molecular relapse is to occur, it happens early. Comparable results have been reported worldwide (Mahon et al, 2014; Mahon et al, 2010; Rea et al, 2012; Ross et al, 2010; Ross et al, 2013; Takahashi et al, 2012). The EURO-SKI trial is the largest study to date, with recruitment of over 800 patients. Most recent analysis demonstrated a molecular-recurrence free survival of 62% at 6 months, 56% at 12 months, and 52% at 24 months (Mahon et al, 2016). The DADI study analysed molecular-relapse free survival after stopping dasatinib as second-line therapy or beyond. The probability of molecular-recurrence free survival was 49% at 6 months, and 48% at 12 months, with all molecular relapses occurring within 7 months of stopping therapy. All patients with molecular relapse regained deep molecular response within 6 months (Imagawa et al, 2015). The UK equivalent trial currently in progress (DESTINY) is analysing the role of dose reduction before complete suspension of TKI treatment. Interim data has suggested that decreasing TKI treatment to half the standard dose was associated with improvement in TKI adverse events, in patients with stable MR3 or more. This suggested that many patients are being overtreated and that there is scope for TKI dose reduction prior to discontinuation to assess response (Clark et al, 2016).

Although these results indicate the possibility for TKI discontinuation in a small subset of CML patients, they highlight an uncertainty surrounding the 'trigger' event(s) in molecular relapse, and question if sustained *BCR-ABL* expression, LSC persistence, microenvironmental factors, or, indeed, multiple factors are contributory factors. It is known that in up to 30% of normal individuals, low levels of *BCR-ABL* expression can be identified (Biernaux et al, 1995; Bose et al, 1998), perhaps suggesting that *BCR-ABL*

transcript level alone is not sufficient in CML maintenance. It is unknown, however, what cell types these transcripts are originating from and if this is significant long-term. Interestingly, a single copy of *BCR-ABL* expressed from the endogenous BCR locus in a knock-in murine model is not sufficient to induce leukaemia (Foley et al, 2013; Huntly & Gilliland, 2005; Huntly et al, 2004). Therefore, although it is clear that a certain level of *BCR-ABL* needs to be expressed at the stem cell level to cause CML, it is unclear if further molecular changes or aberrant signalling is needed to drive disease persistence, molecular relapse and disease progression. Furthermore, it is unknown if *BCR-ABL* is the initiating insult, or if host factors, such as epigenetic and genetic changes influence disease outcome. Regardless, it is clear that eradication of *BCR-ABL* is not a prerequisite for long-term disease free survival, and this suggests that other factors, including CML LSCs, are responsible for molecular relapse.

It has been well documented that CML LSCs are not eradicated by TKIs *in vitro*, with initial studies by the Holyoake group demonstrating that a population of Lin^-CD34^+ CML progenitors have the ability to remain quiescent, are insensitive to the TKI, imatinib, and can engraft into NOD SCID gamma (NSG) mice (Graham, 2002; Hamilton et al, 2012; Verstegen et al, 1999). Furthermore, Bhatia *et al* translated this into the clinical setting by showing that cells of a similar phenotype could be identified in the bone marrow of imatinib-treated CML patients in CCyR (Bhatia et al, 2003b). These studies, amongst others, verify that CML LSCs are not absolutely dependent on *BCR-ABL* activity for their survival and may determine disease persistence (Chomel et al, 2011; Corbin et al, 2011b; Deininger, 2012).

It seems pertinent therefore, that a biomarker of the CML LSC is discovered to enable detection of those individuals that can come off therapy and those that need to remain on therapy, as this will have both financial and psychological implications for the healthcare system and the patient group, respectively. Although many labs have performed extensive analysis to identify markers of a primitive cell population in the preclinical setting, including CD26 (Culen et al, 2016; Herrmann et al, 2015; Warfvinge et al, 2017) and IL1-RAP (Järås et al, 2010; Landberg et al, 2016; Warfvinge et al, 2017; Ågerstam et al, 2016), none have been shown, as yet, to be robust enough for clinical translation. CD26, however, is showing increasing promise in this regard with recent data suggesting a correlation between CD26 expression and treatment response, as well as $Lin^-CD34^+CD38^{-/low}CD45RA^-cKIT^-CD26^+$ population being identified as a potential therapeutic target at a single cell level (Culen et al, 2016; Warfvinge et al, 2017).

Although identification of the CML LSC appears to be within reach, little is known about the biology of the LSC in those patients that are in deep molecular response, with much of our understanding and the previous data coming from a drug-naïve population. Clinically, the therapeutic need will be in those that are on TKI therapy. In keeping with this, (Giustacchini et al, 2017) recently described a novel approach in determining single-cell gene expression within a LSC phenotype between BCR-ABL+ and BCR-ABL negative cells of the same patients, as well as those on TKI treatment. This will advance our understanding of LSC biology within CML and other stem cell diseases.

Within the Copland group, we have sought to understand the biology of CML LSCs compared to normal, in an effort to aid the identification of this subset of cells. Previous unpublished work has demonstrated that the GEP of CML LSCs is more akin to normal stem and progenitor cells, and not normal HSCs, as represented through Principal Component Analyses (PCA) where, when plotted together, LSCs from patients with CP CML (n=6) have a global gene expression signature that appears more mature than normal HSCs (n=3), and is positioned overlapping the progenitor subpopulations' (GSE47927) (figure 6-1).

Within this dataset (GSE47927), 1217 genes were deregulated between CP-CML LSCs and normal HSCs (figure 6-2). We initially utilised this gene expression data to evaluate the expression of cell surface markers. Using z scores to normalise the gene expression for each sample, we plotted heat maps using R/Bioconductor. This demonstrated the variable expression of cell surface markers between CP-CML LSCs and normal HSCs (figure 6-3).

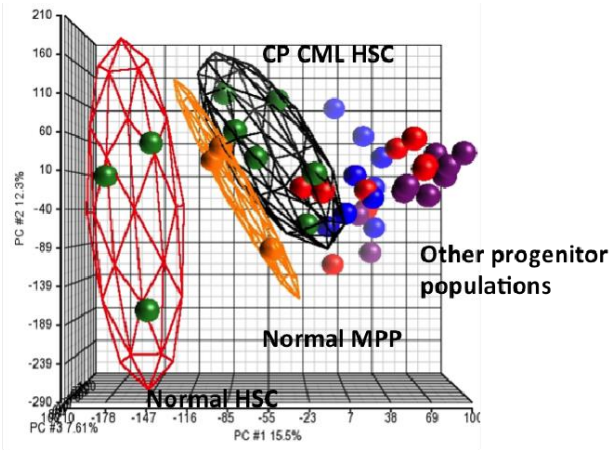

Figure 6 - 1 PCA of normal HSC, CP-CML LSC, and progenitor populations
Data analysed by DI as part of (Irvine, 2013). Each axis represents a principal component of the variability in the normal and CP samples. An individual point within the axes represents each microarray and each subpopulation grouping by a different colour (green for HSC, orange for MPP); an ellipse is positioned at 2 standard deviations around the normal HSC (red), normal MPP (Orange) and CP-CML LSC (black). The other progenitor populations are shown without ellipses.

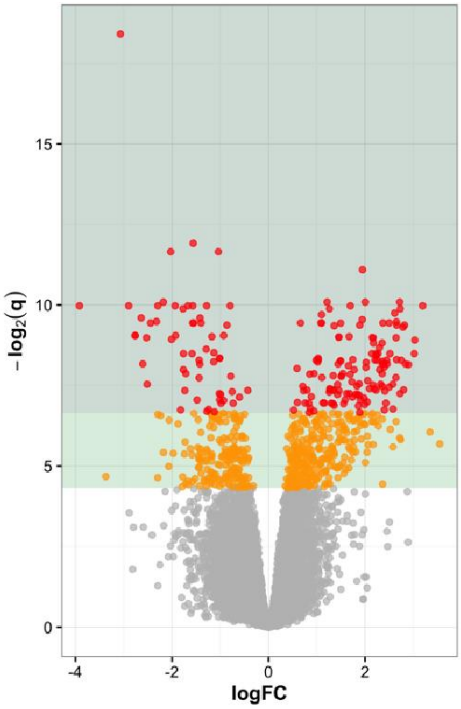

Figure 6 - 2 Gene expression is deregulated between normal and CP-CML LSCs
A volcano plot showing deregulation of genes in a comparison of $Lin^-CD34^+CD38^-CD90^+$ cells from 6 CP-CML samples against the same population derived from 3 normal samples (GSE47927). Areas of significance are indicated by a dark green (equivalent to q<=0.01) or light green (equivalent to q<=0.05) background. Genes reaching significance are coloured red (q<=0.01) or orange (q<=0.05); non-significant genes are grey. Data analysed by GH and LH.

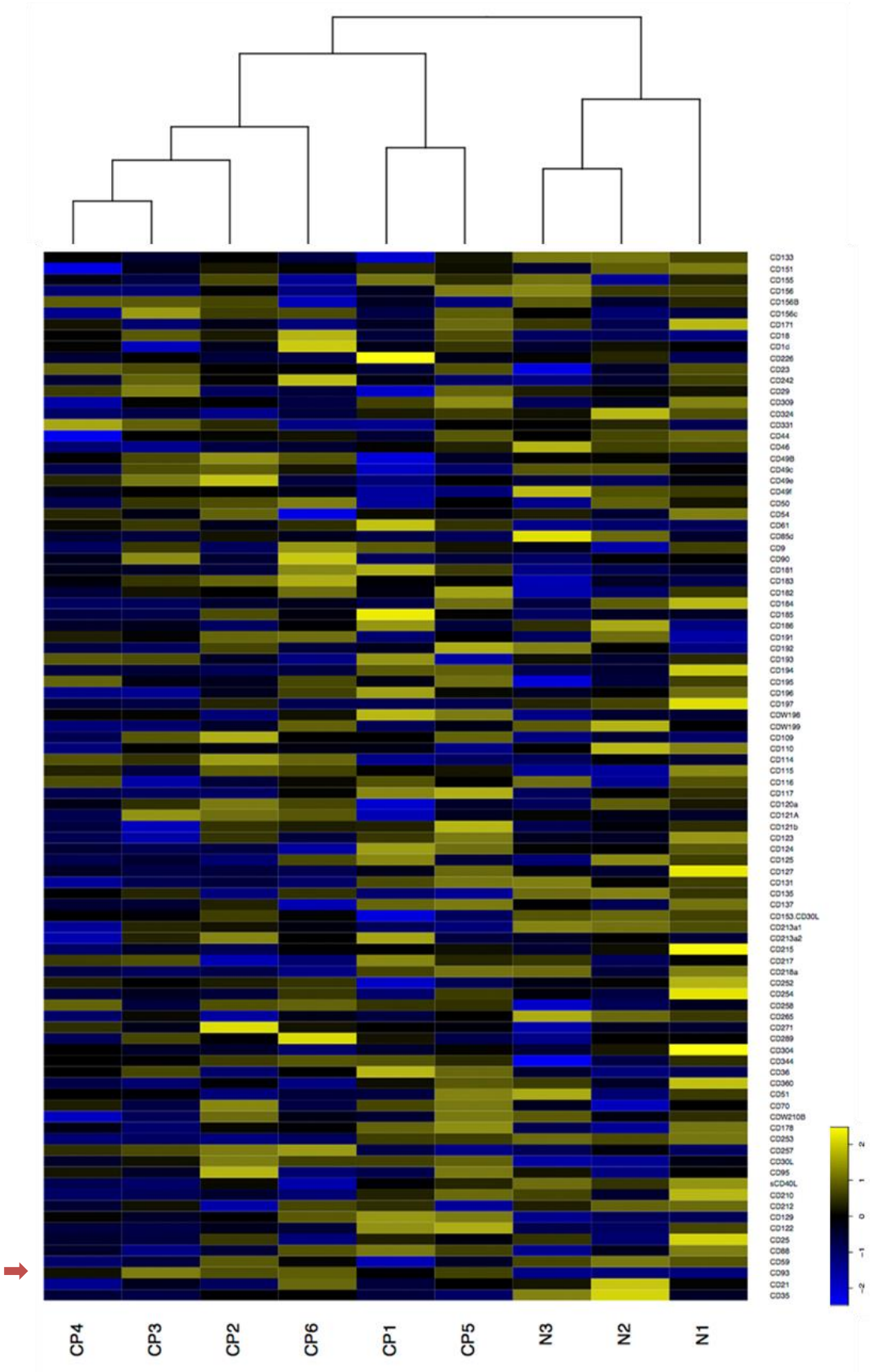

Figure 6 - 3 Cell surface markers are deregulated between normal and CP-CML LSCs
Mean expression levels between normal HSCs (n=3) and CP-CML LSCs (n=6) from GSE47297 were normalised across each gene (z score) and represented using heatmap.2 in R/Bioconductor. Yellow represents increased expression and blue represents decreased expression within the data set. Samples could be clustered into disease process, i.e. normal and CP-CML. Data analysed by GH and HM.

Although there was variable expression noted across the cell surface markers analysed, some cell surface markers were expressed at significant and differential levels between the CML LSC and normal HSC populations (Table 6-1). Of note, *CD93* demonstrated a six-fold increased expression in CP-CML compared to normal HSC and represented an interesting target for further analysis.

	P-value	Fold change CP-CML vs. normal
CD93	$2.5x10^{-6}$	6
CD47	$9.25x10^{-8}$	-1.88
CD96	0.0017	-3.08
CD59	0.0013	-1.63
CD53	0.0011	-1.62
CD62L	0.085	-2.72

Table 6 - 1 Cell surface marker fold change between CP-CML LSC versus normal
Analysis of the microarray, GSE47927, demonstrated significant fold change between CP-CML vs. normal in a number of cell surface markers. The table represents the most statistically significant genes identified. Data analysed by HM and GH.

This was confirmed at the gene level within $CD34^+$-selected PB and BM CML samples compared to normal BM samples, purchased from Stem Cell Technologies (figure 6-4A). A statistically significant increase in $CD93^+$ cells was noted within the LSC population of PB CP-CML samples at the protein level (n=20) compared to normal (figure 6-4B).

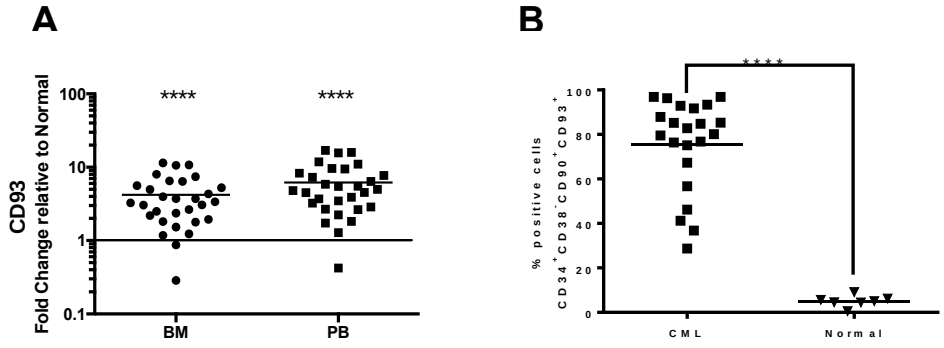

Figure 6 - 4 CD93 is upregulated within CP-CML at gene and protein level
(A) RNA from 30 BM and PB CP-CML samples was utilised to validate the gene expression of *CD93*. All samples were isolated from CD34+-selected cells, and compared to normal BM (n=5). Compared to normal, there was a statistically significant increase in *CD93* gene expression in BM and PB, as determined by an unpaired student's t test ($p<0.001$). (B) CD93 protein expression was assessed by flow cytometry in $CD34^+CD38^-CD90^+$ populations between CML (n=22) and normal (n=7). A statistically significant increase in percentage of $CD93^+$ cells was determined using an unpaired student's t test ($p<0.0001$).

CD93 is a glycoprotein, which comprises a C-type lectin-like domain, five EGF-like domains, a transmembrane domain and a short cytoplasmic tail (Christian et al, 2001; Nepomuceno et al, 1997). It can appear in two forms: a cell-associated full-length and a truncated soluble form (Greenlee-Wacker et al, 2011), which confer functional variability. Although CD93 was previously identified as a receptor for complement component 1, subcomponent q phagocytosis (C1qRp), which was initially shown to be involved in the C1q-mediated enhancement of phagocytosis, several studies have reported the contrary and the functional roles for CD93 are extensive. A variety of functions have been described, including high expression promoting dissemination of malignancy through angiogenesis (Bao et al, 2016; Langenkamp et al, 2015; Orlandini et al, 2014), apoptosis (Norsworthy et al, 2004), and monocyte inflammation (Greenlee-Wacker et al, 2011; Jeon et al, 2010), as well as being implicated in leukocyte migration and cell adhesion (Galvagni et al, 2016). Knockout CD93 murine models remain viable and show no severe developmental abnormalities, although phagocytosis is decreased *in vivo* in these animals (Norsworthy et al, 2004). Furthermore, membrane CD93 protein and mRNA expression has been described in cells of myeloid origin, stem cells, endothelial cells and platelets (Ikewaki et al, 2010; Nepomuceno & Tenner, 1998).

The role of CD93 as an immature cell marker, or biomarker, has been explored in a variety of malignancies (Lee et al, 2009; Olsen et al, 2015), including within multiple myeloma, where a recent study showed that higher gene expression of CD93 was associated with higher survival rates amongst patients with multiple myeloma (MM) treated with bortezomib, indicating that high levels of CD93 may be a possible marker for better outcome in these patients (Stessman et al, 2013).

Within myeloid disease, CD93 has been shown to offer potential as a biomarker for an AML LSC population, where it has been identified as a part of the AML LSC gene signature, and expression confirmed at protein level (Saito et al, 2010). Furthermore, it has been shown, more recently, that CD93 expression can identify a predominantly cycling, non-quiescent leukaemia-initiating cell population in MLL-rearranged AML, providing opportunities for selective targeting and eradication of the AML LSC (Iwasaki et al, 2015b). The functional role of CD93 expressing cells within CML has yet to be identified.

6.2. Aims

In view of the above, the specific aims set out in this chapter were

1. to assess the self-renewal capability of CD93 within the LSC compartment, and
2. to assess the gene expression differences between $Lin^-CD34^+CD38^-CD90^+CD93^+$ and $Lin^-CD34^+CD38^-CD90^+CD93^-$ cells at bulk and single cell level.

6.3. Results

6.3.1. CD93^{+}, but not CD93^{-} CML cells have LIC and self-renewal capacity *in vitro* and *in vivo*

Because CD93 was upregulated within an LSC phenotype at gene and protein level, it was hypothesised that CD93^{+} cells would correlate with the self-renewal properties of CML LSCs. To address this, primary CP-CML samples were sorted into Lin^{-}CD34^{+}CD38^{-}CD90^{+}CD93^{+} and Lin^{-}CD34^{+}CD38^{-}CD90^{+}CD93^{-} populations (figure 6-5).

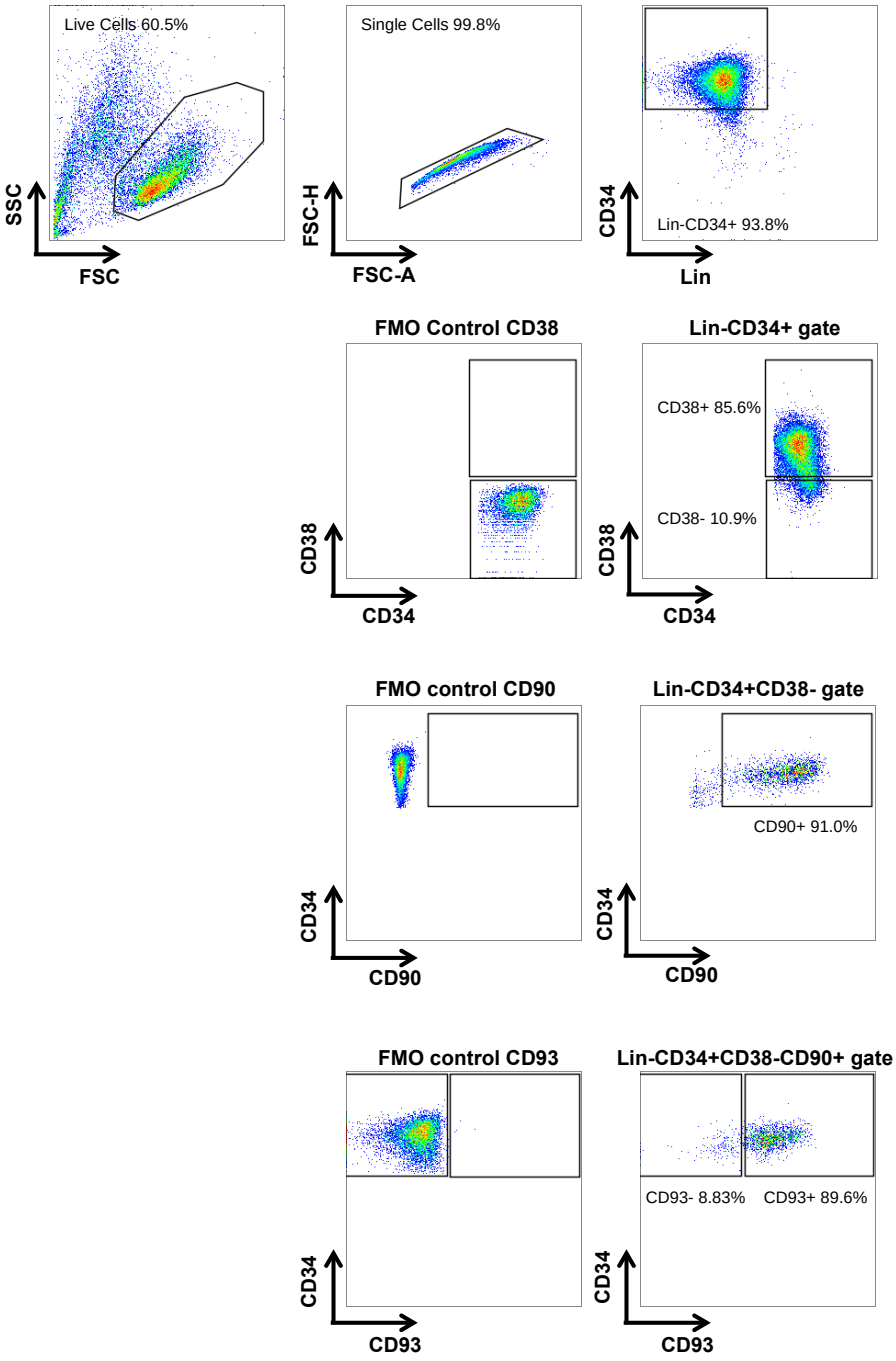

Figure 6 - 5 Sorting strategy for Lin$^-$CD34$^+$CD38$^-$CD90$^+$CD93$^{+/-}$ populations
Cells were thawed and cultured overnight in SFM+5GF. Cells were then washed in PBS/2%FBS and counted. 5x10^4 cells were used within each unstained, single-stained and FMO control, where cells were re-suspended in 100ul PBS/2%FBS prior to the addition of antibody (concentration calculated in previous dilution experiments'). The '5-stain' sample was re-suspended in 450ul PBS/2%FBS prior to the addition of antibody. Samples were stained for 30 minutes at 4°C and then washed twice with PBS/2%FBS before being filtered through a 0.22uM filter. Cells were sorted with a BD FACS Aria with Diva software.

We first sought to identify differential potential of the cells with CFC assays. Two thousand FACS-sorted cells from the Lin$^-$CD34$^+$CD38$^-$CD90$^+$CD93$^+$ and Lin$^-$CD34$^+$CD38$^-$CD90$^+$CD93$^-$ populations were plated in duplicate in Methocult. Plates were incubated at 37°C for 10-12 days before colonies were counted. Colonies were *BCR-ABL* positive as determined by FISH. An increase in number of colonies was noted within the Lin$^-$CD34$^+$CD38$^-$CD90$^+$CD93$^+$ population compared to Lin$^-$CD34$^+$CD38$^-$CD90$^+$CD93$^-$ (n=4 CP-CML samples) (figure 6-6A); however, this was not statistically significant as determined by a paired student's t test, and perhaps reflects the fact that primary colony formation in progenitor assays is largely driven by committed progenitors and not stem cell self-renewal. Up to 50 primary colonies per sample were next individually picked and re-suspended in 200ul fresh Methocult in 96 well plates. Plates were incubated at 37°C for 12 days before positive wells were counted. This demonstrated no statistical change in replatiting capability between Lin$^-$CD34$^+$CD38$^-$CD90$^+$CD93$^+$ population compared to Lin$^-$CD34$^+$CD38$^-$CD90$^+$CD93$^-$ (figure 6-6B); there was, however, a trend towards increased replating potential in the CD93$^+$-selected cells.

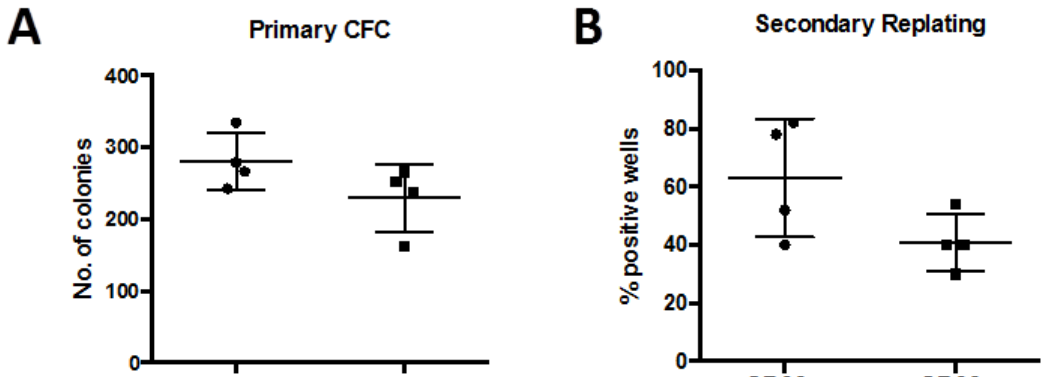

Figure 6 - 6 Lin-CD34+CD38-CD90+CD93+ do not differ in CFC and replating potential
(A) CP-CML samples (n=4) were sorted according to figure 5-3 and plated in duplicate into methocult for 12-14 days prior to colony counts. The graph indicates the mean number of colonies for each CP-CML, with mean and standard deviation for each population. There was no statistical significance between the populations (p>0.05; n=4 CP-CML samples). (B) The graph indicates the percentage of positive wells per population from replating assays (p>0.05; n=4 CP-CML samples), with mean and standard deviation. There was no statistical difference between populations, as determined by a paired student's t test; however, there was an apparent trend towards an increase in percentage of positive wells in the Lin-CD34+38-90+93+ population.

To interrogate this further, LTC-IC assays were utilised. LTC-IC assays represent the most stringent *in vitro* surrogate measure of the functional activity of HSCs. Samples were sorted into $Lin^-CD34^+93^+$ and $Lin^-CD34^+93^-$ populations. 50,000 cells from each sorted population (n=3, CP-CML samples) were cultured in six duplicates on a stromal feeder layer (a 1:1 mix of irradiated (80Gy) SL/SL and M210B4 murine fibroblasts) in long-term myeloid culture medium (MyeloCult supplemented with hydrocortisone). Cultures were maintained for 6 weeks with 50% media changes performed weekly before being harvested into Methocult for 12 days prior to colonies being counted. Results demonstrated a statistically significant increase in colonies within the $Lin^-CD34^+93^+$ arm of the experiment with no, or few, colonies within the $Lin^-CD34^+93^-$ experimental arm (Figure 6-7A and 6-7B). This suggested that $CD93^+$-selected cells have increased self-renewal capacity *in vitro* compared to $CD93^-$-selected cell population.

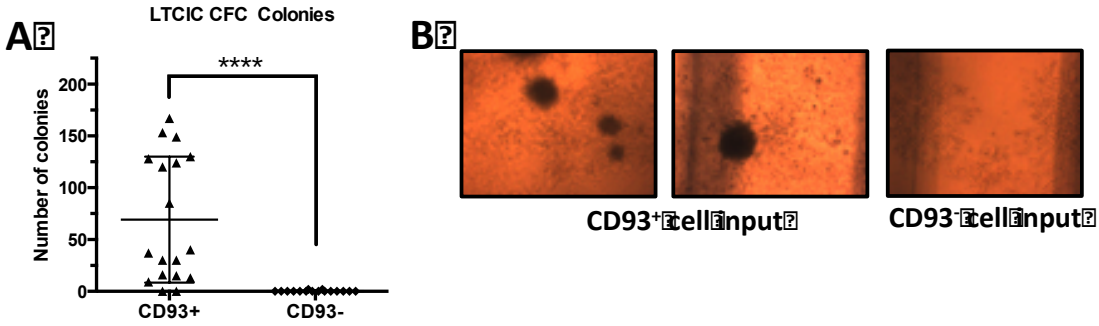

Figure 6 - 7 $Lin^-CD34^+CD93^+$ have greater self-renewal capacity that $Lin^-CD34^+CD93^-$ *in vitro*

3 CP-CML samples were sorted in $Lin^-CD34^+93^+$ and $Lin^-CD34^+93^-$ populations. 50,000 cells from each sorted population were cultured in six duplicates on a stromal feeder layer of irradiated SL/SL and M210B4 in long-term myeloid culture medium. Cultures were maintained for 6 weeks with 50% media changes performed weekly. (A) The graph indicates the number of colonies from each experimental arm (n=3 CPCML samples), with mean and standard deviation. There was a statistical significant difference between $Lin^-CD34^+93^+$ and $Lin^-CD34^+93^-$ populations as demonstrated using a paired students t-test (****, $p<0.0001$).

We next sought to identify if this increased self-renewal capacity could be translated *in vivo* and utilised a NSG engraftment model to evaluate this (figure 6-8). The NSG mouse model was used to assay human LSCs with *in vivo* engraftment capacity (SCID-repopulating cells).

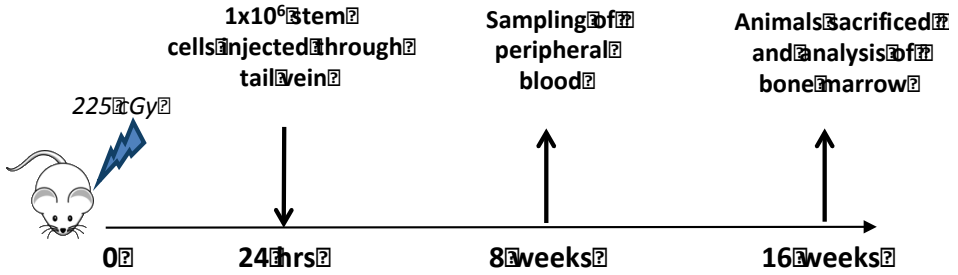

Figure 6 - 8 Schematic of NSG experiment

CP-CML Lin$^-$CD34$^+$CD93$^+$ or Lin$^-$CD34$^+$CD93$^-$ cells were isolated by FACS sorting (1x10^6 cells/mouse), washed and transplanted via tail vein injection into sub-lethally irradiated (2 Gy) 8-12 week old NSG mice. Peripheral blood was sampled at 8 weeks to assess for CD45$^+$33$^+$ expression. All mice were euthanised after 16 weeks and marrow contents of femurs were obtained. To assess human cell engraftment, cells were labeled with anti-human CD45, CD33 and CD19 antibodies prior to analysis by flow cytometry. This allowed for analysis of lineages within the engrafted samples. Performed and analysed by GH and RK.

Prior to sorting, CP-CML samples (n=5) were assessed for *BCR-ABL* expression within a Lin$^-$CD34$^+$ population by FISH (figure 6-9). CP-CML Lin$^-$CD34$^+$CD93$^+$ or Lin$^-$CD34$^+$CD93$^-$ cells were then isolated by FACS sorting (1x10^6 cells/mouse) (figure 6-5), washed and transplanted via tail vein injection into sub-lethally irradiated (2 Gy) 8-12 week old NSG mice. Samples were not selected for CD38 or CD90, as cell numbers were deemed too small to proceed with transplantation.

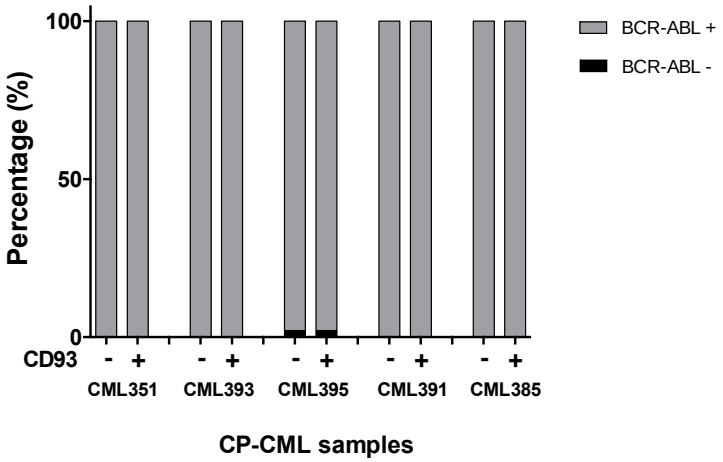

Figure 6 - 9 *BCR-ABL* analysis by FISH prior to NSG engraftment model

FISH was performed as per 2.3.2.13 prior to being analysed using an AXIOvision AX10 fluorescent microscope and AXIOvision software. Chromosome t(9;22) *BCR-ABL* fusion was detected by a dual colour dual fusion probe (Abbott Molecular). Upon thawing, all samples were *BCR-ABL* positive, with only one sample (CML395) being less than 100%.

PB was removed at 8 weeks from the mice utilised for three of the CML samples, and analysed for engraftment using CD45 and CD33 expression by flow cytometry. There was no significant difference in $CD45^{+}33^{+}$ expression between the $Lin^{-}CD34^{+}93^{+}$ and $Lin^{-}CD34^{+}93^{-}$ populations at this time point, suggesting that engraftment had not yet occurred or was not detectable and, therefore, peripheral blood engraftment was not analysed in the further 2 samples (figure 6-10).

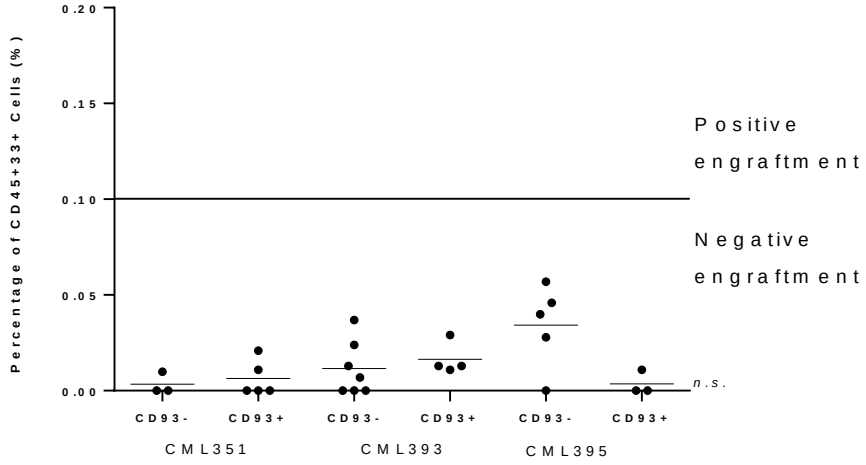

Figure 6 - 10 Significant engraftment was not identified at 8 weeks in CD93+ or CD93- populations

Following transplantation via tail vein injection into sublethally (2 Gy) irradiated NSG mice, blood sampling was performed at 8 weeks. To assess human cell engraftment, cells were labelled with anti-human CD45, CD33 and CD19 antibodies prior to analysis by flow cytometry. $CD45^{+}CD33^{+}$ cells were determined as a percentage of total cells. There was no statistically signficant difference between the experimental arms at 8 weeks, suggesting that engraftment had not yet occurred. n=3 CP-CML samples, p value calculated from paired student's t test between arms of the experimental for each CP-CML sample. Performed and analysed by GH and RK.

All mice were euthanised after 16 weeks and marrow contents of femurs were obtained. To assess human cell engraftment, cells were labeled with anti-human CD45, CD33 and CD19 antibodies prior to analysis by flow cytometry. This allowed for analysis of lineages within the engrafted samples. Within CML395, there was no statistical change in engraftment potential between the $Lin^{-}CD34^{+}CD93^{+}$ and $Lin^{-}CD34^{+}CD93^{-}$ experimental arms (figure 6-11A). However, on closer analysis of the flow cytometry data, it is clear that the engraftment potential in the $CD93^{-}$ population is mixed lineage, suggesting that this is secondary to *BCR-ABL* negative cells, which engraft better than *BCR-ABL* positive cells and engraft with both myeloid and lymphoid lineage cells. This was, indeed, validated in the pre-FISH analysis, which demonstrated a small, but biologically significant, percentage of BCR-ABL negative cells within the sample. Furthermore, on analysis of the post engraftment sort, the $CD34^{+}$ populations were

BCR-ABL negative within the CD93$^-$-selected populations (figure 6-11B). Consequently, within this sample, it is clear that the engraftment potential in the CD93$^-$-selected population is driven by 'normal' stem cells, which have good engraftment potential and engraft both lymphoid and myeloid lineages (figure 6-11C).

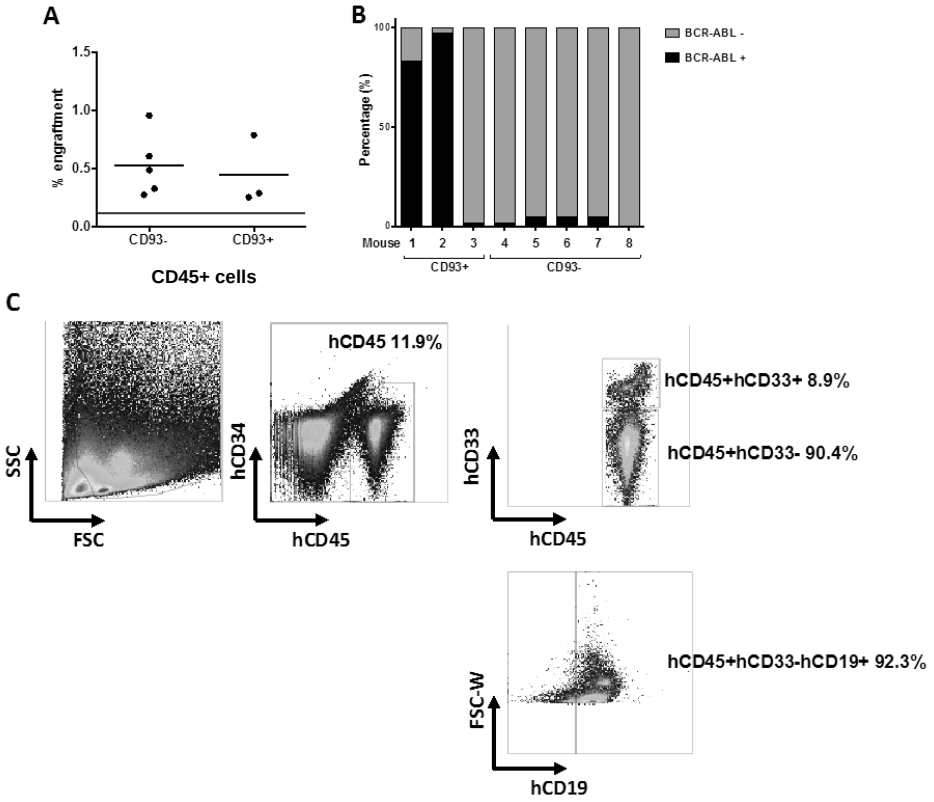

Figure 6-11 Non-*BCR-ABL* engraftment leads to multi-lineage cell potential
Mice were euthanised after 16 weeks and marrow contents of femurs were obtained. (A) To assess human cell engraftment, cells were labeled with anti-human CD45, CD33 and CD19 antibodies prior to analysis by flow cytometry. Human cell engraftment was characterised by percentage of CD45$^+$. (B) Human CD45$^+$ cells were isolated by FACS sorting and analysed by FISH for the *BCR-ABL* gene rearrangement. Percentage of *BCR-ABL* positive cells, as determined from analysis of 100 cells, was assessed for each murine experiment. All mice within the CD93$^-$ experimental arm were predominantly *BCR-ABL* negative, with a mixed *BCR-ABL* population evident within the CD93$^+$ arm. (C) Example of FACS analysis isolating both myeloid and lymphoid lineages within the CD45$^+$ sample.

There was a statistically significant increase in engraftment with CD93$^+$-selected cells, as determined by student's t test, in the further 4 independent CP-CML samples (figure 6-12A), where prior to engraftment there was 100% *BCR-ABL* positive expression with FISH in CD93$^+$- and CD93$^-$-selected ssamples. Human CD45$^+$CD33$^+$ cells were isolated by FACS sorting at 16 weeks and again analysed by FISH for the *BCR-ABL* gene rearrangement. These samples were *BCR-ABL* positive (figure 6-12B) demonstrating again that the CD93$^+$-selected population has an increased leukaemia-

initiating and self-renewal capacity and, ultimately, may represent an immature phenotype within the hierarchy that can be used as a biomarker for the CML LSC.

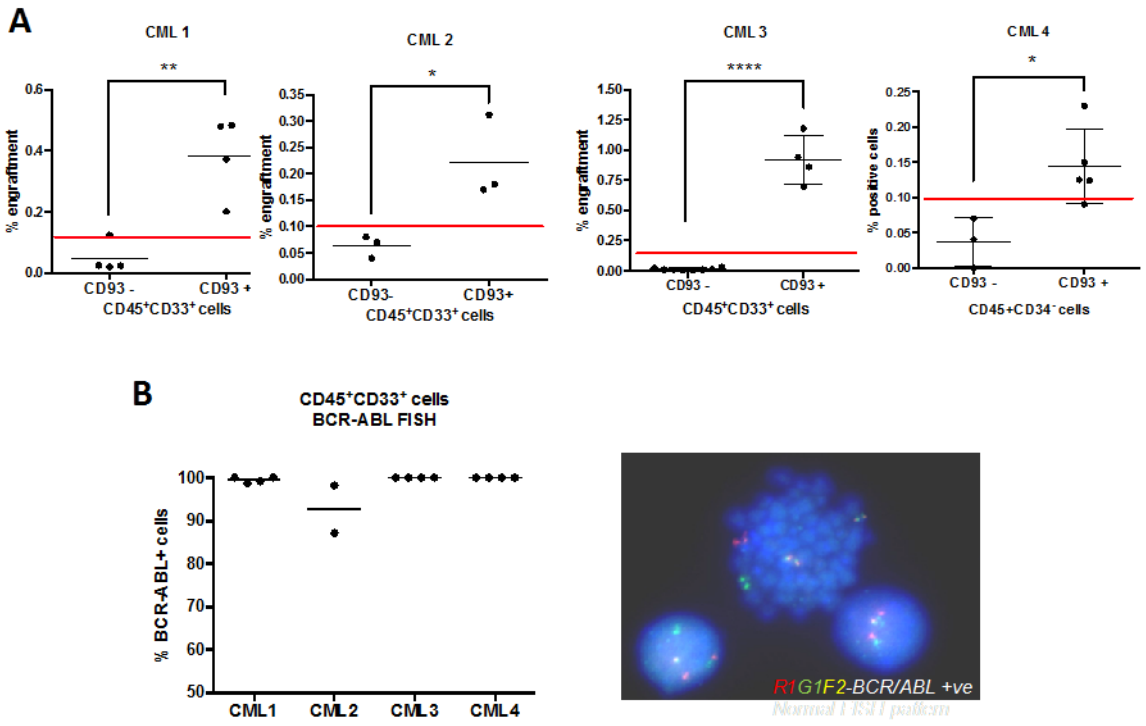

Figure 6 - 12 Lin$^-$CD34$^+$CD93$^+$ cells confer higher rates of engraftment compared to Lin$^-$CD34$^+$93$^-$ cells

Mice were euthanised after 16 weeks and marrow contents of femurs were obtained. (A) Human cell engraftment was characterised by percentage of CD45$^+$CD33$^+$ cells. There was a statistically significantly increased engraftment in the CD93$^+$ experimental arm as determined by the student's t test (*, p<0.05; **, p<0.01; ***, p<0.001). (B) Human CD45$^+$ cells were isolated by FACS sorting and analysed by FISH for the *BCR-ABL* gene rearrangement. Percentage of *BCR-ABL* positive cells, as determined from analysis of 100 cells, was assessed for each murine experiment. Performed and analysed by GH and RK.

6.3.2. Gene expression profiling of CD93$^+$-selected CP-CML stem cells confirms their quiescent character and biomarker potential

These results have demonstrated that CD93$^+$Ph+-selected populations have functional properties of the CML LSC, with evidence of increased self-renewal and engraftment potential. It was subsequently hypothesised that lin$^-$CD34$^+$CD38$^-$CD90$^+$CD93$^-$ CML cells would have a more mature and less lineage restricted gene expression profile compared to lin$^-$CD34$^+$CD38$^-$CD90$^+$CD93$^+$ cells. We next sought to characterise the differences in the lineage gene expression profile between CD93$^+$ and CD93$^-$-selected CML LSC populations and determine gene expression for each population at the single cell level.

To interrogate this, CP-CML subpopulations with the greatest functional capability compared to normal were identified from previous data generated within our lab (Copland, 2007). In brief, normal and CP-CML samples were FACS-sorted into HSC/LSC, CMP, GMP, and MEP subpopulations. Results suggested a significant change in functional status between normal and CP-CML subpopulations within the HSC/LSC compartment ($lin^-CD34^+CD38^-CD45RA^-CD90^+$), where the CML LSC population demonstrated significantly increased proliferation (14 fold expansion; $P<0.001$) compared to normal HSCs (no expansion) after 5 days *in vitro* culture in physiological growth factors. In addition, equivalent numbers of CML LSCs produced approximately 4-fold more colonies in CFC assays than normal HSCs (329±56 versus 86±17 per 2,000 cells, respectively ($p<0.05$)). The LSC compartment was, therefore, utilised in subsequent experiments to accurately characterise the expression between the 93^+ and 93^- populations.

CP-CML cells were sorted into (1) lin^-CD34^+, (2) $lin^-CD34^+CD38^-CD90^+CD93^-$ and (3) $lin^-CD34^+CD38^-CD90^+CD93^+$ populations (figure 5-5). RNA was harvested at baseline from 'bulk' populations (1) to (3) and cDNA generated. cDNA was generated from single cells using the Fluidigm C1 autoprep system. Using Fluidigm technology, quantitative PCR of 90 lineage-specific and cell survival genes was performed within all populations of cells (1) to (3) in 'bulk' samples (n=3), and at single cell level (n=150 $lin^-CD34^+CD38^-CD90^+CD93^+$, n=150 $lin^-CD34^+CD38^-CD90^+CD93^-$ single cells; n=3 samples in total). Multiplex PCR was used to determine if *BCR-ABL* was present at a single cell level following pre-amplification with the Fluidigm C1 autoprep system (figure 6-13)

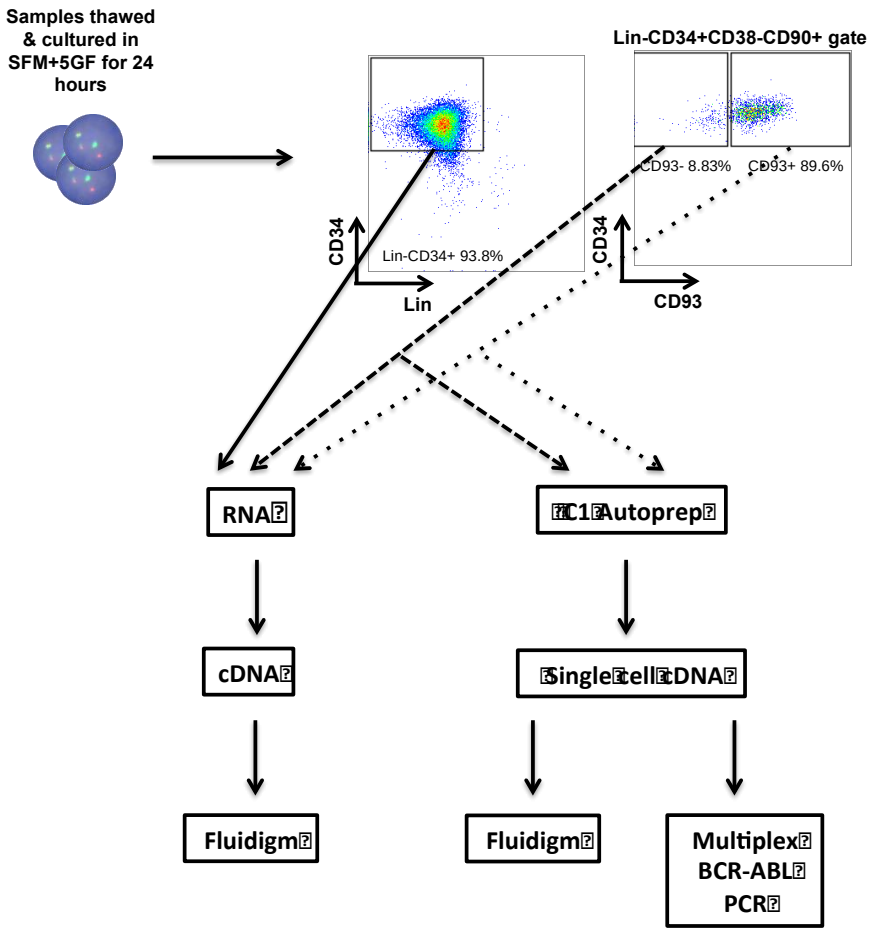

Figure 6 - 13 Schematic experimental design for gene expression profiles between Lin$^-$CD34$^+$CD38$^-$CD90$^+$CD93$^+$ and Lin$^-$CD34$^+$CD38$^-$CD90$^+$CD93$^-$ populations

CP-CML samples were thawed and cultured in SFM+5GF overnight prior to FACS-sorting into (1) Lin$^-$CD34$^+$, (2) Lin$^-$CD34$^+$CD38$^-$CD90$^+$CD93$^+$, and (3) Lin$^-$CD34$^+$CD38$^-$CD90$^+$CD93$^-$. RNA was generated from the 'bulk' populations (1) to (3), and 100ng was used to generate cDNA, prior to Fluidigm gene expression analysis. 5000 cells from the 'bulk' samples were run through the C1 Autoprep to generated pre-amped single cell cDNA. 1ul of this sample was used in a multiplex *BCR-ABL* PCR to identify *BCR-ABL* positive cells, and the rest of the sample was used in the Fluidigm gene expression analysis.

The inherent biological heterogeneity between patient samples can result in a greater variability of gene expression when compared with cell line-based experiments. This can lead to minimal statistically significant difference between populations. Furthermore, any significant changes that were noted between lineage gene expression between CD93$^+$ and CD93$^-$-selected populations were within an already immature LSC population, making them biologically significant. **Δ**CT was determined as an average of 4 housekeeping genes, namely *ATP*, *β-actin*, *B2M*, and *UBE2D2*. Statistical significance was determined through an unpaired student's t-test from **Δ**CT values; results are presented as fold change compared to the CD34$^+$ population.

Gene expression of *CD93* was shown to be upregulated within our Lin$^-$CD34$^+$38$^-$90$^+$93$^+$ population compared to CD34$^+$ control and Lin$^-$CD34$^+$38$^-$90$^+$93$^-$ population (p=0.0068) (figure 6-14).

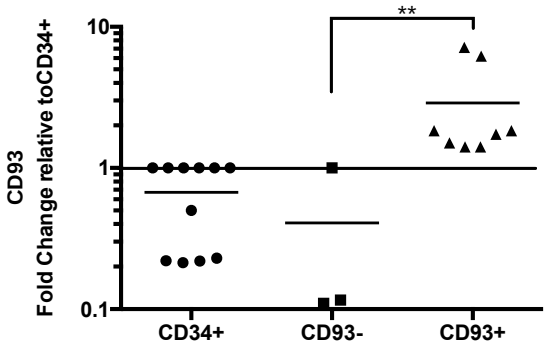

Figure 6 - 14 CD93 gene expression is higher within the Lin$^-$CD34$^+$CD38$^-$CD90$^+$CD93$^+$ population

Gene expression was determined from CD34$^+$ selected CP CML samples (n=3 samples, Lin$^-$CD34$^+$CD38$^-$CD90$^+$CD93$^+$ and Lin$^-$CD34$^+$CD38$^-$CD90$^+$CD93$^-$ CP-CML samples. Gene expression levels were determined by Fluidigm array analysis using the delta delta Ct method with an average of four housekeeping genes as reference. Fold change is relative to CD34$^+$. Increase gene expression of *CD93* was determined in the Lin$^-$CD34$^+$CD38$^-$CD90$^+$CD93$^+$ population compared to CD34$^+$. P values were determined by an unpaired t-test (*, p<0.05; **, p<0.01; ***, p<0.001).

On global gene expression analysis, the two populations could be segregated by differential gene expression through gene clustering of the fold change compared to the CD34$^+$ population, although this was sample-dependent (figure 6-15). Within this expression cluster, the Lin$^-$CD34$^+$CD38$^-$CD90$^+$CD93$^-$ population was associated with overexpression of genes involved in lineage restriction. Included in these were *GATA1* (p=0.0007), and *CBX8* (p=0.0002). Furthermore, there was an overexpression in the cell cycle gene, *CYCLIND2*, and lower expression of *MCM4*, suggesting that these cells have a more active cell cycle pattern (figure 6-16). The lin$^-$CD34$^+$CD38$^-$CD90$^+$CD93$^+$ population displayed a less lineage-restricted profile with increased expression of *CDK6* (p=0.05), *HOXA6* (ns), *CDKN1C* (ns) and *C-KIT* (p=0.0014), compared to the Lin$^-$CD34$^+$CD38$^-$CD90$^+$CD93$^-$ population (figure 6-17). Taken together, this suggests that gene expression profiles of bulk lin$^-$CD34$^+$CD38$^-$CD90$^+$CD93$^+$ population correlates with the primitive functional status of the population, and confirms previous findings that a CD93$^+$-selected population may represent a potential biomarker of the CML LSC.

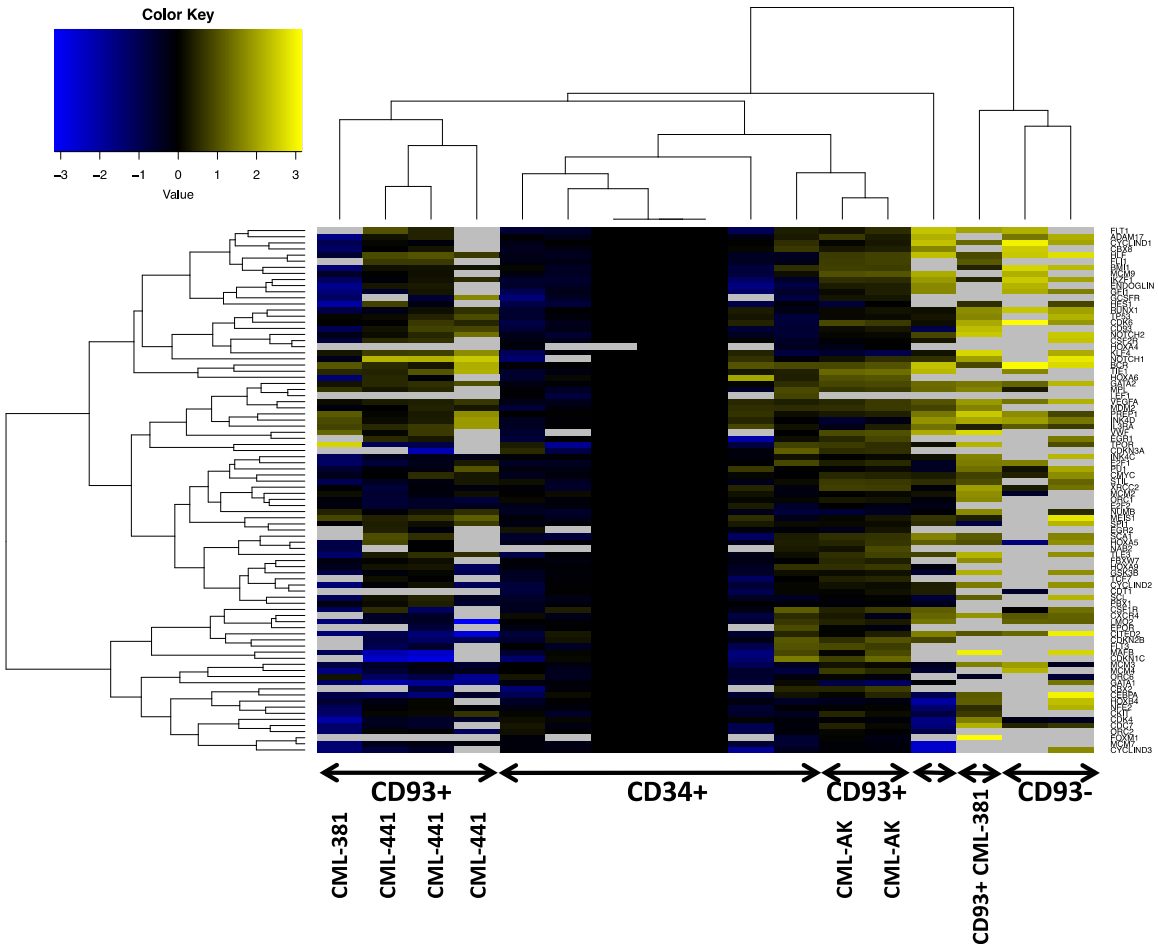

Figure 6 - 15 Gene expression profiling can segregate Lin$^-$CD34$^+$CD38$^-$CD90$^+$CD93$^+$ and Lin$^-$CD34$^+$CD38$^-$CD90$^+$CD93$^-$ populations

Gene expression profiles (GEPs) were determined from CD34$^+$, Lin$^-$CD34$^+$CD38$^-$CD90$^+$CD93$^+$, and Lin$^-$CD34$^+$CD38$^-$CD90$^+$CD93$^-$ populations after thawing in SFM+5GF for 24hours. GEP levels were determined by Fluidigm array analysis. Relative gene expression levels were determined by delta delta Ct method using an average of four housekeeping genes as reference and the average CD34$^+$ value as the calibrator for fold change. Heat maps were produced by using heatmap.2 in R/Bioconductor.

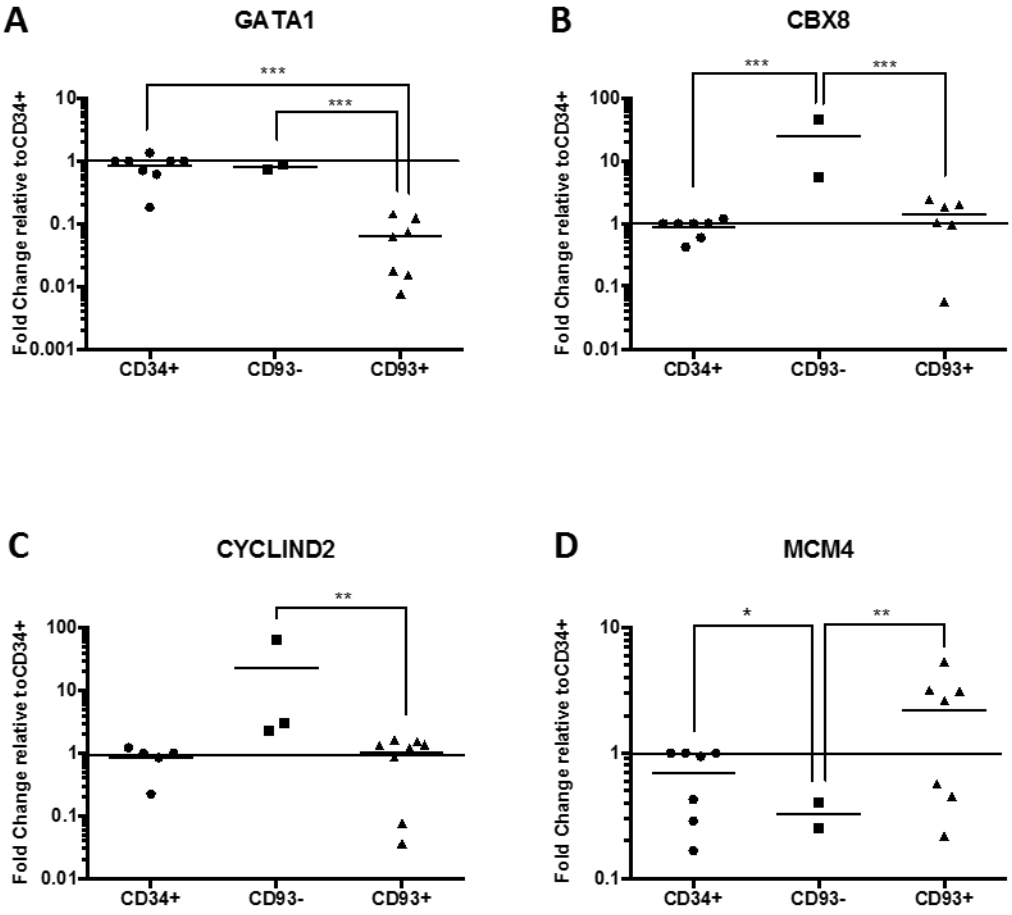

Figure 6-16 Gene expression of Lin-CD93- suggests lineage restriction

Gene expression was determined from CD34+ selected CP CML samples (n=3), Lin-CD34+CD38-CD90+CD93+ and Lin-CD34+CD38-CD90+CD93- CP-CML samples. Gene expression levels were determined by Fluidigm array analysis using the delta delta Ct method with an average of four housekeeping genes as reference. Fold change is relative to CD34+. The $Lin^{-}CD34^{+}CD38^{-}CD90^{+}CD93^{-}$ population was associated with decreased expression of genes involved in lineage restriction. Included in these were *GATA1* (p=0.0007), and *CBX8* (p=0.0002). Furthermore, there was an overexpression in the cell cycle gene, *CYCLIND2*, and lower expression of *MCM4*, suggesting that these cells have a more active cell cycle. P values were determined by an unpaired t-test (*, p<0.05; **, p<0.01; ***, p<0.001)

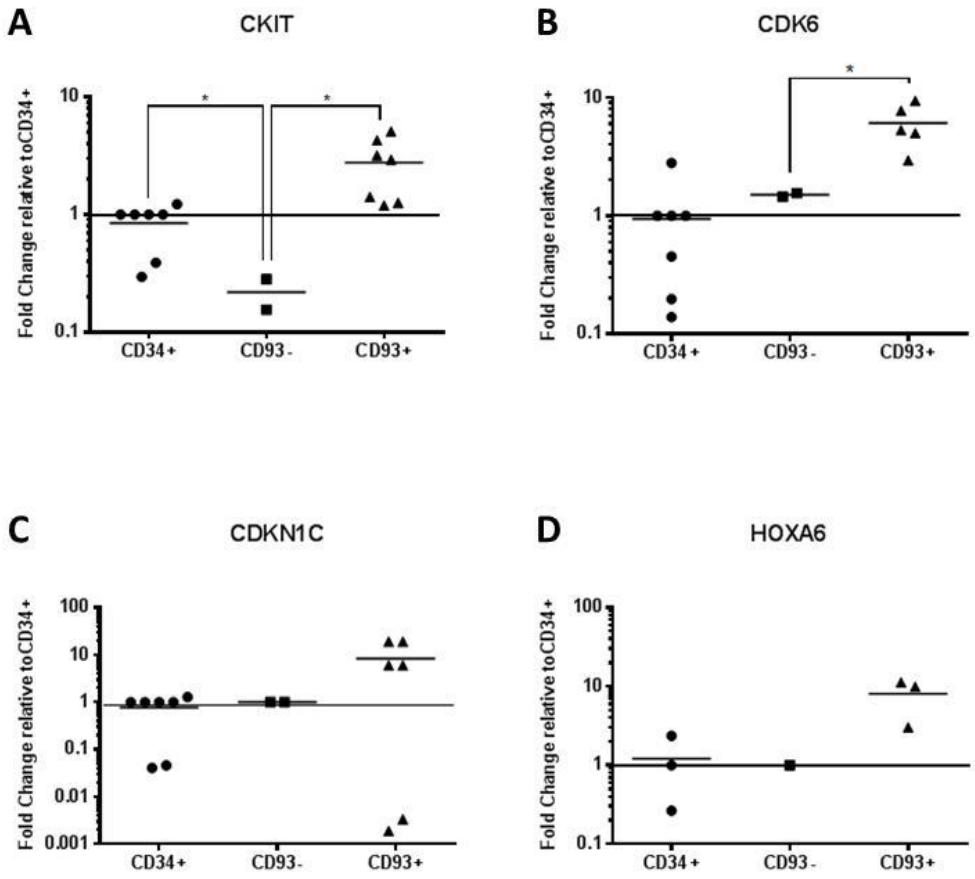

Figure 6 - 17 Gene expression of Lin-CD93+ confers a stem cell signature

Gene expression was determined from CD34+ selected CP CML samples (n=3), Lin-CD34+CD38-CD90+CD93+ and Lin-CD34+CD38-CD90+CD93- CP-CML samples. Gene expression levels were determined by Fluidigm array analysis using the delta delta Ct method with an average of four housekeeping genes as reference. Fold change is relative to CD34+. The $lin^{-}CD34^{+}CD38^{-}CD90^{+}CD93^{+}$ population displayed a less lineage-restricted profile with increased expression of *CDK6* (p=0.05), *HOXA6* (ns), *CDKN1C* (ns) and *CKIT* (p=0.0014), compared to the $Lin^{-}CD34^{+}CD38^{-}CD90^{+}CD93^{-}$ population. P values were determined by an unpaired t-test (*, p<0.05; **, p<0.01; ***, p<0.001).

Advances in single cell analysis have allowed for a more complete investigation of the cellular heterogeneity that may exist within populations and enables a more detailed examination of the homogeneity or heterogeneity of a population than was previously possible. Cells were isolated using fluorescence-activated cell sorting. We then performed targeted expression profiling of 90 genes in 150 single human $lin^-CD34^+CD38^-CD90^+CD93^-$ and $lin^-CD34^+CD38^-CD90^+CD93^+$ cells isolated using Fluidigm C1 technology. Single cells were pooled into each population across 3 individual CP-CML samples. Data was analysed using R/Bioconductor. As only 2 housekeeping genes were consistent across all Fluidigm chips within the single cell experiments, namely *B2M* and *UBE2D2*, these were used to determine ΔΔ Ct levels. False discovery rate was determined at a significance level of 0.05 and all single cell analyses were adjusted for this.

The frequency of expression (i.e. the number of cells with expression for the gene above five events per population per chip) for each gene was first determined. Of the genes eligible for analysis, 20 genes had a higher frequency within the $CD93^+$-selected population, and 53 genes had a higher frequency within the $CD93^-$-selected single cell population (figure 6-18).

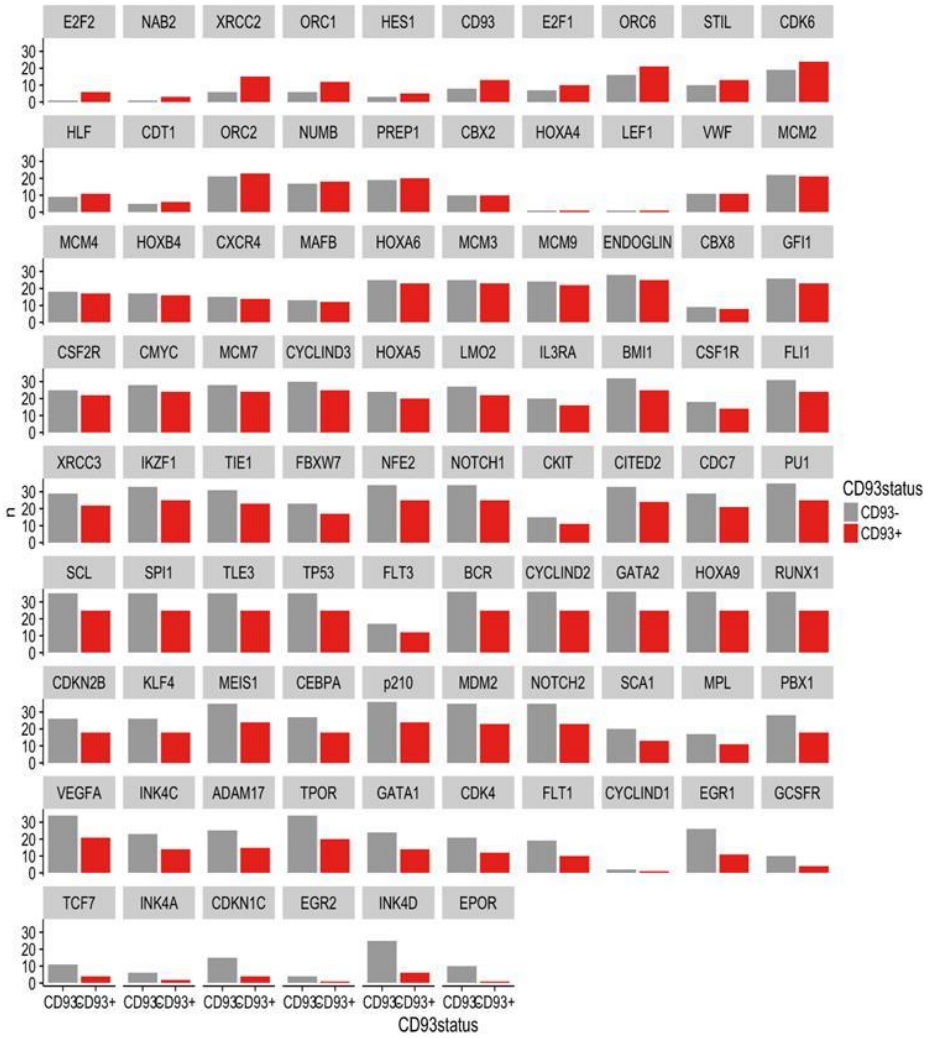

Figure 6 - 18 Frequency of gene expression identifies gene differences between CD93$^+$ and CD93$^-$ single CML cells

Cells were isolated using FACS. Targeted expression profiling of 90 genes in 150 single human lin$^-$CD34$^+$CD38$^-$CD90$^+$CD93$^-$ and lin$^-$CD34$^+$CD38$^-$CD90$^+$CD93$^+$ cells isolated using Fluidigm C1 technology. Single cells were pooled into each population across 3 individual CP-AML samples. Data was analysed using R/Bioconductor. False discovery rate of 0.05 was used within the analysis. Of the genes eligible for analysis, 20 genes had a higher frequency within the CD93$^+$-selected population, and 53 genes had a higher frequency within the CD93$^-$-selected single cell population. An unpaired student's t-test was used to determine significance (*, p<0.05; **, p<0.01; ***, p<0.001).

Gene expression analysis was performed by the ΔΔCt method using *B2M* and *UBE2D2* as a normalisation control. Hierarchical clustering was performed using R/Bioconductor. For the purpose of clustering, only genes that were expressed in all three samples were included in analysis. Hierarchical gene clustering could not clearly discriminate between CD93$^+$ and CD93$^-$ populations at a single cell level, and therefore highlighted the heterogeneity seen within a single cell analysis (figure 6-19). However, on analysis of correlation using Spearman's coefficient between the single cells versus bulk for each individual gene, there was correlation identified, with R^2=0.65 and 0.56 for CD93$^+$ and CD93$^-$, respectively, against bulk samples (figure 6-20). This suggests

that any statistically significant gene changes are true for the selected populations, and not secondary to technical variation between experimental design.

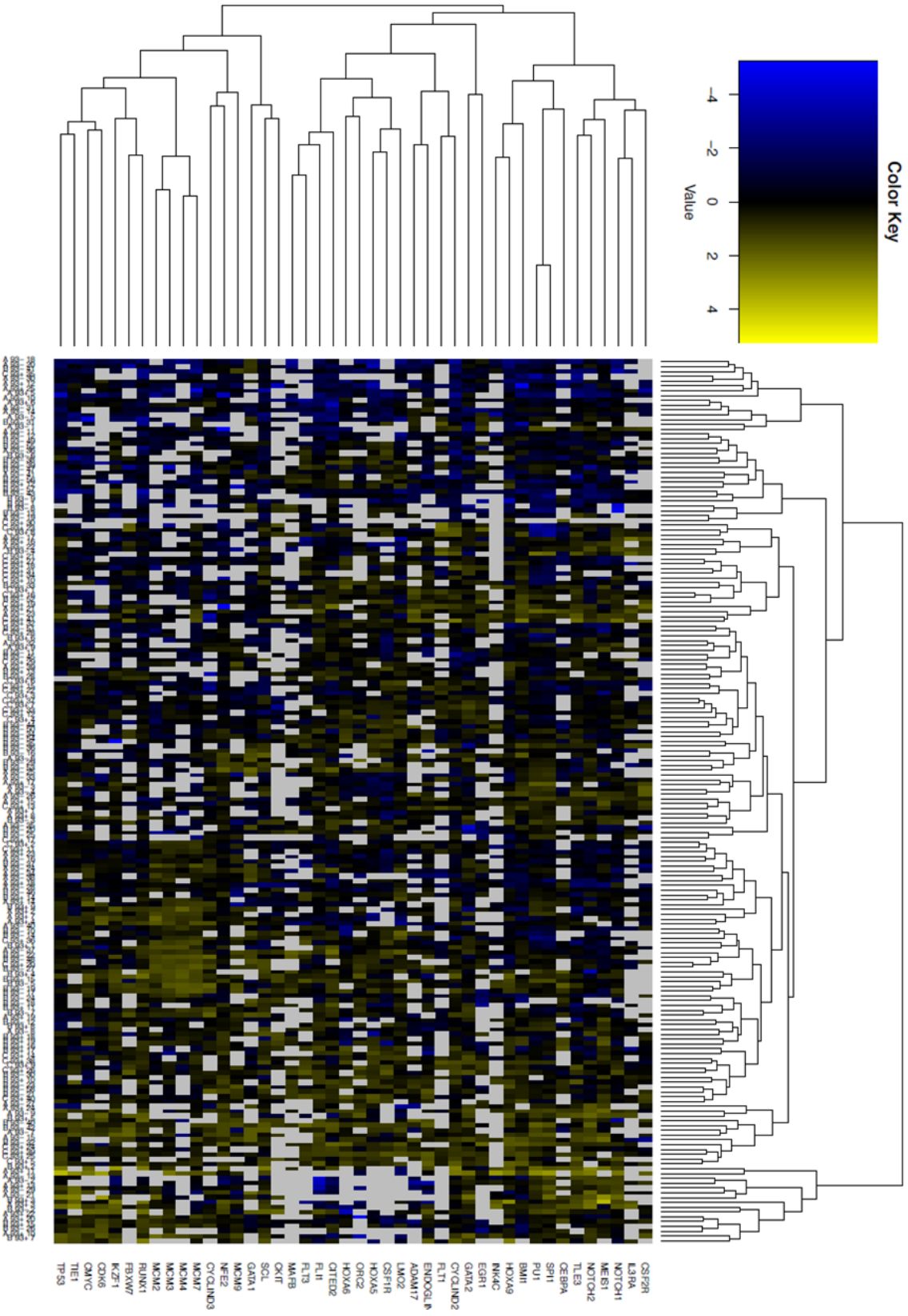

Figure 6 - 19 Gene clustering cannot clearly discriminate between CD93$^+$ and CD93$^-$ populations

Gene expression profiles were determined from CD34$^+$, Lin$^-$CD34$^+$CD38$^-$CD90$^+$CD93$^+$, and Lin$^-$CD34$^+$CD38$^-$CD90$^+$CD93$^-$ populations after thawing in SFM+5GF for 24 hours. GEPs were determined by Fluidigm array analysis. Relative gene expression levels were determined by ΔΔCt method using an average of two housekeeping genes as reference and the average CD34$^+$ value as the calibrator for fold change. Heat maps were produced by using heatmap.2 in R/Bioconductor.

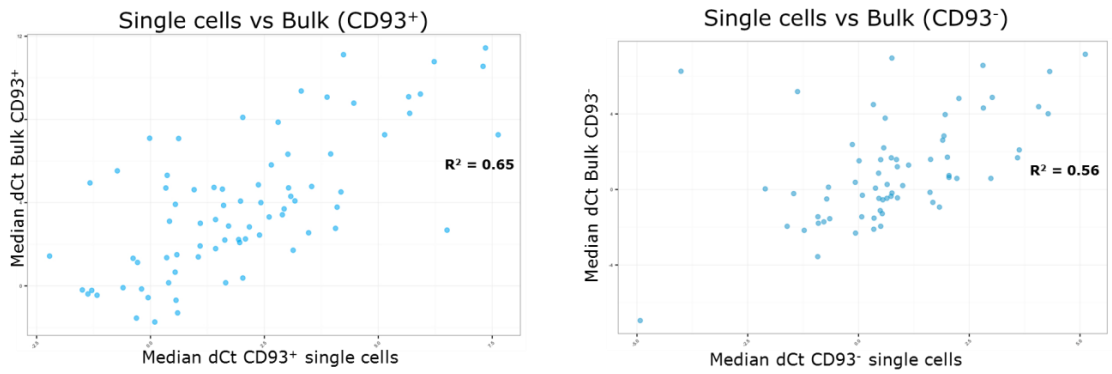

Figure 6 – 20 Correlation is identified between CD93$^+$ and CD93$^-$ samples vs bulk using Spearman's Coefficient

Cells were isolated using FACS. Targeted expression profiling of 90 genes in 150 single human lin$^-$CD34$^+$CD38$^-$CD90$^+$CD93$^-$ and lin$^-$CD34$^+$CD38$^-$CD90$^+$CD93$^+$ cells isolated using Fluidigm C1 technology. Single cells were pooled into each population across 3 individual CP-CML samples. Data was analysed using R/Bioconductor. False discovery rate of 0.05 was used within the analysis. Of the genes eligible for analysis, a Spearman's Correlation Coefficient was identified. R^2 was 0.65 and 0.56 for CD93$^+$ and CD93$^-$ single cells, respectively.

Next, analysis of individual genes between pooled CD93$^+$ and CD93$^-$-selected single cell populations' were conducted. Using a limma modified t-test and correcting for false discovery rate with 0.05, 16 genes were noted to demonstrate statistically significant changes in expression between CD93$^+$ and CD93$^-$-selected populations. Of note, CD93$^+$ genes had lower expression of genes involved in differentiation, namely *SPI1* and *GATA1*, and higher expression of self-renewal genes, *SCA1*, *MAFB*, *LMO2*, *HOXA5*, *SPI1*, *FLT3*, *RUNX1*, *CSF1R*, *MCM7*, *HOXA6*, and *BMI1* (table 6-2). Multiplex PCR was used to determine *BCR*-ABL expression in single cells following pre-amplification. There was no statistical significant change in *BCR*-ABL expression between the CD93$^+$ and CD93$^-$-selected populations, but a trend towards higher *BCR-ABL* expression in the CD93+ population (p=0.13) (figure 6-21).

	logFC	P.Value	adj.P.Val
SCA1	-2.09578	2.27E-07	9.75E-06
MAFB	-1.54523	2.18E-05	0.000313
LMO2	-1.19493	1.89E-05	0.000313
SPI1	0.802386	3.05E-05	0.000328
ORC2	-1.00764	4.74E-05	0.000407
HOXA5	-1.27036	7.31E-05	0.000449
CITED2	-0.978	7.28E-05	0.000449
FLT3	-0.94912	0.000349	0.001876
GATA1	1.914533	0.000529	0.002529
RUNX1	-0.62017	0.000767	0.003298
CSF1R	-1.1231	0.005552	0.019894
FLT1	-1.25481	0.007225	0.020712
MCM7	-0.72342	0.006025	0.019927
HOXA6	-0.78185	0.006518	0.020019
BMI1	-0.52627	0.012059	0.032407

Table 6 - 2 Single cell GEP identifies that CD93$^+$-selected single cells have a stem cell signature

Gene expression profiles were determined from CD34$^+$, Lin$^-$CD34$^+$CD38$^-$CD90$^+$CD93$^+$, and Lin$^-$CD34$^+$CD38$^-$CD90$^+$CD93$^-$ populations after thawing in SFM+5GF for 24 hours. GEP levels were determined by Fluidigm array analysis. Relative gene expression levels were determined by ΔΔCt method using an average of two housekeeping genes as reference. Analysis of individual genes between pooled CD93$^+$ and CD93$^-$ single cell populations' were analysed. Using a limma modified t-test and correcting for false discovery rate with 0.05, 16 genes were noted to demonstrate statistically significant changes in expression between CD93$^-$ and $^+$ populations.

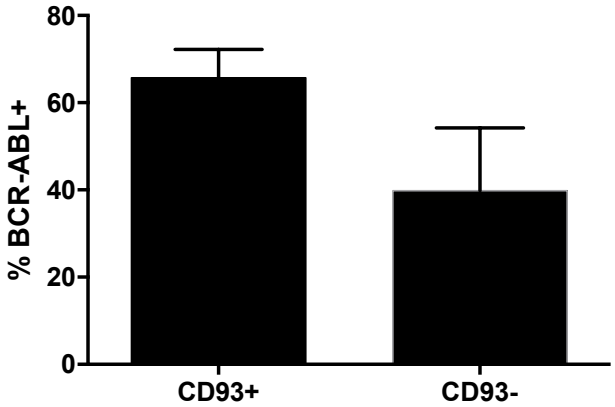

Figure 6 – 21 No significant change of *BCR-ABL* expression was identified between CD93$^+$ and CD93$^-$-selected single cells as determined by multiplex PCR

Following single cell harvest with the Fluidigm C1 autoprep system, 1ul of the preamplified sample was used within a multiplex PCR. Single cell data was pooled across 3 CP-CML samples. Positive expression of *BCR-ABL* as determined through gel electrophoresis allowed identification of *BCR-ABL* expression for each single cell analysed. There was no statistically significant change in expression, as determined by an unpaired student's t-test (p=0.13).

Single cell gene expression demonstrates that, even at a single cell level, there is evidence that $CD93^+$ selection confers cell immaturity and self-renewal capability, although overall gene expression profiling cannot distinguish amongst the populations. In future experiments, it would be prudent to isolate the gene expression for *BCR-ABL+* and *BCR-ABL* negativie cells within the $CD93^+$- and $CD93^-$-selected populations.

6.4. Discussion

Within this chapter, we have presented both functional and gene expression data to support our groups preliminary data that the glycoprotein, CD93, may represent a biomarker for the CML LSC. This was supported using both $Lin^-CD34^+CD38^-CD90^+$ and Lin^-CD34^+ populations. Initial *in vitro* analysis of clonal progenitor assays demonstrated no change in colony forming capacity between $Lin^-CD34^+CD38^-CD90^+CD93^+$ and $Lin^-CD34^+CD38^-CD90^+CD93^-$ populations. This perhaps is not surprising since the ability to form a multi-lineage colony focuses on the populations' ability to differentiate, with only limited involvement from properties of self-renewal. Colony re-plating represents a self-renewal model with re-plating capacity greater in primitive multi-lineage or mixed colonies. This capacity has been shown to decline with cell maturity. Within our model, there was an increased trend towards re-plating efficiency from CFC assays, but this was not statistically significant. This may be, in part, due to inter-patient variability, with previous evidence suggesting that re-plating within CML is variable between different patients and can relate to patient characteristics, such as prognostic index (Gordon et al, 2003). To address this, LTC-IC were utilised to quantitatively assess HSC function. The LTC-IC assay represents the most stringent *in vitro* surrogate measure of the functional activity of HSCs, and relies on more extensive self-renewal capacity that the shorter-duration CFC assay with replates. Our results demonstrated a statistically significant increase in colonies within the $Lin^-CD34^+CD93^+$ arm of the experiment ($p=0.0001$). These results suggest that $CD93^+$-selected cells have increased *in vitro* self-renewal capacity.

Because the *in vitro* measurements of self-renewal do not reflect the complex multi-directional interactions seen within the HSC niche, we utilised an *in vivo* NSG engraftment model to determine if the $CD93^+$-selected population could be truly representative of an increased self-renewal and leukaemia-initiating population. The experiments performed demonstrated that engraftment could only really be evaluated if the BCR-ABL status was known for each population. Furthermore, engraftment data could only be generated at 16 weeks through analysis of BM cells, with no PB engraftment evident at 8 weeks, or 16 weeks. Within four independent CP-CML samples, there was a statistically significant increase in engraftment in the $CD93^+$ compared to the $CD93^-$-selected population. This verified our previous findings that the $CD93^+$-selected population has functional properties of LSCs, with evidence of increased self-renewal and engraftment potential. Our xenograft model allowed for

analysis of the capability of the transplanted cells to initiate CML disease in recipient mice. However, it does not evaluate the long-term potential of the engraftment to lead to a myeloproliferative neoplasm. To determine this serial transplantation experiments' would be needed. However, within the CML xenograft murine model lies an inherent problem in that there is generally low engraftment as demonstrated within our model and others (Eisterer et al, 2005; Lewis et al, 1998).

To support our previous findings, we next sought to characterise the differences in the gene expression profiles between $CD93^+$ and $CD93^-$-selected CML populations and determine heterogeneity of each population at bulk and single cell level. To interrogate this, we initially identified the CP-CML LSC population as having the greatest functional capability compared to normal, and all gene expression experiments were subsequently confined to this population.

We hypothesised that $lin^-CD34^+CD38^-CD90^+CD93^-$ CML cells would have a more mature GEP compared to $lin^-CD34^+CD38^-CD90^+CD93^+$ cells. CP-CML cells were sorted into (1) lin^-CD34^+, (2) $lin^-CD34^+CD38^-CD90^+CD93^-$ and (3) $lin^-CD34^+CD38^-CD90^+CD93^+$ populations. RNA was harvested at baseline from bulk populations (1) to (3) and cDNA was generated from single cells using the Fluidigm C1 autoprep system. Using Fluidigm technology, quantitative PCR of 90 lineage-specific and cell survival genes was performed within all populations of cells (1) to (3) in 'bulk' samples (n=3), and at single cell level (n=123 $CD93^+$, n=120 $CD93^-$single cells; n=3 samples in total).

Bulk sample analysis demonstrated a significant increase in expression of lineage commitment genes within the $lin^-CD34^+CD38^-CD90^+CD93^-$ population, as shown by increased expression of *GATA1* (p=0.0007), and *CBX8* (p=0.0002). The $lin^-CD34^+CD38^-CD90^+CD93^+$ population displayed a less lineage-restricted profile with increased expression of *CDK6* (p=0.05), *HOXA6* (ns), *CDKN1C* (ns) and *CKIT* (p=0.0014), compared to the $lin^-CD34^+CD38^-CD90^+CD93^-$ population. Furthermore, the two populations could be segregated by differential gene expression through gene clustering.

At a single cell level, differences were noted in the frequency of expression between $lin^-CD34^+CD38^-CD90^+CD93^-$ and $lin^-CD34^+CD38^-CD90^+CD93^+$ populations, particularly in *GATA1*, *TPOR*, and *VWF*. Although a statistically significant change was

demonstrated in gene expression between the lin$^-$CD34$^+$CD38$^-$CD90$^+$CD93$^-$ and lin$^-$CD34$^+$CD38$^-$CD90$^+$CD93$^+$ populations in a number of genes, we were not able to segregate the populations by differential expression using gene clustering. This highlights the heterogeneous nature of the cell populations and the inability to distinctly characterise between the two populations at a single cell level by GEP. However, there was positive correlation noted between the bulk and single cell data, suggesting that the gene expression changes determined between CD93$^+$ and CD93$^-$-selected populations are not purely confounding variation caused by patient heterogeneity, or technical variation between bulk and single cell experimental design, but are inherent to the CD93-selectivity.

This heightens the argument that CD93$^+$-selectivity represents an immature LSC phenotype at both gene and functional level.

There is no previous data to suggest that CD93 is a potential marker of a LSC within CML. Although, our group is the first to report a functional role for CD93 within CP-CML, previous reports have demonstrated it to be upregulated within human LSCs in AML (Iwasaki et al, 2015b; Saito et al, 2010). Most recently (Iwasaki et al, 2015b), within AMLs with genomic rearrangements of the MLL gene, it was demonstrated that LSC expression of CD93 is essential for MLL-mediated leukaemogenesis, but, in contrast to our findings, the CD93$^+$ LSCs were cycling, non-quiescent leukaemia-initiating cells, whereby CD93-regulated self-renewal was secondary to silencing of *CDKN2B*, a major tumour suppressor in AML. Within the primary CP-CML samples analysed, *CDKN2B* was upregulated compared to CD34$^+$ bulk within the CD93$^+$ population. These differences may be purely an inherent feature within the disease process.

Based on the above, our results validate CD93 as a potential functional marker of the primitive CP-CML LSC population and highlight key lineage and cell survival pathways that are altered in CML LSC. The results demonstrate the heterogeneity seen within gene expression at the single cell level, which may allow for further insight into the CML LSC compartment with further analyses. An inherent flaw within our data is that both BCR-ABL+ and BCR-ABL- samples are present within the CD93$^+$- and CD93$^-$- selected populations. Recently, (Giustacchini et al, 2017) described a novel technique that combines *BCR-ABL* detection with whole-transcriptome analysis of the same single cell. They demonstrated that significantly higher number of genes were

detected within the BCR-ABL+ stem cells, which correlated with increased proliferation gene expression and reduced quiescence-associated gene expression, compared to normal HSCs and BCR-ABL negative stem cells. This correlates with the activation of BCR-ABL-driven proliferation. This important work has allowed for analysis of samples from patients established already on TKI. Within these samples, a distinct subpopulation of highly quiescent *BCR-ABL+* stem cells were identified, which demonstrated deregulation of specific pathways, including TGF-β, NFKβ, TNF-α, JAK-STAT, and Wnt/β-catenin. Cell cycle quiescence and a capacity for self-renewal are key features that underlie leukaemic initiation, progression, and relapse within CML. Identification, and subsequent, targeting this subset of cells is necessary for complete eradication of the disease.

Recent evidence has suggested that CD26 may represent an interesting target for the CML-LSC; indeed single cell gene analysis confers this notion (Warfvinge et al, 2017). Although, CD93 was analysed within (Warfvinge et al, 2017), analysis of its expression was within an MNC population. Our data similarly demonstrated that within an MNC population there is limited expression of CD93. Our experimental model utilised a more primitive population to include $CD34^{+}CD38^{-}CD90^{+}$ cells. Further work is necessary to establish if there is co-expression between CD93 and CD26 population and if this alters the functionality of the cells. Furthermore, further work is necessary to establish if, as well as identifying the LSC population, CD93 can be targeted to eradicate it.

7. Thesis summary and future directions

Within this thesis, we have presented data for the identification of the cell surface marker, CD93, as a potential marker for the CP-CML LSC. Further to this, we present data for the role of the self-renewal pathway, Notch, in CP-CML LSC eradication. In view of the complexity of the Notch pathway within CP and myeloid BP, we characterised self-renewal pathway deregulation through transcriptional analysis of CML progression to myeloid and lymphoid BP, and offer a comparison between lymphoid BP and Ph+ ALL.

The identification and eradication of LSCs within CML remains an important area clinically. This has been highlighted in recent trials exploring the discontinuation of TKIs in CP patients with sustained deep molecular remission (Mahon et al., 2010, Mahon et al., 2014, Mahon, 2015, Mahon et al., 2016, Rea et al., 2012, Etienne et al., 2017, Ross et al., 2010, Ross et al., 2013, Takahashi et al., 2012). These trials have demonstrated that discontinuation of therapy can be selectively achieved.

Although these results indicate the possibility for TKI discontinuation in a small subset of CML patients, they highlight an uncertainty surrounding the 'trigger' event(s) in molecular relapse, and question if sustained *BCR-ABL* expression, LSC persistence, microenvironmental factors or, indeed, multiple factors are contributing. A single copy of *Bcr-Abl* expressed from the endogenous BCR locus in a knock-in murine model is not sufficient to induce leukaemia (Foley et al., 2013). Therefore, although it is clear that a certain level of *BCR-ABL* needs to be expressed at the stem cell level to cause CML, it is unclear if further molecular changes or aberrant signalling is needed to drive molecular relapse and disease progression. Furthermore, it is unknown if *BCR-ABL* is the initiating insult, or if host factors, such as epigenetic and genetic changes influence disease outcome and precede the acquisition of *BCR-ABL*. Regardless, it is apparent, that further insight into why LSCs survive TKIs is vital in the quest for cure. Furthermore, understanding of the LSC within CML, may offer insight in other CSC driven diseases. This is in view of the fact that CML is an extrememly well understood disease, with numerous well validated experimental *in vitro* and *in vivo* models that can be manipulated , when compared to the heterogeneity seen within AML, for example.

As has been extensively described in previous chapters, identification of the CML LSC population in a clinical setting would enable therapeutic decisions in identifying those

at risk of molecular relapse, and those where TKIs can be stopped. Additionally, it would aid further evaluation of the LSC population at a biological level, that would, in turn, allow for a greater understanding in potential therapeutic targets to help in their eradication. Although many labs have performed extensive analysis to identify markers of a primitive cell population in the preclinical setting, including CD26 (Herrmann et al., 2015, Culen et al., 2016, Warfvinge et al., 2017) and IL1-RAP (Ågerstam et al., 2016, Landberg et al., 2016, Warfvinge et al., 2017, Järås et al., 2010), none have been shown, as yet, to be robust enough at clinical translation. CD26, however, is showing increasing promise in this area with recent data suggesting a correlation between CD26 expression and treatment response, as well as a potential therapeutic target at a single cell level (Warfvinge et al., 2017, Culen et al., 2016).

To determine further markers to identify the CP-CML LSC population, we utilised data from a microarray study where $Lin^-CD34^+CD38^-CD45RA^-CD90^+$ normal HSC (n=3) and CP-CML LSC (n=6 patients at diagnosis) populations were isolated using a FACSAria and applied to Affymetrix HuGene 1.0ST arrays. The raw data (.CEL files) was imported into Partek Genomics Suite and Ingenuity Pathway Analysis software and PCA and gene ontology ANOVA performed. A total of 1217 genes were significantly deregulated between normal HSC and CP-CML LSCs. The most significantly deregulated genes and pathways were involved with the molecular and cellular functions of cell cycle, cell assembly and organisation, cellular movement, cell death and DNA replication, recombination and repair. These results suggested that CML LSCs were less quiescent than normal HSCs. Within this dataset, we further sought to assess if there were differences in expression of cell surface molecules that may be amenable to therapeutic manipulation. Of particular interest, our microarray studies demonstrated that *CD93* was highly upregulated in CP-CML LSCs (6 fold, $p=2.5x10^{-6}$). Increased *CD93* expression was validated by Fluidigm digital PCR (6 fold increase, p=0.02; n=6). Furthermore, using flow cytometry, we demonstrated significant upregulation of CD93 protein expression on $lin^-CD34^+CD38^-CD45RA^-CD90^+$ CML LSCs from PB and BM of CP-CML patients (n= 17; mean = 63.8% CD93+) compared to normal HSC from healthy PB stem cell donors (n=7; mean = 0.8% CD93+) and BM donors (n=4; mean = 0.2% CD93+; $p < 0.0001$). FISH confirmed that 100% of $lin^-CD34^+CD38^-CD90^+CD93^+$ CML cells were *BCR-ABL* positive in all samples assessed. CD93 (also known as C1qRp) is a C-type lectin-like domain (CTLD)-containing glycoprotein which regulates phagocytosis, with roles in cell adhesion and leukocyte

migration. It is normally expressed on endothelial cells, haemopoietic precursors and mature cells including neutrophils, monocytes and platelets.

Within this thesis, we sought to assess the functional capability of the CD93-selected population and ascertain if these cells had 'true' stem cell capability. LTC-IC assays were utilised to quantitatively assess stem cell function. The LTC-IC assay represents the most stringent *in vitro* surrogate measure of the functional activity of HSCs, and relies on more extensive self-renewal capacity than the shorter-duration CFC assay with replates. Our results demonstrated a statistically significant increase in colonies within the $Lin^-CD34^+CD93^+$ arm of the experiment ($p=0.0001$). These results suggest that $CD93^+$-selected cells have increased *in vitro* self-renewal capacity. Furthermore, in xenograft transplantation experiments ($n = 5$), after 16 weeks, $CD34^+CD93^+$ CML LSC engrafted lethally irradiated NSG mice with BCR-ABL positive cells, whereas $CD34^+CD93^-$ cells from the same patient samples failed to engraft to significant levels (3.5-30-fold increase in engraftment with $CD34^+CD93^+$ cells; $p<0.03$). FISH confirmed that engrafted human cells were *BCR-ABL* positive.

We subsequently hypothesised that $CD93^+$-selected cells would represent a more immature functional phenotype compared to $CD93^-$-selected cells. The aim of this aspect of this thesis was to characterise differences in the gene expression profiles between $CD93^+$ and $CD93^-$ CML LSC populations and determine heterogeneity of each population at a single cell level.

To interrogate this, we initially identified CP-CML subpopulations with the greatest functional capability compared to normal from existing data within our lab. Normal and CP-CML samples were FACS-sorted into HSC/LSC, CMP, GMP, and MEP sub-populations. Results suggest a significant change in functional status between normal and CP-CML subpopulations within the HSC/LSC compartment ($lin^-CD34^+CD38^-CD45RA^-CD90^+$), where CML LSC demonstrated significantly increased proliferation (14 fold expansion; $P<0.001$) compared to normal HSC (no expansion) after 5 days *in vitro* culture in physiological growth factors. In addition, equivalent numbers of CML LSC produce ~4-fold more colonies in CFC assays than normal HSC (329±56 versus 86±17 per 2,000 cells, respectively ($p<0.05$)). Furthermore, FISH demonstrated that >90% of $lin^-CD34^+CD38^-CD45RA^-CD90^+$ CML LSC from all patient samples were *BCR-ABL* positive. Subsequent experiments were confined to the LSC population.

We hypothesised that lin$^-$CD34$^+$CD38$^-$CD45RA$^-$CD90$^+$CD93$^-$ CML cells would have a more mature gene expression profile compared to lin$^-$CD34$^+$CD38$^-$CD45RA$^-$ CD90$^+$CD93$^+$ cells. CP-CML cells were sorted into (1) lin$^-$CD34$^+$, (2) lin$^-$CD34$^+$CD38$^-$ CD90$^+$CD93$^-$ and (3) lin$^-$CD34$^+$CD38$^-$CD90$^+$CD93$^+$ populations. Using Fluidigm technology, quantitative PCR of 90 lineage-specific and cell survival genes was performed within all populations of cells (1) to (3) in 'bulk' samples (n=3), and at single cell level (n=123 CD93$^+$, n=120 CD93$^-$ single cells; n=3 samples in total).

Bulk sample analysis demonstrated a significant increase in expression of lineage commitment genes within the lin$^-$CD34$^+$CD38$^-$CD90$^+$CD93$^-$ population, as shown by increased expression of *GATA1* (p=0.0007), and *CBX8* (p=0.0002). The lin$^-$ CD34$^+$CD38$^-$CD90$^+$CD93$^+$ population displayed a less lineage-restricted profile with increased expression of *CDK6* (p=0.05), *HOXA6* (ns), *CDKN1C* (ns) and *C-KIT* (p=0.0014), compared to the lin$^-$CD34$^+$CD38$^-$CD90$^+$CD93$^-$ population. Furthermore, the two populations could be segregated by differential gene expression through gene clustering. At a single cell level, differences were noted in the frequency of expression between lin$^-$CD34$^+$CD38$^-$CD90$^+$CD93$^-$ and lin$^-$CD34$^+$CD38$^-$CD90$^+$CD93$^+$ populations, particularly in *GATA1*. Although a statistically significant change was demonstrated in gene expression between the lin$^-$CD34$^+$CD38$^-$CD90$^+$CD93$^-$ and lin$^-$CD34$^+$CD38$^-$ CD90$^+$CD93$^+$ populations in a number of genes, we were not able to segregate the populations by differential expression using gene clustering. This highlights the heterogeneous nature of the cell populations and the inability to distinctly characterise between the two populations at a single cell level. However, on analysis of correlation using Spearman's coefficient between the single cells versus bulk for each individual gene, there was correlation identified, with R2=0.65 and 0.56 for CD93$^+$ and CD93$^-$, respectively, against bulk samples. This suggested that any statistically significant gene changes are true for the selected populations, and not secondary to technical variation between experimental design. Our data on CD93 heightens the argument of the use of CD93 in the isolation and identification of the CML LSC. Further work needs to ascertain if, as well as its identification, CD93 can be utilised within CML LSCs eradication. This work is currently ongoing, where we have utilised a lentiviral approach to knock-down CD93 within primary CP-CML samples. This will need to be extended to a normal HSC population to ensure no detrimental effect, prior to discussions regarding *in vivo* translation into patients.

Further to the identification of CD93 as a marker for a primitive cell population within CP-CML, we explored the role self-renewal signalling within CML maintenance and progression. In particular, the role of the Notch pathway was evaluated extensively. Firstly, we identified, at gene and protein level, the expression of Notch pathway components within CP-CML primary samples. This identified variable expression between samples, but that the Notch pathway was deemed inactive through utilisation of the gamma secretase inhibitor, DAPT, which upon culture with primary samples, led to no change in cellular functions of proliferation or apoptosis. As $CD34^+$ CP-CML cells abundantly express the Notch receptor, NOTCH2, we investigated whether the pathway could be reactivated through exogenous stimulation upon ligand binding. An OP9 co-culture system was utilised to allow for overexpression of Notch ligands, DLL1 or JAG1, using OP9GFP as control stroma. Compared to non-stromal conditions, culturing over 7 days on OP9GFP led to a significant increase in growth ($p=0.02$, $n=5$). The overexpression of JAG1 led to a further increase compared to OP9GFP ($p=0.002$). We confirmed that activation of the pathway was through JAG1, and not DLL1, by utilising DAPT, where we observed a significant decrease in live cell counts within the OP9GFP ($p=0.01$) and OP9JAG1 ($p=0.018$) experimental arms. Upregulation of the pathway was confirmed with increased expression of *HES1* at the gene level ($n=4$, $p=0.001$), and val1744 protein by IF ($n=5$). CP-CML samples ($n=3$) were FACS-sorted into $Lin^-CD34^+38^+$ and $Lin^-CD34^+38^-$ populations to assess for functional variation in stem and progenitor populations. Following 7 days in culture, live cell counts showed a significant increase in $Lin^-CD34^+38^+$ cells on OP9JAG1 co-culture ($p=0.04$). There was a decrease in cell growth of $Lin^-CD34^+38^-$ cells in the same experimental conditions ($p=0.02$), with an associated increased trend in late apoptotic cells (ns). We hypothesised that Notch activation would have a toxic influence on an immature CML LSC population. LTC-IC assays showed a significant decrease in colonies for $Lin^-CD34^+38^-$ cells co-cultured with OP9JAG1 for 7 days ($p<0.05$). Futher to this, CFSE assays demonstrated an increased trend towards percentage of viable cells in later division on stromal co-culture compared to non-stromal conditions, suggesting that in stromal conditions, cells are protected somewhat to enable increased divisions. This was again confirmed within MSC experiments where co-culture on MSC led to protection of $CD34^+$ against TKI-induced apoptosis. Within our experiments, this was not clearly dependent on activation of Notch through JAG1 expression. This suggested that Notch activation is not solely responsible for protection of LSC within disease states. This data led us to establish that upon JAG1 activation, cells undergo a degree of apoptosis, but more significantly, it causes a push towards early erythroid

differentiation that is blocked in an immature state (i.e. proerythroblast phase). This was determined through cell surface identification of erythroid markers. There was an increase in expression of both CD71 and GlyA with the addition of stromal co-culture. This was only statistically significant with CD71 surface expression. As CD33 expression was maintained, it suggested that although the samples had initiated differentiation, they could not progress beyond an immature phenotype. To corroborate the possible involvement of Notch activation through JAG1 interaction in early differentiation, gene expression was investigated in primary $CD34^+$ CP-CML patient samples. There was a statistically significant increase in overexpression of key genes involved in early erythroid differentiation, namely, *p38* ($p<0.05$) and *PU.1* ($p<0.05$), which have notable involvement in development of (pro)erythroblasts. Furthermore, there was little change in gene expression in regulators of the stem cell phenotype, namely *GATA2* and *NFKB1*. This is the first time this has been proposed within a CML phenotype. This data together allows us to propose that activation of the Notch pathway through JAG1 protein leads to increased differentiation and apoptosis in CP-CML cells, that ultimately leads to LSC exhaustion and a decrease in colony formation.

In order to evaluate the function of Notch activation as a therapeutic modality, we have embarked on translating the *in vitro* findings to an *in vivo* setting. This will allow for evaluation within a BM microenvironment. With thanks to the Aifantis laboratory (NYU), we are in the process of utilising the ROSA26-ICN2 murine model, which was generated by insertion of a loxP flanked splice acceptor NEO-ATG cassette with two polyA sites followed by ICN2 into the ROSA26 locus, allowing the ROSA26 promoter to drive expression of the NEO-ATG cassette. Cre-recombinase–mediated excision of NEO-ATG results in use of the splice acceptor in the ICN2 cassette and irreversible expression of the transgene (Lobry et al. 2013; Klinakis et al. 2011). Following confirmed activation of Notch, animals will be sacrificed and BM cells retrovirally transduced with *BCR-ABL* as described (Mizuno et al. 2008; Li et al. 1999), and monitored for leukaemic development.

In myeloid BP (n=4), in similar experiments, sorted $Lin^-CD34^+CD38^+$ and $Lin^-CD34^+38^-$ populations did not demonstrate this functional profile of Notch activation, despite an overexpression in the *NOTCH2* receptor compared to normal ($p=0.0035$). To investigate this further, we sought to investigate the changes in gene expression of 90 self-renewal and cell survival components in all stages of CML, including CP (n=13), myeloid BP (n=12), and lymphoid BP (n=4). Samples were sorted in stem and

progenitor populations. The self-renewal pathway components were highly deregulated between CP and myeloid BP disease. Of interest, there was a statistically significant upregulation in Wnt components in myeloid BP compared to CP, particularly *TCF7* (p=0.0011). We hypothesise that Wnt upregulation is preventing Notch activation in myeloid BP-CML. Furthermore, there was a statistically significant increase in the DNA replication genes, *MCM7* and *MCM9*, between CP and myeloid BP. The transition of CML from CP to BP is characterised by the accumulation of molecular and chromosomal abnormalities, although the molecular mechanisms are poorly understood. There is accumulating evidence that suggests that BCR-ABL causes this directly through induction of ROS, inducing DNA breaks requiring repair and by interacting directly with the repair machinery to inhibit performance (Skorski, 2008). It has also been shown that BCR-ABL directly drives expression of certain members of the DNA repair pathways resulting in increased DNA instability (Skorski, 2008). The uncontrolled activity of *MCM7* and *MCM9* may represent an interesting therapeutic target in myeloid BP disease in the control of genomic instability and remains an interesting area of future work.

Further to this, we explored the transcriptional changes within the Ph+ acute leukaemias. This led to some interesting observations. Firstly, the differential gene expression of self-renewal and cell survival pathways was comparable between lymphoid BP and myeloid BP, with an inability to segregate the samples by gene clustering. This is perhaps, unsurprising, in view that the disease phenotypes arise from the same cell origin, i.e. the *BCR-ABL* positive HSC. The Notch signalling pathway has a known role within lineage decision, particularly towards a lymphoid bias (Delaney et al., 2010, Ohishi et al., 2002, Ohishi et al., 2003, Jaleco et al., 2001). However, the main comonents of the pathway were not statistically changed between myeloid and lymphoid BP disease. The data of self-renewal gene expression, together, suggests that these pathways are not involved in the lineage decision in myeloid or lymphoid BP development.

Ph+ acute lymphoid-phenotype leukaemias encompass both lymphoid BP CML and Ph+ ALL. These two diseases are clinically distinct, but can often be mislabelled, as suggested within (Hovorkova et al, 2017). In view of this, we next sought to question if there was differing gene expression profiles of self-renewal and cell survival pathways within the Ph+ acute leukaemias'. This was in view of the known differences in cell of origin between them, with lymphoid BP representing a distinctly stem cell disease, and

Ph+ ALL a more differentiated phenotype. Indeed, on global gene expression of the 90 self-renewal and cell survival components, the two diseases could be segregated with gene clustering methods and confirmed that the diseases are distinct entities. Of particular interest, within our dataset, *HIF1A* was statistically significantly increased in Ph+ ALL compared to both lymphoid BP and normal PB. Although further investigation is required to ascertain its importance in Ph+ ALL, it seems an exciting area of development. It has been shown that within ALL, blockade of *HIF1A*-mediated signalling may play an important role in chemo-sensitisation of ALL cells under hypoxic conditions of the BM (Frolova et al., 2012). Furthermore, within childhood B-ALL, high expression of *HIF1A* is associated with a good prognosis (Silveira et al., 2014), as well as being required for active Wnt signalling in T-ALL (Giambra et al., 2015). Although our focussed gene analysis demonstrated no statistical change between lymphoid BP and Ph+ ALL within Wnt pathway components, there appeared to be an increased dependency on the Wnt pathway within Ph+ ALL, with a statistically significant increase in key Wnt components, namely *TCF4*, *TCF7*, and *LEF1*, compared to normal PB. Furthermore, *FBXW7*, a negative regulator of Notch, was statistically significantly increased in Ph+ ALL compared to normal. *FBXW7* is not unique to Notch signalling and has been shown *in vivo* to target many proto-oncogenes, growth promoters, and anti-apoptotic molecules. Furthermore, *FBXW7* has been shown to have an indispensable role in the maintenance of adult HSC quiescence (Matsuoka et al, 2008; Thompson et al, 2008). Deletions of Fbxw7 in HSCs and CML LSCs have been shown to lead to c-Myc accumulation, activation of the TP53 signalling pathway, aberrant cell cycle entry and eventual exhaustion (Reavie et al, 2013; Reavie, 2010). TP53 mutations can accompany disease progression in human CML and TP53 loss in some cases impedes the anti-leukaemic response to BCR-ABL inhibition (Kelman et al, 1989; Wendel et al, 2006), suggesting that loss of p53 in some tumours could constitute an adaptive response to the increase in the levels of c-Myc during CML progression. As there was no statistical change in *TP53* and *MYC*, this suggests that *FBXW7* is acting independently of these survival mechanisms, and may offer a therapeutic target within the disease.

This transciptional data provides some understanding of the differences in self-renewal and cell survival signalling pathway components that may offer interesting areas of future development. Furthermore, it may lead to further work in the identification of a gene expression signature that would allow for a greater diagnositc capability and, subsequently, improvement in patient care.

Overall the work presented in this thesis has furthered our understanding of the role of self-renewal within CML maintenance and progression, as well as further implicating the use of the cell surface marker, CD93, in the identification of the CML-LSC. This data will help guide novel therapeutic approaches towards the CML LSC in future experimental work, as well as guide further development in the transcriptional differences and potential targets in the Ph+ acute leukaemias.

8. Bibliography

Abraham, S. A., Hopcroft, L. E. M., Carrick, E., Drotar, M. E., Dunn, K., Williamson, A. J. K., Korfi, K., Baquero, P., Park, L. E., Scott, M. T., Pellicano, F., Pierce Andrew, Copland, M., Nourse, C., Grimmond, S. M., Vetrie, D., Whetton, A. D. & Holyoake, T. L. (2016) Dual targeting of p53 and c-MYC selectively eliminates leukaemic stem cells. *Nature*, 534(7607), 341-346.

Abrahamsson, A. E., Geron, I., Gotlib, J., Dao, K.-H. T., Barroga, C. F., Newton, I. G., Giles, F. J., Durocher, J., Creusot, R. S., Karimi, M., Jones, C., Zehnder, J. L., Keating, A., Negrin, R. S., Weissman, I. L. & Jamieson, C. H. M. (2009) Glycogen synthase kinase 3beta missplicing contributes to leukemia stem cell generation. *Proc Natl Acad Sci U S A*, 106(10), 3925-9.

Adolfsson, J., Månsson, R., Buza-Vidas, N., Hultquist, A., Liuba, K., Jensen, C. T., Bryder, D., Yang, L., Borge, O. J., Thoren, L. A., Anderson, K., Sitnicka, E., Sasaki, Y., Sigvardsson, M. & Jacobsen, S. E. (2005) Identification of Flt3+ lympho-myeloid stem cells lacking erythro-megakaryocytic potential a revised road map for adult blood lineage commitment. *Cell*, 121(2), 295-306.

Advani, A. S. & Pendergast, A. M. (2002) Bcr-Abl variants: biological and clinical aspects. *Leuk Res*, 26(8), 713-20.

Afar, D. E., Goga, A., McLaughlin, J., Witte, O. N. & Sawyers, C. L. (1994) Differential complementation of Bcr-Abl point mutants with c-Myc. *Science*, 264(5157), 424-426.

Agarwal, P. & Bhatia, R. (2015) Influence of Bone Marrow Microenvironment on Leukemic Stem Cells: Breaking Up an Intimate Relationship. *Adv Cancer Res*, 127, 227-252.

Ågerstam, H., Hansen, N., von Palffy, S., Sandén, C., Reckzeh, K., Karlsson, C., Lilljebjörn, H., Landberg, N., Askmyr, M., Högberg, C., Rissler, M., Porkka, K., Wadenvik, H., Mustjoki, S., Richter, J., Järås, M. & Fioretos, T. (2016) IL1RAP antibodies block IL-1-induced expansion of candidate CML stem cells and mediate cell killing in xenograft models. *Blood*, 128(23), 2683-2693.

Ai, J. & Tiu, R. V. (2014) Practical management of patients with chronic myeloid leukemia who develop tyrosine kinase inhibitor-resistant BCR-ABL1 mutations. *Ther Adv Hematol*, 5(4), 107-20.

Akashi, K., Traver, D., Miyamoto, T. & Weissman, I. L. (2000) A clonogenic common myeloid progenitor that gives rise to all myeloid lineages. *Nature*, 404, 193-197.

Al-Hajj, M., Wicha, M. S., Benito-Hernandez, A., Morrison, S. J. & Clarke, M. F. (2003) Prospective identification of tumorigenic breast cancer cells. *Proc Natl Acad Sci U S A*, 100(7), 3983-8.

Al-Mawali, A., Gillis, D. & Lewis, I. (2016) Immunoprofiling of leukemic stem cells CD34+/CD38-/CD123+delineate FLT3/ITD-positive clones. *J Hematol Oncol*, 9(1), 61.

Alison, M. R., Lim, S. M. L. & Nicholson, L. J. (2011) Cancer stem cells: problems for therapy? *J Pathol*, 223(2), 147-161.

Aljedai, A., Buckle, A. M., Hiwarkar, P. & Syed, F. (2015) Potential Role of Notch Signalling in CD34(+) Chronic Myeloid Leukaemia Cells: Cross-Talk between Notch and BCR-ABL. *Plos One*, 10(4), e0123016.

Anastas, J. N. & Moon, R. T. (2013) WNT signalling pathways as therapeutic targets in cancer. *Nat Rev Cancer*, 13(1), 11-26.

Anastasi, J., Feng, J., Dickstein, J. I., Le Beau, M. M., Rubin, C. M., Larson, R. A., Rowley, J. D. & Vardiman, J. W. (1996) Lineage involvement by BCR/ABL in Ph+ lymphoblastic leukemias: chronic myelogenous leukemia presenting in lymphoid blast vs Ph+ acute lymphoblastic leukemia. *Leukemia*, 10(5), 795-802.

Anjos-Afonso, F., Currie, E., Palmer, H. G., Foster, K. E., Taussig, D. C. & Bonnet, D. (2013) CD34(-) cells at the apex of the human hematopoietic stem cell hierarchy have distinctive cellular and molecular signatures. *Cell stem cell*, 13(2), 161-74.

Antonchuk, J., Sauvageau, G. & Humphries, R. K. (2002) HOXB4-induced expansion of adult hematopoietic stem cells ex vivo. *Cell*, 109(1), 39-45.

Aplenc, R., Blaney, S. M., Strauss, L. C., Balis, F. M., Shusterman, S., Ingle, A. M., Agrawal, S., Sun, J., Wright, J. J. & Adamson, P. C. (2011) Pediatric phase I trial and pharmacokinetic study of dasatinib: a report from the children's oncology group phase I consortium. *J Clin Oncol*, 29(7), 839-44.

Arana-Trejo, R. M., Ruíz Sánchez, E., Ignacio-Ibarra, G., Báez de la Fuente, E., Garces, O., Gómez Morales, E., Castro Granados, M., Ovilla Martínez, R., Rubio-Borja, M. E., Solís Anaya, L., Herrera, P., Delgado Llamas, J. & Kofman, S. (2002) BCR/ABL p210, p190 and p230 fusion genes in 250 Mexican patients with chronic myeloid leukaemia (CML). *Clin Lab Haematol*, 24(3), 145-50.

Arber, D. A., Orazi, A., Hasserjian, R., Thiele, J., Borowitz, M. J., Le Beau, M. M., Bloomfield, C. D., Cazzola, M. & Vardiman, J. W. (2016) The 2016 revision to the World Health Organization classification of myeloid neoplasms and acute leukemia. *Blood*, 127(20), 2391-405.

Askew, D. S., Ashmun, R. A., Simmons, B. C. & Cleveland, J. L. (1991) Constitutive c-myc expression in an IL-3-dependent myeloid cell line suppresses cell cycle arrest and accelerates apoptosis. *Oncogene*, 6(10), 1915-22.

Atallah, E., Talpaz, M., O'brien, S., Rios, M. B., Guo, J. Q., Arlinghaus, R., Fernandes-Reese, S. & Kantarjian, H. (2002) Chronic myelogenous leukemia in T cell lymphoid blastic phase achieving durable complete cytogenetic and molecular remission with imatinib mesylate (STI571; Gleevec) therapy. *Cancer*, 94(11), 2996-9.

Austin, T. W., Solar, G. P., Ziegler, F. C., Liem, L. & Matthews, W. (1997) A role for the Wnt gene family in hematopoiesis: expansion of multilineage progenitor cells. *Blood*, 89(10), 3624-35.

Azevedo, A. P., Reichert, A., Afonso, C., Alberca, M. D., Tavares, P. & Lima, F. (2017) BCR-ABL V280G Mutation, Potential Role in Imatinib Resistance: First Case Report. *Clin Med Insights Oncol*, 11, 1179554917702870.

Baccarani, M., Deininger, M. W., Rosti, G., Hochhaus, A., Soverini, S., Apperley, J. F., Cervantes, F., Clark, R. E., Cortes, J. E., Guilhot, F., Hjorth-Hansen, H., Hughes, T. P., Kantarjian, H. M., Kim, D.-W., Larson, R. A., Lipton, J. H., Mahon, F.-X., Martinelli, G., Mayer, J., Mller, M. C., Niederwieser, D., Pane, F., Radich, J. P., Rousselot, P., Saglio, G., Sauele, S., Schiffer, C., Silver, R., Simonsson, B., Steegmann, J.-L., Goldman, J. M. & Hehlmann, R. (2013) European LeukemiaNet recommendations for the management of chronic myeloid leukemia: 2013. *Blood*, 122(6), 872-84.

Bacher, U., Haferlach, T., Hiddemann, W., Schnittger, S., Kern, W. & Schoch, C. (2005a) Additional clonal abnormalities in Philadelphia-positive ALL and CML demonstrate a different cytogenetic pattern at diagnosis and follow different pathways at progression. *Cancer Genet Cytogenet*, 157(1), 53-61.

Bacher, U., Hochhaus, A., Berger, U., Hiddemann, W., Hehlmann, R., Haferlach, T. & Schoch, C. (2005b) Clonal aberrations in Philadelphia chromosome negative hematopoiesis in patients with chronic myeloid leukemia treated with imatinib or interferon alpha. *Leukemia*, 19(3), 460-3.

Bacher, U., Kern, W., Schnittger, S., Hiddemann, W., Schoch, C. & Haferlach, T. (2005c) Blast count and cytogenetics correlate and are useful parameters for the evaluation of different phases in chronic myeloid leukemia. *Leuk Lymphoma*, 46(3), 357-66.

Bai, L. Y., Chiu, C. F., Lin, C. W., Hsu, N. Y., Lin, C. L., Lo, W. J. & Kao, M. C. (2008) Differential expression of Sonic hedgehog and Gli1 in hematological malignancies. *Leukemia*, 22(1), 226-228.

Bao, L., Tang, M., Zhang, Q., You, B., Shan, Y., Shi, S., Li, L., Hu, S. & You, Y. (2016) Elevated expression of CD93 promotes angiogenesis and tumor growth in nasopharyngeal carcinoma. *Biochem Biophys Res Commun*, 476(4), 467-474.

Baum, C. M., Weissman, I. L., Tsukamoto, A. S., Buckle, A. M. & Peault, B. (1992) Isolation of a candidate human hematopoietic stem-cell population. *Proc Natl Acad Sci U S A*, 89(7), 2804-8.

Beck, J. R., Guilhot, J., Giles, F. J., Aoki, N., Wirt, D. P. & Guilhot, F. (2001) Cytarabine added to interferon improves the cost-effectiveness of initial therapy for patients with early chronic phase chronic myelogenous leukemia. *Leuk Lymphoma*, 41(1-2), 117-24.

Belay, E., Hayes, B. J., Blau, C. A. & Torok-Storb, B. (2017) Human Cord Blood and Bone Marrow CD34+ Cells Generate Macrophages That Support Erythroid Islands. *PLoS One*, 12(1), e0171096.

Belle, J. I., Petrov, J. C., Langlais, D., Robert, F., Cencic, R., Shen, S., Pelletier, J., Gros, P. & Nijnik, A. (2016) Repression of p53-target gene Bbc3/PUMA by MYSM1 is essential for the survival of hematopoietic multipotent progenitors and contributes to stem cell maintenance. *Cell Death Differ*, 23(5), 759-75.

Bennett, J. H. (1845) Case of hypertrophy of the spleen and liver in which death took place from suppuration of the blood. *Edinburgh Medical and Surgical Journal*, 64, 413-423.

Benveniste, P., Serra, P., Dervovic, D., Herer, E., Knowles, G., Mohtashami, M. & Zúñiga-Pflücker, J. C. (2014) Notch signals are required for in vitro but not in vivo maintenance of human hematopoietic stem cells and delay the appearance of multipotent progenitors. *Blood*, 123(8), 1167-77.

Bergua, J. M., Montesinos, P., Martinez-Cuadrón, D., Fernández-Abellán, P., Serrano, J., Sayas, M. J., Prieto-Fernandez, J., García, R., García-Huerta, A. J., Barrios, M., Benavente, C., Pérez-Encinas, M., Simiele, A., Rodríguez-Macias, G., Herrera-Puente, P., Rodríguez-Veiga, R., Martínez-Sánchez, M. P., Amador-Barciela, M. L., Riaza-Grau, R., Sanz, M. A. & group, P. (2016) A prognostic model for survival after salvage treatment with FLAG-Ida +/- gemtuzumab-ozogamicine in adult patients with refractory/relapsed acute myeloid leukaemia. *Br J Haematol*, 174(5), 700-10.

Bertorelle, R., Bonaldi, L., Bianchini, E., Ramazzina, E., Del Mistro, A., Zamboni, S., Chieco-Bianchi, L. & Paolini, R. (2001) The e19a2 BCR/ABL fusion transcript with additional chromosomal aberrations on a new case of chronic myeloid leukemia (CML) of mild type. *Leukemia*, 15(12), 2003-4.

Besseyrias, V., Fiorini, E., Strobl, L. J., Zimber-Strobl, U., Dumortier, A., Koch, U., Arcangeli, M.-L., Ezine, S., Macdonald, H. R. & Radtke, F. (2007) Hierarchy of Notch-Delta interactions promoting T cell lineage commitment and maturation. *J Exp Med*, 204(2), 331-43.

Bettelheim, P., Lutz, D., Majdic, O., Paietta, E., Haas, O., Linkesch, W., Neumann, E., Lechner, K. & Knapp, W. (1985) Cell lineage heterogeneity in blast crisis of chronic myeloid leukaemia. *Br J Haematol*, 59(3), 395-409.

Bhardwaj, G., Murdoch, B., Wu, D., Baker, D. P., Williams, K. P., Chadwick, K., Ling, L. E., Karanu, F. N. & Bhatia, M. (2001) Sonic hedgehog induces the proliferation of primitive human hematopoietic cells via BMP regulation. *Nat Immunol*, 2(2), 172-80.

Bhatia, M., Bonnet, D., Kapp, U., Wang, J. C., Murdoch, B. & Dick, J. E. (1997a) Quantitative analysis reveals expansion of human hematopoietic repopulating cells after short-term ex vivo culture. *J Exp Med*, 186(4), 619-24.

Bhatia, M., Wang, J. C., Kapp, U., Bonnet, D. & Dick, J. E. (1997b) Purification of primitive human hematopoietic cells capable of repopulating immune-deficient mice. *Proc Natl Acad Sci U S A*, 94(10), 5320-5325.

Bhatia, M., Bonnet, D., Murdoch, B., Gan, O. I. & Dick, J. E. (1998) A newly discovered class of human hematopoietic cells with SCID-repopulating activity. *Nat Med*, 4(9), 1038-45.

Bhatia, M., Bonnet, D., Wu, D., Murdoch, B., Wrana, J., Gallacher, L. & Dick, J. E. (1999) Bone morphogenetic proteins regulate the developmental program of human hematopoietic stem cells. *J Exp Med*, 189(7), 1139-48.

Bhatia, R., Holtz, M., Niu, N., Gray, R., Snyder, D. S., Sawyers, C. L., Arber, D. A., Slovak, M. L. & Forman, S. J. (2003) Persistence of malignant hematopoietic progenitors in chronic myelogenous leukemia patients in complete cytogenetic remission following imatinib mesylate treatment. *Blood*, 101(12), 4701-7.

Biernaux, C., Loos, M., Sels, A., Huez, G. & Stryckmans, P. (1995) Detection of major bcr-abl gene expression at a very low level in blood cells of some healthy individuals. *Blood*, 86(8), 3118-3122.

Bixby, D. & Talpaz, M. (2011) Seeking the causes and solutions to imatinib-resistance in chronic myeloid leukemia. *Leukemia*, 25(1), 7-22.

Blair, A., Hogge, D. E., Ailles, L. E., Lansdorp, P. M. & Sutherland, H. J. (1997) Lack of expression of Thy-1 (CD90) on acute myeloid leukemia cells with long-term proliferative ability in vitro and in vivo. *Blood*, 89(9), 3104-3112.

Blair, A., Hogge, D. E. & Sutherland, H. J. (1998) Most acute myeloid leukemia progenitor cells with long-term proliferative ability in vitro and in vivo have the phenotype CD34(+)/CD71(-)/HLA-DR-. *Blood*, 92(11), 4325-4335.

Blank, U. & Karlsson, S. (2011) The role of Smad signalling in hematopoiesis and translational hematology. *Leukemia*, 25(9), 1379-88.

Bonnet, D. & Dick, J. E. (1997) Human acute myeloid leukemia is organized as a hierarchy that originates from a primitive hematopoietic cell. *Nat Med*, 3(7), 730-7.

Bordonaro, S., Romano, F., Lanteri, E., Cappuccio, F., Indorato, R., Butera, A., D'Angelo, A., Ferraù, F. & Tralongo, P. (2014) Effect of a structured, active, home-based cancer-treatment program for the management of patients on oral chemotherapy. *Patient Prefer Adherence*, 8, 917-23.

Bose, S., Deininger, M., Gora-Tybor, J., Goldman, J. M. & V., M. J. (1998) The presence of typical and atypical BCR-ABL fusion genes in leukocytes of normal individuals: biologic significance and implications for the assessment of minimal residual disease. *Blood*, 92(9), 3362-3367.

Bourdieu, A., Avalon, M., Lapostolle, V., Ismail, S., Mombled, M., Debeissat, C., Guérinet, M., Duchez, P., Chevaleyre, J., Vlaski-Lafarge, M., Villacreces, A., Praloran, V., Ivanovic, Z. & Brunet de la Grange, P. (2017) Steady state peripheral blood provides cells with functional and metabolic characteristics of real hematopoietic stem cells. *J Cell Physiol*.

Bower, H., Bjorkholm, M., Dickman, P. W., Hoglund, M., Lambert, P. C. & Andersson, T. M. (2016) Life Expectancy of Patients With Chronic Myeloid Leukemia Approaches the Life Expectancy of the General Population. *J Clin Oncol*, 34(24), 2851-7.

Bowers, M., Zhang, B., Ho, Y. W., Agarwal, P., Chen, C. C. & Bhatia, R. (2015) Osteoblast ablation reduces normal long-term hematopoietic stem cell self-renewal but accelerates leukemia development. *Blood*, 125(17), 2678-2688.

Branford, S., Fletcher, L., Cross, N. C., Müller, M. C., Hochhaus, A., Kim, D. W., Radich, J. P., Saglio, G., Pane, F., Kamel-Reid, S., Wang, Y. L., Press, R. D., Lynch, K., Rudzki, Z., Goldman, J. M. & Hughes, T. (2008) Desirable performance characteristics for BCR-ABL measurement on an international reporting scale to allow consistent interpretation of individual patient response and comparison of response rates between clinical trials. *Blood*, 112(8), 3330-8.

Branford, S., Kim, D. W., Soverini, S., Haque, A., Shou, Y., Woodman, R. C., Kantarjian, H. M., Martinelli, G., Radich, J. P., Saglio, G., Hochhaus, A., Hughes, T. P. & Müller, M. C. (2012) Initial molecular response at 3 months may predict both response and event-free survival at 24 months in imatinib-resistant or -intolerant patients with Philadelphia chromosome-positive chronic myeloid leukemia in chronic phase treated with nilotinib. *J Clin Oncol*, 30(35), 4323-9.

Branford, S., Melo, J. V. & Hughes, T. P. (2009) Selecting optimal second-line tyrosine kinase inhibitor therapy for chronic myeloid leukemia patients after imatinib failure: does the BCR-ABL mutation status really matter? *Blood*, 114(27), 5426-35.

Branford, S., Rudzki, Z., Walsh, S., Parkinson, I., Grigg, A., Szer, J., Taylor, K., Herrmann, R., Seymour, J. F., Arthur, C., Joske, D., Lynch, K. & Hughes, T. (2003) Detection of BCR-ABL mutations in patients with CML treated with imatinib is virtually always accompanied by clinical resistance, and mutations in the ATP phosphate-binding loop (P-loop) are associated with a poor prognosis. *Blood*, 102(1), 276-83.

Brasher, B. B. & Van Etten, R. A. (2000) c-Abl has high intrinsic tyrosine kinase activity that is stimulated by mutation of the Src homology 3 domain and by autophosphorylation at two distinct regulatory tyrosines. *J Biol Chem*, 275(45), 35631-7.

Bray, S. J. (2016) Notch signalling in context. *Nat Rev Mol Cell Biol*, 17(11), 722-735.

Brümmendorf, T. H., Cortes, J. E., de Souza, C. A., Guilhot, F., Duvillié, L., Pavlov, D., Gogat, K., Countouriotis, A. M. & Gambacorti-Passerini, C. (2015) Bosutinib versus imatinib in newly diagnosed chronic-phase chronic myeloid leukaemia: results from the 24-month follow-up of the BELA trial. *Br J Haematol*, 168(1), 69-81.

Burnett, A. K., Hills, R. K., Milligan, D., Kjeldsen, L., Kell, J., Russell, N. H., Yin, J. A., Hunter, A., Goldstone, A. H. & Wheatley, K. (2011) Identification of patients with acute myeloblastic leukemia who benefit from the addition of gemtuzumab ozogamicin: results of the MRC AML15 trial. *J Clin Oncol*, 29(4), 369-77.

Burnett, A. K., Russell, N. H., Hills, R. K., Hunter, A. E., Kjeldsen, L., Yin, J., Gibson, B. E., Wheatley, K. & Milligan, D. (2013) Optimization of chemotherapy for younger patients with acute myeloid leukemia: results of the medical research council AML15 trial. *J Clin Oncol*, 31(27), 3360-8.

Burnett, A. K., Russell, N. H., Hills, R. K., Kell, J., Freeman, S., Kjeldsen, L., Hunter, A. E., Yin, J., Craddock, C. F., Dufva, I. H., Wheatley, K. & Milligan, D. (2012) Addition of gemtuzumab ozogamicin to induction chemotherapy improves survival in older patients with acute myeloid leukemia. *J Clin Oncol*, 30(32), 3924-31.

Busfield, S. J., Biondo, M., Wong, M., Ramshaw, H. S., Lee, E. M., Ghosh, S., Braley, H., Panousis, C., Roberts, A. W., He, S. Z., Thomas, D., Fabri, L., Vairo, G., Lock, R. B., Lopez, A. F. & Nash, A. D. (2014) Targeting of acute myeloid leukemia in vitro and in vivo with an anti-CD123 mAb engineered for optimal ADCC. *Leukemia*, 28(11), 2213-2221.

Cai, H., Qin, X. & Yang, C. (2017) Dehydrocostus Lactone Suppresses Proliferation of Human Chronic Myeloid Leukemia Cells Through Bcr/Abl-JAK/STAT Signalling Pathways. *J Cell Biochem*.

Calabretta, B. a. P. D. (2004) Review in translational hematology The biology of CML blast crisis. *Blood*, 103(11), 4010-4022.

Calvi, L. M., Adams, G. B. & Weibrecht, K. W. (2003) Osteoblastic cells regulate the haematopoietic stem cell niche. *Nature*, 425(6960), 841-846.

Camacho, V., McClearn, V., Patel, S. & Welner, R. S. (2017) Regulation of normal and leukemic stem cells through cytokine signalling and the microenvironment. *Int J Hematol*, 105(5), 566-577.

Campbell, C., Risueno, R. M., Salati, S., Guezguez, B. & Bhatia, M. (2008) Signal control of hematopoietic stem cell fate: Wnt, Notch, and Hedgehog as the usual suspects. *Curr Opin Hematol*, 15(4), 319-25.

Campbell, V. L., Tarafdar, A., Dobbin, E., Horne, G. A., Park, L., Dixon, C., Goodlad, J. R., Wheadon, H. & Copland, M. (2016) Unravelling the complexities of hedgehog mediated signal transduction in acute myeloid leukaemia and normal haematopoiesis. *Blood*, 128, 2881.

Capaccione, K. M. & Pine, S. R. (2013) The Notch signalling pathway as a mediator of tumor survival. *Carcinogenesis*, 34(7), 1420-1430.

Carlesso, N., Aster, J. C., Sklar, J. & Scadden, D. T. (1999) Notch1-induced delay of human hematopoietic progenitor cell differentiation is associated with altered cell cycle kinetics. *Blood*, 93(3), 838-848.

Castaigne, S., Pautas, C., Terré, C., Raffoux, E., Bordessoule, D., Bastie, J. N., Legrand, O., Thomas, X., Turlure, P., Reman, O., de Revel, T., Gastaud, L., de Gunzburg, N., Contentin, N., Henry, E., Marolleau, J. P., Aljijakli, A., Rousselot, P., Fenaux, P., Preudhomme, C., Chevret, S., Dombret, H. & Association, A. L. F. (2012) Effect of gemtuzumab ozogamicin on survival of adult patients with de-novo acute myeloid leukaemia (ALFA-0701): a randomised, open-label, phase 3 study. *Lancet*, 379(9825), 1508-16.

Catlin, S. N., Busque, L., Gale, R. E., Guttorp, P. & Abkowitz, J. L. (2011) The replication rate of human hematopoietic stem cells in vivo. *Blood*, 117(17), 4460-6.

Caussinus, E. & Hirth, F. (2007) Asymmetric stem cell division in development and cancer. *Prog Mol Subcell Biol*, 45, 205-25.

Cavelier, L., Ameur, A., Häggqvist, S., Höijer, I., Cahill, N., Olsson-Strömberg, U. & Hermanson, M. (2015) Clonal distribution of BCR-ABL1 mutations and splice isoforms by single-molecule long-read RNA sequencing. *BMC Cancer*, 15, 45.

Ceredig, R., Rauch, M., Balciunaite, G. & Rolink, A. G. (2006) Increasing Flt3L availability alters composition of a novel bone marrow lymphoid progenitor compartment. *Blood*, 108(4), 1216-22.

Cervantes, F., Villamor, N., Esteve, J., Montoto, S., Rives, S., Rozman, C. & Montserrat, E. (1998) 'Lymphoid' blast crisis of chronic myeloid leukaemia is associated with distinct clinicohaematological features. *Br J Haematol*, 100(1), 123-8.

Chen, B. P., Fraser, C., Reading, C., Murray, L., Uchida, N., Galy, A., Sasaki, D., Tricot, G., Jagannath, S. & Barlogie, B. (1995) Cytokine-mobilized peripheral blood CD34+Thy-1+Lin- human hematopoietic stem cells as target cells for transplantation-based gene therapy. *Leukemia*, 9(1), S17-25.

Chen, P. M., Yen, C. C., Wang, W. S., Lin, Y. J., Chu, C. J., Chiou, T. J., Liu, J. H. & Yang, M. H. (2008) Down-regulation of Notch-1 expression decreases PU.1-mediated myeloid differentiation signalling in acute myeloid leukemia. *Int J Oncol*, 32(6), 1335-1341.

Cheng, J., Baumhueter, S., Cacalano, G., Carver-Moore, K., Thibodeaux, H., Thomas, R., Broxmeyer, H. E., Cooper, S., Hague, N., Moore, M. & Lasky, L. A. (1996) Hematopoietic defects in mice lacking the sialomucin CD34. *Blood*, 87(2), 479-90.

Cheng, X., Huber, T. L., Chen, V. C., Gadue, P. & Keller, G. M. (2008) Numb mediates the interaction between Wnt and Notch to modulate primitive erythropoietic specification from the hemangioblast. *Development*, 135(20), 3447-58.

Cheshier, S. H., Morrison, S. J., Liao, X. & Weissman, I. L. (1999) In vivo proliferation and cell cycle kinetics of long-term self-renewing hematopoietic stem cells. *Proc Natl Acad Sci U S A*, 96(6), 3120-5.

Chiang, M. Y., Shestova, O., Xu, L. W., Aster, J. C. & Pear, W. S. (2013) Divergent effects of supraphysiologic Notch signals on leukemia stem cells and hematopoietic stem cells. *Blood*, 121(6), 905-917.

Chiaramonte, R., Basile, A., Tassi, E., Calzavara, E., Cecchinato, V., Rossi, V., Biondi, A. & Comi, P. (2005) A wide role for NOTCH1 signalling in acute leukemia. *Cancer letters*, 219(1), 113-20.

Chiba, S. (2006) Notch signalling in stem cell systems. *Stem Cells*, 24(11), 2437-2447.

Chomel, J. C., Bonnet, M. L., Sorel, N., Bertrand, A., Meunier, M. C., Fichelson, S., Melkus, M., Bennaceur-Griscelli, A., Guilhot, F. & Turhan, A. G. (2011) Leukemic stem cell persistence in chronic myeloid leukemia patients with sustained undetectable molecular residual disease. *Blood*, 118(13), 3657-60.

Chomel, J. C., Bonnet, M. L., Sorel, N., Sloma, I., Bennaceur-Griscelli, A., Rea, D., Legros, L., Marfaing-Koka, A., Bourhis, J. H., Ame, S., Guerci-Bresler, A., Rousselot, P. & Turhan, A. G. (2016) Leukemic stem cell persistence in chronic myeloid leukemia patients in deep molecular response induced by tyrosine kinase inhibitors and the impact of therapy discontinuation. *Oncotarget*, 7(23), 35293-35301.

Christian, S., Ahorn, H., Koehler, A., Eisenhaber, F., Rodi, H. P., Garin-Chesa, P., Park, J. E., Rettig, W. J. & Lenter, M. C. (2001) Molecular Cloning and Characterization of Endosialin, a C-type Lectin-like Cell Surface Receptor of Tumor Endothelium. *J Biol Chem*, 276(10), 7408-7414.

Chu, S., McDonald, T., Lin, A., Chakraborty, S., Huang, Q., Snyder, D. S. & Bhatia, R. (2011) Persistence of leukemia stem cells in chronic myelogenous leukemia patients in prolonged remission with imatinib treatment. *Blood*, 118(20), 5565-72.

Civin, C. I., Strauss, L. C., Brovall, C., Fackler, M. J., Schwartz, J. F. & Shaper, J. H. (1984) Antigenic analysis of hematopoiesis. III. A hematopoietic progenitor cell surface antigen defined by a monoclonal antibody raised against KG-1a cells. *J Immunol*, 133(1), 157-65.

Clark, R., Polydoros, F., Apperley, J., Pocock, C., Smith, G., Byrne, J., O'Brien, S., Coffey, T., Foroni, L. & Copland, M. (2016) Chronic Myeloid Leukaemia Patients with Stable Molecular Responses (at least MR3) May Safely Decrease the Dose of Their Tyrosine Kinase Inhibitor: Data from the British Destiny Study, American Society of Hematology (ASH).

Clark, S. S., McLaughlin, J., Timmons, M., Pendergast, A. M., Ben-Neriah, Y., Dow, L. W., Crist, W., Rovera, G., Smith, S. D. & Witte, O. N. (1988) Expression of a distinctive BCR-ABL oncogene in Ph1-positive acute lymphocytic leukemia (ALL). *Science*, 239(4841 Pt 1), 775-7.

Clarke, C. J. & Holyoake, T. L. (2017) Preclinical approaches in chronic myeloid leukemia: from cells to systems. *Exp Hematol*, 47, 13-23.

Clevers, H. (2006) Wnt/beta-catenin signalling in development and disease. *Cell*, 127(3), 469-480.

Clift, R. A., Buckner, C. D., Thomas, E. D., Doney, K., Fefer, A., Neiman, P. E., Singer, J., Sanders, J., Stewart, P., Sullivan, K. M., Deeg, J. & Storb, R. (1982) Treatment of chronic granulocytic leukaemia in chronic phase by allogeneic marrow transplantation. *Lancet*, 2(8299), 621-3.

Cobas, M., Wilson, A., Ernst, B., Mancini, S. J., MacDonald, H. R., Kemler, R. & Radtke, F. (2004) Beta-catenin is dispensable for hematopoiesis and lymphopoiesis. *J Exp Med*, 199(2), 221-9.

Cohen, D. J. (2012) Targeting the hedgehog pathway: role in cancer and clinical implications of its inhibition. *Hematol Oncol Clin North Am*, 26(3), 565-88, viii.

Colaluca, I. N., Tosoni, D., Nuciforo, P., Senic-Matuglia, F., Galimberti, V., Viale, G., Pece, S. & Di Fiore, P. P. (2008) NUMB controls p53 tumour suppressor activity. *Nature*, 451(7174), 76-80.

Congdon, K. L., Voermans, C., Ferguson, E. C., DiMascio, L. N., Uqoezwa, M., Zhao, C. & Reya, T. (2008) Activation of Wnt signalling in hematopoietic regeneration. *Stem Cells*, 26(5), 1202-10.

Conneally, E., Cashman, J., Petzer, A. & Eaves, C. (1997) Expansion in vitro of transplantable human cord blood stem cells demonstrated using a quantitative assay of their lympho-myeloid repopulating activity in nonobese diabetic-scid/scid mice. *Proc Natl Acad Sci U S A*, 94(18), 9836-41.

Copland, M. (2007) Novel drug combinations for the eradication of Ph+/BCR-ABL+ haematopoietic stem cells in chronic myeloid leukaemia. *University of Glasgow*.

Copland, M., Pellicano, F., Richmond, L., Allan, E. K., Hamilton, A., Lee, F. Y., Weinmann, R. & Holyoake, T. L. (2008) BMS-214662 potently induces apoptosis of chronic myeloid leukemia stem and progenitor cells and synergizes with tyrosine kinase inhibitors. *Blood*, 111(5), 2843-53.

Corbin, A. S., Agarwal, A., Loriaux, M., Cortes, J., Deininger, M. W. & Druker, B. J. (2011) Human chronic myeloid leukemia stem cells are insensitive to imatinib despite inhibition of BCR-ABL activity. *J Clin Invest*, 121(1), 396-409.

Cornelison, M., Jabbour, E. J. & Welch, M. A. (2012) Managing side effects of tyrosine kinase inhibitor therapy to optimize adherence in patients with chronic myeloid leukemia: the role of the midlevel practitioner. *J Support Oncol*, 10(1), 14-24.

Corrigan, P. M., Dobbin, E., Freeburn, R. W. & Wheadon, H. (2009) Patterns of Wnt/Fzd/LRP gene expression during embryonic hematopoiesis. *Stem Cells Dev*, 18(5), 759-72.

Cortes, J. E., Talpaz, M., Giles, F., O'Brien, S., Rios, M. B., Shan, J., Garcia-Manero, G., Faderl, S., Thomas, D. A., Wierda, W., Ferrajoli, A., Jeha, S. & Kantarjian, H. M. (2003) Prognostic significance of cytogenetic clonal evolution in patients with chronic myelogenous leukemia on imatinib mesylate therapy. *Blood*, 101(10), 3794-800.

Cortes, J. E., Baccarani, M., Guilhot, F., Druker, B. J., Branford, S., Kim, D. W., Pane, F., Pasquini, R., Goldberg, S. L., Kalaycio, M., Moiraghi, B., Rowe, J. M., Tothova, E., De Souza, C., Rudoltz, M., Yu, R., Krahnke, T., Kantarjian, H. M., Radich, J. P. & Hughes, T. P. (2010a) Phase III, randomized, open-label study of daily imatinib mesylate 400 mg versus 800 mg in patients with newly diagnosed, previously untreated chronic myeloid leukemia in chronic phase using molecular end points: tyrosine kinase inhibitor optimization and selectivity study. *J Clin Oncol*, 28(3), 424-30.

Cortes, J. E., Jones, D., O'Brien, S., Jabbour, E., Konopleva, M., Ferrajoli, A., Kadia, T., Borthakur, G., Stigliano, D., Shan, J. & Kantarjian, H. (2010b) Nilotinib as front-line treatment for patients with chronic myeloid leukemia in early chronic phase. *J Clin Oncol*, 28(3), 392-7.

Cortes, J. E., Kim, D. W., Kantarjian, H. M., Brümmendorf, T. H., Dyagil, I., Griskevicius, L., Malhotra, H., Powell, C., Gogat, K., Countouriotis, A. M. & Gambacorti-Passerini, C. (2012) Bosutinib versus imatinib in newly diagnosed chronic-phase chronic myeloid leukemia: results from the BELA trial. *J Clin Oncol*, 30(28), 3486-92.

Cortes, J. E., Kim, D. W., Pinilla-Ibarz, J., le Coutre, P., Paquette, R., Chuah, C., Nicolini, F. E., Apperley, J. F., Khoury, H. J., Talpaz, M., DiPersio, J., DeAngelo, D. J., Abruzzese, E., Rea, D., Baccarani, M., Müller, M. C., Gambacorti-Passerini, C., Wong, S., Lustgarten, S., Rivera, V. M., Clackson, T., Turner, C. D., Haluska, F. G., Guilhot, F., Deininger, M. W., Hochhaus,

A., Hughes, T., Goldman, J. M., Shah, N. P., Kantarjian, H. & Investigators, P. (2013) A phase 2 trial of ponatinib in Philadelphia chromosome-positive leukemias. *N Engl J Med*, 369(19), 1783-96.

Cortes, J. E., Kim, D., Pinilla-Ibarz, J., Le Coutre, P., Paquette , R., Chuah , C., Nicolini , F., Apperley , J., Khoury , H., Talpaz , M., DiPersio , J., DeAngelo , D., Abruzzese , E., Rea , D., Baccarani , M., Müller , M., Gambacorti-Passerini , C., Lustgarten , S., Rivera , V., C lackson , T., Turner , C., Haluska , F., Guilhot , F., Deininger , M., Hochhaus , A., Hughes , T., Shah, N. & Kantarjian, H. (2014a) Long-term follow-up of ponatinib efficacy and safety in the Phase 2 PACE trial *Blood*, 124, 3135.

Cortes, J. E., Carter, B. Z., Quintas-Cardama, A., Inada, T., Morita, K., Fujimori, M., Kouji, H., Mak, P. Y., Ruvolo, V., Borthakur, G., Andreeff, M., Konopleva, M., Ravandi, F. & Kantarjian, H. (2014b) A Phase I Dose-Escalation Study of Pri-724, a Cbp/B-Catenin Modulator in Patients with Advanced Acute Myeloid Leukemia (Aml). *Haematologica*, 99, 222-223.

Cortes, J. E., Heidel, F. H., Heuser, M., Fiedler, W., Smith, D., Robak, T., Fernandez, P. M., Ma, W. W., Shaik, M. N., Zeremski, M., O'Connell, A. & Chan, J. (2016a) A phase 2 randomized study of low dose ara-C with or without glasdegib (PF-04449913) in untreated patients with acute myeloid leukemia ir high-risk myelodysplastic syndrome. *Blood*, 128, 99.

Cortes, J. E., Saglio, G., Kantarjian, H. M., Baccarani, M., Mayer, J., Boqué, C., Shah, N. P., Chuah, C., Casanova, L., Bradley-Garelik, B., Manos, G. & Hochhaus, A. (2016b) Final 5-Year Study Results of DASISION: The Dasatinib Versus Imatinib Study in Treatment-Naïve Chronic Myeloid Leukemia Patients Trial. *J Clin Oncol*, 34(20), 2333-40.

Cortez, D., Reuther, G. & Pendergast, A. M. (1997) The Bcr-Abl tyrosine kinase activates mitogenic signalling pathways and stimulates G1-to-S phase transition in hematopoietic cells. *Oncogene*, 15(19), 2333-42.

Cowart, L. A. (2012) Notch Signalling in Embryology and Cancer. *Springer Science + Business Media, LLC.*

Craig, W., Poppema, S., Little, M. T., Dragowska, W. & Lansdorp, P. M. (1994) CD45 isoform expression on human haemopoietic cells at different stages of development. *Br J Haematol*, 88(1), 24-30.

Craigie, D. (1845) Case of disease and enlargement of the spleen in which death took place from the presence of purulent matter in the blood. *Edinburgh Medical and Surgical Journal*, 64, 400-413.

Crews, L. A. & Jamieson, C. H. M. (2012) Chronic Myeloid Leukemia Stem Cell Biology. *Curr Hematol Malig Rep*, 7(2), 125-132.

Cridland, S. O., Keys, J. R., Papathanasiou, P. & Perkins, A. C. (2009) Indian hedgehog supports definitive erythropoiesis. *Blood Cells Mol Dis*, 43(2), 149-55.

Crisan, M., Kartalaei, P. S., Vink, C. S., Vink, C., Yamada-Inagawa, T., Bollerot, K., van IJcken, W., van der Linden, R., de Sousa Lopes, S. M., Monteiro, R., Mummery, C. & Dzierzak, E.

(2015) BMP signalling differentially regulates distinct haematopoietic stem cell types. *Nat Commun*, 6, 8040.

Cross, N. C., White, H. E., Colomer, D., Ehrencrona, H., Foroni, L., Gottardi, E., Lange, T., Lion, T., Machova Polakova, K., Dulucq, S., Martinelli, G., Oppliger Leibundgut, E., Pallisgaard, N., Barbany, G., Sacha, T., Talmaci, R., Izzo, B., Saglio, G., Pane, F., Müller, M. C. & Hochhaus, A. (2015) Laboratory recommendations for scoring deep molecular responses following treatment for chronic myeloid leukemia. *Leukemia*, 29(5), 999-1003.

Csaszar, E., Wang, W., Usenko, T., Qiao, W., Delaney, C., Bernstein, I. D. & Zandstra, P. W. (2014) Blood stem cell fate regulation by Delta-1-mediated rewiring of IL-6 paracrine signalling. *Blood*, 123(5), 650-8.

Culen, M., Borsky, M., Nemethova, V., Razga, F., Smejkal, J., Jurcek, T., Dvorakova, D., Zackova, D., Weinbergerova, B., Semerad, L., Sadovnik, I., Eisenwort, G., Herrmann, H., Valent, P., Mayer, J. & Racil, Z. (2016) Quantitative assessment of the CD26+ leukemic stem cell compartment in chronic myeloid leukemia: patient-subgroups, prognostic impact, and technical aspects. *Oncotarget*, 7(22), 33016-24.

Cuneo, A., Balboni, M., Piva, N., Carli, M. G., Tomasi, P., Previati, R., Negrini, M., Scapoli, G., Spanedda, R. & Castoldi, G. (1994a) Lineage switch and multilineage involvement in two cases of pH chromosome-positive acute leukemia: evidence for a stem cell disease. *Haematologica*, 79(1), 76-82.

Cuneo, A., Demuynck, H., Ferrant, A., Louwagie, A., Doyen, C., Stul, M., Cassiman, J. J., Dal Cin, P., Negrini, M. & Carli, M. G. (1994b) Minor myeloid component in Ph chromosome-positive acute lymphoblastic leukaemia: correlation with cytogenetic pattern and implication for poor response to therapy. *Br J Haematol*, 87(3), 515-22.

Cutler, J. A., Tahir, R., Sreenivasamurthy, S. K., Mitchell, C., Renuse, S., Nirujogi, R. S., Patil, A. H., Heydarian, M., Wong, X., Wu, X., Huang, T. C., Kim, M. S., Reddy, K. L. & Pandey, A. (2017) Differential signalling through p190 and p210 BCR-ABL fusion proteins revealed by interactome and phosphoproteome analysis. *Leukemia*.

Dahlberg, A., Delaney, C. & Bernstein, I. D. (2011) Ex vivo expansion of human hematopoietic stem and progenitor cells. *Blood*, 117(23), 6083-90.

Daley, G. Q., Van Etten, R. A. & Baltimore, D. (1990) Induction of chronic myelogenous leukemia in mice by the P210bcr/abl gene of the Philadelphia chromosome. *Science*, 247(4944), 824-30.

Danhauser-Riedl, S., Warmuth, M., Druker, B. J., Emmerich, B. & Hallek, M. (1996) Activation of Src kinases p53/56lyn and p59hck by p210bcr/abl in myeloid cells. *Cancer Res*, 56(15), 3589-96.

Danial, N. N. & Rothman, P. (2000) JAK-STAT signalling activated by Abl oncogenes. *Oncogene*, 19(21), 2523-31.

Daynac, M. & Petritsch, C. K. (2017) Regulation of Asymmetric Cell Division in Mammalian Neural Stem and Cancer Precursor Cells. *Results Probl Cell Differ*, 61, 375-399.

de Pooter, R. F., Schmitt, T. M., de la Pompa, J. L., Fujiwara, Y., Orkin, S. H. & Zúñiga-Pflücker , J. C. (2006) Notch signalling requires GATA-2 to inhibit myelopoiesis from embryonic stem cells and primary hemopoietic progenitors. *J Immunol*, 176(9), 5267-5275.

Deangelo, D. J., Stone, R. M., Silverman, L. B., Stock, W., Attar, E. C., Fearen, I., Dallob, A., Matthews, C., Stone, J., Freedman, S. J. & Aster, J. (2006) A phase I clinical trial of the notch inhibitor MK-0752 in patients with T-cell acute lymphoblastic leukemia/lymphoma (T-ALL) and other leukemias. *J Clin Oncol*, 24(18), 357s.

Deininger, M. (2012) Stem cell persistence in chronic myeloid leukemia. *Leukemia Supplements*, 1(S2), S46-S48.

Deininger, M. W., Vieira, S. A., Parada, Y., Banerji, L., Lam, E. W., Peters, G., Mahon, F. X., Köhler, T., Goldman, J. M. & Melo, J. V. (2001) Direct relation between BCR-ABL tyrosine kinase activity and cyclin D2 expression in lymphoblasts. *Cancer Res*, 61(21), 8005-13.

del Álamo, D., Rouault, H. & Schweisguth, F. (2011) Mechanism and significance of cis-inhibition in Notch signalling. *Curr Biol*, 21(1), R40-7.

Delaney, C., Heimfeld, S., Brashem-Stein, C., Voorhies, H., Manger, R. L. & Bernstein, I. D. (2010) Notch-mediated expansion of human cord blood progenitor cells capable of rapid myeloid reconstitution. *Nat Med*, 16(2), 232-6.

Delaney, C., Varnum-Finney, B., Aoyama, K., Brashem-Stein, C. & Bernstein, I. D. (2005) Dose-dependent effects of the Notch ligand Delta1 on ex vivo differentiation and in vivo marrow repopulating ability of cord blood cells. *Blood*, 106(8), 2693-9.

Derynck, R. & Zhang, Y. E. (2003) Smad-dependent and Smad-independent pathways in TGF-beta family signalling. *Nature*, 425(6958), 577-84.

Dexter, T. M., Allen, T. D. & Lajtha, L. G. (1977) Conditions controlling the proliferation of haemopoietic stem cells in vitro. *J Cell Physiol*, 91(3), 335-44.

Dierks, C., Beigi, R., Guo, G. R., Zirlik, K., Stegert, M. R., Manley, P., Trussell, C., Schmitt-Graeff, A., Landwerlin, K., Veelken, H. & Warmuth, M. (2008) Expansion of Bcr-Abl-positive leukemic stem cells is dependent on Hedgehog pathway activation. *Cancer Cell*, 14(3), 238-49.

Ding, L. & Morrison, S. J. (2013) Haematopoietic stem cells and early lymphoid progenitors occupy distinct bone marrow niches. *Nature*, 495(7440), 231-5.

Domogala, A., Blundell, M., Thrasher, A., Lowdell, M. W., Madrigal, J. A. & Saudemont, A. (2017) Natural killer cells differentiated in vitro from cord blood CD34(+) cells are more advantageous for use as an immunotherapy than peripheral blood and cord blood natural killer cells. *Cytotherapy*, 19(6), 710-720.

Donato, N. J., Wu, J. Y., Stapley, J., Gallick, G., Lin, H., Arlinghaus, R. & Talpaz, M. (2003) BCR-ABL independence and LYN kinase overexpression in chronic myelogenous leukemia cells selected for resistance to STI571. *Blood*, 101(2), 690-8.

Dorey, K., Engen, J. R., Kretzschmar, J., Wilm, M., Neubauer, G., Schindler, T. & Superti-Furga, G. (2001) Phosphorylation and structure-based functional studies reveal a positive and a negative role for the activation loop of the c-Abl tyrosine kinase. *Oncogene*, 20(56), 8075-84.

Doulatov, S., Notta, F., Eppert, K., Nguyen, L. T., Ohashi, P. S. & Dick, J. E. (2010) Revised map of the human progenitor hierarchy shows the origin of macrophages and dendritic cells in early lymphoid development. *Nat Immunol*, 11, 585-593.

Drissen, R., Buza-Vidas, N., Woll, P., Thongjuea, S., Gambardella, A., Giustacchini, A., Mancini, E., Zriwil, A., Lutteropp, M., Grover, A., Mead, A., Sitnicka, E., Jacobsen, S. E. & Nerlov, C. (2016) Distinct myeloid progenitor-differentiation pathways identified through single-cell RNA sequencing. *Nat Immunol*, 17(6), 666-76.

Druker, B. J., Guilhot, F., O'Brien, S. G., Gathmann, I., Kantarjian, H., Gattermann, N., Deininger, M. W., Silver, R. T., Goldman, J. M., Stone, R. M., Cervantes, F., Hochhaus, A., Powell, B. L., Gabrilove, J. L., Rousselot, P., Reiffers, J., Cornelissen, J. J., Hughes, T., Agis, H., Fischer, T., Verhoef, G., Shepherd, J., Saglio, G., Gratwohl, A., Nielsen, J. L., Radich, J. P., Simonsson, B., Taylor, K., Baccarani, M., So, C., Letvak, L., Larson, R. A. & Investigators, I. (2006) Five-year follow-up of patients receiving imatinib for chronic myeloid leukemia. *N Engl J Med*, 355(23), 2408-17.

Druker, B. J., Tamura, S., Buchdunger, E., Ohno, S., Segal, G. M., Fanning, S., Zimmermann, J. & Lydon, N. B. (1996) Effects of a selective inhibitor of the Abl tyrosine kinase on the growth of Bcr-Abl positive cells. *Nat Med*, 2(5), 561-6.

Duncan, A. W., Rattis, F. M., DiMascio, L. N., Congdon, K. L., Pazianos, G., Zhao, C., Yoon, K., Cook, J. M., Willert, K., Gaiano, N. & Reya, T. (2005) Integration of Notch and Wnt signalling in hematopoietic stem cell maintenance. *Nat Immunol*, 6(3), 314-22.

Eaves, C., Cashman, J. & Eaves, A. (1998) Defective regulation of leukemic hematopoiesis in chronic myeloid leukemia. *Leuk Res*, 22(12), 1085-96.

Ehninger, A., Kramer, M., Rollig, C., Thiede, C., Bornhauser, M., von Bonin, M., Wermke, M., Feldmann, A., Bachmann, M., Ehninger, G., Oelschlagel, U. & Leukemia, S. A. (2014) Distribution and levels of cell surface expression of CD33 and CD123 in acute myeloid leukemia. *Blood Cancer J*, 4, e218.

Ehninger, A. & Trumpp, A. (2011) The bone marrow stem cell niche grows up: mesenchymal stem cells and macrophages move in. *J Exp Med*, 208(3), 421-8.

Eisterer, W., Jiang, X., Christ, O., Glimm, H., Lee, K. H., Pang, E., Lambie, K., Shaw, G., Holyoake, T. L., Petzer, A. L., Auewarakul, C., Barnett, M. J., Eaves, C. J. & Eaves, A. C. (2005) Different subsets of primary chronic myeloid leukemia stem cells engraft immunodeficient mice and produce a model of the human disease. *Leukemia*, 19(3), 435-41.

Eliasson, L., Clifford, S., Barber, N. & Marin, D. (2011) Exploring chronic myeloid leukemia patients' reasons for not adhering to the oral anticancer drug imatinib as prescribed. *Leuk Res*, 35(5), 626-30.

Elliott, M. A., Hanson, C. A., Dewald, G. W., Smoley, S. A., Lasho, T. L. & Tefferi, A. (2005) WHO-defined chronic neutrophilic leukemia: a long-term analysis of 12 cases and a critical review of the literature. *Leukemia*, 19(2), 313-7.

Ellisen, L. W., Bird, J., West, D. C., Soreng, A. L., Reynolds, T. C., Smith, S. D. & Sklar, J. (1991) Tan-1, the Human Homolog of the Drosophila Notch Gene, Is Broken by Chromosomal Translocations in T-Lymphoblastic Neoplasms. *Cell*, 66(4), 649-661.

Eppert, K., Takenaka, K., Lechman, E. R., Waldron, L., Nilsson, B., van Galen, P., Metzeler, K. H., Poeppl, A., Ling, V., Beyene, J., Canty, A. J., Danska, J. S., Bohlander, S. K., Buske, C., Minden, M. D., Golub, T. R., Jurisica, I., Ebert, B. L. & Dick, J. E. (2011) Stem cell gene expression programs influence clinical outcome in human leukemia. *Nat Med*, 17(9), 1086-1091.

Espinoza, I., Pochampally, R., Xing, F., Watabe, K. & Miele, L. (2013) Notch signalling: targeting cancer stem cells and epithelial-to-mesenchymal transition. *Onco Targets Ther*, 6, 1249-1259.

Etet, P. F. S., Vecchio, L. & Kamdje, A. H. N. (2012) Interactions between bone marrow stromal microenvironment and B-chronic lymphocytic leukemia cells: Any role for Notch, Wnt and Hh signalling pathways? *Cell Signal*, 24(7), 1433-1443.

Etienne, G., Guilhot, J., Rea, D., Rigal-Huguet, F., Nicolini, F., Charbonnier, A., Guerci-Bresler, A., Legros, L., Varet, B., Gardembas, M., Dubruille, V., Tulliez, M., Noel, M. P., Ianotto, J. C., Villemagne, B., Carre, M., Guilhot, F., Rousselot, P. & Mahon, F. X. (2017) Long-Term Follow-Up of the French Stop Imatinib (STIM1) Study in Patients With Chronic Myeloid Leukemia. *J Clin Oncol*, 35(3), 298-305.

Fang, B., Zheng, C., Liao, L., Han, Q., Sun, Z., Jiang, X. & Zhao, R. C. (2005) Identification of human chronic myelogenous leukemia progenitor cells with hemangioblastic characteristics. *Blood*, 105(7), 2733-40.

Fefer, A., Cheever, M. A., Thomas, E. D., Boyd, C., Ramberg, R., Glucksberg, H., Buckner, C. D. & Storb, R. (1979) Disappearance of Ph1-positive cells in four patients with chronic granulocytic leukemia after chemotherapy, irradiation and marrow transplantation from an identical twin. *N Engl J Med*, 300(7), 333-7.

Feldmann, G., Dhara, S., Fendrich, V., Bedja, D., Beaty, R., Mullendore, M., Karikari, C., Alvarez, H., Iacobuzio-Donahue, C., Jimeno, A., Gabrielson, K. L., Matsui, W. & Maitra, A. (2007) Blockade of hedgehog signalling inhibits pancreatic cancer invasion and metastases: a new paradigm for combination therapy in solid cancers. *Cancer Res*, 67(5), 2187-96.

Feller, N., van der Pol, M. A., van Stijn, A., Weijers, G. W. D., Westra, A. H., Evertse, B. W., Ossenkoppele, G. J. & Schuurhuis, G. J. (2004) MRD parameters using immunophenotypic detection methods are highly reliable in predicting survival in acute myeloid leukaemia. *Leukemia*, 18(8), 1380-1390.

Ferrandiz, N., Caraballo, J. M., Albajar, M., Gomez-Casares, M. T., Lopez-Jorge, C. E., Blanco, R., Delgado, M. D. & Leon, J. (2010) p21(Cip1) confers resistance to imatinib in human chronic myeloid leukemia cells. *Cancer Lett*, 292(1), 133-9.

Ferreira, R., Ohneda, K., Yamamoto, M. & Philipsen, S. (2005) GATA1 function, a paradigm for transcription factors in hematopoiesis. *Mol Cell Biol*, 25(4), 1215-27.

Fialkow, P. J., Gartler, S. M. & Yoshida, A. (1967) Clonal origin of chronic myelocytic leukemia in man. *Proc Natl Acad Sci U S A*, 58(4), 1468-71.

Fitzgerald, P. H., Pickering, A. F. & Eiby, J. R. (1971) Clonal origin of the Philadelphia chromosome and chronic myeloid leukaemia: evidence from a sex chromosome mosaic. *Br J Haematol*, 21(4), 473-80.

Foley, S. B., Hildenbrand, Z. L., Soyombo, A. A., Magee, J. A., Wu, Y., Oravecz-Wilson, K. I. & Ross, T. S. (2013) Expression of BCR/ABL p210 from a Knockin Allele Enhances Bone Marrow Engraftment without Inducing Neoplasia. *Cell Reports*, 5(1), 51-60.

Foltz, D. R., Santiago, M. C., Berechid, B. E. & Nye, J. S. (2002) Glycogen synthase kinase-3beta modulates notch signalling and stability. *Curr Biol*, 12(12), 1006-11.

Ford, C. E., Ma, S. S. Q., Quadir, A. & Ward, R. L. (2013) The dual role of the novel Wnt receptor tyrosine kinase, ROR2, in human carcinogenesis. *Int J Cancer*, 133(4), 779-787.

Forsberg, E. C., Passegué, E., Prohaska, S. S., Wagers, A. J., Koeva, M., Stuart, J. M. & Weissman, I. L. (2010) Molecular signatures of quiescent, mobilized and leukemia-initiating hematopoietic stem cells. *PLoS One*, 5(1), e8785.

Friedenstein, A. J., Petrakova, K. V., Kurolesova, A. & , F. G. P. (1968) Heterotopic of bone marrow. Analysis of precursor cells for osteogenic and hematopoietic tissues. *Transplantation*, 6(2), 230-47.

Frolova, O., Samudio, I., Benito, J. M., Jacamo, R., Kornblau, S. M., Markovic, A., Schober, W., Lu, H., Qiu, Y. H., Buglio, D., McQueen, T., Pierce, S., Shpall, E., Konoplev, S., Thomas, D., Kantarjian, H., Lock, R., Andreeff, M. & Konopleva, M. (2012) Regulation of HIF-1α signalling and chemoresistance in acute lymphocytic leukemia under hypoxic conditions of the bone marrow microenvironment. *Cancer Biol Ther*, 13(10), 858-70.

Fukushima, N., Minami, Y., Hayakawa, F., Kiyoi, H., Sadarangani, A., Jamieson, C. H. M. & Naoe, T. (2013) Treatment With Hedgehog Inhibitor, PF-04449913, Attenuates Leukemia-Initiation Potential In Acute Myeloid Leukemia Cells. *Blood*, 122(21).

Fukushima, N., Minami, Y., Kakiuchi, S., Kuwatsuka, Y., Hayakawa, F., Jamieson, C., Kiyoi, H. & Naoe, T. (2016) Small-molecule Hedgehog inhibitor attenuates the leukemia-initiation potential of acute myeloid leukemia cells. *Cancer Sci*, 107(10), 1422-1429.

Gainor, J. F. & Chabner, B. A. (2015) Ponatinib: Accelerated Disapproval. *Oncologist*, 20(8), 847-8.

Gallipoli, P., Cook, A., Rhodes, S., Hopcroft, L., Wheadon, H., Whetton, A. D., Jørgensen, H. G., Bhatia, R. & Holyoake, T. L. (2014) JAK2/STAT5 inhibition by nilotinib with ruxolitinib contributes to the elimination of CML CD34+ cells in vitro and in vivo. *Blood*, 124(9), 1492-501.

Galvagni, F., Nardi, F., Maida, M., Bernardini, G., Vannuccini, S., Petraglia, F., Santucci, A. & Orlandini, M. (2016) CD93 and dystroglycan cooperation in human endothelial cell adhesion and migration adhesion and migration. *Oncotarget*, 7(9), 10090-103.

Galy, A., Travis, M., Cen, D. & Chen, B. (1995) Human T, B, Natural killer, and dendritic cells arise from a common bone marrow progenitor cell subset. *Immunity*, 3, 459-473.

Galán-Díez, M., Isa, A., Ponzetti, M., Nielsen, M. F., Kassem, M. & Kousteni, S. (2016) Normal hematopoiesis and lack of β-catenin activation in osteoblasts of patients and mice harboring Lrp5 gain-of-function mutations. *Biochim Biophys Acta*, 1863(3), 490-8.

Gama-Norton, L., Ferrando, E., Ruiz-Herguido, C., Liu, Z., Guiu, J., Islam, A. B., Lee, S. U., Yan, M., Guidos, C. J., López-Bigas, N., Maeda, T., Espinosa, L., Kopan, R. & Bigas, A. (2015) Notch signal strength controls cell fate in the haemogenic endothelium. *Nat Commun*, 6, 8510.

Gambacorti-Passerini, C., Brümmendorf, T. H., Kim, D. W., Turkina, A. G., Masszi, T., Assouline, S., Durrant, S., Kantarjian, H. M., Khoury, H. J., Zaritskey, A., Shen, Z. X., Jin, J., Vellenga, E., Pasquini, R., Mathews, V., Cervantes, F., Besson, N., Turnbull, K., Leip, E., Kelly, V. & Cortes, J. E. (2014) Bosutinib efficacy and safety in chronic phase chronic myeloid leukemia after imatinib resistance or intolerance: Minimum 24-month follow-up. *Am J Hematol*, 89(7), 732-42.

Gang, E. J., Hsieh, Y. T., Pham, J., Zhao, Y., Nguyen, C., Huantes, S., Park, E., Naing, K., Klemm, L., Swaminathan, S., Conway, E. M., Pelus, L. M., Crispino, J., Mullighan, C. G., McMillan, M., Muschen, M., Kahn, M. & Kim, Y. M. (2014) Small-molecule inhibition of CBP/catenin interactions eliminates drug-resistant clones in acute lymphoblastic leukemia. *Oncogene*, 33(17), 2169-2178.

Gao, J., Graves, S., Koch, U., Liu, S., Jankovic, V., Buonamici, S., El Andaloussi, A., Nimer, S. D., Kee, B. L., Taichman, R., Radtke, F. & Aifantis, I. (2009) Hedgehog signalling is dispensable for adult hematopoietic stem cell function. *Cell Stem Cell*, 4(6), 548-58.

Gelebart, P., Popa, M. & McCormack, E. (2016) Xenograft Models of Primary Acute Myeloid Leukemia for the Development of Imaging Strategies and Evaluation of Novel Targeted Therapies. *Curr Pharm Biotechnol*, 17(1), 42-51.

Gerber, J. M., Gucwa, J. L., Esopi, D., Gurel, M., Haffner, M. C., Vala, M., Nelson, W. G., Jones, R. J. & Yegnasubramanian, S. (2013) Genome-wide comparison of the transcriptomes of highly enriched normal and chronic myeloid leukemia stem and progenitor cell populations. *Oncotarget*, 4(5), 715-728.

Giambra, V., Jenkins, C. E., Lam, S. H., Hoofd, C., Belmonte, M., Wang, X., Gusscott, S., Gracias, D. & Weng, A. P. (2015) Leukemia stem cells in T-ALL require active Hif1α and Wnt signalling. *Blood*, 125(25), 3917-27.

Gibbons, D. L., Pricl, S., Posocco, P., Laurini, E., Fermeglia, M., Sun, H., Talpaz, M., Donato, N. & Quintás-Cardama, A. (2014) Molecular dynamics reveal BCR-ABL1 polymutants as a unique mechanism of resistance to PAN-BCR-ABL1 kinase inhibitor therapy. *Proc Natl Acad Sci U S A*, 111(9), 3550-5.

Giles, F. J., O'Dwyer, M. & Swords, R. (2009) Class effects of tyrosine kinase inhibitors in the treatment of chronic myeloid leukemia. *Leukemia*, 23(10), 1698-707.

Gill, S., Tasian, S. K., Ruella, M., Shestova, O., Li, Y., Porter, D. L., Carroll, M., Danet-Desnoyers, G., Scholler, J., Grupp, S. A., June, C. H. & Kalos, M. (2014) Preclinical targeting of human acute myeloid leukemia and myeloablation using chimeric antigen receptor-modified T cells. *Blood*, 123(15), 2343-54.

Giotopoulos, G., van der Weyden, L., Osaki, H., Rust, A. G., Gallipoli, P., Meduri, E., Horton, S. J., Chan, W. I., Foster, D., Prinjha, R. K., Pimanda, J. E., Tenen, D. G., Vassiliou, G. S., Koschmieder, S., Adams, D. J. & Huntly, B. J. (2015) A novel mouse model identifies cooperating mutations and therapeutic targets critical for chronic myeloid leukemia progression. *J Exp Med*, 212(10), 1551-69.

Giustacchini, A., Thongjuea, S., Barkas, N., Woll, P. S., Povinelli, B. J., Booth, C. A. G., Sopp, P., Norfo, R., Rodriguez-Meira, A., Ashley, N., Jamieson, L., Vyas, P., Anderson, K., Segerstolpe, Å., Qian, H., Olsson-Strömberg, U., Mustjoki, S., Sandberg, R., Jacobsen, S. E. W. & Mead, A. J. (2017) Single-cell transcriptomics uncovers distinct molecular signatures of stem cells in chronic myeloid leukemia. Nat Med, 23(6), 692-702.

Goessling, W., North, T. E., Loewer, S., Lord, A. M., Lee, S., Stoick-Cooper, C. L., Weidinger, G., Puder, M., Daley, G. Q., Moon, R. T. & Zon, L. I. (2009) Genetic Interaction of PGE2 and Wnt Signalling Regulates Developmental Specification of Stem Cells and Regeneration. *Cell*, 136(6), 1136-1147.

Golas, J. M., Arndt, K., Etienne, C., Lucas, J., Nardin, D., Gibbons, J., Frost, P., Ye, F., Boschelli, D. H. & Boschelli, F. (2003) SKI-606, a 4-anilino-3-quinolinecarbonitrile dual inhibitor of Src and Abl kinases, is a potent antiproliferative agent against chronic myelogenous leukemia cells in culture and causes regression of K562 xenografts in nude mice. *Cancer Res*, 63(2), 375-81.

Goldman, J. M., Baughan, A. S., McCarthy, D. M., Worsley, A. M., Hows, J. M., Gordon-Smith, E. C., Catovsky, D., Batchelor, J. R., Goolden, A. W. & Galton, D. A. (1982) Marrow transplantation for patients in the chronic phase of chronic granulocytic leukaemia. *Lancet*, 2(8299), 623-5.

Goodell, M. A., Brose, K., Paradis, G., Conner, A. S. & Mulligan, R. C. (1996) Isolation and functional properties of murine hematopoietic stem cells that are replicating in vivo. *J Exp Med*, 183(4), 1797-806.

Gordon, M. Y., Marley, S. B., Apperley, J. F., Marin, D., Kaeda, J., Szydlo, R. & Goldman, J. M. (2003) Clinical heterogeneity in chronic myeloid leukaemia reflecting biological diversity in normal persons. *Br J Haematol*, 122(3), 424-9.

Graham, S. M. (2002) Primitive, quiescent, Philadelphia-positive stem cells from patients with chronic myeloid leukemia are insensitive to STI571 in vitro. *Blood*, 99(1), 319-325.

Graham, S. M., Jorgensen, H. G., Allan, E., Pearson, C., Alcorn, M. J., Holyoake, T. L. & Richmond, L. (2008) Primitive, quiescent, Philadelphia-positive stem cells from patients with chronic myeloid leukemia are insensitive to STI571 in vitro. *Blood*, 99(1), 319-325.

Graham, S. M., Vass, J. K., Holyoake, T. L. & Graham, G. J. (2007) Transcriptional analysis of quiescent and proliferating CD34+ human hemopoietic cells from normal and chronic myeloid leukemia sources. *Stem cells*, 25(12), 3111-20.

Greenlee-Wacker, M. C., Briseo, C., Galvan, M., Moriel, G., Velzquez, P. & Bohlson, S. S. (2011) Membrane-Associated CD93 Regulates Leukocyte Migration and C1q-Hemolytic Activity during Murine Peritonitis. *J Immunol*, 187(6), 3353-3361.

Gregory, M. A., Phang, T. L., Neviani, P., Alvarez-Calderon, F., Eide, C. A., O'Hare, T., Zaberezhnyy, V., Williams, R. T., Druker, B. J., Perrotti, D. & Degregori, J. (2010) Wnt/Ca2+/NFAT signalling maintains survival of Ph+ leukemia cells upon inhibition of Bcr-Abl. *Cancer Cell*, 18(1), 74-87.

Grier, D. G., Thompson, A., Kwasniewska, A., McGonigle, G. J., Halliday, H. L. & Lappin, T. R. (2005) The pathophysiology of HOX genes and their role in cancer. *J Pathol*, 205(2), 154-171.

Grimes, C. A. & Jope, R. S. (2001) The multifaceted roles of glycogen synthase kinase 3beta in cellular signalling. *Prog Neurobiol*, 65(4), 391-426.

Groffen, J., Stephenson, J. R., Heisterkamp, N., de Klein, A., Bartram, C. R. & Grosveld, G. (1984) Philadelphia chromosomal breakpoints are clustered within a limited region, bcr, on chromosome 22. *Cell*, 36(1), 93-9.

Gunsilius, E., Duba, H. C., Petzer, A. L., Kahler, C. M., Grunewald, K., Stockhammer, G., Gabl, C., Dirnhofer, S., Clausen, J. & Gastl, G. (2000) Evidence from a leukaemia model for maintenance of vascular endothelium by bone-marrow-derived endothelial cells. *Lancet*, 355(9216), 1688-91.

Guo, G., Luc, S., Marco, E., Lin, T. W., Peng, C., Kerenyi, M. A., Beyaz, S., Kim, W., Xu, J., Das, P. P., Neff, T., Zou, K., Yuan, G. C. & Orkin, S. H. (2013) Mapping cellular hierarchy by single-cell analysis of the cell surface repertoire. *Cell Stem Cell*, 13(4), 492-505.

Gustafsson, M. V., Zheng, X., Pereira, T., Gradin, K., Jin, S., Lundkvist, J., Ruas, J. L., Poellinger, L., Lendahl, U. & Bondesson, M. (2005) Hypoxia requires notch signalling to maintain the undifferentiated cell state. *Dev Cell*, 9(5), 617-28.

Gutierrez, A., Sanda, T., Ma, W., Zhang, J., Grebliunaite, R., Dahlberg, S., Neuberg, D., Protopopov, A., Winter, S. S., Larson, R. S., Borowitz, M. J., Silverman, L. B., Chin, L., Hunger, S. P., Jamieson, C., Sallan, S. E. & Look, A. T. (2010a) Inactivation of LEF1 in T-cell acute lymphoblastic leukemia. *Blood*, 115(14), 2845-51.

Gutierrez, A., Tschumper, R. C., Wu, X., Shanafelt, T. D., Eckel-Passow, J., Huddleston, P. M., Slager, S. L., Kay, N. E. & Jelinek, D. F. (2010b) LEF-1 is a prosurvival factor in chronic lymphocytic leukemia and is expressed in the preleukemic state of monoclonal B-cell lymphocytosis. *Blood*, 116(16), 2975-83.

Hahn, W. C. & Weinberg, R. A. (2002) Rules for making human tumor cells. *N Engl J Med*, 347(20), 1593-603.

Haltiwanger, R. S. & Stanley, P. (2002) Modulation of receptor signalling by glycosylation: fringe is an O-fucose-beta1,3-N-acetylglucosaminyltransferase. *Biochim Biophys Acta*, 1573(3), 328-35.

Hamilton, A., Helgason, G. V., Schemionek, M., Zhang, B., Myssina, S., Allan, E. K., Nicolini, F. E., Muller-Tidow, C., Bhatia, R., Brunton, V. G., Koschmieder, S. & Holyoake, T. L. (2012) Chronic myeloid leukemia stem cells are not dependent on Bcr-Abl kinase activity for their survival. *Blood*, 119(6), 1501-1510.

Hanfstein, B., Müller, M. C., Hehlmann, R., Erben, P., Lauseker, M., Fabarius, A., Schnittger, S., Haferlach, C., Göhring, G., Proetel, U., Kolb, H. J., Krause, S. W., Hofmann, W. K., Schubert, J., Einsele, H., Dengler, J., Hänel, M., Falge, C., Kanz, L., Neubauer, A., Kneba, M., Stegelmann, F., Pfreundschuh, M., Waller, C. F., Branford, S., Hughes, T. P., Spiekermann, K., Baerlocher, G. M., Pfirrmann, M., Hasford, J., Saußele, S., Hochhaus, A., SAKK & Group, G. C. S. (2012) Early molecular and cytogenetic response is predictive for long-term progression-free and overall survival in chronic myeloid leukemia (CML). *Leukemia*, 26(9), 2096-102.

Hannon, M. M., Lohan, F., Erbilgin, Y., Sayitoglu, M., O'Hagan, K., Mills, K., Ozbek, U. & Keeshan, K. (2012) Elevated TRIB2 with NOTCH1 activation in paediatric/adult T-ALL. *Br J Haematol*, 158(5), 626-634.

Hantschel, O. (2012) Structure, regulation, signalling, and targeting of abl kinases in cancer. *Genes Cancer*, 3(5-6), 436-46.

Hantschel, O., Rix, U., Schmidt, U., Bürckstümmer, T., Kneidinger, M., Schütze, G., Colinge, J., Bennett, K. L., Ellmeier, W., Valent, P. & Superti-Furga, G. (2007) The Btk tyrosine kinase is a major target of the Bcr-Abl inhibitor dasatinib. *Proc Natl Acad Sci U S A*, 104(33), 13283-8.

Hantschel, O. & Superti-Furga, G. (2004) Regulation of the c-Abl and Bcr-Abl tyrosine kinases. *Nat Rev Mol Cell Biol*, 5(1), 33-44.

Hantschel, O., Warsch, W., Eckelhart, E., Kaupe, I., Grebien, F., Wagner, K.-U., Superti-Furga, G. & Sexl, V. (2012) BCR-ABL uncouples canonical JAK2-STAT5 signalling in chronic myeloid leukemia. *Nat Chem Biol*, 8(3), 285-93.

Hao, Q. L., Shah, A. J., Thiemann, F. T., Smogorzewska, E. M. & Crooks, G. M. (1995) A functional comparison of CD34 + CD38- cells in cord blood and bone marrow. *Blood*, 86(10), 3745-53.

Hasemann, M. S., Lauridsen, F. K., Waage, J., Jakobsen, J. S., Frank, A. K., Schuster, M. B., Rapin, N., Bagger, F. O., Hoppe, P. S., Schroeder, T. & Porse, B. T. (2014) C/EBPα is required for long-term self-renewal and lineage priming of hematopoietic stem cells and for the maintenance of epigenetic configurations in multipotent progenitors. *PLoS Genet*, 10(1), e1004079.

Hehlmann, R., Heimpel, H., Hasford, J., Kolb, H. J., Pralle, H., Hossfeld, D. K., Queisser, W., Löffler, H., Heinze, B. & Georgii, A. (1993) Randomized comparison of busulfan and hydroxyurea in chronic myelogenous leukemia: prolongation of survival by hydroxyurea. The German CML Study Group. *Blood*, 82(2), 398-407.

Hehlmann, R., Ansari, H., Adelberger, V., Heinze, B., Hossfeld, K., Hochhaus, A. & Heimpel, H. (1994a) New perspectives with interferon alpha. The German CML study group experience. *Bone Marrow Transplant*, 14(3), S14-20.

Hehlmann, R., Heimpel, H., Hasford, J., Kolb, H. J., Pralle, H., Hossfeld, D. K., Queisser, W., Löffler, H., Hochhaus, A. & Heinze, B. (1994b) Randomized comparison of interferon-alpha with busulfan and hydroxyurea in chronic myelogenous leukemia. The German CML Study Group. *Blood*, 84(12), 4064-77.

Hehlmann, R., Berger, U., Pfirrmann, M., Hochhaus, A., Metzgeroth, G., Maywald, O., Hasford, J., Reiter, A., Hossfeld, D. K., Kolb, H. J., Löffler, H., Pralle, H., Queisser, W., Griesshammer, M., Nerl, C., Kuse, R., Tobler, A., Eimermacher, H., Tichelli, A., Aul, C., Wilhelm, M., Fischer, J. T., Perker, M., Scheid, C., Schenk, M., Weiss, J., Meier, C. R., Kremers, S., Labedzki, L., Schmeiser, T., Lohrmann, H. P., Heimpel, H. & Group, G. C.-S. (2003) Randomized comparison of interferon alpha and hydroxyurea with hydroxyurea monotherapy in chronic myeloid leukemia (CML-study II): prolongation of survival by the combination of interferon alpha and hydroxyurea. *Leukemia*, 17(8), 1529-37.

Hehlmann, R., Lauseker, M., Jung-Munkwitz, S., Leitner, A., Müller, M. C., Pletsch, N., Proetel, U., Haferlach, C., Schlegelberger, B., Balleisen, L., Hänel, M., Pfirrmann, M., Krause, S. W., Nerl, C., Pralle, H., Gratwohl, A., Hossfeld, D. K., Hasford, J., Hochhaus, A. & Saussele, S. (2011) Tolerability-adapted imatinib 800 mg/d versus 400 mg/d versus 400 mg/d plus interferon-α in newly diagnosed chronic myeloid leukemia. *J Clin Oncol*, 29(12), 1634-42.

Hehlmann, R. (2012) How I treat CML blast crisis. *Blood*, 120(4), 737-47.

Hehlmann, R., Müller, M. C., Lauseker, M., Hanfstein, B., Fabarius, A., Schreiber, A., Proetel, U., Pletsch, N., Pfirrmann, M., Haferlach, C., Schnittger, S., Einsele, H., Dengler, J., Falge, C., Kanz, L., Neubauer, A., Kneba, M., Stegelmann, F., Pfreundschuh, M., Waller, C. F., Spiekermann, K., Baerlocher, G. M., Ehninger, G., Heim, D., Heimpel, H., Nerl, C., Krause, S. W., Hossfeld, D. K., Kolb, H. J., Hasford, J., Saußele, S. & Hochhaus, A. (2014) Deep molecular response is reached by the majority of patients treated with imatinib, predicts survival, and is achieved more quickly by optimized high-dose imatinib: results from the randomized CML-study IV. *J Clin Oncol*, 32(5), 415-23.

Heidel, F. H., Bullinger, L., Feng, Z. H., Wang, Z., Neff, T. A., Stein, L., Kalaitzidis, D., Lane, S. W. & Armstrong, S. A. (2012) Genetic and Pharmacologic Inhibition of beta-Catenin Targets Imatinib-Resistant Leukemia Stem Cells in CML. *Cell Stem Cell*, 10(4), 412-424.

Heisterkamp, N., Stephenson, J. R., Groffen, J., Hansen, P. F., de Klein, A., Bartram, C. R. & Grosveld, G. (1983) Localization of the c-ab1 oncogene adjacent to a translocation break point in chronic myelocytic leukaemia. *Nature*, 306(5940), 239-42.

Herpin, A. & Cunningham, C. (2007) Cross-talk between the bone morphogenetic protein pathway and other major signalling pathways results in tightly regulated cell-specific outcomes. *FEBS J*, 274(12), 2977-85.

Herrmann, H., Sadovnik, I., Cerny-reiterer, S., Thomas, R., Stefanzl, G., Willmann, M., Hoermann, G., Bilban, M., Blatt, K., Herndlhofer, S., Mayerhofer, M., Streubel, B., Sperr, W. R., Holyoake, T. L., Mannhalter, C. & Valent, P. (2015) Dipeptidylpeptidase IV (CD26) defines leukemic stem cells (LSC) in chronic myeloid leukemia. *Blood*, 123(25), 3951-3963.

Hicks, C., Johnston, S. H., diSibio, G., Collazo, A., Vogt, T. F. & Weinmaster, G. (2000) Fringe differentially modulates Jagged1 and Delta1 signalling through Notch1 and Notch2. *Nat Cell Biol*, 2(8), 515-20.

Ho, T. C., LaMere, M., Stevens, B. M., Ashton, J. M., Myers, J. R., O'Dwyer, K. M., Liesveld, J. L., Mendler, J. H., Guzman, M., Morrissette, J. D., Zhao, J. H., Wang, E. S., Wetzler, M., Jordan, C. T. & Becker, M. W. (2016) Evolution of acute myelogenous leukemia stem cell properties after treatment and progression. *Blood*, 128(13), 1671-1678.

Hochhaus, A., O'Brien, S. G., Guilhot, F., Druker, B. J., Branford, S., Foroni, L., Goldman, J. M., Müller, M. C., Radich, J. P., Rudoltz, M., Mone, M., Gathmann, I., Hughes, T. P., Larson, R. A. & Investigators, I. (2009) Six-year follow-up of patients receiving imatinib for the first-line treatment of chronic myeloid leukemia. *Leukemia*, 23(6), 1054-61.

Hochhaus, A., Saglio, G., Hughes, T. P., Larson, R. A., Kim, D. W., Issaragrisil, S., le Coutre, P. D., Etienne, G., Dorlhiac-Llacer, P. E., Clark, R. E., Flinn, I. W., Nakamae, H., Donohue, B., Deng, W., Dalal, D., Menssen, H. D. & Kantarjian, H. M. (2016) Long-term benefits and risks of frontline nilotinib vs imatinib for chronic myeloid leukemia in chronic phase: 5-year update of the randomized ENESTnd trial. *Leukemia*, 30(5), 1044-54.

Hock, H., Meade, E., Medeiros, S., Schindler, J. W., Valk, P. J., Fujiwara, Y. & Orkin, S. H. (2004) Tel/Etv6 is an essential and selective regulator of adult hematopoietic stem cell survival. *Genes Dev*, 18(19), 2336-41.

Hoesel, B. & Schmid, J. A. (2013) The complexity of NF-κB signalling in inflammation and cancer. *Mol Cancer*, 12, 86.

Hoffmann, V. S., Baccarani, M., Hasford, J., Lindoerfer, D., Burgstaller, S., Sertic, D., Costeas, P., Mayer, J., Indrak, K., Everaus, H., Koskenvesa, P., Guilhot, J., Schubert-Fritschle, G., Castagnetti, F., Di Raimondo, F., Lejniece, S., Griskevicius, L., Thielen, N., Sacha, T., Hellmann, A., Turkina, A. G., Zaritskey, A., Bogdanovic, A., Sninska, Z., Zupan, I., Steegmann, J. L., Simonsson, B., Clark, R. E., Covelli, A., Guidi, G. & Hehlmann, R. (2015) The EUTOS population-based registry: incidence and clinical characteristics of 2904 CML patients in 20 European Countries. *Leukemia*, 29(6), 1336-43.

Hofmann, I., Stover, E. H., Cullen, D. E., Mao, J., Morgan, K. J., Lee, B. H., Kharas, M. G., Miller, P. G., Cornejo, M. G., Okabe, R., Armstrong, S. A., Ghilardi, N., Gould, S., de Sauvage, F. J., McMahon, A. P. & Gilliland, D. G. (2009) Hedgehog Signalling Is Dispensable for Adult Murine Hematopoietic Stem Cell Function and Hematopoiesis. *Cell Stem Cell*, 4(6), 559-567.

Hogan, C. J., Shpall, E. J. & Keller, G. (2002) Differential long-term and multilineage engraftment potential from subfractions of human CD34+ cord blood cells transplanted into NOD/SCID mice. *Proc Natl Acad Sci U S A*, 99(1), 413-8.

Holyoake, T., Jiang, X., Eaves, C. & Eaves, A. (1999) Isolation of a highly quiescent subpopulation of primitive leukemic cells in chronic myeloid leukemia. *Blood*, 94(6), 2056-64.

Holyoake, T. L. & Vetrie, D. (2017) The chronic myeloid leukemia stem cell: stemming the tide of persistence. *Blood*, 129(12), 1595-1606.

Hong, S. H., Yang, S. J., Kim, T. M., Shim, J. S., Lee, H. S., Lee, G. Y., Park, B. B., Nam, S. W., Ryoo, Z. Y. & Oh, I. H. (2014) Molecular integration of HoxB4 and STAT3 for self-renewal of hematopoietic stem cells: a model of molecular convergence for stemness. *Stem Cells*, 32(5), 1313-22.

Horne, G. A., Jackson, L., Helgason, V. & Holyoake, T. L. (2017) Stem Cell Guardians - Old and New Perspectives in LSC Biology. *Curr Drug Targets*, 18(4), 405-413.

Horne, G. A., Morrison, H., Campbell, V. L., Kinstrie, R., Cassels, J., Hair, A., Vetrie, D., Wheadon, H., Holyoake, T. L. & Copland, M. (2016) Notch Pathway Activation Targets Leukemic Stem Cells in Chronic-Phase Chronic Myeloid Leukemia (CP-CML). *Blood*, 128, 3057.

Hosen, N., Park, C. Y., Tatsumi, N., Oji, Y., Sugiyama, H., Gramatzki, M., Krensky, A. M. & Weissman, I. L. (2007) CD96 is a leukemic stem cell-specific marker in human acute myeloid leukemia. *Proc Natl Acad Sci U S A*, 104(26), 11008-11013.

Hovorkova, L., Zaliova, M., Venn, N. C., Bleckmann, K., Trkova, M., Potuckova, E., Vaskova, M., Linhartova, J., Machova Polakova, K., Fronkova, E., Muskovic, W., Giles, J. E., Shaw, P. J., Cario, G., Sutton, R., Stary, J., Trka, J. & Zuna, J. (2017) Monitoring of childhood ALL using BCR-ABL1 genomic breakpoints identifies a subgroup with CML-like biology. *Blood*, 129(20), 2771-2781.

Hu, Y., Liu, Y., Pelletier, S., Buchdunger, E., Warmuth, M., Fabbro, D., Hallek, M., Van Etten, R. A. & Li, S. (2004) Requirement of Src kinases Lyn, Hck and Fgr for BCR-ABL1-induced B-lymphoblastic leukemia but not chronic myeloid leukemia. *Nat Genet*, 36(5), 453-61.

Hu, Y., Swerdlow, S., Duffy, T. M., Weinmann, R., Lee, F. Y. & Li, S. (2006) Targeting multiple kinase pathways in leukemic progenitors and stem cells is essential for improved treatment of Ph+ leukemia in mice. *Proc Natl Acad Sci U S A*, 103(45), 16870-5.

Huang, S. & Terstappen, L. W. (1994a) Formation of haematopoietic microenvironment and haematopoietic stem cells from single human bone marrow stem cells. *Nature*, 368(6472), 664.

Huang, S. & Terstappen, L. W. (1994b) Lymphoid and myeloid differentiation of single human CD34+, HLA-DR+, CD38- hematopoietic stem cells. *Blood*, 83(6), 1515-26.

Hughes, T., Deininger, M., Hochhaus, A., Branford, S., Radich, J., Kaeda, J., Baccarani, M., Cortes, J., Cross, N. C., Druker, B. J., Gabert, J., Grimwade, D., Hehlmann, R., Kamel-Reid, S., Lipton, J. H., Longtine, J., Martinelli, G., Saglio, G., Soverini, S., Stock, W. & Goldman, J. M.

(2006) Monitoring CML patients responding to treatment with tyrosine kinase inhibitors: review and recommendations for harmonizing current methodology for detecting BCR-ABL transcripts and kinase domain mutations and for expressing results. *Blood*, 108(1), 28-37.

Hughes, T. P., Hochhaus, A., Branford, S., Müller, M. C., Kaeda, J. S., Foroni, L., Druker, B. J., Guilhot, F., Larson, R. A., O'Brien, S. G., Rudoltz, M. S., Mone, M., Wehrle, E., Modur, V., Goldman, J. M., Radich, J. P. & investigators, I. (2010) Long-term prognostic significance of early molecular response to imatinib in newly diagnosed chronic myeloid leukemia: an analysis from the International Randomized Study of Interferon and STI571 (IRIS). *Blood*, 116(19), 3758-65.

Hughes, T. P., Lipton, J. H., Spector, N., Cervantes, F., Pasquini, R., Clementino, N. C., Dorlhiac Llacer, P. E., Schwarer, A. P., Mahon, F. X., Rea, D., Branford, S., Purkayastha, D., Collins, L., Szczudlo, T. & Leber, B. (2014) Deep molecular responses achieved in patients with CML-CP who are switched to nilotinib after long-term imatinib. *Blood*, 124(5), 729-36.

Hunger, S. P. (2017) CML in blast crisis: more common than we think? *Blood*, 129(20), 2713-2714.

Huntly, B. J. & Gilliland, D. G. (2005) Leukaemia stem cells and the evolution of cancer-stem-cell research. *Nat Rev Cancer*, 5(4), 311-21.

Huntly, B. J., Shigematsu, H., Deguchi, K., Lee, B. H., Mizuno, S., Duclos, N., Rowan, R., Amaral, S., Curley, D., Williams, I. R., Akashi, K. & Gilliland, D. G. (2004) MOZ-TIF2, but not BCR-ABL, confers properties of leukemic stem cells to committed murine hematopoietic progenitors. *Cancer Cell*, 6(6), 587-96.

Ibrahim, A. R., Eliasson, L., Apperley, J. F., Milojkovic, D., Bua, M., Szydlo, R., Mahon, F. X., Kozlowski, K., Paliompeis, C., Foroni, L., Khorashad, J. S., Bazeos, A., Molimard, M., Reid, A., Rezvani, K., Gerrard, G., Goldman, J. & Marin, D. (2011) Poor adherence is the main reason for loss of CCyR and imatinib failure for chronic myeloid leukemia patients on long-term therapy. *Blood*, 117(14), 3733-6.

Ikewaki, N., Yamao, H., Kulski, J. K. & Inoko, H. (2010) Flow cytometric identification of CD93 expression on naive T lymphocytes (CD4+CD45RA+ Cells) in human neonatal umbilical cord blood. *J Clin Immunol*, 30(5), 723-733.

Ilaria, R. L. (2005) Pathobiology of lymphoid and myeloid blast crisis and management issues. *Hematology Am Soc Hematol Educ Program*, 188-94.

Imagawa, J., Tanaka, H., Okada, M., Nakamae, H., Hino, M., Murai, K., Ishida, Y., Kumagai, T., Sato, S., Ohashi, K., Sakamaki, H., Wakita, H., Uoshima, N., Nakagawa, Y., Minami, Y., Ogasawara, M., Takeoka, T., Akasaka, H., Utsumi, T., Uike, N., Sato, T., Ando, S., Usuki, K., Morita, S., Sakamoto, J., Kimura, S. & Group, D. T. (2015) Discontinuation of dasatinib in patients with chronic myeloid leukaemia who have maintained deep molecular response for longer than 1 year (DADI trial): a multicentre phase 2 trial. *Lancet Haematol*, 2(12), e528-35.

Imai, T., Tokunaga, A., Yoshida, T., Hashimoto, M., Mikoshiba, K., Weinmaster, G. & Nakafuku, M. (2001) The Neural RNA-Binding Protein Musashi1 Translationally Regulates

Mammalian numb Gene Expression by Interacting with Its mRNA. *Mol Cell Biol*, 21(12), 3888-3900.

Irvine, D. A. & Copland, M. (2012) Targeting hedgehog in hematologic malignancy. *Blood*, 119(10), 2196-204.

Irvine, D. A., Zhang, B., Kinstrie, R., Tarafdar, A., Morrison, H., Campbell, V. L., Moka, H. A., Ho, Y. W., Nixon, C., Manley, P. W., Wheadon, H., Goodlad, J. R., Holyoake, T. L., Bhatia, R. & Copland, M. (2016) Deregulated hedgehog pathway signalling is inhibited by the smoothened antagonist LDE225 (Sonidegib) in chronic phase chronic myeloid leukaemia. *Scientific Reports*, 6, 25476.

Ischenko, I., Seeliger, H., Schaffer, M., Jauch, K. W. & Bruns, C. J. (2008) Cancer stem cells: how can we target them? *Curr Med Chem*, 15(30), 3171-84.

Ito, T., Kwon, H. Y., Zimdahl, B., Congdon, K. L., Blum, J., Lento, W. E., Zhao, C., Lagoo, A., Gerrard, G., Foroni, L., Goldman, J., Goh, H., Kim, S.-H., Kim, D.-W., Chuah, C., Oehler, V. G., Radich, J. P., Jordan, C. T. & Reya, T. (2010) Regulation of myeloid leukaemia by the cell-fate determinant Musashi. *Nature*, 466(7307), 765-8.

Ivey, A., Hills, R. K., Simpson, M. A., Jovanovic, J. V., Gilkes, A., Grech, A., Patel, Y., Bhudia, N., Farah, H., Mason, J., Wall, K., Akiki, S., Griffiths, M., Solomon, E., McCaughan, F., Linch, D. C., Gale, R. E., Vyas, P., Freeman, S. D., Russell, N., Burnett, A. K., Grimwade, D. & Inst, U. N. C. R. (2016) Assessment of Minimal Residual Disease in Standard-Risk AML. *N Eng J Med*, 374(5), 422-433.

Iwasaki, M., Liedtke, M., Gentles, A. J. & Cleary, M. L. (2015) CD93 Marks a Non-Quiescent Human Leukemia Stem Cell Population and Is Required for Development of MLL-Rearranged Acute Myeloid Leukemia. *Cell Stem Cell*, 17(4), 412-421.

Jabbour, E. & Kantarjian, H. (2014) Chronic myeloid leukemia: 2014 update on diagnosis, monitoring, and management. *Am J Hematol*, 89(5), 547-56.

Jabbour, E., Kantarjian, H., Jones, D., Talpaz, M., Bekele, N., O'Brien, S., Zhou, X., Luthra, R., Garcia-Manero, G., Giles, F., Rios, M. B., Verstovsek, S. & Cortes, J. (2006) Frequency and clinical significance of BCR-ABL mutations in patients with chronic myeloid leukemia treated with imatinib mesylate. *Leukemia*, 20(10), 1767-73.

Jabbour, E., Kantarjian, H. M., Saglio, G., Steegmann, J. L., Shah, N. P., Boqué, C., Chuah, C., Pavlovsky, C., Mayer, J., Cortes, J., Baccarani, M., Kim, D. W., Bradley-Garelik, M. B., Mohamed, H., Wildgust, M. & Hochhaus, A. (2014) Early response with dasatinib or imatinib in chronic myeloid leukemia: 3-year follow-up from a randomized phase 3 trial (DASISION). *Blood*, 123(4), 494-500.

Jaiswal, S., Jamieson, C. H., Pang, W. W., Park, C. Y., Chao, M. P., Majeti, R., Traver, D., van Rooijen, N. & Weissman, I. L. (2009) CD47 is upregulated on circulating hematopoietic stem cells and leukemia cells to avoid phagocytosis. *Cell*, 138(2), 271-85.

Jaleco, A. C., Neves, H., Hooijberg, E., Gameiro, P., Clode, N., Haury, M., Henrique, D. & Parreira, L. (2001) Differential effects of Notch ligands Delta-1 and Jagged-1 in human lymphoid differentiation. *J Exp Med*, 194(7), 991-1002.

Jamieson, C. (2010) Split ends in CML: divergent roles of Hes1. *Blood*, 115(14), 2726-7.

Jamieson, C., Cortes, J. E., Oehler, V., Baccarani, M., Kantarjian, H. M., Papayannidis, C., Rice, K. N., Zhang, X., Shaik, N., Courtney, R., Levin, W. J. & Martinelli, G. (2011) Phase 1 Dose-Escalation Study of PF-04449913, An Oral Hedgehog (Hh) Inhibitor, in Patients with Select Hematologic Malignancies. *Blood*, 118, 424.

Jamieson, C. H., Ailles, L. E., Dylla, S. J., Muijtjens, M., Jones, C., Zehnder, J. L., Gotlib, J., Li, K., Manz, M. G., Keating, A., Sawyers, C. L. & Weissman, I. L. (2004) Granulocyte-macrophage progenitors as candidate leukemic stem cells in blast-crisis CML. *N Engl J Med*, 351(7), 657-67.

Jeon, J. W., Jung, J. G., Shin, E. C., Choi, H. I., Kim, H. Y., Cho, M. L., Kim, S. W., Jang, Y. S., Sohn, M. H., Moon, J. H., Cho, Y. H., Hoe, K. L., Seo, Y. S. & Park, Y. W. (2010) Soluble CD93 induces differentiation of monocytes and enhances TLR responses. *J Immunol*, 185(8), 4921-7.

Jia, J., Amanai, K., Wang, G., Tang, J., Wang, B. & Jiang, J. (2002) Shaggy/GSK3 antagonizes Hedgehog signalling by regulating Cubitus interruptus. *Nature*, 416(6880), 548-52.

Jordan, C. T., Guzman, M. L. & Noble, M. (2006) Mechanisms of disease - Cancer stem cells. *N Eng J Med*, 355(12), 1253-1261.

Jordan, C. T., Upchurch, D., Szilvassy, S. J., Guzman, M. L., Howard, D. S., Pettigrew, A. L., Meyerrose, T., Rossi, R., Grimes, B., Rizzieri, D. A., Luger, S. M. & Phillips, G. L. (2000) The interleukin-3 receptor alpha chain is a unique marker for human acute myelogenous leukemia stem cells. *Leukemia*, 14(10), 1777-1784.

Järås, M., Johnels, P., Hansen, N., Agerstam, H., Tsapogas, P., Rissler, M., Lassen, C., Olofsson, T., Bjerrum, O. W., Richter, J. & Fioretos, T. (2010) Isolation and killing of candidate chronic myeloid leukemia stem cells by antibody targeting of IL-1 receptor accessory protein. *Proc Natl Acad Sci U S A*, 107(37), 16280-5.

Kalaszczynska, I., Geng, Y., Iino, T., Mizuno, S., Choi, Y., Kondratiuk, I., Silver, D. P., Wolgemuth, D. J., Akashi, K. & Sicinski, P. (2009) Cyclin A is redundant in fibroblasts but essential in hematopoietic and embryonic stem cells. *Cell*, 138(2), 352-65.

Kamdje, A. H. N. & Krampera, M. (2011) Notch signalling in acute lymphoblastic leukemia: any role for stromal microenvironment? *Blood*, 118(25), 6506-6514.

Kamdje, A. H. N., Mosna, F., Bifari, F., Lisi, V., Bassi, G., Malpeli, G., Ricciardi, M., Perbellini, O., Scupoli, M. T., Pizzolo, G. & Krampera, M. (2011) Notch-3 and Notch-4 signalling rescue from apoptosis human B-ALL cells in contact with human bone marrow-derived mesenchymal stromal cells. *Blood*, 118(2), 380-389.

Kampen, K. R. (2012) The discovery and early understanding of leukemia. *Leuk Res*, 36(1), 6-13.

Kang, J. A., Kim, W. S. & Park, S. G. (2014) Notch1 is an important mediator for enhancing of B-cell activation and antibody secretion by Notch ligand. *Immunology*, 143(4), 550-9.

Kang, Y., Chao, N. J. & Aversa, F. (2008) Unmanipulated or CD34 selected haplotype mismatched transplants. *Curr Opin Hematol*, 15(6), 561-7.

Kannan, S., Sutphin, R. M., Hall, M. G., Golfman, L. S., Fang, W., Nolo, R. M., Akers, L. J., Hammitt, R. A., McMurray, J. S., Kornblau, S. M., Melnick, A. M., Figueroa, M. E. & Zweidler-McKay, P. A. (2013) Notch activation inhibits AML growth and survival: a potential therapeutic approach. *J Exp Med*, 210(2), 321-337.

Kantarjian, H. & Cortes, J. (2011) Considerations in the management of patients with Philadelphia chromosome-positive chronic myeloid leukemia receiving tyrosine kinase inhibitor therapy. *J Clin Oncol*, 29(12), 1512-6.

Kantarjian, H., Pasquini, R., Lévy, V., Jootar, S., Holowiecki, J., Hamerschlak, N., Hughes, T., Bleickardt, E., Dejardin, D., Cortes, J. & Shah, N. (2009) Dasatinib or high-dose imatinib for chronic -phase chronic myeloid leukemia resistant to imatinib at a dose of 400 to 600 milligrams daily: two-year follow-up of a randomized phase 2 study (START-R). *Cancer*, 115(18), 4137-37.

Kantarjian, H., Shah, N. P., Hochhaus, A., Cortes, J., Shah, S., Ayala, M., Moiraghi, B., Shen, Z., Mayer, J., Pasquini, R., Nakamae, H., Huguet, F., Boqué, C., Chuah, C., Bleickardt, E., Bradley-Garelik, M. B., Zhu, C., Szatrowski, T., Shapiro, D. & Baccarani, M. (2010) Dasatinib versus imatinib in newly diagnosed chronic-phase chronic myeloid leukemia. *N Engl J Med*, 362(24), 2260-70.

Kantarjian, H. M., Giles, F. J., Bhalla, K. N., Pinilla-Ibarz, J., Larson, R. A., Gattermann, N., Ottmann, O. G., Hochhaus, A., Radich, J. P., Saglio, G., Hughes, T. P., Martinelli, G., Kim, D. W., Shou, Y., Gallagher, N. J., Blakesley, R., Baccarani, M., Cortes, J. & le Coutre, P. D. (2011a) Nilotinib is effective in patients with chronic myeloid leukemia in chronic phase after imatinib resistance or intolerance: 24-month follow-up results. *Blood*, 117(4), 1141-5.

Kantarjian, H. M., Hochhaus, A., Saglio, G., De Souza, C., Flinn, I. W., Stenke, L., Goh, Y. T., Rosti, G., Nakamae, H., Gallagher, N. J., Hoenekopp, A., Blakesley, R. E., Larson, R. A. & Hughes, T. P. (2011b) Nilotinib versus imatinib for the treatment of patients with newly diagnosed chronic phase, Philadelphia chromosome-positive, chronic myeloid leukaemia: 24-month minimum follow-up of the phase 3 randomised ENESTnd trial. *Lancet Oncol*, 12(9), 841-51.

Kantarjian, H. M., Shah, N. P., Cortes, J. E., Baccarani, M., Agarwal, M. B., Undurraga, M. S., Wang, J., Ipiña, J. J., Kim, D. W., Ogura, M., Pavlovsky, C., Junghanss, C., Milone, J. H., Nicolini, F. E., Robak, T., Van Droogenbroeck, J., Vellenga, E., Bradley-Garelik, M. B., Zhu, C. & Hochhaus, A. (2012) Dasatinib or imatinib in newly diagnosed chronic-phase chronic myeloid leukemia: 2-year follow-up from a randomized phase 3 trial (DASISION). *Blood*, 119(5), 1123-9.

Kato, Y., Iwama, A., Tadokoro, Y., Shimoda, K., Minoguchi, M., Akira, S., Tanaka, M., Miyajima, A., Kitamura, T. & Nakauchi, H. (2005) Selective activation of STAT5 unveils its role in stem cell self-renewal in normal and leukemic hematopoiesis. *J Exp Med*, 202(1), 169-79.

Keeshan, K., Cotter, T. G. & McKenna, S. L. (2003) Bcr-Abl upregulates cytosolic p21WAF-1/CIP-1 by a phosphoinositide-3-kinase (PI3K)-independent pathway. *Br J Haematol*, 123(1), 34-44.

Kelman, Z., Prokocimer, M., Peller, S., Kahn, Y., Rechavi, G., Manor, Y., Cohen, A. & Rotter, V. (1989) Rearrangements in the p53 gene in Philadelphia chromosome positive chronic myelogenous leukemia. *Blood*, 74, 2318-2324.

Kenney, A. M. & Rowitch, D. H. (2000) Sonic hedgehog promotes G(1) cyclin expression and sustained cell cycle progression in mammalian neuronal precursors. *Mol Cell Biol*, 20(23), 9055-9067.

Kersten, B., Valkering, M., Wouters, R., van Amerongen, R., Hanekamp, D., Kwidama, Z., Valk, P., Ossenkoppele, G., Zeijlemaker, W., Kaspers, G., Cloos, J. & Schuurhuis, G. J. (2016) CD45RA, a specific marker for leukaemia stem cell sub-populations in acute myeloid leukaemia. *Br J Haematol*, 173(2), 219-235.

Keung, Y. K., Beaty, M., Powell, B. L., Molnar, I., Buss, D. & Pettenati, M. (2004) Philadelphia chromosome positive myelodysplastic syndrome and acute myeloid leukemia-retrospective study and review of literature. *Leuk Res*, 28(6), 579-86.

Khorashad, J. S., Kelley, T. W., Szankasi, P., Mason, C. C., Soverini, S., Adrian, L. T., Eide, C. A., Zabriskie, M. S., Lange, T., Estrada, J. C., Pomicter, A. D., Eiring, A. M., Kraft, I. L., Anderson, D. J., Gu, Z., Alikian, M., Reid, A. G., Foroni, L., Marin, D., Druker, B. J., O'Hare, T. & Deininger, M. W. (2013) BCR-ABL1 compound mutations in tyrosine kinase inhibitor-resistant CML: frequency and clonal relationships. *Blood*, 121(3), 489-98.

Khurana, S., Melacarne, A., Yadak, R., Schouteden, S., Notelaers, T., Pistoni, M., Maes, C. & Verfaillie, C. M. (2014) SMAD signalling regulates CXCL12 expression in the bone marrow niche, affecting homing and mobilization of hematopoietic progenitors. *Stem Cells*, 32(11), 3012-22.

Kiel, M. J., Yilmaz, O. H., Iwashita, T., Yilmaz, O. H., Terhorst, C. & Morrison, S. J. (2005) SLAM family receptors distinguish hematopoietic stem and progenitor cells and reveal endothelial niches for stem cells. *Cell*, 121(7), 1109-21.

Kim, S., Lin, L., Brown, G. A., Hosaka, K. & Scott, E. W. (2017) Extended time-lapse in vivo imaging of tibia bone marrow to visualize dynamic hematopoietic stem cell engraftment. *Leukemia*.

Kim, Y. W., Koo, B. K., Jeong, H. W., Yoon, M. J., Song, R., Shin, J., Jeong, D. C., Kim, S. H. & Kong, Y. Y. (2008) Defective Notch activation in microenvironment leads to myeloproliferative disease. *Blood*, 112(12), 4628-38.

King, B., Trimarchi, T., Reavie, L., Xu, L., Mullenders, J., Ntziachristos, P., Aranda-Orgilles, B., Perez-Garcia, A., Shi, J., Vakoc, C., Sandy, P., Shen, S. S., Ferrando, A. & Aifantis, I. (2013) The ubiquitin ligase FBXW7 modulates leukemia-initiating cell activity by regulating MYC stability. *Cell*, 153(7), 1552-66.

Kinstrie, R., Karamitros, D., Goardon, N., Morrison, H., Hamblin, M., Robinson, L., Clark, R. E., Copland, M. & Vyas, P. (2016) Heterogeneous leukemia stem cells in myeloid blast phase chronic myeloid leukemia. *Blood Advances*, 1(3), 160-169.

Kirmizitas, A., Meiklejohn, S., Ciau-Uitz, A., Stephenson, R. & Patient, R. (2017) Dissecting BMP signalling input into the gene regulatory networks driving specification of the blood stem cell lineage. *Proc Natl Acad Sci U S A*, 114(23), 5814-5821.

Kirstetter, P., Anderson, K., Porse, B. T., Jacobsen, S. E. & Nerlov, C. (2006) Activation of the canonical Wnt pathway leads to loss of hematopoietic stem cell repopulation and multilineage differentiation block. *Nat Immunol*, 7(10), 1048-56.

Klinakis, A., Lobry, C., Abdel-Wahab, O., Oh, P., Haeno, H., Buonamici, S., van De Walle, I., Cathelin, S., Trimarchi, T., Araldi, E., Liu, C., Ibrahim, S., Beran, M., Zavadil, J., Efstratiadis, A., Taghon, T., Michor, F., Levine, R. L. & Aifantis, I. (2011) A novel tumour-suppressor function for the Notch pathway in myeloid leukaemia. *Nature*, 473(7346), 230-233.

Kobayashi, Y., Tanaka, T., Kawata, E. & Akaogi, T. (2011) Chronic myelogenous leukemia in the chronic phase with lymph node swelling which represented extramedullary involvement composed of cells at different stages of maturation. *Rinsho Byori*, 59(4), 360-3.

Kobune, M., Iyama, S., Kikuchi, S., Horiguchi, H., Sato, T., Murase, K., Kawano, Y., Takada, K., Ono, K., Kamihara, Y., Hayashi, T., Miyanishi, K., Sato, Y., Takimoto, R. & Kato, J. (2012) Stromal cells expressing hedgehog-interacting protein regulate the proliferation of myeloid neoplasms. *Blood Cancer J*, 2, e87.

Kode, A., Manavalan, J. S., Mosialou, I., Bhagat, G., Rathinam, C. V., Luo, N., Khiabanian, H., Lee, A., Murty, V. V., Friedman, R., Brum, A., Park, D., Galili, N., Mukherjee, S., Teruya-Feldstein, J., Raza, A., Rabadan, R., Berman, E. & Kousteni, S. (2014) Leukaemogenesis induced by an activating beta-catenin mutation in osteoblasts. *Nature*, 506(7487), 240-244.

Kokabu, S., Sato, T., Ohte, S., Enoki, Y., Okubo, M., Hayashi, N., Nojima, J., Tsukamoto, S., Fukushima, Y., Sakata, Y., Katagiri, T., Rosen, V. & Yoda, T. (2014) Expression of TLE3 by bone marrow stromal cells is regulated by canonical Wnt signalling. *FEBS L*, 588(4), 614-9.

Kondo, M., Weissman, I. L. & Akashi, K. (1997) Identification of clonogenic common lymphoid progenitors in mouse bone marrow. *Cell*, 91, 661-672.

Konopka, J. B., Watanabe, S. M. & Witte, O. N. (1984) An alteration of the human c-abl protein in K562 leukemia cells unmasks associated tyrosine kinase activity. *Cell*, 37(3), 1035-1042.

Konstantinov, I. E. (2000) In search of Alexander A. Maximow: the man behind the unitarian theory of hematopoiesis. *Perspect Biol Med*, 43(2), 269-76.

Koschmieder, S., Gottgens, B., Zhang, P., Iwasaki-Arai, J., Akashi, K., Kutok, J. L., Dayaram, T., Geary, K., Green, A. R., Tenen, D. G. & Huettner, C. S. (2005) Inducible chronic phase of myeloid leukemia with expansion of hematopoietic stem cells in a transgenic model of BCR-ABL leukemogenesis. *Blood*, 105(1), 324-34.

Kramer, A. & Challen, G. A. (2017) The epigenetic basis of hematopoietic stem cell aging. *Semin Hematol*, 54(1), 19-24.

Krause, D. S., Fulzele, K., Catic, A., Sun, C. C., Dombkowski, D., Hurley, M. P., Lezeau, S., Attar, E., Wu, J. Y., Lin, H. Y., Divieti-Pajevic, P., Hasserjian, R. P. & Schipani, E. (2013) Differential regulation of myeloid leukemias by the bone marrow microenvironment. *Nat Med*, 19(11), 1513-7.

Krop, I., Demuth, T., Guthrie, T., Wen, P. Y., Mason, W. P., Chinnaiyan, P., Butowski, N., Groves, M. D., Kesari, S., Freedman, S. J., Blackman, S., Watters, J., Loboda, A., Podtelezhnikov, A., Lunceford, J., Chen, C., Giannotti, M., Hing, J., Beckman, R. & LoRusso, P. (2012) Phase I Pharmacologic and Pharmacodynamic Study of the Gamma Secretase (Notch) Inhibitor MK-0752 in Adult Patients With Advanced Solid Tumors. *J Clin Oncol*, 30(19), 2307-2313.

Kunisato, A., Chiba, S., Nakagami-Yamaguchi, E., Kumano, K., Saito, T., Masuda, S., Yamaguchi, T., Osawa, M., Kageyama, R., Nakauchi, H., Nishikawa, M. & Hirai, H. (2003) HES-1 preserves purified hematopoietic stem cells ex vivo and accumulates side population cells in vivo. *Blood*, 101(5), 1777-83.

Lahaye, T., Riehm, B., Berger, U., Paschka, P., Müller, M. C., Kreil, S., Merx, K., Schwindel, U., Schoch, C., Hehlmann, R. & Hochhaus, A. (2005) Response and resistance in 300 patients with BCR-ABL-positive leukemias treated with imatinib in a single center: a 4.5-year follow-up. *Cancer*, 103(8), 1659-69.

Laing, A. F., Lowell, S. & Brickman, J. M. (2015) Gro/TLE enables embryonic stem cell differentiation by repressing pluripotent gene expression. *Dev Biol*, 397(1), 56-66.

Lam, L. T., Ronchini, C., Norton, J., Capobianco, A. J. & Bresnick, E. H. (2000) Suppression of erythroid but not megakaryocytic differentiation of human K562 erythroleukemic cells by notch-1. *J Biol Chem*, 275(26), 19676-84.

Landberg, N., Hansen, N., Askmyr, M., H, A., Lassen, C. A., Rissler, M. A., Hjorth-Hansen, H. A., Mustjoki, S. A., Jaras, M. A., Richter, J. A. & Fioretos, T. (2016) IL1RAP expression as a measure of leukemic stem cell burden at diagnosis of chronic myeloid leukemia predicts therapy outcome. *Leukemia*, 30, 255-258.

Langenkamp, E., Zhang, L., Lugano, R., Huang, H., Elhassan, T. E., Georganaki, M., Bazzar, W., Lööf, J., Trendelenburg, G., Essand, M., Pontén, F., Smits, A. & Dimberg, A. (2015) Elevated expression of the C-type lectin CD93 in the glioblastoma vasculature regulates cytoskeletal rearrangements that enhance vessel function and reduce host survival. *Cancer Res*, 75(21), 4504-16.

Lansdorp, P. M., Sutherland, H. J. & Eaves, C. J. (1990) Selective expression of CD45 isoforms on functional subpopulations of CD34+ hemopoietic cells from human bone marrow. *J Exp Med*, 172(1), 363-6.

Laperrousaz, B., Jeanpierre, S., Sagorny, K., Voeltzel, T., Ramas, S., Kaniewski, B., Ffrench, M., Salesse, S., Nicolini, F. E. & Maguer-Satta, V. (2013) Primitive CML cell expansion relies on abnormal levels of BMPs provided by the niche and on BMPRIb overexpression. *Blood*, 122(23), 3767-3777.

Lapidot, T., Sirard, C., Vormoor, J., Murdoch, B., Hoang, T., Caceres-cortes, J., Minden, M., Paterson, B., Caligiuri, M. A. & Dick, J. E. (1994) A Cell Initiating Human Acute Myeloid-Leukemia after Transplantation into SCID Mice. *Nature*, 367(6464), 645-648.

Larson, R. A., Hochhaus, A., Hughes, T. P., Clark, R. E., Etienne, G., Kim, D. W., Flinn, I. W., Kurokawa, M., Moiraghi, B., Yu, R., Blakesley, R. E., Gallagher, N. J., Saglio, G. & Kantarjian, H. M. (2012) Nilotinib vs imatinib in patients with newly diagnosed Philadelphia chromosome-positive chronic myeloid leukemia in chronic phase: ENESTnd 3-year follow-up. *Leukemia*, 26(10), 2197-203.

Latif, A. L., Cole, J. J., Campos, J. M., Clark, W., McGarry, L., Brock, C., Newcombe, A., Keeshan, K., Copland, M. & Adams, P. D. (2015) Dual Inhibition of MDM2 and BET Cooperate to Eradicate Acute Myeloid Leukemia. *Blood*, 126(23), 674.

Laurenti, E., Doulatov, S., Zandi, S., Plumb, I., Chen, J., April, C., Fan, J. B. & Dick, J. E. (2013) The transcriptional architecture of early human hematopoiesis identifies multilevel control of lymphoid commitment. *Nat Immunol*, 14, 756-763.

LaVoie, M. J. & Selkoe, D. J. (2003) The Notch ligands, Jagged and Delta, are sequentially processed by alpha-secretase and presenilin/gamma-secretase and release signalling fragments. *J Biol Chem*, 278(36), 34427-37.

Le, V. H., Lee, S., Wang, T., Hyuk Jang, W., Yoon, Y., Kwon, S., Kim, H., Lee, S. W. & Hean Kim, K. (2017) In vivo longitudinal visualization of bone marrow engraftment process in mouse calvaria using two-photon microscopy. *Sci Rep*, 7, 44097.

Leatherman, J. (2013) Stem cells supporting other stem cells. *Front Genet*, 4, 257.

Lee, J. Y., Park, A. K., Lee, K. M., Park, S. K., Han, S., Han, W., Noh, D. Y., Yoo, K. Y., Kim, H., Chanock, S. J., Rothman, N. & Kang, D. (2009) Candidate gene approach evaluates association between innate immunity genes and breast cancer risk in Korean women. *Carcinogenesis*, 30(9), 1528-1531.

Lee, S. M., Bae, J. H., Kim, M. J., Lee, H. S., Lee, M. K., Chung, B. S., Kim, D. W., Kang, C. D. & Kim, S. H. (2007) Bcr-Abl-independent imatinib-resistant K562 cells show aberrant protein acetylation and increased sensitivity to histone deacetylase inhibitors. *J Pharmacol Exp Ther*, 322(3), 1084-92.

Lengerke, C., Schmitt, S., Bowman, T. V., Jang, I. H., Maouche-Chretien, L., McKinney-Freeman, S., Davidson, A. J., Hammerschmidt, M., Rentzsch, F., Green, J. B. A., Zon, L. I. &

Daley, G. Q. (2008) BMP and Wnt specify hematopoietic fate by activation of the Cdx-Hox pathway. *Cell Stem Cell*, 2(1), 72-82.

Leong, K. G. & Karsan, A. (2006) Recent insights into the role of Notch signalling in tumorigenesis. *Blood*, 107(6), 2223-33.

Levin, R. H., Whang, J., Tjio, J. H., Carbone, P. P., Frei, E. & Freireich, E. J. (1963) persistent mitosis of transfused homologous leukocytes in children receiving antileukemic therapy. *Science*, 142(3597), 1305-11.

Lewis, I. D., McDiarmid, L. A., Samels, L. M., To, L. B. & Hughes, T. P. (1998) Establishment of a reproducible model of chronic-phase chronic myeloid leukemia in NOD/SCID mice using blood-derived mononuclear or CD34+ cells. *Blood*, 91, 630-640.

Lewis, N. S., Lewis, E. E., Mullin, M., Wheadon, H., Dalby, M. J. & Berry, C. C. (2017) Magnetically levitated mesenchymal stem cell spheroids cultured with a collagen gel maintain phenotype and quiescence. *J Tissue Eng*, 8, 2041731417704428.

Li, L. H., Milner, L. A., Deng, Y., Iwata, M., Banta, A., Graf, L., Marcovina, S., Friedman, C., Trask, B. J., Hood, L. & Torok-Storb, B. (1998) The human homolog of rat Jagged1 expressed by marrow stroma inhibits differentiation of 32D cells through interaction with Notch1. *Immunity*, 8(1), 43-55.

Li, S., Ilaria, R. L., Million, R., Daley, G. Q. & Etten, R. A. V. (1999) The P190, P210, and P230 Forms of the. *J Exp Med*, 189(9).

Li, S. & Li, D. (2007) Stem cell and kinase activity-independent pathway in resistance of leukaemia to BCR-ABL kinase inhibitors. *J Cell Mol Med*, 11(6), 1251-62.

Li, V. S., Ng, S. S., Boersema, P. J., Low, T. Y., Karthaus, W. R., Gerlach, J. P., Mohammed, S., Heck, A. J., Maurice, M. M., Mahmoudi, T. & Clevers, H. (2012a) Wnt signalling through inhibition of β-catenin degradation in an intact Axin1 complex. *Cell*, 149(6), 1245-56.

Li, Y., Hibbs, M. A., Gard, A. L., Shylo, N. A. & Yun, K. (2012b) Genome-wide analysis of N1ICD/RBPJ targets in vivo reveals direct transcriptional regulation of Wnt, SHH, and hippo pathway effectors by Notch1. *Stem Cells*, 30(4), 741-52.

Liang, H., Chen, Q., Coles, A. H., Anderson, S. J., Pihan, G., Bradley, A., Gerstein, R., Jurecic, R. & Jones, S. N. (2003) Wnt5a inhibits B cell proliferation and functions as a tumor suppressor in hematopoietic tissue. *Cancer Cell*, 4(5), 349-60.

Liao, H. F., Su, Y. C., Zheng, Z. Y., Cai, C. J., Hou, M. H., Chao, K. S. C. & Chen, Y. J. (2012) Sonic hedgehog signalling regulates Bcr-Abl expression in human chronic myeloid leukemia cells. *Biomed Pharmacother*, 66(5), 378-383.

Lindauer, M. & Hochhaus, A. (2010) Dasatinib. *Recent Results Cancer Res*, 184, 83-102.

Liu, B., Sun, Y., Jiang, F., Zhang, S., Wu, Y., Lan, Y., Yang, X. & Mao, N. (2003) Disruption of Smad5 gene leads to enhanced proliferation of high-proliferative potential precursors during embryonic hematopoiesis. *Blood*, 101(1), 124-33.

Lobry, C., Ntziachristos, P., Ndiaye-Lobry, D., Oh, P., Cimmino, L., Zhu, N., Araldi, E., Hu, W. H., Freund, J., Abdel-Wahab, O., Ibrahim, S., Skokos, D., Armstrong, S. A., Levine, R. L., Park, C. Y. & Aifantis, I. (2013) Notch pathway activation targets AML-initiating cell homeostasis and differentiation. *J Exp Med*, 210(2), 301-319.

Long, B., Zhu, H., Zhu, C., Liu, T. & Meng, W. (2011) Activation of the Hedgehog pathway in chronic myelogeneous leukemia patients. *J Exp Clin Cancer Res*, 30, 8.

Lu, F. L., Yu, C.-C., Chiu, H.-H., Liu, H. E., Chen, S.-Y., Lin, S., Goh, T.-Y., Hsu, H.-C., Chien, C.-H., Wu, H.-C., Chen, M.-S., Schuyler, S. C., Hsieh, W.-S., Wu, M.-H. & Lu, J. (2013) Sonic hedgehog antagonists induce cell death in acute myeloid leukemia cells with the presence of lipopolysaccharides, tumor necrosis factor-alpha, or interferons. *Invest New Drugs*, 31(4), 823-32.

Lu, L., Xiao, M., Clapp, D. W., Li, Z. H. & Broxmeyer, H. E. (1993) High efficiency retroviral mediated gene transduction into single isolated immature and replatable CD34(3+) hematopoietic stem/progenitor cells from human umbilical cord blood. *J Exp Med*, 178(6), 2089-96.

Lucas, C. M., Harris, R. J., Giannoudis, A. & Clark, R. E. (2015) c-Myc inhibition decreases CIP2A and reduces BCR-ABL1 tyrosine kinase activity in chronic myeloid leukemia. *Haematologica*, 100(5), e179-82.

Luis, T. C., Naber, B. A., Roozen, P. P., Brugman, M. H., de Haas, E. F., Ghazvini, M., Fibbe, W. E., van Dongen, J. J., Fodde, R. & Staal, F. J. (2011) Canonical wnt signalling regulates hematopoiesis in a dosage-dependent fashion. *Cell Stem Cell*, 9(4), 345-56.

Luis, T. C., Weerkamp, F., Naber, B. A., Baert, M. R., de Haas, E. F., Nikolic, T., Heuvelmans, S., De Krijger, R. R., van Dongen, J. J. & Staal, F. J. (2009) Wnt3a deficiency irreversibly impairs hematopoietic stem cell self-renewal and leads to defects in progenitor cell differentiation. *Blood*, 113(3), 546-54.

Luo, Y., Change, L.-J., Hu, Y., Dong, L., Wei, G. & Huang, H. (2015) First-in-Man CD123-Specific Chimeric Antigen Receptor-Modified T Cells for the Treatment of Refractory Acute Myeloid Leukemia. *Blood*, 126:3778.

Magnusson, M., Brun, A. C., Lawrence, H. J. & Karlsson, S. (2007) Hoxa9/hoxb3/hoxb4 compound null mice display severe hematopoietic defects. *Exp Hematol*, 35(9), 1421-8.

Mahmud, N., Devine, S. M., Weller, K. P., Parmar, S., Sturgeon, C., Nelson, M. C., Hewett, T. & Hoffman, R. (2001) The relative quiescence of hematopoietic stem cells in nonhuman primates. *Blood*, 97(10), 3061-8.

Mahon, F. X., Richter, J., Guilhot, J., Muller, M., Dietz, C., Porkka, K., Hjorth-Hansen, H., Gruber, F., Panagoitidis, P., Ossenkoppele, G. J., Mayer, J., Almeida, A., Polakova, K., Ehrencrona, H., Pfirrmann, M. & Saussele, S. (2014) Interim Analysis of a Pan European Stop Tyrosine Kinase Inhibitor Tiral in Chronic Myeloid Leukemia: The EURO-SKI study. *Blood*, 124(21), 151.

Mahon, F. X. (2015) Discontinuation of tyrosine kinase therapy in CML. *Annals of Hematol*, 94(2), 187-193.

Mahon, F. X., Belloc, F., Lagarde, V., Chollet, C., Moreau-Gaudry, F., Reiffers, J., Goldman, J. M. & Melo, J. V. (2003) MDR1 gene overexpression confers resistance to imatinib mesylate in leukemia cell line models. *Blood*, 101(6), 2368-73.

Mahon, F. X., Deininger, M. W., Schultheis, B., Chabrol, J., Reiffers, J., Goldman, J. M. & Melo, J. V. (2000) Selection and characterization of BCR-ABL positive cell lines with differential sensitivity to the tyrosine kinase inhibitor STI571: diverse mechanisms of resistance. *Blood*, 96(3), 1070-9.

Mahon, F. X., Rea, D., Guilhot, J., Guilhot, F., Huguet, F., Nicolini, F., Legros, L., Charbonnier, A., Guerci, A., Varet, B., Etienne, G., Reiffers, J., Rousselot, P. & Intergroupe Francais des Leucemies Myeloides, C. (2010) Discontinuation of imatinib in patients with chronic myeloid leukaemia who have maintained complete molecular remission for at least 2 years: the prospective, multicentre Stop Imatinib (STIM) trial. *Lancet Oncol*, 11(11), 1029-35.

Mahon, F. X., Richter, J., Guilhot, J., Hjorth-Hansen, H., Almeida, A., Janssen, J. J. W. M., Mayer, J., Porkka, K., Panayiotidis, P., Stromberg, U., Berger, M. G., Diamond, J., Ehrencrona, H., Kairisto, V., Polakova, K., Mueller, M. C., Mustjoki, S., Hochhaus, A., Pfirrmann, M. & Saussele, S. (2016) Cessation of Tyrosine Kinase Inhibitors Treatment in Chronic Myeloid Leukemia Patients with Deep Molecular Response: Results of the Euro-Ski Trial, *Blood*, 128, 787.

Maillard, I., Koch, U., Dumortier, A., Shestova, O., Xu, L., Sai, H., Pross, S. E., Aster, J. C., Bhandoola, A., Radtke, F. & Pear, W. S. (2008) Canonical notch signalling is dispensable for the maintenance of adult hematopoietic stem cells. *Cell Stem Cell*, 2(4), 356-66.

Majeti, R., Chao, M. P., Alizadeh, A. A., Pang, W. W., Jaiswal, S., Gibbs, K. D., Jr., van Rooijen, N. & Weissman, I. L. (2009) CD47 is an adverse prognostic factor and therapeutic antibody target on human acute myeloid leukemia stem cells. *Cell*, 138(2), 286-99.

Majeti, R., Park, C. Y. & Weissman, I. L. (2007) Identification of a hierarchy of multipotent hematopoietic progenitors in human cord blood. *Cell Stem Cell*, 1(6), 635-45.

Malide, D., Métais, J. Y. & Dunbar, C. E. (2014) In vivo clonal tracking of hematopoietic stem and progenitor cells marked by five fluorescent proteins using confocal and multiphoton microscopy. *J Vis Exp*, 90, e51669.

Mancini, S. J., Mantei, N., Dumortier, A., Suter, U., MacDonald, H. R. & Radtke, F. (2005) Jagged1-dependent Notch signalling is dispensable for hematopoietic stem cell self-renewal and differentiation. *Blood*, 105(6), 2340-2.

Manz, M. G., Miyamoto, T., Akashi, K. & Weissman, I. L. (2002) Prospective isolation of human clonogenic common myeloid progenitors. *Proc. Natl. Acad. Sci. USA*, 99, 11872-11877.

Mardiros, A., Dos Santos, C., McDonald, T., Brown, C. E., Wang, X., Budde, L. E., Hoffman, L., Aguilar, B., Chang, W. C., Bretzlaff, W., Chang, B., Jonnalagadda, M., Starr, R., Ostberg, J. R., Jensen, M. C., Bhatia, R. & Forman, S. J. (2013) T cells expressing CD123-specific

chimeric antigen receptors exhibit specific cytolytic effector functions and antitumor effects against human acute myeloid leukemia. *Blood*, 122(18), 3138-48.

Marin, D., Bazeos, A., Mahon, F. X., Eliasson, L., Milojkovic, D., Bua, M., Apperley, J. F., Szydlo, R., Desai, R., Kozlowski, K., Paliompeis, C., Latham, V., Foroni, L., Molimard, M., Reid, A., Rezvani, K., de Lavallade, H., Guallar, C., Goldman, J. & Khorashad, J. S. (2010) Adherence is the critical factor for achieving molecular responses in patients with chronic myeloid leukemia who achieve complete cytogenetic responses on imatinib. *J Clin Oncol*, 28(14), 2381-8.

Marin, D., Ibrahim, A. R., Lucas, C., Gerrard, G., Wang, L., Szydlo, R. M., Clark, R. E., Apperley, J. F., Milojkovic, D., Bua, M., Pavlu, J., Paliompeis, C., Reid, A., Rezvani, K., Goldman, J. M. & Foroni, L. (2012) Assessment of BCR-ABL1 transcript levels at 3 months is the only requirement for predicting outcome for patients with chronic myeloid leukemia treated with tyrosine kinase inhibitors. *J Clin Oncol*, 30(3), 232-8.

Martelli, A. M., Evangelisti, C., Chiarini, F., Grimaldi, C., Cappellini, A., Ognibene, A. & McCubrey, J. A. (2010) The emerging role of the phosphatidylinositol 3-kinase/Akt/mammalian target of rapamycin signalling network in normal myelopoiesis and leukemogenesis. *Biochim Biophys Acta*, 1803(9), 991-1002.

Martinelli, G., Oehler, V. G., Papayannidis, C., Courtney, R., Shaik, M. N., Zhang, X. X., O'Connell, A., McLachlan, K. R., Zheng, X. X., Radich, J., Baccarani, M., Kantarjian, H. M., Levin, W. J., Cortes, J. E. & Jamieson, C. (2015) Treatment with PF-04449913, an oral smoothened antagonist, in patients with myeloid malignancies: a phase 1 safety and pharmacokinetics study. *Lancet Haematol*, 2(8), e339-346.

Matsuoka, S., Oike, Y., Onoyama, I., Perry, J. M., Li, L., Matsuoka, S. & Oike, Y. (2008) Fbxw7 acts as a critical fail-safe against premature loss of hematopoietic stem cells and development of T-ALL Fbxw7 acts as a critical fail-safe against premature loss of hematopoietic stem cells and development of T-ALL. *Genes Dev*, 22(8), 986-991.

Matsuoka, Y., Sumide, K., Kawamura, H., Nakatsuka, R., Fujioka, T., Sasaki, Y. & Sonoda, Y. (2015) Human cord blood-derived primitive CD34-negative hematopoietic stem cells (HSCs) are myeloid-biased long-term repopulating HSCs. *Blood Cancer J*, 5, e290.

Mauro, M., Baccarani, M., Cervantes, F., Lipton, J., Matloub, Y., Sinha, R. & Stone, R. (2008) Dasatinib 2-year efficacy in patients with chronic-phase chronic myelogenous leukemia (CML-CP) with resistance or intolerance to imatinib (START-C). *J Clin Oncol*, 7009.

Maximow, A. (1909) Der Lymphozyt als gemeinsame Stammzelle der verschiedenen Blutelemente in der embryonalen Entwicklung und im postfetalen Leben der Säugetiere. *Fol. Haematol.*, 8, 125-134.

McCubrey, J. A., Steelman, L. S., Bertrand, F. E., Davis, N. M., Abrams, S. L., Montalto, G., D'Assoro, A. B., Libra, M., Nicoletti, F., Maestro, R., Basecke, J., Cocco, L., Cervello, M. & Martelli, A. M. (2013) Multifaceted roles of GSK-3 and Wnt/β-catenin in hematopoiesis and leukemogenesis: opportunities for therapeutic intervention. *Leukemia*, 28(1), 15-33.

Melo, J. V. (1997) BCR-ABL gene variants. *Baillieres Clin Haematol*, 10(2), 203-22.

Melo, J. V., Gordon, D. E., Cross, N. C. & Goldman, J. M. (1993) The ABL-BCR fusion gene is expressed in chronic myeloid leukemia. *Blood*, 81(1), 158-65.

Memmi, E. M., Sanarico, A. G., Giacobbe, A., Peschiaroli, A., Frezza, V., Cicalese, A., Pisati, F., Tosoni, D., Zhou, H., Tonon, G., Antonov, A., Melino, G., Pelicci, P. G. & Bernassola, F. (2015) p63 sustains self-renewal of mammary cancer stem cells through regulation of Sonic Hedgehog signalling. *Proc Natl Acad Sci U S A*, 112(11), 3499-504.

Mendler, J. H., Balys, M., Sivagnanalingam, U., Eberhardt, A., Thorne, K., Ho, T. C., LaMere, M. W., Moore, S., McMurray, H., Myers, J. R., Ashton, J. M., O'Dwyer, K., Liesveld, J. L., Calvi, L. M. & Becker, M. W. (2015) Distinct Properties of Leukemia Stem Cells in Primary Refractory Acute Myeloid Leukemia. *Blood*, 126(23), 685.

Meng, L., Bai, Z., He, S., Mochizuki, K., Liu, Y., Purushe, J., Sun, H., Wang, J., Yagita, H., Mineishi, S., Fung, H., Yanik, G. A., Caricchio, R., Fan, X., Crisalli, L. M., Hexner, E. O., Reshef, R. & Zhang, Y. (2016) The Notch Ligand DLL4 Defines a Capability of Human Dendritic Cells in Regulating Th1 and Th17 Differentiation. *J Immunol*, 196(3), 1070-80.

Merchant, A., Joseph, G., Wang, Q., Brennan, S. & Matsui, W. (2010) Gli1 regulates the proliferation and differentiation of HSCs and myeloid progenitors. *Blood*, 115(12), 2391-6.

Meyn, M. A., Wilson, M. B., Abdi, F. A., Fahey, N., Schiavone, A. P., Wu, J., Hochrein, J. M., Engen, J. R. & Smithgall, T. E. (2006) Src family kinases phosphorylate the Bcr-Abl SH3-SH2 region and modulate Bcr-Abl transforming activity. *J Biol Chem*, 281(41), 30907-16.

Miele, L. & Osborne, B. (1999) Arbiter of differentiation and death: Notch signalling meets apoptosis. *J Cell Physiol*, 181(3), 393-409.

Milne, T. A. (2017) Mouse models of MLL leukemia: recapitulating the human disease. *Blood*, 129(16), 2217-2223.

Milner, L. A., Bigas, A., Kopan, R., BrashemStein, C., Bernstein, I. D. & Martin, D. I. K. (1996) Inhibition of granulocytic differentiation by mNotch1. *Proc Natl Acad Sci U S A*, 93(23), 13014-13019.

Milojkovic, D., Apperley, J. F., Gerrard, G., Ibrahim, A. R., Szydlo, R., Bua, M., Reid, A., Rezvani, K., Foroni, L., Goldman, J. & Marin, D. (2012) Responses to second-line tyrosine kinase inhibitors are durable: an intention-to-treat analysis in chronic myeloid leukemia patients. *Blood*, 119(8), 1838-43.

Minami, Y., Stuart, S. A., Ikawa, T., Jiang, Y., Banno, A., Hunton, I. C., Young, D. J., Naoe, T., Murre, C., Jamieson, C. H. & Wang, J. Y. (2008) BCR-ABL-transformed GMP as myeloid leukemic stem cells. *Proc Natl Acad Sci U S A*, 105(46), 17967-72.

Miyamoto, K., Araki, K. Y., Naka, K., Arai, F., Takubo, K., Yamazaki, S., Matsuoka, S., Miyamoto, T., Ito, K., Ohmura, M., Chen, C., Hosokawa, K., Nakauchi, H., Nakayama, K., Nakayama, K. I., Harada, M., Motoyama, N., Suda, T. & Hirao, A. (2007) Foxo3a is essential for maintenance of the hematopoietic stem cell pool. *Cell Stem Cell*, 1(1), 101-12.

Miyanari, Y. & Torres-Padilla, M. E. (2012) Control of ground-state pluripotency by allelic regulation of Nanog. *Nature*, 483(7390), 470-473.

Miyazono, K. (2012) Tumour promoting functions of TGF-β in CML-initiating cells. *J Biochem*, 152(5), 383-385.

Miyazono, K., Maeda, S. & Imamura, T. (2005) BMP receptor signalling: Transcriptional targets, regulation of signals, and signalling cross-talk. *Cytokine and Growth Factor Rev*, 16(3), 251-263.

Mizuno, T., Yamasaki, N., Miyazaki, K., Tazaki, T., Koller, R., Oda, H., Honda, Z., Ochi, M., Wolff, L. & Honda, H. (2008) Overexpression/enhanced kinase activity of BCR/ABL and altered expression of Notch1 induced acute leukemia in p210BCR/ABL transgenic mice. *Oncogene*, 27(24), 3465-74.

Mochizuki-Kashio, M., Mishima, Y., Miyagi, S., Negishi, M., Saraya, A., Konuma, T., Shinga, J., Koseki, H. & Iwama, A. (2011) Dependency on the polycomb gene Ezh2 distinguishes fetal from adult hematopoietic stem cells. *Blood*, 118(25), 6553-61.

Monteiro, R. M., de Sousa Lopes, S. M., Bialecka, M., de Boer, S., Zwijsen, A. & Mummery, C. L. (2008) Real time monitoring of BMP Smads transcriptional activity during mouse development. *Genesis*, 46(7), 335-46.

Morgan, T. (1917) The theory of the gene. *Am Naturalist*, 51, 513-544.

Morrison, S. J. & Kimble, J. (2006) Asymmetric and symmetric stem-cell divisions in development and cancer. *Nature*, 441(7097), 1068-74.

Mullighan, C. G. (2012a) Molecular genetics of B-precursor acute lymphoblastic leukemia. *J Clin Invest*, 122(10), 3407-15.

Mullighan, C. G. (2012b) The molecular genetic makeup of acute lymphoblastic leukemia. *Hematology Am Soc Hematol Educ Program*, 2012, 389-96.

Mullighan, C. G., Miller, C. B., Radtke, I., Phillips, L. A., Dalton, J., Ma, J., White, D., Hughes, T. P., Le Beau, M. M., Pui, C. H., Relling, M. V., Shurtleff, S. A. & Downing, J. R. (2008) BCR-ABL1 lymphoblastic leukaemia is characterized by the deletion of Ikaros. *Nature*, 453(7191), 110-4.

Murray, L., Chen, B., Galy, A., Chen, S., Tushinski, R., Uchida, N., Negrin, R., Tricot, G., Jagannath, S. & Vesole, D. (1995) Enrichment of human hematopoietic stem cell activity in the CD34+Thy-1+Lin- subpopulation from mobilized peripheral blood. *Blood*, 85(2), 368-78.

Månsson, R., Hultquist, A., Luc, S., Yang, L., Anderson, K., Kharazi, S., Al-Hashmi, S., Liuba, K., Thorén, L., Adolfsson, J., Buza-Vidas, N., Qian, H., Soneji, S., Enver, T., Sigvardsson, M. & Jacobsen, S. E. (2007) Molecular evidence for hierarchical transcriptional lineage priming in fetal and adult stem cells and multipotent progenitors. *Immunity*, 26(4), 407-19.

Nacheva, E. P., Grace, C. D., Brazma, D., Gancheva, K., Howard-Reeves, J., Rai, L., Gale, R. E., Linch, D. C., Hills, R. K., Russell, N., Burnett, A. K. & Kottaridis, P. D. (2013) Does BCR/ABL1 positive acute myeloid leukaemia exist? *Br J Haematol*, 161(4), 541-50.

Nagar, B., Hantschel, O., Young, M. A., Scheffzek, K., Veach, D., Bornmann, W., Clarkson, B., Superti-Furga, G. & Kuriyan, J. (2003) Structural basis for the autoinhibition of c-Abl tyrosine kinase. *Cell*, 112(6), 859-71.

Naka, K., Hoshii, T., Muraguchi, T., Tadokoro, Y., Ooshio, T., Kondo, Y., Nakao, S., Motoyama, N. & Hirao, A. (2010) TGF-beta-FOXO signalling maintains leukaemia-initiating cells in chronic myeloid leukaemia. *Nature*, 463(7281), 676-680.

Nakahara, F., Sakata-Yanagimoto, M., Komeno, Y., Kato, N., Uchida, T., Haraguchi, K., Kumano, K., Harada, Y., Harada, H., Kitaura, J., Ogawa, S., Kurokawa, M., Kitamura, T. & Chiba, S. (2010) Hes1 immortalizes committed progenitors and plays a role in blast crisis transition in chronic myelogenous leukemia. *Blood*, 115(14), 2872-81.

Nakamura, I., Fernandez-Barrena, M. G., Ortiz-Ruiz, M. C., Almada, L. L., Hu, C., Elsawa, S. F., Mills, L. D., Romecin, P. A., Gulaid, K. H., Moser, C. D., Han, J. J., Vrabel, A., Hanse, E. A., Akogyeram, N. A., Albrecht, J. H., Monga, S. P., Sanderson, S. O., Prieto, J., Roberts, L. R. & Fernandez-Zapico, M. E. (2013) Activation of the transcription factor GLI1 by WNT signalling underlies the role of SULFATASE 2 as a regulator of tissue regeneration. *J Biol Chem*, 288(29), 21389-98.

Nakaseko, C., Takahashi, N., Ishizawa, K., Kobayashi, Y., Ohashi, K., Nakagawa, Y., Yamamoto, K., Miyamura, K., Taniwaki, M., Okada, M., Kawaguchi, T., Shibata, A., Fujii, Y., Ono, C. & Ohnishi, K. (2015) A phase 1/2 study of bosutinib in Japanese adults with Philadelphia chromosome-positive chronic myeloid leukemia. *Int J Hematol*, 101(2), 154-64.

Naughton, R., Quiney, C., Turner, S. D. & Cotter, T. G. (2009) Bcr-Abl-mediated redox regulation of the PI3K/AKT pathway. *Leukemia*, 23(8), 1432-1440.

Negrin, R. S., Atkinson, K., Leemhuis, T., Hanania, E., Juttner, C., Tierney, K., Hu, W. W., Johnston, L. J., Shizurn, J. A., Stockerl-Goldstein, K. E., Blume, K. G., Weissman, I. L., Bower, S., Baynes, R., Dansey, R., Karanes, C., Peters, W. & Klein, J. (2000) Transplantation of highly purified CD34+Thy-1+ hematopoietic stem cells in patients with metastatic breast cancer. *Biol Blood Marrow Transplant*, 6(3), 262-71.

Nepomuceno, R. & Tenner, A. (1998) C1qRP, the C1q receptor that enhances phagocytosis, is detected specifically in human cells of myeloid lineage, endothelial cells, and platelets. *J Immunol*, 160(4), 1929-1935.

Nepomuceno, R. R., Henschen-Edman, A. H., Burgess, W. H. & Tenner, A. J. (1997) cDNA Cloning and Primary Structure Analysis of C1qR/MBL/SPA Receptor That Mediates Enhanced Phagocytosis In Vitro. *Immunity*, 6, 119-129.

Neuendorff, N. R., Burmeister, T., Dörken, B. & Westermann, J. (2016) BCR-ABL-positive acute myeloid leukemia: a new entity? Analysis of clinical and molecular features. *Ann Hematol*, 95(8), 1211-21.

Nicolini, F. E., Corm, S., Lê, Q. H., Sorel, N., Hayette, S., Bories, D., Leguay, T., Roy, L., Giraudier, S., Tulliez, M., Facon, T., Mahon, F. X., Cayuela, J. M., Rousselot, P., Michallet, M., Preudhomme, C., Guilhot, F. & Roche-Lestienne, C. (2006) Mutation status and clinical outcome of 89 imatinib mesylate-resistant chronic myelogenous leukemia patients: a retrospective analysis from the French intergroup of CML (Fi(phi)-LMC GROUP). *Leukemia*, 20(6), 1061-6.

Nilsson, S. K. (2001) Spatial localization of transplanted hemopoietic stem cells: inferences for the localization of stem cell niches. *Blood*, 97(8), 2293-2299.

Noens, L., van Lierde, M. A., De Bock, R., Verhoef, G., Zachée, P., Berneman, Z., Martiat, P., Mineur, P., Van Eygen, K., MacDonald, K., De Geest, S., Albrecht, T. & Abraham, I. (2009) Prevalence, determinants, and outcomes of nonadherence to imatinib therapy in patients with chronic myeloid leukemia: the ADAGIO study. *Blood*, 113(22), 5401-11.

Noort, W. A., Kruisselbrink, A. B., in't Anker, P. S., Kruger, M., van Bezooijen, R. L., de Paus, R. A., Heemskerk, M. H., Löwik, C. W., Falkenburg, J. H., Willemze, R. & Fibbe, W. E. (2002) Mesenchymal stem cells promote engraftment of human umbilical cord blood-derived CD34(+) cells in NOD/SCID mice. *Exp Hematol*, 30(8), 870-8.

Norsworthy, P. J., Fossati-Jimack, L., Cortes-Hernandez, J., Taylor, P. R., Bygrave, A. E., Thompson, R. D., Nourshargh, S., Walport, M. J. & Botto, M. (2004) Murine CD93 (C1qRp) contributes to the removal of apoptotic cells in vivo but is not required for C1q-mediated enhancement of phagocytosis. *J Immunol*, 172(6), 3406-3414.

Notari, M., Neviani, P., Santhanam, R., Blaser, B. W., Chang, J.-s., Galietta, A., Willis, A. E., Roy, D. C., Caligiuri, M. A., Marcucci, G. & Perrotti, D. (2006) A MAPK/HNRPK pathway controls BCR/ABL oncogenic potential by regulating MYC mRNA translation. *Blood*, 107(6), 2507-16.

Notta, F., Doulatov, S., Laurenti, E., Poeppl, A., Jurisica, I. & Dick, J. E. (2011) Isolation of single human hematopoietic stem cells capable of long-term multilineage engraftment. *Science*, 333(6039), 218-21.

Notta, F., Zandi, S., Takayama, N., Dobson, S., Gan, O. I., Wilson, G., Kaufmann, K. B., McLeod, J., Laurenti, E., Dunant, C. F., McPherson, J. D., Stein, L. D., Dror, Y. & Dick, J. E. (2016) Distinct routes of lineage development reshape the human blood hierarchy across ontogeny. *Science*, 351(6269), aab2116.

Noubissi, F. K., Goswami, S., Sanek, N. A., Kawakami, K., Minamoto, T., Moser, A., Grinblat, Y. & Spiegelman, V. S. (2009) Wnt signalling stimulates transcriptional outcome of the Hedgehog pathway by stabilizing GLI1 mRNA. *Cancer Res*, 69(22), 8572-8.

Nowell, P. C. (1962) The minute chromosome (Phl) in chronic granulocytic leukemia. *Blut*, 8, 65-6.

Nowell, P. C. & Hungerford, D. A. (1960) Chromosome studies on normal and leukemic human leukocytes. *J Natl Cancer Inst*, 25, 85-109.

Nusslein-Volhard, C. a. W. E. (1980) Mutations affecting segment number and polarity in Dosophila. *Nature*, 287(5785), 795-801.

Nutt, S. L., Heavey, B., Rolink, A. G. & Busslinger, M. (1999) Commitment to the B-lymphoid lineage depends on the transcription factor Pax5. *Nature*, 401(6753), 556-62.

Nwabo Kamdje, A. H., Mosna, F., Bifari, F., Lisi, V., Bassi, G., Malpeli, G., Ricciardi, M., Perbellini, O., Scupoli, M. T., Pizzolo, G. & Krampera, M. (2011) Notch-3 and Notch-4 signalling rescue from apoptosis human B-ALL cells in contact with human bone marrow-derived mesenchymal stromal cells. *Blood*, 118(2), 380-9.

Nygren, J. M., Bryder, D. & Jacobsen, S. E. (2006) Prolonged cell cycle transit is a defining and developmentally conserved hemopoietic stem cell property. *J Immunol*, 177(1), 201-8.

O'Brien, S. G., Guilhot, F., Larson, R. A., Gathmann, I., Baccarani, M., Cervantes, F., Cornelissen, J. J., Fischer, T., Hochhaus, A., Hughes, T., Lechner, K., Nielsen, J. L., Rousselot, P., Reiffers, J., Saglio, G., Shepherd, J., Simonsson, B., Gratwohl, A., Goldman, J. M., Kantarjian, H., Taylor, K., Verhoef, G., Bolton, A. E., Capdeville, R. & Druker, B. J. (2003) Imatinib compared with interferon and low-dose cytarabine for newly diagnosed chronic-phase chronic myeloid leukemia. *N Eng J Med*, 348(11), 994-1004.

O'Brien, S. G., Guilhot, F., Goldman, J. M., Hochhaus, A., Hughes, T. P., Radich, J., Rudoltz, M., Filian, J., Gathmann, I., Druker, B. J., Larson, R. (2008) International randomized study of interferon versus STI571 (IRIS) 7-year follow-up: sustained survival, low rate of transformation and increased rate of major molecular response (MMR) in patients (pts) with newly diagnosed chronic myeloid leukemia in chronic phase treated with imatinib. Blood, 112(11), 76.

O'Dwyer, M. E., Mauro, M. J., Kurilik, G., Mori, M., Balleisen, S., Olson, S., Magenis, E., Capdeville, R. & Druker, B. J. (2002) The impact of clonal evolution on response to imatinib mesylate (STI571) in accelerated phase CML. *Blood*, 100(5), 1628-33.

O'Hare, T., Shakespeare, W. C., Zhu, X., Eide, C. A., Rivera, V. M., Wang, F., Adrian, L. T., Zhou, T., Huang, W. S., Xu, Q., Metcalf, C. A., Tyner, J. W., Loriaux, M. M., Corbin, A. S., Wardwell, S., Ning, Y., Keats, J. A., Wang, Y., Sundaramoorthi, R., Thomas, M., Zhou, D., Snodgrass, J., Commodore, L., Sawyer, T. K., Dalgarno, D. C., Deininger, M. W., Druker, B. J. & Clackson, T. (2009) AP24534, a pan-BCR-ABL inhibitor for chronic myeloid leukemia, potently inhibits the T315I mutant and overcomes mutation-based resistance. *Cancer Cell*, 16(5), 401-12.

Oehler, V. G. (2013) Update on current monitoring recommendations in chronic myeloid leukemia: practical points for clinical practice. *Hematology Am Soc Hematol Educ Program*, 2013, 176-83.

Oh, P., Lobry, C., Gao, J., Tikhonova, A., Loizou, E., Manent, J., van Handel, B., Ibrahim, S., Greve, J., Mikkola, H., Artavanis-Tsakonas, S. & Aifantis, I. (2013) In Vivo mapping of notch pathway activity in normal and stress hematopoiesis. *Cell stem cell*, 13(2), 190-204.

Ohishi, K., Katayama, N., Shiku, H., Varnum-Finney, B. & Bernstein, I. (2003) Notch signalling in hematopoiesis. Seminars in Cell & Developmental Biology, 14(2), 143-150.

Ohishi, K., Varnum-finney, B. & Bernstein, I. D. (2002) Delta-1 enhances marrow and thymus repopulating ability of human CD34 + CD38 – cord blood cells. *J Clin Invest*, 110(8), 1165-1174.

Ohnishi, H., Sasaki, H., Nakamura, Y., Kato, S., Ando, K., Narimatsu, H. & Tachibana, K. (2013) Regulation of cell shape and adhesion by CD34. *Cell Adh Migr*, 7(5), 426-33.

Oldenborg, P. A. (2013) CD47: A Cell Surface Glycoprotein Which Regulates Multiple Functions of Hematopoietic Cells in Health and Disease. *ISRN Hematol*, 2013, 614619.

Olsen, R. S., Lindh, M., Vorkapic, E., Andersson, R. E., Zar, N., Lofgren, S., Dimberg, J., Matussek, A. & Wagsater, D. (2015) CD93 gene polymorphism is associated with disseminated colorectal cancer. *Int J Colorectal Dis*, 30(7), 883-890.

Orford, K. W. & Scadden, D. T. (2008) Deconstructing stem cell self-renewal: genetic insights into cell-cycle regulation. *Nat Rev Genet*, 9(2), 115-28.

Orlandini, M., Galvagni, F., Bardelli, M., Rocchigiani, M., Lentucci, C., Anselmi, F., Zippo, A., Bini, L. & Oliviero, S. (2014) The characterization of a novel monoclonal antibody against CD93 unveils a new antiangiogenic target. *Oncotarget*, 5(9), 2750-2760.

Osborne, W., O'Brien, S., Hedgley, C., Foroni, L., Apperley, J., Terril, P., Rowe, P., McCullough, J., Holyoake, T., Pocock, C., Byrne, J., Bescoby, R., Copland, M. & Clark, R. (2015) SPIRIT 2: an NCRI randomised study comparing dasatinib with imatinib in patients with newly diagnosed chronic myeloid leukaemia-2 year follow up, *British Society of Haematology*.

Oshima, M., Endoh, M., Endo, T. A., Toyoda, T., Nakajima-Takagi, Y., Sugiyama, F., Koseki, H., Kyba, M., Iwama, A. & Osawa, M. (2011) Genome-wide analysis of target genes regulated by HoxB4 in hematopoietic stem and progenitor cells developing from embryonic stem cells. *Blood*, 117(15), e142-50.

Osterberg, L. & Blaschke, T. (2005) Adherence to medication. *N Engl J Med*, 353(5), 487-97.

Ottmann, O., Charbonnier, A., Stegelmann, F., Breccia, M., Steegmann, J. L., Olavarria, E., Jevtic, S., Cota, M., Scheuer, N. & Lipton, J. H. (2015) Smoothened (Smo) Inhibitor Lde225 Combined with Nilotinib in Patients with Chronic Myeloid Leukemia (Cml) Resistant/Intolerant (R/I) to at Least 1 Prior Tyrosine Kinase Inhibitor: A Phase 1b Study. *Haematologica*, 100, 62-63.

Pajor, L., Vass, J. A., Kereskai, L., Kajtár, P., Szomor, A., Egyed, M., Iványi, J. & Jáksó, P. (2000) The existence of lymphoid lineage restricted Philadelphia chromosome-positive acute lymphoblastic leukemia with heterogeneous bcr-abl rearrangement. *Leukemia*, 14(6), 1122-6.

Pancewicz, J. & Nicot, C. (2011) Current views on the role of Notch signalling and the pathogenesis of human leukemia. *Bmc Cancer*, 11, 502.

Pang, Y., Tsigkou, O., Spencer, J. A., Lin, C. P., Neville, C. & Grottkau, B. (2015) Analyzing Structure and Function of Vascularization in Engineered Bone Tissue by Video-Rate Intravital Microscopy and 3D Image Processing. *Tissue Eng Part C Methods*, 21(10), 1025-31.

Passegué, E., Wagers, A. J., Giuriato, S., Anderson, W. C. & Weissman, I. L. (2005) Global analysis of proliferation and cell cycle gene expression in the regulation of hematopoietic stem and progenitor cell fates. *J Exp Med*, 202(11), 1599-611.

Pasto, A., Serafin, V., Pilotto, G., Lago, C., Bellio, C., Trusolino, L., Bertotti, A., Hoey, T., Plateroti, M., Esposito, G., Pinazza, M., Agostini, M., Nitti, D., Amadori, A. & Indraccolo, S. (2014) Notch3 Signalling Regulates Musashi-1 Expression in Metastatic Colorectal Cancer Cells. *Cancer Res*, 74(7), 2106-18.

Pendergast, A. M., Quilliam, L. A., Cripe, L. D., Bassing, C. H., Dai, Z., Li, N., Batzer, A., Rabun, K. M., Der, C. J. & Schlessinger, J. (1993) BCR-ABL-induced oncogenesis is mediated by direct interaction with the SH2 domain of the GRB-2 adaptor protein. *Cell*, 75(1), 175-85.

Perkins, A., Kongsuwan, K., Visvader, J., Adams, J. M. & Cory, S. (1990) Homeobox Gene-Expression Plus Autocrine Growth-Factor Production Elicits Myeloid-Leukemia. *Proc Natl Acad Sci U S A*, 87(21), 8398-8402.

Perrotti, D., Silvestri, G., Stramucci, L., Yu, J. & Trotta, R. (2017) Cellular and Molecular Networks in Chornic Myeloid Leukemia: the leukemic ste, progenitor and stromal cell interplay. *Curr Drug Targets*, 18(4), 377-388.

Petersdorf, S. H., Kopecky, K. J., Slovak, M., Willman, C., Nevill, T., Brandwein, J., Larson, R. A., Erba, H. P., Stiff, P. J., Stuart, R. K., Walter, R. B., Tallman, M. S., Stenke, L. & Appelbaum, F. R. (2013) A phase 3 study of gemtuzumab ozogamicin during induction and postconsolidation therapy in younger patients with acute myeloid leukemia. *Blood*, 121(24), 4854-60.

Petropoulos, K., Arseni, N., Schessl, C., Stadler, C. R., Rawat, V. P., Deshpande, A. J., Heilmeier, B., Hiddemann, W., Quintanilla-Martinez, L., Bohlander, S. K., Feuring-Buske, M. & Buske, C. (2008) A novel role for Lef-1, a central transcription mediator of Wnt signalling, in leukemogenesis. *J Exp Med*, 205(3), 515-22.

Poulos, M. G., Guo, P., Kofler, N. M., Pinho, S., Gutkin, M. C., Tikhonova, A., Aifantis, I., Frenette, P. S., Kitajewski, J., Rafii, S. & Butler, J. M. (2013) Endothelial Jagged-1 is necessary for homeostatic and regenerative hematopoiesis. *Cell Rep*, 4(5), 1022-34.

Prasetyanti, P. R., Zimberlin, C. D., Bots, M., Vermeulen, L., Melo Fde, S. & Medema, J. (2013) Regulation of stem cell self-renewal and differentiation by Wnt and Notch are conserved throughout the adenoma-carcinoma sequence in the colon. *Mol Cancer*, 12(1), 126.

Pronk, C. J., Rossi, D. J., Månsson, R., Attema, J. L., Norddahl, G. L., Chan, C. K., Sigvardsson, M., Weissman, I. L. & Bryder, D. (2007) Elucidation of the phenotypic, functional, and molecular topography of a myeloerythroid progenitor cell hierarchy. *Cell Stem Cell*, 1(4), 428-42.

Ptasznik, A., Nakata, Y., Kalota, A., Emerson, S. G. & Gewirtz, A. M. (2004) Short interfering RNA (siRNA) targeting the Lyn kinase induces apoptosis in primary, and drug-resistant, BCR-ABL1(+) leukemia cells. *Nat Med*, 10(11), 1187-9.

Puttini, M., Coluccia, A. M., Boschelli, F., Cleris, L., Marchesi, E., Donella-Deana, A., Ahmed, S., Redaelli, S., Piazza, R., Magistroni, V., Andreoni, F., Scapozza, L., Formelli, F. & Gambacorti-Passerini, C. (2006) In vitro and in vivo activity of SKI-606, a novel Src-Abl inhibitor, against imatinib-resistant Bcr-Abl+ neoplastic cells. *Cancer Res*, 66(23), 11314-22.

Radich, J. P. (2007) The Biology of CML blast crisis. *Hematology Am Soc Hematol Educ Program*, 384-391.

Radich, J. P., Dai, H., Mao, M., Oehler, V., Schelter, J., Druker, B., Sawyers, C., Shah, N., Stock, W., Willman, C. L., Friend, S. & Linsley, P. S. (2006) Gene expression changes associated with progression and response in chronic myeloid leukemia. *Proc Natl Acad Sci U S A*, 103(8), 2794-9.

Radtke, F., Wilson, A., Stark, G., Bauer, M., Meerwijk, J. V., Macdonald, H. R. & Aguet, M. (1999) Deficient T Cell Fate Specification in Mice with an Induced Inactivation of. *Immunity*, 10, 547-558.

Ramasamy, S. K., Kusumbe, A. P., Wang, L. & Adams, R. H. (2014) Endothelial Notch activity promotes angiogenesis and osteogenesis in bone. *Nature*, 507(7492), 376-380.

Rassi, F. E. & Khoury, H. J. (2013) Bosutinib: a SRC-ABL tyrosine kinase inhibitor for treatment of chronic myeloid leukemia. *Pharmgenomics Pers Med*, 6, 57-62.

Rea, D., Rousselot, P., Guilhot, J., Guilhot, F. & Mahon, F. X. (2012) Curing chronic myeloid leukemia. *Curr Hematol Malig Rep*, 7(2), 103-108.

Reavie, L., Buckley, S. M., Loizou, E., Takeishi, S., Aranda-Orgilles, B., Ndiaye-Lobry, D., Abdel-Wahab, O., Ibrahim, S., Nakayama, K. I. & Aifantis, I. (2013) Regulation of c-Myc ubiquitination controls chronic myelogenous leukemia initiation and progression. *Cancer Cell*, 23(3), 362-375.

Reavie, L. A. (2010) Regulation of hematopoietic stem cell differentiation by a single ubiquitin ligase-substrate complex. *Nat Immunol*, 11(3), 207-215.

Reddiconto, G., Toto, C., Palamà, I., De Leo, S., de Luca, E., De Matteis, S., Dini, L., Passerini, C. G., Di Renzo, N., Maffia, M. & Coluccia, A. M. (2012) Targeting of GSK3β promotes imatinib-mediated apoptosis in quiescent CD34+ chronic myeloid leukemia progenitors, preserving normal stem cells. *Blood*, 119(10), 2335-45.

Reya, T. (2003) Regulation of hematopoietic stem cell self-renewal. *Recent Prog Horm Res*, 58, 283-95.

Reya, T., Duncan, A. W., Ailles, L., Domen, J., Scherer, D. C., Willert, K., Hintz, L., Nusse, R. & Weissman, I. L. (2003) A role for Wnt signalling in self-renewal of haematopoietic stem cells. *Nature*, 423(6938), 409-14.

Reya, T., Morrison, S. J., Clarke, M. F. & Weissman, I. L. (2001) Stem cells, cancer, and cancer stem cells. *Nature*, 414(6859), 105-111.

Reynaud, D., Lefort, N., Manie, E., Coulombel, L. & Levy, Y. (2003) In vitro identification of human pro-B cells that give rise to macrophages, natural killer cells, and T cells. *Blood*, 101(11), 4313-21.

Richter, J., Mahon, F. X., Guilhot, J., Hjorth-Hansen, H., Almeida, A., Janssen, J. J., Mayer, J., Porkka, K., Panayiotidis, P., Olsson-Stromberg, U., Berger, M. G., Diamond, J., Ehrencrona, H., Kairisto, V., Polakova, K. M., Muller, M. C., Mustjoki, S., Hochhaus, A., Pfirrmann, M. & Saussele, S. (2016) Stopping Tyrosine Kinase Inhibitors in a Very Large Cohort of European Chronic Myeloid Leukemia Patients: Results of the Euro-Ski Trial. *Haematologica*, 101, 22-23.

Richter, J., Traver, D. & Willert, K. (2017) The role of Wnt signalling in hematopoietic stem cell development. *Crit Rev Biochem Mol Biol*, 1-11.

Riether, C., Schurch, C. M., Flury, C., Hinterbrandner, M., Druck, L., Huguenin, A. L., Baerlocher, G. M., Radpour, R. & Ochsenbein, A. F. (2015) Tyrosine kinase inhibitor-induced CD70 expression mediates drug resistance in leukemia stem cells by activating Wnt signalling. *Sci Transl Med*, 7(298), 298ra119.

Robert-Moreno, A., Espinosa, L., Sanchez, M. J., de la Pompa, J. L. & Bigas, A. (2007) The notch pathway positively regulates programmed cell death during erythroid differentiation. *Leukemia*, 21(7), 1496-1503.

Roche-Lestienne, C., Deluche, L., Corm, S., Tigaud, I., Joha, S., Philippe, N., Geffroy, S., Laï, J. L., Nicolini, F. E., Preudhomme, C. & group, F.-L. (2008) RUNX1 DNA-binding mutations and RUNX1-PRDM16 cryptic fusions in BCR-ABL+ leukemias are frequently associated with secondary trisomy 21 and may contribute to clonal evolution and imatinib resistance. *Blood*, 111(7), 3735-41.

Roma, J., Almazán-Moga, A., Sánchez de Toledo, J. & Gallego, S. (2012) Notch, wnt, and hedgehog pathways in rhabdomyosarcoma: from single pathways to an integrated network. *Sarcoma*, 2012, 695603.

Rosenthal, S., Schwartz, J. H. & Canellos, G. P. (1977) Basophilic chronic granulocytic leukaemia with hyperhistaminaemia. *Br J Haematol*, 36(3), 367-72.

Ross, D. M., Branford, S., Seymour, J. F., Schwarer, A. P., Arthur, C., Bartley, P. A., Slader, C., Field, C., Dang, P., Filshie, R. J., Mills, A. K., Grigg, A. P., Melo, J. V. & Hughes, T. P. (2010) Patients with chronic myeloid leukemia who maintain a complete molecular response after stopping imatinib treatment have evidence of persistent leukemia by DNA PCR. *Leukemia*, 24(10), 1719-1724.

Ross, D. M., Branford, S., Seymour, J. F., Schwarer, A. P., Arthur, C., Yeung, D. T., Dang, P., Goyne, J. M., Slader, C., Filshie, R. J., Mills, A. K., Melo, J. V., White, D. L., Grigg, A. P. & Hughes, T. P. (2013) Safety and efficacy of imatinib cessation for CML patients with stable undetectable minimal residual disease: results from the TWISTER study. *Blood*, 122(4), 515-22.

Rowe, J. M. & Lowenberg, B. (2013) Gemtuzumab ozogamicin in acute myeloid leukemia: a remarkable saga about an active drug. *Blood*, 121(24), 4838-4841.

Rowley, J. D. (1973) Letter: A new consistent chromosomal abnormality in chronic myelogenous leukaemia identified by quinacrine fluorescence and Giemsa staining. *Nature*, 243(5405), 290-3.

Roy, S. & Ingham, P. W. (2002) Hedgehogs tryst with the cell cycle. *J Cell Sci*, 115(Pt 23), 4393-7.

Rudin, C. M., Hann, C. L., Laterra, J., Yauch, R. L., Callahan, C. A., Fu, L., Holcomb, T., Stinson, J., Gould, S. E., Coleman, B., LoRusso, P. M., Von Hoff, D. D., de Sauvage, F. J. & Low, J. A. (2009) Brief Report: Treatment of Medulloblastoma with Hedgehog Pathway Inhibitor GDC-0449. *N Eng J Med*, 361(12), 1173-1178.

Sadarangani, A., Pineda, G., Lennon, K. M., Chun, H. J., Shih, A., Schairer, A. E., Court, A. C., Goff, D. J., Prashad, S. L., Geron, I., Wall, R., McPherson, J. D., Moore, R. A., Pu, M., Bao, L., Jackson-Fisher, A., Munchhof, M., VanArsdale, T., Reya, T., Morris, S. R., Minden, M. D., Messer, K., Mikkola, H. K., Marra, M. A., Hudson, T. J. & Jamieson, C. H. (2015) GLI2 inhibition abrogates human leukemia stem cell dormancy. *J Transl Med*, 13, 98.

Saglio, G., Kim, D. W., Issaragrisil, S., le Coutre, P., Etienne, G., Lobo, C., Pasquini, R., Clark, R. E., Hochhaus, A., Hughes, T. P., Gallagher, N., Hoenekopp, A., Dong, M., Haque, A., Larson, R. A., Kantarjian, H. M. & Investigators, E. (2010) Nilotinib versus imatinib for newly diagnosed chronic myeloid leukemia. *N Engl J Med*, 362(24), 2251-9.

Saito, Y., Kitamura, H., Hijikata, A., Tomizawa-Murasawa, M., Tanaka, S., Takagi, S., Uchida, N., Suzuki, N., Sone, A., Najima, Y., Ozawa, H., Wake, A., Taniguchi, S., Shultz, L., Ohara, O. & Ishikawa, F. (2010) Identification of therapeutic targets for quiescent, chemotherapy-resistant human leukemia stem cells. *Sci Transl Med*, 2(17), 17ra9.

Salati, S., Zini, R., Bianchi, E., Testa, A., Mavilio, F., Manfredini, R. & Ferrari, S. (2008) Role of CD34 antigen in myeloid differentiation of human hematopoietic progenitor cells. *Stem Cells*, 26(4), 950-9.

Samadani, A. A. & Akhavan-Niaki, H. (2015) Interaction of sonic hedgehog (SHH) pathway with cancer stem cell genes in gastric cancer. *Med Oncol*, 32(3).

Sarmento, L. M., Huang, H., Limon, A., Gordon, W., Fernandes, J., Tavares, M. J., Miele, L., Cardoso, A. A., Classon, M. & Carlesso, N. (2005) Notch1 modulates timing of G(1)-S progression by inducing SKP2 transcription and p27(Kip1) degradation. *J Exp Med*, 202(1), 157-168.

Sarry, J. E., Murphy, K., Perry, R., Sanchez, P. V., Secreto, A., Keefer, C., Swider, C. R., Strzelecki, A. C., Cavelier, C., Recher, C., Mansat-De Mas, V., Delabesse, E., Danet-Desnoyers, G. & Carroll, M. (2011) Human acute myelogenous leukemia stem cells are rare and heterogeneous when assayed in NOD/SCID/IL2R gamma c-deficient mice. *J Clin Invest*, 121(1), 384-395.

Sato, N., Meijer, L., Skaltsounis, L., Greengard, P. & Brivanlou, A. H. (2004) Maintenance of pluripotency in human and mouse embryonic stem cells through activation of Wnt signalling by a pharmacological GSK-3-specific inhibitor. *Nat Med*, 10(1), 55-63.

Sattler, M., Mohi, M. G., Pride, Y. B., Quinnan, L. R., Malouf, N. A., Podar, K., Gesbert, F., Iwasaki, H., Li, S., Van Etten, R. A., Gu, H., Griffin, J. D. & Neel, B. G. (2002) Critical role for Gab2 in transformation by BCR/ABL. *Cancer Cell*, 1(5), 479-92.

Sauvageau, G., Thorsteinsdottir, U., Hough, M. R., Hugo, P., Lawrence, H. J., Largman, C. & Humphries, R. K. (1997) Overexpression of HOXB3 in hematopoietic cells causes defective lymphoid development and progressive myeloproliferation. *Immunity*, 6(1), 13-22.

Saußele, S. & Silver, R. T. (2015) Management of chronic myeloid leukemia in blast crisis. *Ann Hematol*, 94(2), S159-65.

Sawyers, C. L. (1999) Chronic myeloid leukemia. *N Engl J Med*, 340(17), 1330-40.

Scheller, M., Huelsken, J., Rosenbauer, F., Taketo, M. M., Birchmeier, W., Tenen, D. G. & Leutz, A. (2006) Hematopoietic stem cell and multilineage defects generated by constitutive beta-catenin activation. *Nat Immunol*, 7(10), 1037-47.

Schenk, T. M., Keyhani, A., Bottcher, S., Kliche, K. O., Goodacre, A., Guo, J. Q., Arlinghaus, R. B., Kantarjian, H. M. & Andreeff, M. (1998) Multilineage involvement of Philadelphia chromosome positive acute lymphoblastic leukemia. *Leukemia*, 12(5), 666-74.

Schepers, K., Pietras, E. M., Reynaud, D., Flach, J., Binnewies, M., Garg, T., Wagers, A. J., Hsiao, E. C. & Passegué, E. (2013) Myeloproliferative neoplasia remodels the endosteal bone marrow niche into a self-reinforcing leukemic niche. *Cell Stem Cell*, 13(3), 285-99.

Schiavone, E. M., Lo Pardo, C., Di Noto, R., Manzo, C., Ferrara, F., Vacca, C. & Del Vecchio, L. (1995) Expression of the leucocyte common antigen (LCA, CD45) isoforms RA and RO in acute haematological malignancies: possible relevance in the definition of new overlap points between normal and leukaemic haemopoiesis. *Br J Haematol*, 91(4), 899-906.

Schindler, T., Bornmann, W., Pellicena, P., Miller, W. T., Clarkson, B. & Kuriyan, J. (2000) Structural mechanism for STI-571 inhibition of abelson tyrosine kinase. *Science*, 289(5486), 1938-42.

Schmittgen, T. D. & Livak, K. J. (2008) Analyzing real-time PCR data by the comparative C(T) method. *Nat Protoc*, 3(6), 1101-8.

Schofield, R. (1978) The relationship between the spleen colony-forming cell and the haemopoietic stem cell. *Blood Cells*, 4(1-2), 7-25.

Scholl, C., Bansal, D., Dohner, K., Eiwen, K., Huntly, B. J. P., Lee, B. H., Rucker, F. G., Schlenk, R. F., Bullinger, L., Dohner, H., Gilliland, D. G. & Frohling, S. (2007) The homeobox gene CDX2 is aberrantly expressed in most cases of acute myeloid leukemia and promotes leukemogenesis. *J Clin Invest*, 117(4), 1037-1048.

Schroeder, T., Geyh, S., Germing, U. & Haas, R. (2016) Mesenchymal stromal cells in myeloid malignancies. *Blood Res*, 51(4), 225-232.

Schroeder, T., Kohlhof, H., Rieber, N. & Just, U. (2003) Notch signalling induces multilineage myeloid differentiation and up-regulates PU.1 expression. *J Immunol*, 170(11), 5538-5548.

Schurch, C., Riether, C., Matter, M. S., Tzankov, A. & Ochsenbein, A. F. (2012) CD27 signalling on chronic myelogenous leukemia stem cells activates Wnt target genes and promotes disease progression. *J Clin Invest*, 122(2), 624-638.

Schuringa, J. J., Chung, K. Y., Morrone, G. & Moore, M. a. S. (2004a) Constitutive activation of STAT5A promotes human hematopoietic stem cell self-renewal and erythroid differentiation. *J Exp Med*, 200(5), 623-35.

Schuringa, J. J., Wu, K., Morrone, G. & Moore, M. A. (2004b) Enforced activation of STAT5A facilitates the generation of embryonic stem-derived hematopoietic stem cells that contribute to hematopoiesis in vivo. *Stem Cells*, 22(7), 1191-204.

Schwanbeck, R. & Just, U. (2011) The Notch signalling pathway in hematopoiesis and hematologic malignancies. *Haematologica*, 96(12), 1735-1737.

Scott, M. T., Korfi, K., Saffrey, P., Hopcroft, L. E., Kinstrie, R., Pellicano, F., Guenther, C., Gallipoli, P., Cruz, M., Dunn, K., Jorgensen, H. G., Cassels, J. E., Hamilton, A., Crossan, A., Sinclair, A., Holyoake, T. L. & Vetrie, D. (2016) Epigenetic Reprogramming Sensitizes CML Stem Cells to Combined EZH2 and Tyrosine Kinase Inhibition. *Cancer Discov*, 6(11), 1248-1257.

Secker-Walker, L. M. (1984) The prognostic implications of chromosomal findings in acute lymphoblastic leukemia. *Cancer Genet Cytogenet*, 11(2), 233-48.

Secker-Walker, L. M., Lawler, S. D. & Hardisty, R. M. (1978) Prognostic implications of chromosomal findings in acute lymphoblastic leukaemia at diagnosis. *Br Med J*, 2(6151), 1529-30.

Seke Etet, P. F., Vecchio, L. & Nwabo Kamdje, A. H. (2012) Interactions between bone marrow stromal microenvironment and B-chronic lymphocytic leukemia cells: any role for Notch, Wnt and Hh signalling pathways? *Cell Signal*, 24(7), 1433-43.

Sengupta, A., Banerjee, D., Chandra, S., Banerji, S. K., Ghosh, R., Roy, R. & Banerjee, S. (2007) Deregulation and cross talk among Sonic hedgehog, Wnt, Hox and Notch signalling in chronic myeloid leukemia progression. *Leukemia*, 21(5), 949-55.

Shah, N. P., Cortes, J. E., Martinelli, G., Smith, B. D., Clarke, E., Copland, M., Strauss, L. & Talpaz, M. (2014) Dasatinib Plus Smoothened (SMO) Inhibitor BMS-833923 in Chronic Myeloid Leukemia (CML) with Resistance or Suboptimal Response to a Prior Tyrosine Kinase Inhibitor (TKI): Phase I Study CA180323. *Blood*, 124(21), 4539.

Shah, N. P., Nicoll, J. M., Nagar, B., Gorre, M. E., Paquette, R. L., Kuriyan, J. & Sawyers, C. L. (2002) Multiple BCR-ABL kinase domain mutations confer polyclonal resistance to the tyrosine kinase inhibitor imatinib (STI571) in chronic phase and blast crisis chronic myeloid leukemia. *Cancer Cell*, 2(2), 117-25.

Shah, N. P., Tran, C., Lee, F. Y., Chen, P., Norris, D. & Sawyers, C. L. (2004) Overriding imatinib resistance with a novel ABL kinase inhibitor. *Science*, 305(5682), 399-401.

Sharma, S., Gurudutta, G. U., Satija, N. K., Pati, S., Afrin, F., Gupta, P., Verma, Y. K., Singh, V. K. & Tripathi, R. P. (2006) Stem cell c-KIT and HOXB4 genes: critical roles and mechanisms in self-renewal, proliferation, and differentiation. *Stem Cells Dev*, 15(6), 755-78.

Shen, Y. L., Luo, Q., Guo, Y. X., Zheng, G. H., Yu, J. & Xu, Y. H. (2014) Bone marrow mesenchymal stem cell-derived Wnt5a inhibits leukemia cell progression in vitro via activation of the non-canonical Wnt signalling pathway. *Oncol Lett*, 8(1), 85-90.

Sheng, W. W., Dong, M., Zhou, J. P., Li, X., Liu, Q. F., Dong, Q. & Li, F. (2013) Cooperation among Numb, MDM2 and p53 in the development and progression of pancreatic cancer. *Cell Tissue Res*, 354(2), 521-532.

Shet, A. S., Jahagirdar, B. N. & Verfaillie, C. M. (2002) Chronic myelogenous leukemia: mechanisms underlying disease progression. *Leukemia*, 16(8), 1402-11.

Shimamoto, T., Ohyashiki, J. H., Ohyashiki, K., Kawakubo, K., Kimura, N., Nakazawa, S. & Toyama, K. (1994) GATA-1, GATA-2, and stem cell leukemia gene expression in acute myeloid leukemia. *Leukemia*, 8(7), 1176-80.

Shtivelman, E., Lifshitz, B., Gale, R. P. & Canaani, E. (1985) Fused transcript of abl and bcr genes in chronic myelogenous leukaemia. *Nature*, 315(6020), 550-4.

Silveira, V. S., Freire, B. M., Borges, K. S., Andrade, A. F., Cruzeiro, G. A., Sabino, J. P., Glass, M. L., Yunes, J. A., Brandalise, S. R., Tone, L. G. & Scrideli, C. A. (2014) Hypoxia-related gene expression profile in childhood acute lymphoblastic leukemia: prognostic implications. *Leuk Lymphoma*, 55(8), 1751-7.

Sinclair, A., Latif, A. L. & Holyoake, T. L. (2013) Targeting survival pathways in chronic myeloid leukaemia stem cells. *Br J Pharmacol*, 169(8), 1693-707.

Singh, M., Chaudhry, P. & Merchant, A. A. (2016) Primary cilia are present on human blood and bone marrow cells and mediate Hedgehog signalling. *Exp Hematol*, 44(12), 1181-7.

Skorski, T. (2008) BCR/ABL, DNA damage and DNA repair: implications for new treatment concepts. *Leuk Lymphoma*, 49(4), 610-4.

Smith, J. N. & Calvi, L. M. (2013) Concise review: Current concepts in bone marrow microenvironmental regulation of hematopoietic stem and progenitor cells. *Stem Cells*, 31(6), 1044-50.

Soekarman, D., van Denderen, J., Hoefsloot, L., Moret, M., Meeuwsen, T., van Baal, J., Hagemeijer, A. & Grosveld, G. (1990) A novel variant of the bcr-abl fusion product in Philadelphia chromosome-positive acute lymphoblastic leukemia. *Leukemia*, 4(6), 397-403.

Somervaille, T. C. P., Matheny, C. J., Spencer, G. J., Iwasaki, M., Rinn, J. L., Witten, D. M., Chang, H. Y., Shurtleff, S. A., Downing, J. R. & Cleary, M. L. (2009) Hierarchical Maintenance of MLL Myeloid Leukemia Stem Cells Employs a Transcriptional Program Shared with Embryonic Rather Than Adult Stem Cells. *Cell Stem Cell*, 4(2), 129-140.

Sontakke, P., Jaques, J., Vellenga, E. & Schuringa, J. J. (2016) Modeling of Chronic Myeloid Leukemia: An Overview of In Vivo Murine and Human Xenograft Models. *Stem Cells Int*, 2016, 1625015.

Soupir, C. P., Vergilio, J. A., Dal Cin, P., Muzikansky, A., Kantarjian, H., Jones, D. & Hasserjian, R. P. (2007) Philadelphia chromosome-positive acute myeloid leukemia: a rare aggressive leukemia with clinicopathologic features distinct from chronic myeloid leukemia in myeloid blast crisis. *Am J Clin Pathol*, 127(4), 642-50.

Soverini, S., Colarossi, S., Gnani, A., Rosti, G., Castagnetti, F., Poerio, A., Iacobucci, I., Amabile, M., Abruzzese, E., Orlandi, E., Radaelli, F., Ciccone, F., Tiribelli, M., di Lorenzo, R., Caracciolo, C., Izzo, B., Pane, F., Saglio, G., Baccarani, M., Martinelli, G. & Leukemia, G. W. P. o. C. M. (2006) Contribution of ABL kinase domain mutations to imatinib resistance in different subsets of Philadelphia-positive patients: by the GIMEMA Working Party on Chronic Myeloid Leukemia. *Clin Cancer Res*, 12(24), 7374-9.

Soverini, S., Hochhaus, A., Nicolini, F. E., Gruber, F., Lange, T., Saglio, G., Pane, F., Müller, M. C., Ernst, T., Rosti, G., Porkka, K., Baccarani, M., Cross, N. C. & Martinelli, G. (2011) BCR-ABL kinase domain mutation analysis in chronic myeloid leukemia patients treated with tyrosine kinase inhibitors: recommendations from an expert panel on behalf of European LeukemiaNet. *Blood*, 118(5), 1208-15.

Spangrude, G. J., Heimfeld, S. & Weissman, I. L. (1988) Purification and characterization of mouse hematopoietic stem cells. *Science*, 241(4861), 58-62.

Staal, F. J., Chhatta, A. & Mikkers, H. (2016) Caught in a Wnt storm: Complexities of Wnt signalling in hematopoiesis. *Exp Hematol*, 44(6), 451-7.

Stanglmaier, M., Warmuth, M., Kleinlein, I., Reis, S. & Hallek, M. (2003) The interaction of the Bcr-Abl tyrosine kinase with the Src kinase Hck is mediated by multiple binding domains. *Leukemia*, 17(2), 283-9.

Stanley, P. (2007) Regulation of Notch signalling by glycosylation. *Curr Opin Struct Biol*, 17(5), 530-535.

Steelman, L. S., Pohnert, S. C., Shelton, J. G., Franklin, R. A., Bertrand, F. E. & McCubrey, J. A. (2004) JAK/STAT, Raf/MEK/ERK, PI3K/Akt and BCR-ABL in cell cycle progression and leukemogenesis. *Leukemia*, 18(2), 189-218.

Stessman, H. A. F., Mansoor, A., Zhan, F., Linden, M. A., Van Ness, B. & Baughn, L. (2013) Bortezomib resistance can be reversed by induced expression of plasma cell maturation markers in a mouse in vitro model of multiple myeloma. *PloS One*, 8(10), e77608.

Stier, S., Cheng, T., Dombkowski, D., Carlesso, N. & Scadden, D. T. (2002) Notch1 activation increases hematopoietic stem cell self-renewal in vivo and favors lymphoid over myeloid lineage outcome. *Blood*, 99(7), 2369-78.

Stirewalt, D. L., Kopecky, K. J., Meshinchi, S., Appelbaum, F. R., Slovak, M. L., Willman, C. L. & Radich, J. P. (2001) FLT3, RAS, and TP53 mutations in elderly patients with acute myeloid leukemia. *Blood*, 97(11), 3589-3595.

Su, W., Meng, F., Huang, L., Zheng, M., Liu, W. & Sun, H. (2012) Sonic hedgehog maintains survival and growth of chronic myeloid leukemia progenitor cells through beta-catenin signalling. *Exp Hematol*, 40(5), 418-27.

Suman, S., Das, T. P. & Damodaran, C. (2013) Silencing NOTCH signalling causes growth arrest in both breast cancer stem cells and breast cancer cells. *Br J Cancer*, 109(10), 2587-96.

Suresh, S. & Irvine, A. E. (2015) The NOTCH signalling pathway in normal and malignant blood cell production. *J Cell Commun Signal*, 9(1), 5-13.

Sutherland, H. J., Eaves, C. J., Eaves, A. C., Dragowska, W. & Lansdorp, P. M. (1989) Characterization and partial purification of human marrow cells capable of initiating long-term hematopoiesis in vitro. *Blood*, 74(5), 1563-70.

Sutherland, H. J., Lansdorp, P. M., Henkelman, D. H., Eaves, A. C. & Eaves, C. J. (1990) Functional characterization of individual human hematopoietic stem cells cultured at limiting dilution on supportive marrow stromal layers. *Proc Natl Acad Sci U S A*, 87(9), 3584-8.

Szankasi, P., Schumacher, J. A. & Kelley, T. W. (2016) Detection of BCR-ABL1 mutations that confer tyrosine kinase inhibitor resistance using massively parallel, next generation sequencing. *Ann Hematol*, 95(2), 201-10.

Tabatabai, G., Frank, B., Möhle, R., Weller, M. & Wick, W. (2006) Irradiation and hypoxia promote homing of haematopoietic progenitor cells towards gliomas by TGF-beta-dependent HIF-1alpha-mediated induction of CXCL12. *Brain*, 129(9), 2426-35.

Takahashi, N., Kyo, T., Maeda, Y., Sugihara, T., Usuki, K., Kawaguchi, T., Usui, N., Okamoto, S., Ohe, Y., Ohtake, S., Kitamura, K., Yamamoto, M., Teshima, H., Motoji, T., Tamaki, T., Sawada, K. & Ohyashiki, K. (2012) Discontinuation of imatinib in Japanese patients with chronic myeloid leukemia. *Haematologica*, 97(6), 903-96.

Takeishi, S., Matsumoto, A., Onoyama, I., Naka, K., Hirao, A. & Nakayama, K. I. (2013) Ablation of Fbxw7 eliminates leukemia-initiating cells by preventing quiescence. *Cancer Cell*, 23(3), 347-61.

Talpaz, M., Kantarjian, H. M., McCredie, K., Trujillo, J. M., Keating, M. J. & Gutterman, J. U. (1986) Hematologic remission and cytogenetic improvement induced by recombinant human interferon alpha A in chronic myelogenous leukemia. *N Engl J Med*, 314(17), 1065-9.

Tan-Pertel, H. T., Walker, L., Browning, D., Miyamoto, A., Weinmaster, G. & Gasson, J. C. (2000) Notch signalling enhances survival and alters differentiation of 32D myeloblasts. *J Immunol*, 165(8), 4428-4436.

Taussig, D. C., Pearce, D. J., Simpson, C., Rohatiner, A. Z., Lister, T. A., Kelly, G., Luongo, J. L., Danet-Desnoyers, G. A. & Bonnet, D. (2005) Hematopoietic stem cells express multiple myeloid markers: implications for the origin and targeted therapy of acute myeloid leukemia. *Blood*, 106(13), 4086-4092.

Taussig, D. C., Vargaftig, J., Miraki-Moud, F., Griessinger, E., Sharrock, K., Luke, T., Lillington, D., Oakervee, H., Cavenagh, J., Agrawal, S. G., Lister, T. A., Gribben, J. G. & Bonnet, D. (2010) Leukemia-initiating cells from some acute myeloid leukemia patients with mutated nucleophosmin reside in the CD34(-) fraction. *Blood*, 115(10), 1976-1984.

Taylor, M. D., Liu, L., Raffel, C., Hui, C. C., Mainprize, T. G., Zhang, X., Agatep, R., Chiappa, S., Gao, L., Lowrance, A., Hao, A., Goldstein, A. M., Stavrou, T., Scherer, S. W., Dura, W. T., Wainwright, B., Squire, J. A., Rutka, J. T. & Hogg, D. (2002) Mutations in SUFU predispose to medulloblastoma. *Nat Genet*, 31(3), 306-10.

Thomas, G. B. & van Meyel, D. J. (2007) The glycosyltransferase Fringe promotes Delta-Notch signalling between neurons and glia, and is required for subtype-specific glial gene expression. *Development*, 134(3), 591-600.

Thomas, X. (2012) Philadelphia chromosome-positive leukemia stem cells in acute lymphoblastic leukemia and tyrosine kinase inhibitor therapy. *World J Stem Cells*, 4(6), 44-52.

Thompson, B. J., Jankovic, V., Gao, J., Buonamici, S., Vest, A., Lee, J. M., Zavadil, J., Nimer, S. D. & Aifantis, I. (2008) Control of hematopoietic stem cell quiescence by the E3 ubiquitin ligase Fbw7. *J Exp Med*, 205(6), 1395-1408.

Thorsteinsdottir, U., Mamo, A., Kroon, E., Jerome, L., Bijl, J., Lawrence, H. J., Humphries, K. & Sauvageau, G. (2002) Overexpression. of the myeloid leukemia-associated Hoxa9 gene in bone marrow cells induces stem cell expansion. *Blood*, 99(1), 121-129.

Till, J. E. & McCulloch, E. A. (1961) A direct measurement of the radiation sensitivity of normal mouse bone marrow cells. *Radiat Res*, 14, 213-22.

Ting, H. A., Schaller, M. A., de Almeida Nagata, D. E., Rasky, A. J., Maillard, I. P. & Lukacs, N. W. (2017) Notch Ligand Delta-like 4 Promotes Regulatory T Cell Identity in Pulmonary Viral Infection. *J Immunol*, 198(4), 1492-1502.

Tohda, S. & Nara, N. (2001) Expression of Notch1 and Jagged1 proteins in acute myeloid leukemia cells. *Leuk Lymph*, 42(3), 467-472.

Toofan, P., Irvine, D., Hopcroft, L., Copland, M. & Wheadon, H. (2014) The role of the bone morphogenetic proteins in leukaemic stem cell persistence. *Biochem Soc Trans*, 42, 809-815.

Tosello, V. & Ferrando, A. A. (2013) The NOTCH signalling pathway: role in the pathogenesis of T-cell acute lymphoblastic leukemia and implication for therapy. *Ther Adv Hematol*, 4(3), 199-210.

Tran, H. T., Sekkali, B., Van Imschoot, G., Janssens, S. & Vleminckx, K. (2010) Wnt/beta-catenin signalling is involved in the induction and maintenance of primitive hematopoiesis in the vertebrate embryo. *Proc Natl Acad Sci U S A*, 107(37), 16160-5.

Trentin, J. J. (1971) Determination of bone marrow stem cell differentiation by stromal hemopoietic inductive microenvironments (HIM). *Am J Pathol*, 65(3), 621-8.

Trowbridge, J. J., Scott, M. P. & Bhatia, M. (2006a) Hedgehog modulates cell cycle regulators in stem cells to control hematopoietic regeneration. *Proc Natl Acad Sci U S A*, 103(38), 14134-9.

Trowbridge, J. J., Xenocostas, A., Moon, R. T. & Bhatia, M. (2006b) Glycogen synthase kinase-3 is an in vivo regulator of hematopoietic stem cell repopulation. *Nat Med*, 12(1), 89-98.

Van Den Berg, D. J., Sharma, A. K., Bruno, E. & Hoffman, R. (1998) Role of members of the Wnt gene family in human hematopoiesis. *Blood*, 92(9), 3189-202.

Van Etten, R. A. (1999) Cycling, stressed-out and nervous: cellular functions of c-Abl. *Trends Cell Biol*, 9(5), 179-86.

Van Etten, R. A. (2001) Models of chronic myeloid leukemia. *Curr Oncol Rep*, 3(3), 228-37.

Van Galen, P., Kreso, A., Mbong, N., Kent, D. G., Fitzmaurice, T., Chambers, J. E., Xie, S., Laurenti, E., Hermans, K., Eppert, K., Marciniak, S. J., Goodall, J. C., Green, A. R., Wouters, B. G., Wienholds, E. & Dick, J. E. (2014) The unfolded protein response governs integrity of the haematopoietic stem-cell pool during stress. *Nature*, 510(7504), 268-72.

Van Rhenen, A., Feller, N., Kelder, A., Westra, A. H., Rombouts, E., Zweegman, S., van der Pol, M. A., Waisfisz, Q., Ossenkoppele, G. J. & Schuurhuis, G. J. (2005) High stem cell frequency in acute myeloid leukemia at diagnosis predicts high minimal residual disease and poor survival. *Clin Cancer Res*, 11(18), 6520-6527.

Van Rhenen, A., Moshaver, B., Kelder, A., Feller, N., Nieuwint, A. W. M., Zweegman, S., Ossenkoppele, G. J. & Schuurhuis, G. J. (2007) Aberrant marker expression patterns on the CD34+CD38-stem cell compartment in acute myeloid leukemia allows to distinguish the malignant from the normal stem cell compartment both at diagnosis and in remission. *Leukemia*, 21(8), 1700-1707.

Vanegas, N. P. & Vernot, J. P. (2017) Loss of quiescence and self-renewal capacity of hematopoietic stem cell in an in vitro leukemic niche. *Exp Hematol Oncol*, 6, 2.

Varnum-Finney, B., Brashem-Stein, C. & Bernstein, I. D. (2003) Combined effects of Notch signalling and cytokines induce a multiple log increase in precursors with lymphoid and myeloid reconstituting ability. *Blood*, 101(5), 1784-9.

Varnum-Finney, B., Halasz, L. M., Sun, M., Gridley, T., Radtke, F. & Bernstein, I. D. (2011) Notch2 governs the rate of generation of mouse long- and short-term repopulating stem cells. J Clin Invest, 121(3), 1207-16.

Verstegen, M. M., Cornelissen, J. J., Terpstra, W., Wagemaker, G. & Wognum, A. W. (1999) Multilineage outgrowth of both malignant and normal hemopoietic progenitor cells from individual chronic myeloid leukemia patients in immunodeficient mice. Leukemia, 13(4), 618-28.

Virchow, R. (1845) Weisses Blut. *Froriep's Notizen*, 36, 151-6.

Vogel, W., Scheding, S., Kanz, L. & Brugger, W. (2000) Clinical applications of CD34(+) peripheral blood progenitor cells (PBPC). *Stem Cells*, 18(2), 87-92.

Von Hoff, D. D., LoRusso, P. M., Rudin, C. M., Reddy, J. C., Yauch, R. L., Tibes, R., Weiss, G. J., Borad, M. J., Hann, C. L., Brahmer, J. R., Mackey, H. M., Lum, B. L., Darbonne, W. C., Marsters, J. C., de Sauvage, F. J. & Low, J. A. (2009) Inhibition of the Hedgehog Pathway in Advanced Basal-Cell Carcinoma. *N Eng J Med*, 361(12), 1164-1172.

Vukovic, M., Sepulveda, C., Subramani, C., Guitart, A. V., Mohr, J., Allen, L., Panagopoulou, T. I., Paris, J., Lawson, H., Villacreces, A., Armesilla-Diaz, A., Gezer, D., Holyoake, T. L., Ratcliffe, P. J. & Kranc, K. R. (2016) Adult hematopoietic stem cells lacking Hif-1α self-renew normally. *Blood*, 127(23), 2841-6.

Walkley, C. R., Olsen, G. H., Dworkin, S., Fabb, S. A., Swann, J., McArthur, G. A., Westmoreland, S. V., Chambon, P., Scadden, D. T. & Purton, L. E. (2007) A microenvironment-induced myeloproliferative syndrome caused by retinoic acid receptor gamma deficiency. *Cell*, 129(6), 1097-110.

Wang, L., Kamocka, M. M., Zollman, A. & Carlesso, N. (2017) Combining Intravital Fluorescent Microscopy (IVFM) with Genetic Models to Study Engraftment Dynamics of Hematopoietic Cells to Bone Marrow Niches. *J Vis Exp*, 121.

Wang, W., Yu, S., Zimmerman, G., Wang, Y., Myers, J., Yu, V. W., Huang, D., Huang, X., Shim, J., Huang, Y., Xin, W., Qiao, P., Yan, M., Scadden, D. T., Stanley, P., Lowe, J. B., Huang, A. Y., Siebel, C. W. & Zhou, L. (2015) Notch Receptor-Ligand Engagement Maintains Hematopoietic Stem Cell Quiescence and Niche Retention. *Stem Cells*, 33(7), 2280-93.

Wang, Y. Z., Krivtsov, A. V., Sinha, A. U., North, T. E., Goessling, W., Feng, Z. H., Zon, L. I. & Armstrong, S. A. (2010) The Wnt/beta-Catenin Pathway Is Required for the Development of Leukemia Stem Cells in AML. *Science*, 327(5973), 1650-1653.

Warfvinge, R., Geironson, L., Sommarin, M. N. E., Lang, S., Karlsson, C., Roschupkina, T., Stenke, L., Stentoft, J., Olsson-Strömberg, U., Hjorth-Hansen, H., Mustjoki, S., Soneji, S., Richter, J. & Karlsson, G. (2017) Single-cell molecular analysis defines therapy response and immunophenotype of stem cell subpopulations in CML. *Blood*, 129(17), 2384-2394.

Weisberg, E., Manley, P. W., Breitenstein, W., Brüggen, J., Cowan-Jacob, S. W., Ray, A., Huntly, B., Fabbro, D., Fendrich, G., Hall-Meyers, E., Kung, A. L., Mestan, J., Daley, G. Q., Callahan, L., Catley, L., Cavazza, C., Azam, M., Mohammed, A., Neuberg, D., Wright, R. D., Gilliland, D. G. & Griffin, J. D. (2005) Characterization of AMN107, a selective inhibitor of native and mutant Bcr-Abl. *Cancer Cell*, 7(2), 129-41.

Weli, S. C., Fink, T., Cetinkaya, C., Prasad, M. S., Pennisi, C. P. & Zachar, V. (2010) Notch and hedgehog signalling cooperate to maintain self-renewal of human embryonic stem cells exposed to low oxygen concentration. *Int J Stem Cells*, 3(2), 129-37.

Wellbrock, J., Latuske, E., Kohler, J., Wagner, K., Stamm, H., Vettorazzi, E., Vohwinkel, G., Klokow, M., Uibeleisen, R., Ehm, P., Riecken, K., Loges, S., Thol, F., Schubert, C., Amling, M., Jucker, M., Bokemeyer, C., Heuser, M., Krauter, J. & Fiedler, W. (2015) Expression of Hedgehog Pathway Mediator GLI Represents a Negative Prognostic Marker in Human Acute

Myeloid Leukemia and Its Inhibition Exerts Antileukemic Effects. *Clin Cancer Res*, 21(10), 2388-98.

Wendel, H. G., de Stanchina, E., Cepero, E., Ray, S., Emig, M., Fridman, J. S., Veach, D. R., Bornmann, W. G., Clarkson, B., McCombie, W. R., Kogan, S. C., Hochhaus, A. & Lowe, S. W. (2006) Loss of p53 impedes the antileukemic response to BCR-ABL inhibition. *Proc Natl Acad Sci U S A*, 103(19), 7444-9.

Willert, K. & Nusse, R. (1998) Beta-catenin: a key mediator of Wnt signalling. *Curr Opin Genet Dev*, 8(1), 95-102.

Winter, G. E., Rix, U., Carlson, S. M., Gleixner, K. V., Grebien, F., Gridling, M., Mller, A. C., Breitwieser, F. P., Bilban, M., Colinge, J., Valent, P., Bennett, K. L., White, F. M. & Superti-Furga, G. (2012) Systems-pharmacology dissection of a drug synergy in imatinib-resistant CML. *Nature Chem Biol*, 8(11), 905-912.

Wu, J., Meng, F., Kong, L. Y., Peng, Z., Ying, Y., Bornmann, W. G., Darnay, B. G., Lamothe, B., Sun, H., Talpaz, M. & Donato, N. J. (2008) Association between imatinib-resistant BCR-ABL mutation-negative leukemia and persistent activation of LYN kinase. J *Natl Cancer Inst*, 100(13), 926-39.

Wu, M., Kwon, H. Y., Rattis, F., Blum, J., Zhao, C., Ashkenazi, R., Jackson, T. L., Gaiano, N., Oliver, T. & Reya, T. (2007) Imaging hematopoietic precursor division in real time. *Cell Stem Cell*, 1(5), 541-54.

Xie, S., Lin, H., Sun, T. & Arlinghaus, R. B. (2002) Jak2 is involved in c-Myc induction by Bcr-Abl. *Oncogene*, 21(47), 7137-7146.

Yaccoby, S., Barlogie, B. & Epstein, J. (1998) Primary myeloma cells growing in SCID-hu mice: A model for studying the biology and treatment of myeloma and its manifestations. *Blood*, 92(8), 2908-2913.

Yamamoto, R., Morita, Y., Ooehara, J., Hamanaka, S., Onodera, M., Rudolph, K. L., Ema, H. & Nakauchi, H. (2013) Clonal analysis unveils self-renewing lineage-restricted progenitors generated directly from hematopoietic stem cells. *Cell*, 154, 1112-1126.

Yamazaki, S., Ema, H., Karlsson, G., Yamaguchi, T., Miyoshi, H., Shioda, S., Taketo, M. M., Karlsson, S., Iwama, A. & Nakauchi, H. (2011) Nonmyelinating Schwann cells maintain hematopoietic stem cell hibernation in the bone marrow niche. *Cell*, 147(5), 1146-58.

Yang, D. G., Cao, F. L., Ye, X. M., Zhao, H., Liu, X. H., Li, Y., Shi, C., Wang, H. L. & Zhou, J. (2013) Arsenic Trioxide Inhibits the Hedgehog Pathway Which Is Aberrantly Activated in Acute Promyelocytic Leukemia. *Acta Haematologica*, 130(4), 260-267.

Yang, L. T., Nichols, J. T., Yao, C., Manilay, J. O., Robey, E. A. & Weinmaster, G. (2005) Fringe glycosyltransferases differentially modulate Notch1 proteolysis induced by Delta1 and Jagged1. *Mol Biol Cell*, 16(2), 927-42.

Yeung, J., Esposito, M. T., Gandillet, A., Zeisig, B. B., Griessinger, E., Bonnet, D. & So, C. W. E. (2010) beta-Catenin Mediates the Establishment and Drug Resistance of MLL Leukemic Stem Cells. *Cancer Cell*, 18(6), 606-618.

Yin, D. D., Fan, F. Y., Hu, X. B., Hou, L. H., Zhang, X. P., Liu, L., Liang, Y. M. & Han, H. (2009) Notch signalling inhibits the growth of the human chronic myeloid leukemia cell line K562. *Leuk Res*, 33(1), 109-14.

Ysebaert, L., Chicanne, G., Demur, C., De Toni, F., Prade-Houdellier, N., Ruidavets, J. B., Mansat-De Mas, V., Rigal-Huguet, F., Laurent, G., Payrastre, B., Manenti, S. & Racaud-Sultan, C. (2006) Expression of beta-catenin by acute myeloid leukemia cells predicts enhanced clonogenic capacities and poor prognosis. *Leukemia*, 20(7), 1211-1216.

Yu, H., Neale, G., Zhang, H., Lee, H. M., Ma, Z., Zhou, S., Forget, B. G. & Sorrentino, B. P. (2014) Downregulation of Prdm16 mRNA is a specific antileukemic mechanism during HOXB4-mediated HSC expansion in vivo. *Blood*, 124(11), 1737-47.

Yu, K. R., Yang, S. R., Jung, J. W., Kim, H., Ko, K., Han, D. W., Park, S. B., Choi, S. W., Kang, S. K., Schöler, H. & Kang, K. S. (2012) CD49f enhances multipotency and maintains stemness through the direct regulation of OCT4 and SOX2. *Stem Cells*, 30(5), 876-87.

Yugaw, T., Nishino, K., Ohno, S. I., Nakahara, T., Fujita, M., Goshima, N., Umezawa, A. & Kiyono, T. (2013) Noncanonical NOTCH Signalling Limits Self-Renewal of Human Epithelial and Induced Pluripotent Stem Cells through ROCK Activation. *Mol Cell* Biol, 33(22), 4434-47.

Yugawa, T., Nishino, K., Ohno, S.-I., Nakahara, T., Fujita, M., Goshima, N., Umezawa, A. & Kiyono, T. (2013) Non-canonical NOTCH signalling limits self-renewal of human epithelial and iPS cells through ROCK activation. *Mol Cell Biol*, 33(22). 4434-47.

Zanjani, E. D., Almeida-Porada, G., Livingston, A. G., Flake, A. W. & Ogawa, M. (1998) Human bone marrow CD34- cells engraft in vivo and undergo multilineage expression that includes giving rise to CD34+ cells. *Exp Hematol*, 26(4), 353-60.

Zeng, H., Yücel, R., Kosan, C., Klein-Hitpass, L. & Möröy, T. (2004) Transcription factor Gfi1 regulates self-renewal and engraftment of hematopoietic stem cells. *EMBO J*, 23(20), 4116-25.

Zeuner, A., F., F., Signore, M., Venneri, M. A., Pedini, F., Felli, N., Pagliuca, A., Conticello, C. & De Maria, R. (2011) The Notch2-Jagged1 interaction mediates stem cell factor signalling in erythropoiesis. *Cell Death Differ*, 18(2), 371-380.

Zhan, X., Shi, X., Zhang, Z., Chen, Y. & Wu, J. I. (2011) Dual role of Brg chromatin remodeling factor in Sonic hedgehog signalling during neural development. *Proc Natl Acad Sci U S A*, 108(31), 12758-12763.

Zhang, B., Ho, Y. W., Huang, Q., Maeda, T., Lin, A., Lee, S. U., Hair, A., Holyoake, T. L., Huettner, C. & Bhatia, R. (2012) Altered microenvironmental regulation of leukemic and normal stem cells in chronic myelogenous leukemia. *Cancer Cell*, 21(4), 577-92.

Zhang, B., Li, L., Ho, Y. W., Li, M., Marcucci, G., Tong, W. & Bhatia, R. (2016) Heterogeneity of leukemia-initiating capacity of chronic myelogenous leukemia stem cells. *J Clin Invest*, 126(3), 975-991.

Zhang, B., Li, M., McDonald, T., Holyoake, T. L., Moon, R. T., Campana, D., Shultz, L. & Bhatia, R. (2013) Microenvironmental protection of CML stem and progenitor cells from tyrosine kinase inhibitors through N-cadherin and Wnt-beta-catenin signalling. *Blood*, 121(10), 1824-1838.

Zhang, J., Niu, C., Ye, L., Huang, H., He, X., Tong, W.-G., Ross, J., Haug, J., Johnson, T., Feng, J. Q., Harris, S., Wiedemann, L. M., Mishina, Y. & Li, L. (2003a) Identification of the haematopoietic stem cell niche and control of the niche size. *Nature*, 425, 836-841.

Zhang, Y., Li, C., Jiang, X., Zhang, S., Wu, Y., Liu, B., Tang, P. & Mao, N. (2004) Human placenta-derived mesenchymal progenitor cells support culture expansion of long-term culture-initiating cells from cord blood CD34+ cells. *Exp Hematol*, 32(7), 657-64.

Zhao, C., Blum, J., Chen, A., Kwon, H. Y., Jung, S. H., Cook, J. M., Lagoo, A. & Reyal, T. (2007) Loss of beta-catenin impairs the renewal of normal and CML stem cells in vivo. *Cancer Cell*, 12(6), 528-541.

Zhao, C., Chen, A., Jamieson, C. H., Fereshteh, M., Abrahamsson, A., Blum, J., Kwon, H. Y., Kim, J., Chute, J. P., Rizzieri, D., Munchhof, M., VanArsdale, T., Beachy, P. A. & Reya, T. (2009) Hedgehog signalling is essential for maintenance of cancer stem cells in myeloid leukaemia. *Nature*, 458(7239), 776-9.

Zhao, Y., Masiello, D., McMillian, M., Nguyen, C., Wu, Y., Melendez, E., Smbatyan, G., Kida, A., He, Y., Teo, J. L. & Kahn, M. (2016) CBP/catenin antagonist safely eliminates drug-resistant leukemia-initiating cells. *Oncogene*, 35(28), 3705-3717.

Zhou, H.-S., Carter, B. Z. & Andreeff, M. (2016) Bone marrow niche-mediated survival of leukemia stem cells in acute myeloid leukemia: Yin and Yang. *Cancer Biol Med*, 13(2), 248-259.

Zhou, T., Commodore, L., Huang, W. S., Wang, Y., Thomas, M., Keats, J., Xu, Q., Rivera, V. M., Shakespeare, W. C., Clackson, T., Dalgarno, D. C. & Zhu, X. (2011) Structural mechanism of the Pan-BCR-ABL inhibitor ponatinib (AP24534): lessons for overcoming kinase inhibitor resistance. *Chem Biol Drug Des*, 77(1), 1-11.

Zon, L. I. (2008) Intrinsic and extrinsic control of haematopoietic stem-cell self-renewal. *Nature*, 453(7193), 306-13.